

Western Australian School of Mines

Department of Mining Engineering and Mine Surveying

**An Integrated Approach to Span Design in Open Stope
Mining**

by

Peter M Cepuritis

B.App.Sc. (App. Geol.) Royal Melbourne Institute of Technology, Australia

M.Eng.Sc. (Min. Geomech.) Curtin University of Technology, Australia

This thesis is presented for the Degree of
Doctor of Philosophy
of Curtin University of Technology

August 2010

DECLARATION

To the best of my knowledge and belief this thesis contains no material previously published by any other person except where due acknowledgement has been made.

This thesis contains no material which has been accepted for the award of any other degree or diploma in any university.

Signed:

Date:

ABSTRACT

In order to develop an appropriate mine design, a thorough understanding of the rock mass conditions and its potential response to mining is required. Rock mass characterisation is a key component in developing models of the rock mass and its engineering behaviour, and relies on disparate data collected by exploration geologists, mine geologists, rock mechanics engineers and technicians, in a variety of formats. Optimal rock mass model development requires the effective integration of all data sources, which currently requires considerable effort in collecting, managing, collating, validating and analysing this data.

The importance of understanding the spatial variability of rock mass conditions has been highlighted as a major issue. The traditional approach of using simplistic models of “average” rock mass conditions can lead to sub-optimal designs, which may result in unplanned additional costs or economic implications of dilution and ore loss. The design of stope and pillars should be optimised for the prevailing rock mass conditions in the various regions of the mine.

Some of the existing design tools used for open stope design have shown poor reliability in their performance predictions. Though some may have been originally developed to assist in initial stope size selection (i.e. pre-feasibility and feasibility levels), they are potentially being inappropriately relied upon for detailed design. Consideration of large scale structures on stability and their influence on local rock mass conditions are also important aspects of open stope design that are commonly over-looked. There is a need to select design methodologies that are optimised for the stage of project development. It is also important to emphasise the iterative, evolutionary and interdisciplinary nature of open stope design.

This thesis proposes a framework that attempts to integrate different rock mass characterisation models, numerical modelling and stope performance data to assist in improving the overall excavation design process. The key philosophy behind design optimisation is the continual reduction in uncertainty in collected data, analysis and design methods used with a view to improving the overall reliability of the design. A stope span design optimisation approach is proposed which attempts to ensure that the

appropriate methodologies in data collection, data analysis, rock mass model formulation and stope design are utilised at relevant project stages in order to minimise uncertainty and maximise design reliability. The design optimisation approach recognises that the appropriateness of a particular design methodology is highly dependant on the availability of an appropriate rock mass model, which is in turn dependant on the availability of quality rock mass data. With respect to the design of spans in open stope mining, the key aims of the proposed integrated approach are to;

- Assess the suitability of data for analysis
- If data is unsuitable, assess the most appropriate data collection strategy
- Assess the most appropriate approach to rock mass modelling
- Assess the most appropriate design methodologies
- Assess the reliability of the design criteria and quantify the potential economic impact of the design on the project

Optimisation of the design process also requires integration of state-of-the-art techniques in data collection, analysis, modelling and engineering analysis and design at the appropriate stage of project development. During development of this thesis a number of improvements have been proposed in key areas in the rock engineering design process which can be incorporated into the integrated approach, including;

- A rock mass data model has been developed that assists in facilitating the ongoing rock mass characterisation process. The data model is capable of integrating rock mass data from various sources, which promotes sharing of data and avoids duplication of data collection efforts. The data model is able to query rock mass data, define relationships between data types, apply bias corrections, and perform basic analysis for use in subsequent detailed analysis and rock mass modelling.
- An implicit based approach to spatial rock mass and deterministic discontinuity modelling can be employed to improve understanding of the spatial variability of rock mass parameters, inter-relationships between rock mass characteristics on their role in design. For example, understanding the influence of large-scale structures on rock mass characteristics and excavation performance.
- Improved scale independent geometrical assessments of stope performance have been proposed that maximise the use of stope performance data.

-
- An integrated back analysis framework has been presented that is able to account for structural complexity, scale and features that cannot be directly incorporated into linear elastic numerical modelling codes.
 - With regard to linear elastic back analyses, a number of improvements have been proposed, as well as a suggested method to assess appropriateness of continuum models based on discontinuity intensity and critical span.

ACKNOWLEDGEMENTS

This thesis was prepared under the supervision of Prof E. Villaescusa. I would like to thank Prof Villaescusa for giving me the opportunity to undertake this research and for having faith in me. His support, guidance and encouragement is gratefully appreciated. I am grateful to the following organisations for their financial support of this work;

- BHP Billiton Cannington Mine
- Barrick Gold Australia Kanowna Belle Gold Mine
- Commonwealth of Australia - ARC Linkage Grant
- Western Australian School of Mines

I would also like to thank the following individuals;

Dr Alan Thompson for his assistance in turning my mathematical ideas into the reality of macros and computer code. Mr Chris Windsor for initiating my understanding and passion for all things related to discontinuities. Dr Graham Baird for helping me understand that linear algebra is easy, once you understand it. Denise Magee (nee Mead), Luke Malatesta and Dylan Coles for their hard work and persistence in undertaking the *CMS* back analyses of stopes at Kanowna Belle Gold Mine and Cannington Mine.

BHP Billiton Cannington; Jody Todd, Christian Holland, Scott Jeffery, Rhett de Vries, Peter Knights, Steve Homer, Paul Tozer, Justin Walsh, Riek Muller, Anna Gentle, Tanya Nayda and Jianping Li. Barrick Gold Australia's Kanowna Belle Gold Mine; Dave Finn, Oleg Belov, Ronald Lachenicht, Richard Varden and Dave Twaddle.

Beck Engineering Pty Ltd for preparing and running the numerical models, especially Dave Beck for his enthusiasm and encouragement. Zaparo Pty Ltd for the research licence of their Leapfrog3D software. I especially would like to thank Jun Cowan, Hugh Ross and Glen Richards.

I'd like to thank all my friends at WASM, especially Mr Kelly Fleetwood for working with me and keeping my morale up at certain times and in certain places, and Mr Andrés Brzovic for being a good friend and listening to my ideas.

Lastly, I'd like to thank Ellen and Snappa, for without their support and encouragement I would not have persevered.

AUTHOR'S STATEMENT OF PREVIOUS PUBLICATIONS

Some results of data analyses and approaches discussed in this thesis have been previously published by the author during the time of thesis preparation. No references to these publications have been made in the body of the thesis, as the ideas and analysis techniques were developed as part of the thesis background work by the author prior to publication. The following list details the previous publications by the author at the time of submission of this thesis.

Villaescusa, E. and Cepuritis, P.M. 2005. The effects of large scale faults on narrow vein stope stability: A Case Study. Proceedings of the 40th US Rock Mechanics Symposium, Anchorage, Alaska, 25-29 June. Paper 05-714, 6p.

Cepuritis, P.M. and Villaescusa, E. 2006. Back Analysis Techniques for Assessing Open Stope Performance. 2006 Australian Mining Technology Conference. Hunter Valley, NSW. 26-27 September. pp. 261-271.

Cepuritis, P.M. and Villaescusa, E. 2006. Comprehensive Back Analysis Techniques for Assessing Factors Affecting Open Stope Performance. Proceedings of the 4th Asian Rock Mechanics Symposium. Singapore. 8-10 November. 8p.

Cepuritis, P.M., Villaescusa, E. and Lachenicht, R. 2007. Back Analysis and Performance of Block A Long Hole Open Stopes - Kanowna Belle Gold Mine. Rock Mechanics: Meeting Society's Challenges and Demands. Proceedings of the 1st Canada-US Rock Mechanics Symposium, Vancouver, Canada, 27-31 May. Eberhardt, E., Stead, D. and Morrison, T. (eds). Taylor & Francis, pp. 1431-1445.

Cepuritis, P.M. 2008. Techniques to assist in back analysis and assess open stope performance. MassMin2008 - Proceedings of the 5th International Conference on Mass Mining. Lulea, Sweden. 9-11 June. pp. 203-212.

Cepuritis, P.M., Villaescusa, E., Beck, D.A. and Varden, R. 2010. Back analysis of Over-break in a Longhole Open Stope Operation using Non-linear Elasto-Plastic Numerical Modelling. In Proceedings of the 44th US Rock Mechanics Symposium, Salt Lake City, 27-30 June.

TABLE OF CONTENTS

Declaration.....	i
Abstract.....	ii
Acknowledgements.....	v
Author's Statement of Previous Publications.....	vi
List of Symbols.....	xxiii
Flowchart Symbols.....	xxv
Chapter 1 - Introduction.....	1
1.1 Background.....	1
1.2 Objectives of the Research.....	3
1.2.1 Rock Mass Data collection and Data Management.....	3
1.2.2 Rock Mass Characterisation and Rock Mass Modelling Techniques.....	4
1.2.3 Rock Mass Classifications and Empirical Design Methodologies.....	5
1.2.4 Stope Performance Data Collection and Analysis.....	5
1.2.5 Numerical Modelling and Development of Instability Criteria.....	6
1.3 Structure of Thesis.....	7
Chapter 2 - A Review of Rock Engineering in Mine Design.....	11
2.1 Introduction.....	11
2.2 Overview of the Rock Engineering Design Process.....	11
2.3 Rock Engineering Design Methodologies.....	13
2.3.1 Empirical.....	13
2.3.2 Observational.....	13
2.3.3 Analytical.....	13
2.3.4 Numerical.....	15
2.4 Choice of Design Methodology.....	16
2.5 Rock Engineering in Open Stope Design	17
2.5.1 Planning and Design of Open Stopes.....	19
2.6 Uncertainty and Design Reliability.....	20
2.6.1 Reliability-based Design Analysis.....	22
2.7 BHP Billiton Cannington Mine.....	25
2.7.1 Geotechnical Objectives.....	27
2.7.2 Preliminary Stope Shape Review.....	27
2.7.3 Stope Stability Analysis.....	27
2.7.4 Draft Stope Note and Risk Assessment.....	29
2.7.5 Geotechnical Report.....	30
2.7.6 Discussion.....	31
2.8 Conclusions.....	32
Chapter 3 - Rock Mass Characterisation.....	35
3.1 Introduction.....	35
3.2 Rock Mass Characteristics.....	35

3.2.1 Geological Characteristics.....	36
3.2.2 Rock Fabric Engineering Properties.....	36
3.2.3 Assessment of In Situ Stress.....	37
3.2.4 Discontinuity Properties.....	39
3.3 Rock Mass Data Collection.....	42
3.3.1 Subjective versus Objective Techniques.....	43
3.3.2 Rock Mass Sampling Methods.....	44
3.3.3 Accuracy, Bias, Precision and Error.....	44
3.3.4 Remote Data Collection Methods.....	48
3.4 Rock Mass Data Analysis.....	48
3.4.1 Data Validation and Bias Corrections.....	48
3.4.2 Statistical Moments.....	50
3.4.3 Analysis of Discontinuity Data.....	51
3.4.4 Improving Accuracy and Precision in Rock Mass Data Collection.....	51
3.5 Conclusions.....	52
3.5.1 Rock Fabric Characterisation Investigations.....	53
3.5.2 Discontinuity Characterisation Investigations.....	54
3.5.3 Integrating available data sources.....	57
Chapter 4 - A Review of Empirical Methods in Open Stope Mine Design.....	59
4.1 Introduction.....	59
4.2 Rock Mass Classification Systems.....	59
4.2.1 Engineering Applications and Objectives.....	59
4.2.2 Classification Parameters.....	61
4.2.3 Extending Classifications for Other Applications.....	61
4.2.4 RQD.....	62
4.2.5 NGI - Q Rock Mass Classification System.....	63
4.3 Geological Strength Index.....	64
4.4 Empirical Open Stope Span Stability Graph Methods.....	66
4.4.1 Mathews Stability Graph Method.....	66
4.4.2 Modified Stability Graph Method.....	73
4.4.3 Nickson (1992).....	78
4.4.4 Stewart and Forsyth (1995).....	79
4.4.5 Recent Australian Mining Industry Experience.....	80
4.4.6 Modifications and Extensions to the Modified Stability Graph Method.....	82
4.5 Excavation Design using Empirical Methods.....	85
4.5.1 Critical Span.....	87
4.5.2 Hydraulic Radius.....	87
4.5.3 Radius Factor.....	88
4.5.4 Comparison of Span Parameters.....	89
4.6 Development of Empirical Design Lines.....	90
4.7 Conclusions.....	92
Chapter 5 - Assessments of Stope Performance.....	95
5.1 Introduction.....	95
5.1.1 Economic Performance.....	95

5.1.2 Rock Mechanics Performance.....	96
5.2 Qualitative Assessments of Performance	97
5.3 Quantitative Assessments of Performance	98
5.3.1 Dilution and Ore Loss.....	98
5.3.2 Over-break and Under-break estimation using Cavity Monitoring Systems.....	100
5.3.3 Volume of Over-break and Under-break.....	102
5.3.4 Area of Over-break and Under-break.....	104
5.3.5 Depth of Over-break and Under-break.....	105
5.3.6 ELOS and ELLO.....	107
5.4 Qualitative and Quantitative Assessments of Performance.....	108
5.5 Quantitative and Economic Assessments of Performance.....	109
5.6 Conclusions.....	110
Chapter 6 - Proposed Geometric Performance Measures.....	111
6.1 Introduction.....	111
6.2 Shape and Size.....	111
6.3 Shape, Size and Dimensionality.....	112
6.4 Existing Measures of Shape and Size in Open Stope Design.....	114
6.5 A Scale Independent Measure of the Extent of Over/Under-break.....	114
6.6 Two dimensional Shape Measures.....	114
6.6.1 Circularity.....	116
6.7 Three-dimensional Shape Measures.....	116
6.7.1 Hemi-sphericity.....	117
6.8 A Geometrical Classification of Over-break and Under-break.....	118
6.8.1 Inter-sectional Area.....	119
6.8.2 Hemi-sphericity and Circularity.....	119
6.8.3 Relative Volume.....	119
6.9 Conclusions.....	125
Chapter 7 - Continuum Based Numerical Modelling In Open Stope Mine Design.....	127
7.1 Introduction.....	127
7.2 Continuum and Discontinuum Numerical Models	128
7.2.1 Excavation Scale and Rock Mass Structure.....	129
7.3 Equivalent Continuum Modelling.....	131
7.3.1 Constitutive Models.....	131
7.3.2 Rock Mass Failure Criteria.....	132
7.3.3 Summary.....	133
7.4 Empirical Deformability and Peak Strength Failure Criteria for Rock Masses.....	134
7.5 Continuum Based Back Analysis.....	135
7.5.1 Site-Specific Linear Elastic Damage Models.....	136
7.5.2 Non-linear Elasto-Plastic Damage Models.....	140
7.6 Reliability of Stope Performance Back Analysis Using Linear Elastic Modelling.....	142
7.6.1 Back Analysis using Excavation Profiles.....	144
7.6.2 Variability in Confinement.....	145
7.7 Conclusions.....	147

Chapter 8 - Rock Mass Modelling	149
8.1 Introduction.....	149
8.2 Stochastic Representations of Rock Mass Properties.....	149
8.2.1 Classical Statistics.....	149
8.2.2 Regionalised Variables and Geostatistics.....	150
8.3 Rock Mass Model Processes.....	151
8.4 Spatial Model Types.....	152
8.5 Spatial Interpolation Methods.....	153
8.5.1 Basic Principles of Interpolation.....	153
8.5.2 Interpolation Methods.....	153
8.5.3 Geostatistical Interpolation Methods.....	154
8.5.4 Non-Geostatistical Interpolation Methods.....	155
8.5.5 Geostatistical and Spatial Modelling in Mining Rock Mechanics.....	155
8.5.6 Radial Basis Functions.....	156
8.5.7 Model Reliability.....	157
8.6 Rock Mass Structure Modelling.....	158
8.6.1 Joint Network Models.....	160
8.7 Rock Mass Domains.....	163
8.7.1 Trend Analysis via Cumulative Sums.....	163
8.7.2 Statistically Homogeneous Domains.....	164
8.7.3 Data Density using Distance Buffers and Voxel Counts.....	165
8.7.4 Structural Orientation Domains.....	165
8.7.5 Structural Geology Approach to Domain Definition.....	167
8.8 Model Validation.....	169
8.9 Conclusions.....	170
Chapter 9 - A Rock Mass Characterisation Framework.....	171
9.1 Introduction.....	171
9.2 The Rock Mass Characterisation Data Model.....	175
9.2.1 Fact Data versus Interpretative Data.....	176
9.2.2 Data Source Details.....	177
9.2.3 Data Dimensions and Coordinates.....	177
9.2.4 Domain Tagging.....	178
9.2.5 Summary.....	179
9.3 Conclusions.....	180
Chapter 10 - An Implicit Function Based Approach to Rock Mass Modelling.....	181
10.1 Introduction.....	181
10.2 Spatial Modelling of Discontinuity Intensity.....	181
10.2.1 Models based on One-Dimensional Data.....	182
10.2.2 Models based on Two-Dimensional Data.....	192
10.3 A Deterministic Discontinuity Modelling Framework.....	194
10.3.1 Traditional Three-dimensional Wireframe Modelling.....	194
10.3.2 A Hierarchical Implicit Surface Approach.....	195
10.3.3 Modelling Process.....	195
10.3.4 Discontinuity Trace Data.....	197

10.3.5	Discontinuity Persistence and Hierarchy.....	197
10.3.6	Genetic Classification.....	197
10.3.7	Orientation Grouping.....	198
10.3.8	Generation of fact glyphs.....	198
10.3.9	Fact Data Selection and Interpolation.....	198
10.3.10	Model Validation.....	199
10.3.11	Comparison with Traditional Digital Discontinuity Models.....	201
10.4	Conclusions.....	201
10.4.1	Spatial Models of Discontinuity Intensity.....	202
10.4.2	Deterministic Discontinuity Modelling Framework.....	203
Chapter 11	- An Integrated Approach to the Geotechnical Design of Spans in Open Stope Mining.....	205
11.1	Introduction.....	205
11.2	Design Optimisation Through an Integrated Approach.....	205
11.3	Project Development Stage and Objectives.....	207
11.4	Data Collection.....	210
11.4.1	Data Suitability and Reliability.....	211
11.4.2	Data Collection Programmes.....	212
11.4.3	Rock Mass Characterisation Framework.....	213
11.5	Rock Mass Models.....	213
11.5.1	Deterministic Discontinuity Models.....	213
11.5.2	Stochastic Discontinuity Models.....	214
11.5.3	Rock Fabric / Continuum Models.....	214
11.5.4	Rock Mass Modelling Techniques and Domain Definition.....	215
11.5.5	Assessing Model Suitability and Reliability.....	216
11.6	Design Methods.....	216
11.6.1	Empirical Methods.....	217
11.6.2	Analytical Methods.....	219
11.6.3	Numerical Methods.....	219
11.6.4	Integrating Rock Mass Models and Numerical Codes.....	220
11.7	Design Reliability.....	221
11.7.1	Estimates of Open Stope Design Reliability for Initial Forward Analysis.....	223
11.7.2	Confirming Design Reliability Based on Back Analysis.....	224
11.8	An Integrated Back Analysis Framework.....	226
11.8.1	Integrated Spatial Model and Relational Databases.....	227
11.8.2	Proposed Techniques for Improved Linear Elastic Back Analysis in Open Stope Design.....	230
11.8.3	Back Analysis Process.....	232
11.8.4	Candidate Instability Criteria.....	234
11.9	Quantifying the Potential Economic Impact of the Design on the Project.....	235
11.10	Conclusions.....	237
11.10.1	Continual Reduction in Uncertainty.....	237
11.10.2	Improvements to Existing Techniques.....	238
11.10.3	Practical Applications.....	238
Chapter 12	- Case Study: BHP Billiton Cannington Mine.....	241
12.1	Introduction.....	241

12.1.1 Cannington Mine.....	241
12.2 Geology.....	242
12.2.1 Regional Geology.....	242
12.2.2 Mine Geology.....	243
12.2.3 In Situ Stress.....	248
12.3 Mine Scale Rock Mass Model.....	248
12.3.1 Previous Rock Mass Modelling.....	249
12.3.2 Resolution Issues in Slope Design.....	249
12.3.3 Scope of Current Modelling.....	250
12.3.4 Data Sources.....	251
12.3.5 Unconfined Compressive Strength Modelling.....	252
12.3.6 Discontinuity Intensity Modelling.....	255
12.3.7 Relationships between rock mass parameters.....	257
12.4 Identification of Large-scale Structures from Discontinuity Intensity Modelling.....	259
12.4.1 Background.....	259
12.4.2 Geological Mapping.....	259
12.4.3 Deterministic Modelling of the Squirrel Hills Fault Zone.....	260
12.4.4 Establishing Model Reliability.....	261
12.4.5 Summary.....	264
12.5 Two-Dimensional Discontinuity Intensity Model.....	264
12.6 Empirical and Geometrical Back Analysis of Slope Performance.....	267
12.6.1 Scale independent empirical back analysis.....	268
12.6.2 Forward analysis.....	271
12.6.3 Risk-based Design.....	274
12.6.4 Assessment of Existing Empirical Methods.....	279
12.7 Conclusions.....	281
Chapter 13 - Case Study: Kanowna Belle Gold Mine.....	283
13.1 Introduction.....	283
13.2 Kanowna Belle Gold Mine Underground Operations.....	284
13.3 Geology.....	284
13.3.1 Regional Geology.....	284
13.3.2 Generalised Mine Geology.....	287
13.3.3 In Situ Stress.....	289
13.4 Deterministic Discontinuity Modelling.....	289
13.4.1 Geological Fact Data.....	289
13.4.2 Interpretation.....	290
13.4.3 Model Validation.....	290
13.4.4 Summary.....	292
13.5 Improved Rock Mass Domaining using Large-scale Discontinuities.....	292
13.5.1 Orientation Analysis.....	293
13.6 Discontinuity Intensity Model.....	298
13.6.1 Domains and Interpolation Parameters.....	298
13.6.2 Variability of Rock Mass Characteristics on Large-Scale Discontinuities.....	300
13.6.3 Summary.....	302

13.7 Linear Elastic Back Analysis.....	302
13.7.1 Initial Modelling Parameters.....	303
13.7.2 Assumptions.....	303
13.7.3 Structures.....	304
13.7.4 Results.....	304
13.7.5 Summary.....	307
13.8 Non-Linear Numerical Modelling and Back Analysis.....	308
13.8.1 Modelling package.....	308
13.8.2 Constitutive Model.....	309
13.8.3 Modelling Approach.....	309
13.8.4 Rock Mass Domains.....	309
13.8.5 Excavation Steps.....	309
13.8.6 Stope-scale structural model.....	310
13.8.7 Modelling Output.....	310
13.8.8 Stochastic Analysis of Instability.....	311
13.8.9 Results of Stochastic Analysis.....	315
13.8.10 Instability Criteria as a Predictor and Design Tool.....	319
13.8.11 Discussion.....	325
13.9 Conclusions.....	326
Chapter 14 - Conclusions.....	329
14.1 An integrated approach to the geotechnical design of open stopes.....	329
14.2 Main Findings and Achievements of Research.....	329
14.3 Thesis Limitations and Recommendations for Future Work.....	333
References.....	337
Appendix A - Rock Mass Data Collection and Analysis Methods.....	355
Appendix B - Comparison of Empirical Methods in Open Stope Design.....	395
Appendix C - Validation Plans for the Squirrel Hills Structural Interpretation.....	399
Appendix D - Cannington Window Mapping Data.....	407
Appendix E - Cannington Empirical Back Analysis Data.....	413
Appendix F - Kanowna Belle Back Analysis Data.....	421

LIST OF TABLES

Table 2.1 - Common numerical methods used in rock engineering (Jing, 2003)	15
Table 2.2 - Suggested data requirements, rock mass model reliability and design techniques based on project stage (Haile, 2004)	23
Table 2.3 - Risk management factors considered in the design of stopes at BHP Cannington Mine	30
Table 3.1 - Comparison of common stress measurement techniques (Villaescusa et al., 2003b)	38
Table 3.2 - Comparison of Subjective versus Objective data collection techniques	44
Table 3.3 - Summary of common rock mass data collection methods in mining	45
Table 3.4 - Summary of Common Rock Mass Data Analysis Tasks	50
Table 4.1 - Example objectives for two tunnelling projects	60
Table 6.2 - Stope Performance Classification based on Relative Volume	121
Table 6.3 - Summary of over-break shape measures and performance classification for example stope surfaces shown in Figure 6.6	123
Table 6.4 - Summary of stope performance by mining block based on Relative volume	125
Table 7.1 - Comparison of Numerical Methods (modified after Coggan et al, 1998)	128
Table 7.2 - Empirical relations of deformation modulus of rock masses (Li, 2004)	134
Table 7.3 - Empirical peak strength failure criteria for intact rock and rock masses (after Li, 2004) ..	135
Table 8.1 - Example joint network models and their characteristics	162
Table 9.1 - Example capabilities of the rock mass data model	179
Table 10.1 - Discontinuity Linear Intensity by orientation groups for Sites A and B	190
Table 10.2 - Summary of the influence of sampling and rock mass anisotropy on spatial models of discontinuity intensity	203
Table 11.1 - Example open stope span design criteria	222
Table 11.2 - Proposed qualitative assessment of the appropriateness of continuum models based on discontinuity linear frequency and critical span	232
Table 12.1 - Discontinuity sets at Cannington by rock type (after Power, 2004)	247
Table 12.2 - In situ stress model for the Cannington Mine (Windsor, 2006)	248
Table 12.3 - Summary of intact unconfined compressive strength by rock type at Cannington Mine	252
Table 12.4 - Identified development intercepts of the "Squirrel Hills" fault zone from geological fact mapping	262
Table 12.5 - Significance statistics for the probabilistic linear regression models of over-break	273
Table 12.6 - Input parameters for example economic assessment	277
Table 12.7 - Sensitivity and Specificity of the Cannington Logistic Regression Model	280
Table 13.1 - In situ stress model for Kanowna Belle Gold Mine	289
Table 13.2 - Summary of linear elastic critical stress-based criteria	306
Table 13.3 - Non-linear rock mass modelling parameters	309
Table 13.4 - Anticipated stability and bounds to instability criteria for velocity and plastic strain	313

LIST OF FIGURES

Figure 2.1 - Outline flowchart for mine design with multiple feedback loops (Brown, 1985).....	12
Figure 2.2 - Suitability of various numerical modelling methods with respect to scale of excavation a) continuum, b) either continuum with discontinuity elements or discrete method c) discrete method and c) equivalent continuum method - modified from (Jing, 2003)	16
Figure 2.3 - Flowchart for a) Rock Engineering Design Process and b) supporting Rock Mechanics Modelling Techniques (Hudson and Feng, 2007).....	18
Figure 2.4 - Slope design methodology from data collection to slope reconciliation (Villaescusa, 2004)	20
Figure 2.5 - Generic process to ascertain data uncertainty and risk for mining projects (Haile, 2004)...	24
Figure 2.6 - Conceptual representation of the distribution of uncertainty in load (Q) and resistance (R) (modified after Hoek, 1992).....	25
Figure 2.7 - Detailed slope design process at BHP Billiton Cannington Mine (Roberts, 2005).....	26
Figure 3.1 - Grouping of the ten discontinuity parameters into Geometric and Strength parameters....	40
Figure 3.2 - Demonstration of scale effects on ubiquitous representation of discontinuities utilising the General Rock Structure Scheme (Pusch, 1994).....	41
Figure 3.3 - Representative elemental volume (REV) concept (modified from Hudson, 1989).....	46
Figure 3.4 - Comparison of sampling methods and their ability to capture various rock mass characteristics (modified from Hudson, 1989).....	49
Figure 3.5 - Sample number versus precision of the mean discontinuity estimate for negative exponential distributions of spacing (Priest and Hudson, 1981).....	52
Figure 3.6 - Illustrative concept showing strength characterisation based on data density and its relation to method precision.....	53
Figure 4.1 - Variation of theoretical RQD with mean discontinuity spacing for a range of threshold values (after Priest and Hudson, 1976).....	62
Figure 4.2 - Range of applicability of GSI with respect to scale limitations of Hoek-Brown failure criterion (modified from Hoek and Brown, 1997).....	65
Figure 4.3 - Summary of the chronology of some rock mass classifications and empirical open slope span design methods (modified from Stewart and Forsyth, 1995).....	67
Figure 4.4 - Rock Stress Factor (A) (after Mathews et al, 1981).....	69
Figure 4.5 - Mathews stability chart with data points and stability zones (modified after Mathews et al, 1981).....	71
Figure 4.6 - Unsupported Modified Stability Graph (after Potvin, 1988).....	76
Figure 4.7 - Supported Modified Stability Graph (after Potvin, 1988).....	76
Figure 4.8 - Modified Stability Graph (Potvin, 1988) stability zones with Mount Charlotte unsupported data (after Trueman et al, 2000).....	81
Figure 4.9 - Modified Stability Graph (Potvin, 1988) with Cannington unsupported and supported data, with the Cannington Line (after Streeton, 2000).....	81
Figure 4.10 - Modified Stability Graph (Potvin, 1988) with Olympic Dam unsupported data (after Oddie	

and Pascoe, 2005).....	83
Figure 4.11 - Comparison of relative influence of intact compressive strength to induced stress for a number of empirical systems (modified from Villaescusa et al, 2003).....	84
Figure 4.12 - Revised Stress Factor (A) including effect of tensile stress (Diederichs and Kaiser, 1999).	85
Figure 4.13 - An example of Effective Radius Factor for two locations on a stope surface (Milne et al, 2004).....	89
Figure 4.14 - Correlation of elastic deformation with Radius Factor (Pascoe and Oddie, 2003).....	89
Figure 4.15 - Comparison of Hydraulic Radius and Radius Factor (Milne et al, 1996).....	90
Figure 4.16 - Extended Mathews' stability graph based on logistic regression (Mawdesley et al., 2001)	92
Figure 5.1 - Planned and unplanned dilution (after Scoble and Moss, 1994).....	99
Figure 5.2 - Classification of dilution and ore loss (Villaescusa, 1998).....	100
Figure 5.3 - Schematic showing effects of shadowing and accuracy issues when amalgamating CMS surveys.....	101
Figure 5.4 - Example calculation of volume of over-break and under-break using a) set operations and boolean operations (b-f).....	102
Figure 5.5 - Schematic showing definition of area of intersection between stope surface and over-break volume (enclosed by dashed line) and denoted as AOB.....	105
Figure 5.6 - Schematic showing measurement of a) depth of over-break for planar surfaces, and b) effect of irregular shapes on determining direction of depth of over-break.....	106
Figure 5.7 - Calculating depth of over-break from a) CMS (red) and reference volume (blue) by b) discretising both surfaces, c) shows detailed discretisation and d) shows contoured values of isotropic distance to CMS from the reference volume.....	106
Figure 5.8 - Example schematic showing inability of ELOS to capture geometry of over-break.....	108
Figure 6.1 - Plots of a) proposed measure of Circularity versus number of sides and b) SFC versus proposed Circularity measure, for a variety of 2-dimensional shapes.....	115
Figure 6.2 - Relationship between hemi-sphericity and normalised volume for a spherical segment... ..	118
Figure 6.3 - Plot of hemi-sphericity versus circularity for some example 3-dimensional geometrical shapes.....	119
Figure 6.4 - Plot of Circularity versus Extensivity for some example 2-dimensional shapes of over-break shown with an example stope surface shape, together with a classification.....	120
Figure 6.5 - Plot of hemi-sphericity versus circularity with a generalised shape classification.....	120
Figure 6.6 - Stope surface over-break at Cannington mine plotted by a) hemi-sphericity, circularity and extensivity, b) hemi-sphericity versus extensivity (classified by Relative Volume), and c) re-scaled example stope surfaces (labelled A-F) shown in elevation and cross-section with CMS and design profiles.....	122
Figure 6.7 - Box plots displaying statistical distribution of scale independent stope performance parameters (for over-break) for various mining blocks at Kanowna Belle Gold Mine.....	124
Figure 6.8 - Frequency-probability plots of Relative volume of over-break on stope surfaces for (a) mining Block A, (b) Block C, and (c) Block D at Kanowna Belle Gold Mine.....	124
Figure 7.1 - Relationship between P21 and Axial strength reduction of modelled pillars (after Elmo and	

Stead, 2010).....	129
Figure 7.2 - Strength variability as a function of discontinuity linear intensity and critical span. Data based on Elmo and Stead (2010).....	130
Figure 7.3 - Influence of constitutive model on stress-strain relationships.....	132
Figure 7.4 - Differences of forward and back analyses (Sakurai, 1997).....	136
Figure 7.5 - a) Linear elastic stress damage model (after Wiles, 2001) for monotonically increasing stresses, together with assumed strain damage, b) generalised damage model (after Wiles, 2001) and c) showing various stress paths to over-stressing.....	137
Figure 7.6 - Stope Damage Assessment Chart for stope pillars at the Kidd Mine (after Board, 2000)...	138
Figure 7.7 - Damage and failure criteria (after Villaescusa et al, 2003).....	139
Figure 7.8 - Common damage scale with indicative levels of equivalent plastic strain shown on left (Beck and Duplancic, 2005).....	142
Figure 7.9 - Prediction error for linear elastic back analysis (modified from Wiles, 2006).....	143
Figure 7.10 - Stress path in linear elastic modelling (modified after Beck, 2003).....	144
Figure 7.11 - Inability of CMS profiles to accurately define zone of yielded rock mass.....	145
Figure 7.12 - Typical 2D linear elastic stress analysis contour plot of confinement (σ_3), showing coefficient of variation for σ_1 (CV1) and σ_3 (CV3) along various sampling regimes.....	146
Figure 8.1 - Example of multivariate representation down a borehole (Maerz and Zhou, 2005).....	167
Figure 8.2 - Generalised procedure for using multi-scale data sources for sub-surface modelling (de Kemp, 2000).....	169
Figure 9.1 - Conceptual dependency diagram showing influence of common rock mass characterisation data types on development of a robust rock mass model.....	172
Figure 9.2 - Ability to characterise the rock mass based solely on unoriented drill core. Dimmed items indicate partial characterisation.....	173
Figure 9.3 - Ability to characterise the rock mass based solely on mapping. Dimmed items indicate partial characterisation.....	174
Figure 10.1 - 2-dimensional plane (vertical, oriented east-west) of the 3-dimensional discontinuity intensity locus showing a) directions for maximum and minimum discontinuity intensity, together with possible maximum and minimum b) tensor representations and c) isotropic representations.....	183
Figure 10.2 - Plot of corrected versus uncorrected discontinuity linear intensity data (left) and cumulative frequency plot of corrected versus uncorrected data.....	184
Figure 10.3 - Section at 11050mN showing contours of isotropically modelled discontinuity linear intensity for a) uncorrected and b) corrected data	186
Figure 10.4 - Section at 4690mN showing variability of drill hole sampling directions.....	187
Figure 10.5 - Isometric view of a) total sampling volume based on 5.64m isotropic distance from boreholes , compared with b) the isotropically sampled volume based on spherical variance.....	189
Figure 10.6 - Isometric view of the query isosurface (where spherical variance = 0.05 and number samples per unit cell > 15), together with discontinuity traces from window mapping data showing test areas A and B.....	190

Figure 10.7 - Isometric view of test cell locations A and B, a) and b) respectively, with borehole orientation groups and traces from window mapping data, together with the orientation analysis of window mapping data from areas A and B, c) and d) respectively.....	191
Figure 10.8 - Diagram showing circular sub-sampling windows for analysis of discontinuity areal intensity from two-dimensional data.....	193
Figure 10.9 - Isometric view of an interpreted fault surface generate by a) traditional sectional interpretation and wire-frame triangulation and b) by implicit surface defined by a RBF with user defined resolution for triangulation, together with the fault intercept data set (red spheres).....	195
Figure 10.10 - Flowchart for the generation of deterministic discontinuity models.....	196
Figure 10.11 - Clipped isometric view showing a) classified fact data, b) "pseudo" fact glyphs and c) interpolated structures.....	197
Figure 10.12 - Angular validation criteria for unoriented structural data.....	200
Figure 10.13 - Perspective view of models of Fitzroy Fault a) using original data and traditional modelling techniques and b) proposed implicit function based approach (see text for details).....	202
Figure 11.1 - Interaction and progression of design objectives, design methods, rock mass models and data collection with project development.....	208
Figure 11.2 - General rock engineering design process for span design.....	209
Figure 11.3 - Plot of a) depth of failure versus hydraulic radius for Mt Marion data (Villaescusa, 2010) and b) probability of depth of failure versus hydraulic radius for 1m, 2m and 3m.....	225
Figure 11.4 - Isometric view showing some components of the integrated spatial model.....	229
Figure 11.5 - Example stress path classification for excavations steps in linear elastic modelling.....	231
Figure 11.6 - Example of pillar rock mass damage rating (after Roberts et al, 1998).....	231
Figure 11.7 - Framework for back analysis of stope performance utilising numerical modelling, volumetric queries and stope performance databases.....	233
Figure 11.8 - Results of intersection of multiple candidate criteria (gold) for stope AP02 looking a) west and b) east, compared against CMS profile (dark grey).....	236
Figure 12.1 - Location of a) the Eastern Fold Belt of the Mt Isa inlier, b) Cannington Mine with regional geology (Chapman and Williams, 1998).....	243
Figure 12.2 - Cross section at 4700mN showing local mine geology and mineralisation (courtesy BHP Billiton Cannington Mine).....	244
Figure 12.3 - Plan of interpreted geology at approximately 300mLV, showing the major brittle structures (after McCarthy, 1996).....	246
Figure 12.4 - Sectional view of stope 24jc6 showing discontinuity linear intensity values for a) existing Cannington block model and b) high resolution RBF surface interpolant	250
Figure 12.5 - Modelled UCS (MPa) values a) cross-section at 4700mN also showing valid UCS samples (spheres) and b) correlation between laboratory and modelled UCS values (dashed line represents equivalence).....	253
Figure 12.6 - Modelled DLF values a) cross-section at 4700mN also showing logged DLF samples (spheres) and b) Q-Q plot between logged and modelled DLF values.....	255

Figure 12.7 - Development at 350mLV showing interpolated a) UCS and b) DLF values for the Central Zone domain.....	256
Figure 12.8 - Plot of a) UCS (MPa) for validated geomechanics laboratory data versus logged DLF (m-1) at the sample position, and b) modelled UCS (MPa) versus modelled DLF (m-1) for the integrated model data based on equally spaced (15m) sampling points along the 350mLV development	257
Figure 12.9: Isometric view of Trepell and Hamilton faults and discontinuity intensity modelled at 450mLV showing alignment of high intensity along the "Squirrel Hills" zone.....	259
Figure 12.10 - Perspective (looking north east) of digitised fact mapping in vicinity of interpreted "Squirrel Hills" fault zone.....	260
Figure 12.11 - Perspective (looking north east) of three-dimensional "pseudo" fact models of digitised geology.....	260
Figure 12.12 - Lower hemisphere stereographic projection of poles to planes for identified mapped intercepts of the Squirrel Hills structure.....	261
Figure 12.13 - Long section of interpreted "Squirrel Hills" fault zone (looking perpendicular to the south west), showing identified intercepts (red) for each level.....	262
Figure 12.14 - Sectional view of north east wall of drive C8WX3 showing window mapping traces and calculated discontinuity areal intensity values.....	264
Figure 12.15 - a) Isometric view of mapped traces around stope 20ec8HL and Trepell Fault b) relationship between distance to Trepell Fault and increase in corrected areal intensity (P'21).....	265
Figure 12.16 - Relationship between a) uncorrected linear intensity and distance to Trepell Fault b) proportionality relationship between areal and linear intensity.....	265
Figure 12.17 - Plot of modified stability number (N') versus hydraulic radius, classified by depth of over-break (after Coles, 2007).....	266
Figure 12.18 - Isometric view of a) modelled UCS and b) DLF on selected back analysed stopes.....	268
Figure 12.19 - Plot of a) Relative volume versus UCS (MPa) and b) Percentage of "Poor" stope performance versus UCS (MPa).....	269
Figure 12.20 - Plot of a) Relative volume versus discontinuities per span and b) Percentage of "Poor" stope performance versus discontinuities per span.....	269
Figure 12.21 - Plot of a) Relative volume versus discontinuities per span divided by UCS and b) Percentage of "Poor" stope performance versus discontinuities per span divided by UCS.....	270
Figure 12.22 - Probabilistic models of over-break stope performance a) exponential model, and b) linear model.....	271
Figure 12.23 - Comparison of UCS for "under-broken" and "over-broken" stopes, showing a) cumulative distribution and b) Q-Q plot.....	272
Figure 12.24 - Comparison of discontinuities per span for "under-broken" and "over-broken" stopes, showing a) cumulative distribution and b) Q-Q plot.....	272
Figure 12.25 - Relative volume versus a) UCS, b) discontinuities per span and c) discontinuities per span divided by UCS with data segregated into predominantly "under-broken" and "over-broken" stopes, with empirical probabilistic models for performance prediction based on	

predominantly “over-broken” stopes for b) UCS, d) discontinuities per span and f) discontinuities per span divided by UCS.....	274
Figure 12.26 - a) combined probabilistic model of stope performance for over-break and under-break, and b) distribution of probability for example in text.....	275
Figure 12.27 - Isometric view of stope 22h.c6HL looking a) north east and b) south west, and stope 47b.70FZ looking c) north west and d) east contoured by predicted probability of "poor" performance due to over-break together with CMS geometries.....	275
Figure 12.28 - Plot of cost per tonne for a) over-break, under-break and mining costs, with b) total cost against stope span, together with lower and upper bounds based on 95% confidence intervals for the probabilistic models.....	278
Figure 12.29 - Cannington stability graph data with the stability zone defined by logistic regression..	280
Figure 13.1 - Summary location showing a) the Yilgarn Craton of Western Australia, b) regional geology of the Norseman-Wiluna belt, and c) the local geology around the Kanowna Belle Gold Mine. (modified after Gee and Swager, 2008 and Ross et al, 2004).....	286
Figure 13.2 - Local mine geology in plan (top) and section (bottom).....	288
Figure 13.3 - Isometric view (looking south east) showing deterministic discontinuity models with the Kanowna Belle Open Pit for reference.....	290
Figure 13.4: Lower hemisphere equal area stereographic projections comparing a) small scale structural orientations, b) geological fact mapping scale orientations and c) orientations of modelling structures for Block D and E.....	291
Figure 13.5 - Size distribution of deterministic discontinuity models.....	291
Figure 13.6 - Conolly diagram of the Fitzroy Fault (long section looking north).....	293
Figure 13.7 - Plots of dip and dip direction versus coordinate axis for Set 1 a) Easting , b) Northing and RL.....	294
Figure 13.8 - Schematic plan showing delineation of structural domains based on inflection of the Fitzroy Fault.....	294
Figure 13.9 - Stereographic projections for structural domains a) Zone 4, b) Zone 5 and c) Zone 6 together with the axial plane and its pole.....	295
Figure 13.10 - Conceptual structural model showing clockwise rotation of mean poles of Set 1 across structural domains along the axial plane, with a corresponding increase in intensity of Set 2.....	296
Figure 13.11 - a) isometric slice showing structural data in Zone 6 and isosurfaces at a number of distances from Inflection axis plane 1, b) change of dip and dip direction of Set 1 in zone 6 with distance from Inflection axis plane 1.....	297
Figure 13.12 - a) original orientations and Fisher's K constants for Set 1 in zones 5 and 6, and b) updated orientations and Fisher's K constants with change of domain boundary.....	298
Figure 13.13 - Lower hemisphere equal angle projection showing intersection of Fitzroy Fault and Felsic Contacts, with pitch angle relative to Felsic Contact.....	299
Figure 13.14: Plot of discontinuity linear frequency versus distance to a modelled structure for Block A rock mass showing discrimination zones used in linear elastic modelling.....	300
Figure 13.15 - Deterministic discontinuity models colour contoured by DLF showing lines of intersection	

with the Fitzroy Fault.....	301
Figure 13.16 - Discontinuity linear frequency characteristics for modelled structures, showing a) bivariate kernel density estimation of modelled uncorrected discontinuity linear frequency versus intersection distance from the Fitzroy fault, b) example cumulative probability curves for various distances from the fault intersection.....	301
Figure 13.17 - Longitudinal view showing stoping sequence for Block A.....	303
Figure 13.18 - Linear elastic critical stress-based criteria for a) all data, b) DLF < 7m-1 and greater than 5m to a structure, c) DLF > 7m-1 and less than 5m to a structure.....	306
Figure 13.19 - Plot of σ_1 versus σ_3 for a) moderately jointed rock and b) very highly jointed rock <5m from structure, showing contours of over-break and loading conditions (thin dashed lines), theoretical Hoek-Brown rock mass strength (thick solid line) and estimated rock mass damage initiation criteria (thick dashed line).....	307
Figure 13.20 - Arrangement and distribution of results points for a) Block C stopes, showing b) detail for stope CD0062.....	311
Figure 13.21 - Example data for stope CP0074 showing plastic strain and maximum velocity values versus mining step for a) a stable point and b) an unstable point, with locations shown in c) an isometric view of a 10m horizontal slice (mid-span) showing stope design, CMS, hangingwall data points and some stope scale structures (looking south west).....	312
Figure 13.22 - Plastic strain versus maximum velocity during mining for unstable points indicating data independence.....	313
Figure 13.23 - Plan at 10006mRL showing influence of structure on contours of plastic strain.....	314
Figure 13.24 - Long section and selected sections of Block A stopes showing zones of incomplete representation of the final excavation from CMS data.....	315
Figure 13.25 - Percentage of unstable points (left-hand y-axis) versus velocity for a) Block A and b) Block C stopes, with relative frequency of unstable data points (right-hand y-axis).....	316
Figure 13.26 - Instability criteria based on velocity only.....	317
Figure 13.27 - Percentage of unstable points (left-hand y-axis) versus plastic strain for a) Block A and b) Block C stopes, with relative frequency of unstable data points (right-hand y-axis).....	318
Figure 13.28 - Location of 'stable' data points in Block A where plastic strain > 0.03.....	318
Figure 13.29 - Instability criteria based on plastic strain only.....	319
Figure 13.30 - Cross-section at 20032mE showing design and CMS geometries together with modelled a) velocity (m/step), b) plastic strain for the hangingwall.....	320
Figure 13.31 - Long section of Block C stopes showing probability of hangingwall instability, estimated from the velocity instability criteria.....	321
Figure 13.32 - Isometric section of stope CP0380 showing isosurfaces of probabilities of hangingwall instability based on velocity criteria.....	322
Figure 13.33 - Probability density function for volume of instability for stope CP0380.....	322
Figure 13.34 - Plot of predicted volume of instability versus probability of instability for stopes CP0380 and C9380, showing actual and expected volumes of instability.....	323
Figure 13.35 - Plot of a) Actual relative volume versus expected (predicted) relative volume, and b) cumulative percent of over-/under- estimations based on relative volume.....	324

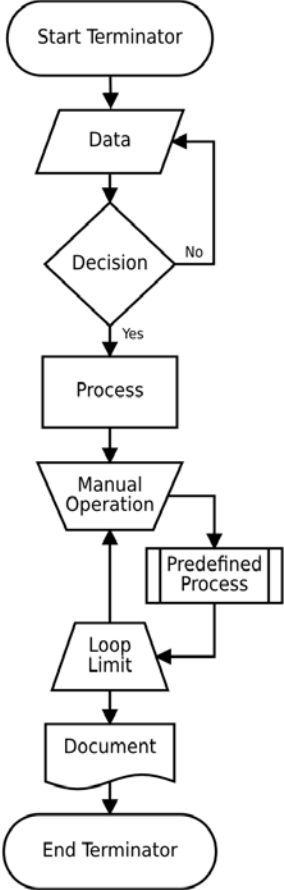
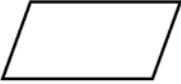
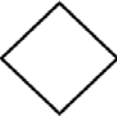
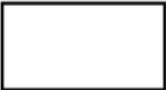
Figure 13.36 - Long section of Block C stopes showing percentages of over- and under-estimation of instability based on velocity instability criteria.....325

LIST OF SYMBOLS

δ	Acute angle between vectors, usually the discontinuity normal and the sampling line
λ	Lame's constant
λ_a	Areal frequency
λ_n	Normal set discontinuity linear frequency
λ_s	Set discontinuity linear frequency
λ_t	Total discontinuity linear frequency
λ'_t	Total discontinuity linear frequency (bias corrected)
λ_v	Volumetric frequency
$\vec{\lambda}$	Discontinuity frequency along a line of known direction
μ	Lame's constant
ν	Poisson's Ratio
σ_1	Major principal stress
σ_2	Intermediate principal stress
σ_3	Minor principal stress
σ_c	Uniaxial compressive strength of intact rock
σ_{cc}	Crack closure stress level (Eberhardt, 1998)
σ_{cd}	Crack damage stress level (Eberhardt, 1998)
σ_{ci}	Crack initiation stress level (Eberhardt, 1998)
σ_{cm}	Uniaxial compressive strength of the rock mass
σ_{peak}	Peak strength (Eberhardt et al, 1998)
σ_t	Uniaxial tensile strength
τ_{max}	Maximum shear stress
A	Rock stress factor (Mathews et al, 1981) or Factor A (Potvin, 1988)
A_{OB}	Area of over-break for a designated stope surface
AR	Stope aspect ratio (Suorineni, 1998)
A_S	Surface area of a designated stope surface
A_{SOB}	Total stope surface area of over-break
A_{stope}	Total stope surface area (excluding floor)
A_{SUB}	Total stope surface area of under-break
A_{UB}	Area of under-break for a designated stope surface
B	Rock defect orientation factor (Mathews et al, 1981) or Factor B (Potvin, 1988)
C	Design surface orientation factor (Mathews et al, 1981) or Factor C (Potvin, 1988)
C_{OB}	Circularity of over-break on a stope surface
C_{P2}	Areal proportionality constant (Dershowitz and Herda, 1992)
C_{P3}	Volumetric proportionality constant (Dershowitz and Herda, 1992)
C_S	Circularity of a stope surface
C_{UB}	Circularity of under-break on a stope surface
CMS	Cavity monitoring system (Miller et al, 1992)
D	Dilution (Scoble and Moss, 1994)
DFN	Discrete fracture network
DLF	Discontinuity linear frequency
D_{OB}^{MAX}	Maximum depth of over-break
D_{UB}^{MAX}	Maximum depth of under-break
D_{OB}	Depth of over-break
D_{UB}	Depth of under-break
E	Young's Modulus
EFN	Explicit fracture network
EHR	Equivalent hemispherical radius
$ELOS$	Equivalent linear over-break sloughage (Clark and Pakalnis, 1997)
$ELLO$	Equivalent linear lost ore (Clark and Pakalnis, 1997)
ERF	Effective radius factor (Milne et al, 1996)
ESR	Excavation support ratio (Barton et al, 1974) or Equivalent spherical radius (Windsor and Thompson,

	1997)
<i>F</i>	Fault factor (Suorineni, 1998)
<i>GSI</i>	Geological strength index (Hoek, 1994)
<i>H_{OB}</i>	Hemi-sphericity of over-break on a stope surface
<i>HR</i>	Hydraulic radius (Potvin, 1988)
<i>HSR</i>	Hangingwall Stability Rating (Villaescusa et al, 1997)
<i>H_{UB}</i>	Hemi-sphericity of over-break on a stope surface
<i>J_a</i>	Joint alteration number (Barton et al, 1974)
<i>J_n</i>	Joint set number (Barton et al, 1974)
<i>J_r</i>	Joint roughness number (Barton et al, 1974)
<i>J_w</i>	Joint water number (Barton et al, 1974)
<i>K</i>	Fisher's constant
<i>N</i>	Stability number (Mathews et al, 1981)
<i>N'</i>	Modified stability number (Potvin, 188)
<i>N'_f</i>	Modified stability number with fault factor (Suorineni, 1998)
<i>P₁₀</i>	One-dimensional measure of discontinuity density and intensity
<i>P'₁₀</i>	One-dimensional measure of discontinuity density and intensity (bias corrected)
<i>P₂₀</i>	Two-dimensional measure of discontinuity density
<i>P₂₁</i>	Two-dimensional measure of discontinuity intensity
<i>P'₂₁</i>	Two-dimensional measure of discontinuity intensity (bias corrected)
<i>P₃₁</i>	Three-dimensional measure of discontinuity density
<i>P₃₂</i>	Three-dimensional measure of discontinuity intensity
<i>POB</i>	Probability of over-break (Wiles, 2001)
<i>Q</i>	NGI - Q rock mass classification number (Barton et al, 1974)
<i>Q'</i>	Modified NGI - Q rock mass classification number (Mathews et al, 1981)
<i>REV</i>	Representative elemental volume
<i>RF</i>	Radius factor (Milne et al, 1996)
<i>RMR</i>	Rock mass rating (Bieniawski, 1973)
<i>R_{OB}</i>	Volumetric percentage of over-break
<i>RQD</i>	Rock Quality Designation (Deere, 1964)
<i>R_{UB}</i>	Volumetric percentage of under-break
<i>R_V</i>	Void ratio
<i>S</i>	Shape factor (Mathews et al, 1981)
<i>S_c</i>	Critical span
<i>SLOS</i>	Sub-level open stoping
<i>SF_C</i>	Circularity shape factor
<i>S_n</i>	Normal set spacing
<i>SRF</i>	Stress reduction factor (Barton et al, 1974)
<i>S_s</i>	Set spacing
<i>S_t</i>	Total spacing
<i>TIN</i>	Triangulated irregular network
<i>UCS</i>	Unconfined compressive strength or Uniaxial compressive strength
<i>VCR</i>	Vertical crater retreat mining method
<i>V_{OB}</i>	Volume of over-break
<i>V_{Ref}</i>	Reference volume
<i>V_{UB}</i>	Volume of under-break
<i>V_{Void}</i>	Void volume
<i>X_{OB}</i>	Extensivity of over-break
<i>X_{UB}</i>	Extensivity of under-break

FLOWCHART SYMBOLS

Symbol	Symbol Definition	Example Use
	Terminator: An oval flow chart shape indicating the start or end of the process	
	Data: A parallelogram that indicates data input or output (I/O) for a process	
	Decision: A diamond flow chart shape indicating a branch in the process flow	
	Process: A rectangular flow chart shape indicating a normal process flow step	
	Predefined Process: A rectangle for another process step or series of process flow steps that are formally defined elsewhere	
	Manual Operation: show which process steps are not automated. Indicates a looping operation along with a loop limit symbol (inverted)	
	Document: used to indicate a document or report	

CHAPTER 1 - INTRODUCTION

1.1 BACKGROUND

The selection of the most appropriate underground mining method is largely a function of geometry and the geomechanical properties of the ore-body and surrounding rock. Open stoping methods are generally appropriate for massive competent orebodies or steeply-dipping tabular orebodies surrounded by competent host rocks. Open stoping methods are attractive in that they involve low cost, safe and efficient non-entry production. Efficiencies are created by the large-scale use of mechanised mobile drilling and loading production equipment, leading to high production rates with a minimum level of personnel. The success of the method relies on the stability of large (mainly un-reinforced) stope walls and crowns as well as the stability of any fill masses exposed (Villaescusa, 2004). Stope sizes should be as large as possible to obtain high productivity and low unit costs, yet also be small enough to achieve sustained production rates (Ponierwierski, 2005) and be sufficiently stable to achieve maximum extraction with minimal dilution and ore loss. Stope size optimisation is therefore critical to economic viability of the method.

In order to develop an appropriate mine design, a thorough understanding of the rock mass conditions is required. Typically, geotechnical data (i.e. engineering rock mass data) are often limited, with models of ground conditions based on “average” values and some appreciation of the range of expected conditions to be encountered. Using these relatively simplistic models of ground conditions may lead to situations where, upon excavation, stope designs appear too conservative for local rock mass conditions, potentially resulting in additional development or unnecessary ground support costs. More importantly, situations can also arise where stopes are designed too aggressively, causing significant rock mass failure and subsequent economic implications of unplanned dilution.

A number of challenges currently face the Australian mining industry; strict environmental laws and safety regulations, skilled workforce shortages, high labour and production costs, increased expectation to mine geometrically complicated and low-grade ore bodies and, in particular, difficult mining conditions due to current depths of mining and high in situ stress regimes. These challenges will only become more difficult in the future as mining depths increase. In light of this, optimisation of the open stope design process has been identified as a high priority.

A major stumbling block in the slope design process is the way in which geotechnical data are collected, analysed, interpreted and used to construct a geotechnical model. In most cases mine site geotechnical engineers are not in a position to dedicate significant portion of their time to data collection, as they are mainly involved in production and planning tasks. In addition, the level of geotechnical information at their disposal is often limited. The vast majority of rock mass data for engineering design are collected in the Pre-feasibility, Feasibility and initial construction stages, whilst little emphasis is placed on routine “on going” data collection during production stages. In addition, rock mass data are collected by a variety of personnel (e.g. exploration geology, mine geology and geotechnical personnel), each having differing objectives to rock mass characterisation. It is therefore difficult to integrate all data sources into the geotechnical modelling process, considering the different formats and collection methods and levels of reliability. In some cases data collection efforts may be duplicated, or information is lost or not accessible to all disciplines. It has been identified that tools are needed to assist in rapid collection and management of geotechnical data, as well as statistical and interpretative tools to assist in model development.

The importance of understanding the spatial variability of rock mass conditions has been highlighted as a major issue, as the traditional approach of using “average” rock mass conditions can lead to sub-optimal designs. There is a demonstrated need to adequately design slope and pillar dimensions such that they are optimised for the prevailing rock mass conditions in the various regions of the mine. In this respect, more robust geotechnical models need to be developed that will allow for the spatial variability of rock mass conditions to be incorporated into the design process. A robust geotechnical model should contain sufficient geotechnical information to confidently assess the variability and continuity of certain geotechnical characteristics, within acceptable levels of uncertainty. An analogy can be drawn from geological and resource modelling. Here, the robustness of the resource model can be categorised, for example; inferred, indicated, measured (JORC, 2004). These categories are based on the level of available geological information to confidently understand the geological complexity and ascertain geological continuity. In addition, modelling methods used and resulting model reliability need to be appropriate for the stage of project development. No standard method or guidelines exist for generating geotechnical models to the required level of detail and reliability for use in open slope design.

In terms of open slope design, there are a variety of design tools employed in industry today. Many of these tools are empirical methodologies, based on mining experience gained in Canadian and South African mines. There are concerns about the direct applicability of some of these tools for Australian mining conditions and practices. In addition, there is also a sense of ambiguity amongst some Australian practitioners in the use of certain empirical

methodologies, potentially leading to inappropriate designs. Many of these empirical methods were developed to assist in initial stope size selection (i.e. pre-feasibility and feasibility levels), however, there is a concern that these tools are potentially being inappropriately relied on for detailed design. Another issue with these tools is their inability in properly accounting for all influences on stope performance. For example, large-scale structures have been identified as a major contributor to poor stope performance (Adu-Acheampong, 2003; Villaescusa and Cepuritis, 2005), however, the ability to directly account for them is still lacking in a number of stope design methodologies. There is a need for a better understanding of the role of large scale structures on stability and their influence on local rock mass conditions.

Another major problem perceived in industry is the lack of quantifying the economic effect of dilution and ore loss. In order to implement adequate dilution control and management systems it is necessary to regularly monitor stope performance by measuring dilution and ore loss (i.e. use of post-mining surveys). Once dilution is quantified, it is possible to introduce and financially justify any necessary modifications to mine planning and design, such as; changes to the sequence and/or stope dimensions, drill and blast practices, rock reinforcement and support requirements, rate of mining and other engineering parameters.

1.2 OBJECTIVES OF THE RESEARCH

The main objective of the research is to investigate and develop an integrated system of improved techniques for span design in open stope mining, principally in the areas of;

- Rock mass data collection and management
- Rock mass characterisation and rock mass modelling techniques
- Collection and analysis of stope performance data and its integration into the mine-design process
- Selection of appropriate and reliable open stope mine design techniques

Initially, an extensive literature review was undertaken in each of these key areas. The objectives of this review were to identify the strengths and weaknesses of existing techniques and methodologies as they apply to hard rock open stope mining. These reviews enabled investigation of proposed improvements in each of the key areas. A brief outline of some individual research questions, as well as proposed investigation methodologies, are provided in the following sections.

1.2.1 Rock Mass Data collection and Data Management

With regard to rock mass data collection and data management in open stope design, a

number of questions were identified for investigation;

- What information is required to adequately characterise the rock mass for open stope design?
- How can different engineering objectives be accounted for and prioritised in rock mass data collection programmes?
- Rock mass characterisation cannot be carried out in “one go”, yet is an “on going” procedure that should be carried out throughout the life of the project. In this regard, how is this process effectively managed in a production environment?
- Are there ways of maximising the value of rock mass data?
- How is the degree of uncertainty in the data measured and accounted for in the design?

In order to attempt to answer these questions a literature review was undertaken to determine the key rock mass parameters and how they may influence open stope design. A detailed literature review was then undertaken to investigate existing and suggested rock mass data collection methods and examine their ability to capture these key parameters. Methods to improve geotechnical logging and mapping productivity were then investigated. This included a review of rock mass data and collection methods from a number of selected mines including; intact rock properties (e.g. laboratory test data, index tests, etc.), geological and geotechnical drill core logging data and mapping data for geological discontinuities and their properties (e.g. location, size, orientation, frequency, surface characteristics, spacing, etc.). The review also included an investigation of data entry and database systems capable of achieving quick and easy manipulation of geotechnical logging, mapping and other data. Finally, methods of statistical analysis of rock mass property data, including treatment of biases, were investigated.

1.2.2 Rock Mass Characterisation and Rock Mass Modelling Techniques

Rock mass characterisation and rock mass models are generally required to ascertain likely rock mass responses to mining. In order to understand the characterisation and modelling process, the following questions were identified;

- What methods are available to characterise the rock mass for engineering purposes?
- Which methods are most appropriate for identifying and modelling spatial variability of rock mass parameters?
- How can discontinuities and rock mass structure be incorporated at a number of scales?
- What are the most appropriate rock mass models for open stope design, given

available data and stage of mine development?

Firstly, a review was undertaken of the discontinuity characteristics, particularly; orientation, spacing, terminations, persistence, and intensity. The review highlighted the different processes of organising discontinuity data into families of orientations, quantifying their characteristics and using these to generate various models of the rock mass structure. The review also included an investigation of the use of geostatistical and other spatial modelling tools for development of 3-dimensional spatial models of engineering rock mass data. This also included evaluation of the most suitable way of displaying raw and modelled information for mine design purposes. Methods for generating statistically homogeneous regions of the rock mass (i.e. “domains”) were evaluated, with a number of improvements proposed. New approaches to spatial modelling were also proposed, and a method for generating 3-dimensional models of large-scale structures using implicit functions was developed. These developments were demonstrated by development of models of various rock mass characteristics for a number of case study mines.

1.2.3 Rock Mass Classifications and Empirical Design Methodologies

Rock mass classifications and empirical open stope design tools are used extensively in the mining industry. With regards to optimising their use in the stope design process, the following questions were identified;

- What is the reliability of rock mass classifications and empirical of existing empirical methods in open stope design today?
- Can reliability be improved?
- How can their use be optimised in the stope design process?

The history and development of a number of key rock mass classifications and empirical stope design methods were examined in detail in order to develop an understanding of the original purposes and objectives of the methods, their range of applicability and some of their limitations. In this way their applicability and relevance to open stope design can be examined. The review enabled a number guidelines to be developed regarding implementing empirical methods in excavation design and establishing their reliability.

1.2.4 Stope Performance Data Collection and Analysis

Once a stope design has been implemented, feedback on the stope's performance is required in order to quantify its success or otherwise. In addition, any lessons learnt during implementation of the design can be recorded and used as a future experience base to improve future design and implementation processes. In this respect, retrospective analyses that are required to improve design performance rely on quantification of stope performance;

- How can open stope performance be measured or quantified?
- How can this data be integrated into the design process?

Methods for collecting stope performance data were investigated, as well as methods for storing and managing this data. This involved the development of a computer database that stores the stope details, excavation dimensions and performance data for each excavation. Methods for integrating rock mass models and the stope performance database were investigated. This enables relationships between various rock mass parameters, excavation geometries and stope performance to be analysed. This allows for identification and ranking of the critical factors that influence stability such that they can be used in development of design tools and critical “instability criteria”. A critical review of existing measures of stope performance was undertaken to identify where improvements can be made to improve predictive performance by reducing bias and scale effects. A number of methods were investigated to calculate various geometric parameters (i.e. volumes, areas, perimeters) of over-break and under-break from cavity monitoring surveys (*CMS*) using proprietary mine planning and other software. To facilitate this, a number of computer macros/scripts needed to be developed to increase efficiency of extracting geometric parameters for stope surface geometries, as well as over-break and under-break parameters from *CMS* data. Stope performance data for a number of case study mines were collected, stored and presented accordingly to assist in back analyses for determination of instability criteria

1.2.5 Numerical Modelling and Development of Instability Criteria

Numerical modelling is an important tool for the design of open stopes, mainly as they are capable of incorporating additional complexities over analytical and empirical methods, such as; effects of in situ and induced stresses, complex excavation geometries, non-linear behaviour, material anisotropy and the influence of complex rock structure. Typically, site specific “instability criteria” are developed which are then used in forward analysis and design to minimise rock mass damage and optimise performance. However, optimal and reliable predictive performance requires certainty in the input parameters. In this regard, model calibration through back analysis is a vital process;

- What are the benefits and limitations of existing numerical methods?
- What are the methods used to develop site specific instability criteria?
- How can the predictive performance of numerical modelling using back analysis data be established and can it be improved?

A review of common numerical modelling approaches used in metalliferous mining was undertaken to highlight advantages and disadvantages of the various methods. The approach taken to numerical modelling and back analysis can then be optimised based on the available rock mass and performance data, identified modes of instability, scale and

level of reliability required. The limitations of the linear elastic continuum methods were also highlighted along with some typical approaches to back analysis using this method. A number of suggested improvements to the method were also investigated as well as methods for establishing reliability of derived design criteria. Finally, the suggested improvements were demonstrated on actual sequences from case study mines, using modelling outputs and rock response data, to develop a number of instability criteria to improve reliability in performance prediction.

1.3 STRUCTURE OF THESIS

The following sections outline the structure of the thesis.

Chapter 2 provides a general review of the rock engineering design process and how it relates to the practical design of open stopes. It summarises the overall design process, from initial data collection, data analysis, geotechnical model development, design analysis, implementation to retrospective analysis. The review highlights the importance of data collection on geotechnical model development and its impact on identification of failure modes and choice of design method. The role of data uncertainty on design reliability is also discussed. The review also identifies a need for improved selection of appropriate design methodologies. A detailed review of a stope design process at a particular mine has been provided to highlight the iterative and inter-disciplinary nature of the process. The chapter concludes with the identification of a number of suggested improvements to the rock engineering design process for use in the design of open stope mines.

Chapter 3 provides a review of rock mass characterisation. The chapter includes a brief review of both rock fabric and discontinuity data collection methods commonly employed in the Australian mining industry, with particular emphasis on metalliferous underground operations. The chapter also reviews the various sampling biases associated with the data collection methods such as drill core logging, and manual and remote mapping of rock mass exposures. This chapter also highlights the need to systematically integrate data from a number of sources and disciplines to maximise the potential for improved rock mass characterisation and subsequent design. The chapter acknowledges that laboratory and fields tests are only indexes of certain engineering properties under specific loading and geometrical conditions, and are influenced by anisotropy, sample selection and scale effects. The review also outlines typical data analysis techniques and the treatment of biases.

Chapter 4 provides a detailed review and critique of empirical stope design methodologies,

including rock mass classification and stability graph methods and their use in open stope design. The chapter highlights the deficiencies and weaknesses of these methods and how they cannot be relied upon for detailed dimensioning of stope excavations, especially in a production environment.

Chapter 5 provides a discussion on the geometrical aspects used to assess stope performance. Existing methods used to assess performance principally range from subjective and qualitative assessments through to quantitative measures, such as percent dilution.

Chapter 6 introduces a new scale independent geometrical approach to assessing stope performance, together with a demonstration of its application with example data.

Chapter 7 provides a review of some continuum-based rock mass damage and failure criteria used in design and back analysis of open stopes. The review highlights some of the limitations of linear elastic continuum modelling for detailed stope design.

Chapter 8 provides a brief review of some techniques and models used to represent the rock mass and its characteristics, with special emphasis on spatial modelling. The chapter also reviews a number of techniques for the definition of rock mass domains.

Chapter 9 introduces a digital rock mass characterisation data model. The purpose of the data model is to provide an organisational and analysis framework for engineering rock mass data.

Chapter 10 introduces a novel approaches to spatial modelling of rock engineering characteristics utilising implicit functions. The chapter also introduces a novel deterministic discontinuity modelling technique to enable modelling of discrete large-scale geological features. The chapter also highlights some of the issues with respect to the spatial modelling of discontinuity intensity.

Chapter 11 proposes an integrated approach to open stope design. The methodology involves integrating rock mass models, stope performance data and results from numerical models in order to develop reliable instability criteria for stope design which are appropriate

for the stage of mine development. The chapter also introduces an improved approach to linear elastic modelling in back analysis for open stope design. Case studies from two mines (**Chapter 12** and **Chapter 13**) are utilised to highlight various aspects of the methodology.

Chapter 14 highlights the developments made in this research, discusses the limitations of the approach taken and provides some future research directions.

CHAPTER 2 - A REVIEW OF ROCK ENGINEERING IN MINE DESIGN

2.1 INTRODUCTION

In some ways, rock engineering design requires a different approach to other engineering disciplines such as mechanical or civil engineering. Conventional engineering design requires material strengths and deformability properties to be prescribed in order to sustain calculated loads from designed structural geometries. In rock engineering, designers are required to deal with complex rock masses at a given site. The engineer has to try to determine the rock mass structure and properties, which in itself poses a major problem. In mining this is further complicated as the geometry of the proposed engineering structures are generally fixed, governed by the geometry of the orebody and local geological structures. A fundamental aspect of rock engineering therefore, is a thorough appraisal of the geological conditions and especially geological hazards (Bieniawski, 1993).

2.2 OVERVIEW OF THE ROCK ENGINEERING DESIGN PROCESS

(Brown, 1985) proposed a generalised process for rock engineering in mine design consisting of five integral processes; site characterisation, geotechnical model formulation, design analysis, rock mass performance monitoring and retrospective analysis (see Figure 2.1). An important aspect of Figure 2.1, is the multiple feedback loops carried out at a number of stages. The feedback loops provide a number of important functions. Site characterisation needs to be recognised as an **ongoing process**, as initial site characterisation studies are unable to adequately characterise the rock mass for all engineering activities over the life of the mine. The feedback loops also recognise that the mine design process is evolutionary, with design changes made in response to observed performance throughout the mines operation (Brady and Brown, 2004).

The site characterisation process involves the collection of rock mass characterisation data, from drill cores, mapping of exposures and other methods. Data from site characterisation programmes then needs to be formulated into a conceptual model of the rock mass. This generally entails establishing the range and variability of a number of rock fabric properties, as well as the structure and properties of the rock mass discontinuities.

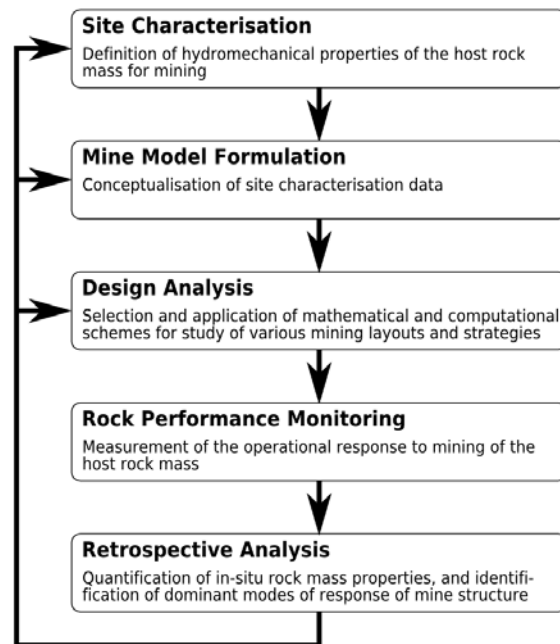


Figure 2.1 - Outline flowchart for mine design with multiple feedback loops (Brown, 1985)

From this model, the likely geological factors affecting the performance of the proposed excavation can be evaluated in the design analysis. An important realisation is that the geotechnical model will dictate the methodologies and approach taken in the design analysis, as these are related to the knowledge of the anticipated failure modes and rock mass response, scale of the excavation with respect to the rock structure system and the level of geological uncertainty.

Once the design is finalised, it is implemented and the excavation proceeds with the rock mass response monitored and measured during and after construction. Throughout the mine design process, a retrospective analysis is continually conducted and provides an important calibration and optimisation function. It is designed to provide an improved understanding of the mechanisms, check validity of assumptions and generally refine the geotechnical parameters used in the design analysis. It is also used as a tool to **continually improve** each aspect of the overall mine operation process;

- data collection methods, quality and quantity
- update and improve the geotechnical model,
- improvements to design approaches and methods,
- improvements in implementation and procedures (reinforcement, drill and blast, backfill, sequencing, performance monitoring requirements, etc.).

It is therefore important that any lessons learnt during implementation of the design are

recorded and used as a future experience base for designers (Bieniawski, 1993).

2.3 ROCK ENGINEERING DESIGN METHODOLOGIES

Analysis and design in rock engineering can be evaluated using a variety of approaches, each with varying degrees of sophistication. The following sections briefly outline some common design methodologies.

2.3.1 Empirical

These methods attempt to relate certain rock mass characteristics and some geometric parameters to the excavation performance experienced at a number of sites. The use of these methods can be useful in the initial evaluation of mining method selection, however, their use in detailed stope design may not necessarily lead to an optimal design solution. Due to their popularity in the mining industry, a more thorough examination of these methods is presented in Chapter 4.

2.3.2 Observational

Observational methods are those that rely on continual monitoring of excavation displacements during construction, modifying rock reinforcement and ground support requirements accordingly. These methods were initially developed for tunnelling where detailed monitoring of a simple excavation geometry can take place over relatively long periods with reinforcement and support installed as required. The concept of observational design is generally incompatible with the functional requirements of an open stope. In addition, reinforcement needs to be estimated in advance of excavation and cannot be modified as excavation takes place. However, ground-support interactions may provide useful insight into design of rock reinforcement and support in access development around stopes where large strains may be experienced.

2.3.3 Analytical

Analytical approaches utilise the analyses of stresses and strains around an excavation boundary, as well as the potential for displacements of rock blocks into the excavation. Techniques include the use of closed form solutions and analysis of vectors and forces, where solutions are determinable.

Classical Stress Analyses

A number of closed-form solutions exists for determining the stresses and strains around simple geometric shapes such as circular or elliptical tunnels (Obert and Duvall, 1967). These simple models rely on a number of theoretical assumptions, such as plane strain

conditions, complete continuum, known constitutive and strain compatibility equations. These rudimentary analyses provide insights into the analysis of stress, however, are often of limited use in the design of more complex excavation geometries such as interacting open stopes.

Voussior Beams

Voussior beams and similar bedded roof methods assume that the rock mass can be represented by a series of stiff parallel layers, or beams, of rock. There are a number of analysis techniques, each with their own assumptions and limitations (Brady and Brown, 2004; Diederichs and Kaiser, 1999a; Sofianos, 1996). These methods are only applicable to highly anisotropic rock masses, and rely on known parameters such as bed thickness and deformation modulus. In bedded rock masses, these methods are especially useful in undertaking 'parametric' studies (Brady and Brown, 2004).

Block Theory

The concept of this method assumes that instability of the excavation is controlled by a number of "key" rock blocks on the excavation surface. Once a key-block is removed, by rotation and/or translation into the excavation, the potential for further rock block unravelling into the excavation is increased. A number of analysis methods have been proposed. Methods can generally be categorised into two main approaches (Windsor, 1999).

- Specific approaches involve assessing the stability of a rock block given the geometry of the discontinuities and excavation at a specific location. This enables the exact rock block geometry to be ascertained using vector techniques (Warburton, 1983).
- Ubiquitous, or non-specific, approaches assume that the discontinuities and excavation have the potential to exist in all locations. If we assume that the discontinuities are continuous, stereographic techniques can be used to define all the shapes of 'removable' blocks on an excavation plane (Goodman and Shi, 1985). By including details about the range of discontinuity orientations and traces lengths the range of probable 'removable' block sizes can then be estimated (Windsor, 1999).

Specific approaches may not necessarily be the optimal methodology in initial stope design, as they are dependant on the exact location of the discontinuities with respect to the geometry of a specific excavation, which are difficult to know in advance. In this case, ubiquitous approaches are probably more useful. However, specific approaches may prove better suited in more detailed stope design phases where the specific locations, orientations, and potential size of discontinuities may be ascertained from improved rock mass models.

2.3.4 Numerical

With the computational power available today at a reasonable cost, it is possible to solve increasingly sophisticated problems. The recent advances in computing capacity has lead to the development and popularity of a number of numerical methods that can be called upon to assist in the rock engineering design process. There are many numerical methods available, however, the principal concepts are similar. Numerical models attempt to solve complex problems by sub-dividing a region into smaller discrete elements, whose behaviour is **approximated** by simpler mathematical descriptions. In some respects, numerical methods are extensions to analytical techniques, where solutions of discrete elements are generally determinable.

A summary of the main numerical methods that are used in typical mining applications is presented in Table 2.1. A detailed description of each method is beyond the scope of this study, however, it is important to understand the capabilities and limitations of each method in its relationship to rock engineering design. In order to select the most appropriate numerical method for the design problem, an appraisal of the capabilities, limitations and advantages of each method is highly recommended. It may be found that a single numerical method cannot provide the required solution. In this case, an integrated or hybrid approach may be required, where different numerical methods are used at a number of scales and for various purposes. The role of scale in the fundamental choice of methods, either continuum or discontinuum approaches is alluded to in Figure 2.2.

Table 2.1 - Common numerical methods used in rock engineering (Jing, 2003)

Continuum Methods
Finite Difference Method (FDM)
Finite Element Method (FEM)
Boundary Element Method (BEM)
Discontinuum Methods
Discrete Element Method (DEM)
Discrete Fracture Network (DFN)
Hybrid Continuum/Discontinuum Methods
Hybrid FEM/BEM
Hybrid DEM/DEM
Hybrid FEM/DEM
Other hybrid models

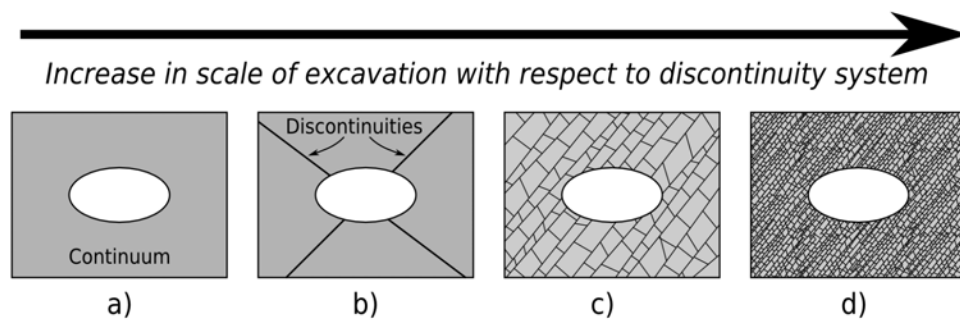


Figure 2.2 - Suitability of various numerical modelling methods with respect to scale of excavation
a) continuum, b) either continuum with discontinuity elements or discrete method c) discrete method and d) equivalent continuum method - modified from (Jing, 2003)

(Starfield and Cundall, 1988) state that the purpose of numerical modelling is not to create a complex and detailed model that tries to imitate reality. Numerical models are simplifications of reality that can be used as tools to try to answer specific questions involving specific mechanisms and conditions. In this light, it is necessary to choose the most simplistic model that is capable of modelling these mechanisms. In construction of numerical models, it is also necessary to determine what aspects of the rock mass are important to include in the model to understand the specific rock mass behaviour under investigation. This appraisal can be used to influence the choice of continuum or discontinuum approaches.

From a practical point of view, continuum methods are generally more appealing as the data input requirements for discontinuum models require substantial knowledge of the various characteristics of the rock mass structure, which may not be readily available. This is perhaps why the use of equivalent continuum criteria, such as the Hoek-Brown failure criteria (Hoek and Brown, 1980), and linear elastic methods are popular with rock mechanics practitioners. The appropriateness of continuum approaches and their ability to capture the required rock-excitation interactions must be carefully considered when developing modelling strategies. This is especially relevant at particular excavation scales (represented by Figure 2.2b and Figure 2.2c).

2.4 CHOICE OF DESIGN METHODOLOGY

Although the processes proposed by (Brown, 1985) and (Bieniawski, 1993) provide a general framework for rock engineering design, they do not provide information on precise data required for design, the rock-excitation interactions nor the actual analysis methods to be used. In order to provide more guidance on the selection of appropriate design methodologies (Hudson and Feng, 2007) provide a series of updated flowcharts for the rock engineering design process (Figure 2.3a), as well as a flowchart for selecting design

methodologies (Figure 2.3b). The design methodologies generally increase in complexity from left to right (i.e. Method A → Method D) and are separated into two classes; those that involve 1:1 mapping where the problem and rock mass interactions can be explicitly modelled (e.g. analytical - key block analysis), and those where they are not (e.g. empirical - rock mass classifications). The framework proposed by (Hudson and Feng, 2007) serves to illustrate that rock engineering can be evaluated using a variety of methodologies, depending on the required degree of sophistication and level of reliability.

2.5 ROCK ENGINEERING IN OPEN STOPE DESIGN

The main objectives in the overall planning and design of open stope mines are (Brady and Brown, 2004);

- ensure safe operation
- maximise recovery and minimise dilution
- ensure cost efficient, timely and continuous production

The open stoping mining method relies on the ability to create and maintain a *series* of large, relatively self-supporting, excavations for the extraction of the contained ore. In general, most underground excavations are manifested by a zone of damaged or yielded rock mass around their periphery. Successful excavation requires that large uncontrolled displacements of rock into the excavation do not occur (Brady and Brown, 2004). Rock reinforcement can generally be utilised to minimise these uncontrolled displacements, however, there are a number of geometrical and practical issues that may limit their effectiveness in open stope excavations.

The main objective of rock engineering in stope design therefore, is to ensure that the series of stope excavations and associated access, haulage and ventilation infrastructure remain serviceable for their duty life. The rock engineering component of the stope design process must consider potential rock mass damage not only of isolated individual stopes, yet for all proximal and future stopes in the planned extraction sequence. During the continual of extraction of the stopes, it may be found that there is a progressive increase in rock mass yielding, displacement and associated dilution, which left unchecked may potentially eventuate in an uneconomic scenario for the mine. In addition, extraction of stoping blocks may cause unacceptable displacements of key infrastructure. These scenarios are critical operational risks that need to be identified or managed in the design and operation of open stope mines. An important role of the rock engineering design process is to identify in advance at what stage, or under what conditions, self-supporting methods such as open stoping are no longer economically viable, or at what point key infrastructure may be at risk.

In this regard, rock mass monitoring and retrospective analyses are critical components of the rock engineering design process.

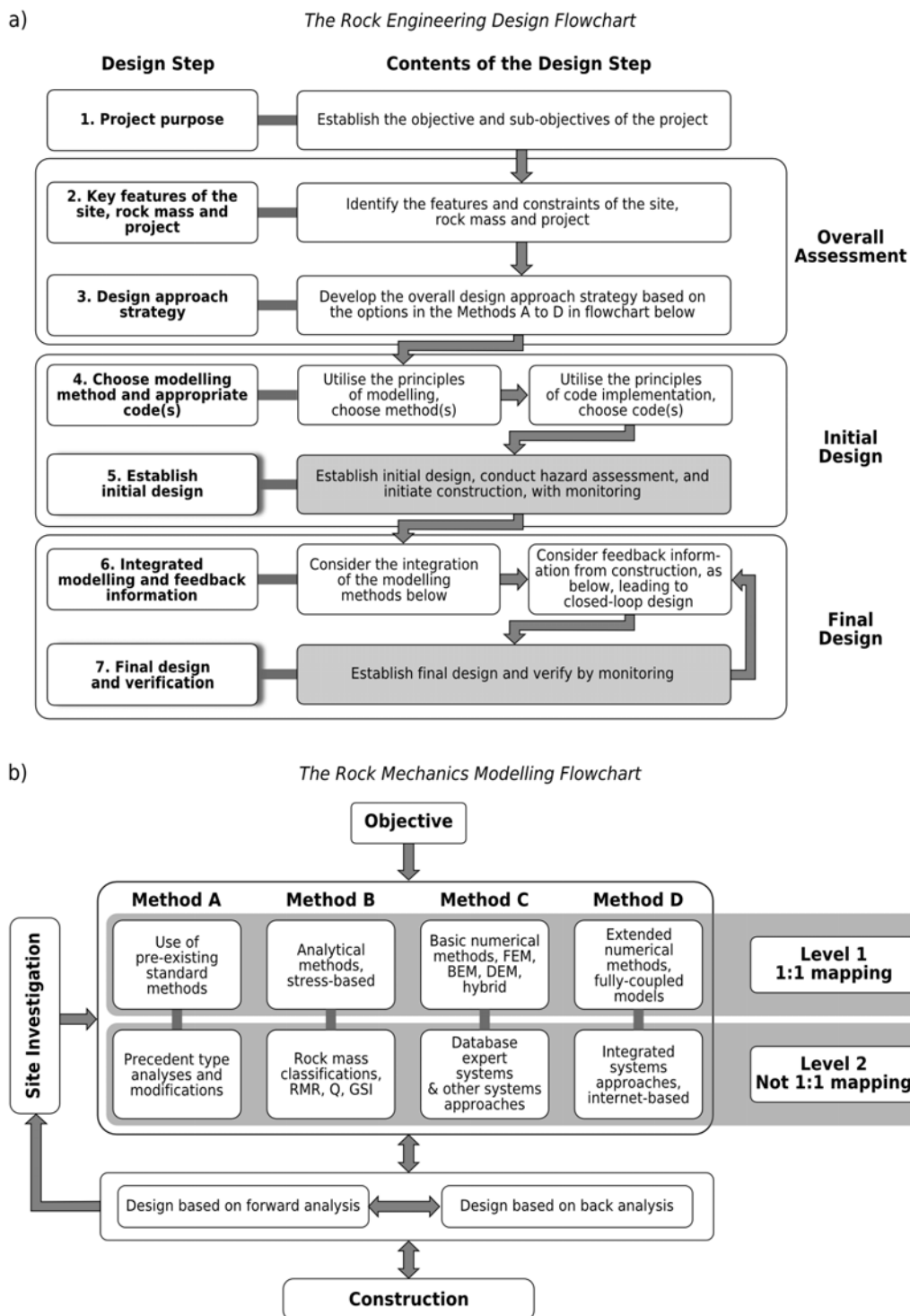


Figure 2.3 - Flowchart for a) Rock Engineering Design Process and b) supporting Rock Mechanics Modelling Techniques (Hudson and Feng, 2007)

2.5.1 Planning and Design of Open Stopes

In the overall planning and design of open stope mines, a multitude of technical and financial aspects need to be considered. The engineering processes in open stope mine design involves technical input from a variety of disciplines such as geology, rock mechanics, mine planning, and operation/production engineering. As described earlier, the role of rock engineering in the design of open stopes is primarily concerned with the design of stable, mainly unreinforced, stope walls and crowns. Rock engineering aspects in open stope mining also concern the stability of regional and local pillars, exposed fill masses, fill barricade systems, access development, ore passes and major mine infrastructure such as crusher chambers, shafts and haulage systems. These rock engineering aspects need to be integrated with other organisational functions in the mine planning process.

(Villaescusa, 1998; Villaescusa, 2004) provides an overview of the main processes in the planning and design of open stope mines, from initial orebody delineation from drill holes to reconciliation of stope performance (see Figure 2.4). It can be seen that the process involves a number of number of iterative steps undertaken at a number of scales. The initial steps involve delineating the geometry and grade of the orebody and undertaking rock engineering characterisation of the rock mass. The general strategy for access and infrastructure layout, definition of stoping blocks and required regional pillars, and the mine-scale extraction sequence is then devised and reviewed. A more detailed assessment is then carried out at the stope scale in each region or mine block. The purpose of the detailed design stage is to provide an optimal stope design and extraction method subject to a number of variables and constraints. Rock engineering inputs into the detailed stope design assist in a number of key areas, such as;

- development layout and reinforcement requirements.
- stope wall and crown reinforcement requirements.
- drill and blast design and firing sequence.
- Back fill requirements.

Importantly, all these required planning and design functions are dependant on the stope geometry. It therefore must be recognised that ***the key design parameter in open stope design is stope span definition.***

In the assessment of the above, there are quite a number interactions and variables that need to be considered; ventilation, design and capacity of back fill systems, backfill curing rates and stability, drilling equipment capabilities, position of existing development and other planned or backfilled stopes, etc. An important aspect of rock engineering in the stope

design process is to find the **optimal** design considering limitations, conflicting requirements and resources available.

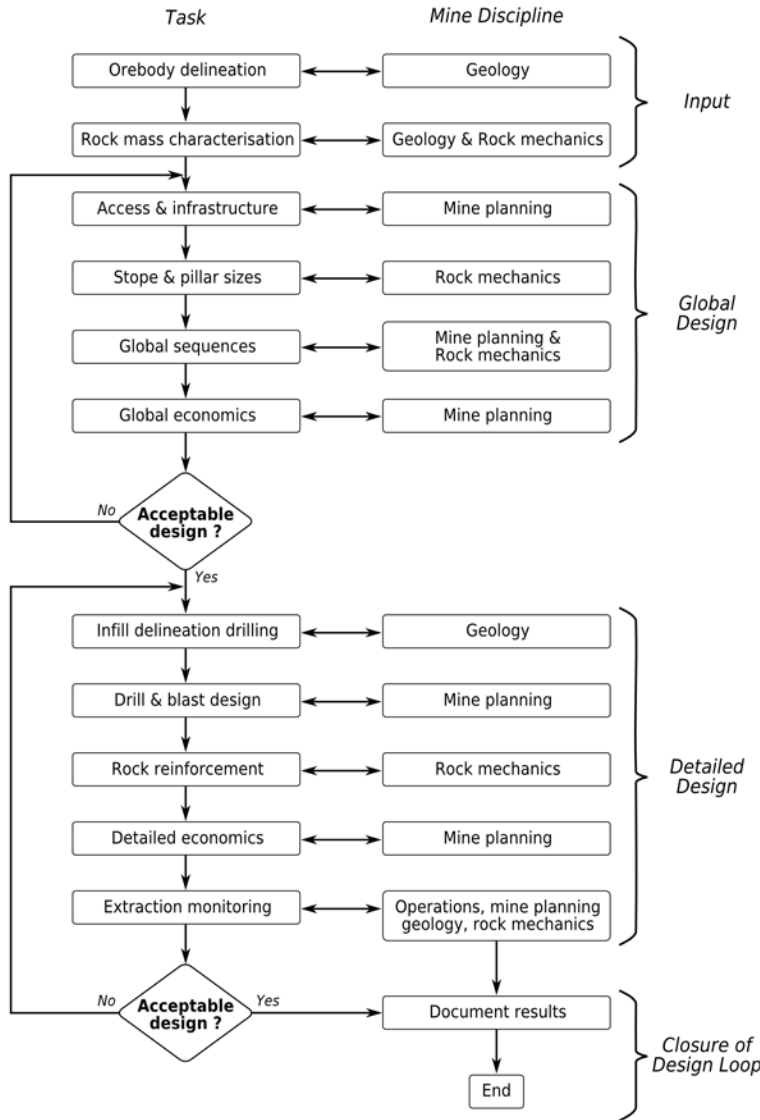


Figure 2.4 - Stope design methodology from data collection to stope reconciliation (Villaescusa, 2004)

Once the stope design is finalised and implementation begins, all activities are monitored as extraction progresses, such as; drill and blast performance, ore fragmentation and flow, mucking, grade and tonnage variability, dilution, ore loss, fill rates, etc. An important aspect of the process outlined in Figure 2.4 is the final element where stope performance is documented. The purpose of this activity ensure that any lessons learnt during stope extraction (good or bad) can be used to improve future designs.

2.6 UNCERTAINTY AND DESIGN RELIABILITY

Due to the variable nature of natural materials, uncertainty is an inherent characteristic of

rock engineering design that needs to adequately addressed. Uncertainty can be categorised into three main types (McMahon, 1985);

- **Type 1:** The risk of encountering an unknown geological condition, such as a fault or weak zone.
- **Type 2:** The risk of using the wrong rock engineering parameters, incorrect interpretation of failure mechanism and selection of analysis and design methods.
- **Type 3:** The risk of bias and/or variation in the design parameters being greater than expected.

The design processes described in the previous sections address the general approaches to be taken for analysis, planning and design in open stope mining, however, they do not specifically address rock mass data requirements (i.e. amount and type) and data reliability (data quality) and their potential impact on the ability to; develop reliable rock mass models, undertake meaningful rock engineering analyses and to develop reliable mine design parameters.

(Haile, 2004) proposed a reporting framework that classifies mining projects based on the level of understanding of the overall rock engineering environment and how this may affect its economic viability. The framework includes general guidelines for establishing appropriate levels of rock mass data collection and types of analysis/design methodologies employed for broadly defined orebody types and mining methods, at any particular stage of development (Table 2.2). The reporting framework also recognises that uncertainty in rock engineering is generally accounted for either by;

- improving reliability of data, analysis methods and design parameters, or
- applying appropriate safety margins to derived design criteria (such as pit slope angles and stope spans) to manage the risk of potential adverse performance (either financial or safety related).

The economic impact of uncertainty in mining projects is inherently related to the mining method and orebody characteristics. For example, a pit wall failure, or a reduction in pit wall slope angle, will generally have an insignificant economic impact for a wide shallow open pit (i.e. shallow dipping orebody) compared to a steep walled open pit (i.e. steeply dipping orebody) with narrow pit floors and single ramp access. Similarly in underground environments, uncertainty can be accommodated in flexible selective mining methods, such as narrow vein cut and fill, yet uncertainty will have a far greater economic impact in more inflexible bulk mining methods that require fixed and committed layouts, such as open stoping or block caving methods. In non-entry open stope mining, the economic

consequences of poor performance brought about by uncertainty and poor reliability of selected design parameters can be significant (i.e. unplanned additional costs and the implications of dilution and ore loss). Although the acceptability of poor stope performance is generally a company management responsibility, the risk of poor stope performance still needs to be quantified in the design.

(Haile, 2004) provides a generic process map for assessing data requirements, model reliability and accounting for uncertainty and risk in the development of mining projects (Figure 2.5). The key questions asked in advancing a project include;

- Is the available data suitable for analysis needs?
- If data is not sufficient for analysis can more be collected, or can the down-side risk associated with the uncertainty be mitigated by selecting conservative design criteria?
- Do the economic and operational risks detrimentally impact on the project and can they be mitigated?

2.6.1 Reliability-based Design Analysis

Reliability-based design analysis is one method used in rock engineering which attempts to incorporate uncertainty and risk into the design process (Hoek, 1992). Reliability analysis in rock engineering design deals with the relationship between loads a rock engineering system must carry and its ability to sustain those loads. In this regards, 'loads' are taken to mean forces, stresses, displacements or other phenomena that are required to be assessed and considered in analysis and design. Reliability-based design recognises that both the loads (Q) on the system as well as resistance (R) to those loads are uncertain, such that the result of their interaction is also uncertain. A state of 'failure' is generally defined where loads (Q) exceed resistance (see Figure 2.6), and can either be measured by a margin of safety (M) (Baecher and Christian, 2003);

$$M=R-Q \quad (2.1)$$

or, more traditionally, as a factor of safety;

$$F=R/Q \quad (2.2)$$

Table 2.2 - Suggested data requirements, rock mass model reliability and design techniques based on project stage (Haile, 2004)

Requirement / Data Type	Conceptual (Implied*)	Pre-Feasibility (Qualified*)	Feasibility (Justified*)	Operations (Verified*)
Data requirements and geotechnical model reliability	No site-specific geotechnical data necessary	Project specific data are broadly representative of the main geological units and inferred geotechnical domains, although local variability or continuity cannot be readily accounted for.	Project specific data are of sufficient spatial distribution (density) to identify geotechnical domains and to demonstrate continuity and variability of geotechnical properties within each domain	Site-specific data are derived from local in-situ rock mass
Analysis techniques and level of rigour	Design recommendations are typically based on broad industry experience	Design recommendations are typically based on a combination of empirical guidelines and broad industry experience	Design recommendations are justified by rigorous analyses, which account for the measured intrinsic and/or extrinsic variability in the geotechnical characteristics	Design recommendations are based on site-specific experience and analysis of in-situ characteristics, which are probably derived by back analysis of local excavation performance
Geological model				
Stratigraphic boundaries	Inferred from regional geology	Reasonable knowledge of major units and geometry	Well constrained in the vicinity of the mine excavations and infrastructure	Mapped in the field
Weathering/alteration boundaries	Inferred from regional geology	Based on geology model	Well defined grading of weathering and local variability	Mapped in the field
Major structural features	Inferred from regional geology	Major 'dislocations' interpreted	Drilling sufficient to be well constrained in continuity, dip and dip direction	Mapped in the field
Rock mass data				
Discontinuity	Based on general rock type characteristics	Estimates of RQD / FF and number of defect sets from resource data (will probably contain directional bias)	RQD / FF statistics and number of defect sets representative of all geotechnical domains and directions	Multi-directional FF from in-situ mapping and visual count of defect sets
Intact material characteristics	Based on general rock type characteristics	Field estimates	Field and laboratory estimates and variability	Field and laboratory estimates and variability
Defect data				
Orientation	Inferred from regional geology	Orientation inferred from geological model	Dip and dip direction statistical data from drill holes	In-situ measurement of dip and dip direction from excavation mapping
Surface characteristics	Estimated on precedent experience	Estimated on precedent experience	Statistical estimates from core logging for all defect sets. Laboratory shear strength testing of critical defects	Statistical estimates from in-situ measurements. Laboratory shear strength testing of critical defects
Volumetric distribution (continuity and spacing)	Estimated on precedent experience	Estimated on precedent experience	Estimated on precedent experience	Persistence and spacing measurements
Stress regime				
Principal stress field	Estimated on precedent experience	Mean regional trend	Local magnitude and orientation based on local experience or modelling	Measured or inferred from in-situ performance
seismicity/earthquake	Based on general experience	Based on general experience	Based on regional trends	In-situ experience
Geotechnical model/domains	Based on geology model	Based on geology model	Based on geotechnical data	Based on in-situ data
Hydrogeological model	Based on general experience	Based on general experience	Hydrogeological study	Local observations / measurements

Notes: * - Geotechnical classification proposed by Haile (2004) and corresponding project stage in relation to open stope mining methods

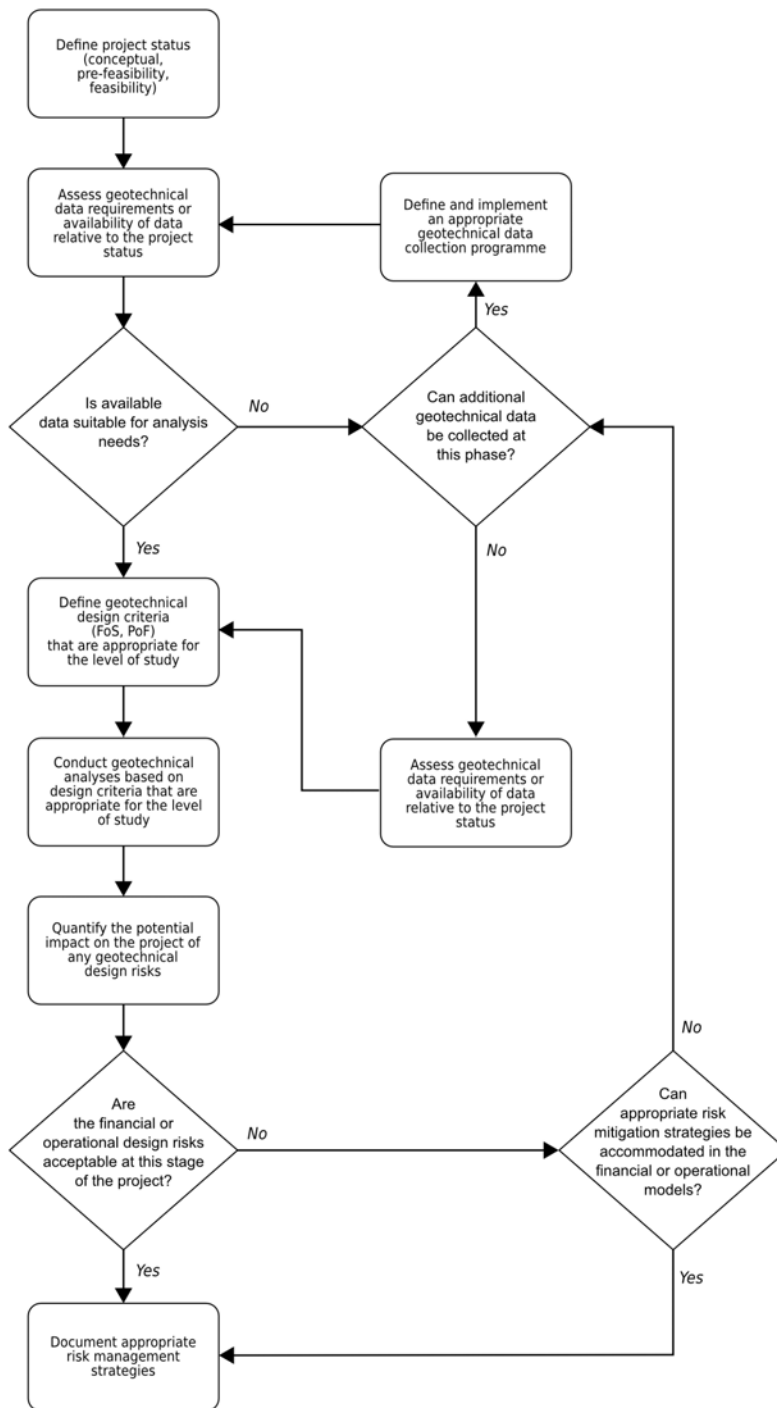


Figure 2.5 - Generic process to ascertain data uncertainty and risk for mining projects (Haile, 2004)

Either M or F describe the performance of the engineering structure, so either can be called the *performance function*. The probability of 'failure' (P_f) can be assessed by the determining the likelihood of either M being less than 0 or F less than 1. 'Failure' can represent any instance of poor or unacceptable performance. Reliability is generally the complement of probability of failure;

$$Reliability = 1 - P_f \tag{2.3}$$

Unfortunately, there are many difficulties in performing practical reliability-based approaches in rock-engineering design. As we have seen, some analyses may involve simplistic equations, whilst others involve complex computational processes, and approximations may be necessary in all or some steps of the analysis and design. In this case, one would expect that different analysis methods should produce different means and variances in the *performance function*, and thus different *probabilities of failure* and design reliability. Comparison of results from a number of methods can provide an insight into the errors involved in the computational procedures as well as an appreciation of the relative reliability of each design method (Baecher and Christian, 2003).

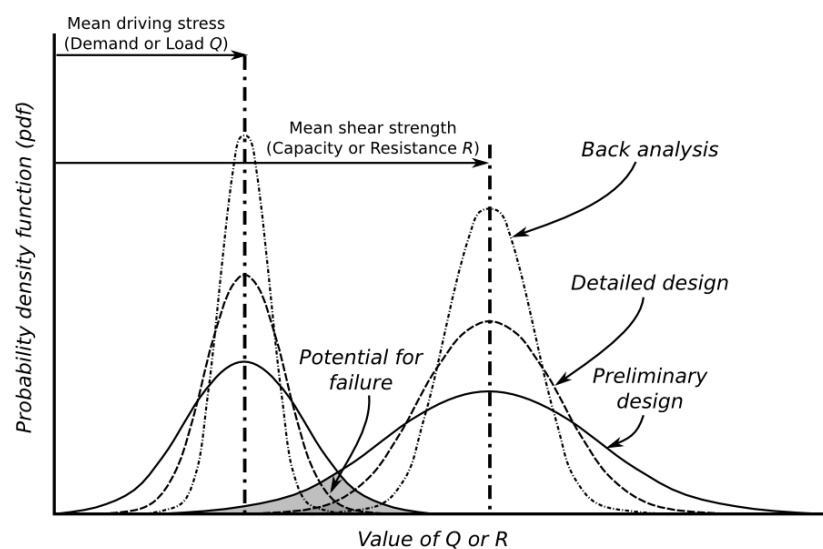


Figure 2.6 - Conceptual representation of the distribution of uncertainty in load (Q) and resistance (R) (modified after Hoek, 1992)

2.7 BHP BILLITON CANNINGTON MINE

In order to demonstrate how the slope design process is currently implemented in practice a detailed review of slope design at BHP Billiton Cannington Mine was undertaken. The review also serves to illustrate some of the state-of-the-art rock engineering methods and practices currently employed in the Australian mining industry, particularly at an advanced stage of project development (i.e. “operational” level). The Technical Services Department at BHP Billiton Cannington mine is responsible for the design of stable and economic open stopes. This process is controlled by Cannington's “Stope Design Procedure” (Roberts, 2005), which has been implemented to ensure that corporate safety and business risks are adequately managed in all aspects of the design of open stopes. A schematic flow chart of the mine planning process and detailed design of open stopes is shown in Figure 2.7. The following sections summarise the key points relating to rock engineering inputs, analyses and decisions in the open stope design process at the Cannington mine.

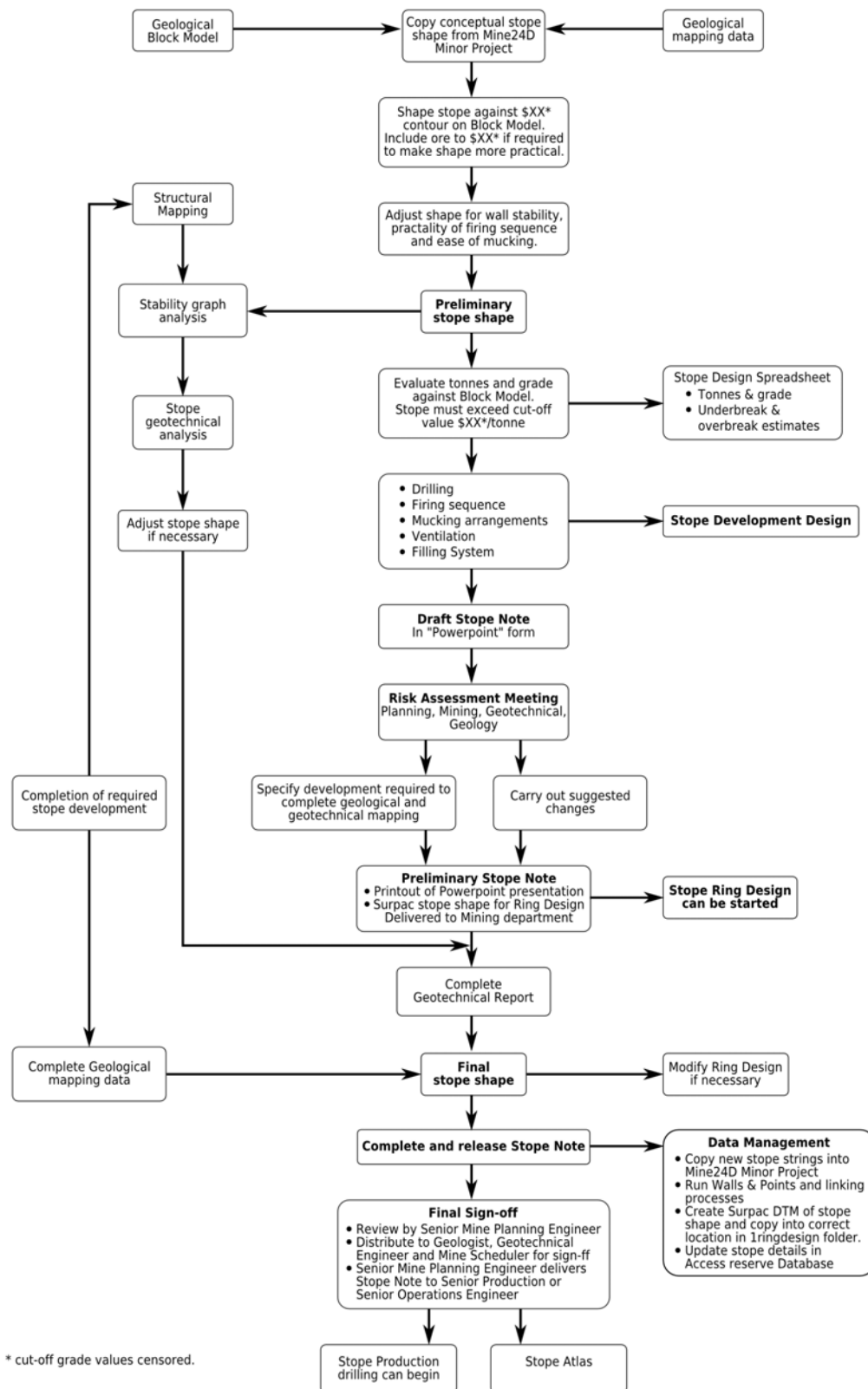


Figure 2.7 - Detailed stope design process at BHP Billiton Cannington Mine (Roberts, 2005)

2.7.1 Geotechnical Objectives

Throughout the entire open stope design process, the geotechnical engineering department are required to consider the following;

- The design and mining of the individual stope in question will **not impact on the safety of any personnel** during the entire life cycle of the stope, including; ventilation, service crews, surveying, drill and blast, load and haul, backfilling, etc.
- The design and mining of the individual stope will **not cause significant instability** issues that may impact on adjacent infrastructure (e.g. escape-ways, ore passes, return airways, workshops, etc.) or significantly impact on stope access, drives and draw-points.
- Consideration given to **minimise dilution** for the stope in question and adjacent future stopes.

2.7.2 Preliminary Stope Shape Review

The detailed stope design process usually begins with the production of Preliminary stope shapes, provided by the mine planning engineers, which are based on ore value cut-off grades (\$/tonne). The cut-off grade is set by BHP Billiton's Business Evaluation and Economics commodity price and exchange rate forecasts. The mine planning engineers provide Preliminary stope shapes to the geotechnical engineers for review. The primary purpose of the Preliminary stope shape review is to identify serious flaws in the geometry of these stope shapes that may have a significant impact on stope stability, such as; excessive draw-point spans, re-entrants, over-hangs and/or substantial convex stope wall profiles. The geotechnical engineers then provide verbal recommendations to the mine planning engineers for changes to the Preliminary stope shapes.

2.7.3 Stope Stability Analysis

Once the Preliminary shape, and therefore extents of the proposed stope have been established, the geotechnical engineers will begin compiling all relevant geological and geotechnical information in the immediate vicinity of the proposed stope. This also usually entails the geotechnical engineer reviewing the geological fact mapping and undertaking reconnaissance mapping in the development around the proposed stope for the presence of large scale geological structures and zones of poor quality rock mass (e.g. lenses of sillimanite schist and/or gneiss) and any rehabilitation requirements. After completion of the compilation, the geotechnical engineers firstly conduct a stability analysis utilising the Modified Stability Graph method (Potvin, 1988). The data for this analysis are based mainly on drill core logging in the immediate vicinity of each wall and on the mapping data. The drill core data are utilised for calculating RQD (Deere, 1964), and to some extent J_n values

(Barton et al., 1974). In some circumstances, there may not be any drill holes located near the stope wall of concern. In this case, the geotechnical engineer may take the opportunity to “map” *RQD* from the development in the immediate vicinity of the stope wall in question. The mapping data are also used to provide information on the joint condition and further assessment of the number of joint sets present (i.e. joint orientation data are collected), as well as for *Factor B* (Potvin, 1988) estimations. The data from the reconnaissance mapping are generally entered into personal notebooks and small format (A4) paper level plans of the area and then subsequently filed. The mapping data are not always shared with geologists to supplement the geological mapping data set.

The geomechanics laboratory dataset is used to estimate the intact rock strength for *Factor A* estimations. The intact rock strength is estimated by assessing the percentage of the various rock types around the stope surface under consideration, and weight averaging the intact rock strength based on their relative abundance. The maximum induced stresses used in *Factor A* estimations are based on likely stress concentration factors for each stope surface. After calculation of the modified stability number (N'), these values and the proposed hydraulic radius values for each wall surface are plotted on a site specific stability graph and compared to the “Cannington Stability Line”, suggested by (Streeton, 2000). If the stability numbers plot on or beneath this line, then these walls are targeted for further evaluation. This may include a review of the individual components, such as intact strength, stress or discontinuities, to indicate the primary cause to the low stability number.

Recently, as of February 2007, linear elastic numerical modelling of individual stopes has been used to complement the stability assessment by defining the likely location and extent of over-stressed and/or areas of confinement loss. The strength criteria for over-stressing is based on (Kalamaras and Bieniawski, 1995) rock mass compressive strength criteria and is described as;

$$\sigma_{cm} = 0.5 \frac{(RMR_{89} - 15)}{85} \sigma_c \quad (2.4)$$

The friction angle for the rock mass strength is estimated using (Trueman, 1988):

$$\phi_t = 0.5 RMR + 5 \quad (2.5)$$

For evaluating the effects of low confinement and tensile stress conditions, the tensile strength of the rock mass is typically estimated using (Sheorey, 1997);

$$\sigma_{tm} = -\sigma_t e^{\frac{(RMR_{89} - 100)}{27}} \quad (2.6)$$

Induced stress values from the linear elastic *BEM* numerical modelling are compared to the

rock mass strength criteria, in order to evaluate the likelihood of significant stress related damage and/or over-break. The numerical modelling also attempts to consider the effect of stoping on nearby development and infrastructure.

After the initial stability graph assessment has been performed, the geotechnical engineers may request that the geometry of the shape be altered to provide more “stable” behaviour. This assessment is also based on past experience with stopes in the same mining area under similar conditions. This may include changing the area/perimeter parameters (i.e. hydraulic radius), or changing the angle of the walls to improve stability.

2.7.4 Draft Stope Note and Risk Assessment

During the planning process, the mine planning engineer responsible for the stope will start to prepare a formal “Stope Note” prior to commencement of stope production. This process firstly involves the generation of a Draft Stope Note. The Draft Stope Note includes details on:

- Proposed stope shape
- Tonnes and grade
- Geotechnical issues
- Required development
- Drilling design and firing pattern
- Mucking and ore haulage arrangements
- Ventilation
- Paste and rock fill requirements

The Draft Stope Note is then presented at a meeting to Technical Services and Mining Operations personnel for group peer review or “Stope Risk Assessment Meeting”. As described in the Cannington Stope Design Procedures (Roberts, 2005), the main objectives of the risk assessment meeting are to;

- Carry out a formal Risk Management process and complete a semi-quantitative risk assessment for inclusion in the stope note
- Determine the modifications required to the design such that a Preliminary Stope Note can be produced and a stope Ring Design can be carried out.

Some technical factors that are considered in the risk assessment process are shown in Table 2.3 (Roberts, 2005). Any proposed additional development to access the stope (e.g. for access for additional mapping, extraction and/or production drilling requirements) will be

checked and signed off by the geotechnical engineers, geologists, surveyors and mining operations. The review will check for proximity to other excavations, ensure minimum pillar widths and intersection spans are not exceeded. In some circumstances, the rock reinforcement and ground support in the area has been identified to not comply with design performance, either due to poor installation, or deterioration due to excessive displacement, unravelling or corrosion issues. In this case, additional support may be required to minimise safety and business risks and to ensure completion of the stope design and production process. The geotechnical engineers will assess the rehabilitation requirements, conduct a peer review and pass on for review and sign-off by the Senior Engineer and they then issue the designs to the shift engineers. If cable bolting of the stope is deemed necessary, the geotechnical engineers will estimate the cable bolting requirements (i.e. type, length, number, orientation) and hand draft the cable bolt ring designs onto sections and plans.

Table 2.3 - Risk management factors considered in the design of stopes at BHP Cannington Mine

Risk Management Factor	Typical considerations
Geological	Mapping, diamond drill hole, block model, potential dilution.
Geometric	Rill angle, practicality of shape for drilling and mucking, design outside cut-off, protruding (convex) angles, drawpoint trough.
Geotechnical	Large and minor structures, rock mass quality (using rock mass classifications), hangingwall dip, hydraulic radii, stress concentration or relaxation, support installation.
Drill and blast	Hole length, drill rig set-up, reduce set-ups, practical firing sequence, safe charging access, drilling near paste walls, undercut drives.
Ventilation	Adequate fresh air, effect of open stope on primary ventilation system, heat, emergency egress, gases, dust and fumes.
Production	Mucking access, ore handling, undercut drives, remote mucking, filling, services, drainage, rehabilitation.

2.7.5 Geotechnical Report

After the Draft Stope Note and Risk Assessment Meeting the geotechnical engineers commence documentation into a formal stope assessment report. This stope assessment report will be included in the final "Stope Note". Any adjustments to the geometry of the stope are then made and a final "Stope Note" produced. Once a final "Stope Note" has been

produced, it is reviewed and signed-off by section representatives from Technical Services and Operations, and then it is handed over to Operations. The Stope Note is placed in a Stope Atlas, which also includes information on any problems encountered during implementation including; drilling, mining and filling of the stope. This information can be used to develop a set of key learnings that may be applied to improve the performance of future adjacent stopes.

2.7.6 Discussion

This review has shown that the stope design process, as operationally implemented at BHP Billiton Cannington mine, generally follows the process outlined by (Villaescusa and Li, 2004). It can be observed that the overall process is more closely related to the "Detailed Design" portion of Figure 2.7. The following observations can be made from the review;

- It can be seen that the practical implementation of the stope planning and process involves substantial iterative interaction between mine disciplines, including geology, geotechnical engineering, mine planning, production or 'construction' engineering. The main purpose of the stope design flowchart shown in Figure 2.7 is to document the main tasks and inter-discipline interactions and is not intended to provide detail of technical methods to be used.
- Rock mass characterisation data used in the stope design consists primarily of *RQD* values from diamond drill holes, *UCS* summaries from major rock types, geological structures from geological plans and from additional reconnaissance mapping. The results from the reconnaissance mapping for individual stopes are recorded on paper plans, filed separately and generally not used to supplement and improve the existing geological database where it may enhance geological interpretations or prove useful for the design of future stopes.
- The principal design methods used to assess stope stability include initial empirical methods supplemented with linear elastic *BEM* continuum modelling. Linear elastic failure criteria are based on empirical rock mass classifications. At the time of writing, deterministic design analyses are conducted using mean input parameters, (i.e. the impact of uncertainty is not taken into account in the design process), with no modification of failure criteria based on site specific back analyses.
- Data regarding stope performance include mining physicals and qualitative assessments of mining related problems. These are recorded in document format in the Stope Atlas for individual stopes. This could potentially be more useful if collated into a central database which could be easily accessed and analysed in greater detail. The role of monitoring and retrospective analyses were not included in the design process.

2.8 CONCLUSIONS

A common theme from all the rock engineering design processes reviewed shows that optimal design is achieved through continual re-assessment, or retrospective analysis, manifested as a series of multiple feedback loops at a number of design stages. One of the primary reasons for the requirement of such analyses is the variable and uncertain nature of the engineering properties of the rock mass and their impact on the engineering reliability.

It is essential that the mining environment is adequately characterised in terms of both data quality and quantity before key decisions are made on mining feasibility and the mine design is finalised (Brown and Rosengren, 2000). An important key to minimising uncertainty is to maximise efforts in rock mass data collection and characterisation. The iterative and evolutionary nature of stope design indicates that detailed stope design cannot rely solely on data collected at the initial feasibility study. In line with this philosophy, ***it is imperative that rock mass characterisation is treated as an essential on going process***. In light of this, there is a need for a data management framework capable of managing regular updates of rock mass characterisation data from a variety of sources and formats, and to maximise utilisation of rock mass data by enabling sharing of data between various technical disciplines.

Rock mass characterisation provides the factual basis for the formulation of any models that are used to represent rock-excavation interaction and potential failure mechanisms. ***A thorough understanding of the rock-excavation interactions are critical*** in determining the most appropriate strategy and methodologies to be used in the design analysis. Therefore, appropriate rock mass models that reliably capture these interactions need to be developed at each stage of project development.

The example rock engineering design processes (Bieniawski, 1993; Brown, 1985; Haile, 2004; Hudson and Feng, 2007) provide a useful yet generalised approach to rock engineering design and indicate that the appropriateness of one design methodology over another is largely a function of;

- the level of detail of the study, usually related to project development stage (i.e. conceptual versus feasibility),
- specific objectives of the engineering design,
- level of reliability or tolerance required,
- quality and quantity of input data,

- spatial representation and complexity of conceptual rock mass models,
- level of understanding of the engineering problem.

The example from BHP Billiton Cannington Mine highlighted that open stope design process involves a multi-discipline approach and requires consideration of a multitude of design functions and constraints. The key objective, in stope design is to **find the optimal design** considering limitations, conflicting requirements and resources available. This example also highlighted that contemporary state-of-the-art rock engineering mine design practice at operational project levels are still highly dependant on both empirical methods and linear elastic *BEM* numerical modelling techniques. The popularity of these methods is mainly due to the relative ease of use, however, there are a number of shortcomings associated with both of these methods that impact on their ability to produce reliable designs (see Chapters 4 and 7). It is also noted that uncertainties associated with design input parameters are not readily incorporated into the design approach.

It is considered that development and use of design process check lists are important tools in guiding the design engineer in the required tasks for formulating the best design option. Whilst the process map proposed by Haile (2004) is purposely generic in nature, it is considered that open stope design would also benefit significantly from adopting this strategy, especially considering its staged and evolutionary nature. It is therefore considered that **there is a need to develop a more detailed rock engineering design process specifically targeted for the design of open stopes**. Furthermore, the process should be sufficiently detailed for the various stages of mine development and specifically address the following in relation to open stope design;

- How do we assess whether the data are suitable for the analysis needs?
- How do we define the “appropriate” analysis for the level of study?
- How can we capture uncertainty in analysis and design?
- How do we quantify the potential impact of rock engineering risks on the project?
- How do we determine if the risks are acceptable?

Overall, the review has highlighted how **an integrated, adaptive and staged approach to open stope design is required, using a combination of appropriate data collection, analysis and design methods, and to maximise the use of excavation performance data**.

CHAPTER 3 - ROCK MASS CHARACTERISATION

3.1 INTRODUCTION

The engineering properties of the rock fabric, as well as the geometrical and mechanical properties of the discontinuities, will significantly influence rock mass behaviour and subsequent excavation performance, and generally dictate the choice of mining method and design layout (Brady and Brown, 2004). In order to gain an understanding of the potential rock mass response, it is necessary to understand the engineering properties and characteristics of both the intact rock material, discontinuities and boundary conditions, such as in situ stresses and the groundwater regime. Rock mass characterisation is the detailed study and analysis of rock mass properties and attributes and involves the disciplines of geology, engineering geology and rock mechanics. Characterisation can be done at a number of scales and for a variety of purposes, from excavation design to rock reinforcement and support design. The general rock mass characterisation process involves a number of activities, including;

- Planning and execution of rock mass data collection programmes - sampling strategies are devised and data collection methods selected to ensure that all key rock mass properties are well represented and that uncertainty and biases are minimised.
- Collation and basic analysis of rock mass data - quality of the collected data is ensured by firstly removing erroneous data points. Analyses are then undertaken to remove or reduce the effects of bias, assess accuracy and precision of key parameters and establish their reliability.
- Synthesis of rock mass data - combined analysis of rock mass parameters is undertaken to improve knowledge of the engineering characteristics and potential behaviour.
- Development of a number of rock mass models appropriate for use in engineering analysis and design (see Chapter 8).

The following sections briefly describe the rock mass characterisation process relating to the design of open stope spans.

3.2 ROCK MASS CHARACTERISTICS

There are a multitude of rock mass characteristics that are required for rock engineering design. A detailed account of each rock mass characteristic and methods for their estimation is beyond the scope of this thesis, however, a brief review of some features that are typically required in rock engineering design is presented below.

3.2.1 Geological Characteristics

Lithology is the study and description of rocks, especially at the macroscopic level (hand specimen to outcrop scale), in terms of their colour, texture (i.e. grain geometry), and composition (i.e. mineralogy) and is an integral part of understanding the geology of a project site. The general process for the study and description of rocks firstly involves establishing the origin or genesis of the rock (i.e. sedimentary, igneous and metamorphic). The rock can then be classified into more detailed genetic sub-divisions. Lithology therefore aims to identify and convey this genetic, chemical and physical information. The lithological features of the rock, such as its physical and chemical properties, can have a significant influence on the engineering properties and behaviour (Attewell and Farmer, 1976; Rzhnevsky and Novik, 1971). Determining and delineating the various lithologies at a project site also provides the initial basis for “domaining” or dividing the rock mass into regions of similar rock mass characteristics and comparative mechanical behaviour. The degree of severity of alteration and weathering will also have a significant impact on rock engineering behaviour. Alteration minerals, such as phyllosilicates (e.g. chlorite, sericite and clay minerals), can have a detrimental effect on the rock engineering properties. Conversely, silicification generally produces a stronger and more elastic rock mass (Watters et al., 2000).

3.2.2 Rock Fabric Engineering Properties

Engineering properties of the rock mass cannot readily be accounted for due to our inability to sample and test at the engineering scale. Therefore engineering properties of the rock mass are generally estimated by assessing results from small scale tests of the rock fabric and discontinuities at a limited number of locations. The most important engineering properties of the rock fabric in open stope mine design are strength and deformability. Intact rock strength generally refers to the peak strength of the rock fabric on a small scale, excluding the influence of discontinuities. In effect, intact rock strength can be construed to represent the strength of the rock mass between discontinuities, or the “rock block strength”. Strength can be defined in many number of ways, yet is principally related to the loading conditions, such as; shear, tension, compression, level of confinement and loading rate. It is also important to realise that strength can vary with scale, orientation, and location within the rock fabric. In order to gain an understanding of the strength characteristics of the rock fabric, it is necessary to sample and undertake a number of different laboratory and

index tests. Some typical rock fabric strength tests include (ISRM, 1981);

- Uniaxial Compressive Strength (*UCS*) tests
- Triaxial Strength tests
- Direct Tensile Strength tests
- Indirect Tensile Strength (Brazilian) tests
- Direct Shear tests (either on rock fabric or rock discontinuities)
- Point Load Index Tests
- Schmidt Hammer Rebound tests

Whilst undertaking laboratory strength tests such as *UCS* or triaxial tests, it is also possible to determine the elastic properties of the rock fabric and some post peak behaviour characteristics. Typical elastic properties include;

- Young's Modulus (e.g. tangent, secant or average)
- Poisson's Ratio for the selected Young's Modulus

Additional rock fabric properties that can be determined in the laboratory include; moisture content, porosity, unit weight, and ultrasonic shear and compression wave velocities. A popular and authoritative text on rock property testing is provided by the (ISRM, 1981).

3.2.3 Assessment of In Situ Stress

Knowledge of the *in situ* stress field is a fundamental requirement in rock engineering excavation design process as it assists in developing an understanding of the potential rock mass response to excavation. Stress measurements are a fundamental tool for obtaining knowledge of the *in situ* stress field. Stress measurement techniques can be classified into three generic groups (Windsor, 1993);

- De-stressing techniques
- Destressing-Restressing techniques
- Overstressing techniques

A number of techniques are shown in Table 3.1. The choice of stress measurement technique is dependent on a number of practical, economic and technical issues. Some of these are provided by (Windsor, 1993);

- logistical and practical issues
- number of measurements required to determine the full stress tensor
- the volume of rock sampled to estimate the stress tensor

- assumptions with regard to material properties and constitutive relationships
- issues regarding perturbations and erroneous results due to the excavation, geological structures or the technique itself

Table 3.1 - Comparison of common stress measurement techniques (Villaescusa et al., 2003b)

Stress Measurement Technique	Required Access	Sensing Method	Dimensional Extent
Destressing Techniques			
Overcoring			
Stiff inclusion	B	S	2D
Soft inclusion	B	S	3D
Hollow inclusion	B	S	3D
Strain gauge rosettes	B	S	3D
Hemispherical inclusion	B	S	3D
Photoelastic inclusion	B	S	2D
Deformeter	B	S	2D
Doorstopper	B&F	S	2D
Borehole slotter	B	S	2D
Differential strain relaxation	C	S	2D
Undercoring			
Pin array undercoring	F	D	2D
Tunnel undercoring	T	D	2D
Hole deepening	B	D	2D
Destressing-Restressing Techniques			
Flat jack	F	P&D	1D
Circular jack	F	P&D	1D/2D
Acoustic emission	C	A	1D/3D
Overstressing Techniques			
Hydraulic fracturing	B	P	2D
Jack fracturing	B	P&D	2D
Borehole breakout	B	I	O/2D
Core dinking	B	I	O/2D
Earthquake focal mechanisms	-	I	O
Geological features	F, C&E	I	O

F=rock face, B=borehole, C=core, E=exposure, T=tunnel/shaft/chamber

S=strain, D=displacement, P=pressure, C=calliper, I=interpretation, A= AE count

O=orientations, 1D=one dimensional, 2D=2 dimensional, 3D=3 dimensional

The results from stress measurements are generally reported as principal stresses, with the orientation of the principal stress axes related to the mines Cartesian coordinate system. The key components involve;

- the trend and plunge of the derived principal stress directions for each measurement

on a lower equal angle hemispherical projection

- a graph of the magnitude of the principal stresses versus depth
- linear relationships of the magnitude of the principal stresses versus depth (z)
- The first and last aspects are essential input parameters for use in numerical and analytical design techniques.

Although there are a number of stress measurement techniques available to the mining industry, those that offer *in situ* stress determination at an early stage are highly sought after. This is especially significant when planning high investment, and potentially high risk, mining methods at great depths.

3.2.4 Discontinuity Properties

Discontinuities are described as the collective term for low strength geological features such as joints, faults, shears, bedding planes, schistosity and foliation, or any zone of weakness within a rock mass (ISRM, 1978). Discontinuities can be classified in a variety of ways; by geological classification and geological origin, size or by one or more individual characteristics.

Quantitative Discontinuity Characteristics

The geometric and strength characteristics of discontinuities have a strong influence on the mechanical properties of a rock mass, including its strength and deformability. The rock mass structure therefore needs to be quantified by assessing various aspects, such as;

- the number of discontinuities (or discontinuity centres) within a given rock mass volume (i.e. discontinuity density)
- the orientation, size and shape of the discontinuities
- the spatial relationship between discontinuities
- the arrangement or topological hierarchy
- their strength and deformability which is dependent on;
 - surface geometries (e.g. large and small scale profiles, anisotropy)
 - composition, form and arrangement of discontinuity infill, and
 - effective stresses, loading directions and conditions.

A detailed account of the quantification of these aspects is beyond the scope of this thesis, however, the International Society of Rock Mechanics (ISRM, 1978) provides a suggested methodology for quantitatively describing discontinuities in the field, as well as a number of sampling methods. Of the ten (10) most important parameters influencing the behaviour and

potential response of the rock mass (ISRM, 1978), five can be considered 'geometric' parameters, and five as 'strength' parameters (Figure 3.1). Although characterisation of the strength parameters is important, in the design of excavations the need to focus on the geometric components cannot be overstated, as the geometric parameters define the rock structure system. **Without knowledge of the rock structure system and how it interacts with the excavation, the strength parameters essentially become redundant.** It is considered that the **most important geometric parameters than can be measured** are;

- Orientation
- Persistence
- Spacing

These parameters can be subsequently used to derive the 'Number of sets' and 'Block size'.

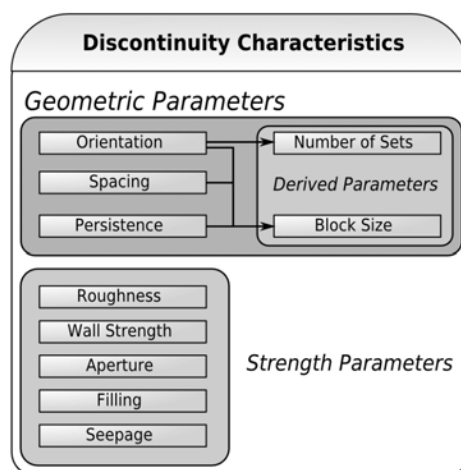


Figure 3.1 - Grouping of the ten discontinuity parameters into Geometric and Strength parameters

Scale Of Discontinuities

From a rock engineering point of view, it is convenient to describe discontinuities in terms of their scale and subsequent importance to rock mass behaviour and excavation performance. Scale can be used to represent the various types of structural features, classified as (Windsor and Thompson, 1997);

- **Primary** features include large scale discontinuities such as faults, folds, bedding planes, dykes and sills, and
- **Secondary** features include smaller discontinuities such as joints, foliation and lineations.

This terminology also includes an evolutionary aspect, which implies that 'Primary' structures are the principal structures that may control the subsequent development of 'Secondary' structures and their associated physical, geometrical and mechanical characteristics. The identification and delineation of large-scale 'Primary' structures therefore is a key element in the rock mass characterisation process. Another classification of discontinuities based on scale is provided (Cruden, 1977);

- **Major discontinuities** include features such as faults, folds, dykes, contacts and related features that are generally in the same order of magnitude as the project site. The location, physical properties and geometrical characteristics can usually be established for each individual discontinuity, and
- **Minor discontinuities** include features such as joints, bedding planes, small scale shears which, at the scale of the project site, cannot be individually described, and thus can be assumed to represent an infinite population. In this case, the properties of these features have to be generalised by a statistical assessment of a small sample of the population.

The definitions above essentially imply that scale is a very important geometric characteristic that determines whether discontinuities are represented deterministically ('Major' discontinuities) or stochastically ('Minor' discontinuities). It may be found that, for a particular engineering objective, there is a certain scale of discontinuity that has a significant control on rock mass behaviour and excavation performance. In this case, it is important that the sampling strategy is devised to adequately identify and characterise these features 'deterministically' within the study area for this scale. For example, Figure 3.2a shows 'First-order' structures which can usually be easily identified and treated deterministically at the 'mine-scale', with second- and 'higher'-order features too numerous to individually account for.

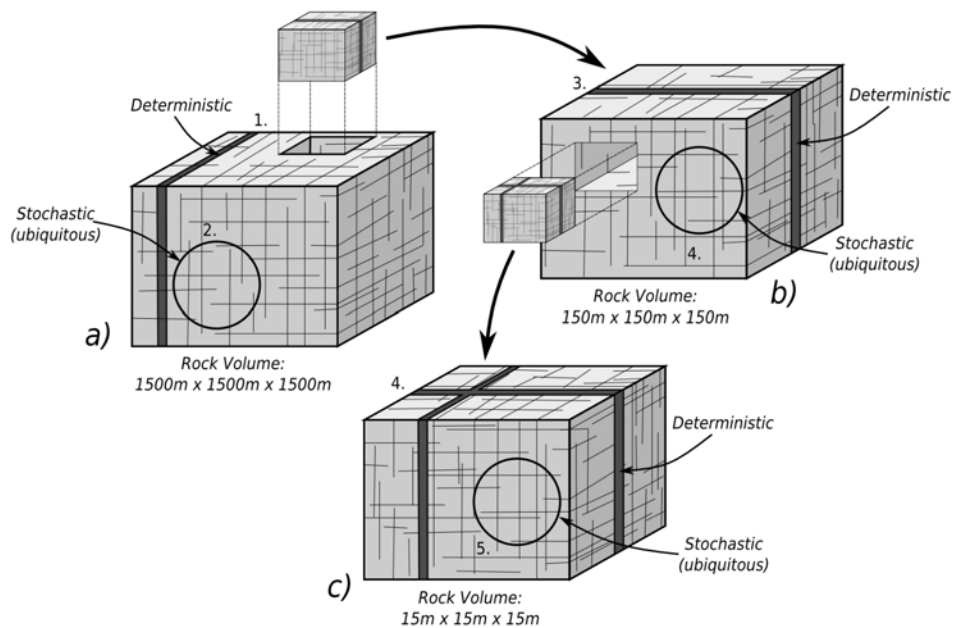


Figure 3.2 - Demonstration of scale effects on ubiquitous representation of discontinuities utilising the General Rock Structure Scheme (Pusch, 1994).

At the 'stope-scale' (Figure 3.2b), a smaller volume of rock is sampled, being a subset of the previous rock mass volume. This volume can be further sub-divided to represent the rock mass at the 'development-scale' (Figure 3.2c). Therefore, from a practical and economic point of view, given the specific scale of the rock engineering project, project objectives and budget for rock mechanics investigations, the optimum scale threshold for discrimination and treatment of 'minor' discontinuities should be determined.

3.3 ROCK MASS DATA COLLECTION

The rock mass properties can be collected from a variety of sources and at various levels of detail. The amount of data collected and methods employed primarily depends on;

- **development phase of the project.** At an early stage of the project, initial rock mass data collection generally consists of reconnaissance style mapping exercises. As the project develops, more systematic and detailed methods are generally employed.
- **scale of engineering project.** The size of a project may dictate the volumetric coverage of the rock mass to be sampled. For example, rock engineering of a cave mine requires significantly more sampling coverage than, for example, shaft sinking investigations.
- **engineering objectives and reliability.** The engineering objectives will dictate the level of detail and degree of rigour involved in the data collection methods and subsequent engineering analysis. For example, the data and analysis requirements

will be different for a conceptual level stability analysis for a small open pit compared to the detailed design of rock reinforcement for a crusher chamber, where analysis techniques might range from simple rock mass classifications to detailed probabilistic kinematic analysis of key-block instability.

- **access to rock mass exposures.** In some environments, or for certain projects, there are limited exposures for direct access to the rock mass. In this case, the rock mass may be sampled solely using diamond drill core or other remote methods.
- **variability of the rock mass.** For certain projects, the rock mass may contain a complex array of rock mass 'domains', relative to the scale of the project. The complexity and size of these 'domains' may not allow for certain sampling techniques, such as line mapping, to be conducted. In this case, the sampling programme will need to be modified to accommodate the configuration of rock mass 'domains'. In addition, the project may contain many domains. The data collection programme will need to be designed such that each domain is adequately sampled.

It also must be noted that, from a practical and operational perspective, the amount and detail of rock engineering data collected can also depend on the availability of skilled personnel, as well as budgetary and time constraints. This may have an influence on the data collection methods employed for a particular project.

Once the objectives of a rock engineering project are clearly understood, a carefully considered and appropriate sampling programme should be devised. Unfortunately in the mining industry, the rock mechanics engineer may have limited input into the design and specification of initial rock mass data collection programmes. Indeed, in most circumstances, the rock mechanics engineer usually obtains initial rock mass data from resource diamond drilling, where the primary objective is assessing the mineral economic potential of the rock mass. This programme may be optimal for this purpose, yet may be inappropriate for rock engineering purposes and may contain a number of biases that will affect the results and ability to undertake analyses specific to the engineering objective. In this case, it is necessary to supplement this information with additional data collection programmes designed to capture the required information and minimise biases.

Importantly, the types of data collection methods employed, as well as the amount of data collected by each method, has a significant impact on the ability to develop a robust rock mass characterisation models for the engineering objective at hand.

3.3.1 Subjective versus Objective Techniques

Broadly speaking, data collection methods can be classified by the into two main categories, primarily based on the way the data are collected (Windsor and Thompson, 1997);

- **Subjective.** Only **selected** discontinuities and features that are deemed important are described or tested. This introduces bias and, because the full range of conditions are not sampled, the level of uncertainty is generally unknown.
- **Objective.** **All** discontinuities and features of the rock mass in an area are systematically described or tested. The survey locations are usually selected in an unbiased manner. This type of survey allows for the range, level of confidence and uncertainty to be known.

Importantly, the data collection technique will control the type of any subsequent analyses that can be undertaken. That is, data from subjective data collection techniques can only be used for deterministic analyses at specific locations, whilst objective data can be used for *both* deterministic and stochastic analysis techniques. This highlights the importance of **maximising the amount of objective data techniques employed**. The decision of the style of data collection is also influenced by the time and effort required to collect the data. Subjective techniques are often the easiest to undertake, and large outcrops or exposures of rock masses can be covered relatively quickly. Objective techniques, on the other hand, are extremely time consuming. The main differences between the two techniques are summarised in Table 3.2.

Table 3.2 - Comparison of Subjective versus Objective data collection techniques

Subjective	Objective
Only some selected features collected	All features within a particular region collected
Biased towards "important" features	Unbiased selection
Unknown level of reliability	Level of Confidence known
Large volumes of rock mass can be assessed, yet in limited detail	Less volumetric coverage - more detailed
Useful for delineating rock mass domains	Applicability effected by configuration of rock mass domains
Relatively quick and inexpensive	Very time consuming - costly
Deterministic analysis at specific locations	Suitable for detailed deterministic and stochastic analyses

3.3.2 Rock Mass Sampling Methods

There are a wide range of rock fabric and discontinuity sampling methods available to characterise various components of the rock mass. A summary of the most common

methods is presented in Table 3.3. A more detailed review of rock mass characterisation data collection methods utilised in the mining industry are presented in Appendix A.

3.3.3 Accuracy, Bias, Precision and Error

Data reliability can generally be expressed in terms of accuracy and precision. Accuracy refers to the degree to which the calculated mean differs from the true mean. The difference between the two is generally due to some persistent factor, or bias (i.e. a systematic error). Precision is a measure of how close measurements are to each other, or the variation between readings (i.e. random errors). Imprecision is generally caused by small sample sizes. As more samples are collected, the more precise the estimate of the mean will become. The practical problem facing the rock mechanics engineer is to balance precision with effort required, that is, determine the optimal sample size. Increasing the sample size may increase precision but does not improve accuracy. Eliminating the systematic error improves accuracy but does not change precision. In order to provide reliable estimates of rock engineering parameters, all attempts must be made to improve both accuracy (i.e. remove or reduce biases) and precision. However, the ability to provide reliable estimates is hindered by a number of factors that need to be understood and addressed in the planning and execution of rock mass characterisation programmes.

Table 3.3 - Summary of common rock mass data collection methods in mining

Sampling Method	Rock Mass Characteristics	Technique Classification
Drill core logging	Rock fabric and all discontinuities	Objective
Spot Mapping	Rock fabric and discontinuities	Subjective
Scanline Mapping	Discontinuities [#]	Objective
Window Mapping	Discontinuities [#]	Objective
Geological Mapping	Major discontinuities and lithology/alteration	Subjective
Geophysical methods	Rock fabric and discontinuities [^]	Objective
Laser scanning	Discontinuities [^]	Objective
Photogrammetric Methods	Discontinuities [^]	Objective
Sub-sampling of drill core for laboratory tests	Indices of small scale rock fabric and discontinuity strength and deformability	Subjective

Notes: [#] - some aspects of rock fabric may be collected at the same time, [^] - only some aspects of discontinuities measured

Small Scale Laboratory Tests

Engineering properties of the rock fabric are generally ascertained using a limited number of physical tests on **small scale** samples. A variety of small scale test methods can be utilised, with each method providing a specific aspect or **index** of engineering behaviour. That is,

these small scale tests do not provide the full range of rock fabric engineering behaviour under all conditions. Nevertheless, different index tests can be used to derive a number of rock fabric performance criteria in engineering design, such as; peak failure criteria, post-peak failure, or yield criteria. These criteria can be based on critical stresses, critical strains or critical energy inputs. In conjunction with the rock mass geometry and discontinuity properties, it is possible to estimate these criteria at the rock mass scale.

The use of small scale samples may make sample handling and transportation easier and allows for laboratory specimens to be prepared in a systematic manner. This enables test methods to be standardised, which assists in removing biases, as well as improving accuracy and repeatability. Standardised testing allows for the determination of the mean and the range of variability of specific indices for a certain rock type, or allows for comparisons to be made between different rock types under identical test conditions. However, the reliance on small scale samples brings with it many disadvantages;

- **Scale and Shape effects** - certain index parameters, such as strength, are biased by size and shape of the sample. Corrections need to be made in order to ensure indices are comparable between specimens of differing sizes and shapes.
- **Inhomogeneity** - in order to test for inhomogeneity within a rock volume, sampling and testing in a large number of locations is required. Test methods that are rapid and low-cost, such as Point Load tests or Schmidt Hammer Rebound tests are more appropriate in this situation, however, the accuracy and precision of the method must also be considered.
- **Anisotropy** - in order to assess anisotropy, sampling and testing in a number of orientations is required. Attempts should be made to establish the test index variation with orientation, or at least to establish an “anisotropy ratio”. Care should be undertaken when assessing the results of all test methods on apparent isotropic material.
- **Precision** - due to the small size of the sample relative to the volume of rock to be tested, a large number of tests are required to establish precision. Progressively testing larger scale samples is required to find the representative elemental volume (*REV*), or scale at which variability is minimised (Figure 3.3), however, this is not a practical solution for most mining applications and studies. In this case, the only option is to rely on small scale samples. Biases (and variability) can be minimised by eliminating samples that contain obvious discontinuities.

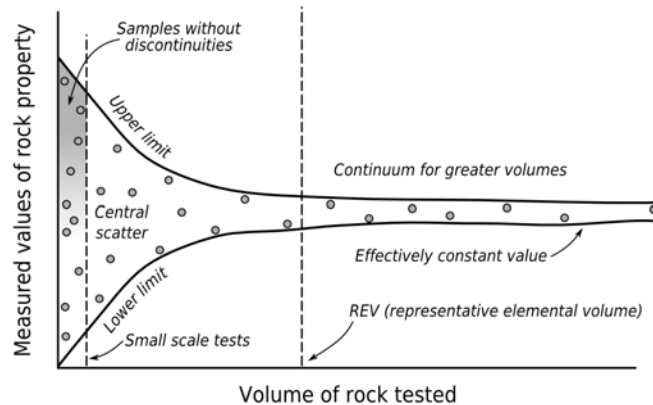


Figure 3.3 - Representative elemental volume (REV) concept (modified from Hudson, 1989)

Discontinuity Sampling Biases

Depending on the sampling technique used and its relation to the rock mass configuration, a number of biases can be introduced during data collection. It is important to realise that, in developing any statistical model, we are attempting to provide an inferred model of the **target population** from a series of smaller populations (**sampled populations**). In rock mass characterisation studies, the **sampled population** is only observed in one- and two-dimensions from an **exposed population** (i.e. rock faces and boreholes) where only a partial view of rock mass features are available, especially discontinuities. As we can only directly view and measure the rock mass in two-dimensions at best, intrinsic discontinuity properties such as shape, size and density cannot be measured directly. These parameters have to be estimated from other measurements, such as spacing and persistence, which can introduce a number of biases, depending on how they are collected. It is important to be aware of these biases such that they can be minimised and/or accounted for in subsequent analysis of discontinuity mapping data. The main forms of bias include;

- **Orientation Bias.** The probability of a discontinuity appearing in an outcrop depends on the relative orientation between the outcrop and the discontinuity (Terzaghi, 1965). Therefore, discontinuities oriented sub-perpendicular to the sampling direction are more likely to be intersected than those oriented sub-parallel. In order to minimise orientation bias, sampling for discontinuities needs to be undertaken at a number of different orientations.
- **Size Bias.** The larger the discontinuity, is more likely to appear in an outcrop than a smaller one (Baecher and Lanney, 1978). In addition, a longer trace is more likely to appear in a sampling area than a shorter one.
- **Truncation Bias.** Smaller discontinuities are difficult, if not impossible to measure. If these are not recorded then biases will exist in means and erroneous statistical models may be developed. Trace lengths below some known “cut-off” need to be

recorded and taken into account in rigorous statistical analysis (Villaescusa, 1991).

- **Censoring Bias.** Trace lengths limited by artificial boundaries imposed by, say excavations. Censored lengths provide the lower bounds to true trace lengths, as one or both ends are no longer visible (Cruden, 1977). Recording of censored ends can reduce biases in the estimation of mean trace lengths.
- **Sample Size Bias.** The reliability of mean discontinuity spacing, linear frequency and trace length values are directly related to quality and quantity of the sample population. For example, if we restrict the length of scan lines below a certain value, say L , then we will be unable to obtain spacing values in excess of L and bias the data set towards smaller spacing values. Alternatively, if we neglect to record spacing values smaller than some minimum value we bias the data set towards larger spacing values. These biases in the sample population directly lead to inaccurate estimations of the mean (Sen and Kazi, 1984). Sen and Kazi (1984) also demonstrated the effects of short scan lines on spacing values for negative exponential and log-normal distributions and provided a method for determining the percentage of relative error between the true and calculated means based on the scan line length. Their work also allows for the determination of the optimal scan line length, based on an acceptable level of relative error. Unfortunately, exposure and access limitations may not allow for required scanline lengths within the geological domain under investigation. In this case, an estimate of the relative error can be made and corrections can be applied accordingly.

3.3.4 Remote Data Collection Methods

Sampling can generally be categorised by either direct or remote methods. Direct methods involve human interaction with the rock mass by physically inspecting the rock fabric and discontinuities, measuring their attributes. Examples of direct methods include line mapping, window mapping and drill core logging. In some circumstances, the rock mass cannot be accessed manually, as exposures are practically inaccessible (cliff or pit wall face) or due to safety concerns (i.e. rock fall hazards). A number of technologies have been devised to partially overcome these issues by collecting rock mass data remotely, including photogrammetry and laser scanning technologies. The advantages of remote methods, is that they are able to sample much larger and potentially inaccessible rock exposures. Although these methods allow for reasonably quick, accurate and detailed capture of discontinuity data, there are a number of shortcomings in their ability to capture all necessary rock mass characterisation data to the required level of detail (see Figure 3.4). A more detailed account of the most important criticisms of the remote methods are provided in Appendix A.

3.4 ROCK MASS DATA ANALYSIS

Once rock mass data is collected it needs to be checked, analysed and then synthesised into information such that it can be used in engineering analysis and design. The following sections provide a brief outline of the methods used in rock mass data analysis, including derivation of statistical moments, treatment of a number of biases, and common discontinuity analysis methods. A summary of some basic rock mass data analysis techniques is shown in Table 3.4, with a more detailed description provided in Appendix A.

3.4.1 Data Validation and Bias Corrections

The first task in data analysis is to check and ensure the quality of the collected data. This is done by checking data for correctness and removing erroneous data points;

- correct codes used
- check for missing values
- check values are within proper ranges (e.g. $0 < RQD < 100$)
- no overlaps in interval data (i.e. from/to distances)
- application of any necessary correction factors

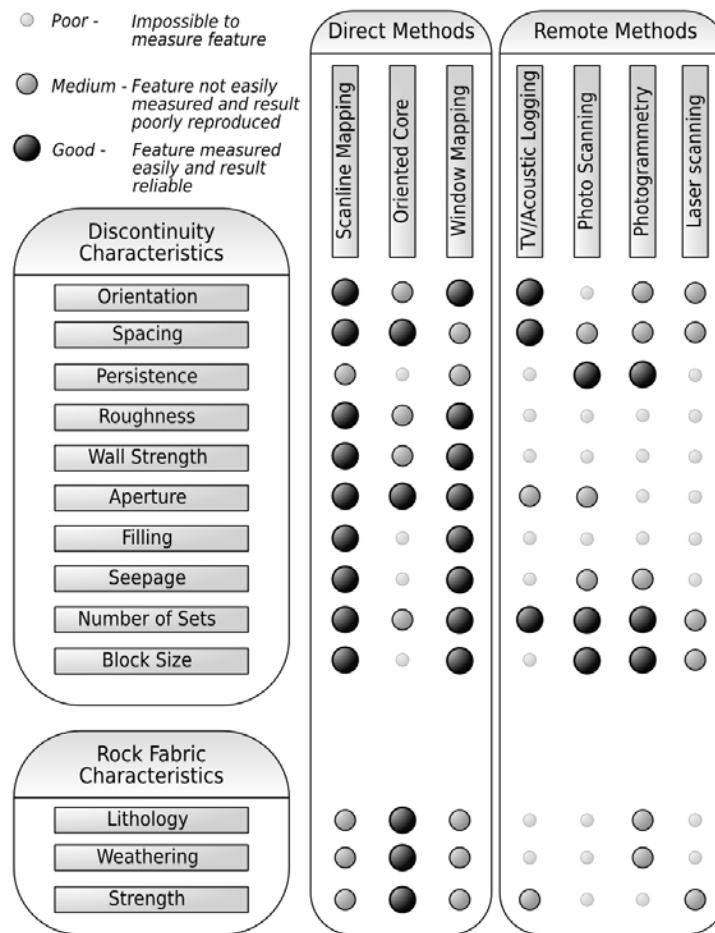


Figure 3.4 - Comparison of sampling methods and their ability to capture various rock mass characteristics (modified from Hudson, 1989)

After validation all attempts must be made to remove or reduce bias in rock fabric and discontinuity data. Some basic methods include;

- removing rock fabric tests that have failed on existing discontinuities
- evaluate and account for anisotropy in rock fabric tests by grouping results based on angle to penetrative fabric
- apply bias corrections and weightings to orientation data prior to analysis

Table 3.4 - Summary of Common Rock Mass Data Analysis Tasks

Task	Parameters or Characteristic	Equations or Method
Validation	<i>RQD</i> vs Discontinuity frequency	See Appendix A
Bias Corrections	<i>UCS</i> test aspect ratio	A.2
	<i>UCS</i> diameter	A.3
	Point Load	A.4 & A.5
	Orientation	A.7, A.8, A.9 & A.10
Correlations	<i>UCS</i> vs Point Load	A.6
	<i>UCS</i> vs Schmidt Hammer	
	<i>UCS</i> vs Field Index Tests	
	<i>UCS</i> vs alteration type	Regression and Multivariate analysis
Set Definition	<i>UCS</i> vs rock type	
	Mean Orientations	See Appendix A
	Dispersion (K-values)	A.11 & A.12
Isotropy/Orthogonality	% unassigned (i.e. % random)	See Appendix A
	No. of sets	See Appendix A
	Angles between sets	See Appendix A
	Eigenvalue analysis	See Appendix A
	Contour analysis	See Appendix A
Total Spacing	Tensor analysis	A.14
	Arithmetic mean	A.15
Normal Spacing	Arithmetic mean	A.16
	Standard deviation	A.28
Set Spacing	Arithmetic mean	A.17
Linear Intensity	Total discontinuity linear intensity	A.19
	Corrected discontinuity linear intensity	A.21
Areal Intensity	Total discontinuity areal intensity	A.22
	Corrected discontinuity areal intensity	A.23
Volumetric Intensity	Total discontinuity volumetric intensity	A.24
Anisotropic Intensity	Three-dimensional locus	A.31, A.32, A.33 & A.34
	Intensity tensor	A.36, A.37 & A.38
	Anisotropy factor	A.39
Discontinuity Size	Maximum likelihood trace length	A.40
	End-point estimator (circular windows)	A.41
Terminations	Termination index	A.42 & A.43
	Termination probabilities	A.44 & A.45

3.4.2 Statistical Moments

All rock engineering parameters are classified as random variates or stochastic variables. They cannot be predicted with absolute certainty, and each possible range of values has an associated likelihood, or probability, of occurrence. A statistical sample of data needs to be presented in a form that is useful for further analysis. This usually includes some measure of central tendency:

- average (or arithmetic mean)
- median
- mode

and some measure of dispersion about the central value:

- variance
- standard deviation
- coefficient of variation

Coefficient of variation is useful to compare dispersion between sets of variables with different absolute means. In this case, it provides the design engineer with a quantifiable measure of precision, irrespective of the variable and its range of values. It is also useful when absolute information on a variable is not known but typical values for coefficient of variation are known which can then be applied to the analysis.

3.4.3 Analysis of Discontinuity Data

Statistical analysis of discontinuity data are of vital importance in development of discontinuity network models (see Chapter 8). Analysis and synthesis of these data can provide valuable information on the characteristics of the rock mass structure which need to be understood prior to rock engineering analysis and design;

- define the number of sets
- define mean orientations and degree of dispersion
- assess anisotropy and/or angles between mean orientations (i.e. sets)
- define mean spacing (or discontinuity intensity) and degree of dispersion
- define mean trace lengths and degree of dispersion
- define mean discontinuity size and its distribution (assuming a certain shape)
- define termination characteristics (to identify persistent and non-persistent sets)
- establish mean and range of discontinuity surface and infill characteristics

3.4.4 Improving Accuracy and Precision in Rock Mass Data Collection

Analysis of rock mass data can also be used to determine additional data collection requirements in order to improve accuracy and precision. In order to accomplish this, it is necessary to be able to;

- i) quantify precision in some way
- ii) specify the required precision, and
- iii) calculate the sample size that provides this precision (Priest, 1993)

For example, precision of the mean spacing can be estimated using the central limit theorem (Priest and Hudson, 1981). Here, mean values \bar{X} , of random samples n , taken from a

population that follows any distribution and has some definite, yet unknown mean value μ_x , and variance σ_x^2 , will tend to be normally distributed with a mean μ_x and a standard deviation (or standard error of the mean) of $\sigma_x/\sqrt{n}(\sigma_x^2/n)$. From this, it can be seen that as n increases the standard deviation, or standard error about the mean, approaches zero.

Where spacing values are characterised by negative exponential distribution, the mean and standard deviation are equal. In this case, the central limit theorem can be used to, for a given sample, determine how confident one can be (e.g. 95% confidence limit) that the unknown population mean μ_x lies within some range of the sample mean, \bar{X} . Alternatively, this situation can be used to define the number of samples n required to provide an estimate of the population mean to a certain level of precision, or allowable proportionate error ϵ ;

$$n = \left(\frac{z}{\epsilon} \right)^2 \quad (3.1)$$

where z is the standard normal variable associated with a certain value (or percent confidence) of $\Phi(z)$. This approach is illustrated in Figure 3.5. This approach can be used on any parameter where the underlying distribution is known.

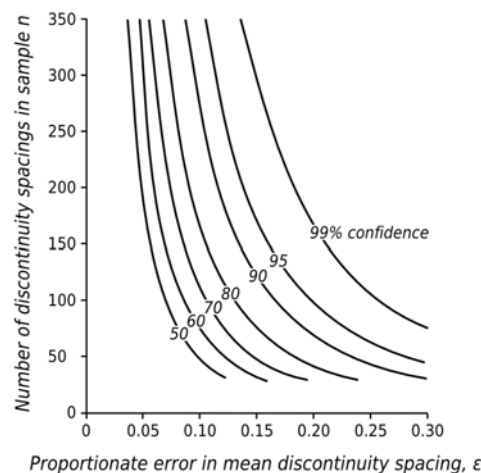


Figure 3.5 - Sample number versus precision of the mean discontinuity estimate for negative exponential distributions of spacing (Priest and Hudson, 1981)

3.5 CONCLUSIONS

This review has described some common data collection and analysis techniques utilised in the mining industry for rock fabric and discontinuity characterisation. In developing a rock mass characterisation investigation programme, the rock mechanics engineer will need to plan and collect data in a systematic and cost effective way. The rock mechanics engineer will ultimately need to decide on where and how many samples to take and what kind of

tests are required and the test configurations. These are generally a function of;

- Engineering objectives of the project
- Establishing the most important rock fabric parameters
- The level of reliability required
- The variability of the site geology (size, spatial distribution, variability and anisotropy of the major rock types) with respect to the scale of the project

3.5.1 Rock Fabric Characterisation Investigations

There are many methods available to the rock mechanics engineer to characterise rock mass fabric. Each method will have a number of advantages and disadvantages. Some test methods are more accurate and precise than others. Accuracy and precision of the various test methods are generally proportional to cost and effort. The engineer will need to **carefully consider and compare, the accuracy and precision, ease and speed, and cost of each method**. In order to cover a large volume of rock efficiently and cost effectively, lower reliability methods are generally preferred. This concept is illustrated in Figure 3.6.

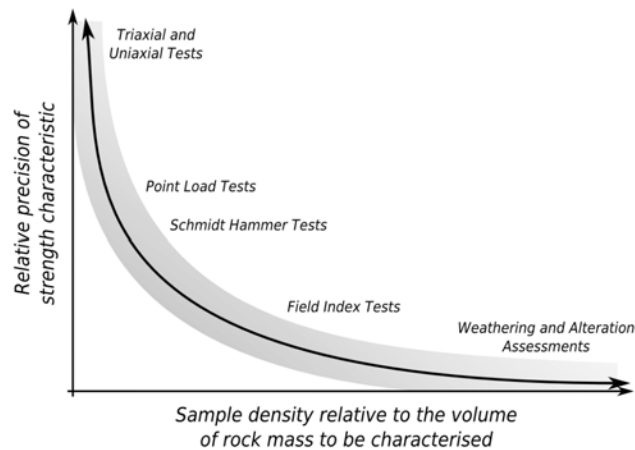


Figure 3.6 - Illustrative concept showing strength characterisation based on data density and its relation to method precision

As noted previously, strength and deformability characteristics are influenced by physical and chemical rock fabric properties, such as; density, moisture content, lithology and mineralogy, alteration and weathering. It is therefore also important to record this information to understand the extent to which these factors influence engineering behaviour. One approach would be to ascertain correlations between the degree of weathering and alteration, and rock fabric properties for various rock types. In this way, the rock type and extent and severity of alteration and weathering can be used to delineate volumes of rock mass with potentially similar rock mass behaviours (i.e. “domaining”). This concept is

discussed in more detail in Chapter 8.

In developing a sampling and testing programme, a key aim of rock fabric characterisation is **to maximise both reliability and volumetric coverage** utilising the various test methods available, within budget and time constraints. A suggested approach could involve;

- Utilising less accurate and precise methods, such as field index strength tests to broadly categorise gross variations in the rock fabric properties across the site, together with weathering alteration and geological descriptions of any anisotropy to categorise the rock fabric **qualitatively**.
- Utilising more precise methods, such as Point Load or Schmidt Hammer tests to **quantify** the likely strength range of the major rock types and possibly highlight spatial variations and anisotropy.
- Utilising accurate methods, such as UCS methods, as a standard to gauge the accuracy and precision of the Point Load and Schmidt Hammer Rebound tests. This can not only be used as a correlation tool, yet maximise the volume of rock fabric that can be characterised.

3.5.2 Discontinuity Characterisation Investigations

The purpose of discontinuity investigations is to improve our understanding of the rock structure system by quantifying a number of discontinuity parameters. The review has shown how reliability is improved by minimising biases and improving precision. This can be achieved by optimal planning of sampling locations and orientations as well as the appropriate selection of collection methods. A number of techniques were also explored for the removal of biases in discontinuity data analysis. Some additional aspects that should be considered in discontinuity characterisation programmes are suggested below.

Recording Of Discontinuity Characteristics

The review has highlighted that the geometric properties of discontinuities (e.g. orientation, size, shape, location) can be regarded as the most important discontinuity characteristics effecting excavation performance. Unfortunately, true measures of discontinuity size and shape are unattainable, however, size can be estimated from 2-dimensional measures (Warburton, 1980). The importance of recording discontinuity orientation and location should not be overlooked. For example, deterministic analysis of large-scale discontinuities or any spatial analysis of discontinuity data requires that the location of each data point is determinable.

If a variety of rock engineering objectives are to be undertaken at a site, one may not be able consider which discontinuities constitute “important geological features” for all objectives. For example, closed and filled discontinuities may not appear significant for excavation and rock reinforcement design, however, in the assessment of fragmentation and comminution these may be of vital importance (Brzovic and Villaescusa, 2007). A prudent approach therefore, would be to **record all information with provisions to discriminate “important geological features” at a later date** rather than just recording discontinuities considered important for the task at hand. This is especially relevant where core samples may potentially be destroyed and rock mass exposures lost. Taking more time and effort in the data collections stages far out ways the time and expense of re-drilling or generating fresh exposures.

The increased popularity of rock mass classification systems in the Australian mining industry has lead to the situation where rock mass data, and in particular quantitative descriptions of discontinuities, are immediately interpreted and categorised in terms of input parameters of rock mass classification systems. Some mines interpret and categorise the surface characteristics of discontinuities to the NGI Q-system (Barton et al., 1974) or Geomechanics classifications systems (Bieniawski, 1973; Bieniawski, 1978; Bieniawski, 1989; Laubscher, 1990). It must be noted that the there are a number of issues that need to be **carefully considered** when deciding to collect and then treat information in this manner. Firstly, the surface characteristics, as categorised and rated in rock mass classification systems, are **simplifications** and **interpretations** of the full descriptive quantification of the surface features. Once discontinuity data are interpreted and recorded only as rock mass classification parameters, the complete descriptive quantification of the discontinuity can no longer be obtained. This information is lost and can only be recovered by re-logging the core, which may longer be available due to assaying requirements. Importantly, the decision to adopt such an approach to data collection **severely limits the choice of rock mass characterisation techniques and subsequent engineering design methods available to the rock mechanics engineer.**

Structural Analysis Of Large-scale Discontinuities

From a rock engineering point of view, the configuration and properties of discontinuities would appear to be more important rather than the processes that formed them. However, an understanding of the geological processes can lead to a better understanding, and potentially the prediction, of the structural characteristics of the rock mass. Collection and detailed analysis of the structural geology is imperative to understanding the structure of the rock mass and the geological processes involved in its formation. Careful analysis of structural data may allow for the identification of the chronology of discontinuity evolution,

including families (or sets) that have developed, together with their topological arrangement and characteristics, and the conditions required to form them (Price and Cosgrove, 1990).

The concept of 'stochastic' representation of discontinuities was also introduced. The concept explains that each discontinuity cannot be individually accounted for but rather a small sample of discontinuities within a volume of rock mass is used to model and statistically predict discontinuity system characteristics for a larger region. If detailed structural analysis can establish that discontinuities from an area have undergone the same geological history and processes, then it may be possible to assume that a 'stochastic' approach is valid (Piteau, 1973).

Development of large-scale 'Primary' discontinuities can influence the location and development of 'secondary' structures (Moody and Hill, 1956; Price, 1966; Riedel, 1929). Analysis of structural data can also indicate controls on the development, location, geometry and intensity of families of 'Secondary' or 'Minor' discontinuities. Thus, detailed analysis of large-scale structures may assist in understanding the occurrence and spatial correlation of different families of discontinuities. Careful and detailed study of the origin of discontinuities can assist in;

- determining the validity of extrapolating sampled data to regions of rock mass
- predicting discontinuity characteristics;
 - predominant discontinuity orientations, or sets
 - morphology, mechanical properties
 - topology and age relationships
- indicating spatial correlations between the type and abundance of discontinuities

Some of these aspects are covered in more detailed in Chapter 8.

Orientation Analyses

The emphasis of orientation data analysis is to define the number of sets and establish their mean orientations and degree of dispersion. This type of orientation analysis forms the basis of most rock characterisation studies for open slope design purposes. It is important to note that other discontinuity attributes such as shear strength properties, persistence and spacing, as well as spatial and hierarchical relationships between discontinuities are generally ignored in orientation analyses. In addition, the scale of the discontinuity is not considered such that large, persistent, discontinuities (e.g. faults, shears, etc.) will be represented as having the same importance as smaller, impersistent discontinuities. It is

therefore important to keep these limitations in mind when conducting a “orientation only” characterisation of the rock mass structure. For example, one project site may be characterised by two distinctly different types of discontinuities, one being a persistent with low shear strength, the other being impersistent with high shear strength, yet each having the same orientation. Stability in this case most likely will be controlled by the longer, weaker discontinuities.

Geological Complexity, Sample Size And Statistical Homogeneity

As we have seen, the accuracy and precision of spacing and persistence analyses are heavily influenced by the adopted sampling regime and quantity of data collected. Information about the shape and orientation of the sampling domain, as well as adopted or imposed truncation and censoring levels, are required in order to account for biases to improve accuracies of estimated parameter means and distributions. Accuracy and precision of spacing and trace length estimates are generally improved by increasing the size of the data set. All of the analysis methods described in this chapter assume that the data belong to a statistically homogeneous region. However, the required accuracy and precision may not be achieved due to the lack of rock mass exposures or the complexity and small size of the rock mass domain.

3.5.3 Integrating available data sources

Rock engineering staff often rely on data obtained from other disciplines, such as the exploration or mining geology teams, whose primary function is to understand the geology of the mine environs. As such, they have more resources dedicated to sampling the rock mass and subsequently have the potential to collect vast amounts of rock mass data. The review has shown that this data may not be entirely suitable for rock engineering analysis and design partially due to the differing rock mass characterisation objectives (i.e. economic versus engineering), the subjective nature of the data and the inability to correctly account for biases.

In the current mining environment, particularly in Australia, it is becoming increasingly difficult to adequately source adequately trained personnel to conduct basic geotechnical data collection. It is therefore becoming increasingly ***important to maximise the utilisation of all available rock mass data sources***. In terms of contemporary rock mass data collection practices in metalliferous mining, this should at least involve integrating and utilising the following data sources;

- Diamond drill core logging (oriented, unoriented)
- Line and Window mapping

- Digital Photogrammetry and Laser scanning
- Geological face and backs mapping

Each of the data sources above are only capable of capturing necessary rock mass parameters to varying degrees. In this case, **reliance on one data collection method alone may not necessarily provide all of the required rock mass information**. In addition, data may have specific biases that may need to be treated, depending on the data method employed. It is therefore essential that, in the formulation of any discontinuity data collection programme, **there is a thorough understanding of the limitations and biases of each sampling technique** and how it impacts on subsequent rock mass characterisation studies. In order to maximise utilisation of the collected rock mass data by various mine staff, it should be **organised and stored in an accessible format that enables sharing of information**. In this way, staff members from various disciplines can access and evaluate all information and potentially avoid duplication of rock mass data collection efforts.

In order to overcome some of the issues concerning rock mass characterisation and its application in mine excavation design, a number of areas for further development have been recognised;

- There is a need to develop efficient, semi-automatic data collection and analysis methods to ensure that data are captured in a reliable, time and cost effective manner.
- Development of a standardised methodology for correct statistical treatment of biases and analysis of geometric discontinuity parameters (i.e. spacing, persistence and orientation) which directly based on the adopted sampling technique. This is particularly relevant for 3-dimensional remote data collection methods, such as photogrammetry and laser scanning technologies where it is uncertain whether current 2-dimensional bias correction approaches are applicable (see Appendix A).
- Development of a rock mass characterisation data management framework that allows for spatial data analysis and complex multivariate analysis techniques. The data management framework should be capable of extraction and preparation of digital rock mass data from various data sources based on a number of queries.

CHAPTER 4 - A REVIEW OF EMPIRICAL METHODS IN OPEN STOPE MINE DESIGN

4.1 INTRODUCTION

Rock mass classifications and empirical methods have been utilised in design of rock engineering structures, such as open stopes, for well over 25 years. The use of these methods do appear superficially attractive, because of their apparent ease of use and wide range of application, however they have a number of serious shortcoming and must be used only with extreme care (Brady and Brown, 2004). Rock mass classifications can be an “economical and extremely useful basis for determining properties, but there are dangers in uncritical application” (Pine and Harrison, 2003). With these cautions in mind, a review of the most common empirical methodologies utilised in the design of open stopes is presented.

4.2 ROCK MASS CLASSIFICATION SYSTEMS

Rock mass classification systems were developed as a means of evaluating the quality and expected behaviour of rock masses, by utilising experience gained on other, similar rock engineering projects (Hoek and Brown, 1980). The principal reason for the development of these systems was a need to quickly determine the potential rock mass behaviour at an early stage of project development, where typically there is limited information on the properties of the rock mass. There is a danger to rely too heavily on rock mass classifications for the detailed design of rock reinforcement and ground support, and excavation dimensioning. One author of a rock mass classification system has warned that “*Rock mass classifications are not to be taken as a substitute for engineering design. They should be applied intelligently and used in conjunction with observational and analytical studies to formulate an overall design rationale compatible with the design objectives and site geology*” (Bieniawski, 1989).

4.2.1 Engineering Applications and Objectives

A number of different rock mass classification systems have been developed over the years for a variety of specific engineering applications. Some of these applications include;

- specification of steel sets in tunnelling (Terzaghi, 1946)
- stand-up time determination (Lauffer, 1958)
- estimation of span determination and reinforcement and ground support in mining (Laubscher, 1977)
- estimation of cavability (Laubscher, 1990; Laubscher and Taylor, 1976)

- blastability (Lilly, 1986)

The engineering applications listed above may involve controlling, or exploiting, specific aspects of rock mass behaviour. For example, tunnel excavation design requires guaranteeing the stability of the rock mass and/or limiting rock mass deformations, whereas blastability aims to assess the susceptibility of the rock mass to breakage by drill and blast methods. The aims of each of these two example applications can be considered as being incompatible. It is important to note that the factors that contribute to stability may not necessarily be the same as those that make for good blastability, and vice versa.

Even for specific engineering applications, such as tunnelling, there may be a number of different objectives that drive the project. For example, one project may require the rapid completion of an auxiliary service tunnel, whereas another project may require construction of a large diameter tunnel for a dual carriage railway. Although both may represent the same engineering application, the objectives between the two projects can be quite different, as shown in Table 4.1;

Table 4.1 - Example objectives for two tunnelling projects

Auxiliary Tunnel	Rail Tunnel
Small diameter tunnelling (i.e. small-scale), low precision	Large diameter tunnelling (i.e. large-scale), high precision
Low public exposure, moderate to high risk tolerated	High public exposure, very low risk tolerated
Post-excavation displacement tolerated	Little displacement tolerated
Rapid excavation versus quality	Quality versus speed

It can be seen that the objectives of the project will influence a number of practices in the execution of the engineering project, including;

- strategy for data collection and site characterisation
- excavation methodology
- reinforcement and support methodology
- quality control requirements

In addition, site specific conditions, such as logistical constraints, labour skills and occupational health and safety laws, will also influence the practices used in execution of the project. With regard to the development of rock mass classifications, it is unclear if, or how, the various practices determined by project objectives and site specific conditions have been accounted for in the case history databases. The use of empirical data, without knowledge of

the case history project objectives, engineering practices and site conditions, may provide an outcome that is both inaccurate and imprecise for the intended objectives of the project under consideration.

One of the objectives of rock mass classifications is to assess rock mass “quality” by utilising a number of recordable observations about the site geology and site conditions which are then rated, expressed as numbers and finally combined, formulated by sum or product, into a final number (Palmstrøm and Broch, 2006). This approach appears to be superficially attractive for engineering design, as it provides for a single number, or qualitative term, to represent the complex nature of site geology, site conditions and engineering behaviour. However, it is hard to justify how a single number, or qualitative term, can be used to describe rock mass behaviour that can involve a variety of factors that influence stability, which may be represented by multitude of distinctly different failure mechanisms.

4.2.2 Classification Parameters

It must be noted that there are a number of factors that have influenced the selection, and subsequent treatment, of particular aspects of the site geology and conditions during the development of rock mass classifications. At an early stage of project development, due to time and cost constraints, not all of the geological and site condition parameters influencing engineering performance can be described in detail. In light of this, presumably the developers of rock mass classification systems were required to decide on which properties of the rock mass and site conditions were the most important in relation to the specific engineering application and design objectives, which in turn would have influenced data collection and analysis requirements. It is therefore not clear whether all of the important aspects of the rock mass that contribute to a specific rock mass behaviour have been included and properly accounted for (Windsor et al., 1995). This aspect may be a major factor that contributes to the inability of rock mass classifications to function with a high degree of accuracy and/or precision.

4.2.3 Extending Classifications for Other Applications

Because of their apparent ease of use, it would be tempting to use existing rock mass classifications for other engineering applications. In fact, this has been shown to have occurred by the multitude of extensions to existing rock mass classification systems. By using existing classification systems as the basis for new extended applications, a risk exists where the existing parameters, and their respective weightings, may have little relevance to the extended application. A brief description of some issues related to some widely used rock mass classification systems is provided below.

4.2.4 RQD

One basic rock mass classification system that has been adopted and extended in other systems is *RQD* (Deere, 1964). Hutchinson and Diederichs (1996) describe the development of *RQD* "in response to the need for a quick and objective technique for estimating rock mass quality from diamond drill core logs during the initial exploratory phase of construction". The intention of this qualitative index was to be used as a "red-flag" to identify low-quality rock zones requiring further scrutiny (Bieniawski, 1989). *RQD* has become a de facto standard for assessing discontinuity intensity, however, its inclusion in the NGI *Q*-system (as well as other rock mass classification systems) has never been thoroughly explained. Figure 4.1 shows that *RQD*, with a threshold value of 0.1m (as proposed by Deere et al, 1967), is almost completely insensitive after discontinuity spacings greater than 0.3m. However, due to the scale of excavations in large-scale mining, such as open pit slopes, open stoping or caving, discontinuity intensities that may control stability may be beyond the sensitivity afforded by *RQD*. Indeed, the choice of a 100mm threshold level reduces the ability of *RQD* to give meaningful results as the scale increases (Mostyn and Douglas, 2000). For excavations greater than several tens of metres, *RQD* has questionable value. For example, back analysis of stope performance of large open stopes at Mount Charlotte Gold Mine (mean spans of 49m) showed quite varied rock mass responses, however, in all most all cases (99%) ground conditions are typified by *RQD*'s of 100% (Ullah, 1997).

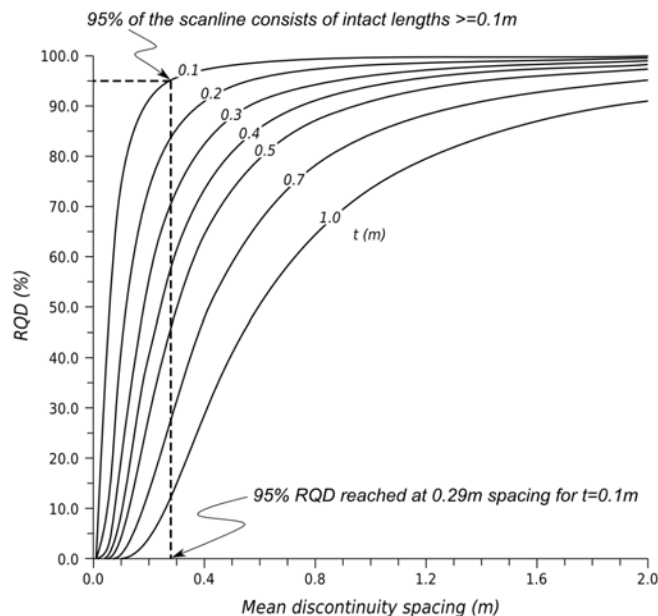


Figure 4.1 - Variation of theoretical *RQD* with mean discontinuity spacing for a range of threshold values (after Priest and Hudson, 1976)

4.2.5 NGI - Q Rock Mass Classification System

The NGI (Norwegian Geotechnical Institute) *Q*-system was developed by Barton et al (1974). This rock mass classification system was developed to provide guidelines on rock reinforcement and ground support requirements for hard rock tunnelling and underground excavation design. The system was based on a large number of civil engineering underground tunnel and construction projects, principally at relatively shallow depths in Sweden and Norway (Barton, 1988). The system involves calculation of a rating (*Q*), also termed Rock Tunnelling Index, based on a number of engineering geology and site parameters, and using this rating to select appropriate rock reinforcement and support requirements based on the excavation span and intended purpose. The *Q*-system has gained wide acceptance in the civil engineering and mining industries, however, there are some serious shortcomings of the system that must be fully understood before uncritically applying this classification system in engineering design. The main issues stem from the choice of parameters included, how they have been collected and rated, and the relative importance between parameters and their perceived contribution on rock mass quality and behaviour;

- Joint set number (J_n) - a parameter adjustment related to the number of joint sets present in a rock mass. In specifying the number of joint sets for J_n determination, a user of the *Q*-system may include sets identified for the specific locality, or all identified sets for a domain. The latter will obviously result in a higher joint set number. The user of the system must therefore consider the scale of the final excavation, as larger excavations will have a higher probability of intersecting more discontinuity sets.
- Joint roughness number (J_r) - an adjustment parameter related to the surface characteristics of the “critical joint set” (i.e. the set “most likely to allow failure to initiate”). There are a number of issues trying to determine this parameter from the small sample size, or area of the discontinuity, afforded by core (i.e. censoring bias) relative to the scale of open stope spans. It also requires a subjective assessment of selecting the “critical joint set”.
- Joint alteration number (J_a) - an adjustment parameter related to the joint alteration and infill characteristics and joint geometry configuration of the “critical joint set”. Without having a detailed understanding of joint waviness and amplitude, as well as a presumption of the shearing direction and conditions (such as normal load applied), it would be difficult to make an assessment of which category to select, especially using core.
- Joint water reduction factor (J_w) - an adjustment parameter related to generic qualitative descriptions from only six different cases, based on a limited range of

water pressures and water inflows.

- Stress reduction factor (*SRF*) - an adjustment parameter related to the general stress conditions. The prescriptive guidelines may only be applicable for some excavation geometries, for example, “circular” openings sub-perpendicular to major and minor stresses. Interpretations need to be made for larger, rectangular opening oriented at other directions. The *SRF* can influence the resulting *Q*-System rating by up to 2 orders of magnitude and is based, largely, on qualitative assessments and, where qualitative assessments are provided, they only apply under a restrictive set of conditions.

Due to the serious shortcomings of this system, it is concurred that this classification system “only be used for general use in the preliminary design of underground excavations” (Hoek and Brown, 1980).

4.3 GEOLOGICAL STRENGTH INDEX

The Geological Strength Index, or *GSI* (Hoek, 1994), was developed for the determination of a number of parameters in the Generalised Hoek-Brown rock mass failure criterion (Hoek et al., 1995; Hoek et al., 1992). The need to develop the *GSI*, was based on the perceived difficulty in applying the *RMR* system to very poor quality rock masses. In addition, it was felt by Hoek (1994), that a rock mass strength system needed to be developed based more heavily “*on fundamental geological observations and less on 'numbers'*”. It is considered that the application of the *GSI* involves even more subjectivity and simplification than either *RMR* or the *Q*-System, which at least attempt to *quantify* certain discontinuity characteristics.

There are a number of limitations to applying the Hoek-Brown failure criterion, mainly due to scale and isotropy issues. It is recommended that the failure criterion be used where there are “*sufficient number of closely spaced discontinuities that isotropic behaviour involving failure on discontinuities can be assumed*” (Hoek and Brown, 1997). In this regard, at least four discontinuity sets have been suggested (Hoek, 1988) to obtain “isotropic” conditions, and that “closely spaced” should be defined in terms of the scale of the potential failure surface that could develop through the rock mass (Mostyn and Douglas, 2000). The limitations placed on the Hoek-Brown failure criterion have a number of ramifications when assessing and utilising *GSI* for rock mass strength estimation.

It is not clear how scale is directly incorporated into the *GSI* method. It is therefore up to the user to decide what scale, degree of isotropy and “blockiness” the diagrams represent with

respect to the scale of excavation. Figure 4.2 attempts to place the *GSI* in context with the limitations of the Hoek-Brown failure criterion. It can be seen that the range of potential *GSI* values should be assessed with respect to the range of applicable scales and degrees of isotropy for the Hoek-Brown failure criterion, which, as Figure 4.2 suggests, are at least on the same scale of the excavation. Indeed, from a data collection perspective, a paradox may exist where the size of the excavation, and hence scale of potential failure surface, is an unknown and the *GSI* can only be assessed at the scale of an exploratory excavation exposure. Furthermore, the rock mass may be divided into a number of units/domains of varying “blockiness” and isotropy, each providing significantly differing *GSI* values at the mapping scale. The task for the design engineer therefore is to assess the engineering design scale and estimate the most likely *GSI* for design based on the various mapping scale *GSI* values.

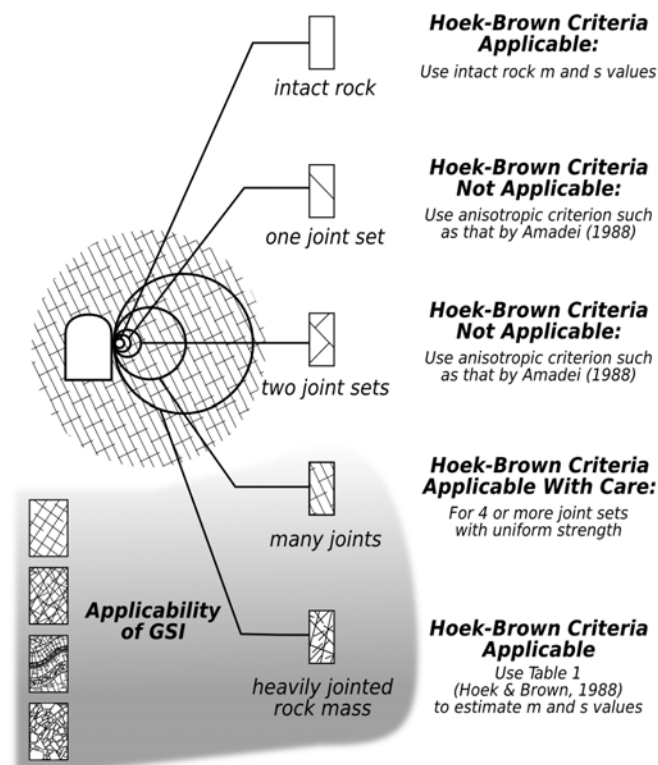


Figure 4.2 - Range of applicability of *GSI* with respect to scale limitations of Hoek-Brown failure criterion (modified from Hoek and Brown, 1997)

An assumption of the Hoek-Brown failure criterion is “isotropic behaviour involving failure on discontinuities”. This indicates that the criterion is strictly only applicable to domains with isotropic discontinuity orientations, or as suggested by Hoek and Brown (1988), with four or more sets. There are some novel guidelines to classify the degree of rock mass orientation isotropy, based on the percentage area of 1% pole concentration and the maximum pole concentration from stereographic projections (Read et al., 2003). Read et al (2003) also devise a methodology to modify the Hoek-Brown criterion in anisotropic or rock masses with

moderately regular discontinuity patterns. This process involves identifying the orientation of concentrations of poles to discontinuities, as well as lines of intersection of discontinuities, and utilising an anisotropic criterion, such as using the discontinuity shear strength, where the potential failure surface lies sub-parallel to these orientations.

4.4 EMPIRICAL OPEN STOPE SPAN STABILITY GRAPH METHODS

A number of empirical open stope span design methodologies have been devised over a number of years (Mathews et al., 1981; Potvin, 1988) to assist in the preliminary dimensioning of open stope spans and to provide preliminary guidelines for rock reinforcement requirements. The evolution of empirical open stope span design methods from basic classifications is concisely summarised in Figure 4.3, together with some recent site specific applications in the Australian mining industry.

Empirical open stope span design methods fundamentally rely on categorising the performance of open stope span case histories, and relating this to the size/shape of particular excavation surface and the perceived rock mass quality and conditions that control stability of that surface. These empirical open stope span design methodologies are based on extensions to existing rock mass classification systems, and as such, include and sometimes even exacerbate the limitations and biases of the original classification systems. Indeed, some of the extensions to these systems have introduced a number of additional parameters which were intended to overcome the limitations of the latter in their applicability to the design of large-scale openings. However, some of these additional parameters themselves have their own limitations and biases that need to be addressed.

As we have seen with rock mass classifications, there are a number of aspects, regarding the original case history databases, that have directly influenced the development, limitations and applicability of these systems. It is therefore important to understand the influence of the case history database on the development of empirical stope span design methodologies. A review of some of these methodologies was undertaken to highlight these aspects. The review has concentrated on systems based on the *Q*-system, mainly due to its relative wide acceptance in the mining industry.

4.4.1 Mathews Stability Graph Method

Mathews et al (1981) describe classifying stope span performance based on qualitative descriptions based on 47 open stope case studies. The main aim of the study was to “determine whether an empirical relationship existed between rock mass properties, mining depth and maximum stable open stope spans” (Mathews et al., 1981). This study reviewed

the existing rock mass classification systems of the time and assessed their applicability to the design of open stopes.

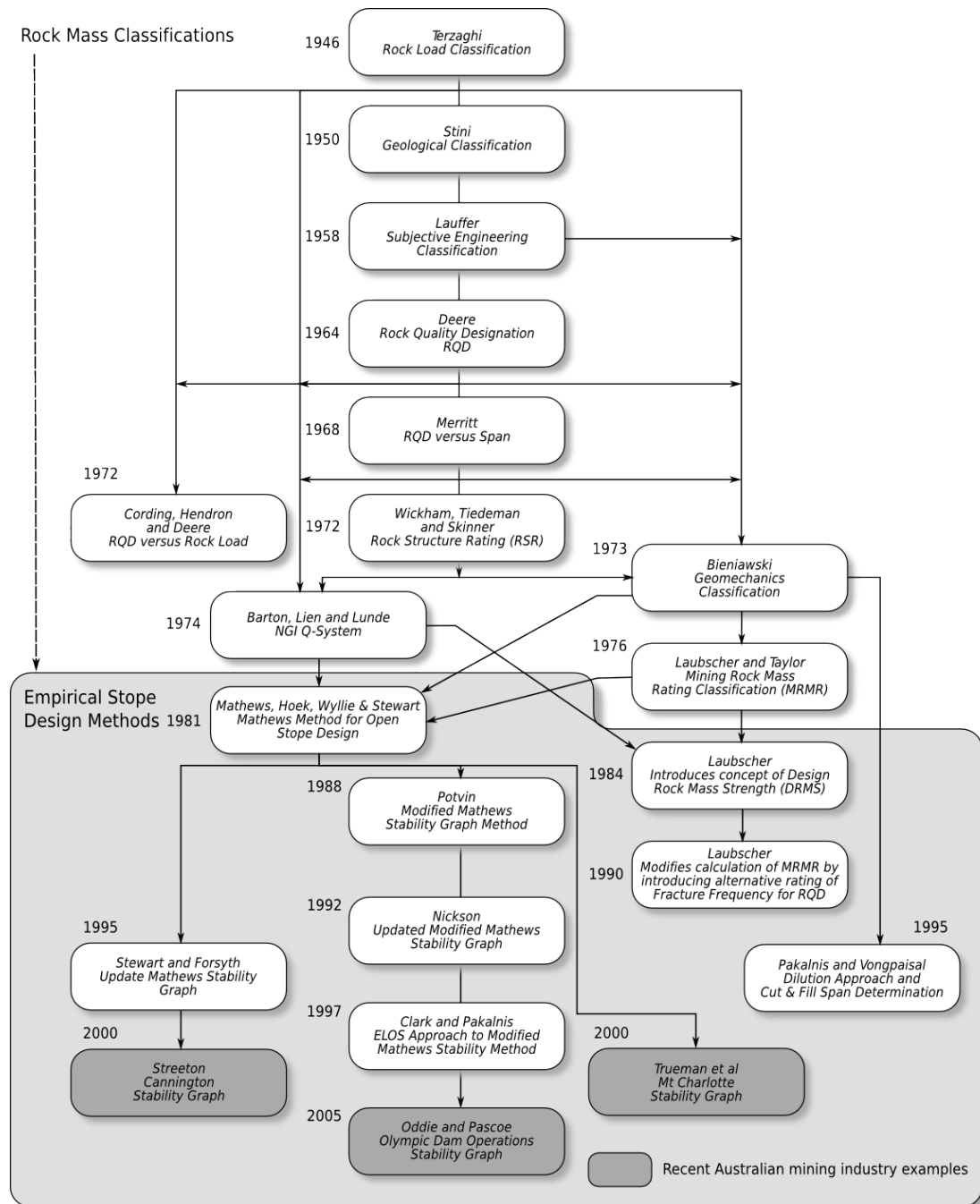


Figure 4.3 - Summary of the chronology of some rock mass classifications and empirical open stope span design methods (modified from Stewart and Forsyth, 1995)

Their review was reasonably comprehensive and considered a number of classification systems (Barton et al., 1974; Bieniawski, 1973; Deere, 1964; Laubscher and Taylor, 1976; Lauffer, 1958; Patching and Coates, 1968; Terzaghi, 1946), as well as their potential application to open stope design. Although the authors found some limitations and shortcomings with the NGI Q Rock Tunnelling Index, they decided to utilise this system as

the basis for a new extended application in the design of open stope spans. The decision was based “mainly on the background and experience of the authors” and does not suggest that NGI Q -system is superior to Bieniawski's (1973) Geomechanics Classification system. The extension of the NGI Q -system included modifications and additions in an attempt to overcome these limitations;

- “modifications to the stress reduction factor to permit the assessment of the ratio of intact rock strength to induced stress acting parallel to the exposed surface”
- “incorporation of additional features to reflect the effects of persistent structure paralleling or intersecting exposed surfaces and unfavourable inclination of those surfaces”

The NGI Q index was firstly modified by arbitrarily setting the SRF and J_w quotients to unity, with this new index termed Modified NGI Rock Mass Rating Q' . This modified index Q' was intended to “account for the rock mass strength and structure only”, without the influence of boundary conditions (i.e. stress and groundwater). The new modified Q' value, together with the new adjustments and modifications was termed Stability Number (N), defined as follows;

$$N = Q' \times A \times B \times C \quad (4.1)$$

where Q' is the modified NGI Q Rock Tunnelling Index, A is the rock stress factor, B is the rock defect orientation factor and C is the design surface orientation factor.

Rock Stress Factor (A)

The rock stress factor (A), was intended to replace the SRF term in the NGI Q -system with a more robust measure of the ratio of intact rock strength to the induced stress (parallel to the excavation surface). The rock stress factor diagram is shown in Figure 4.4. The authors suggest that stress controlled instability will occur as the ratio of intact rock strength to induced (compressive) stress approaches unity. For this case, they chose to set the rock stress factor (A) to zero. Conversely, the authors suggest that stress controlled instability should not occur where the ratio of intact rock strength to induced stress exceeds 10. The authors reason that above this ratio, stress controlled failure of rock bridges (i.e. intact rock between discontinuities) should not occur, and any failure that should occur would be related to movement along defined structure and in this case the rock stress factor should be set to 1.0. It is then postulated that stress and structurally controlled failure modes can occur between these two levels, and a straight line relationship between these extremes has been assumed. In addition, from the authors' experience, where the induced stress to intact rock strength ratio is less than 2.0, it is considered that potential problems should be flagged and the rock stress factor (A) should be set to zero. Where induced stresses are tensile, the authors suggest that “block fallout by gravity will be the condition of failure”. In this case stress factor (A) will be set to one, as it is assumed to be a structurally controlled failure and

not stress driven. No consideration has been given to the role of confining stress on rock mass damage and/or failure, or its influence on block instability.

For the practical determination of rock stress factor (*A*), the authors provide a series of charts in order to assist the user with estimating the induced stresses at the midpoint on vertical and horizontal planes for end walls and backs, and for hangingwalls and footwalls. The charts are based on providing stress concentration factors for various in situ principal stress ratios and excavation dimension ratios. It is unclear why the authors have chosen the induced stresses at the mid-point of the wall as being important in controlling the potential for stress induced failure. Depending on the configuration of boundary stresses, for typical stope surfaces, it may well be that it is the stress concentrations in stope corners that ultimately control the potential for stress induced failure. The user of the system is then required to select the lowest resulting rock stress factor (*A*) for each surface.

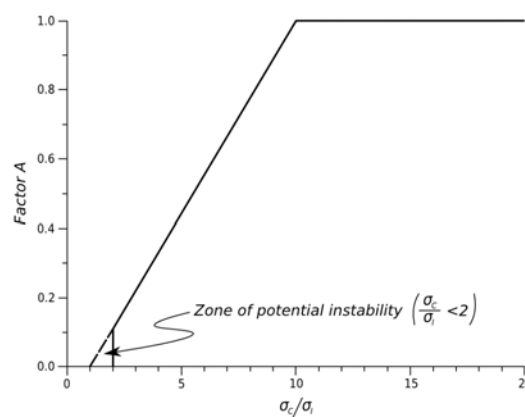


Figure 4.4 - Rock Stress Factor (*A*) (after Mathews et al, 1981)

Rock Defect Orientation Factor (*B*)

The purpose of this adjustment factor is to “account for the presence of persistent discontinuities paralleling or intersecting exposed surfaces” (Mathews et al., 1981). This factor ranges from 0.3 to 1.0 for discontinuities angled from 20 degrees to 90 degrees with respect to the exposed surface, respectively. This factor should also be set to 0.5 where the discontinuity parallels the excavation surface. The authors also recommend utilising stereographic projections to ascertain the acute angle between the “persistent set” and the design surface. The rock defect orientation factor (*B*) should be applied to the most persistent set of fractures, “based on relative spacing and continuity”. It must be noted that, without spacing and continuity data, a user may be tempted to select the discontinuity set that provides the lowest corresponding factor *B* value, however, the authors note that the intent of the rock orientation factor is to assess overall stability, and accept that some “block fallout or spalling” may occur. It must be noted that the likelihood of “block fallout” is also

dependent of the existence, orientation, and persistence of additional discontinuities, which is not accounted for here.

Design Surface Orientation Factor (C)

The purpose for this factor is to account for the de-stabilising influence of gravity and relies on the assumption that stope backs or roofs are inherently less stable than sidewalls. The authors justify the rating of this parameter by using suggestions provided by Barton et al (1974) that “rock quality in a wall is hypothetically improved 5 times compared to a roof”. The authors have also adopted Barton et al's (1974) “*ESR*” term, which represents a safety factor for “permanent mine openings”. The authors reason that a vertical wall should be “at least $5 \times 1.6 = 8$ times as stable as a horizontal roof”. The authors recommend a range of factor (C) of 1.0 to 8.0 for horizontal and vertical surfaces, respectively. They also provide the following formula for evaluating factor (C);

$$\text{Factor } C = 8 - 7 \cos(\text{Angle of dip}) \quad (4.2)$$

As the authors have adopted Barton et al's (1974) *ESR* term, it is unclear why they have not made the lowest value 1.6 for the horizontal roof. It is also unclear why they have classified an open stope as a permanent mine opening, rather than a temporary mine opening.

Shape Factor (S)

Mathews et al (1981) highlighted that the shape of an opening influences its stability. They classify tunnels being “one way spanning” openings, as their length is very long compared to their width (i.e. length:width ratios greater than 4:1) and stope surfaces classified as “two way spanning” openings. In order to account for this shape relationship, they utilised a term called Shape Factor (S);

$$S = \frac{\text{Design surface area}}{\text{Design surface perimeter}} \quad (4.3)$$

The Shape Factor (S) was used to “account for the shape and size of the opening”. This measure was adopted from Laubscher and Taylor's (1976) “hydraulic radius” term, which was originally used “only as a guide” to define the undercut area required to initiate caving.

Stability Chart

The authors of this method then postulated that the stability of exposed stope surfaces from their case history database could be assessed empirically by plotting the stability number (N) against the Shape Factor (S). The resulting data is shown in Figure 4.5. The authors decided to plot the Stability Number (N) on a log scale in keeping with Barton et al's (1974) presentation of the Q Rock Tunnelling Index. It is interesting to note that whilst Barton et al (1974) consider span to be a function of “rock mass quality” in their charts, Mathews et al

(1981) plot the stability number (N) (the dependent variable) against the Shape Factor (S).

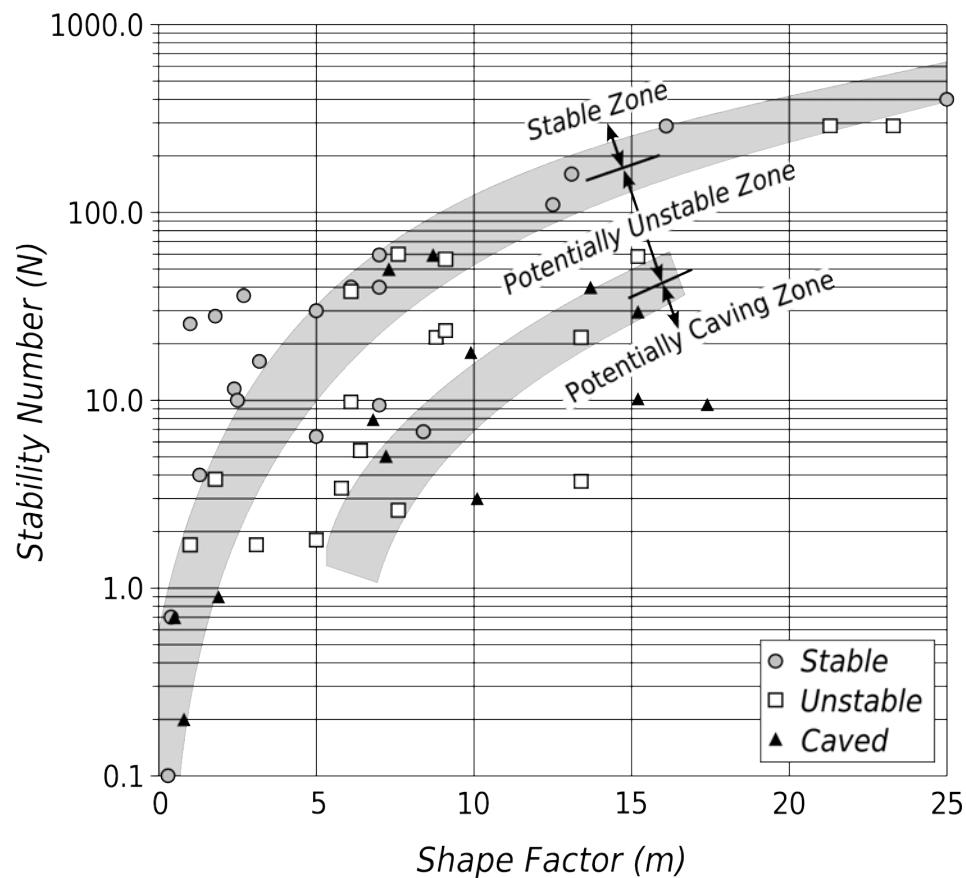


Figure 4.5 - Mathews stability chart with data points and stability zones (modified after Mathews et al, 1981)

The definitions of “stability” provided by the authors are as follows;

- **Stable:** The excavation will stand unsupported with occasional localised ground support to control slabbing
- **Unstable:** The excavation will experience some localised caving but will tend to form a stable arch. Open stoping is feasible if localised caving can be prevented by modifying extraction sequence, installing cable bolts, etc.
- **Caving:** The excavation will cave and will not stabilise until the void is full

It is considered that the three definitions of “stability” listed above cover the entire range of performance expected to be encountered in open stoping operations. The “caving” condition in *SLOS* mining method is one to be avoided at all costs. The definition of “unstable” here also represents an extremely undesirable condition in open stope mining. It is considered that this definition would potentially result in significant amounts of dilution, leading to closure of the stope, compromise grade and production rates and has the potential to seriously affect stability of neighbouring stopes. It must be highlighted that the definitions of “stable” and “unstable” do not lend themselves to providing any additional degree of

resolution between “acceptable” and “unacceptable” performance. The authors then utilised the data points plotting on the stability chart to define “stability” zones. Three zones were identified; “stable zone”, “potentially unstable zone” and “potentially caving zone”. These zones were delineated by reasonably broad grey or shaded boundaries. The following conclusions are made from analysis of the chart data;

- an absence of “stable” points plotting in the “potentially caving zone”
- an absence of “caved” points plotting in the “stable zone”
- “unstable” data points are randomly distributed between the “stable zone” and “potentially caving zone”

The authors concluded that the method defining stability zones based on the rock mass quality and shape factor are conceptually sound, however insufficient data were collected to confirm this. This is perhaps reflected in their decision to use broad boundaries to highlight the low level of confidence in defining these three zones.

The authors attempted to account for the limitations of *Q*-system, by introducing new parameters to account for additional factors such as joint orientation, design surface orientation and for the influence of intact strength and induced stress. Although the inclusion of these new parameters does have some merit, and perhaps offer some improvement to the *Q*-system, there still are concerns regarding these new parameters. The main criticisms include;

- influence of orientation and persistence of more than one joint set
- assumption of linear relationship between the ratio of maximum induced stress and intact rock strength to rock mass damage
- poor treatment of the role of tensile or confining stresses

Doubts also exist regarding the justification for the rating, and therefore relative influence, of each of these new parameters. In addition, the method does not account for any previous stress or blast induced rock mass damage.

It is concluded that, as a proof of concept, this work has shown that a weak empirical relationship may exist between rock mass properties and maximum stable open stope spans. The authors state that the relationship developed is only applicable for single, isolated openings, and advise that numerical modelling should be undertaken to assess the influence of induced stress from multiple and adjacent openings. The aim of the research was to predict stable excavations below 1000m, however, considering the reliability and precision of the results, it is considered that this aim was not achieved. It is also interesting

to note that all the case histories used in the study were taken from mines where depths did not exceed 675m below surface.

4.4.2 Modified Stability Graph Method

The Modified Mathews Stability Graph method for open stope design (Potvin, 1988) is essentially an extension to the original work done by Mathews et al (1981). This study substantial increases to the case history database (249 case histories) and makes a number of modifications to Mathews et al's (1981) parameters. A summary of the main points is as follows;

- Modification to the Rock Stress Factor (*A*)
- Modification to the Rock Defect Orientation Factor (*B*)
- Modification to the assessment of Design Surface Orientation Factor (*C*)
- Termed resulting new classification as Modified Stability Number (*N'*)
- Substantial increase in the case history database (176 unsupported and 73 supported)
- Separation of data with respect to supported and unsupported cases

Modifications To Rock Stress Factor (*A*)

Potvin (1988) recommends that where the ratio of intact rock uniaxial compressive strength to maximum induced stress is less than 2.0, the Rock Stress Factor (*A*) be set to 0.1, rather than zero, as proposed by Mathews et al (1981). As pointed out by Nickson (1992), Potvin (1988) proposes that the lower bound for the stress factor be kept at 0.1, based on the observation that “several highly stressed backs that remained stable due to their *small size*”. This observation may be understandable where the geometrical arrangement with respect to the stress tensor may provide a confining effect on damaged or yielded rock mass, or rock wedges. However, this will not necessarily always be the case, as it is dependant on the actual arrangement of;

- the geometry of all surfaces of the excavation (including scale)
- geometry and characteristics of all discontinuities
- ratio, magnitude and direction of all components of the stress tensor

It is considered that this argument cannot be justified for complete generic use. It must be noted that the modified Stress Factor (*A*) still assumes a linear relationship between the ratio of maximum induced stress and intact rock strength to rock mass damage, where this ratio is greater than 2.0. There also is still no mechanism to account for the role of confining and/or tensile stress on stability with this modified Stress Factor (*A*).

Modifications To Rock Defect Orientation Factor (B)

Potvin (1988) made some adjustments to the rather simplistic treatment of rock defect orientation as provided by Mathews et al (1981). The modifications include a name change to "Joint Orientation Factor" and the introduction of the "critical joint" concept, which represents the joint set "most likely to detract from the stability of a particular surface". Potvin (1988) considers that the least favourable condition for stability is where the angle between this set and the design surface is between ten and thirty degrees. It is assumed that, between this angular range, the chance of failure of the rock bridge between the joint and excavation surface is increased. The method for determining the Joint Orientation Adjustment Factor (*B*) includes a chart for considering both the strike and dip of the "critical joint" with respect to the stope surface. No consideration is given to the role of other discontinuity sets on stability.

Modifications To Gravity Adjustment Factor (C)

Potvin (1988) modifies the name of the "Orientation of Design Surface Factor" to "Gravity Adjustment Factor". He also identifies five "modes" of failure encountered in open stoping;

- gravity fall
- slabbing
- buckling
- sliding
- shearing

Potvin (1988) considers that these modes can be reduced by eliminating buckling and shearing, which he considers as stress driven failures and therefore accounted for by the Stress Factor (*A*). This leaves three gravity driven modes; gravity falls, slabbing and sliding, which are taken into account by the Gravity Adjustment Factor (*C*).

Modified Stability Number (N')

In order to avoid confusion with Mathews et al's (1981) Stability Number (*N*), Potvin combines his modified adjustments, in a similar way to his predecessors, and terms this the Modified Stability Number (*N'*).

Case Histories

A major improvement over the original stability graph method was the inclusion of 176 unsupported and 73 supported case histories. These are predominantly from 34 Canadian hard rock underground mines and from literature. The biggest improvement over the original

stability graph method was the separation and individual treatment of unsupported and supported case histories. The unsupported case histories were divided into a main database (84 case histories collected from mines) and a complimentary database consisting of 92 case histories from literature, with the latter involving some degree of uncertainty in determining one or more of the component parameters. Potvin (1988) utilised the main database to develop his unsupported stability graph, and utilised the complimentary database only for confirmation. Potvin (1988) utilised 66 supported case histories consisting of cable reinforced (most dominant type of support), rebar reinforced and cable-plus-rebar reinforced surfaces. The case histories consisted predominantly of backs where, due to the mining method employed, the reinforcement was installed evenly across the entire stope surface.

Stability Graphs

A similar approach to Mathews et al (1981) was made in plotting data points on a stability chart, however, the Modified Stability Number (N') was plotted against "Hydraulic Radius" (HR) rather than the term Shape Factor (S). It must be noted that the definitions of stability have changed from the original approach;

- **Stable:** "low" amounts of dilution
- **Unstable:** Experienced dilution and ground-falls causing operational problems. Unravelling between cables.
- **Caved:** This term was not adequately defined, however Potvin (1988) offers "Severe ground control problems, Support system failure"

On the basis of the unsupported data, new "stability zones" were developed as shown in Figure 4.6. This consisted of firstly of defining a "caved zone", which is assumed to be similar to Mathews et al's (1981) "potentially caving zone". One must note that the new terminology used implies that behaviour within this zone can be predicted with more certainty or reliability. The new stability chart also introduces a new zone termed "transition zone" between the "caved zone" and "stable zone". It implies that within this region stopes are neither completely "stable" nor "caved", and should predominantly contain "unstable" case histories. The last modification sees a narrowing between the "stable zone" and "caved zone", also implying an increase in precision over Mathews et al (1981). It is considered that, based on the spread of unsupported data points, and the overlap of "stable" and "caved" data points, it is difficult to justify the positioning of these "design lines".

From a practical mining perspective, it is difficult to understand the positioning of some the data points on the stability chart. The scatter in the stable zone is understandable, as this may represent a number of conservative design configurations necessary by the mine operators. For example, conservative stopes could represent extraction of small stopes on

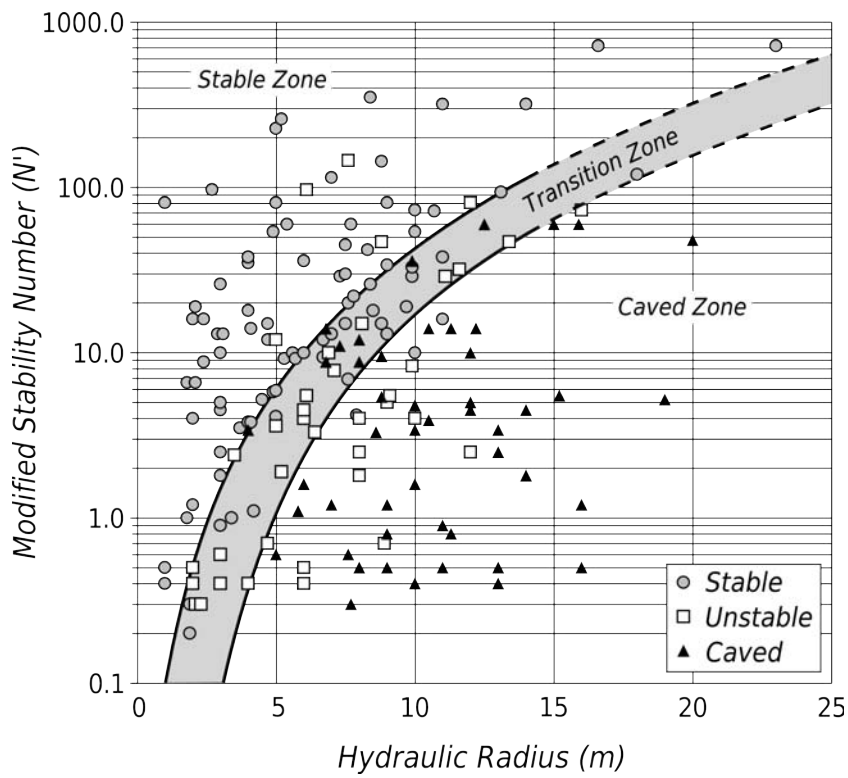


Figure 4.6 - Unsupported Modified Stability Graph (after Potvin, 1988)

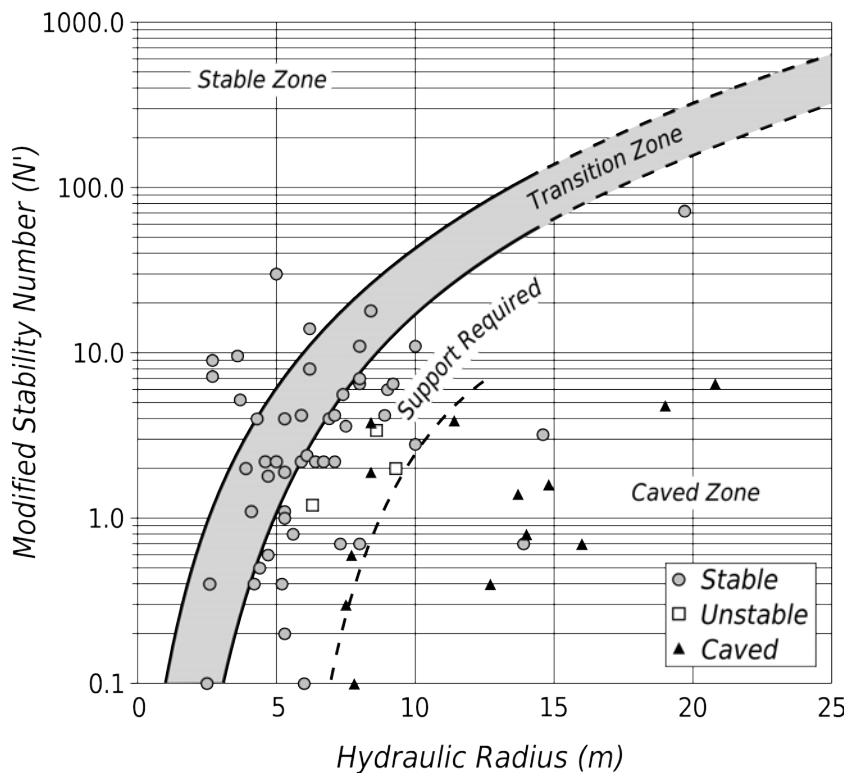


Figure 4.7 - Supported Modified Stability Graph (after Potvin, 1988)

the ore reserve abutments. However, the scatter in the “caved” data points is unintuitive. Intuitively, when a slope is progressively mined (i.e. in sub-levels or along strike ring firing) mine operators will tend to stop production and place a pillar to decrease potential rock mass instability and limit dilution. This would indicate that, if the stability graph is a realistic representation, the majority of “caved” points should lie just immediately to right of this line. Even if stopes were mined as a series of “mass blasts”, mine operators should quickly realise the optimal stope dimensions, and the scatter should therefore not be as severe as depicted in Figure 4.6.

As an example, consider a N' value of, say, 0.5 (i.e. very poor quality) and a sub-level interval of around 25m, the size of a stope plotting in the stable region can be progressively increased until it reaches an “unstable” configuration with a HR of around 5 (i.e. immediately to the right of the “transition-caved” line). This would equate to a maximum stope strike length of around 17m. Given that the last “caved” data point shown in Figure 4.6 has a N' of 5, it would appear incredulous why a mine operator would, and more importantly could, extend the strike of the stope in such poor ground conditions to a HR of in excess of 15. A Hydraulic Radius of 15, for a 25m sub-level interval, represents an “infinite” strike length, which is truly not plausible in such apparently poor ground conditions. The most plausible explanation for the scatter of the “caved” data points is an incorrect calculation of the modified stability number (N'), and that the data point should plot much higher on the y-axis, and therefore closer to “transition-caved” zone. This scatter may suggest that the weighting system used in the Q-System - Modified Stability Number (N') may be the cause of this erroneous downgrading of rock mass quality.

For the supported case history database, a region below the unsupported “transition zone” was identified where supported case histories remained stable. This region is highlighted by the dashed line in Figure 4.7. In this case, it was postulated that this region can be utilised for the design of cable bolt reinforced stopes. Indeed, the data does show that “stable” supported surfaces (mainly backs) occur with higher Hydraulic Radius values and lower Modified Stability Numbers than do the unsupported case histories. The same issues with regard to excessive scatter in “caved” points is also apparent in the supported database.

Potvin (1988) also provides a design chart to estimate the required cable bolt density for *stope backs* in order to maintain stability. This design chart utilises cable bolt density versus $(RQD/J_n)/HR$. The explanation provided for the latter term is to account for the “relative block size” and increased span. Given the questionable nature of the “relative block size” quotient, the validity of this latter term is also in doubt. Further updates to the chart were done

(Potvin and Milne, 1992), which included 30 new case histories, however the new data did not alter the positioning of the cable bolt density design lines. The authors stress that this empirical method is only suitable for stope surfaces which are fully covered by the cable bolting pattern, making it unusable for most cases of hangingwall design.

The Modified Stability Graph Method essentially extended the work of Mathews et al (1981) by including more case histories, plus a number of modifications to each of the adjustment parameters. Pakalnis et al (1995) notes that the reason for the Modified Stability Graph Method's wide acceptance in the mining industry was primarily because the increase the case history database and the modifications made by Potvin (1988). One improvement over the original method was Potvin's (1988) attempt to provide cable bolt design guidelines for open stopes. However, the suggested guidelines were only applicable to stope backs having a uniform pattern of cables over the entire surface. This practice of uniform pattern cable bolting is restricted to open stoping methods employed in Canada in the late 1980's. Typically, as is the case in most Australian underground mines, access limitations and mining layouts may prohibit the use of such an approach.

4.4.3 Nickson (1992)

Nickson (1992) expanded the Modified Stability Graph Method by inclusion of an additional 13 unsupported and 46 supported case histories, from Western Canada, the United States and Ireland. This work presents revised design guidelines for cable reinforcement of stope surfaces for evenly distributed cable patterns and develops an initial approach for point anchor design of cable reinforcement for hangingwall surfaces. In development of stability graphs it was recognised that the division of "stability" zones in the previous work was done by visually assigning boundaries (Nickson, 1992). Rather than rely on a subjective technique, Nickson (1992) utilises discriminant analysis (based on Mahalanobis distance) in order to provide a statistical basis to the design lines. Due to excessive variance, the "unstable" case histories were not included. Three cases were investigated;

- Stable-Caved for unsupported cases histories
- Stable-Caved for supported case histories
- Stable-Caved for supported backs case histories

The results of the statistical analysis show that the division line between Stable and Caved case histories compares reasonably well with Potvin's (1988) "transition" line, and can be expressed mathematically as follows;

$$HR = 10^{(0.573 + 0.338 \log N')} \quad (4.4)$$

Nickson (1992) also found that there was no statistical significance to Potvin's (1988) cable

bolt density design guidelines based on $RQD/J_n/HR$. The study also re-investigated the proposed relationship between cable bolt length and hydraulic radius (Potvin and Hudyma, 1989) using the updated database, however, a very low correlation was found ($r^2=0.245$).

4.4.4 Stewart and Forsyth (1995)

This paper briefly reviews the historical evolution of rock mass classification systems and the empirical stability graph methods. The paper emphasises that, with particular reference to stability graph techniques, that they represent non-rigorous design methods and must be recognised as such. The authors consider that the modifications proposed by Potvin (1988) “*appear to be lending too great a sophistication to the method and may be leading less experienced users into falling into the trap of a 'false feeling of adequacy of design procedures'*”. In addition, the authors consider that the division of design lines by Potvin (1988) imply a degree of accuracy that cannot be warranted. The authors consider that, based on their experience, the narrow zone provided by Potvin (1988) does not accurately represent a realistic transition from “stable” to “caved” conditions.

Stewart and Forsyth (1995) therefore recommend that the design lines be modified into more broader zones that more accurately represent the degree of precision afforded by the empirical and non-rigorous nature of this methodology. The authors also proposed new and more precise definitions of stability than Potvin (1988). The paper also recognised that, although the method may be generally applied, the design curves provided by Potvin (1998) and Nickson (1992) are based on a biased set of data, principally from North America where case histories are typified by medium to good quality, and that very little data comes from mines with very weak or poor quality rocks and small excavation dimensions. This highlights the dangers of applying the methodology outside the range of experience, where reliability of the method is unknown.

Stewart and Forsyth (1995) also indicate that one benefit of the methodology is to “*lead the designer to examine the rock in a systematic and objective manner and logically collate local experience*”, rather than use it to directly determine stable stope surfaces from a graph. It was again highlighted that the method does not account for geological peculiarities, such as faults, folds or inclusions of weak rock, which if present “*would invalidate the method*”. In this case, it was recommended that these situations be dealt with on an individual basis, with a possible approach being to design on general rock quality conditions and provide additional reinforcement or other measures as required.

4.4.5 Recent Australian Mining Industry Experience

Because of its acceptance in the wider mining industry, the Modified Stability Graph method has been applied quite extensively in the Australian mining industry to assist in the design of open stope mining operations. However, a number of published back analysis studies using the Modified Stability Graph method in Australia have raised concerns about the accuracy and applicability of method in the Australian mining industry. The following examples have been used to illustrate some of these shortcomings.

Mount Charlotte Mine

Trueman et al (2000) present a significant back analysis database from the Mount Charlotte Mine, Kalgoorlie, Western Australia. Their database generally consists of case histories with much higher rock mass quality (i.e. higher modified stability numbers) and larger stope sizes (i.e. higher Hydraulic Radius values) compared to the Canadian database. The study attempts to test the validity of using two variants of the Mathews Stability graph, namely Potvin (1998) and recommendations used by Stewart and Forsyth (1995), using the case history database at Mount Charlotte. The study also attempted to improve the predictive capability of these techniques by providing updated design lines based on a combined Australian and Canadian case history database.

The study showed that there were no significant differences in the two variant methods and the authors concluded that the modifications made by Potvin (1988) to the calculation of Stability Number made *“no appreciable difference in the predictive capability of the technique for unsupported excavations”*. This conclusion was in general agreement with that of Stewart and Forsyth (1995). Notwithstanding this, they considered that *“there appears to be some validity in using these methods as a non-rigorous design technique”*. In addition, Trueman et al (2000) indicate that the methods appear to be *“adequate for preliminary design”*, however they also recommend that site-specific design lines be developed. With regard to developing site-specific zones of stability, Trueman et al (2000) recommend that data from at least 20 stopes (i.e. 100 stope surfaces) are collected and analysed. The study also highlighted that, for both methods, there were a significant proportion of “stable” stopes predicted as being “unstable”, as demonstrated in Figure 4.8. More importantly, from a design point of view, utilising the recommended design lines will not necessarily result in optimal stope sizes, and may well result in a significant proportion of stopes being conservative (i.e. much smaller than need be).

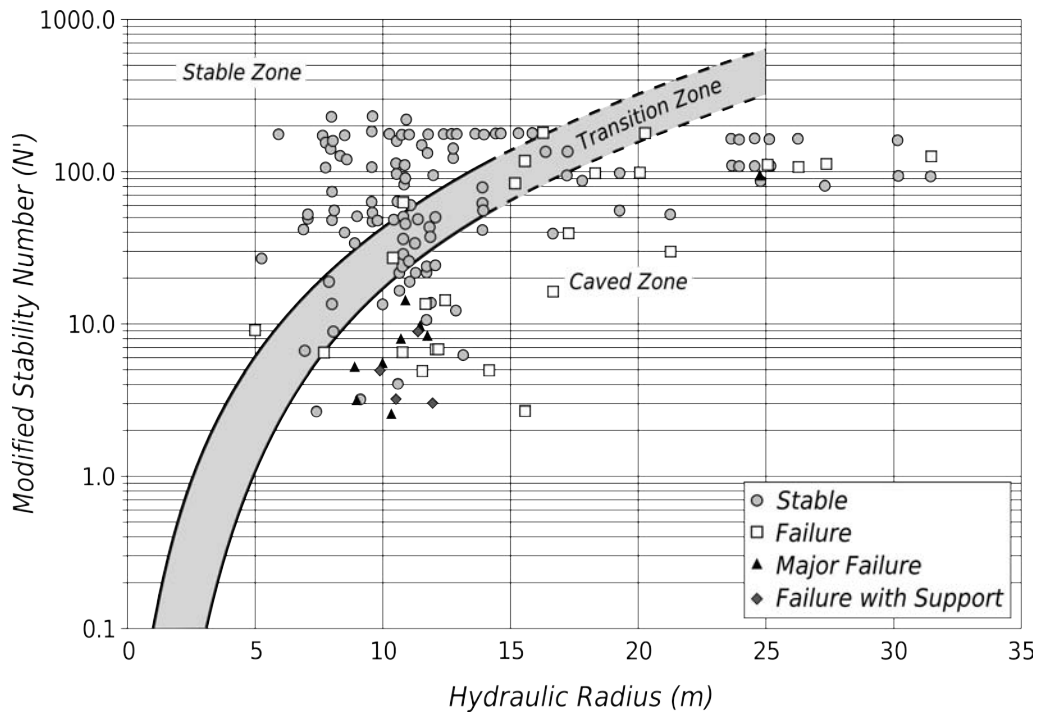


Figure 4.8 - Modified Stability Graph (Potvin, 1988) stability zones with Mount Charlotte unsupported data (after Trueman et al, 2000)

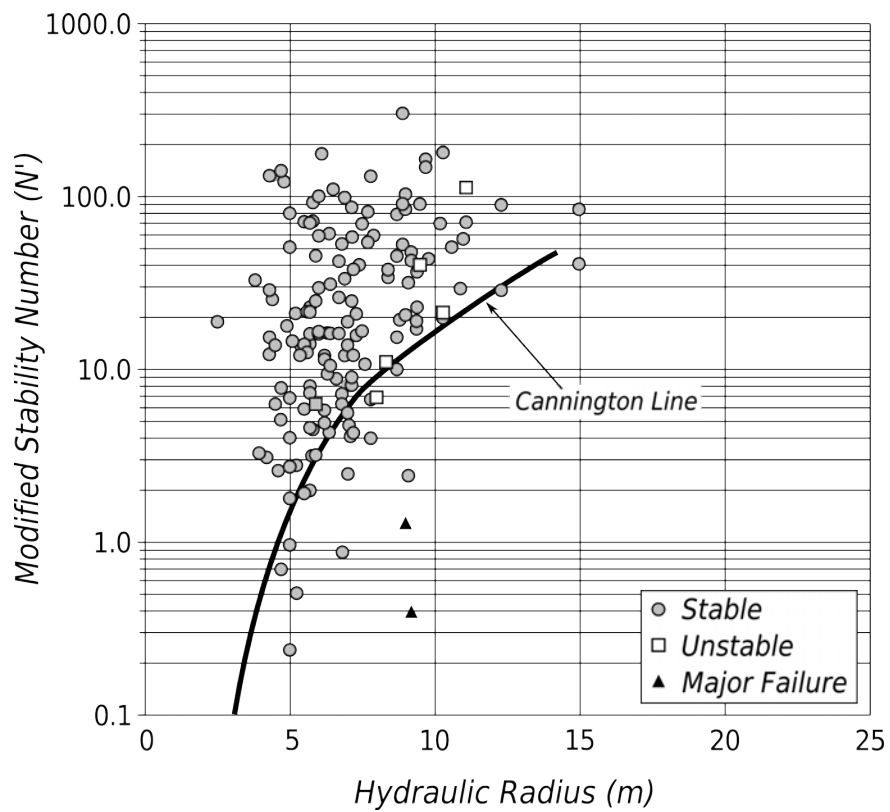


Figure 4.9 - Modified Stability Graph (Potvin, 1988) with Cannington unsupported and supported data, with the Cannington Line (after Streeton, 2000)

Cannington Mine

Streeton (2000) published some data on preliminary open stoping at Cannington Mine, Queensland, Australia, together with the general open stope design principals used at the mine. The Modified Mathews Method was utilised to conduct back analysis from around 20 stopes.

From this back analysis, Streeton (2000) proposed a design curve (named the “Cannington design line”) which closely approximates Potvin's (1988) “Transition-Caved” line, as shown in Figure 4.9. What is immediately apparent from this figure is that, although there are around 100 case histories, the database is heavily biased towards “stable” stopes. In this case, it could be argued that the stopes, up until this point in the mine's life, have been designed too conservatively and that there is room to increase spans and optimise the dimensioning of stopes. This highlights the difficulty in reliably designing future stopes with such a biased data set with few “unstable” or “major failure” stopes.

Olympic Dam Operations

Oddie and Pascoe (2005) present the results of back analysis of open stope performance at Olympic Dam Operations, South Australia, using the Modified Stability Graph Method. The back analysis method utilised the results of linear elastic numerical modelling to estimate the maximum induced tangential stress for stope wall surfaces, based on a number of primary, secondary and tertiary stope layouts. In selecting the database for the back analysis study, the authors removed case histories where the stability of the stope wall surface may have been unduly influenced by the presence of large scale geological structures. The database for subsequent analysis consisted of 460 case histories. The data were separated into supported and unsupported case histories. Figure 4.10 shows the unsupported case histories for both walls and backs. It is immediately apparent from Figure 4.10 that there a significant proportion of “stable” case studies plotting in the predicted “caved” region of the graph. Oddie and Pascoe (2005) estimated that approximately 63% of unsupported walls plotting in this region were classified as displaying “acceptable” performance. This figure highlights the highly unreliable nature of this method and its ineffectiveness to optimise unsupported stope dimensions, as it applies to Olympic Dam Operations.

4.4.6 Modifications and Extensions to the Modified Stability Graph Method

In an attempt to improve the reliability, and to overcome some of the identified shortcomings of the Modified Stability Graph Method, a number of authors have proposed extensions or modifications to the method. A review of recent literature has shown that these modifications and extensions have not been widely accepted by the mining industry to date. The following section briefly outlines some of the recent modifications and extensions.

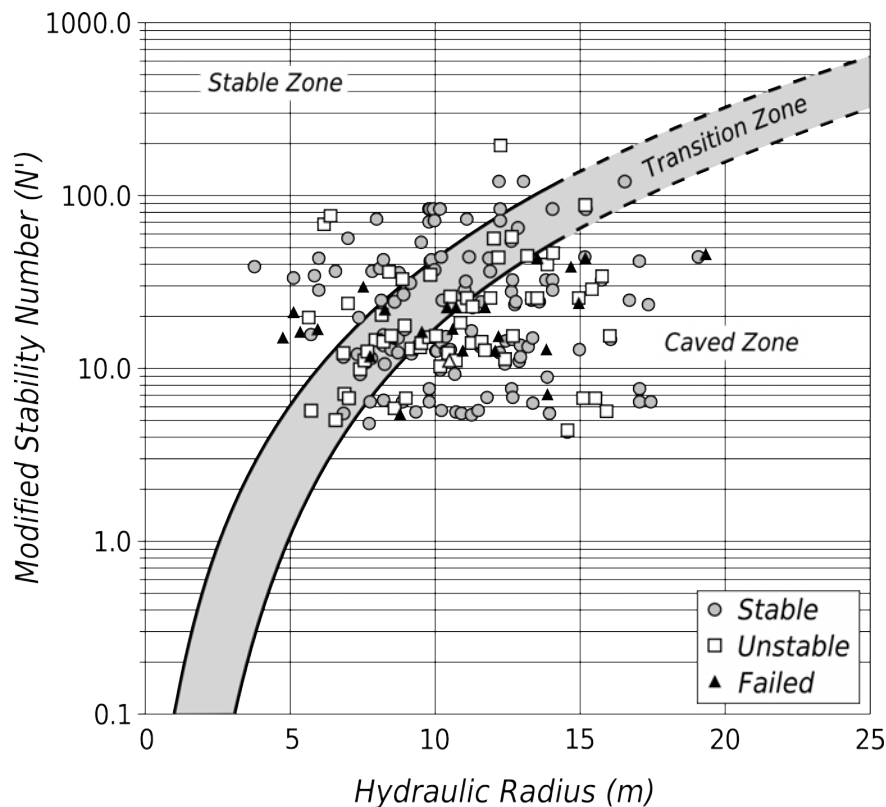


Figure 4.10 - Modified Stability Graph (Potvin, 1988) with Olympic Dam unsupported data (after Oddie and Pascoe, 2005)

Stress Factor (A)

Attempts have been made to improve the Stress Factor (A), by questioning the assumption of a linear relationship between strength/stress ratios and rock mass damage and by also extending its range of application to include the influence of induced tensile stresses.

Villaescusa et al (2003) utilised the data from many years of numerical modelling and observations of underground stoping at Mount Isa (Villaescusa et al., 1997), as the original stress reduction factor (Barton et al, 1974) to review the validity of the Stress Factor (A). From the Mount Isa Mines open slope database, Villaescusa et al (1997) developed a Hangingwall Stability Rating (*HSR*). The rating considered a number of aspects in relation to predicting hangingwall stability of bench stopes. The influence of induced compressive stress change on rock mass damage was also included in this rating (termed the "Mining Induced Stress" component). In order to compare the Mining Induced Stress component from the *HSR* with Potvin's (1988) Stress Factor (A), Villaescusa et al (2003) normalised the Mining Induced Stress component rating over the same range of σ_d/σ_i ratios as the Stress Factor (A). In able to do so, Villaescusa et al (2003) utilised an intact rock strength of 180MPa, which is typical of rock strengths at Mount Isa, where the *HSR* was developed. In addition, Barton et al's (1974) *SRF* term was inverted and normalised to range from 0.0 (where $\sigma_d/\sigma_i = 1.0$) to

1.0 (where $\sigma_c/\sigma_i = 10$). Villaescusa et al (2003) show that Potvin's (1988) Stress Factor A is significantly more conservative than the stress reduction factor used in the Q -system, which is somewhat similar to the results from Mount Isa Mines (see Figure 4.11). Villaescusa et al's (2003) main criticism of Potvin's (1988) Stress Factor A is that it heavily penalises σ_c/σ_i ratios in excess of 5 (i.e. 60% penalty). Significantly, this may lead to the generation of very conservative stope spans. Villaescusa et al (2003) proposed a new Factor A allows for calculations within the overstressed region where the ratio of UCS to stress ranges from 1 to 2.

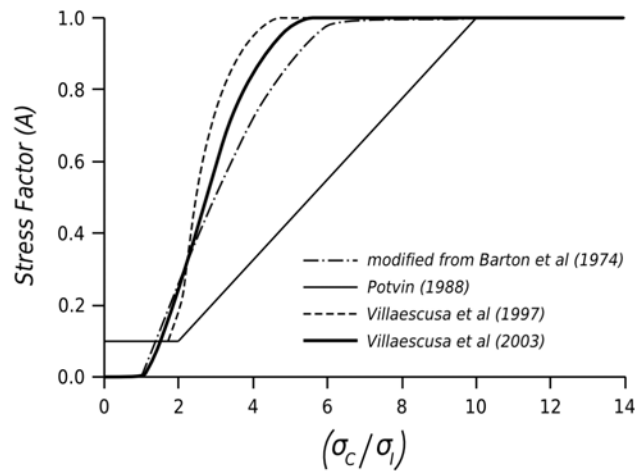


Figure 4.11 - Comparison of relative influence of intact compressive strength to induced stress for a number of empirical systems (modified from Villaescusa et al, 2003)

Another simple and general correction to Stress Factor (A) is proposed (Diederichs and Kaiser, 1999b);

$$A = 0.9 e^{11 \left(\frac{\sigma_T}{UCS} \right)}, \quad \sigma_T < 0 \quad (4.5)$$

where σ_T is the tensile stress tangential to the excavation surface and UCS is the unconfined compressive strength of intact rock. Diederichs and Kaiser (1999b) also incorporate this tensile stress component with the compressive component for Stress Factor (A) in a revised design chart shown in Figure 4.12. It must be noted that compressive stress component has been normalised and inverted in this figure. Also, the above work was undertaken as an exercise to demonstrate the role of abutment relaxation on voussoir beam stability, and therefore the approach may only be applicable for laminated rock masses.

Fault Factor (F)

Suurinen (1998) identified that the influence of faults has a significant influence on stability and performance and was not accounted for in the Modified Stability Graph Method. The effects of faults on dilution were investigated by utilising 2D finite element modelling of stopes of varying stope aspect ratios (AR) (i.e. width:height ratios), and faults located at

various positions (top, middle, bottom) and angles relative to the stope hangingwall.

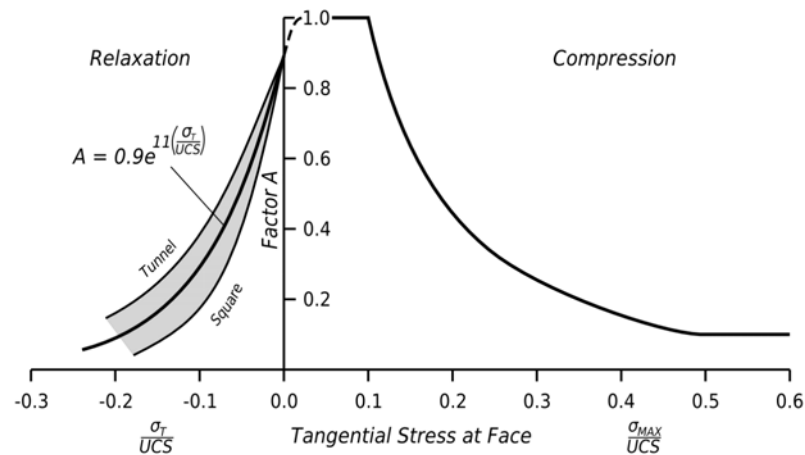


Figure 4.12 - Revised Stress Factor (A) including effect of tensile stress (Diederichs and Kaiser, 1999)

The study also looked at varying fault distance to the stope, which was normalised as the distance to stope height ratio (d/h), as well as various fault strength parameters and in situ stress ratios. The results of the numerical modelling exercise indicated that the most significant impact on the increase in the tensile yield zone was the included angle (i.e. the angle between the fault and the stope surface) and the distance between the fault and the stope surface. Utilising Modified Stability Graph dilution curves prepared by Clark and Pakalnis (1997), it was proposed that a Fault Factor (F) is required to lower the Modified Stability Number (N') to obtain this increased level of dilution. A series of generic Fault Factor (F) curves were then developed for the numerical modelling case scenarios. The Fault Factor (F) can then be applied to the Modified Stability Number (N') to account for the influence of faulting;

$$N'_f = Q' \times A \times B \times C \times F \quad (4.6)$$

where N'_f is the Modified Stability Number, taking into account the Fault Factor (F). The proposed Fault Factor (F) can have a significant weighting on the adjustment of N' (i.e. from 0.02 to 1). Suorineni et al (2001) therefore suggest that the inclusion of a fault factor within the stability graph method is potentially more important than the original factors, as these reduce the N' by only an order of magnitude or less. Furthermore, as concluded by Suorineni (1998), “the most important factors parameters required for application of the fault factor curves are the included angle between the fault and the stope surface, and the position at which the fault intersects the stope surface”.

4.5 EXCAVATION DESIGN USING EMPIRICAL METHODS

The stability of underground openings is controlled by a number of factors, such as rock mass and intact rock strength relative to induced stresses, rock mass discontinuities,

damage caused by blasting and undercutting, etc. The complete geometrical configuration of an excavation plays a significant role on the relative impact of these on excavation performance. More specifically, the geometry of an excavation can be defined in terms of its;

- size
- shape
- orientation
- location

Each of these geometrical attributes will have an impact on the interaction with other factors. For example, the orientation of an excavation surface relative to the orientation of the rock mass discontinuities will influence the likelihood, shape and size of potential structurally controlled failures. Similarly, the orientation and shape of the excavation relative to the principal stresses will control the boundary stress concentration factors, and hence the potential location and extent of stress related rock mass failure. In the design of excavations, one goal of empirical methods is to determine the maximum size and shape allowable for an excavation surface such that it can perform adequately for its intended purpose and service life. Typically, the fundamental geometric size parameters that define the stope size include; stope height (level interval), width and length. In addition to size, the ratio between these geometric size parameters can provide information about the shape of an individual stope surface. The shape of each wall can be defined by an aspect ratio of two components of its geometric size parameters.

Empirically based stope design methodologies have utilised relationships between perceived rock mass conditions (using rock mass classifications and extended classifications) and obtainable stope surface geometries to assist in the design stable stope spans. These current methodologies consider each stope wall separately and imply that the stope wall edges, or abutments, provide support (Milne et al., 2004). It could therefore be considered that the abutments define the boundary conditions for the surface under consideration and that there is minimal interaction between stope surfaces. However, considering the complex interaction of rock mass structure, stress and strains with the geometrical configuration of the entire stope, the validity of this assumption must be questioned. The most common geometric parameters for the stope surface under consideration in empirical stability graph methods include;

- Critical Span
- Hydraulic Radius or Shape Factor
- Radius factor

The following sections briefly summarise the definition of each of these geometric parameters for individual slope wall surfaces.

4.5.1 Critical Span

In terms of slope design, critical span (S_c) could be considered analogous to maximum unsupported span in tunnelling, and is defined as the maximum linear dimension between the closest “supporting” abutments, or smallest dimension. For example, for tall, narrow slope end walls, the slope width would define the critical span. Span can be defined as the largest diameter circle that can fit between abutments (Pakalnis and Vongpaisal, 1993).

4.5.2 Hydraulic Radius

Hydraulic Radius (HR), also known as Shape Factor (S), attempts to capture both the size and shape of the excavation surface. Hydraulic Radius was originally termed by Laubscher and Taylor (1976), re-introduced by Potvin (1988), and is defined below;

$$HR = \frac{A_s}{P_s} \quad (4.7)$$

where A_s is the slope wall surface area and P_s is the perimeter of the slope wall. Alternatively, hydraulic radius can be simply calculated using the following equation;

$$HR = \frac{AB}{2(A+B)} \quad (4.8)$$

Where A and B are the sidewall lengths for a rectangular surface. The origin of this parameter, in terms of its direct influence on stability and dimensioning of excavation surfaces, appears to be unclear. However, Hustrulid (2000) attempts to relate HR to shear failure of a rectangular prism through a limiting equilibrium analysis. He found that shear strength required to keep a slab stable can be related in terms of its area and perimeter and density. It must be remembered, however, that this explanation is based on a very simple analysis, which assumes that the rectangular slab or plug fails through shear at the edges as one solid mass. Hustrulid (2000) goes on to caution that “great care must be exercised when using the shape factor or alternately the hydraulic radius as a descriptor of the exposed opening in a stability analysis”.

A number of authors, (Oddie and Pascoe, 2005; Stewart, 2005) suggest that hydraulic radius is only applicable for “rectangular” slope surfaces. However, the area contributed by a pillars can be subtracting from the area defined by the outer slope surface boundary. As the pillar boundaries also act as an abutment this perimeter length is added to the outer perimeter length. This process can be termed “corrected hydraulic radius”;

$$HR_{corrected} = \frac{A_o - A_p}{P_o + P_p} \quad (4.9)$$

where A_o is the stope surface area bounded by the outside perimeter, A_p is the area within pillars, P_o is the outer stope surface perimeter and P_p is the perimeter of the internal pillars.

4.5.3 Radius Factor

Several factors are suggested to influence hangingwall deformation with increased hangingwall size (Milne et al., 2004);

1. The volume of destressed rock in the hangingwall will increase causing deformation towards the stope opening
2. The deformation modulus of the rock mass may decrease with continued deformation of the hangingwall, due to deterioration of the rock mass, leading to increased movement
3. With further deformation, the rock mass may stop acting like a continuous linear elastic material

Milne et al (1996) observed, as noted in Hoek and Brown (1980), that the zone of elastic relaxation in an excavation surface increases in depth as the distance to excavation abutments increases. In order to reflect this observed phenomenon, Milne et al (1996) introduced the geometric term “harmonic radius” to estimate the average distance to the abutments. The Radius Factor is based on “half the maximum harmonic radius” of a stope surface and is defined as follows (Milne et al., 1996);

$$RF = \frac{Rh_{max}}{2} = \frac{1}{\frac{1}{2n} \sum_{\theta=1}^n \frac{1}{r_{\theta}}} \quad (4.10)$$

Where Rh_{max} is the maximum harmonic radius and r_{θ} are the distances, measured at a number (n) of small angular increments (θ), from a point inside the surface to the abutments. The harmonic radius can be applied to a number of points inside the boundary of the excavation surface, usually in a grid-like fashion. The values at each of these points are termed the effective radius factor (ERF), as shown in Figure 4.13.

Pascoe and Oddie (2003) describe the comparison of ERF values for a simple geometry with the results of linear elastic numerical modelling using an isotropic stress field. The results indicate a good correlation between the calculated Radius Factor values and elastic displacement (Figure 4.14). From this exercise, it was surmised that linear elastic modelling, under an isotropic stress field, could be used as a tool to estimate the “inherent stability” of points surrounding a complex three-dimensional stope surface.

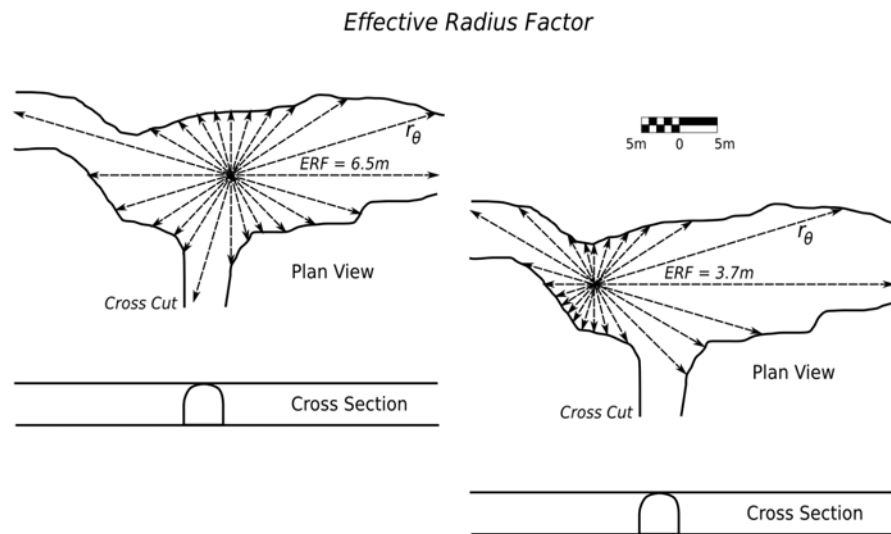


Figure 4.13 - An example of Effective Radius Factor for two locations on a stope surface (Milne et al, 2004)

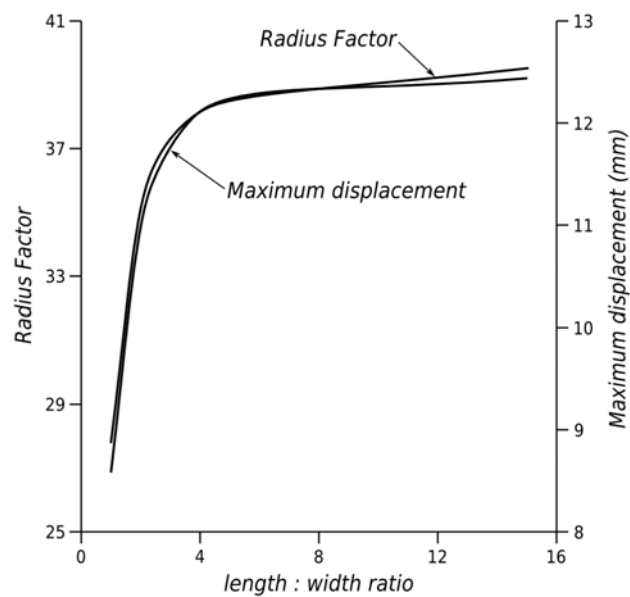


Figure 4.14 - Correlation of elastic deformation with Radius Factor (Pascoe and Oddie, 2003)

4.5.4 Comparison of Span Parameters

The geometric span parameters presented above were developed in an attempt to relate a stope surface's size, and to some extent its shape, with its "inherent degree of instability". The examples provided by Pascoe and Oddie (2003) suggest that *ERF* correlates well with linear elastic deformation of an isolated excavation surface in an isotropic stress field. Intuitively, calibration of this relationship is dependent on the principal stress tensor and elastic properties of the rock mass, and of course, is only applicable assuming a linear elastic continuum. Hydraulic radius was an early attempt, to account for size and shape of a stope

wall surface. A comparison of Hydraulic Radius and Radius Factor is shown in Figure 4.15. It can be seen from Figure 4.15 that, as the length:width aspect ratio exceeds 5, the change in Radius Factor is minor compared to Hydraulic Radius. This reduction in Radius Factor after length:width ratios greater than 5 would therefore suggest a similar reduction in the rate of correlated elastic displacement at the centre of the excavation surface. This length:width ratio limit could be construed as imitating the effects of the geometry tending towards plain-strain conditions. From Figure 4.15, Radius Factor may be a more reliable geometric parameter under these conditions than Hydraulic Radius. What is also interesting to note is that, where length:width ratios are less than 3, there is really no appreciable difference between Hydraulic Radius and Radius Factor.

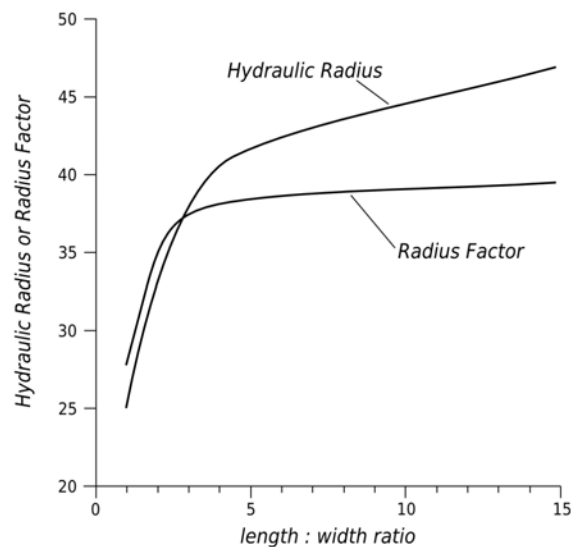


Figure 4.15 - Comparison of Hydraulic Radius and Radius Factor (Milne et al, 1996)

The above results would also suggest that, where the length:width aspect ratio of a stope surface exceeds approximately 5, then the critical span, which is far easier geometric parameter to obtain than Radius Factor for simple geometries (i.e. rectangular surface areas without isolated internal pillars), may be just as an effective parameter to assess geometrical influences under similar conditions. Therefore, the critical span could be considered as capturing the “controlling” dimension for excavations with length:width ratios greater than 5.

4.6 DEVELOPMENT OF EMPIRICAL DESIGN LINES

As mentioned previously, empirical open stope design methods rely on categorising the performance of open stope case histories, and relating this to the geometry of particular excavation surface and the perceived rock mass quality. The categories and their distribution on a “stability graph” are then used to infer or predict future performance. As we have seen in the above examples, authors of these systems have developed a series of

“design lines” that act as boundaries, separating categories of likely stope performance. From an engineer's perspective, it would be inconsequential to accept that a “design line” on a chart represents a valid and accurate measure. It is interesting to note that Stewart and Forsyth (1995) cautioned against the use of “lines” *per se* and instead proposed broad “zones”. A variety of techniques have been used by a number of authors to discriminate the performance category data in order to develop “design lines”, each with varying degrees of sophistication;

- Visually assigning (Mathews et al., 1981; Potvin and Hudyma, 1989)
- Discriminant analysis and regression utilising Mahalanobis distance squared (Nickson, 1992)
- Logit regression and development of isoprobability contours (Mawdesley et al., 2001)
- Bayesian likelihood discriminant analysis (Suorineni et al., 2001)

There a variety of definitions in the published literature used to categorise “stability”. For example, the definitions of “caved” provided by both (Mathews et al., 1981) and (Potvin and Hudyma, 1989) differ significantly in terms of acceptable open stope performance. There is a risk that, when combining data sets, that the definitions may be incompatible, thereby invalidating any discriminant analysis technique employed. The variability in the definitions used to categorise stability and the various methods employed to devise “design lines” for a number of stability graph examples are summarised in Appendix B. Although the development of empirical methods has seen an increase in the use of sophisticated discriminant techniques, one must question the validity of using statistical techniques considering the categories that they try to discriminate are highly subjective and qualitative terms. Notwithstanding this, statistical and likelihood approaches (Mawdesley et al., 2001; Suorineni et al., 2001) can provide the design engineer with a tool to “indicate” the reliability of the derived design parameters, based on the empirical database. Indeed, the precision of the Mathew's method can be gauged from Figure 4.16. For example, stopes designed on the “stable-failure” boundary have a 40% chance of incurring “failure” and “0% chance of “major failure”, whilst those designed on the “failure-major failure” boundary have a 46% chance of “failure” and 46% chance of “major failure”.

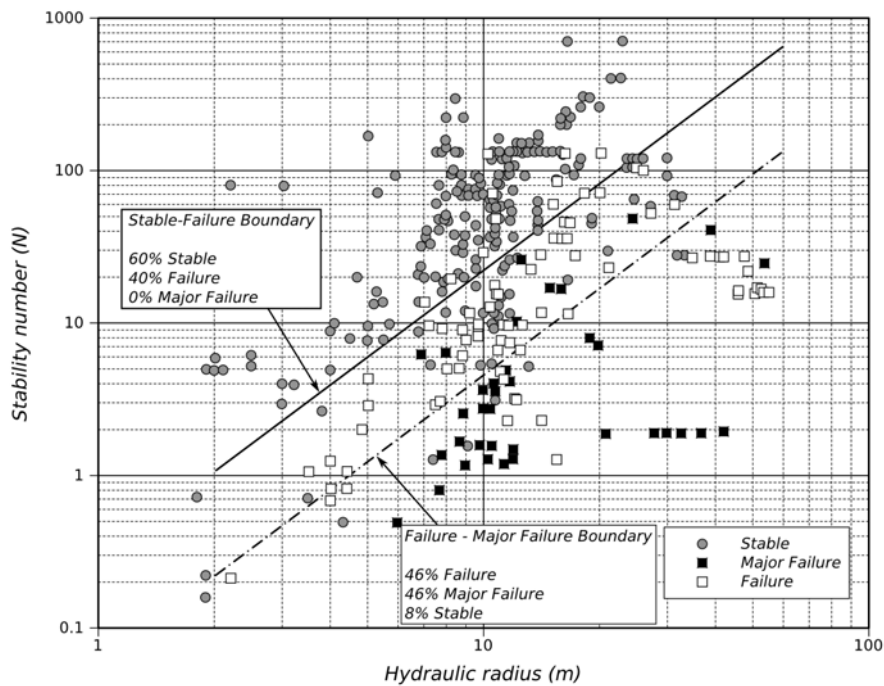


Figure 4.16 - Extended Mathews' stability graph based on logistic regression (Mawdesley et al., 2001)

4.7 CONCLUSIONS

Rock mass classifications and empirical stope design methods can be described as non-rigorous engineering performance rating systems, which include *interpretation* and *simplification* of only *some* of the engineering geology, rock mechanics and rock engineering parameters. In this respect, they are unable to completely capture the complex rock mass interactions and behaviour under all geological regimes and boundary conditions, which may involve any number of failure mechanisms. The review has shown that the development of early rock mass classification systems was influenced by the initial engineering application and objectives, as well as local site conditions. There is a risk of extending existing classification systems to alternative engineering applications that parameters essential to adequately capture rock mass behaviour of the new application may be missing, or existing parameters are weighted inappropriately. In particular, the review has highlighted **the inappropriateness of RQD as a measure of discontinuity intensity as the excavation scale increases.**

The accuracy and precision of empirical methods are also a function of the case history database. The location or origin of case histories will influence a variety of factors, including the range of geological conditions, legal and logistical conditions and mining methods and practices employed. For example, the case histories in the stability graph methods have not specified or categorised the style of stoping, e.g. VCR, mass blasts versus "slotting and ring firing", which can have a significant effect on the amount of blast induced rock mass

damage and hence stope performance. The precise definition and degree of subjectivity when categorising case studies has also shown to be extremely important on accuracy and precision. **One must therefore be cognisant of the accuracy and precision of the method, not to employ it outside of the experience base, and be aware of any limitations placed on the method.**

The Modified Stability Graph Method can perhaps be useful in initial stope size selection, however, it has often been relied on too heavily for detailed stope dimensioning and especially in the design of cable reinforcement. One of the biggest criticisms of this method by Stewart and Forsyth (1995) was that it *“appears to be lending too great a sophistication to the method and may be leading less experienced users into falling into the trap of a ‘false feeling of adequacy of design procedures’”*. Recent experience within the Australian mining industry has shown that the method can be considered unacceptably imprecise and ineffective at optimising stope dimensions.

Although empirical studies have shown the relative effectiveness of cable bolting on stope performance (Oddie and Pascoe, 2005; Potvin, 1988), the guidelines proposed by empirical methods may only apply under restrictive conditions (such as even distribution of reinforcement across an exposed surface) and lack sufficient reliability (such as those that relate hydraulic radius to cable length). In addition, the levels of over-break and dilution, as a consequence of designing stopes in “transitional” and “unstable” zones on the stability graph, have not been adequately addressed. It must be noted that none of the empirical stability graph methods have differentiated their case history database (as presented on published stability charts) on whether stopes were primaries or secondaries, nor have they accounted for any previous potential stress or blast induced rock mass damage.

The review has also shown that the **presence of large-scale discontinuities (such as faults and folds) potentially invalidate the method**. In this case, alternative methodologies that include the influence of are advisable. A number of authors have attempted to rectify some of the shortcomings, providing improvements or enhancements to the stability graph methods. Some of these recognise the importance of the **influence of large-scale structures on stope stability and consideration of all stress conditions rather than just the maximum induced compressive stress**. Furthermore, recent empirical studies recognised that the most important factor controlling stope stability was the **geometrical arrangement of large-scale structure** with the stope, specifically orientation and location (Suorineni, 1998).

With regard to modifications of empirical methods, it is considered that each addition or enhancement must be justified relative to the overall precision of the method. This is not to say that new classifications, or extending existing systems, are without merit. Hudson (1992) describes how rock mass classifications should be based on specific engineering objectives, on a **sound understanding of site conditions, project objectives, mechanisms of behaviour and parameter interactions**. Pine and Harrison (2003) highlighted that the development of ratings for parameters within classification systems and the inter relationship between parameters may not necessarily lead to an optimum formulation under all site conditions.

Finally, it must be remembered that empirical methods are only one of the design tools that can be employed by the rock mechanics engineer. The most important aspect of this review is to highlight that existing empirical design methods represent **non rigorous design approaches and may only be appropriate for preliminary design and initial construction**.

CHAPTER 5 - ASSESSMENTS OF STOPE PERFORMANCE

5.1 INTRODUCTION

Performance is generally defined as the measure of “success” of an actual outcome versus the planned outcome. Stope excavation performance can be defined in a number of ways. From a mine production perspective, performance can be defined as the measure of success of a number of production characteristics, such as;

- mining physicals (i.e. volume, tonnage and grade of ore extracted)
- costs (i.e. mining and milling costs), and
- time (i.e. stope extraction and completion compared to schedule)

This definition of stope excavation performance generally refers to single stopes, however, the combined performance of single stopes has an impact on the performance of mining blocks and subsequently on total mine production performance. Continuing with this definition, optimal stope performance could therefore be one which maximises ore recovery and/or reduces ore loss, reduces dilution and minimises disruption to the mine schedule.

5.1.1 Economic Performance

Dilution and ore loss adversely impact on a mines profitability and productivity, however, this is often difficult to quantify. In order to improve mine profitability, it is firstly necessary to quantify and place an economic consequence on dilution and ore loss. In this way the relative merits of dilution control measures, such as design and/or procedural changes, can be economically evaluated.

Dilution and ore loss can have a significant impact on re-scheduling and changes to the mine plan. For example, most mines cannot afford to have a shortfall on budgeted tonnes (i.e. metal content), as a consequence stopes may be brought into production out of schedule. It may become necessary for the mine to exploit tonnes planned for future months, or radically re-sequence mining to obtain the required tonnes (i.e. open up areas that were planned for next quarter/year, etc.). This has two major follow on effects; firstly, it may require that capital development is brought forward or re-designed, potentially requiring additional un-budgeted development metres, and secondly, re-scheduling stopes may contribute to out-of-sequencing, thereby potentially increasing the risk of further dilution and stress related issues (i.e. increased ground support costs, increased seismic risk, increased pillar sizes, reduced recovery, etc.). This may lead to an increased risk of reduction in global ore

recovery, thereby reducing the overall mine life. It can be seen that dilution and ore loss not only affect short term production, yet can present a significant risk to potential future development areas and the viability of a project. Therefore, an economic evaluation the impact of dilution and/or ore loss can be conducted at a variety of levels; from short term (i.e. monthly) changes to grade, production rate and re-scheduling issues, through to quarterly, annual and even life of mine. Some operational and long-term aspects that could be evaluated should at least include;

- Production grade/tonnes and respective changes to the mines grade/tonnage curve
- Secondary blasting, loading and haulage, backfill costs
- Processing costs
- Micro and macro re-scheduling and sequencing
- Production rate decrease and ability to achieve target budgets/schedules (monthly, quarterly, annual)
- Reserve reduction effecting mine life and project viability
- Cash flow, IRR and NPV, corporate risk profile and shareholder value

Development of economic impact for various levels of dilution and ore loss can be used to quantify geotechnical risk in a financial manner. The cost of dilution and ore loss can then be used in predictive mine planning and financial assessments. For example, establishing the cost of dilution/ore loss can be used as justification to implement design/procedural changes relative to the economic impact of accepting the dilution and ore losses.

5.1.2 Rock Mechanics Performance

From a rock mechanics perspective, stope performance is usually defined in terms of the rock mass response to mining. In this regard, it is necessary to reconcile the actual response with the anticipated response during excavation. Back analysis is therefore required to improve understanding of mechanisms, check validity of assumptions and generally refine geotechnical parameters used in the design. The design of future excavations can then be optimised by using the improved understanding and refined parameters.

Back analysis techniques in rock mechanics generally rely on measurements of strains, displacements, or rotations of the excavation or rock mass internal to the excavation (Cividini and Gioda, 1993). However, it is generally impractical and expensive to instrument all stopes within a mine. As such a strategic approach to instrumentation and monitoring is generally adopted, with instrumentation concentrated on a small number of stopes where

specific types of rock mass response are anticipated.

Cavity Monitoring System

Unfortunately, in some circumstances, a strategic mine instrumentation and monitoring plan cannot be undertaken. Under these conditions, slope excavation performance is primarily assessed from the final excavation geometry against the planned slope geometry. The post-production slope excavation geometry is generally established from a Cavity Monitoring System (*CMS*) survey. This has been a well established method for surveying inaccessible open cavities in underground mining operations for well over 10 years. The *CMS* was developed jointly by Noranda Technology Centre (NTC) and OPTECH Systems, Canada (Miller et al., 1992). This system is widely used in Australia's underground operations, especially in Western Australia (Jarosz and Shepherd, 2000) where *CMS* data are collected routinely by mines during production.

As will be shown in later chapters, the final excavation profile may not necessarily provide an optimal indicator for rock mass response and calibration in rock mechanics back analyses. Firstly, rock mass damage and yielding can occur well beyond the excavation surface. In this case, *CMS* profiles do not represent the extent of rock mass damage due to blasting or stress redistribution. Secondly, it must be recognised that the response of the yielded rock mass at the excavation surface is not always predictable (see Chapter 7). Nevertheless, *CMS* profiles provide a gross measure of the success or otherwise of the anticipated rock mass response.

5.2 QUALITATIVE ASSESSMENTS OF PERFORMANCE

Slope performance is often referred to in terms of its “stability” or rock mass response. Excavation performance can be characterised in subjective terms such as “good” or “poor” performance. As mentioned in Chapter 4, early empirical open slope design methods principally relied upon these types of qualitative measures of slope performance. A summary of some published literature on empirical stability graph methods, shows a variety of performance classifications (as shown in Appendix B).

The table in Appendix B clearly demonstrates the variability of categories used to classify slope performance of the various case history data. In addition, in some studies, the same category names have been used yet the definitions and meanings of categories are different. For example, the term “caved” as used by Mathews et al (1981) and Potvin (1988) describe very different examples of rock mass response. The choice of category name and definition are therefore subjective and are thought largely due to;

- Differences in the range of rock mass conditions experienced between sites/studies
- Differences in “acceptable” rock mass response between mine sites and/or studies

Another issue with qualitative assessments is that the range of rock mass response, even within a category, may not allow for sufficient discrimination of performance between stopes. In summary, the use of qualitative assessments makes direct comparison of the case study data difficult, and highlights the problems using subjective classification categories to describe stope performance.

5.3 QUANTITATIVE ASSESSMENTS OF PERFORMANCE

In order to obtain a detailed understanding of stope performance it becomes necessary to measure physical characteristics that can be used to quantify performance. The most commonly used quantifiable measures of stope performance are dilution and ore loss. In addition, a number of other quantifiable measures are described in the following sections.

5.3.1 Dilution and Ore Loss

Dilution essentially is a reduction of the grade of the mine reserve, which can be in a number of forms and attributed to a number of process, from exploration, mining and processing operations (Scoble and Moss, 1994). Ore loss generally refers to economic material that is left in place (i.e. not extracted) or extracted yet accidentally classified and treated as waste. The sources of dilution and ore loss occur during all phases of mineral exploitation, from exploration to mining, through to ore processing (Elbrond, 1994). In exploration and subsequent geological modelling processes, dilution and ore loss is usually caused by uncertainty in delineating the ore boundary, as well as inability to define internal waste (i.e. non or low grade material) within the orebody. It has been indicated that, depending on the ore body complexity, dilution arising from improper orebody delineation and modelling may account for up to 30% of all sources of dilution (Lappalainen and Pitkajarvi, 1996).

During mining, dilution and ore loss can occur from expected or unexpected sources. Scoble and Moss (1994) classify the “planned” dilution as the identified “expected” dilution within the mining reserve, and “unplanned” dilution the additional “unexpected” waste material extracted from the stope outside the planned stope boundary (see Figure 5.1). Planned dilution is generally a function of the mining method, stope design and ore body complexity. These include all waste internal to the planned mining geometry, including waste pockets. Unplanned dilution includes sources outside the planned stope boundary, including fall-off from stope walls, contamination from backfill, leaving ore behind in the stope and mismanagement of down stream ore and waste handling. Villaescusa (1998) provides a classification of dilution, which includes the source of dilution relative to the mining

boundaries and the primary causes, as shown in Figure 5.2.

From a rock mechanics and slope performance perspective, the internal dilution (i.e. planned dilution) cannot be avoided and what interests us most is the amount and form of the unplanned dilution. It must be noted that there are a number of ways to quantitatively define of dilution (Pakalnis, 1986), however the dilution is usually described as the percentage of mass of uneconomic material (i.e. waste) extracted from the stope to the mass of the total material extracted. Scoble and Moss (1994) define two equations for dilution (D) based on tonnage mined;

$$D = \frac{\text{waste}}{\text{ore}} \quad (5.1)$$

$$D = \frac{\text{waste}}{(\text{ore} + \text{waste})} \quad (5.2)$$

It must be note that equation 5.2 is insensitive to external dilution (from wall fall-off), depending on orebody width, and can over only have a maximum value of 100% (Pakalnis et al., 1995). In this case, it is preferable to estimate tonnage based dilution on equation 5.1. Tonnage based dilution is usually calculated by reconciling the amount and grade of mucked tonnes to the planned tonnage and grade. However, practical difficulties arise in estimating the grade of the mucked material (i.e. head grade) due to ore transport, stockpiling and sampling issues. Without measuring the volume and shape of the excavated profile, and evaluating the contained grade using a resource model, it is very difficult to ascertain the grade of the external dilution. In most circumstances, this material is usually assumed to carry zero grade.

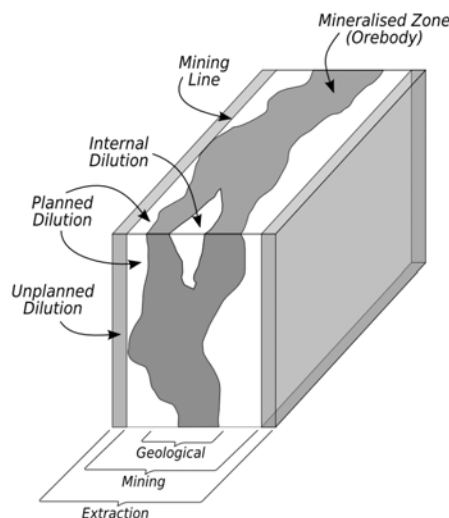


Figure 5.1 - Planned and unplanned dilution (after Scoble and Moss, 1994)

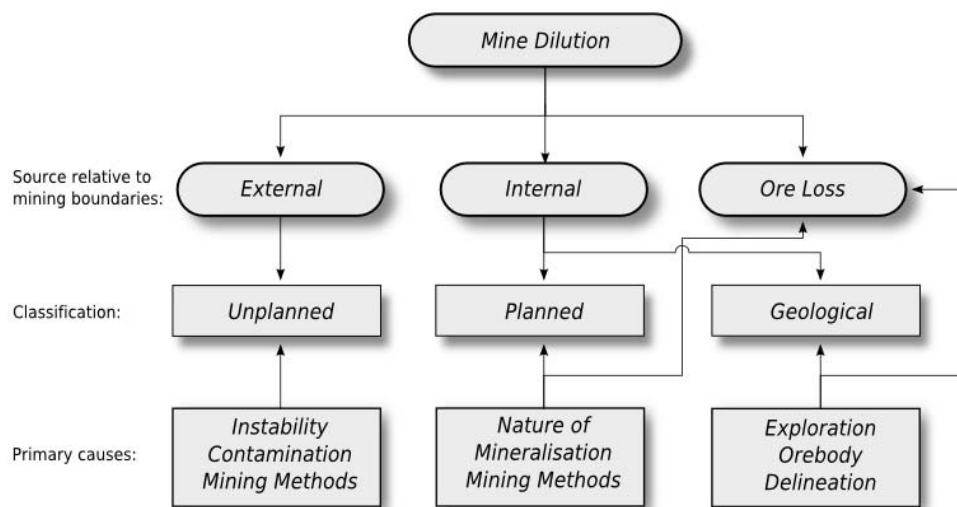


Figure 5.2 - Classification of dilution and ore loss (Villaescusa, 1998)

5.3.2 Over-break and Under-break estimation using Cavity Monitoring Systems

To obtain a quantitative measure stope performance, final excavated volumes need to be obtained and compared to the stope design boundaries. *CMS* surveys can be used to ascertain the final excavated stope volumes. The two main criteria for assessing stope performance using *CMS* data are over-break and under-break.

Over-break

The amount (i.e. depth, volume or tonnage) of material excavated in excess of planned mining geometry is termed “over-break”. Over-break that considers the mineral economics of this material is therefore termed “Unplanned dilution”. If the economic value of the material excavated outside the planned volume is unknown, then it is more appropriate to use the term “over-break” than “dilution”.

Under-break

The amount (depth, volume or tonnage) of material left unbroken within the planned excavation geometry is termed “under-break”. Under-break and/or broken material left within the stope that is of economic value, is therefore termed “Ore loss”.

Void Model

In generating an accurate void model with a cavity monitoring system (*CMS*), it is necessary to undertake the survey when the stope has been fully extracted and to ensure that no broken stocks remain within the stope. Once the *CMS* survey has been undertaken and the raw data has been downloaded, it first needs to be ‘geo-referenced’ using the OPTECH

proprietary software. 'Geo-referencing' refers to the process of transforming data points from the Cartesian coordinate system of the survey instrument to that of the local mine Cartesian coordinate system. The *CMS* results can then be made readily available (i.e. 'imported') to mine planning systems. In some cases, due to limited access, a number of *CMS* surveys are required to be undertaken at various locations within the void. In this case, a number of composite *CMS* surveys are required to define the full stope void. Differences can exist between the each *CMS* survey, which are mainly due to set-up errors between sites and can be exacerbated by a number of other issues, such as void "shadows" or re-entrants, as well as ore/mullock left in the stope (see Figure 5.3).

In generating a complete final stope void, it may be necessary to utilise a number of *CMS* stope surveys, often taken at various stages of stope extraction. Piecing this information together can involve a substantial amount of time and interpretation by the surveyor. In order to conduct meaningful and time efficient void intersection algorithms (i.e. to calculate ore loss and over-break), surveyors often filter the *CMS* cloud data, to reduce the amount of data points. The final void is then usually an amalgam of filtered data points from a number *CMS* surveys, and therefore only represents a "model" of the stope volume, which may vary from the "actual" stope volume. Over-break and under-break, hence dilution and ore loss can be obtained by comparing *CMS* void volume (V_{Void}) to the planned excavation or "reference" volume.

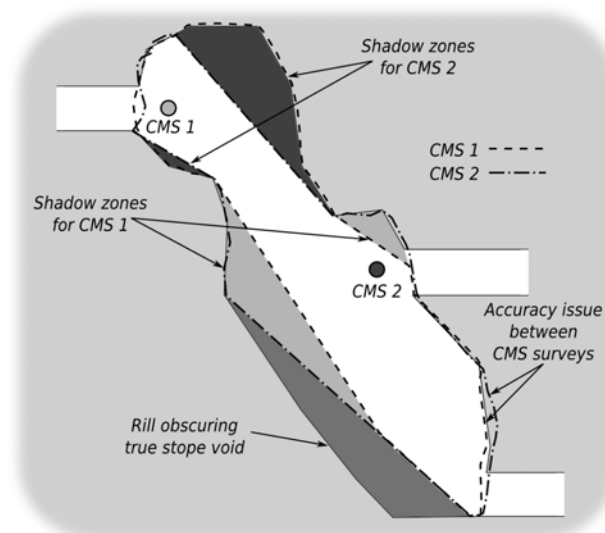


Figure 5.3 - Schematic showing effects of shadowing and accuracy issues when amalgamating *CMS* surveys

Reference Volume

The "reference" volume (V_{Ref}) usually consists of the union of the stope design and in-place

development, however, this may need to be modified if any changes were implemented during excavation. For example, additional holes may have been drilled and fired that were not on the production plan or, conversely, drilled holes were not fired due to bridging/blockages or due to a decision to leave a pillar. The “reference” volume is typically represented by a primitive triangulated irregular network (*TIN*) wire-frame model in mine planning software.

5.3.3 Volume of Over-break and Under-break

Over-break and under-break volumes are generally calculated by intersecting the “reference” volume with the final stope void volume utilising mine planning software, typically using boolean triangulation intersections of the relevant *TIN* wire-frames. A representation of this calculation using set and boolean operations is provided in Figure 5.4.

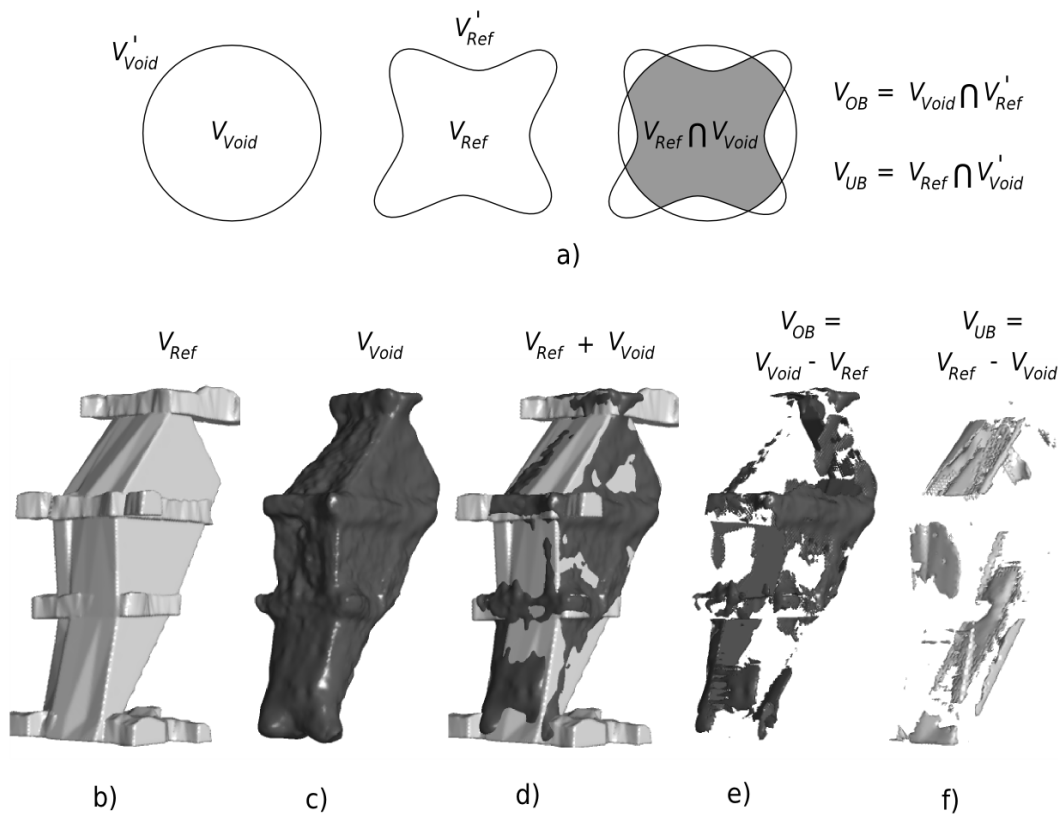


Figure 5.4 - Example calculation of volume of over-break and under-break using a) set operations and boolean operations (b-f).

Depending on the relative configuration and aspect ratios of individual triangles within the wire-frame models, errors may occur during triangulation intersection process (principally due to floating point precision), resulting in an unsolvable volume intersection.

Tonnage and grade values of dilution and ore loss can subsequently be calculated from the

“reference” and final stope void volumes in conjunction with a block model of reserve grades and densities, including backfill materials. These data can then be stored in a database for further reconciliation reporting and presentation (Morin, 2006).

It may firstly be useful to quantify the performance of a stope by comparing the actual volume against the planned volume. The void ratio (R_v) provides a quick indication of whether the drill and blast and mucking activities achieved design;

$$R_v = \frac{V_{Void}}{V_{Ref}} \quad (5.3)$$

where V_{Void} represents the volume of the void and V_{Ref} volume of the “reference” volume. However, this performance indicator does not tell us about the percentage of over-break or under-break, and subsequent dilution and ore loss. It is therefore necessary to define the percentage of over-break and under-break, which are provided in equations 5.4 and 5.3.

$$R_{OB} = \frac{V_{OB}}{V_{Void}} \quad (5.4)$$

$$R_{UB} = \frac{V_{UB}}{V_{Void}} \quad (5.5)$$

where V_{OB} and V_{UB} represent the volume of over-break and under-break, respectively.

Performance By Stope Surface

On a general level, volumes and percentages of over-break and under-break may be sufficient in determining the relative performance of one stope versus another. This level of generality may also be sufficient in determining whether a stope has performed to some basic dilution performance criteria. However, presenting this information alone does not provide any information on where the majority of over-break and under-break has occurred within the stope. It therefore, may be necessary to identify the location and amount of any over/under-break relative to each stope surface, such as hangingwall, footwall, end walls, and crown. Geotechnical factors (such as stress redistributions, unfavourably oriented geological structures, poor rock mass quality, etc.) as well as engineering design and implementation factors (such as position of development, cut-off slots, ring design, blasting, etc.) may have a significant impact on the location and amount of over-break and ore loss. Obtaining and documenting information on where over-break and under-break occur is therefore fundamental in understanding these contributing factors.

In an attempt to improve this understanding, one may assign volume of over-break and under-break to the major stope surfaces. For tabular parallelepiped shaped stopes, this is

relatively straight forward, with the lines of intersection between the surface planes defining the perimeters of each stope surface. Difficulty arises in delineating the “boundary” of surfaces for irregular or “rounded” stope shapes. There is also the issue of assigning the volume of over-break or under-break to where it extends across both surfaces. In this case, some arbitrary division is required.

The volume of over-break and under-break occurring on each wall can be used to define the relative performance of each wall;

$$R_{OB}^S = \frac{V_{OB}^S}{V_{OB}} \quad (5.6)$$

$$R_{UB}^S = \frac{V_{UB}^S}{V_{UB}} \quad (5.7)$$

where V_{OB}^S and V_{UB}^S is the volume of over-break and under-break, respectively, assigned to a particular surface. Where the size stope surfaces are significantly different, it may be necessary to normalise these indicators, by the percentage of the contributing area of the stope surface under investigation;

$$\bar{R}_{OB}^S = \left(\frac{V_{OB}^S}{V_{OB}} \right) \times \left(\frac{A_S}{A_{Stope}} \right) \quad (5.8)$$

$$\bar{R}_{UB}^S = \left(\frac{V_{UB}^S}{V_{UB}} \right) \times \left(\frac{A_S}{A_{Stope}} \right) \quad (5.9)$$

where A_S is the area of the stope surface under consideration and A_{Stope} is the total area of the surfaces that can contribute to over/under-break which can be measured (e.g. typically all walls and the crown, excluding the floor).

5.3.4 Area of Over-break and Under-break

Along with volume of over-break and under-break, mine planning software or CAD systems are capable of determining the area of over-break and under-break. This firstly involves establishing the volumes of over/under-break, and by utilising the surface areas of the individual triangles of the TIN, areas can be quickly ascertained. Areas can be defined by;

- the total surface area of over-break or under-break (A_{SOB} and A_{SUB} , respectively), or
- the area of intersection of over-break or under-break with the stope surface under consideration of the “reference” volume (A_{OB} and A_{UB} , respectively)

A_{SOB} and A_{SUB} represent the total surface areas of the volumes depicted in Figure 5.4d and Figure 5.4e, respectively. The definition of the area of intersection is illustrated in Figure 5.5.

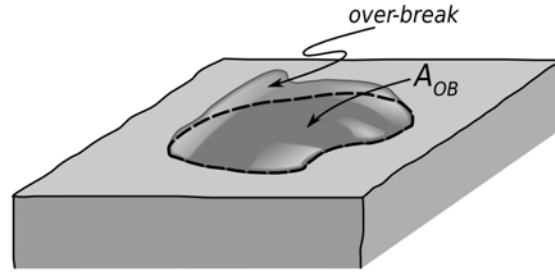


Figure 5.5 - Schematic showing definition of area of intersection between stope surface and over-break volume (enclosed by dashed line) and denoted as A_{OB}

5.3.5 Depth of Over-break and Under-break

The performance of individual stope surfaces may be quantified by the depth of over-break and under-break, relative to the “reference” volume. The direction of depth can be taken as approximately normal to the stope surface under investigation. For tabular or parallelepiped shaped stopes, the derivation of depth direction is relatively straight forward. The depth of over-break can be calculated at regular intervals over the surface under investigation, in the direction perpendicular to the plane of best fit of the surface, as shown in Figure 5.6a. For circular excavations such as tunnels, depth of failure can be defined as a radial measure from the centre of the excavation and plotted with direction (Maerz et al., 1996). However, difficulties can arise where the stope shape is irregular, making the decision for the direction of depth ambiguous (see Figure 5.6b). In this case, the surface of the “rounded” reference geometry and void model can be discretised into a large number of evenly spaced points. The depth of over/under-break at each point on one surface can be evaluated by finding the minimum isotropic (i.e. in all directions) distance to all points on the other surface. These can then be contoured by interpolation (see Figure 5.7), with a finer discretisation providing more accurate results. It must be noted that “depth of over/under-break” is directional in nature, and hence represents a vector quantity. Stope surface performance, in terms of depth of over/under-break, can be quantified by the maximum depth of over/under-break;

$$D_{OB}^{MAX} = \max(D_{OB}^i), \quad \forall D_{OB}^i \quad (5.10)$$

$$D_{UB}^{MAX} = \max(D_{UB}^i), \quad \forall D_{UB}^i \quad (5.11)$$

where D_{OB}^i and D_{UB}^i are the individual depth values calculated for the surface under investigation. The maximum depth of over/under-break can be used to highlight which stope surfaces have experienced deeper over/under-break against those with shallow over/under-break. The average depth of over/under-break can be expressed as follows;

$$\bar{D}_{OB} = \frac{1}{N} \sum_i^N D_{OB}^i \quad (5.12)$$

$$\bar{D}_{UB} = \frac{1}{N} \sum_i^N D_{UB}^i \quad (5.13)$$

Alternatively, the average depth of over/under-break can be calculated from the intersected volumes of over/under-break and the intersection areas for the slope surface under consideration;

$$\bar{D}_{OB} = \frac{V_{OB}^S}{A_{OB}} \quad (5.14)$$

$$\bar{D}_{UB} = \frac{V_{UB}^S}{A_{UB}} \quad (5.15)$$

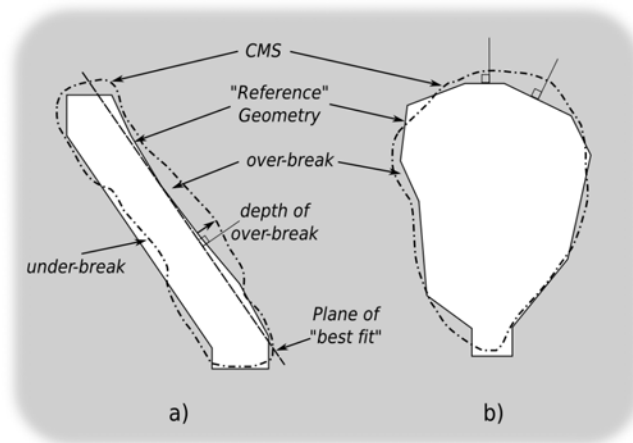


Figure 5.6 - Schematic showing measurement of a) depth of over-break for planar surfaces, and b) effect of irregular shapes on determining direction of depth of over-break

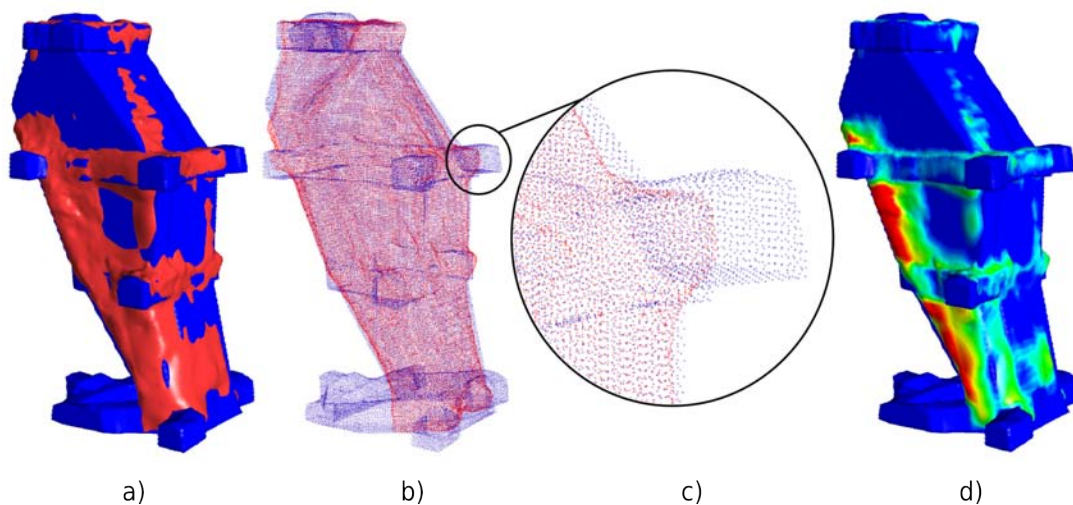


Figure 5.7 - Calculating depth of over-break from a) CMS (red) and reference volume (blue) by b) discretising both surfaces, c) shows detailed discretisation and d) shows contoured values of isotropic distance to CMS from the reference volume

It is considered that quantification of slope performance in terms of the depth of over/under-break is a more useful evaluator than % dilution, which is of course dependant on slope width. Depth of over/under-break provides more detailed information such that comparative performance between slope surfaces can be made. It can indicate where most of the over/under-break has concentrated on slope surface and, by using contour plots (as shown in Figure 5.7d) of the individual measures of depth of over/under-break, the shape characteristics can also be ascertained. In addition, an empirical evaluation of depth of failure for slope walls can also assist in providing necessary design criteria for cable reinforcement lengths.

5.3.6 ELOS and ELLO

Clark and Pakalnis (1997) propose the use of equivalent linear over-break/slough (*ELOS*) to quantify the amount of over-break;

$$ELOS = \frac{V_{OB}^S}{A_S} \quad (5.16)$$

Where A_S is the surface area of a particular slope surface. Similarly, the amount of under-break can be quantified using equivalent linear lost ore (*ELLO*);

$$ELLO = \frac{V_{UB}^S}{A_S} \quad (5.17)$$

Clark and Pakalnis (1997) state that “They represent conversions of the true volumetric measurements into an average depth (*ELOS*) or thickness (*ELLO*) over the entire slope surface.”

The perceived attractiveness of using such a parameter, is that firstly it provides quantitative measures of over-break and under-break that are independent of slope width (Clark and Pakalnis, 1997). This can potentially allow for comparisons of slope performance between slopes of varying widths. Additionally, Clark and Pakalnis (1997) state that “a benefit of using the *ELOS* parameter for empirical design is that it allows comparisons with other mining operations. This is not possible if dilution values are used since the values determined are a function of: slope width, grade of wall rock, and the associated tonnage which cannot be done with dilution percentages”. Secondly, they provide measures that can be applied to individual slope surfaces, such that relative performance comparisons can be made between slope surfaces.

These parameters, however, cannot provide all the information about the nature or “geometry” of over-break/under-break (e.g. shape, size, position, orientation). For example,

shallow and extensive over-break can provide the same value of *ELOS* as localised, yet deep-seated, over-break value, as illustrated in Figure 5.8. In terms of the design of rock reinforcement for open stoping, predicted *ELOS* values are perhaps of limited use, as the indicative depth is required to evaluate cable reinforcement lengths and geometry of failure (i.e. yielded rock mass or block geometry) is required to ascertain the potential demand placed on the reinforcement scheme.

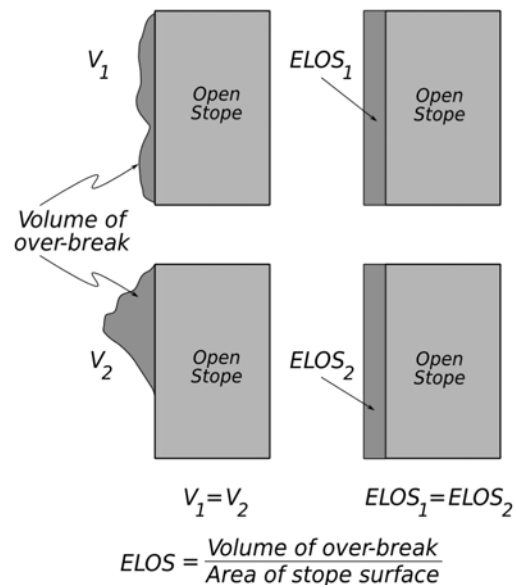


Figure 5.8 - Example schematic showing inability of *ELOS* to capture geometry of over-break

Quantifiable measures, such as dilution and/or *ELOS* have been used by a number of authors to assess and even classify stope performance. This is more attractive than a classification system based purely on ambiguous qualitative terms. Pakalnis and Vongpaisal (1993) were the first to utilise dilution values (in percentage) directly on stability graphs (utilising *RMR* versus Hydraulic Radius) to quantify performance. These values were visually estimated (not measured) and were then used to develop anticipated performance (dilution levels), by regressing the case history database, for a number of stope layout configurations for the Ruttan Mine (Pakalnis and Vongpaisal, 1993).

5.4 QUALITATIVE AND QUANTITATIVE ASSESSMENTS OF PERFORMANCE

Clark and Pakalnis (1997) quantified observed stope performance using the *ELOS* measure. They then utilised the data to develop design lines, to anticipated likely stope performance. The categorised stope span design zones were based mainly on qualitative measures, using the following classification;

- Blast damage (*ELOS* < 0.5m)
- Minor Sloughing (*ELOS* = 0.5m to 1.0m)

- Moderate Sloughing ($ELOS = 1.0\text{m to }2.0\text{m}$)
- Severe Sloughing / Possible Wall Collapse ($ELOS > 2.0\text{m}$)

Clark and Pakalnis (1997) also provided additional qualitative descriptions of performance for each class.

A number of back analysis studies of stope performance have been undertaken at the Cannington Mine (Scott and Power, 1998; Streeton, 2000). The data set contains both supported and unsupported case histories. Stope performance was assessed by quantifying dilution of each surface, classifying the performance based on the amount of dilution, whether the stope surface was supported, as well as qualitative behaviour;

- Stable: No or minimal fall-off, with support dilution estimated at less than 10%
- Unstable: Substantial amounts of fall-off, a stable unsupported configuration reached after 10 to 30% dilution
- Major Failure: Large amounts of wall fall-off, stable unsupported configuration reached after greater than 30% dilution
- Caving: Void forms uncontrollably until filled with fallen material
- Stable/caved: Wall performs as stable, but is supported by cable bolts to some degree

It is unclear how the quantitative measures of percent dilution were assigned to individual stope wall surfaces. It is assumed that the dilution values stated above were attributed solely to the stope surface under investigation.

5.5 QUANTITATIVE AND ECONOMIC ASSESSMENTS OF PERFORMANCE

Oddie and Pascoe (2005) utilised the results of *CMS* stope performance data at Olympic Dam Operations (ODO) to ascertain the stability classifications for this particular mine. In this study, the mine management suggested that an acceptable performance for a stope would be “ten per cent dilution”. In general, according to ODO’s ten per cent dilution criteria, any stope accruing less than 10 percent dilution could be classified as ‘stable’, and has performed acceptably.

The *CMS* data were used to calculate three parameters for each stope surface; maximum over-break depth, indicative over-break depth and the area of the face over which the over-break occurred. From these three parameters, the volume of the over-break was estimated and the *ELOS* parameter calculated using the following equation:

$$ELOS = \frac{(\text{Indicative depth} \times \text{area of over-break})}{\text{Area of slope surface}} \quad (5.18)$$

It must be noted that no information was provided on how the “indicative depth” was derived. *ELOS* was used to categorise the performance of each slope surface. The following criteria was adopted:

- stable (little or no deterioration) – *ELOS* <0.75,
- unstable (limited failure) – *ELOS* 0.75 to 2.0, and
- failed (unacceptable failure) – *ELOS* >2.0.

5.6 CONCLUSIONS

The above examples show the progression of describing slope performance in terms of qualitative terms, then a mix of quantitative and qualitative terms to purely quantitative terms. It also shows how economic considerations are utilised to quantify slope performance. The degree of sophistication of assessments of slope performance are listed below (in ascending order);

- qualitative assessments of performance
- quantitative assessments of performance
- qualitative and quantitative assessments of performance
- quantitative and economic assessments of performance

The review has shown that there are a number of issues with existing quantitative assessments of performance, such as dilution and *ELOS*. Both measures have difficulty in capturing shape characteristics of over-break and may lead to ambiguous interpretations of over-break geometry. These quantitative measures should therefore be site-specific and care should be used to ensure that it is only applied to similar size-slopes and that economic assessments based on dilution include the influence of variable ore-widths.

CHAPTER 6 - PROPOSED GEOMETRIC PERFORMANCE MEASURES

6.1 INTRODUCTION

We have seen that both economic and rock mechanics assessments of slope performance can involve comparing geometrical aspects of the proposed and actual excavations. However, comparisons of complex slope geometries are non-trivial and it is considered that this has led to a variety of means of simplifying geometrical slope performance comparison, such as volume, area or depth. These comparisons can also be made on individual slope wall surfaces to ascertain whether there is any differential performance between walls. It is therefore important to fully understand the impact of all aspects of geometry, namely;

- orientation
- location
- size
- shape

The first two aspects of geometry are relatively simple to ascertain. However, size and shape are more difficult to quantify. It must be noted that the quantitative measures discussed previously depend on the size and shape of an object, in this case the volume representing over-break or under-break.

6.2 SHAPE AND SIZE

Shape is one of the most difficult parameters to measure, as it may be defined in a number of ways for various purposes, each with various degrees of precision. The basic definition of “**shape**” is provided by Kendall (1977); “**Shape** is all the geometrical information that remains when location, scale and rotation effects are filtered out from an object.” Essentially this means that two geometrical objects will have the same “**shape**” if, after being rotated, translated and rescaled, they match perfectly.

Sometimes, it is also necessary to see if geometrical objects of the same “**shape**” are of different sizes. In this case, the definition of “**size-and-shape**” must be considered (Kendall, 1977); “**Size-and-shape** is all the geometrical information that remains when location and rotation effects are filtered out from an object”. That is, two objects are of the same **size-and-shape** if, after rotation and translation, they match perfectly.

The difficulty lies in finding a “measure” or “index” of shape and/or size that adequately captures the required characteristics for the geometrical comparison. Table 6.1 shows a number of characteristics defining “**shape**” that have been developed in the discipline of geology (Davis, 2002).

The most important aspect to note in all of the measures of shape listed above in Table 6.1, is that they represent “dimensional-less” or “**scale-independent**” measures. That is, these measures can be applied to an object of any “size” and, providing they are the same shape, they will result in the same value of the chosen index. In geology, for example, this allows for shape comparisons, such as “roundness”, of pebbles (small scale) and cobbles (large scale) to identify whether they are of the same origin or have undergone the same transportation mechanisms.

6.3 SHAPE, SIZE AND DIMENSIONALITY

Consider a measure of three-dimensional “sphericity” for rounded objects based on the volume divided by the surface area. The total surface area (A_s) of a sphere is denoted by;

$$A_s = 4\pi r^2 \quad (6.1)$$

Whilst the volume (V) is denoted by;

$$V = \frac{4\pi r^3}{3} \quad (6.2)$$

The example measure of “sphericity” therefore becomes the volume divided by the surface area;

$$\frac{V}{A_s} = \frac{r}{3} \quad (6.3)$$

The value of this measure will change with scale (i.e. radius), even if the “shape” remains constant, therefore will be “**scale-dependent**”, and therefore “dimensional”, as the resulting measure will be in units of length. Other examples of “dimensional” measures include;

- volume of a sphere on it's surface area
- area of a triangle on it's base length
- area of a rectangle on it's perimeter

Table 6.1 - Measures of shape (after Davis, 2002)

Shape Measure	Equation
Circularity	$C_1 = \sqrt{\frac{lw}{l^2}}$
	$C_2 = \frac{4A}{p^2}$
	$C_3 = \frac{4A}{lp}$
	$C_4 = \sqrt{\frac{A}{A_c}}$
	$C_5 = \sqrt{\frac{D_i}{D_c}}$
Compactness	$K_1 = \frac{2\sqrt{\pi A}}{p}$
	$K_2 = \frac{p^2}{4\pi A}$
Thinness Ratio	$TR = 4\pi \left(\frac{A}{p^2} \right)$
Shape Factor	$SF_1 = \frac{p_c}{p}$
	$SF_2 = \frac{p}{p_c} \times 100$
	$SF_3 = \frac{A_i}{A}$
	$SF_4 = \frac{A_c - A_i}{A}$
	$SF_5 = \frac{A}{A_c} \times 100$

Key:

A	Area of object
A_c	Area of smallest enclosing circle
A_i	Area of largest inscribed circle
D_c	Diameter of smallest enclosing circle
D_i	Diameter of largest inscribed circle
l	Length of long axis
p	Perimeter of object
p_c	Perimeter of a circle having the same area as object
ww	Width of object perpendicular to long axis

6.4 EXISTING MEASURES OF SHAPE AND SIZE IN OPEN STOPE DESIGN

Clark and Pakalnis (1997) utilised the volume of over-break or under-break and the size of stope surfaces as a measure of stope performance, deriving *ELOS* and *ELLO* respectively. Clark and Pakalnis (1997) plot these measures on a stability graph, using modified stability number, N' , (Potvin 1988) versus “Hydraulic Radius”, which was intended to account for the “size and shape of the opening” (Mathews et al, 1981). The premise of this dilution approach is that, as the area of the stope surface is increased (i.e. an increase in Hydraulic Radius) and the rock mass quality is decreased, there should be a corresponding increase in the observed over-break, in this case represented by the *ELOS* parameter. All of these shape and size measures used in existing empirical stope stability methodologies, result in a “dimensional” parameter and therefore are termed “**scale-dependent**” measures.

ELOS and *ELLO* are a function of the geometry of over-break and under-break, as well as the geometry of the stope surface under consideration. It is therefore difficult to determine whether a change in the *ELOS* or *ELLO* parameter alone is due to a change in **Shape** or a change in **Size** of either the over-break/under-break or the stope surface. In light of this, Hydraulic Radius, *ELOS* and *ELLO* can be considered as poor measures of “Shape” or “Size”, or both “Size-and-shape”.

6.5 A SCALE INDEPENDENT MEASURE OF THE EXTENT OF OVER/UNDER-BREAK

As mentioned in the previous chapter, the intersection areas of over-break (A_{OB}) and under-break (A_{UB}) can define how extensive the over-break or under-break is across the stope surface under investigation. It is proposed to introduce a scale independent measure for ascertaining for the degree of areal coverage, or **extensivity**, of over/under-break;

$$X_{OB} = \frac{A_{OB}}{A_S} \quad (6.4)$$

$$X_{UB} = \frac{A_{UB}}{A_S} \quad (6.5)$$

An extensivity value approaching unity indicates that the over/under-break covers the majority of the stope surface. This can simply be considered as the percentage of the stope surface effected by over/under-break.

6.6 TWO DIMENSIONAL SHAPE MEASURES

The over-break (or under-break) volume that intersects a planned stope surface usually leaves a line of intersection. This line of intersection may be closed, or extend past the

edges of the nominal design surface boundary. Although there are a multitude of 2-dimensional shape descriptors, it is proposed to utilise a simple circularity measure for describing the 2-dimensional shape of these closed polygonal lines of intersection;

$$Circularity = \frac{4\pi A}{P^2} \quad (6.6)$$

where A and P are the total area and total perimeter, respectively, of the closed polygonal line(s) of intersection. This measure can be used to describe the two-dimensional of over-break and under-break as it intersects a slope surface, designated C_{OB} and C_{UB} , respectively. The reason for this proposed measure is the relative ease at which areas and perimeters can be established, compared to other measurements such as axial ratios, side or radial lengths. This especially true for irregularly shaped polygons. Alternatively, the shape of a polygon can be described by a circularity shape factor;

$$SF_c = \frac{A}{A_c - A_i} \quad (6.7)$$

where A_c is the area of the smallest enclosing circle, A_i is the area of the largest inscribed circle and A is the area of the object. Although this provides a measure of how compact and circular an object is, it can only be applied on individual fully enclosed shapes. Some typical 2-dimensional geometric shapes are characterised by the proposed circularity measure and compared to the number of individual side lengths making up the polygons and their compactness (see Figure 6.1). Generally, as the number of sides of an object increases (i.e. complexity and irregularity), the circularity decreases. Figure 6.1b highlights that as an object becomes more compact (i.e. resembling a circle) the circularity measure increases, as expected.

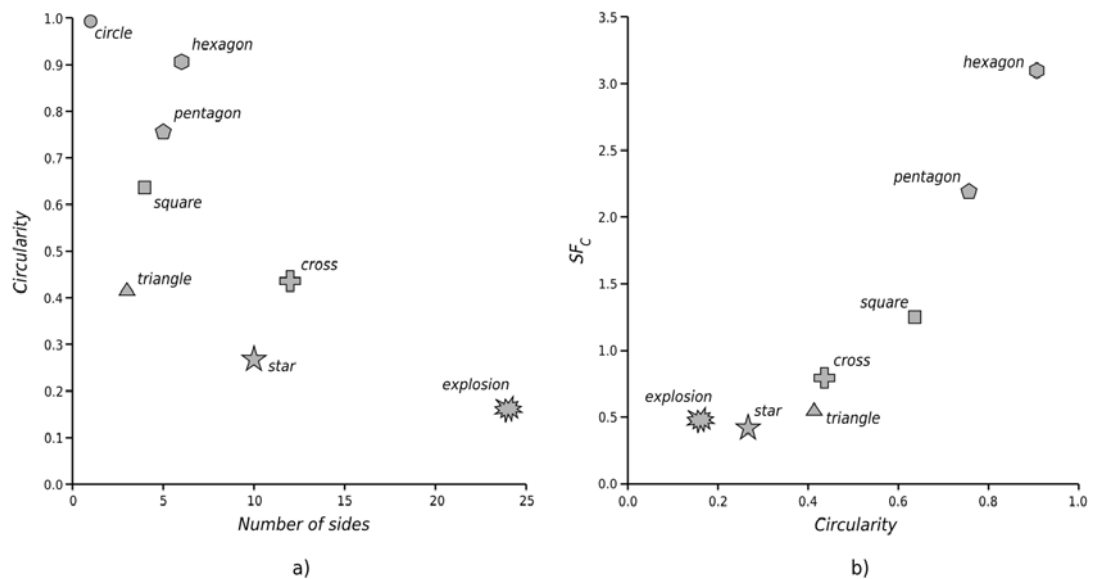


Figure 6.1 - Plots of a) proposed measure of *Circularity* versus number of sides and b) SF_c versus proposed *Circularity* measure, for a variety of 2-dimensional shapes

Where values of circularity fall below approximately 0.4, shapes are typified by highly irregular and/or elongated shapes. Above this value, shapes become more regular/polyhedral, with elliptical to circular shapes above 0.7.

6.6.1 Circularity

It is proposed to utilise the circularity measure to characterise the 2-dimensional shape of the over-break/under-break (as it intersects the slope surface), as well as the shape of the slope surface under investigation. The ratio between the circularity of the over/under-break and the circularity of the slope surface provides a measure for how similar these two shapes are to one another;

$$C_{OB}^R = \frac{C_{OB}}{C_S} \quad (6.8)$$

where C_{OB} is the circularity of over-break (C_{UB} for under-break) and C_S is the circularity of the slope surface. Where the circularity ratio is near unity, indicates that the 2-dimensional shapes of both the over/under-break and the slope surface are similar.

6.7 THREE-DIMENSIONAL SHAPE MEASURES

As seen in the previous sections, area and perimeter parameters can be utilised to devise shape descriptors to characterise the two-dimensional shape of specific geometries. However, difficulties arise in adequately characterising three-dimensional geometry using simple shape descriptors. A number of authors in the field of rock mechanics have used a variety of techniques to characterise the 3-dimensional geometry. For example, the Block Shape Characterization Method (Kalenchuk et al., 2006) takes into account two quantitative measures: the first, α , describes the shortening of the minor principal axis of a rock block while β describes the elongation of the major axis. The method also investigates the rock block volume distribution, to formally describe and classify both the size and shape distributions of a jointed rock mass assembly.

Instead of formally describing the size-and-shape of a rock block, Windsor and Thompson (1997) introduce a representative linear dimension, termed Equivalent Spherical Radius (*ESR*), using the surface area or volume of the rock block compared to radius of a sphere. The *ESR* value can be determined by two methods;

$$ESR = \left(\frac{A_{RB}}{4\pi} \right)^{\frac{1}{2}} \quad (6.9)$$

$$ESR = \left(\frac{3V_{RB}}{4\pi} \right)^{\frac{1}{3}} \quad (6.10)$$

where A_{RB} is total surface area of a rock block and V_{RB} is rock block volume. The *ESR* for a rock block can be determined by either equation. The resulting values from either equation will only be identical in the case of a sphere. In this case, by dividing *ESR* determined from the volume by that determined by surface area will provide a scale independent value, with a value of unity indicating a perfect sphere. The ratios of the *ESR* values derived from surface area and volume can therefore be used to provide a scale independent assessment of rock block shape.

6.7.1 Hemi-sphericity

It is proposed that a similar approach to the *ESR* rock block shape index be used to assess the shape of over-break or under-break. Instead of using a sphere, a hemisphere can be substituted. Here, it may be more appropriate to compare the flat basal area of the hemisphere or cross-sectional area (i.e. the area formed on a plane bisecting a sphere) to the volume of the hemisphere, and denote this as Equivalent Hemispherical Radius (*EHR*);

$$EHR = \left(\frac{A_c}{\pi} \right)^{\frac{1}{2}} \quad (6.11)$$

$$EHR = \left(\frac{3V}{2\pi} \right)^{\frac{1}{3}} \quad (6.12)$$

where A_c is base area and V is volume of a hemisphere. Dividing the *EHR* derived by volume with the *EHR* derived from basal area will result in unity for a hemisphere, with values higher indicating an elongated semi-ellipsoid (with major or semi-major axis perpendicular to the base area) and values lower than unity indicating flatter or prismatic shapes. It is proposed to define a simple scale independent measure to describe the three-dimensional shape relative to a hemi-sphere, and term this "hemi-sphericity";

$$Hemi-sphericity = \frac{\left(\frac{3V^s}{2\pi} \right)}{\left(\frac{A}{\pi} \right)^{\frac{3}{2}}} \quad (6.13)$$

where V^s is the intersected volume of over/under-break and A is the intersected area with the stope surface under consideration. It is proposed to utilise hemi-sphericity as a scale independent measure of the 3-dimensional shape of over-break and under-break, designated H_{OB} and H_{UB} , respectively, by using the intersected volume of over/under-break (V^s_{OB} and V^s_{UB}) and the intersected area with the stope surface under consideration (A_{OB} and A_{UB}).

It must be noted that relationship between hemi-sphericity and volume is not linear. For example, Figure 6.2 shows a plot of normalised volume versus hemi-sphericity for a

spherical segment. Indeed, a hemi-sphericity value below 0.2 represents a negligible volume compared to geometries with higher values.

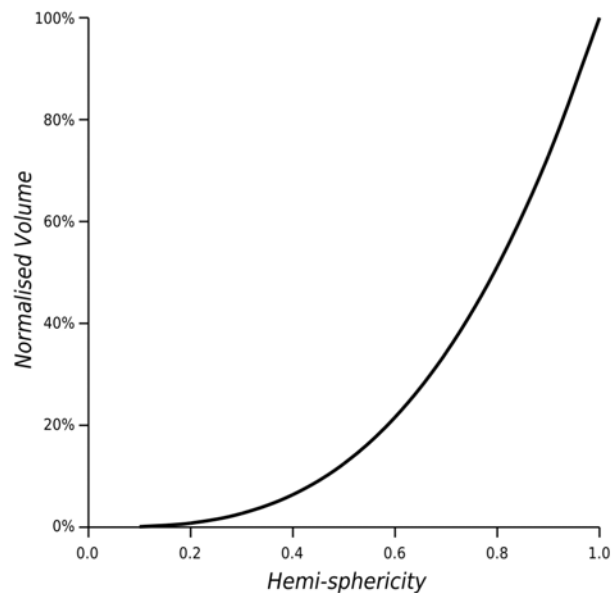


Figure 6.2 - Relationship between hemi-sphericity and normalised volume for a spherical segment

It can also be shown that the 3-dimensional shape of over/under-break is dependent, to some extent, on the 2-dimensional inter-sectional area of over/under-break. Figure 6.3 displays hemi-sphericity versus circularity for a number of example 3-dimensional geometrical shapes. Here, the 2-dimensional shape, as well as the apex heights (providing the third dimension), were varied to provide a large range of potential over-break geometries. It can be seen that, as the 2-dimensional inter-sectional area becomes more elongated or irregular (i.e. circularity decreases), the ability to generate deeper prismatic shapes decreases.

6.8 A GEOMETRICAL CLASSIFICATION OF OVER-BREAK AND UNDER-BREAK

In order to ascertain whether the over-break from one stope surface represents more favourable performance to the over-break from another stope surface, irrespective of the size of the two surfaces, one needs to compare the relative shapes and coverage of over-break across the respective stope surfaces. Intuitively, over-break that is deep and arcuate in shape and covers the entire stope surface represents more severe stope performance conditions than that represented by over-break that is thin and platy in shape and covers only a small portion of the stope surface.

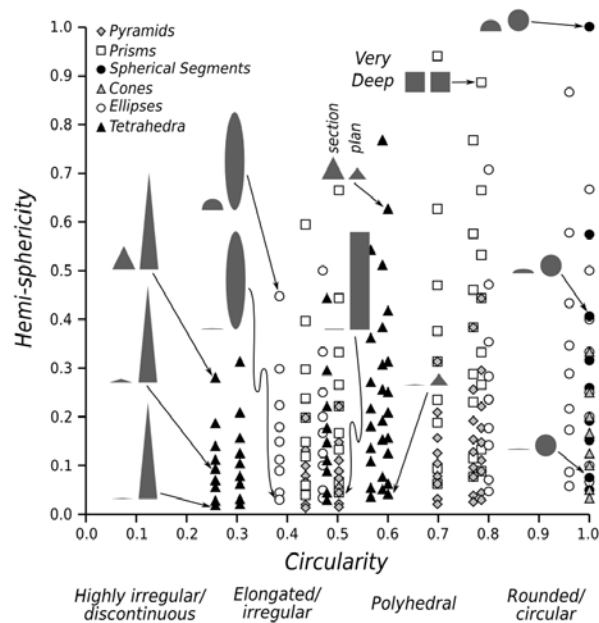


Figure 6.3 - Plot of hemi-sphericity versus circularity for some example 3-dimensional geometrical shapes

6.8.1 Inter-sectional Area

It is proposed to characterise the geometry of over-break and under-break firstly by the circularity and extensivity of the inter-sectional area. An example plot of circularity versus extensivity is shown in Figure 6.4, for a variety of example over-break shapes, together with a simple classification. It must be noted that total intersected areas and perimeters are utilised to calculate the circularity measure. In addition, the circularity ratio can be plotted against extensivity and can indicate where 2-dimensional over/under-break shapes have both similar shapes and similar relative sizes, with a value of unity for both measures indicating a perfect match between the over/under-break shape and the slope surface.

6.8.2 Hemi-sphericity and Circularity

It is proposed to utilise the hemi-sphericity parameter to characterise the “depth” of over-break or under-break. As shown previously in Figure 6.3, hemi-sphericity is to some extent dependant on the 2-dimensional shape, or circularity. In light of this, a classification based on hemi-sphericity and circularity is proposed and shown in Figure 6.5.

6.8.3 Relative Volume

It is also proposed to utilise the measures of extensivity and hemi-sphericity to evaluate the relative severity of over/under-break between two slope surfaces. In this regard, hemi-sphericity and extensivity of over/under-break for a slope surface can be evaluated relative

to the volume of a hemisphere with 100% extensivity;

$$Relative\ Volume = 2\pi \times Hemi-sphericity \left(\frac{Extensivity}{\pi} \right)^{\frac{3}{2}} \quad (6.14)$$

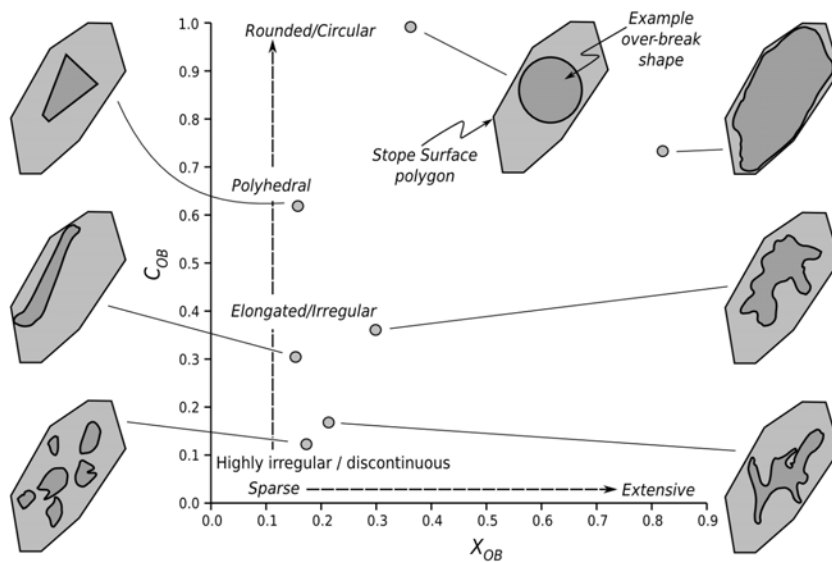


Figure 6.4 - Plot of Circularity versus Extensivity for some example 2-dimensional shapes of over-break shown with an example slope surface shape, together with a classification

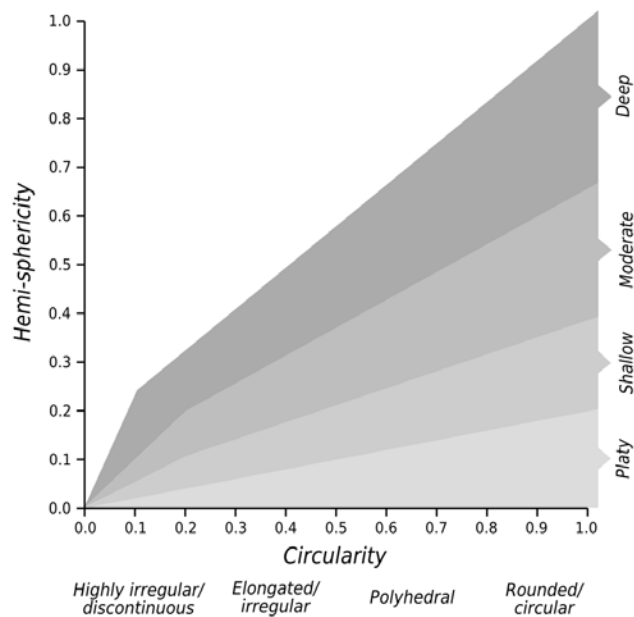


Figure 6.5 - Plot of hemi-sphericity versus circularity with a generalised shape classification

The relative volume can be used to quantify and subsequently classify relative stope performance, irrespective of scale. A simple stope performance classification, based on relative volume, is shown in Table 6.2. It must be noted that this classification has not been optimised for the economic and production constraints for any particular mine and is for illustration purposes only.

Table 6.2 - Stope Performance Classification based on Relative Volume

Relative Volume	Stope Performance Classification
<0.02	Very Good
0.02 - 0.05	Good
0.05 - 0.1	Fair
0.1 - 0.2	Poor
0.2 - 0.5	Very Poor
>0.5	Exceptionally Poor

The geometrical measures defined above have been applied to stope performance data from a recent geometrical back analysis study of open stopes at BHP Billiton's Cannington mine (Coles, 2007). A total of 76 stope surfaces were analysed. It must be noted that the stope surfaces analysed came from a variety of mining blocks across the mine, each with differing rock mass conditions, cable reinforcing intensities, extraction ratios and degrees of local rock mass damage. However, the emphasis of this exercise was to verify that the proposed shape measures could provide a useful scale independent assessment of stope performance.

Figure 6.6 displays the results of the various shape measures applied to the back analysed stope surfaces. A number of example *CMS* geometries and design surfaces have been highlighted, labelled A to F and represented graphically in Figure 6.6c. It must be noted that these shapes have been re-scaled to similar sizes. A summary of the shape measures for the labelled example stope surfaces, together with a brief description based on the simple classifications provided for in Figure 6.4 and Figure 6.5, is shown in Table 6.3. From Table 6.3 and Figure 6.6c, it can be seen that the classifications based on the proposed shape measures are in good agreement with the observable geometries of over-break.

The proposed shape measures and stope performance classification have also been applied to stope performance data collected at Barrick Australia's Kanowna Belle Gold Mine (Magee, 2005; Malatesta, 2006). Stopping activity at Kanowna Belle has been divided into a number of mining blocks with depth. A comparison of stope performance between a number of mining blocks, namely; Block A, Block C and Block D.

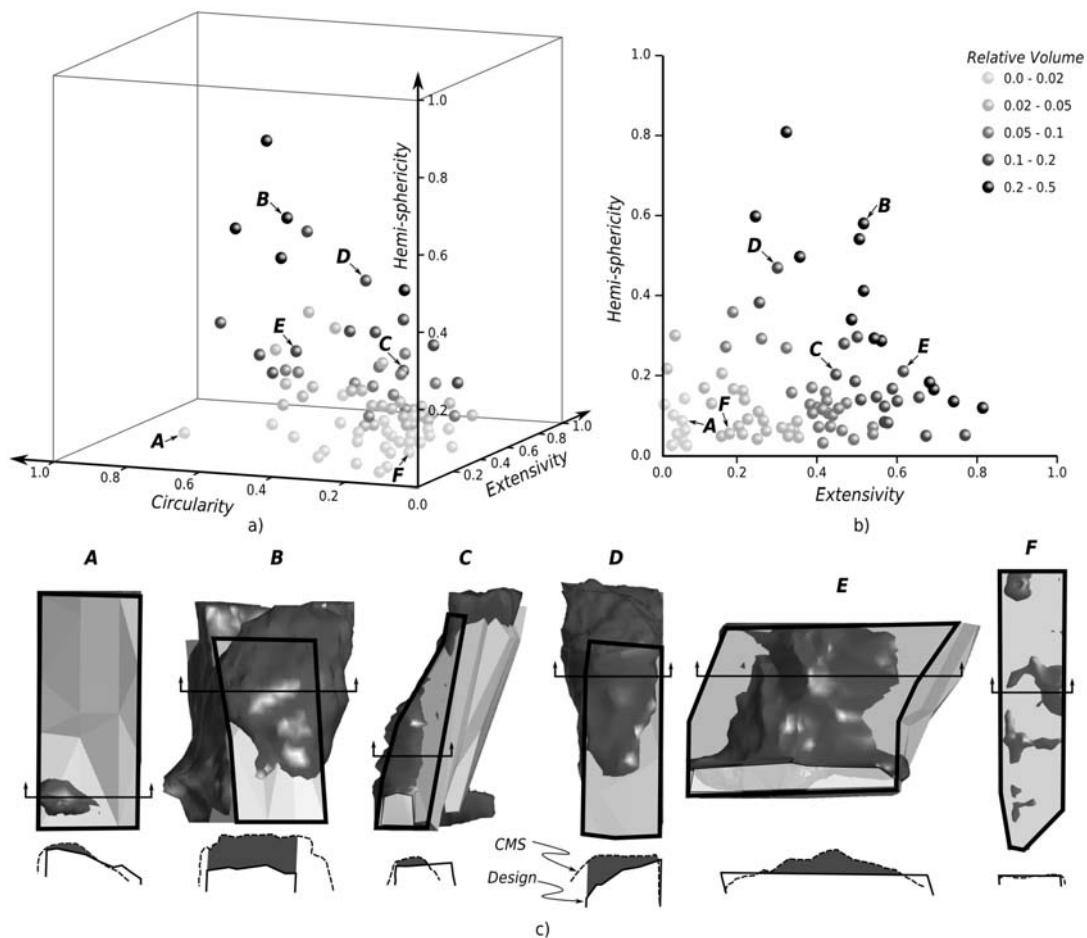


Figure 6.6 - Stope surface over-break at Cannington mine plotted by a) hemi-sphericity, circularity and extensivity, b) hemi-sphericity versus extensivity (classified by Relative Volume), and c) re-scaled example stope surfaces (labelled A-F) shown in elevation and cross-section with CMS and design profiles

Block A typically contains large, multi-lift primary-secondary stopes (approximately 120m in height), ranging from 20 to 30m in length and up to 35m wide. Primary stopes were typically filled with cemented rock fill, with secondaries filled with rock fill. Block C stopes are generally much smaller than Block A stopes, with stopes heights ranging from 40m to 100m, lengths from 15m to 20m with stope widths generally around 20m. These stopes were initially mined in a 1-3-5 sequence, then the sequence switch to a centre-out pyramidal sequence to control stress-related production issues and dilution. Block D stopes typically are smaller than both Block C and Block A stopes, with sizes ranging from 30m to 65m in height, with stope widths around 20m. Block D stopes are mined in a bottom-up centre-out pyramidal sequence, with stopes filled with cemented pastefill. In addition, in thicker sections of the orebody, stopes are mined in panels (up to 3), from the hangingwall to the footwall.

Table 6.3 - Summary of over-break shape measures and performance classification for example stope surfaces shown in Figure 6.6

Example	Extensivity	Circularity	Hemi-sphericity	Relative Volume	Shape and Performance Classification
A	0.06	0.66	0.09	0.001	Sparse, polyhedral, platy to shallow - Very good performance
B	0.51	0.56	0.58	0.239	Moderately extensive, irregular to polyhedral, very deep - Very poor performance
C	0.44	0.22	0.20	0.068	Sparse, highly irregular/discontinuous, moderately deep - Fair performance
D	0.30	0.26	0.47	0.087	Sparse to moderately extensive, elongated/irregular, very deep - Fair performance
E	0.61	0.58	0.21	0.116	Moderately extensive, irregular, moderately deep- Poor performance
F	0.18	0.09	0.05	0.005	Sparse, highly irregular/discontinuous, shallow - Very good performance

Figure 6.7 shows the distribution of performance parameters for stope surfaces for Blocks A, C and D at Kanowna Belle. The box plots represent 10%, 25%, 50%, 75% and 90% percentiles, with outliers presented as markers. Visual analysis of *CMS* profiles indicate that over-break in Block A is typically manifested as irregular, patchy and discontinuous zones, typically of very shallow depths. These zones, however, can be quite extensive over the stope surface. On rare occasion, over-break is manifested by irregular elongated zones of over-break, corresponding to over-break along large-scale geological structures where local rock mass quality is poor. Figure 6.7 reflects this qualitative assessment, with Block A stope surfaces generally exhibiting low circularity, moderate to high extensivity, and generally very low hemisphericity. An assessment of stope performance for each mining block, based on relative volume is shown in Figure 6.8 and Table 6.4. Stope surfaces displaying relative volumes in excess of 0.1 and 0.2 can generally be considered as displaying “poor” and “very poor” performance, respectively. It can be seen that, despite Block A stopes being much larger than Block C and Block D stopes, the stopes from this mining block performed much better, with a probability of not more than 2.4% of stopes classified as poor, and no more than 2.3% classified as “very poor”. This compares to Block C and D which both display similar performance, with at least 16% of stopes displaying “poor” performance and at least 7% displaying “very poor” performance.

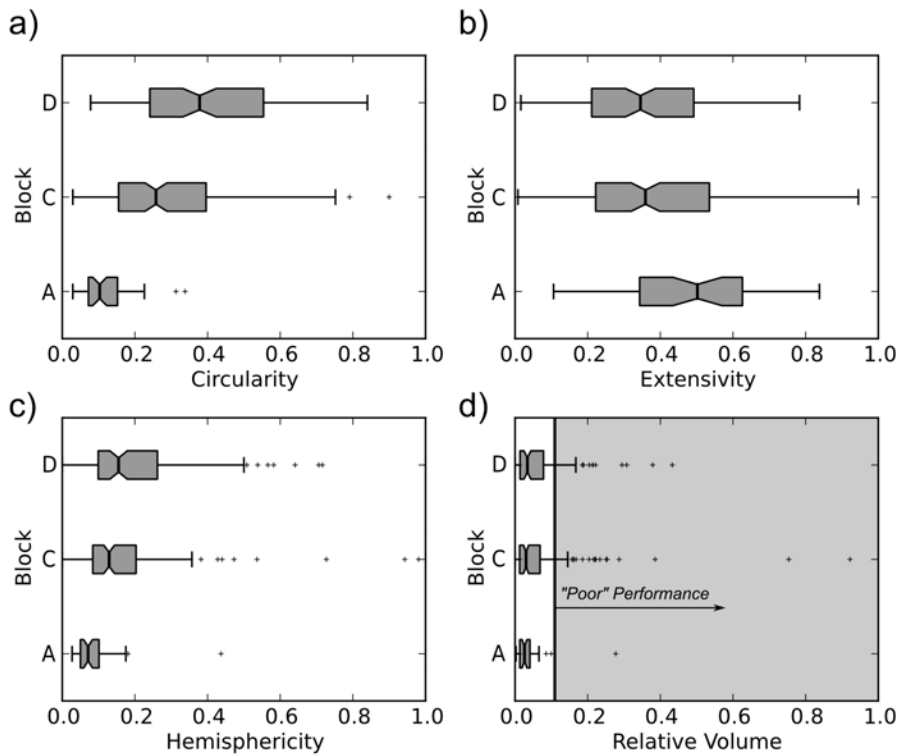


Figure 6.7 - Box plots displaying statistical distribution of scale independent stope performance parameters (for over-break) for various mining blocks at Kanowna Belle Gold Mine.

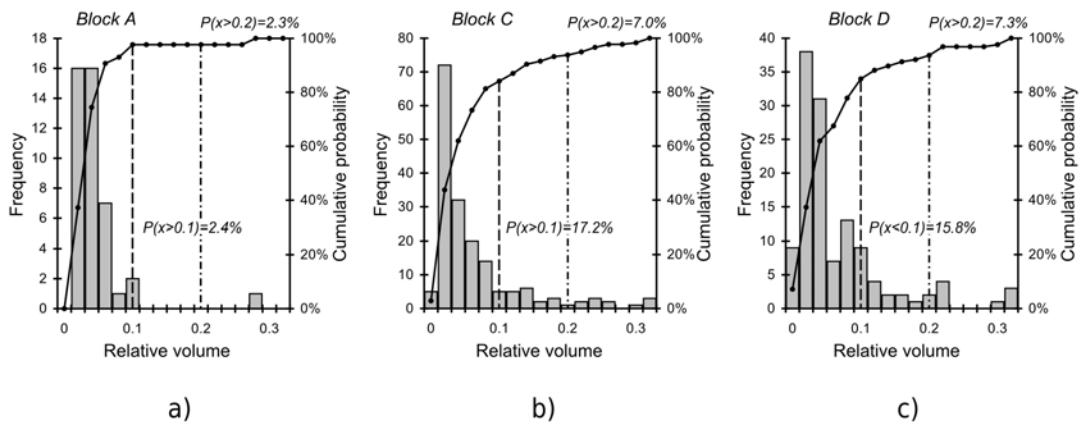


Figure 6.8 - Frequency-probability plots of Relative volume of over-break on stope surfaces for (a) mining Block A, (b) Block C, and (c) Block D at Kanowna Belle Gold Mine.

Figure 6.8 also shows that Block D stopes, although having very similar performance (in terms of relative volume) to Block C stopes, over-break is generally more circular or rounded and less extensive than Block C. The tail of the relative volume distribution also shows that there are more outlier stopes that exhibit much deeper over-break than other mining blocks.

Table 6.4 - Summary of stope performance by mining block based on Relative volume

Block	No. of surfaces	P (X > 0.1) “Poor” performance	P (X > 0.2) “Very poor” performance
A	43	2.4%	2.3%
C	157	17.2%	7.0%
D	114	15.8%	7.3%

6.9 CONCLUSIONS

Traditional stope performance measures that rely on dimensional parameters, such as *ELOS*, are unable to accurately make performance comparisons for stope surfaces of vastly differing sizes. In addition, these measures do not describe certain geometrical aspects of over/under-break, such as shape. Indeed, ***it is difficult to determine whether a change in ELOS is due to a change in “shape” or a change in “size” of either the over-break/under-break or the stope surface.***

This chapter has proposed a number of geometrical performance measures that can be obtained from measuring a number of quantifiable parameters of over/under-break, such as intersectional area, perimeter and volume. Importantly, the proposed geometrical measures offer significant advantages over traditional performance measures in that they are;

- Quantifiable - (c.f. performance measures in existing empirical techniques)
- Scale Independent - quantification of the relative performance of stope surfaces, irrespective of their size.
- Shape Descriptors - provide additional shape information that can be used to assist in rock reinforcement design.

Statistical analysis of the proposed measures can also provide detailed information on the shape of over/under-break. This information can possibly be used to provide useful insights into the mechanisms involved. For example, high circularity, high extensivity, high hemisphericity stope surfaces may indicate stope surfaces affected by significant rock mass failure, whereas low circularity, low extensivity, high hemisphericity may indicate localised block instability.

CHAPTER 7 - CONTINUUM BASED NUMERICAL MODELLING IN OPEN STOPE MINE DESIGN

7.1 INTRODUCTION

Excavation design is based on a sound understanding of the potential rock mass failure modes that may potentially de-stabilise and effect excavation performance. Failure modes generally can be classified into; failure through the rock mass substance, or by translation and rotation of rock blocks, or by some combination of both. The design engineer needs to assess the likely modes of failure using a variety of tools at their disposal. Numerical methods are generally favoured over analytical methods and empirical methods as they are capable of simulating some of these modes of failure to various degrees. In addition, they are capable of incorporating additional complexities over analytical and empirical methods, such as; effects of *in situ* and induced stresses, complex excavation geometries, non-linear behaviour, material anisotropy and the influence of complex rock structure.

Although there are a number of numerical modelling approaches that can be adopted, the practical use of numerical modelling in regular open stope design is limited by a number of factors. Ultimately, the choice of modelling approach is constrained by;

- the features of the numerical code and availability of input data.
- the ability of the selected code to adequately model the rock mass characteristics and anticipated rock mass behaviour.
- complexity of problem geometry - whether the problem geometry can be satisfactorily represented in two dimensions or whether a three-dimensional approach is required.
- the complexity of model construction, general ease of use of modelling package and licensing costs.
- the availability of experienced staff capable of constructing and analysing the results of models in view of the assumptions and limitations of the specific code used.
- the availability of adequate computing resources to enable multiple runs within time constraints.

The following sections briefly describe some of the issues regarding numerical modelling in the design of excavations, particularly with respect to current open stope mine design practice.

7.2 CONTINUUM AND DISCONTINUUM NUMERICAL MODELS

The most popular numerical methods for mining applications are continuum and discontinuum methods. Hybrid methods are generally impractical for regular use and are typically only used for specialist stand alone models. A comparison of the main numerical methods is provided in Table 7.1 (Coggan et al., 1998).

Table 7.1 - Comparison of Numerical Methods (modified after Coggan et al, 1998)

Analysis Method	Critical Parameters	Advantages	Limitations
Continuum Modelling (e.g. Boundary element, Finite element, finite difference)	Representative stope geometry; constitutive criteria (e.g. Elastic, elasto-plastic, creep, etc.), groundwater characteristics, shear strength of discontinuities, <i>in situ</i> stress state	Allows for material deformation and failure (factor of safety concepts incorporated), can model complex behaviour and mechanisms, 3-D capabilities, creep deformation and/or dynamic loading, able to assess effects of parameter variations, computer hardware advances allow complex models to be solved with reasonable run times	User must be well trained, experienced and observe good modelling practice, need to be aware of model and software limitations (e.g. Boundary effects, mesh dependency, hardware memory and time restrictions), availability of input data generally poor, required parameters not routinely measured inability to model effects of highly jointed rock, can be difficult to perform sensitivity analysis due to run time constraints.
Discontinuum Modelling (e.g. Distinct element, discrete element)	Represent stope and discontinuity geometry, intact constitutive criteria, discontinuity stiffness and shear strength, groundwater characteristics, <i>in situ</i> stress state	Allows for block deformation and movement of blocks relative to each other, can model complex behaviour and mechanisms (combined material and discontinuity behaviour coupled with hydro-mechanical and dynamic analysis), able to assess effects of parameter variations on instability.	As above, user required to observe good modelling practice, general limitations similar to those above, need to be aware of scale effects, need to simulate representative discontinuity geometry (spacing, persistence, etc.), limited data on joint properties available (e.g. J_{k_1} , J_{k_2}).
Hybrid Modelling	Combination of input parameters listed above for stand-alone models	Coupled finite-/distinct element models able to simulate intact fracture propagation and fragmentation of jointed and bedded rock.	Complex problem geometry require high memory capacity, comparatively little practical experience in use, requires ongoing calibration and constraints.

From a practical point of view, discontinuum models tend to be more cumbersome than continuum methods, generally requiring more input parameters than are usually available on most mines. Another important aspect to consider with popular discontinuum codes, such as *UDEC* (Itasca Consulting Group Inc, 1984) and *3DEC* (Itasca Consulting Group Inc, 1988), is that they are more suitable for rock masses that are characterised by a high percentage of fully formed rock blocks. Continuum methods therefore tend to be more popular, with the most popular three-dimensional *BEM* codes being *Map3D* (Wiles, 1993) and *Examine^{3D}* (Rocscience, 1990). However, there are a number of aspects of continuum methods that limited their reliability in being able to accurately capture the rock mass behaviour. In this respect, the applicability and use of continuum methods in all aspects of open stope design needs to be continually assessed by the design engineer.

7.2.1 Excavation Scale and Rock Mass Structure

As alluded to in Chapter 2, the fundamental choice of continuum over discontinuum approaches can be related to the anticipated rock mass behaviour which depends on the intensity and arrangement of discontinuities with respect to the scale of the excavation. In order for the design engineer to assess the applicability of a continuum approach, it is therefore necessary to find the optimum excavation scale such that the discontinuities and the intact rock material can be treated as an “equivalent continuum” for the rock mass.

Hoek (1988) suggests that equivalent continuum failure criteria, such as the Hoek-Brown failure criterion (Hoek and Brown, 1980), should only be used when the span or height is at least two-three times the discontinuity spacing. It is also acknowledged that the Hoek-Brown failure criterion does not provide a parameter for spacing of discontinuities or excavation size and suggest that it is up to the user to decide on the applicability of its use (Hoek, 1988). Elmo and Stead (2010) also investigated the influence of scale and discontinuity intensity on the results from numerical modelling. The authors integrated *DFN* models with 2-dimensional hybrid finite element/discrete element code to model pillar behaviour. Although their work was conducted only under 2-dimensions, the authors demonstrated that two-dimensional discontinuity intensity (P_{21}) can be used to assess strength reduction due to scale effects and that P_{21} can be used to determine the *REV* for a given combination of excavation scale and discontinuity geometries (see Figure 7.1).

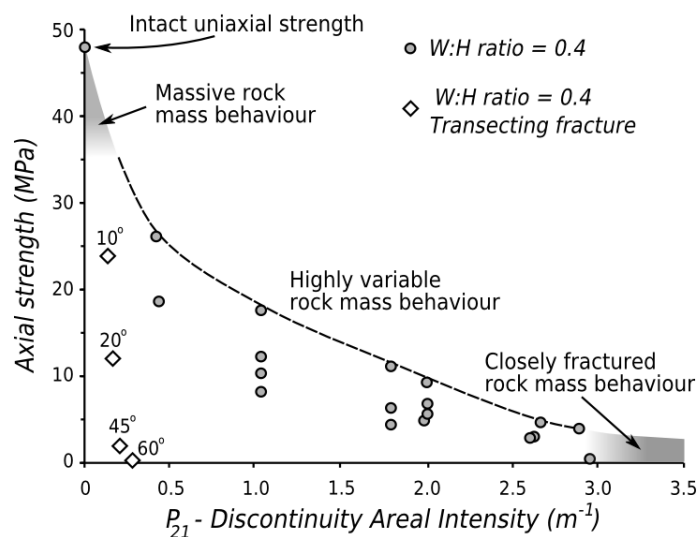


Figure 7.1 - Relationship between P_{21} and Axial strength reduction of modelled pillars (after Elmo and Stead, 2010)

It must be noted that it may not be possible to practically evaluate the *REV* for a given excavation geometry using the approach above, as discontinuity areal intensity values (P_{21})

may not be available. In this case, discontinuity linear intensity (P_{10}) may be used in lieu, providing an appropriate C_{p2} can be estimated. In addition, to make this approach more amenable for span design, an alternative to pillar width:height ratio needs to be provided to assess the influence of excavation scale relative to discontinuity intensity.

The modelling results from Elmo and Stead (2010) were re-evaluated in order to assess the influence of discontinuity intensity on strength variability, rather than strength reduction. Strength coefficient of variation values were calculated based on grouping modelling results with similar pillar width:height ratios and P_{21} values. The results were then plotted as a function of coefficient of variation versus the discontinuity linear intensity with respect to pillar width or critical span (i.e. discontinuities per span). For this analysis a C_{p2} value of 2.0 was selected to convert P_{21} value to P_{10} values. Figure 7.2 shows that there is significant strength variability between 1.0 and 7.0 discontinuities per span, with variability generally consistently lower after around 10 discontinuities per span.

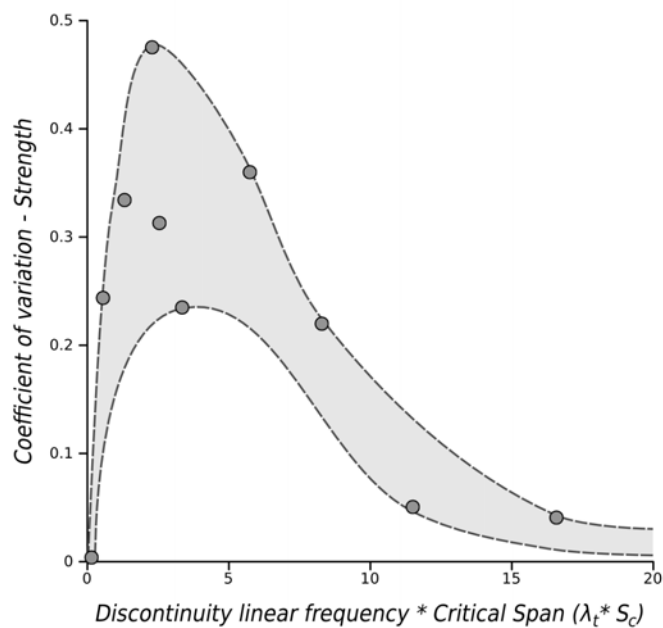


Figure 7.2 - Strength variability as a function of discontinuity linear intensity and critical span. Data based on Elmo and Stead (2010)

Board (1989) also investigated the role of discontinuity intensity and excavation scale using discontinuum modelling. The results suggest that where discontinuity spacing to excavation radius ratios are less than 0.1 (i.e. 10 discontinuities per span) failure representing continuum yield can be approximated. Under these conditions it may be appropriate to model the rock mass as an “equivalent continuum” (Board, 1989).

It is therefore recommended that, for each “equivalent continuum” model constructed, the scale of the excavations, with respect to the geometry of the discontinuity system, is checked in order to gauge the appropriateness of the approach, and hence the likely reliability of the model in predicting the anticipated rock mass response.

7.3 EQUIVALENT CONTINUUM MODELLING

'Failure' of the rock mass can be defined and described in a number of ways. From a structural point of view, failure is the condition at which rock mass ceases to fulfil its functional purpose or reaches a critical limit state. The actual mechanisms involved in 'failure' can be quite complex, ranging from fracturing, buckling, rupturing, creep and yielding. Mechanisms can also be described whether they occur dynamically or statically. For equivalent continuum modelling in rock engineering design, one typically has to assume a relatively simple static yielding 'failure' mechanism.

Of fundamental importance in equivalent continuum modelling is to define or quantify under what conditions the rock mass 'fails' and its subsequent behaviour after failure. Firstly, the constitutive behaviour of the material needs to be selected. The constitutive behaviour is of primary interest as it provides the relation between stresses and strains that can be sustained by the rock mass. Secondly, we need to postulated a failure mechanism (i.e. yield) and derive a model that defines the 'failure' threshold, which is typically based on;

- A critical stress state
- A critical strain state
- A critical energy input

7.3.1 Constitutive Models

Constitutive relationships can range from simple isotropic linear elastic models to anisotropic non-linear inelastic models. Simple isotropic models are generally preferred over anisotropic models. This is mainly due to the fact that the anisotropic elastic constants are generally impractical to obtain (21 independent elastic constants versus 2 for isotropic media). However, some interesting research has been conducted using the fracture intensity tensor as a means to determine the elasticity tensor (Oda et al, 1986; Kulatilake et al, 1993). Another important characteristic of the constitutive model is whether the material behaves linear elastically or inelastically. From Figure 7.3 it can be seen that all models generally behave in a linear elastic fashion up to some critical strain value ($\epsilon_{critical}$). With the linear elastic model, the stress increases linearly with increasing strain, however non-linear inelastic models are incapable of sustaining stress in this fashion. For the non-linear inelastic

model, the strain at peak stress (ϵ_f) can be significant. The choice of constitutive model is therefore extremely important when trying to understand the post-yield behaviour of rock masses.

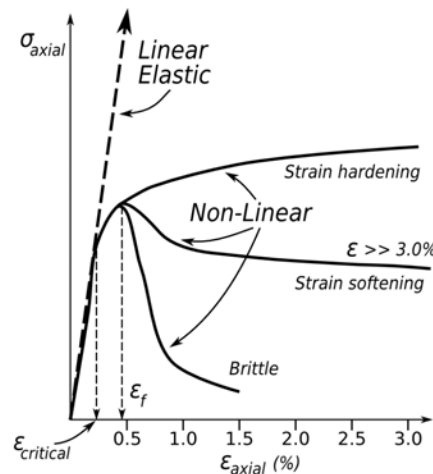


Figure 7.3 - Influence of constitutive model on stress-strain relationships

7.3.2 Rock Mass Failure Criteria

For the purposes of excavation design using equivalent continuum yield models, the following definitions of 'failure' may be used;

- **Damage** - rock mass damage is the irrecoverable static strain. Dynamic strains (i.e. due to blasting, etc.) are not considered.
- **Peak Strength** - in terms of static stress-based criteria, peak strength is the ultimate stress level that the rock mass can sustain.
- **Yield Strength** or **Critical Strain** - the point at which the rock mass material is observed to display non-linear behaviour, expressed in either terms of stress (strength) or strain. It must be noted that, depending on the constitutive properties and other parameters, the difference between the critical strain and the strain at peak stress (strength) can quite substantial (see Figure 7.3).

There are a number of 'failure' criteria used in rock engineering and can be classified as follows;

- Theoretical or Empirical;
 - Theoretical models are closely related to those developed in the field of materials engineering, which postulate yield mechanisms for ductile and brittle materials. These theories consider concepts such as distortion energy, maximum principal strain, total strain energy, linear elastic fracture mechanics (Drucker and Prager, 1952; Griffith, 1921; Tresca, 1864; von

Mises, 1913).

- Empirical models are those that do not assume a known failure mechanism, yet simply fit a mathematical model to observed phenomenon. A number of empirical peak strength criteria for intact rock and rock masses are shown in Table 7.3.
- Yield or Peak Strength - Yield criteria define the onset of non-linear behaviour. Due to the difficulty in empirically determining the yield point for rock masses, yield criteria for rock masses are generally theoretical, whilst the majority of peak strength criteria in rock engineering are empirical.
- Linear versus non-linear - the shape of the line/surface defining the failure criterion.
- Representative stress space - yield or peak strength criteria can be expressed or visualised in a number of stress spaces;
 - Normal and shear stresses - an example is the Mohr-Coulomb criterion.
 - Principal stresses;
 - Maximum and minor principal stresses only (σ_1, σ_3 principal stress space) - the influence of the intermediate stress is ignored. An example is the Hoek-Brown failure criterion (1980).
 - Maximum, intermediate and minor ($\sigma_1, \sigma_2, \sigma_3$ principal stress space), sometimes termed "three-dimensional" stress space.
 - Other stress spaces;
 - First, second and third invariants to the Cauchy stress
 - Haigh-Westergaard stress coordinates

7.3.3 Summary

Due to the difficulty in determining the various parameters in more sophisticated non-linear/inelastic constitutive models and for the various theoretical yield criteria, practical rock engineering equivalent continuum modelling tends to rely on simple empirical models. Constitutive models are generally isotropic linear elastic, with the elastic parameters derived empirically. As it is almost impossible to derive the yield point from large scale *in situ* tests, empirical elastic parameters are based on deformation modulus (i.e. include both pre-peak elastic and inelastic strains). Failure criteria in equivalent continuum modelling in rock engineering predominantly tend to be empirical, non-linear and based on peak strength. These are typically represented in (σ_1, σ_3) principal stress space which is considered largely to be a function of the triaxial methods used to derive them.

7.4 EMPIRICAL DEFORMABILITY AND PEAK STRENGTH FAILURE CRITERIA FOR ROCK MASSES

A number of empirical constitutive models and peak strength criteria have been developed to model the deformability and strength characteristics of intact rock and rock masses. These methods are based on the results of laboratory tests on various rock types at a limited number of scales and at a range of triaxial confining stresses, as well as a number of large-scale *in situ* tests. A number of empirical relationships for deformation modulus and peak strength failure criteria are shown in Table 7.2 and Table 7.3.

Table 7.2 - Empirical relations of deformation modulus of rock masses (Li, 2004)

Empirical Relation	Reference	Equation
$E_m = 2RMR_{76} - 100$ ($RMR > 50$) (GPa)	(Bieniawski, 1978)	(7.1)
$E_m = 25 \log Q$ ($Q > 1$) (GPa)	(Barton et al., 1980)	(7.2)
$E_m = 10^{(RMR_{76} - 10)/40}$ (GPa)	(Serafim and Pereira, 1983)	(7.3)
$\frac{E_m}{E_d} = 0.0028 RMR^2 + 0.9 e^{RMR_{89}/22.82}$ (%)	(Nicholson and Bieniawski, 1990)	(7.4)
$\frac{E_m}{E} = 0.5 [1 - \cos(\pi * RMR_{89}/100)]$	(Mitri et al., 1994)	(7.5)
$E_m = \sqrt{\frac{\sigma_c}{100}} 10^{(GSI - 10)/40}$ ($\sigma_c < 100$ MPa)	(Hoek and Brown, 1997)	(7.6)

For the equations listed in Table 7.3, a , a' , b' , α , m_i , m_b , and s are constants used to statistically fit empirical data, together with the intact rock uniaxial compressive strength (σ_c) and tensile strength (σ_t). The Generalised Hoek-Brown (1997) failure criterion is popular as it allows for the constants m_b , a and s to be estimated from rock mass classifications.

The heavy reliance of these failure criteria on laboratory tests (which involve contrived boundary and loading conditions at small scales) severely limited their ability to accurately predict mining induced rock mass response, which may involve all manner of loading conditions (such as stress rotation, confinement loss, etc.). This is especially true for rock mass failure close to excavation boundaries where excavation geometry can have a significant influence on *in situ* boundary conditions.

Table 7.3 - Empirical peak strength failure criteria for intact rock and rock masses (after Li, 2004)

Criterion	Reference	Equation
$\sigma_1 = \sigma_c \left(1 + \frac{\sigma_3}{\sigma_c} \right)^{b'}$	(Sheorey et al., 1989)	(7.7)
$\sigma_1 = \sigma_c + \sigma_3 + a' \sigma_3^{b'}$	(Hobbs, 1964)	(7.8)
$(\sigma_1 - \sigma_3)^2 = a' + b'(\sigma_1 + \sigma_3)$	(Fairhurst, 1964)	(7.9)
$\sigma_1 = \sigma_c + a' \sigma_3^{b'}$	(Murrel, 1965)	(7.10)
$\sigma_1 = \sigma_c + a' \sigma_3$	(Bodonyi, 1970)	(7.11)
$\sigma_1 = \sigma_3 + a'(\sigma_1 + \sigma_3)^{b'}$	(Franklin, 1971)	(7.12)
$\frac{\sigma_1}{\sigma_c} = a' + b' \left(\frac{\sigma_3}{\sigma_c} \right)^\alpha$	(Bieniawski, 1974); (Yudhbir et al., 1983)	(7.13)
$\sigma_1 = \sigma_3 + (m_i \sigma_c \sigma_3 + s \sigma_c^2)^{1/2}$	Hoek and Brown, 1980	(7.14)
$\sigma_1 = \sigma_3 + a' \sigma_3 \left(\frac{\sigma_c}{\sigma_3} \right)^{b'}$	(Ramamurthy et al., 1985)	(7.15)
$\sigma_1 = \sigma_3 + \sigma_c \left(m_b \frac{\sigma_3}{\sigma_c} + s \right)^a$	Hoek and Brown, 1997	(7.16)

Nevertheless, empirical methods can provide approximations of deformation modulus and peak rock mass strength under similar loading conditions (i.e. monotonic increase in maximum principal stress) and are useful as a starting point where no previous rock mass response data exists. This latter aspect makes criteria such as the Hoek-Brown criteria (1990;1997) especially popular for initial design purposes. For rock mass deformability, Li (2004) recommends the use of Serafim and Pereira (1983) (equation 7.3) where $\sigma_c \geq 100\text{MPa}$, and Hoek and Brown (1997) (equation 7.4) where $\sigma_c < 100\text{MPa}$.

7.5 CONTINUUM BASED BACK ANALYSIS

Effective utilisation of continuum modelling requires deriving a reliable rock mass response model. Generally, this can be assisted to some degree by conducting a site specific back analysis where observable rock mass behaviour is correlated to outputs from an assumed model. Back analysis fundamentally involves using measured displacements from instrumentation, such as extensometers, to derive mechanical properties of the rock mass such as deformability (Sakurai, 1981). In forward analysis, all input parameters, boundary conditions and excavation geometries are given, and assuming a particular failure model, the uniqueness of the solution (i.e. calculated stresses and strains, etc.) is guaranteed. However, in back analysis, we are given the rock mass response (i.e. displacements, stresses and strains from instrumentation) and excavation geometry only, with no knowledge of the correct failure model. In some circumstances we are only provided with

limited data, such as displacement data on the excavation surface. In back analysis, the same observed response may potentially be derived using a variety of failure models (i.e. continuum or discontinuum) and from a range of input parameters. In other words, the uniqueness of the solution in back analysis cannot be confirmed (Sakurai, 1997). This concept is illustrated in Figure 7.4.

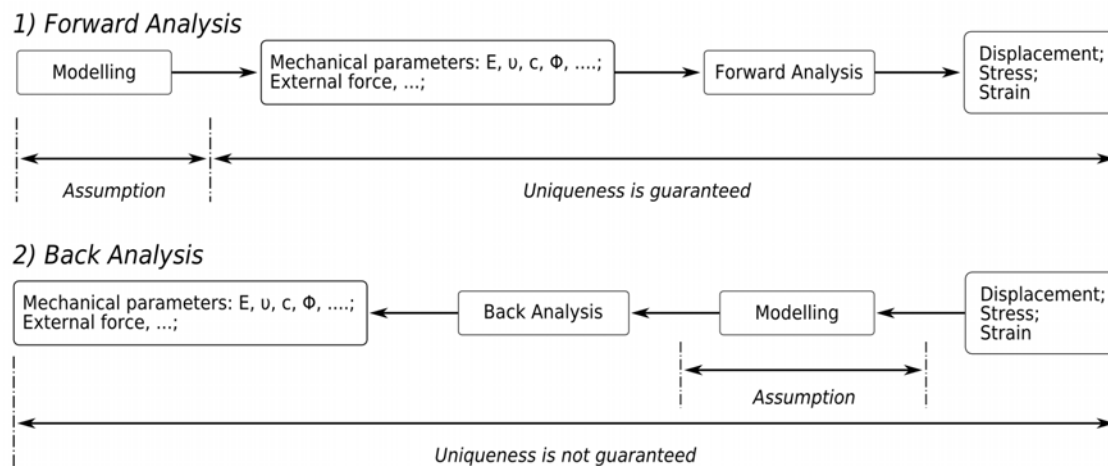


Figure 7.4 - Differences of forward and back analyses (Sakurai, 1997)

This highlights the importance of determining the most appropriate failure mode for the observed rock mass response, and also suggests that “equivalent continuum” modelling may not be able to provide the optimal solution.

7.5.1 Site-Specific Linear Elastic Damage Models

Due to the relative ease of use, linear elastic *BEM* modelling packages (such as *Examine^{3D}* and *Map3D*) are commonly used in the Australian mining industry for open stope design and back analysis studies. Linear elastic continuum models for stress related damage, and their impact on excavation and performance have been proposed by numerous authors (Baczynski, 1980; Diederichs et al., 2004; Martin, 1997). It has been suggested (Wiles, 2001) that rock mass damage can be related to the relative level of linear elastic over-stressing (Figure 7.5). These various stress levels are dependant on site specific parameters and it is suggested that they can be correlated using observed response and the results from numerical modelling. This model anticipates that below a site specific damage threshold the response is elastic and usually very little damage can be observed. As the level of over-stressing is increased, the observed damage (i.e. irrecoverable strain) should increase, leading to a zone of potential over-break (*POB*). Increased over-stressing beyond this level may cause stress driven failures and eventually the rock mass may become unsupportable.

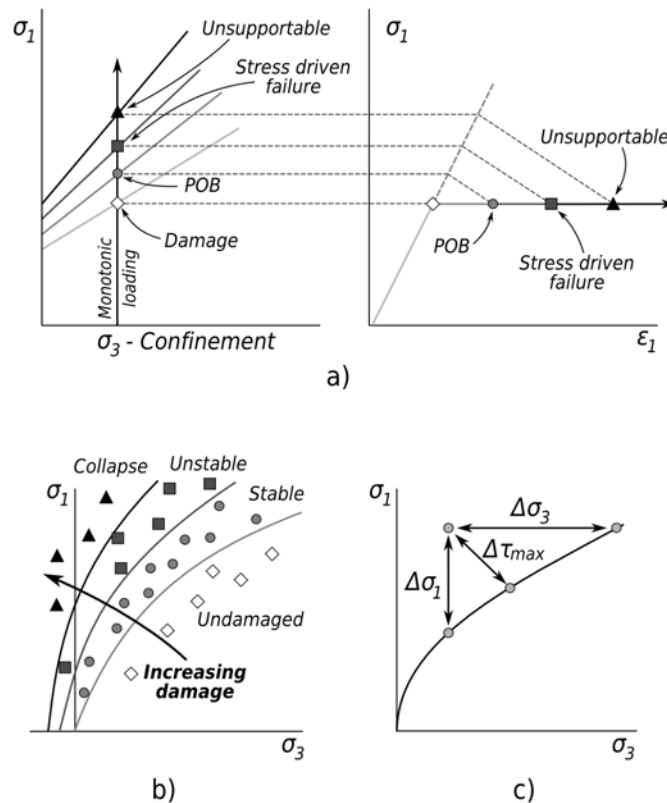


Figure 7.5 - a) Linear elastic stress damage model (after Wiles, 2001) for monotonically increasing stresses, together with assumed strain damage, b) generalised damage model (after Wiles, 2001) and c) showing various stress paths to over-stressing

Wiles (2001) proposed that this methodology could be incorporated into a comprehensive back analysis technique to assist in quantitative mine design (Figure 7.5b). Using criteria developed from back analyses, numerical modelling can then be used in a forward analysis to identify the location of extent of each “damage level” for various mining configurations and layouts, and as such, assist in mine planning activities. The fundamental assumption with the linear elastic “damage criteria” method is that there is a *direct correspondence* between the amount of over-stressing to the amount of damage observed.

Stress Path To Failure

The damage model illustrated in Figure 7.5a assumes that the level of overstressing is a direct cause of monotonic increase in σ_1 , whilst confinement (σ_3) is kept constant. However, the stress path experienced by the rock mass can vary considerably (see Figure 7.5c), with “excess stress” generated by either;

- A loss of confinement, for example a stope wall or back ($-\Delta\sigma_3$),
- An increase in load, for example a pillar ($+\Delta\sigma_1$), or

- A combination of both, typical of an abutment failure ($+\Delta\tau_{max}$)

It must be kept in mind that rock mass damage and response mechanisms are stress path dependent. The damage criteria developed must therefore be related, or even classified, to the stress path observed. Indeed, Board (2000) correlated the observational response of stope pillars at the Kidd Mine to various stress path histories. This correlated behaviour was used to predict a "Stope Damage Assessment" for various mining sequences and stope dimensions for future mining options, shown in Figure 7.6. Depending on the loading conditions and the stress path to failure, the amount and type of observed damage can differ significantly.

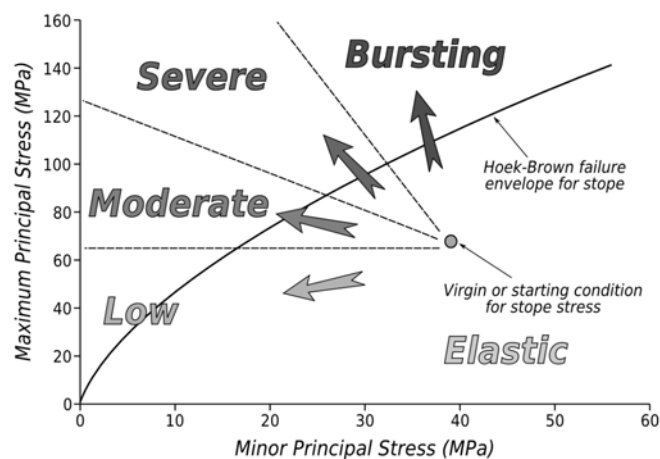


Figure 7.6 - Stope Damage Assessment Chart for stope pillars at the Kidd Mine (after Board, 2000)

Increasing Load With Constant Confinement

This damage model assumes that, for similar confinement conditions, the rock mass will experience increasing levels of damage as loading increases. It must be noted that this model is valid for monotonic increases in the major principal stress at a certain level of confinement (i.e. biaxially confined uniaxial loading). Villaescusa et al (2003) suggest that the initial damage threshold is defined as;

$$\sigma_1 - \sigma_3 = A \quad (7.17)$$

where A is a site dependent constant. This generalised form has been suggested independently by a number of authors (Diederichs et al., 2004; Martin, 1997) represents the initiation of damage, characteristically manifested by the onset of observed seismicity in massive, brittle rocks (Martin, 1997). Over-stressing, and subsequent increase in rock mass damage, beyond this threshold can be directly observed by an increase in rock mass fracture frequency (Sharrock et al., 2002).

When this stress level is exceeded a loss of rock mass cohesion is experienced (Martin, 1997), however, a considerable degree of residual frictional strength (i.e. interlocking) is still available if moderate levels of confinement are provided. Nevertheless, the rock mass is damaged and can unravel if it is not reinforced and contained by a ground support scheme or restrained by tangential confining stresses. Increasing the loading stress ultimately leads to failure. In this case a simple failure criterion can be used, such as the Mohr-Coulomb rock mass strength envelope, which can be generalised as follows;

$$\sigma_1 = B + q \sigma_3 \quad (7.18)$$

where B is the Uniaxial Compressive Strength (σ_{cm}) of the rock mass and q is related to the rock mass friction angle (Φ_m) by $\tan^2(45 + \Phi_m/2)$. When the stresses reach this level the interlocking is overcome and the rock mass undergoes considerable non-linear deformation. The rock mass located within the zone defined between the two criteria can be considered to be damaged (see Figure 7.7). As over-stressing is increased from the lower criterion to the upper one, the rock mass becomes progressively more sensitive, in that it is easier to trigger an unravelling failure, for example, by rapid loss of confinement or by vibration from nearby blasting.

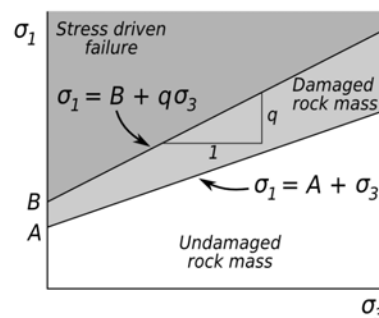


Figure 7.7 - Damage and failure criteria (after Villaescusa et al, 2003)

Brittle Rock Mass Damage Model

Intact rock yield at low levels of confinement are generally manifested by brittle responses and tend toward more ductile responses with increasing levels of confinement. A number of authors have observed that moderately to sparsely jointed rock masses can display similar brittle rock mass responses at low confinement levels (Diederichs, 1999; Martin et al., 1999). In addition, there are a number of other factors, such as site specific boundary and loading conditions, that also influence this response.

Diederichs et al (2004) attempt to explain the discrepancies between the observed brittle response of excavation surfaces in massive to moderately jointed rocks compared to the

expected response using traditional Hoek-Brown Failure criterion (1980) using a linear elastic fracture mechanics approach, combined with theories developed from discrete element micro-mechanical modelling. Diederichs et al (2004) indicate that the Hoek-Brown criterion may not be appropriate in some circumstances, due to the perceived inability of the criterion to incorporate damage initiation, crack propagation and inability of brittle materials to mobilise friction at low confining stresses (i.e. near excavation surfaces). That is, they suggest that a shear strength yield model may be inappropriate for brittle rock mass failure at low confinement. This conclusion has been supported by a number of authors ((Martin, 1997; Martin and Maybee, 2000). In addition, they also showed that brittle failure (stress induced fracturing around tunnels) initiates at around $0.3-0.5\sigma_c$. The basis for this lower bound strength envelope, or damage envelope (equation 7.2), appears to be confirmed by a number of researchers (Martin et al, 1999; Diederichs et al, 2004). Diederichs et al (2004) summarised these findings and proposed a simple linear relationship;

$$\sigma_1 = (0.3 - 0.5)\sigma_c + (1 - 1.5)\sigma_3 \quad (7.19)$$

The main ideas behind damage initiation and propagation for brittle rock mass proposed by Diederichs et al (2004), is that a number of key criteria control this lower bound strength threshold. Once rock mass damage initiation has occurred, rock mass strength degradation to this lower bound strength is possible and is postulated to be a function of rock fabric heterogeneity, near surface effects (i.e. excavation shape), previous damage and stress rotation. The act of stress rotation after the damage threshold has been reached, even without induced stress magnification, can have a significant impact on internal crack propagation and damage (Wu and Pollard, 1995), subsequently leading to an apparent reduction in the strength envelope. This aspect is not considered in existing empirical peak strength criteria. Experimental results from full triaxial tests indicated that elevated levels of σ_2 can provide a significant increase in peak strength (Mogi, 2007). The Hoek-Brown criterion, as well as damage criteria provided in the preceding section, do not consider the influence of σ_2 (i.e. all only consider σ_1, σ_3 space) and its influence of peak rock mass strength. This may also explain discrepancies between observed and predicted performance. It is therefore important to keep aspects such as these in mind when developing site specific damage and failure criteria. A site specific back analysis process is therefore important as it negates the need for a 'strength degradation' procedure, as required in the Hoek-Brown criteria (1980;1997).

7.5.2 Non-linear Elasto-Plastic Damage Models

The benefits of using non-linear elasto-plastic constitutive models over linear elastic models is the ability to model irrecoverable inelastic strains, as well as rock mass behaviour in the 'post-peak' region. The theory of incremental plasticity (Hill, 1950) attempted to analytically model plastic deformations in metal, which generally display perfectly plastic behaviour after

yield (i.e. deformation with constant volume under constant loading conditions). However, most geomaterials do not display perfect-plastic behaviour, but rather strain softening behaviour. That is, deformation occurs with a corresponding decrease in supportable load. In addition, geomaterials generally display dilatant characteristics (i.e. positive increases in volumetric strain) at yield. The dilatant and post-yield strain behaviour is also influenced by confinement (Crouch, 1970; Wawersik and Fairhurst, 1970).

A number of strain softening and dilatant constitutive models have been developed specifically for geomaterials, which allow accumulated damage (i.e. strength degradation) to be modelled (Ottosen, 1977; Frantziskonis and Desai, 1987; Bigoni and Piccolroaz, 2003). One recent model is the *LR2* constitutive model (Levkovitch et al, 2010), which has been developed in order to better account for the influence of confinement on the yield criterion and the plastic strain potential. The yield criterion in *LR2* uses a modified form of the Menétrey/William strength criterion (Menétrey and Willam, 1995). In the *LR2* model, the Menétrey-William criterion has been modified to represent a circumscribed approximation of the modified Hoek-Brown strength criterion (Hoek et al, 1992). The main advantage of the *LR2* model is that it can explicitly account for the intermediate principal stress allowing material parameters to be adjusted to match the true triaxial failure data, if required. The plastic strain component of the *LR2* material model utilises a plastic strain potential that incorporates a flow potential parameter (based on dilation) resulting in either associative or non-associative flow rules, again explicitly accounting for the influence of the intermediate principal stress. A demonstration of the use of this model in stope performance back analysis studies is provided in Chapter 13.

The back analysis process using non-linear modelling, generally requires the observed damage level to be calibrated with modelled plastic strain. In order to facilitate this, a scalar approximation of the plastic strain tensor, or equivalent plastic strain, can be utilised (Coppola et al, 2009);

$$\varepsilon_p = \sqrt{\frac{2}{3}} \sqrt{\varepsilon_1^2 + \varepsilon_2^2 + \varepsilon_3^2} \quad (7.20)$$

where ε_1 , ε_2 , ε_3 , are the principal strain components. The calibration procedure requires observed damage (e.g. changes in physical appearance and rock mass behaviour) to be recorded in terms of when in the mining sequence and its location. This damage can then be related, or matched to predicted equivalent plastic strain levels. An example of this calibration is provided by Beck and Duplancic (2005) and shown in Figure 7.8.

	Class	Description
5.0%	Very Significant	Drive surface heavily deformed, drill holes crushed, support visibly loaded. → Substantial rehabilitation required to prevent frequent falls of ground
3.2%	Significant	Any or all of: Buckling, dilation of existing structure or induced fractures, failed corners and brows, hole problems. Bulking of the mesh is present in some areas. → "Spot" rehabilitation required to maintain access, more substantial rehabilitation required for drill and blast activity etc. Hole problems develop
1.8%		
1.0%	Moderate	Shearing on existing structure, visible yield. Frequent scats in the mesh, or material may be spalling under mesh. → Rehabilitation required only when intense activity will be undertaken in the area (ie drill and blast). Drive still safe for travel. Holes show more frequent signs of damage, sometimes requiring re-drilling.
0.6%	Minor	Minor signs of strain or displacement on persistent structures, some occasional scats in mesh. → No rehabilitation required.
0.3%		
0.0%	None	Blast damage/virgin stress damage only → Primary support controls drive surface

Figure 7.8 - Common damage scale with indicative levels of equivalent plastic strain shown on left (Beck and Duplancic, 2005)

7.6 RELIABILITY OF STOPE PERFORMANCE BACK ANALYSIS USING LINEAR ELASTIC MODELLING

Back analysis is a fundamental requirement in establishing the reliability of any instability criteria used in design. It is considered that the back analysis process using numerical modelling is more attractive than empirical methods as it inherently includes the site specific effects such as rock mass scale, complex excavation geometry and boundary conditions. It could be argued that the back analysis procedure quantifies the reliability of the entire predictive system rather than any of its individual components (Wiles, 2006). For linear elastic back analysis, Wiles (2006) proposes to utilise the coefficient of variation around the line of best fit for the Mohr-Coulomb rock mass strength envelope (equation 7.1) as a measure of reliability. In this case, the distance from any stress point to the best-fit line (excess stress) for a linear (Mohr-Coulomb) criterion is given by;

$$\Delta\sigma_1 = \sigma_1 - B - q\sigma_3 \quad (7.21)$$

where $\Delta\sigma_1$ is positive above the line and negative below the line (see Figure 7.9).

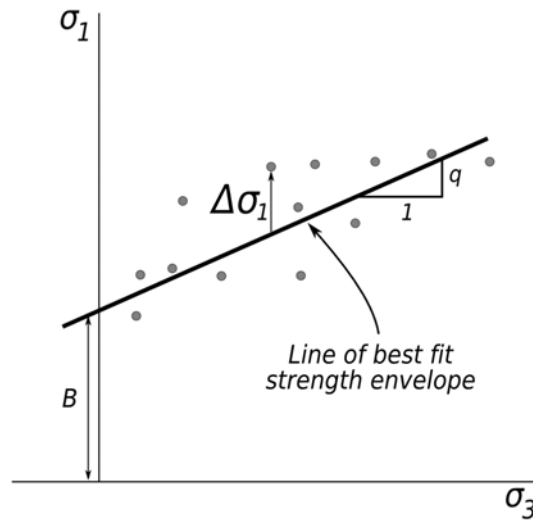


Figure 7.9 - Prediction error for linear elastic back analysis (modified from Wiles, 2006)

The standard deviation for the back analysis data points for σ_1 and σ_3 can be written;

$$s_1 = \sqrt{\sum (\sigma_1 - \bar{\sigma}_1)^2 / (n-1)} \quad (7.22)$$

$$s_3 = \sqrt{\sum (\sigma_3 - \bar{\sigma}_3)^2 / (n-1)} \quad (7.23)$$

where $\bar{\sigma}_1$ and $\bar{\sigma}_3$ represent the mean values of σ_1 and σ_3 and n represents the number of back-analysis points. The combined standard deviation can be written;

$$s = \sqrt{(s_1^2 - q^2 s_3^2)(n-1) / (n-2)} \quad (7.24)$$

with the coefficient of variation for the predictive system defined as;

$$C_v = s / \bar{\sigma}_1 \quad (7.25)$$

If the values are assumed to follow a normal distribution then confidence intervals around the mean can easily be established (Wiles, 2006). Wiles (2006) also suggests that if the coefficient of variation of the linear elastic based predictive system is large (say, greater than 30%), then alternative approaches may need to be adopted.

Because of the limited number of input parameters, the use of linear elastic techniques appears attractive, however, a number of aspects of linear elastic modelling need to be kept in mind when evaluating instability criteria reliability. A key objective of linear elastic numerical modelling back-analysis is to determine the site-specific best-fit damage threshold line. Unfortunately, because of the limitations of linear elastic modelling, the rock mass can be over-stressed well beyond the damage threshold line (see Figure 7.10). This has a significant impact on the back analysis process as, without knowing the damage threshold in advance, the precise degree of over-stressing is therefore unknown. The relationship between over-stressing and rock mass response are fundamentally dependant on the post-

peak properties of the rock mass, which are also generally unknown. Notwithstanding these issues, there are a number of additional complications in the use of linear elastic techniques for back analysis of open stopes that need to be considered. Wiles (2006) suggests that some sources of variability in back analysis may include, but not limited to;

- Incorrect pre-mining stress state orientation or stress ratio assumptions,
- Geometric construction errors in the model between actual and modelled geometries,
- Chaotic rock mass behaviour,
- Influence of large-scale structures not included in the modelling,
- Significant rock mass strength heterogeneity across the study area.

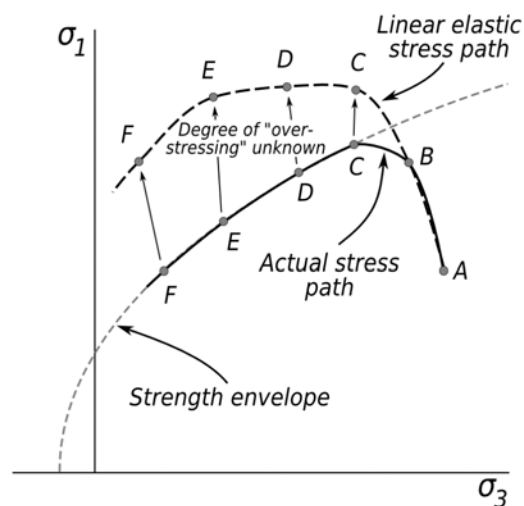


Figure 7.10 - Stress path in linear elastic modelling (modified after Beck, 2003)

7.6.1 Back Analysis using Excavation Profiles

The principal assumption of numerical modelling back analysis with excavation profiles is that the *CMS* data are meant to represent points in the rock mass where stress induced 'failure' has occurred as a direct result of induced stresses exceeding the local rock mass strength. This 'failure' is then assumed to be manifested as over-break at this location. Unfortunately, this assumption may lead to significant variability in back analysis results, **as the *CMS* profile does not necessarily define the excavation damage zone (EDZ) or yield zone of rock mass** (see Figure 7.11). *CMS* points could actually represent "yielded" yet "un-removed" rock mass, where the local shape and span may arch and hold up yielded material. This also depends on the geometry (i.e. orientation, size and shape) and intensity of existing and created discontinuities (Villaescusa et al., 2003a). In this case, if the surface points are used to represent the *EDZ*, then linear elastic modelling may tend to overestimate the stress state required to initiate failure.

Back analysis of *CMS* profiles only allows the depth of failure to be ascertained where *CMS* data exists. That is, an incomplete void model (due to shadows or rill in the stope) will not be able to represent the true extent and range of stress induced failure "events".

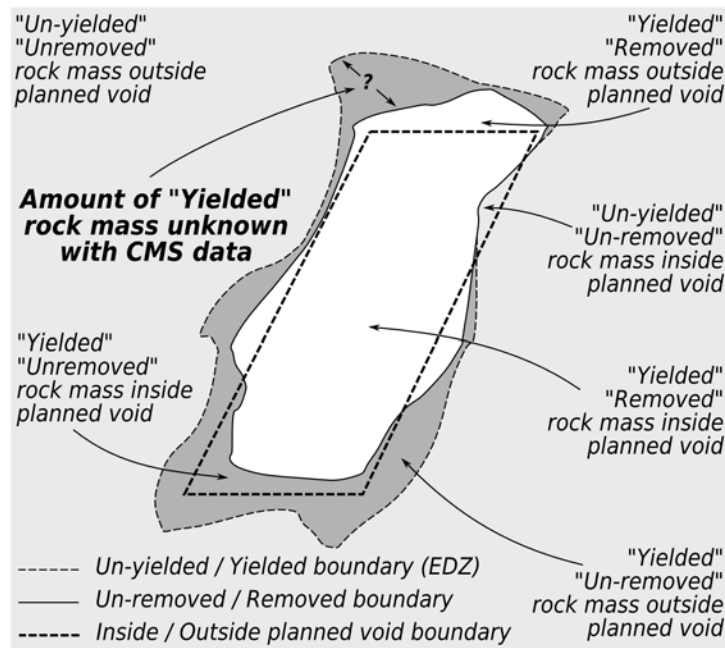


Figure 7.11 - Inability of *CMS* profiles to accurately define zone of yielded rock mass

7.6.2 Variability in Confinement

In the numerical back analysis of pillars, the degree of over-stressing can generally be correlated to the severity of rock mass behaviour (Wiles, 2006). Stress values used for pillar back analysis are usually taken at the mid-point (i.e. centre of the pillar core), where the local, or mean, pillar stress does not vary significantly. In contrast, back analyses conducted on stope surfaces will potentially contain *CMS* data points from all regions close to the excavation wall where stress conditions can vary quite significantly, affecting the reliability of results. As a brief demonstration of this, results from 2-dimensional linear elastic boundary element modelling of a pillar between two excavations are shown in Figure 7.12. The model consists of a pillar with a W:H ratio of 1:0.75, and an *in situ* horizontal to vertical stress ratio of 2:1. Figure 7.12 displays contours of σ_3 together with a number of graphs depicting the values of σ_1 and σ_3 versus the distance along a sampling line for a variety of sampling regimes. It can be seen that, depending on the sampling regime (i.e. where *CMS* profile lies), there is significant variability in both σ_1 and σ_3 values, with points closer to the abutments showing more variability.

Figure 7.12 highlights the dilemma of choosing the representative stress level on, or near, the excavation boundary for back analysis of over-break using linear elastic techniques. Selecting stress points defined by the over-break profile (i.e. *CMS* data points) introduces significant variability in the stresses used to represent failure in the back analysis. In this case, σ_1 will not be normally distributed and, as such, a probability of failure approach (as proposed by Wiles, 2006) may no longer be valid.

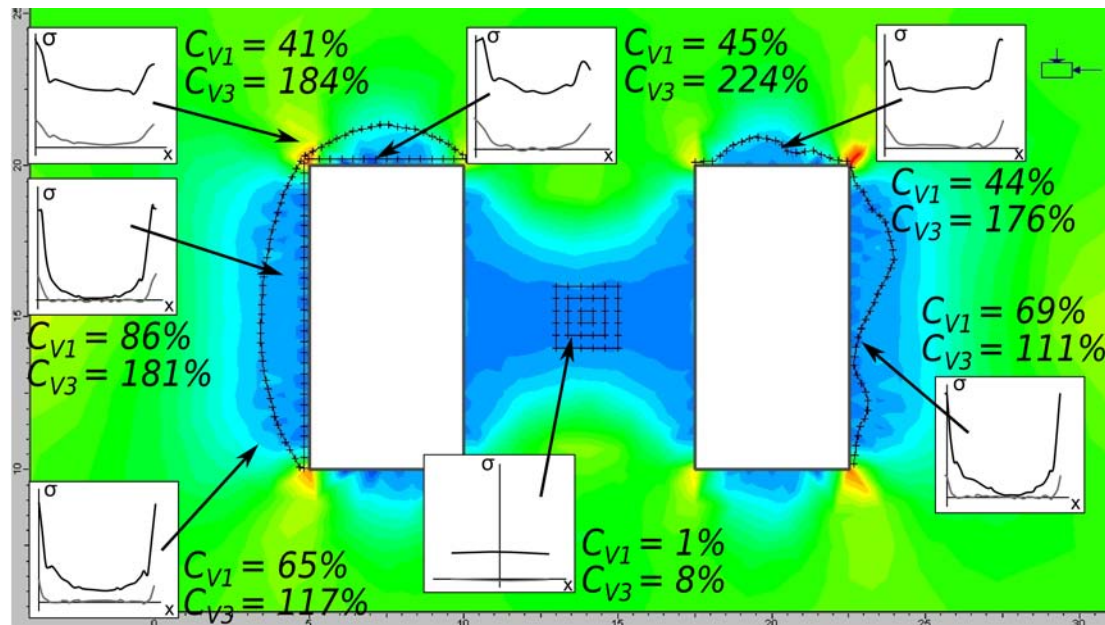


Figure 7.12 - Typical 2D linear elastic stress analysis contour plot of confinement (σ_3), showing coefficient of variation for σ_1 (C_{V1}) and σ_3 (C_{V3}) along various sampling regimes

In terms of unpredictable or “chaotic” rock mass behaviour, it must be recognised that the data set utilised in back analysis includes all *CMS* data points, and assumes that all points are associated with stress driven failure. However, not all points are associated with purely stress induced failure and may represent;

- Structurally controlled fall-off (i.e. discontinuum response)
- Yield due to drilling inaccuracies and blast induced damage (i.e. dynamic strain)

The difficulty lies in trying to discriminate the data points to be used in a “stress driven” back analysis. For example, “non-events” where no failure has occurred, or ‘failed’ due to other causes, may still be included in the data set. It should also be kept in mind that, unless the *EDZ* consistently represents the actual yield surface, site-specific damage criteria developed from *CMS* back analyses will be unreliable due to the fact that post yield behaviour and ‘fall-off’ is “unpredictable” in nature. It is suggested that a high proportion “chaotic” rock mass behaviour may indicate predominantly discontinuity-controlled rock mass response. In this case, the effectiveness and validity of continuum modelling should be questioned.

7.7 CONCLUSIONS

In the design of open stopes, numerical methods are generally favoured over analytical methods and empirical methods as they are capable of incorporating additional complexities such as; effects of *in situ* and induced stresses, complex excavation geometries, non-linear behaviour, material anisotropy and the influence of complex rock structure. Continuum methods are generally preferred due to their relative ease of use and, depending on model complexity and computing resources, can conduct multiple simulations within a suitable time frame.

Although these are still popular in contemporary mine design a number of limitations with their use need to be understood and, if possible, addressed;

- Continuum model - these models may not be able to adequately represent the fundamental 'failure' mechanisms involved, or may only be able to represent these mechanisms over a limited range of scales. Assumptions of isotropy also need to be tested and verified.
- Elastic assumption - Fundamentally, the elastic assumption negates the possibility of modelling post-peak behaviour of rock. When using 'excavation steps' in linear elastic continuum modelling, the extent and amount of rock mass damage is not remembered and included for each subsequent step. Rock mass damage and resultant redistribution of stress therefore cannot be accurately modelled.
- Constitutive models - the existing empirical models are highly dependent on the rock mass properties, range and levels of confinement and amount of non-linear deformation from the case history database.
- Peak Strength Criteria - Existing peak strength criteria assume that shear strength can be mobilised at low confinement (which may not be the case), do not consider the influence of the intermediate principal stress or effects of stress rotation. In addition, these criteria were developed from specific boundary and loading conditions that may not necessarily match the *in situ* configuration.

We have also seen that additional issues face the design engineer when trying to use existing modelling tools for back analysis of excavation surfaces, such as stress variability close to excavation surfaces and the fact that *CMS* profiles do not necessarily represent the yield surface of the rock mass.

It is suggested that improvement in reliability of continuum modelling may be gained by

using more sophisticated material models, such as non-linear inelastic models. However, these require additional input information for the yield criteria and plastic potentials, which may not be readily available or their accuracies uncertain. In this case, it could be argued that the added complexities involved with inelastic material models may not necessarily yield more reliable predictions (Wiles, 2006). However, the main effort of modelling should be to reduce assumptions, not necessarily to minimise complexity. In this regard, linear elastic methods contain many (unrealistic) assumptions about material behaviour. The model with the most assumptions is least likely to be correct. Notwithstanding this, it is desirable to maximise the use of existing tools before resorting to more sophisticated tools which mine operators may not be able to afford nor have the expertise to utilise on a regular basis.

CHAPTER 8 - ROCK MASS MODELLING

8.1 INTRODUCTION

In order to develop an understanding of the potential rock mass behaviour, it is necessary for the rock mechanics engineer to have a robust model of the rock mass in terms of its rock fabric and discontinuities. A variety of approaches to rock mass modelling can be made, from simple tabulation of the descriptive statistics of the rock fabric and discontinuity parameters to 3-dimensional geostatistical modelling of various components of the rock mass, or even geometrical models of discontinuities to represent the rock mass structure at a number of scales. The approach taken to developing a rock mass model is dependent on;

- engineering objective and scale
- design methodology
- complexity and detail required
- quality and quantity of data available
- justification in terms of time and cost

The following sections describe some common rock mass modelling approaches available to the rock engineer for use in open stope design. This chapter also introduces a number of concepts in rock mass “domaining”.

8.2 STOCHASTIC REPRESENTATIONS OF ROCK MASS PROPERTIES

Stochastic processes can be used to describe physical systems (e.g. geological processes) where the behaviour is non-deterministic in that the physical system's ultimate state (i.e. its rock mass properties) is determined both by the process's predictable actions and by some random element. In this case, most rock engineering properties can be treated using probability theory and statistics, as either discrete or continuous random variables.

8.2.1 Classical Statistics

Classical statistical techniques, such as descriptive or inductive statistics, are used to describe sample data sets or to make inferences and predictions about populations, respectively. Rock fabric and rock mass properties such as results from laboratory testing of rock fabric strength, shear strength of discontinuities, rock fabric density, can be treated simply using classical statistics.

A central requirement of classical statistics is the assumption of independence of sampling

points of the random variables within a sampling region or volume. In terms of probability theory, there is the assumption that the value of a random variable is equally likely to occur anywhere within the sampling volume. However, this assumption may only be valid for geological parameters within a certain specific volume of rock and at certain scales. The choice of sampling volume, or *domain*, in terms of geometry (i.e. location, size, shape), and how it is sampled (i.e. sample size and method, sampling density and orientation) will have a significant impact on the validity of these assumptions and the use of classical statistical techniques.

8.2.2 Regionalised Variables and Geostatistics

Spatial data dependency, however, leads to the spatial autocorrelation problem which violates classical statistics, which assumes independence among observations. There are a number of spatial statistical models that are able to capture these relationships that do not suffer from these weaknesses. In terms of gaining a better understanding of rock mass parameters, it is better to view spatial data dependency as a source of information rather than something to be corrected.

The concept of regionalised variables is the fundamental basis for the theory of geostatistics (Matheron, 1962). The main idea behind geostatistics is the observation that values of variables sampled in the field often resemble each other more as the distance between sampling points is decreased. With increasing distance, the spatial influence of neighbouring samples becomes smaller, and above a certain limit, the so-called “range”, variables are spatially independent in a statistical sense. Spatial correlation is measured using the variogram function (Journel and Huijbregts, 1978);

$$2\gamma(x+h)=E\{[Z(x)-Z(x+h)]^2\} \quad (8.1)$$

where $Z(x)$ defines a random function defining the variable, say ore grade, where x is a point in 3-dimensions and h is some distance from x .

Stationarity

The theory of geostatistics also requires that the statistical spatial model representing the sampled data observes certain requirements of “stationarity”. $Z(x)$ is stationary if, for any finite number n of points x_1, \dots, x_n and any h , the joint distribution of $Z(x_1), \dots, Z(x_n)$ is the same as the joint distribution of $Z(x_1 + h), \dots, Z(x_n + h)$ (Cox and Miller, 1965). This form of strict (strong) stationarity does not imply the existence of means, variances, or covariances. In reality, strict stationarity cannot be tested, as the data are represented as a (non random) sample from one realization of the random function. There are at least three variations of the stationary hypothesis. These are;

- Strict stationarity,
- Second order stationarity, and
- Intrinsic stationarity

To work within the framework of linear geostatistics, the second order and intrinsic stationary hypotheses are sufficient (Journel and Huijbregts, 1978). Second-order stationary is where $cov[Z(x + h), Z(x)]$ exists and depends only on h . This implies that $var[Z(x)]$ exists and does not depend on x ; furthermore, $E[Z(x)]$ exists and does not depend on x (Cox and Miller, 1965). That is, second order stationarity hypothesis requires that the first and secondary moments of the distribution are invariant under translation and that covariance is dependant on the separation distance h . Intrinsic stationarity hypothesis requires that the first and second moments of the distribution of increments between two sampled locations at distance h are invariant under translation. That is, for any two sampling points in a sampling volume, the difference in the measured values depends only on the distance between the two points (i.e. the “lag”), independently of where the two samples were collected.

It is important to note that the assumption of “stationarity” is a property of the geostatistical model being used, not of the rock mass or rock mass variable being considered. This assumption is often problematic, especially in areas with rapid changes in rock mass properties. The correctness of the decision to assume secondary and intrinsic stationarity in the model cannot be validated, however its plausibility can be investigated (see Section 8.7.2). Any trends and structural discontinuities render the geostatistical analysis more difficult. Such situations may be caused by short-range, sharp gradients in variables within a rock mass system as well as by marked changes in the gross rock mass system (i.e. a *domain* change). In this case, geostatistics may not be an appropriate methodology if appropriate measures are not taken into account (such as identification and geostatistical treatment of “domains”, as well as utilisation of nested or anisotropic geostatistical models).

8.3 ROCK MASS MODEL PROCESSES

The main objective of 3-dimensional modelling is to develop a synthetic model of an entire area or volume of a rock mass from a limited number of sample points. Generally speaking, most model formats consist of a regular series of 3-dimensional lattice points, to which sample values are interpolated. Each point within the model has the following attributes;

- Cartesian coordinate (i.e. x, y, z position relative to mine coordinate system).
- Rock mass variable of interest

The main steps in the modelling process are summarised below;

- Evaluation of input data sources, data accuracy and reliability and data distribution
- Preliminary domain definition
- Determination of the most appropriate modelling types for each domain
- Compositing input parameters into regularly sized data intervals
- Statistical analysis and sub- or re-domaining (if required)
- Defining and applying interpolation techniques
- Model validation

8.4 SPATIAL MODEL TYPES

A number of spatial model types have been developed in the geology discipline that are equally applicable to the field of rock engineering. The main types are (Cepuritis, 2004);

- Polygonal model - consists of a 2-dimensional representation of polygon centred on a data point, with its boundary equidistant between neighbouring data points. The value of each data point are assumed to apply equally to the entire area of the polygon.
- Gridded surface model - based on a series of equally spaced grid points. The grid can be represented by a convex 3-dimensional surface, providing a true 3-dimensional model. The value of each grid point can be determined by a variety of methods, including interpolating values from nearby drill holes. These models can represent geological surfaces (i.e. faults, lithological and weathering boundaries, hangingwall/footwall contacts, etc.).
- Columnar model - Columnar (also called “seam” or “reef”) model consists of a series of regular square shaped columns with the top and bottom extents truncated or bounded by a surface.
- Block Model - Block models consist of a series of blocks or cells. Each cell has a centroid and extends in 3-dimensions to form a volume. Cells within a block model can consist of regularly sized cells (sometimes called voxels) or may be divided into sub-cells. Sub-celling is a technique used to define resolution around complex shapes and close to boundaries. The type and amount of sub- celling allowed within the block model can also be controlled
- Triangulated Irregular Network (*TIN*) meshes - Other models include the volumetric representations of domains, or “solids”, based on fully enclosed triangulated meshes. These are particularly useful for representing complex 3-dimensional geometries, and are generally the basis for delineating different domains in block models.

8.5 SPATIAL INTERPOLATION METHODS

The fundamental requirement in developing models that are capable of representing spatial variability is the ability to reliably interpolate data from sampled locations to other points within the area of study. There are a multitude of choices available for the spatial interpolation of data. The choice of interpolation method may vary, mainly according to the type and nature of data, and the aim of modelling. However, each method has its specific assumptions and features, which need to be addressed and understood, in order to correctly interpret interpolation results.

8.5.1 Basic Principles of Interpolation

Nearly all spatial interpolation methods represent estimations (i.e. points to be estimated) as weighted averages of the sampled data. They all share the same general estimation formula, as follows:

$$\hat{z}(x_0) = \sum_{i=1}^n \lambda_i z(x_i) \quad (8.2)$$

where \hat{z} is the estimated value of an attribute at the point of interest x_0 , z is the observed value at the sampled point x_i , λ_i is the weight assigned to the sampled point, and n represents the number of sampled points used for the estimation (Webster and Oliver, 2001).

8.5.2 Interpolation Methods

The principal difference between interpolation methods is in the formulation of the weighting system. Interpolation methods can basically be divided into geostatistical and non-geostatistical methods. Interpolation methods can be further classified according to (Li and Heap, 2008);

- global versus local interpolators - Global methods use all available data of the region of interest to derive the estimation and capture the general trend. Local methods operate within a small area around the point being estimated and capture the local or short-range variation .
- Exact versus Inexact interpolators - A method that generates an estimate that is the same as the observed value at a sampled point is called an exact method. All other methods are inexact, which means that their predicted value at the point differs from its known value.
- Deterministic versus Stochastic - Stochastic methods incorporate the concept of randomness and provide both estimations (i.e., deterministic part) and associated errors (stochastic part, i.e., uncertainties represented as estimated variances). All

other methods are deterministic because they do not incorporate such errors and only produce the estimations. Deterministic methods have no assessment of errors with the predicted values, while stochastic methods provide an assessment of the errors associated with the predicted values.

- Gradual versus Abrupt - Some methods produce a discrete and abrupt surface, while some other methods (e.g., distance-based weighted averages) produce a smooth and gradual surface. The smoothness depends on the criteria used in the selection of the weight values in relation to the distance. Criteria include simple distance relations, minimisation of variance and minimisation of curvature and enforcement of smoothness.

The appropriateness or comparison of interpolation methods can also be assessed based on criteria as goodness of representation (errors in honouring control points), dependency on data distribution, number of control points that can be handled, ease of implementation, and speed of computation (Rusu and Rusu, 2006).

8.5.3 Geostatistical Interpolation Methods

Geostatistical interpolation methods utilise spatial correlation models of the regionalised variable to interpolate values at specified points in space. A multitude of methods are available, however, the most common geostatistical interpolation method is kriging, named after Danie Krige (Krige, 1951), which describes a family of generalised least-squares regression algorithms. Kriging provides estimates of a regionalised variable using a linear or non-linear combination of weights obtained from a model of spatial correlation (i.e. variogram models). The weights are specifically chosen to minimise the estimation variance. It can be described as an exact interpolator that produces a minimum variance unbiased estimate. A multitude of variations exist, however, the most common varieties include; simple kriging (*SK*), ordinary kriging (*OK*), indicator kriging (*IK*) and co-kriging (*CK*).

Conditional simulation is a relatively new geostatistical method whereby \hat{z} estimates are based on a form of stochastic simulation. The technique generates multiple (and equally probable) realisations of a regionalised variable where the measured data values are honoured at their locations. It is “conditional” based on the actual control data being honoured. By relaxing some of the kriging constraints (e.g. minimised square error), conditional simulation is able to reproduce the variance of the control data. The goal of simulation is to characterise variability or risk. This feature is particularly attractive in assessing reliability of spatial models. In comparison to other kriging methods, which tend to smooth out local details of spatial variation, conditional simulation is able to highlight sharp spatial discontinuities (i.e. can be classified as an “abrupt” interpolator).

8.5.4 Non-Geostatistical Interpolation Methods

A detailed description of non-geostatistical interpolation methods is beyond the scope of this thesis, however, some common methods include;

- Nearest neighbour (*NN*)
- Natural neighbour (*NaN*)
- Inverse distance weighted (*IDW*)
- Regression models
- Trend surface analysis (*TSA*)
- Splines and local trends
- Radial basis functions (*RBF*)

8.5.5 Geostatistical and Spatial Modelling in Mining Rock Mechanics

By and large, the use of geostatistics in mining has been restricted to the field of ore grade estimation. However, geostatistical techniques have also been utilised to model rock engineering properties and characteristics such as rock strength (Miller and Luark, 1993), weathering (Ayalew et al., 2002) and Schmidt Hammer Hardness (Ozturk and Nasuf, 2002), even attempts at modelling rock mass classification data and rock mass strength (Bye, 2006; Cepuritis, 2004; Luke and Edwards, 2004). Geostatistical techniques have been used to measure discontinuity characteristics such as spacing (Villaescusa, 1991) and orientation (Young, 1987), as well as discontinuity surface characteristics (Lopez et al., 2003). Geostatistical techniques have also been used to model measures of discontinuity intensity in 1- and 2-dimensions (Escuder Viruete et al., 2001; Liu et al., 2004). The greatest impact geostatistics has had to the field of rock mechanics is the recognition of spatial dependence of rock engineering properties and characteristics. We must therefore take full advantage of this approach where at all possible.

Geostatistical models have been shown to provide insights into the spatial variability of rock mass properties, however, there still are a number of aspects that hinders its full and comprehensive inclusion into rock mechanics applications. In order to spatially interpolate data, a variographic study is required. This is not a simple undertaking requiring a detailed understanding and application of advanced statistical concepts. Firstly, experimental variograms (based on input data) need to be derived for a variety of orientations and volumes of rock mass. Appropriate variogram models and their associated parameters need to be derived, sometimes involving 'nested' directional variogram models. An incorrect interpolation may result from inappropriate selection of variogram models and parameters

(Rusu and Rusu, 2006).

8.5.6 Radial Basis Functions

Radial basis functions (*RBF's*) are a relatively new alternative non-geostatistical spatial interpolation technique that offer a number of advantages over traditional geostatistical techniques.

Formulation

RBF's try to approximate the random function $f(x)$ by $s(x)$ given the set of values $f=(f_1, \dots, f_n)$ at distinct points $X=\{x_1, \dots, x_n\} \in \mathbb{R}^3$, where $s(x)$ is a radial basis function (Carr et al., 2001);

$$s(x) = p(x) + \sum_{i=1}^n \lambda_i \phi(|x - x_i|) \quad (8.3)$$

where p is a polynomial of low degree, λ_i is a real-valued weight, and the basic function ϕ is a real valued function on $[0, \infty]$ and is the distance between x and x_i . In this context, the points x_i are referred to as the centres of the *RBF*. In this case, an *RBF* is a weighted sum of translations of a radially symmetric *basic function* augmented by a polynomial term. A number of basic functions can be selected, including thin plate splines;

$$\phi(r) = r^2 \log(r) \quad (8.4)$$

which are useful for fitting smooth function for two variables, multi-quadratic;

$$\phi(r) = \sqrt{(r^2 + c^2)} \quad (8.5)$$

which are useful for fitting topographic data. Biharmonic splines;

$$\phi(r) = r \quad (8.6)$$

combined with a linear quadratic are useful for fitting functions with three variables. In order to solve the *RBF* interpolant $s(x)$ the λ_i weights to be obtained from the values $f=(f_1, \dots, f_n)$ are required so that the *RBF* satisfies;

$$s(x_i) = f_i \quad i=1, \dots, n \quad (8.7)$$

In addition, the orthogonality conditions are defined by;

$$\sum_{j=1}^n \lambda_j p(x_j) = 0 \quad (8.8)$$

for all polynomials of degree k at most. This results in an under-determined system, as there are more parameters than data. These conditions are imposed on the coefficients $\lambda=(\lambda_1, \dots, \lambda_n)$. Then let $\{p_1, \dots, p_k\}$ be a basis for polynomials of degree at most k and let $c = (c_1, \dots, c_k)$ be the coefficients that give p in terms of this basis. Equation 8.3 and 8.1 can be written in matrix notation as;

$$\begin{pmatrix} A_T & P \\ P^T & 0 \end{pmatrix} \begin{pmatrix} \lambda \\ c \end{pmatrix} = \begin{pmatrix} f \\ 0 \end{pmatrix} \quad (8.9)$$

where

$$A_{i,j} = \phi(|x_i - x_j|) \quad i, j = 1, \dots, n$$

$$P_{i,j} = p_j(x_i) \quad i = 1, \dots, n, \quad j = 1, \dots, l$$

This can be solved as a linear system of equations to determine c , λ and finally $s(x)$.

Advantages Of Using RBF Interpolation Techniques

RBFs are useful for interpolating scattered data as the associated system of linear equations is guaranteed to be invertible under very mild conditions on the locations of the data points. For example, the thin-plate spline only requires that the points are not co-linear while the Gaussian and multi-quadric place no restrictions on the locations of the points. In particular, *RBF's* do not require that the data lie on any sort of regular grid (Carr et al, 2001). This makes them particularly attractive for modelling rock mass properties which may have been sparsely and/or irregularly sampled. Some additional advantages for using *RBF's* in spatial interpolations include (Rusu and Rusu, 2006):

- depending on the radial function type, the *RBF* model may offer a localised response (therefore is able to identify the local characteristics of the surface to be modelled), or a global response (identifying this way the global characteristics of the surface to be modelled)
- *RBF's* are exact interpolators, honouring the control points when the data point coincides with the grid node being interpolated
- smoothing factors can be employed in order to reduce the effects of small-scale variability (i.e. noisy data) between neighbouring data points. Therefore they may also act as inexact interpolators if needed.

8.5.7 Model Reliability

A number of tools are available to estimate the reliability of spatial models. For geostatistical techniques, estimation variance is commonly used to assess model reliability. Cross-validation is a simple procedure to check the compatibility between a data set and its spatial estimation model. Cross-validation generally involves running a number of estimations, where sample data points are removed in turn, predicts a value at that location based on the rest of the data, and compares the measured and predicted values (e.g. “leave-one-out” procedure). This technique is also used to check for biased estimates produced by poor model. A measure of the error size can be estimated using the root mean square error or average standard error (Li and Heap, 2008);

$$RMSE = \left[\frac{1}{n} \sum_{i=1}^n (p_i - o_i)^2 \right]^{\frac{1}{2}} \quad (8.10)$$

$$ASE = \left[\frac{1}{n} \sum_{i=1}^n (p_i - (\sum_{i=1}^n p_i) / n)^2 \right]^{\frac{1}{2}} \quad (8.11)$$

where p_i is the predicted value and o_i is the observed value and n is the number of samples. Significant differences between estimated values and true values may be influenced by outliers or other anomalies. Unfortunately, $RMSE$ is sensitive to outliers as it places a lot of weight on large errors (Hernandez-Stefanoni and Ponce-Hernandez, 2006). Apart from the error size, one may also be interested whether the interpolation method overestimates or underestimates the variable. In this case, if $ASE > RSME$ then the method overestimates the variable and, conversely, underestimates the variable if $ASE < RSME$.

Alternatively, the distribution of predicted versus actual values can be compared using Q-Q plots. The Q-Q plot is a plot of matching quantiles, and is a powerful graphical tool for comparing the quantiles of two distributions. The method can provide more insight into the nature of the difference between distributions than analytical methods such as the chi-squared or Kolmogorov-Smirnov 2-sample tests (NIST/SEMATECH, 2009). If the two sets come from a population with the same distribution, the points should fall approximately along the $Y=X$ or 45° reference line. The greater the departure from this reference line, the greater the evidence for the conclusion that the two data sets have come from populations with different distributions. Many distributional aspects can be simultaneously tested. For example, shifts in location, shifts in scale, changes in symmetry, and the presence of outliers can all be detected from this plot. A shift above the 45° line implies that the Y -distribution has a higher value than the X -distribution, and *vice-versa* (Deutsch, 2002).

Conditional simulation techniques offer advantages in that they are able to produce a

measure of error (standard deviation) and other measures of uncertainty, such as iso-probability and uncertainty maps. Uncertainty maps show, at each grid node, the probability that a value is either above or below a certain threshold.

8.6 ROCK MASS STRUCTURE MODELLING

The rock mass structure, or discontinuity system, is perhaps the most difficult aspect of the rock mass to model. There are many approaches to characterising the rock mass structure. The simplest approach is to describe the rock mass structure of a given rock mass volume based on the classical statistical summaries of key discontinuity attributes. That is, these characteristics are assumed to be independent and to occur ubiquitously within a region of the rock mass.

More sophisticated approaches represent the rock mass structure by 'discrete' discontinuities, where the geometric and other characteristics are specified stochastically or deterministically. Whether discrete discontinuities within a rock mass are treated stochastically or deterministically, is largely a function of the scale of the structure with respect to the volume of rock mass to be modelled. This concept was discussed earlier in Chapter 3. The choice of approach is also heavily dependant on the quality and quantity of available data. A summary of the approaches to discontinuity system modelling are provided below, modified from (La Pointe, 1993);

- Stochastic Method - descriptive statistics and qualitative assessments for each sampled discontinuity set are assumed to be ubiquitous over a region or volume of rock mass, with the results summarised in tabular format.
- Stochastic-Geometric Methods - these methods describe geometric models of the discontinuity system using statistical data from the sampled population. That is the location, orientation and size of discontinuities are represented as discrete points, lines, or polygons (typically a convex disc) in 1-, 2- or 3-dimensional space. The approach taken in these methods can be categorised as;
 - Spatially Uncorrelated Methods - orientation and size are defined by a marked Poisson process. In this manner the location of discontinuities are essentially uncorrelated in space and assumed to be "random". Orientation and size can be either statistically independent or dependent. These methods form the basis of "Joint Network Models" or "Discrete Fracture Networks" (see Section 8.6.1)
 - Geostatistical Methods - these models assume that all or some geometrical aspects of discontinuities are spatially correlated. This spatial correlation

implies that some characteristics are similar between neighbouring discontinuities and less similar for distant features. Some of these aspects, such as discontinuity location, have been incorporated into some joint network models.

- Fractal Methods - these models try to quantify how certain discontinuity characteristics vary spatially and with scale. These methods are attractive in that they require less rigorous data requirements, yet can provide useful information about the rock structure system, such as size relations, spatial relations and hierarchical relations with scale.
- Rule-based Methods - these models involve construction of the rock mass structure using sequential application of heuristically derived rules. These methods can be described as using a combination of statistics and empirical observation that are capable of achieving local estimation accuracy of discontinuity system characteristics. The method involves using a detailed understanding the local geological context of fracturing to establish rules required to spatially extrapolate discontinuity characteristics. Given the detailed local context required for rule generation, this approach is considered to be rock mass specific.
- Stochastic-Mechanistic Methods - These methods try to link the mechanical, or geological processes to the likely characteristics of the rock mass structure;
 - Structural Setting Methods - this approach utilises the postulated regional deformational framework (i.e. stresses, strains, rheological characteristics) at the time of structure formation to predict the likely characteristics of the rock structure system. This method has been applied in sedimentary environments, however, it may still be applicable to igneous rock masses where formation mode, abutting (i.e. terminations), relative ages and mineralising relationships can be established.
 - Local Bed Thickness, Curvature and Lithology - these methods utilise specific geological and geometrical characteristics of the host geology to provide locally accurate estimates of size and spacing of discontinuities based on relationships with bed thickness, curvature and lithology. These methods are generally only applicable for sedimentary rock masses.
- Deterministic Discontinuity Models - discrete discontinuities are treated 'deterministically' with the geometry of individual structures modelled as 2- or 3-dimensional convex planar or non-planar surfaces. The variability of a number of discontinuity attributes over the line / surface representing the discontinuity can also be introduced, such as; thickness, type and strength of infill, local rock mass fracture

intensity, etc. This method is generally restricted to individual large-scale features where their continuity and characteristics can be sampled from a number of relatively large exposures.

- Hybrid Models – these models utilise a number of aspects from stochastic-geometric, stochastic-mechanistic, rule-based and deterministic modelling techniques.

8.6.1 Joint Network Models

A number of Stochastic-Geometric characterisation techniques have been developed to generate three dimensional models of discontinuity network systems. Examples of a number of joint network modelling approaches are shown in Table 8.1. With each of the example models, there are a number of assumptions in the way the joint network has been developed. These assumptions will limit the models ability to accurately describe the true characteristics of the rock structure system it is trying to represent. For example, the assumption of orthogonality or random co-planarity may be appropriate for stratiform or sedimentary rock masses, yet inappropriate for rock masses form by other geological process. Therefore, the model methodology must be matched to the geological setting and specific rock mass structure characteristics.

Dershowitz and Herda (1988) highlight the importance of “disaggregate characterisation” of discontinuities during data collection and subsequent data analysis has on our ability to effectively generate realistic joint network models. That is, a number of individual characteristics from individual discontinuities are collected from localised samples and statistical analyses are then undertaken on these parameters, without regard to any possible inter-relationships (Dershowitz and Einstein, 1988).

The results of the statistical analyses are then used as input into stochastically derived joint network models under the assumption of independence between parameters and discontinuities. This assumed independence allows us to apply a number of statistical techniques in conjunction with the rock mass model, such as links between sampled one- or two-dimensional properties collected through mapping and three-dimensional properties of the model. Paradoxically, however, this assumption of independence between parameters and discontinuities restricts the possibility to develop more realistic rock mass structure models. In order to develop more realistic joint network models, it is considered that the following aspects need to be incorporated into the joint network model formulation process;

- spatial correlation and parameter dependence
- incorporation of non-geometric discontinuity characteristics (e.g. mineralogical

and/or genetic characteristics)

- persistence, termination and hierarchical relationships
- more realistic geometric modelling of individual discontinuities (i.e. non-planar, curved surfaces)

Table 8.1 - Example joint network models and their characteristics

Model Type	Author	Space	Bias Correction	Location / Density	Size	Shape	Orientation	Terminated at Intersection	Co-planarity
Orthogonal	(Snow, 1965)	3D	-	U - D	B & U	rectangle	parallel-orthogonal	Yes & No	Yes
Random Disc	(Baecher et al., 1977)	3D	-	R - P	B	circle/ellipse	stochastic	No	No
	(Hester, 1982)	2D	-	R - P	B	line	stochastic	No	No
	(Priest and Samaniego, 1988)	2D	-	R - P	U	line	stochastic	No	No
	(Chan, 1986)	3D	O	R - P	B - Log. norm	circle	regular	No	No
	(Massoud, 1987)	3D	O	G	B - Log. norm	circle	stochastic - Fisher	No	No
	(Mathis, 1988)	3D	O, C-S	R - P	B	circle	stochastic - Fisher	No	No
	(Villaescusa, 1991)	3D	O, T-C-S	R - P	B	circle	stochastic - Fisher	No	No
Random Coplanar Polygons	(Harries, 2001)	3D/ 2D*	O, T-C-S	R - P	B	circle	stochastic - Fisher	Yes*	No
	(Veneziano, 1978)	3D	O	R - P	B	polygon	stochastic - Fisher	No	Yes
Random Non-coplanar Polygons	(Dershowitz, 1984)	3D	O	R - P	B	polygon	stochastic	No	Yes
	(Santalo, 1976)	3D	O	R - P	B	polygon	stochastic & regular	Yes	Yes
	(Serra, 1982)	3D	O	R - P	B	polygon	stochastic	Yes	Yes

Notes: 2D; 2-dimensional, 3D; 3-dimensional

O; orientation bias corrected, C; censoring bias corrected, T; truncation bias corrected, S; sampling shape bias corrected

U - D; undefined-discrete, R - P; random poisson process, G; geostatistical

B; bounded, B- Log. norm.; bounded by log normal distribution, U; unbounded

* terminations and hierarchy modelled in 2-dimensions only

The development of joint network models generally rely on data from small localised, yet highly detailed and time consuming, data collection programs. Models which are based on geostatistical methods are hindered by the inability to sample and generate reliable variograms for discontinuity characteristics in all directions. Sampling lengths generally need

to be twice as long as the estimation region under consideration in order to produce a reliable variogram (Miller, 1979). Long boreholes inclined perpendicular to the discontinuity under investigation may provide sufficient sampling, however, other discontinuities may be severely under-sampled. In other circumstances, such long exposures may not be available within all rock mass domains, especially when using scan line or window mapping data where structurally complex geology can change rapidly over small distances. The ability to sample large volumes of the rock mass to ascertain spatial variability also represents a significant issue.

8.7 ROCK MASS DOMAINS

Rock masses can generally be considered inhomogeneous and anisotropic at a number of scales. To reduce uncertainty and variability there is a need to partition the rock mass into regions, or domains, where rock mass properties are essentially considered constant. This is especially important in parameter estimation in rock engineering analysis and design. There are many approaches to domain definition (Hudson and Harrison, 2002), however, it is important to understand the purpose or basis for partitioning, and whether it can be justified and is sufficiently robust for the intended purpose. The authors also provide a set of principles to assist in partitioning the rock mass into domains, however, there are practical limits to this approach which are highly dependent on data quality and quantity. The emphasis for domain definition in excavation design should be;

- developing interpreted boundaries that define areas of statistical homogeneity
- boundaries developed for each of the rock mass parameters that are critical for the engineering objectives
- boundaries are defined to a sufficient resolution that can be supported by the quality and quantity of data. This implies that domains should also be defined based on the amount and quality of data in the various regions of the mine.

It must be noted that as the size of the rock mass domain (i.e. sampling domain) is decreased the likelihood of maintaining a statistically homogeneous region increases. Paradoxically, the ability to test for statistical homogeneity dramatically decreases with a decreasing sampling volume. Accordingly, there is a need to optimise the domain geometry. The following sections describe some techniques that can be used to derive domain boundaries.

8.7.1 Trend Analysis via Cumulative Sums

Cumulative sums technique involves sequential analysis along the length of a borehole or scan line to identify changes in a particular rock mass variable (Piteau, 1973). Firstly, the mean of the data set for which the analysis is being undertaken is obtained (call it K in this

case). Let $x_1, x_2, x_3, \dots, x_n$ be a series of values measured in sequence. Subtract K from each value and then add the differences in a series of partial sums; that is $S_1 = x_1 - K$, $S_2 = (x_1 - K) + (x_2 - K) = S_1 + (x_2 - K)$, $S_n = S_{n-1} + (x_n - K) = x_1 + x_2 + x_3 + \dots + x_n - nK$. The S values represent a cumulative sum series (or *cusum*). The *cusum* is then plotted against the position in the sequence. If there is no trend in the values, the negative S values will more or less cancel out the positive ones and the *cusum* plot will be more or less constant (horizontal). If the local mean value is greater than K , more of the differences will be positive and the *cusum* will slope upwards. The reverse will occur where the local mean is less than K . The steeper the line, the greater the difference between the local mean and K . The position of significant changes in the variable can be used to define possible domain changes. Piteau (1973) applied this method to assist in determining changes in discontinuity characteristics.

It is considered that the *cusum* method would be difficult to apply to large data sets, especially those containing data from a variety of locations and orientations, especially if the rock mass is anisotropic or the variable under consideration is effected by orientation bias. Applying domain boundary choices based on the same gradient criteria for all data may also be problematic, as it is dependent on the local K . A gradient criteria based on a global K (i.e. for the entire data set) may not provide sufficient resolution for domain boundary definition.

8.7.2 Statistically Homogeneous Domains

The definition of statistically homogeneous zones is a fundamental requirement to safely apply geostatistical estimation techniques, which assume that the underlying distribution of the variable of interest is "stationary". The correctness of the decision to assume stationarity in the model cannot be validated, however its plausibility can be investigated.

Domain stationarity are generally closely related to geological, structural and/or weathering units. In general, the definition of domains for geostatistical estimation needs to take into account some or all of the following factors;

- Distribution of lithology and weathering surfaces
- Stratigraphic sequence and depositional or emplacement environment
- Significant geological structures (faulting, folding)
- Sampling and analytical precision, and
- Spatial distribution of variables

A simple way of assessing the viability of the stationary assumptions is by slicing the data

into sub-regions (usually aligned parallel to one axis of the local coordinate systems) and plotting the slice statistics of a variable against the coordinate of the physical space. A domain is assumed to satisfy the second order stationarity hypothesis if the mean and variance are invariant under translation, which will result in the mean and variance being approximately constant as the coordinate changes. Plotting variables against coordinates can help identify presence of outliers and ascertain the existence of spatial dependence of the variable under consideration. The change in the first moment after a certain range can be established. If it occurs after a certain distance (i.e. greater than area of interest) then it may not be crucial and stationarity may be assumed below this.

Fixed Slices

Data for the variable under consideration can be sliced into a sequence of zones or windows of fixed size, usually perpendicular to a local mine coordinate axis. The size of the slice window will dictate the precision of establishing the domain boundary. For example, large slices will tend to over smooth the data, conversely smaller slices will effect precision due to insufficient data points. In addition, the choice of the position of the window limits will also effect precision and bias results.

Moving Slices

In order to remove some of the biases and improve precision, the position of the slices can be continually stepped, ensuring that there is sufficient overlap as the slice is advanced. This method can be considered analogous to a moving average. Precision may be improved by using this method, however, it is still dependent on the size of the slice, the size of the overlap, the step size of the slices.

8.7.3 Data Density using Distance Buffers and Voxel Counts

As mentioned previously, domains may be established based on data quality and quantity. Distance buffers and voxel counts may be used for calculating data density in the various regions of the mine. Distance buffers usually refer to the 3-dimensional isotropic distance field around a sample. By setting a specific distance buffer the 3-dimensional region (i.e. volume) corresponding to a set sample density can be found. Alternatively, the mine region can be sub-divided into a series of regular sized voxels (i.e. cubes/blocks) and the number of samples within each voxel counted, allowing for 3-dimensional distribution of sample density to be established.

8.7.4 Structural Orientation Domains

Another method of domain creation considers discriminating portions of the rock mass that

display different discontinuity orientation patterns into 'structural' domains. In some circumstances, domain boundaries are clearly defined with distinctly different discontinuity patterns between each delineated rock mass volume. In this case defining 'structural' domains is relatively straightforward. Unfortunately, the controls on dominant discontinuity orientations are not always so clear and methods are therefore required to identify where changes occur. This especially problematic when discontinuity patterns appear highly dispersed or random.

Miller (1983) proposed a test method to compare and determine differences between samples of orientation data. The method involves dividing the stereographic projection into a number of equal area 'patches' and comparing the number of observed frequencies of poles contained within each patch between data sets using the χ^2 test. Mahtab and Yegulalp (1984) proposed a method that uses a Poisson randomness test of the density of poles in 'patches' in order to generate clusters (or sets) along with their mean orientation and dispersion (assuming a hemispherical normal distribution). The angle between the means of clusters from the different samples is then compared with the angles of their cones of confidence. If the angle between means is found to be less than the confidence cone angles, then the two clusters are declared similar. If one similar cluster can be found in another sample, the two samples are considered statistically homogeneous. It must be noted that the use of parametric statistical tests imposes restrictions on the minimum amount of data required to confidently use these methods. In addition, the number of patches and their arrangement with respect to north can influence test statistics even with the same data sets (Kulatilake et al., 1990).

Martin and Tannant (2004) proposed a novel method that uses a 'patch' approach similar to Miller (1983) and Mahtan and Yegulalp (1984), however, comparison between data sets is made directly by comparing the standardised covariance ρ (or correlation coefficient), with no assumption of an underlying distribution;

$$\rho = \frac{\sum_{i=1}^n X_i Y_i / n - \left(\sum_{i=1}^n X_i / n \right) \left(\sum_{i=1}^n Y_i / n \right)}{\sqrt{\left[\sum_{i=1}^n X_i X_i / n - \left(\sum_{i=1}^n X_i / n \right)^2 \right] \left[\sum_{i=1}^n Y_i Y_i / n - \left(\sum_{i=1}^n Y_i / n \right)^2 \right]}} \quad (8.12)$$

where n is the number of equal area patches, X_i and Y_i represent the percentage of samples in corresponding patches from each data set (Martin and Tannant, 2004). This method has additional advantages in that 'patches' containing no discontinuities are easily accounted for and clustering of poles into joints sets is not required. The authors applied the method by

looking at fixed slices, moving slices and radial arc slice comparisons in order to locate the position of domain boundaries. It must be noted that use of the standardised covariance method proposed by Martin and Tannant (2004) for domain boundary definition is not without its drawbacks. The combined effects of a poorly selected critical correlation coefficient and the choice of a sequential volume comparison method may lead to continual subtle orientation changes going unnoticed. These effects could be exacerbated in particular rock masses, such as gently folded sediments.

Zhou and Maerz (2002) proposed a multivariate approach to identifying discontinuity clusters. The method creates a 3-dimensional stereograph along a line of particular orientation (i.e. borehole) where discontinuity clusters can be defined not only by orientation, yet other characteristics such as, including surface geometry, mineralogy and location (see Figure 8.1). This multivariate approach has been used to delineate structural sub-domains along boreholes after lithologically based domain definition (Maerz and Zhou, 2005).

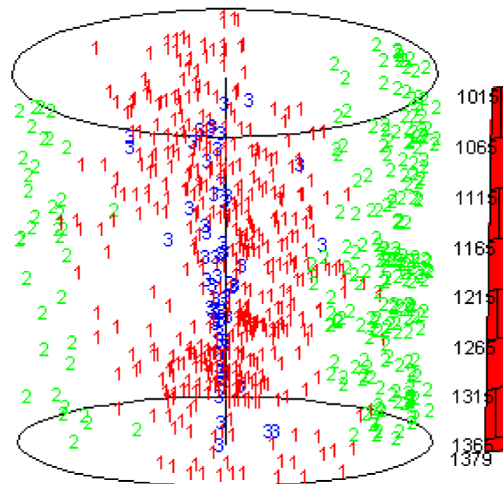


Figure 8.1 - Example of multivariate representation down a borehole (Maerz and Zhou, 2005)

All of the methods above require that orientation data be well distributed throughout the rock mass under investigation. Unfortunately, the ubiquity of quality scan line and window mapping data is lacking for most mining projects. The above methods are therefore better suited to bias corrected oriented drill core and geological backs mapping data.

8.7.5 Structural Geology Approach to Domain Definition

This approach to rock mass domain definition is based on an assessment of the structural geology. The method requires a combined understanding of structural geology analysis techniques and a thorough evaluation of the local and regional geology of the project area.

The objective of structural geology is to determine the mechanism of formation of the geological features. This allows geological features to be assigned to a specific stress or geological setting, critically important in determining the structural evolution of a region and in understanding the changes in the regional and local stress fields with time (Hudson and Cosgrove, 1997). An understanding of the geological processes is also important to assist in determining the likely range of geological features and their properties within various regions of the project area. In regards to domain definition, structural geology allows us to define regions of the mine that constrain the formation of certain types of structures and their associated characteristics.

The methodology relies on interpretation of all available sources of structural geology at a number of scales. The primary objective of a structural interpretation is to obtain an internally consistent 3-dimensional model of the structure that agrees with all available data. Interpretation can be made difficult due to the lack of available data and the number of inferences that are required to be made. However, interpretations should be bound by a number of constraints (e.g. topological and mechanical) that limit erroneous inferences.

There are many methods available for the construction of computerised three-dimensional structural models, however, there are a number of rules and guidelines to this process ensure that consistent and reliable representations are developed (Caumon et al., 2009). Traditional structural geometric methods (Conolly, 1936) are finding increasingly new applications in computerised structural modelling techniques (de Kemp, 2000; Harris, 2001). Integrating field based measurements at a number of scales (namely; outcrop scale, mine scale and regional scale) allows the geologist to develop extended 3-dimensional digital sub-surface models of the structural geology (Figure 8.2), which is of particular interest in underground rock mass characterisation for mine design applications.

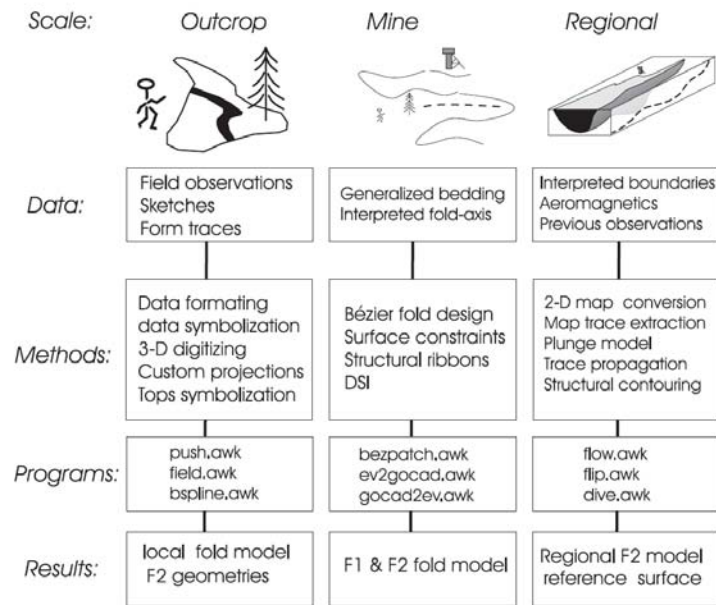


Figure 8.2 - Generalised procedure for using multi-scale data sources for sub-surface modelling (de Kemp, 2000)

A brief overview of the use of structural geology for domain definition is provided below (modified from Winsor, 1998);

- Define largest scale structural controls including major geological units and contacts. This requires a review of the regional structural history, geometry and scale of events (papers, maps, reports, regional geology)
- Determine the geometry and nature of penetrative fabrics (bedding, cleavage, foliation) at the outcrop scale.
- Determine the geometry of mine-scale faults and contacts and their influence on penetrative fabrics. The methods outlined in Chapter 10 can be used to assist in developing mine-scale faults and fold axes.
- Place the outcrop scale measurements into context with mine-scale geology and undertake structural analysis of mine- folding and faulting; geometry, scale and timing. Revise, reinterpret and re-model if required.
- Determine orientation, spacing, frequency of mine-scale faults and potential application as a predictive tool. Establish their impact on discontinuity intensity, development of sets and their orientations.
- Make idealised discontinuity characteristic predictions for selected positions in relation to mine-scale structure.
- Carefully select positions for objective mapping locations relative to mine-scale structures and undertake surveys for validation.

- Compare discontinuity predictions with analysis of mapping data. Review interpretation and model if discrepancies exist.

8.8 MODEL VALIDATION

Model validation usually involves comparison of the predictive model with actual measurements to ascertain the accuracy and precision of the model and any biases that may exist. This necessitates the collection of actual data on the parameter of interest, such as discontinuity spacing for example, as mining progresses. Validation of 3-dimensional models of lithological boundaries, or other geological features, can also be done by comparing its expected location/characteristics with data obtained from observations of the feature as it is intersected during mining. Inaccuracies in the model may indicate that the following may be required;

- changes to mapping/logging, sampling or testing procedures
- re-interpretation of the model
- re-domaining or sub-domaining may be required
- changes to modelling and interpolation methods may be required

8.9 CONCLUSIONS

This chapter has described a number of different modelling methods used to characterise the rock mass and its structure. The choice of modelling approach is generally related to engineering objective and scale, analysis methods to be used and design methodology, and the level of complexity and detail required. However, more importantly, this chapter has demonstrated that the selection and appropriateness of a modelling approach is highly dependent on data type, quantity and quality, as well as spatial availability.

One of the key concepts in developing sophisticated 3-dimensional spatial rock mass models is the reliable definition of domain boundaries. The previous sections have indicated that there many different approaches domain definition, and that they depend on the engineering objectives, analysis methods and rock mass model requirements. It must be also noted that boundaries may also change with inclusion of additional data. In this respect, we need a flexible rock mass data model able to accommodate these requirements and treat domain definition as an ongoing iterative process. Finally, this section also highlighted the importance of the understanding of structural geology in reliable domain definition. In this regard, identification and modelling of large-scale geological structures are critical in the effective domaining of the rock mass.

CHAPTER 9 - A ROCK MASS CHARACTERISATION FRAMEWORK

9.1 INTRODUCTION

As we have seen, the quantity and quality of the underlying data has a significant impact on the reliability of any subsequent analysis or modelling. The previous sections have shown that there are many rock mass modelling techniques available to the rock mechanics engineer to characterise the rock mass. The rock engineer must therefore be cognisant of the limitations of each method, and its impact on the development of a robust geotechnical model and understanding of rock mass behaviour.

Figure 9.1 shows a diagrammatic representation of how rock mass characterisation data can be used, in combination with proposed excavation configurations and boundary conditions, to develop an understanding of potential rock mass behaviour. Importantly, Figure 9.1 can be described as a rock mass characterisation *data dependency diagram*, and shows how specific pieces of data are required to be combined to develop meaningful characteristics and models, and without such specific pieces of data, further more detailed understanding cannot be achieved. In order to assess potential failure modes, data from all of the major groups need to be available; boundary conditions, excavation details, discontinuities and rock fabric properties. Generally speaking, items located on the right of the diagram *depend* on items to the left. For example, set spacing *depends* on orientation *and* discontinuity location (i.e. intersection position on the sampling line).

What is immediately apparent from Figure 9.2, is that reliance alone on unoriented diamond drill core one will never be able to adequately characterise the rock mass or its potential behaviour. The data from unoriented drill core may provide sufficient rock fabric data and the location/position of discontinuities, yet only provides partial characterisation of surface characteristics, certainly provides no information regarding the most important geometrical aspects of discontinuities. The ability to characterise the rock mass, in terms of detail and additional characteristics, improves with the use of 2-dimensional methods such as photogrammetry and mapping (see Figure 9.3). These figures highlight that reliance on data from one data collection method alone will not necessarily provide all of the required rock mass information from either a quality (i.e. level of detail) or quantity (i.e. volumetric coverage) perspective.

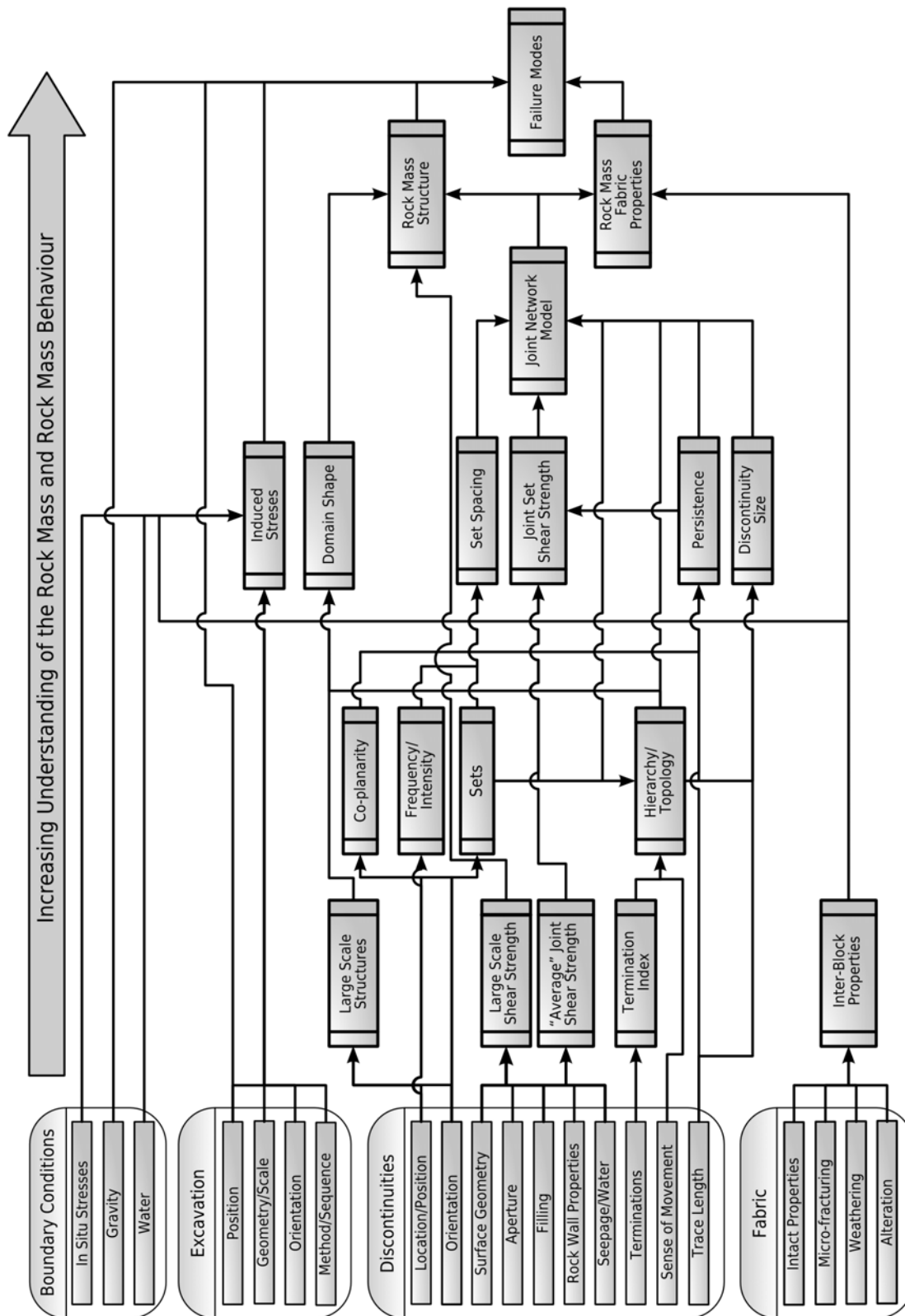


Figure 9.1 - Conceptual dependency diagram showing influence of common rock mass characterisation data types on development of a robust rock mass model

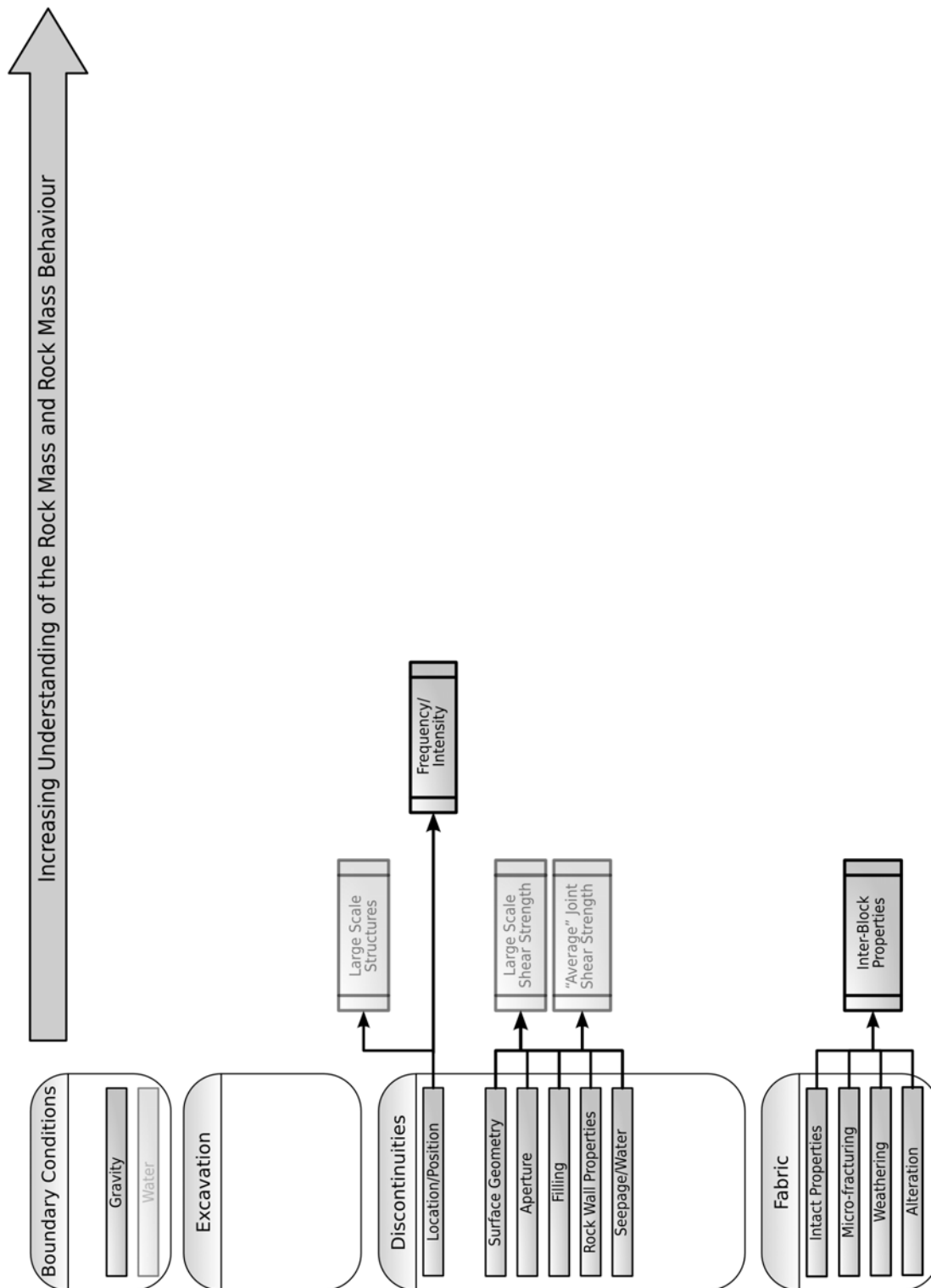


Figure 9.2 - Ability to characterise the rock mass based solely on unoriented drill core. Dimmed items indicate partial characterisation

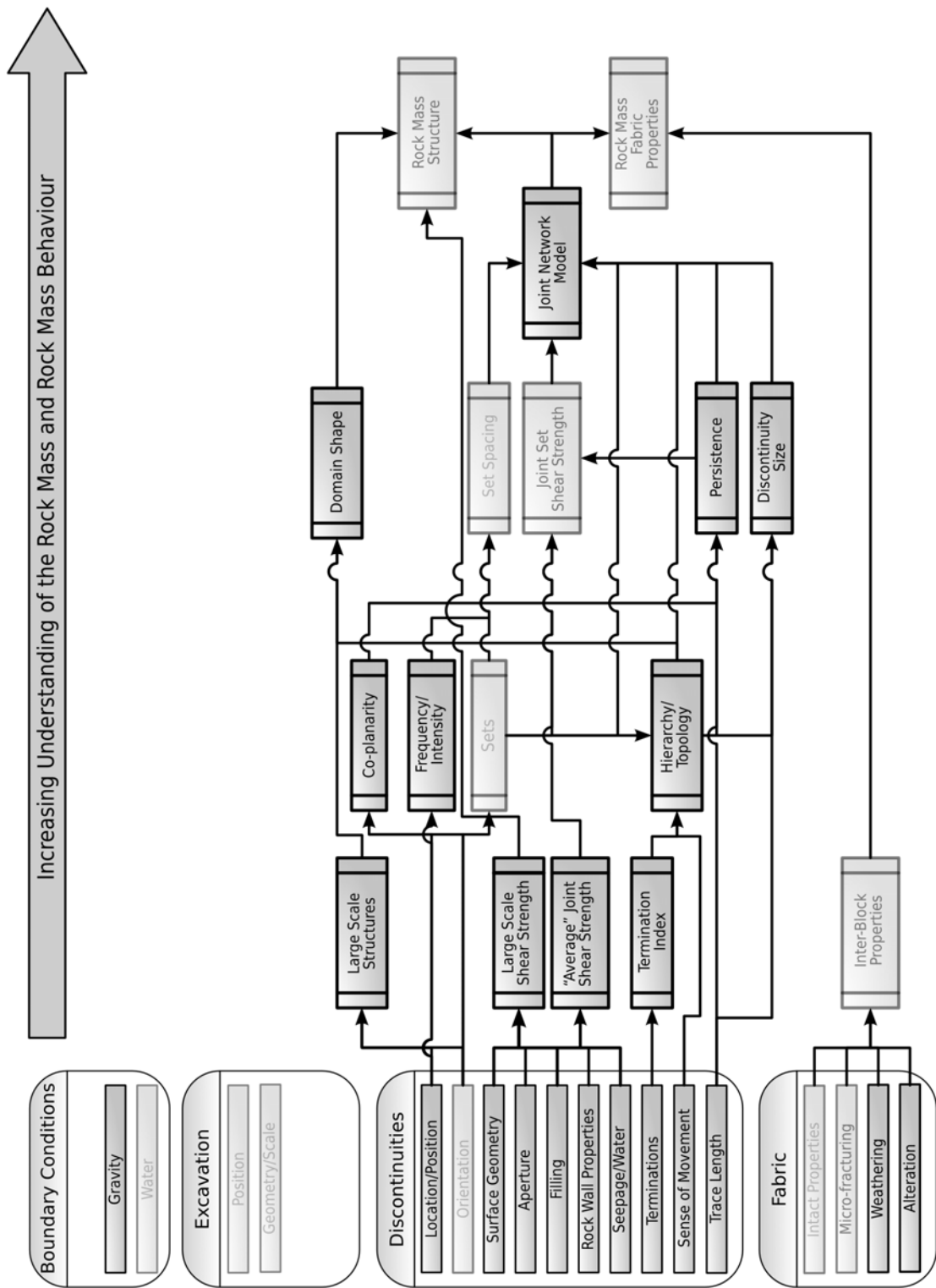


Figure 9.3 - Ability to characterise the rock mass based solely on mapping. Dimmed items indicate partial characterisation

Due to the incremental costs and time associated with orienting drill core, usually only a small portion of rock characterisation programme contains oriented drill core. This severely limits the ability to adequately characterise the rock mass structure. In some circumstances, only sections of selected drill holes are oriented. However, the inclusion of this data is important to our ability to construct meaningful models. It is therefore necessary to have the ability to combine data from all available sources to assist in complete discontinuity characterisation.

Unfortunately, sometimes the rock mechanics engineer will inherit the rock mass characterisation database and is expected to generate a workable solution to an engineering objective given the data. The dependency diagram in Figure 9.1 can be used as a tool to establish additional data collection requirements based on; the engineering objectives, analysis methods to be used and required rock mass models. A balanced approach to data collection is therefore required. Importantly, resources dedicated to the use of more sophisticated geotechnical data collection methods should be optimised for the engineering objectives and the level of project development.

9.2 THE ROCK MASS CHARACTERISATION DATA MODEL

The previous chapters have highlighted that it is imperative that rock mass characterisation, in terms of both data collection and model development, is treated as a continual on going process in the optimisation of open stope design. This necessitates a data model that is able to continually accept and integrate new data as it becomes available. It is also important to maximise the utilisation of all available rock mass data sources, in order to improve both reliability and volumetric coverage by using site specific correlations. To facilitate this data should be stored into a centralised database that has the following basic attributes;

- Allows integration of rock mass data from a variety of sampling schemes (subjective and objective), such as; drill core logging, scanline and window mapping, geological mapping and digital photogrammetry
- Organised and stored in an accessible digital format that enables sharing of information
- Undertake basic data validation
- Calculation of statistical moments of variables based on domain assignment to establish data reliability
- Extraction and preparation of rock mass data from various data sources based on a number of queries
- Allows for spatial data analysis and complex multivariate analysis techniques

- Correct statistical treatment of biases and analysis of geometric discontinuity parameters (i.e. spacing, persistence and orientation) which is directly based on the adopted sampling technique.

In order to facilitate these objectives a specific data model structure is required. A rock mass characterisation data model has been developed to store, query, define relationships between data types, apply bias corrections, and perform basic analysis for use in subsequent detailed analysis and rock mass modelling. The data model has been developed as a Relational Database Management System (RDBMS). The data model was originally developed using Microsoft Access[®] software, however the system has since been migrated to MySQL cross-platform open source server software. The data model is also available as a lightweight standalone SQLite database for use in smaller devices, such as hand-held logging devices. A full description of the development of this data model is beyond the scope of this thesis, however, its development has been based on the ideas and methodologies developed by the author during preparation of this work. The majority of the algorithms used in the data model for validation and applying bias corrections are found in Appendix A. The following sections describe some of the more important aspects that required consideration during the design and development of the data model.

9.2.1 Fact Data versus Interpretative Data

Prior to using any data in the data model, care must be taken to distinguish fact from interpretative data. For example, two exposed fault intersections may be mapped at two distinct locations. If these pieces of fact data have similar orientations and an apparent alignment, the temptation exists to interpret that the two separate fault intersections represent the same structural feature. Any attempt to establish a connection between the two pieces of data becomes a hypothesis or an interpretation. A line on a map or plan linking the two pieces of fact data *always will be* an interpretation. These interpretations are important as they aid our understanding of the rock mass, however, they need to be separated and treated as such.

It must also be remembered that no single interpretation may be correct. In this regard there are many interpretations that can be made using the same fact data. In some circumstances, one geological interpretation may geologically invalidate another which uses the same fact data. Alternatively, two distinctly different geological features may be interpreted, yet they both share the same piece of fact data. In this case, only one of the interpretations is correct and the other may need to be modified by removing this piece of shared data. Therefore, in order to avoid conflict and to aid in auditing and validation of models, it is recommended that each interpretation contains information on what fact data has been used in its formulation. Interpretative data, therefore, can be stored alongside fact

data, however they should be flagged as “interpretations” and also be linked to the fact data which they have been based on.

9.2.2 Data Source Details

The data model requires that the source of information is recorded and that each piece of data is linked to its source. Source details include information on how, when, where, why and by whom the data was collected. Some of these details include;

- Dimension of the sampling regime;
 - Discrete – e.g. point load test
 - Linear – e.g. boreholes and scan lines
 - Areal – e.g. window mapping, geological backs mapping
- Orientation of sampling regime – e.g. trend/plunge of linear sampling regime, dip and dip direction for window mapping / backs mapping plane
- Length or size of sampling domain – drill hole or scanline lengths recorded, window dimensions (censoring limits) recorded for trace length bias determinations
- Truncation level – e.g. 100mm for core, 0.5m for window mapping, 2m for geological mapping
- Sampling approach – e.g. objective versus subjective.
- Fact or Interpretative

The collection of this information is useful for the following;

- De-surveying data (see Section 9.2.3)
- Classifying and separating data by scale for statistical analysis, automatically applying default truncation and censoring corrections to data, managing the validity and reliability of any statistical analyses
- Identification of the data source's 'blind-zone' and orientation bias corrections to the data
- Validating or correcting data taken by specific persons, or during specific time frames, as required.

9.2.3 Data Dimensions and Coordinates

It is important to point out that data also can also be represented in the data model by its dimensions and three-dimensional coordinates. For example, discontinuities can be represented as either points, lines, planes or surfaces at specific points in the rock mass.

Point Data

Refers to data taken as point measurements, or samples taken at a point. For example, discontinuities from drill holes are essentially defined by a point where the discontinuity was intersected.

Line Data

This refers to data digitised on an exposure as a line or line segments, or represented as an interval between two points down a drill hole (e.g. depth from - depth to). Mapped or digitised traces of discontinuities can be represented by a series of lines segment between points. Outcrops of sections of the rock mass or mapping exposure, such as censored zones (i.e. shotcrete), zones of alteration or differing intact rock strength, can be digitised as polygons (closed lines) as a series of sequential points.

Surface And Volumetric Data

This type of data is usually represented as a *TIN* for use in 3-D visualisation software. Discontinuity data can be represented convex planar discs or as non-planar irregular geometries.

De-surveying

For data to be useful in many spatial applications, the actual coordinates of data are required. For the most part, this information can be obtained through direct survey during/after data collection. However, the spatial information for data from drill holes are usually specified solely by depth from the collar. The collar is the only true known location in terms of coordinates. Positional information is specified from in-hole survey measurements, single-shot photographs or semi-continuous optical survey methods such as Reflex Maxibor[®], to establish borehole trend and plunge at known depths. Algorithms are then used to convert survey information to 3D-cartesian coordinates. The choice of algorithm can have a significant influence over the estimation of the real trace and position of the hole.

9.2.4 Domain Tagging

An important process in rock mass data analysis is the ability to group and conduct analyses on data from the same domain, or to test for statistical homogeneity. The rock mass

characterisation data model has provisions for “tagging” all data within a domain with a “domain flag”. In this way, data from certain domains can be queried on the domain flag and analysed separately. Data can be re-combined to form new domains. This allows for rapid generation of statistical moments and testing for statistical homogeneity. The domain tagging process firstly involves assessing whether data points are located within a certain volume or rock mass, usually defined by a 3-dimensional wire-frame surface. This can be done using mine planning software, with the results imported into the rock mass characterisation data model. Alternatively, domains can be created by querying rock mass data model for the location of data or by specific characteristics, such as; rock type, lithology, alteration and weathering.

9.2.5 Summary

The following table outlines some of the more salient features of the proposed data model that attempt to accomplish the previously identified objectives. The specific equations for bias corrections and calculations are found in Appendix A.

Table 9.1 - Example capabilities of the rock mass data model

Requirement	Examples
Make bias corrections	Discontinuity orientation Discontinuity length Specimen scale/shape (<i>UCS</i> , Point Load)
Validation	<i>RQD</i> and discontinuity linear frequency Geomechanics data Check fact data used in interpretations
Calculations	Alpha/Beta to dip/dip direction Rock Mass Classifications Corrected spacing Corrected set spacing Corrected discontinuity linear frequency
Site specific correlations	Point load vs <i>UCS</i> Schmidt Hammer vs <i>UCS</i> <i>UCS</i> /Strength anisotropy Weathering, Alteration, Field Index Strength vs <i>UCS</i>
Complex queries and multivariate analysis	Selection of discontinuities based on orientation, genetic type, mineral infill, thickness.

9.3 CONCLUSIONS

The chapter describes the development of a rock mass characterisation framework that can

be used to understand the role of data dependency on our ability to characterise the rock mass and understand its potential behaviour. A number of data dependency diagrams have been developed to assist in identifying the ability of various rock mass sampling methods to collect various data and develop various rock mass models.

The chapter also summarises the development and key features of a digital rock mass characterisation data model. The data model has the capability to store and query rock mass data, define relationships between data types, apply bias corrections, and perform basic analysis for use in subsequent detailed analysis and rock mass modelling. Importantly, the data model allows for systematic organisation of data to enable rapid statistical analyses and development of a variety of rock mass characterisation models. The data model is capable of managing regular updates of rock mass characterisation data from a variety of sources and formats, and maximises the utilisation of rock mass data by enabling sharing of data between various technical disciplines. The use of the digital rock mass characterisation data model has been pivotal in the development of novel rock mass models, as presented in Chapter 10. The data model has also been applied in analysis of rock mass data and the creation of various rock mass models using case history data in Chapters 11 and 12.

CHAPTER 10 - AN IMPLICIT FUNCTION BASED APPROACH TO ROCK MASS MODELLING

10.1 INTRODUCTION

The previous chapters have shown that there are a variety of rock mass data analysis and rock mass modelling techniques, each with their advantages and disadvantages. Spatial modelling of rock mass parameters is becoming more important in rock engineering as it can allow for the design to be optimised according to local rock mass conditions. There are a number of practical issues with trying to apply traditional geostatistical approaches to spatial modelling of engineering rock mass data. Geostatistics can be easily applied to geological assay data, which tend to be highly concentrated close to the orebody. Unfortunately, rock engineering data are typically poorly sampled, compared to assay data, and more sparsely located. Rock engineering data are generally located at planned excavations, sometimes quite remote from the orebody.

Implicit functions, using *RBF*'s, provide a means to spatially model irregularly sampled and sparse data sets. One may produce an implicit surface from known points by interpolating an embedding function within which the surface is implicitly defined (i.e. a mathematical formulation of the surface). In addition, an implicit surface can be defined at *any value* in a 3-dimensional scalar field (i.e. as an “isosurface”). Because of its mathematical basis, it is extremely easy to regenerate a surface with inclusion, or removal, of data. This makes it very attractive for model updating as new data become available. It also makes it attractive for trialling various scenarios or for model validation.

10.2 SPATIAL MODELLING OF DISCONTINUITY INTENSITY

Compared to other rock mass data, *RQD*, discontinuity spacing and linear frequency data are generally the most abundant, and therefore can be used to develop 3-dimensional spatial models of the density or intensity of discontinuities. From a rock mechanics and rock engineering perspective, the density and size of discontinuities will potentially control a number of rock mass behaviour characteristics. For example, the “degree of fracturing” can have an influence on rock mass properties, such as rock mass strength and rock mass modulus. In addition, an increase in the number and size of discontinuities within a rock mass intuitively leads to an increase in the probability of structurally controlled instability of an excavation surface. Changes in the local discontinuity intensity can therefore provide an insight to potential changes in rock mass properties and rock mass behaviour.

The following sections describe some of the difficulties and considerations in the spatial modelling of discontinuity intensity from one- and two-dimensional data and some suggested approaches using implicit functions. *RQD* data can be modelled in a similar fashion, however, it is not recommended due to its insensitivity and inability to adequately describe discontinuity intensity at all scales.

10.2.1 Models based on One-Dimensional Data

The most important aspect to note is that discontinuity linear intensity is a vector variable rather than a scalar variable. That is, discontinuity linear values obtained along a borehole are unique to the boreholes orientation. Using data from a number of differently oriented boreholes within the same rock mass will potentially result in erroneous predictions in the model. Figure 10.1a shows a 2-dimensional slice through the 3-dimensional discontinuity intensity locus diagram for a certain rock mass. It can be seen that, depending on the orientation of the borehole sampling this region, any value between the maximum and minimum may be selected. As there is currently no practical way of spatially modelling the 3-dimensional discontinuity intensity locus in three dimensions, simplifications to the locus must be made. Figure 10.1b shows a graphic presentation of the discontinuity intensity tensor as an ellipsoid, indicating some possible variations that attempt to capture the 3-dimensional locus. It must be noted that in order to provide a tensor representation, the one-dimensional intensity needs to be sampled in at least 6 different directions. However, depending on the degree of anisotropy, many more sampling directions (>10) may be required, to provide a realistic tensor (Margulies et al., 2002). Figure 10.1c shows isotropic representations (i.e. spheres). It can be seen that both tensors and isotropic models can either over-estimate or under-estimate the discontinuity intensity for a wide range of sampling orientations. The degree of over- or under-estimation is also dependant on the degree of anisotropy of the rock mass. ***Therefore, the validity of spatial modelling of discontinuity linear intensity is dependant on the direction the data was taken and the degree of anisotropy of the rock mass.*** In terms of assessing model validity, assessment of sampling directions is relatively straightforward. However, determining whether the rock mass is isotropic (and spatially remains isotropic) is far more problematic.

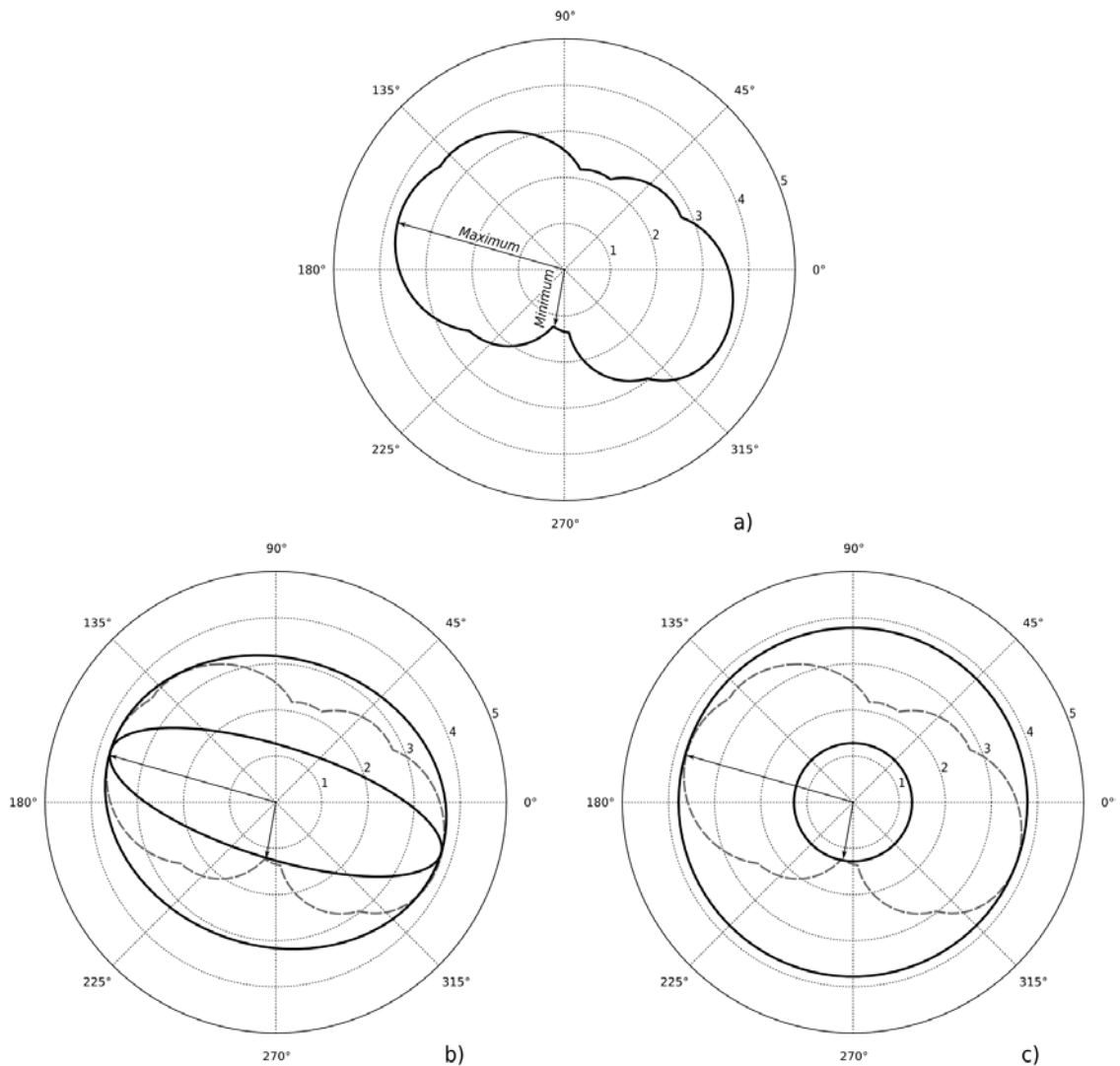


Figure 10.1 - 2-dimensional plane (vertical, oriented east-west) of the 3-dimensional discontinuity intensity locus showing a) directions for maximum and minimum discontinuity intensity, together with possible maximum and minimum b) tensor representations and c) isotropic representations

Bias Corrections To One-dimensional Data

For isotropic representations of discontinuity intensity, bias corrections can be applied to data from all boreholes in an attempt to improve accuracy. This requires that the discontinuity angle to the borehole axis be recorded and used for orientation bias corrections.

Boreholes need not necessarily be oriented to apply corrections. Data from unoriented boreholes can be used as the alpha angle can still be measured. The effect of utilising corrected discontinuity linear intensity versus uncorrected values was evaluated via a modelling exercise. Discontinuity logging data from combined oriented and unoriented drill

holes from the Telfer Gold Mine were utilised. This logging data was unique in that, apart from small isolated intensely fractured zones, the position and alpha angle (i.e. the acute angle from the discontinuity to the core axis) of discontinuities were recorded during logging. Importantly, this enables corrected discontinuity linear intensities to be calculated, regardless of the core being oriented or unoriented.

Data were restricted to an area of the mine where data were most concentrated locally termed the “Main Dome” area. Data consisted of around 29,000m of core logging from 313 holes. Total discontinuity intensity was calculated by counting number of discontinuities intersected over an interval, which typically was one metre to provide consistent sampling support for geostatistical interpolation. Some smaller intervals (<3% of total data) were recorded to delineate small, highly fractured zones (e.g. Faults). Corrected discontinuity linear intensity were calculated by apply a correction weighting to each discontinuity based on its angle to the core axis (according to equation 6.18). Figure 10.2 shows a plot of corrected versus uncorrected discontinuity linear intensity from the core samples. What is immediately apparent is that the uncorrected linear intensities severely underestimate the true linear intensity. It can be seen that, on average, the corrected linear intensity is 140% of the uncorrected value. The distribution of corrected to uncorrected values is influenced by the distribution of discontinuity angles to the core axis, which is in turn a function of the of the discontinuity system pattern and the principal drilling directions. For example, logging data from anisotropic discontinuity systems with a single dominant drilling direction will provide highly skewed distributions.

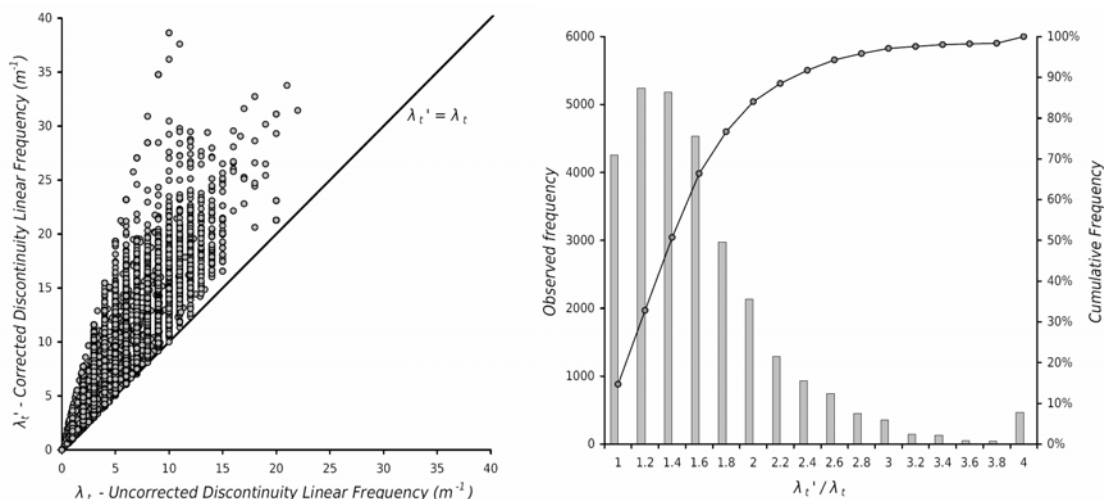


Figure 10.2 - Plot of corrected versus uncorrected discontinuity linear intensity data (left) and cumulative frequency plot of corrected versus uncorrected data

A contouring modelling exercise was undertaken on the uncorrected and corrected discontinuity data sets. Modelling parameters were identical for each data set which consisted of an isotropic inverse-distance weighting applied to data points for interpolation.

Figure 10.3 shows a sample section through the model at 11050mN. It can be seen that there is a significant difference between the two models, with the model based on corrected data showing larger zones of higher linear intensity. The isotropic modelling results tend to reflect the distribution of corrected versus uncorrected sample data. For example, zones delineated by the 2-4m⁻¹ contour interval in Figure 10.3a are similar in size and shape to those displayed by the 4-6m⁻¹ contour interval in Figure 10.3b, that is, approximately 150% difference between the two contour intervals. This analysis highlights how **uncorrected discontinuity linear intensity values from standard unoriented drill core represent a significantly biased estimate of the isotropic discontinuity linear intensity model**. This has an impact on the validity of any model developed from this data.

Isotropically Sampled Rock Mass

In mining, optimal sampling orientations for geology and resource objectives are generally opposite for rock mechanics. The former objective requires consistent orientations to minimise interception thickness bias and the latter requires variable sampling orientations to minimise orientation bias. Notwithstanding this, there are some cases where sampling has been undertaken in a number of directions. It could be argued that a rock mass that has been sampled sufficiently in a number of directions (i.e. “isotropically” sampled) will *potentially* provide a more accurate isotropic representation or tensor representation of the 3-dimensional discontinuity intensity locus.

It is proposed that the spherical variance of sampling directions be used to determine the degree of isotropy of sampling. In this case, each sample's direction can be described by a unit vector (i.e. directional cosines are calculated from trend and plunge of the borehole where the sample is taken). Spherical variance is a descriptive statistic to aid in the analysis of directional data. The mean orientation of sampling can be established from the direction of the resultant of the sum of sampling vectors (Mardia and Jupp, 1999);

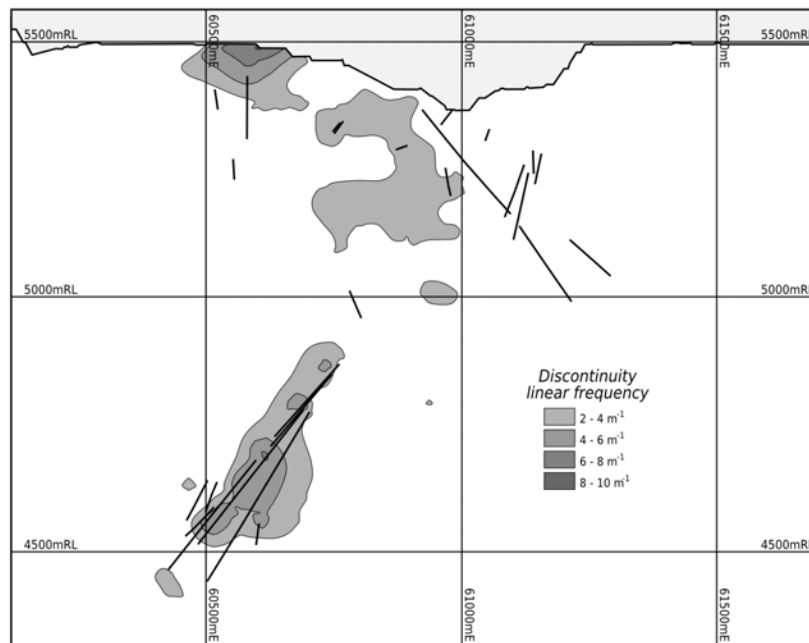
$$\bar{\rho} = \frac{1}{n} \sum_{i=1}^n v_i \quad (10.1)$$

where v_i are the unit vectors of the sampling lengths. The length of the sample mean resultant vector is;

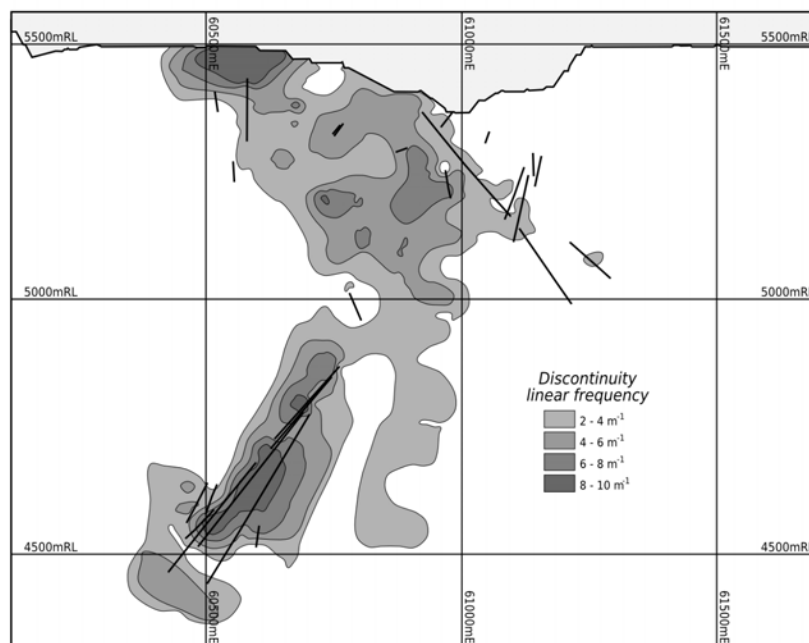
$$\bar{R} = |\bar{\rho}| \quad (10.2)$$

and will have a value between 0 and 1, with a longer resultant length indicating more uniform orientations of the samples. The sample spherical variance is;

$$\hat{\sigma} = 1 - \bar{R} \quad (10.3)$$



a)



b)

Figure 10.3 - Section at 11050mN showing contours of isotropically modelled discontinuity linear intensity for a) uncorrected and b) corrected data

In order to ascertain the variability of sampling spherical variance throughout the rock mass, the sampling volume must be divided into regular sub-volumes, or unit cells of pre-determined volume. The sampling spherical variance can then be determined within these unit cells. A minimum number of samples within each unit cell is required to calculate a meaningful spherical variance.

Statistical inference testing for isotropy could be undertaken, however, this requires an assumption of a spherical distribution. Alternatively, a randomisation test for isotropy can be developed. This requires defining a null hypothesis test against a test statistic of a certain predetermined significance level representing “non-randomness” or anisotropy. We can test the validity of the null hypothesis, by calculating the probability of observing a value of the test statistic greater than the one actually observed. In this case, we can use the spherical variance to assess our assumptions. If the spherical variance is small, that is, if the spherical variance is less than a predetermined significance level (say, 0.05), then the null hypothesis is rejected and we have reason to believe the directions are not purely random, or by chance, and therefore anisotropy can be assumed.

An example exercise of this approach was undertaken using one-dimensional discontinuity intensity data from BHP Billiton's Cannington Mine. Here, core logging data from the diamond drill hole data base were used, and contained approximately 680km of discontinuity logging data. The database could be considered a reasonably isotropic sampling regime due to the orebody geometry and the combined surface and multi-access underground drilling (Figure 10.4).

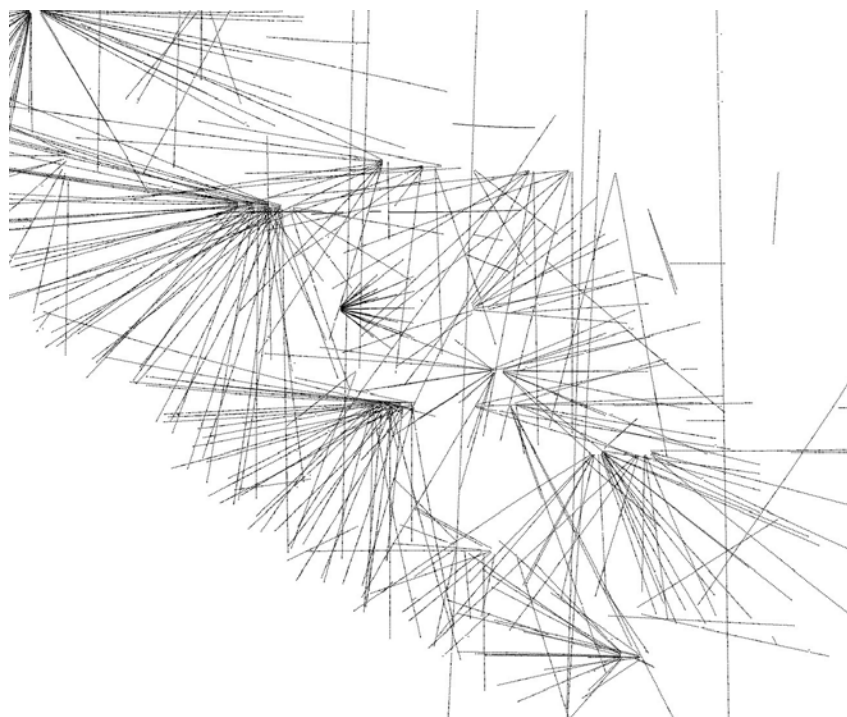


Figure 10.4 - Section at 4690mN showing variability of drill hole sampling directions

The spatial variation of sampling spherical variance was determined by generating a series of unit test cells throughout the sampling volume, and generating the spherical variance and calculating the number of contained samples. The unit cell size was 1000m^3 (e.g. $10\text{m} \times 10\text{m}$

x 10m) and an arbitrary minimum of 5 samples were required to calculate a meaningful spherical variance. An isotropic biharmonic-linear *RBF* was then used to interpolate the spherical variance throughout the rock mass. In addition, the one-dimensional discontinuity drill hole data were used to create an isotropic discontinuity intensity model.

An isosurface at 0.05 spherical variance was then generated and used to constrain the discontinuity intensity model to isotropically sampled regions (i.e. greater or equal than the significance level). The total volume of rock mass sampled versus that sampled “isotropically” was then compared. This was done by generating a volume around each borehole comparable to the volume of the unit test cell;

$$\pi r^2 L = V_T \quad (10.4)$$

where r is a distance from the borehole, L is the length of borehole passing through the unit test cell (i.e. minimum of 10m intersection length) and V_T is is volume of the test cell (i.e. 1000m³) In this case, the equivalent distance (i.e. radius) is 5.64m. Figure 10.5a shows the total sampled volume, based on a 5.64m isotropic distance from the borehole. Figure 10.5b shows the isosurface at the 0.05 spherical variance significance level. From Figure 10.5, it can be seen that the “isotropically” sampled rock mass volume only represents approximately 22% of the total sampled volume. This exercise has shown, even for rock mass which appear to be isotropically sampled (i.e. sampled in a multitude of directions), there is an inability to generate sufficient volumes of “isotropically” sampled rock mass over the area of interest. In most cases, therefore, the accuracy of isotropic representations of discontinuity intensity for the majority of the model must be questioned. Furthermore, generation of accurate tensor representations of discontinuity intensity will be almost impossible in most circumstances, considering the number of sampling directions required. It must also be noted that these issues are further exacerbated for tabular orebodies, where drilling is typically oriented sub-perpendicular to the orebody.

Identifying Rock Mass Anisotropy

If boreholes were oriented, it may also be possible to utilise discontinuity orientation data and the spherical variance approach to ascertain rock mass isotropy. This approach would assume that size distributions are independent of orientation. Alternatively, it is proposed to utilise one-dimensional data from unoriented core data to indicate the degree of rock mass anisotropy using a “test-cell” method;

1. A number of test cells are selected where the rock mass has been sufficiently “isotropically” sampled.
2. Each test cell also needs to have a sufficient number of samples from each sampling

direction.

3. The average discontinuity intensity is firstly ascertained with all samples. It is proposed that, if the average discontinuity intensity does not change significantly with between data from a number of sampling orientations, then the rock mass can be assumed to be isotropic.
4. Scan line or window mapping data taken near the unoriented one-dimensional intensity data can be used to check the validity of anisotropy assumptions, using the methodology of Read et al (2003) or the anisotropy index (A_f) from equation A.39.

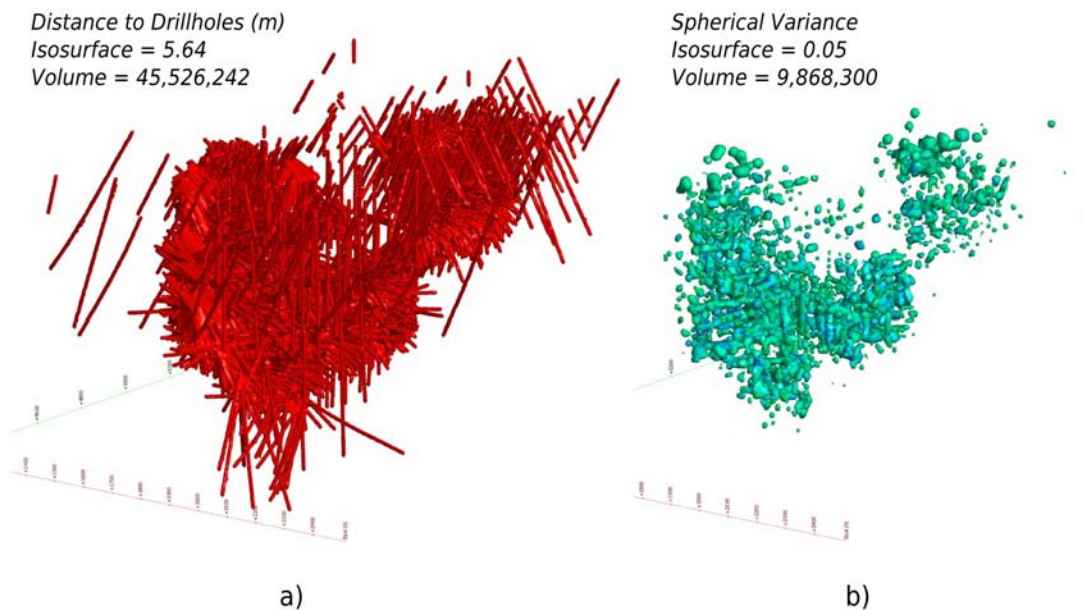


Figure 10.5 - Isometric view of a) total sampling volume based on 5.64m isotropic distance from boreholes , compared with b) the isotropically sampled volume based on spherical variance

As a demonstration of this technique, drill hole and window mapping data from the Cannington Mine were used. An isosurface volume was generated representing where the sampling spherical variance was greater than 0.05 and where the number of discontinuity linear frequency samples per unit test cell were greater than 15 (i.e. sampled isotropically and sufficiently). Only drill hole samples lying within this volume were extracted from the database. The window mapping data were then compared to the drill hole data and two separate areas were selected where there was good volumetric coverage of both types of data (Figure 10.6). For each test area, the drill hole data was divided into orientation groups, based on approximately 30° increments, resulting in a maximum of 6 different directions. The locations of the samples and the orientation groupings are shown in Figure 10.7a and Figure 10.7b. The discontinuity linear intensity measures for each orientation group and test area are shown in Table 10.1. It can be seen from Table 10.1 that Site A has more varied discontinuity linear intensity values with orientation, indicating more anisotropic conditions than Site A.

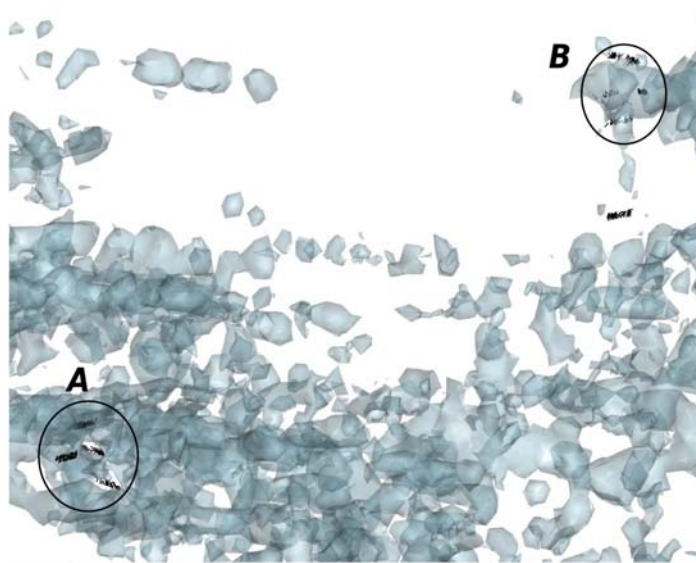


Figure 10.6 - Isometric view of the query isosurface (where spherical variance = 0.05 and number samples per unit cell > 15), together with discontinuity traces from window mapping data showing test areas A and B.

Table 10.1 - Discontinuity Linear Intensity by orientation groups for Sites A and B

Site A						
Orientation Group	Trend (°)	Plunge (°)	Samples	Mean	Std. Dev.	Difference from Site Mean
A	178	24	96	7.56	6.69	38.8%
B	340	9	28	7.46	6.81	37.0%
C	258	18	291	4.69	4.78	-14.0%
D	93	44	214	5.01	4.29	-7.9%
E	280	76	91	6.70	5.49	23.1%
F	96	13	174	5.09	4.8	-6.4%
Total			894	5.45	5.01	

Site B						
Orientation Group	Trend (°)	Plunge (°)	Samples	Mean	Std. Dev.	Difference from Site Mean
A	272	63	283	2.88	2.180	-1.60%
B	270	19	152	2.88	2.550	-1.70%
C	90	12	120	3.08	2.090	5.20%
D	91	42	51	2.83	2.750	-3.30%
E	189	48	16	3.45	3.400	17.70%
Total			622	2.93	2.320	

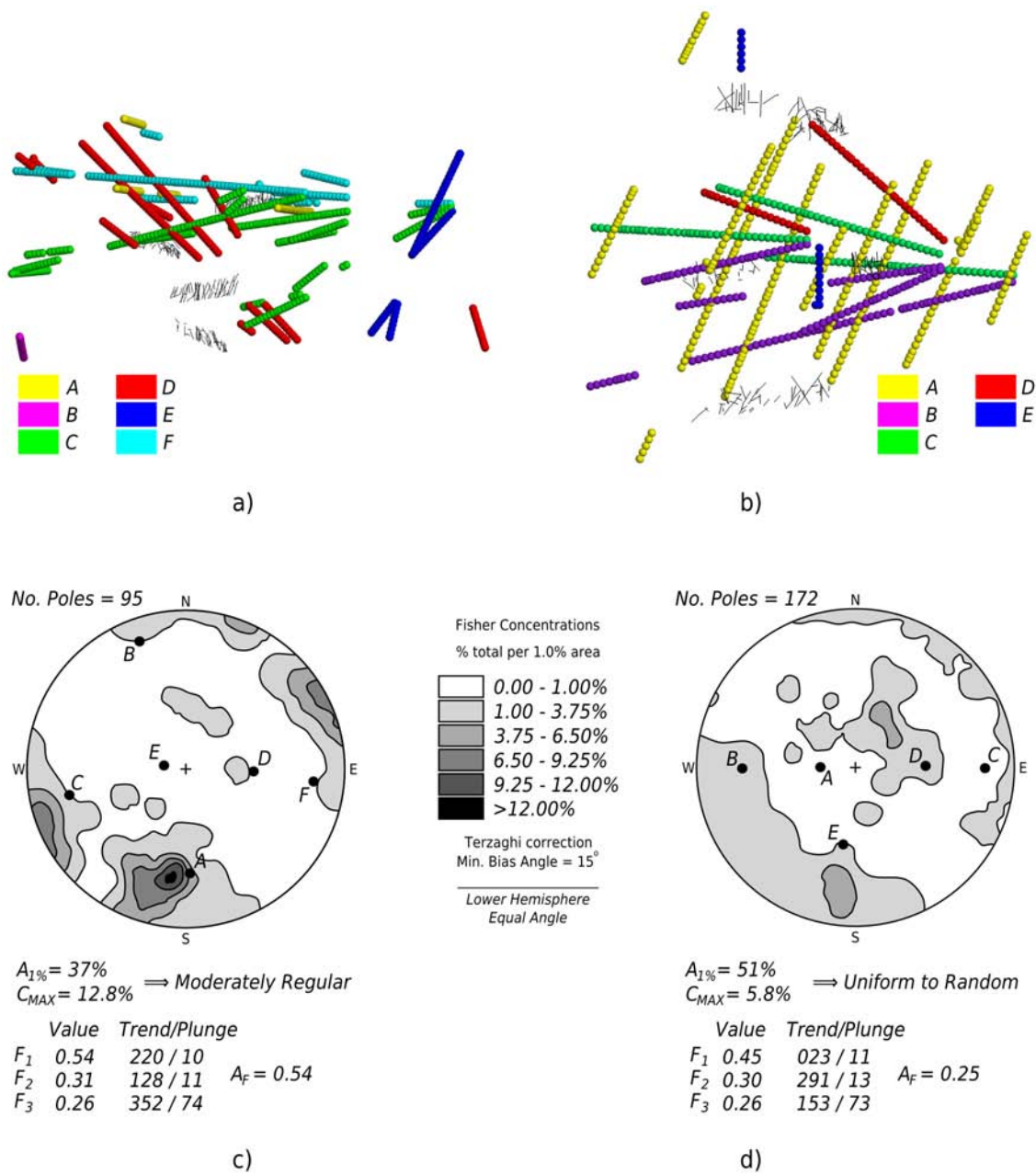


Figure 10.7 - Isometric view of test cell locations A and B, a) and b) respectively, with borehole orientation groups and traces from window mapping data, together with the orientation analysis of window mapping data from areas A and B, c) and d) respectively.

To compare the drilling results with more accurate assessments of rock mass anisotropy, the window mapping data from each area were also analysed. In this case, the orientations from each group are represented as contoured plots, shown in Figure 10.7c and Figure 10.7d, with Terzaghi corrections applied and shown using the same contour intervals for comparison. The lower hemisphere stereographic projections also display the mean drill hole orientation groups (as trend/plunge poles). The anisotropy of the window mapping orientation data was first assessed using the stereographic contour method (Read et al., 2003), which indicated that Site A could be considered “Moderately Regular” which suggests a moderate degree of

anisotropy. Site B data can be considered “Uniform” to “Random”, suggesting a more isotropic characterisation discontinuity orientation compared to Site A. Orientation tensors for both window mapping sites were also generated using equation A.14. The degree of anisotropy was then established using the anisotropy factor (A_F) from equation A.39. From Figure 10.7, it can be seen that Site A has a much larger anisotropy factor than Site B, indicating more anisotropic conditions. These results confer with the stereographic contour method.

This demonstration has shown that, if the rock mass is sufficiently sampled in a number of directions, unoriented discontinuity linear intensity data can be used to indicate rock mass anisotropy. Unfortunately, it is difficult to apply this approach for all areas of the mine. For example, less than 15% of the total Cannington Mine drill hole data set matches the selection criteria used in the above example. This was further exacerbated by the lack of quality window mapping data for validation purposes within these areas of the mine.

10.2.2 Models based on Two-Dimensional Data

A similar approach to interpolation of discontinuity intensity can be adopted for data from 2-dimensional sampling schemes, such as window mapping. Window mapping or even larger scale discontinuity trace mapping, such as geological backs mapping, may be used to obtain estimates of discontinuity areal intensity (P_{21}) at a point (length per m^2 on a plane with an orientation). The use of data from subjective methods, such as geological backs mapping, may provide inaccurate measures of discontinuity areal intensity due to the biased nature of data collection.

A methodology for developing a spatial model of areal discontinuity intensity measure (P_{21}) from 2-dimensional window mapping data is proposed. The method utilises sub-sampling of window mapping traces using a circular sub-sampling windows. The use of circular windows overcomes the issue of bias due to the geometry of the sampling window. In this manner, the shape of the initial sampling region has little influence on local estimation of discontinuity areal intensity. The following method has been incorporated into a computer algorithm, and is described as follows;

1. The 2-dimensional surface exposures of the window mapping locations were first examined for shotcrete with the shotcrete-rock boundary delineated by digitising.
2. Centrelines were automatically created between the lower and upper censoring limits, which were the floor and shotcrete-rock boundary, respectively.
3. For each window mapping location, the centrelines were then sampled at 1m

sampling intervals to determine the minimum distance between the lower and upper censoring limits.

4. The minimum distance was then selected as the circular sampling diameter. This was done to ensure that sampling of discontinuities did not include those that were censored by either the floor or shotcrete in the shoulders. The minimum distance between censoring limits was typically around 4.0m.
5. Sub-sampling points were then created at regular intervals along each centreline at half the minimum censoring distance. This distance was typically around 2.0m. This was to ensure some overlap between circular sampling windows (see Figure 10.8).
6. To reduce bias due to end effects, the first and last centreline sampling points were removed.
7. The circular sub-sampling windows were then overlain over the window mapping data, with the lengths of the individual structures falling within the circular sub-sampling window ascertained. In addition, for each structure within the sub-sampling window, a bias correction was applied to its length. The bias corrected lengths within the circular sub-sampling window were then summed and divided by the circular plane area to obtain the corrected 2-dimensional fracture intensity;

$$P'_{21} = \frac{1}{A} \sum_{i=1}^n \frac{L_i}{\sin \delta_i} \quad (10.5)$$

where δ_i is the acute angle between the i^{th} discontinuity normal and the normal of the circular sub-sampling plane. The bias correction was restricted to a minimum acute angle of 15° .

8. Interpolate resulting P'_{21} values in 3-dimensions using *RBF*'s.

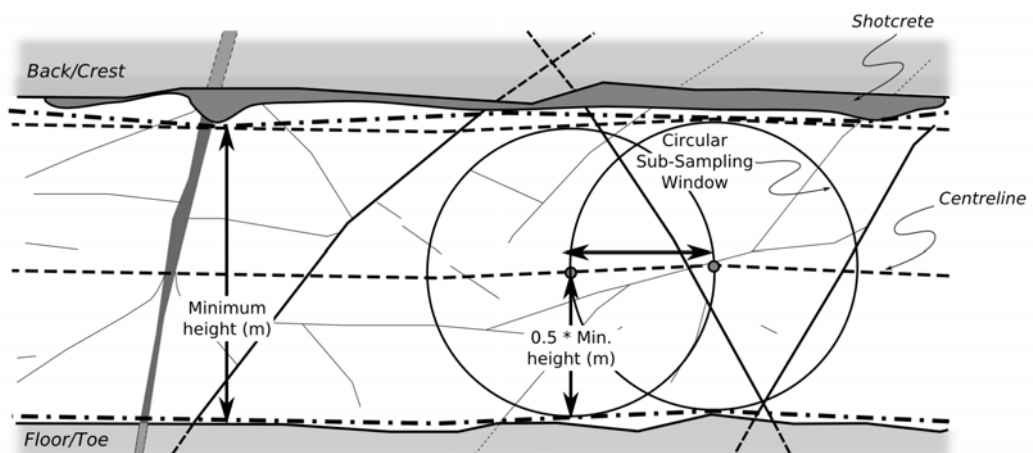


Figure 10.8 - Diagram showing circular sub-sampling windows for analysis of discontinuity areal intensity from two-dimensional data

10.3 A DETERMINISTIC DISCONTINUITY MODELLING FRAMEWORK

In order to investigate the influence of large-scale geological structures on local rock mass conditions and rock mass behaviour, it is necessary to construct models of large, discrete discontinuities. Individual large-scale discontinuities are generally treated 'deterministically' and 'explicitly'. That is, their geometry (location, orientation and size) are explicitly determined from data at specific subjectively sampled points within the rock mass and does not change (c.f. Stochastic-geometric discrete models). In addition, depending on the amount of sample points used to generate the modelled discontinuity, geometrical information, such as the 3-dimensional surface shape, can be captured. This method is generally restricted to individual large-scale features where their continuity and characteristics can be sampled from a number of exposures, typically exposed at the excavation surface.

10.3.1 Traditional Three-dimensional Wireframe Modelling

Traditional geometric surface and solid modelling in mining tends to involve a number of manual processes to construct a three-dimensional surface representing a geological feature;

- Generally speaking, this initially requires the manual sectional interpretation of the structure. Here, the geologist explicitly determines the interpreted position of the fault, based on the location of various data and his/her experience.
- This smoothed interpretation (usually a line on section) is then simplified and digitised as a series of line segments or polygons defined by points. The resolution of these objects is explicitly defined by the subjective choice of the number and spacing of points.
- These line segments are then joined to other line segments or polygons, using tie-lines between the digitised lines to indicate how triangulation should be constrained. The placement of the tie-lines also involves a degree of subjective interpretation.
- A triangulation algorithm is then used to generate a surface (or solid) based on this information.

This process often results in jagged and unrealistic appearances of 3-dimensional surfaces (see Figure 10.9). This is because the number and arrangement of triangles is directly determined from the number and spacing of nodes on digitised lines/polygons and on the rules regarding whether triangles can cross tie-lines and where tie-lines are placed.

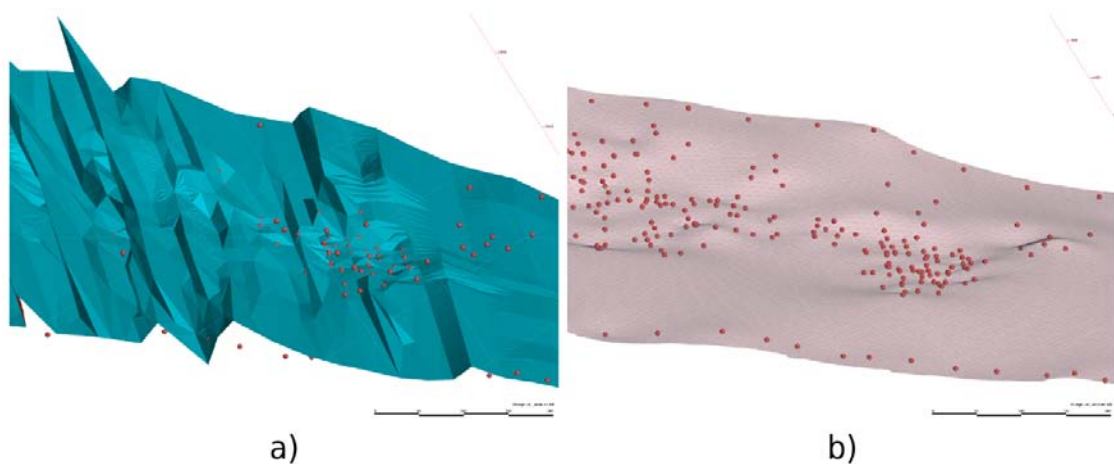


Figure 10.9 - Isometric view of an interpreted fault surface generate by a) traditional sectional interpretation and wire-frame triangulation and b) by implicit surface defined by a *RBF* with user defined resolution for triangulation, together with the fault intercept data set (red spheres)

10.3.2 A Hierarchical Implicit Surface Approach

An alternative way of developing deterministic models from geological data is to use implicit surfaces. *RBFs* can be used as the embedding function for spatial interpolation of fact data (Figure 10.9b). The following sections describe a proposed methodology for generating realistic 3-dimensional models of large-scale structures for incorporation into rock mass characterisation analysis, numerical modelling studies and rock engineering design.

10.3.3 Modelling Process

The main phases of the interpretation and modelling process are as follows;

- Selection of all digital “fact” data representing large-scale discontinuities under consideration (i.e. point data from drill hole and scanline intersections and trace data from geological and window mapping)
- Classifying discontinuity trace data
- Generation of fact glyphs from trace data
- Defining hierarchical relationships of trace data
- Interpolation of a sequence of fact glyphs as implicit surfaces representing structures
- Generation of the implicit surface as triangulated irregular network (*TIN*)
- Model validation utilising drill hole discontinuity intensity and geological logging data
- limiting size of discontinuities

A flowchart of this process is summarised in Figure 10.10.

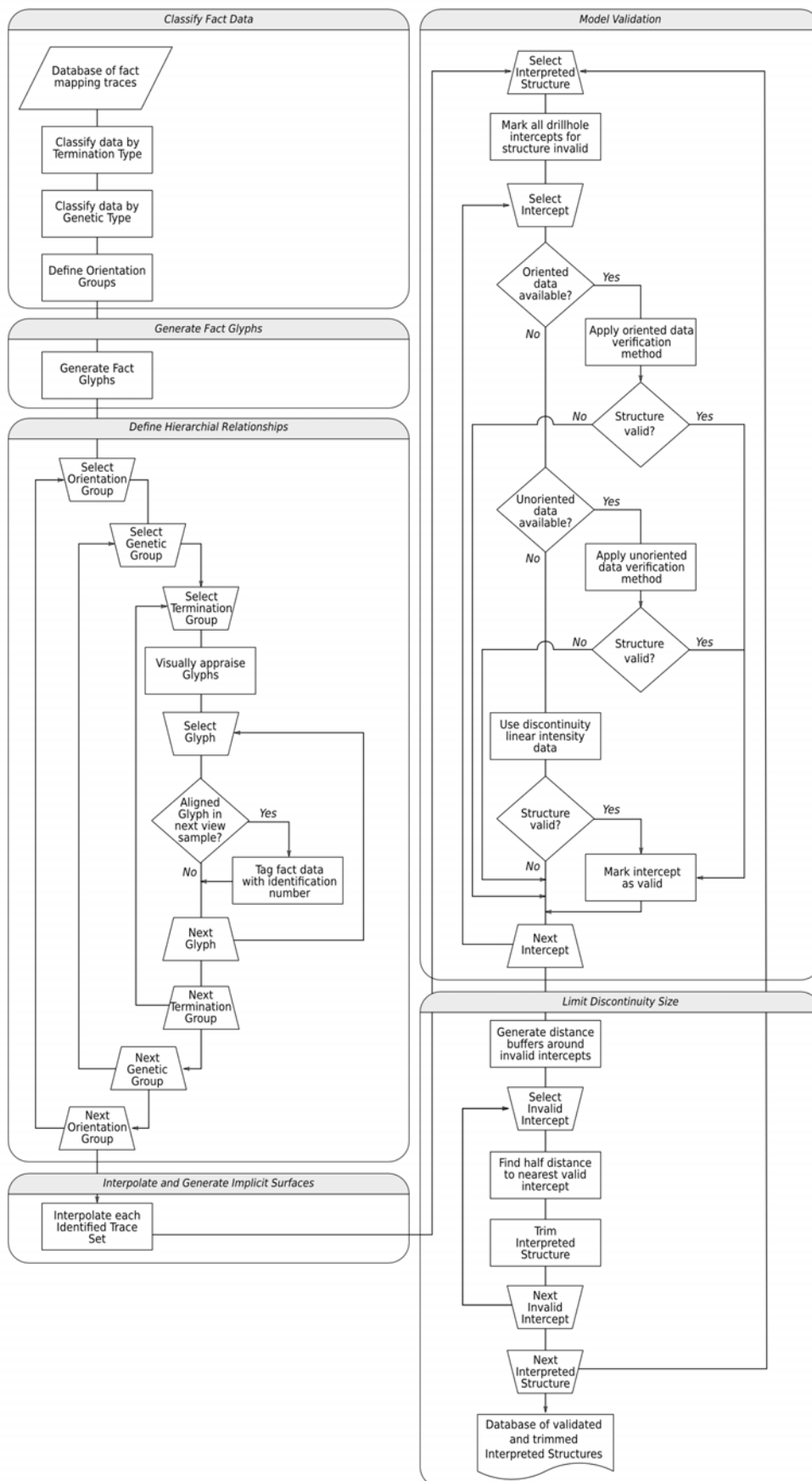


Figure 10.10 - Flowchart for the generation of deterministic discontinuity models

10.3.4 Discontinuity Trace Data

The data for this methodology primarily consists of traces from subjective mapping (such as geological backs mapping), supplemented by traces from objective sampling schemes (i.e. window mapping data). The traces are the three-dimensional lines of intersection that geological structures make with the excavation boundary. Along with x, y and z coordinates (i.e. the local mine Cartesian coordinate system) of each point representing the trace, geological information, such as dip, dip direction and feature type, are generally recorded during mapping.

10.3.5 Discontinuity Persistence and Hierarchy

In order to attempt to preserve the geological hierarchy, the modelling was undertaken sequentially, with discontinuities with the largest persistence were modelled first, followed by modelling of less persistent discontinuities. Termination type was used to assist in determining the persistent primary features from impersistent and/or secondary features. To assist in this process, discontinuity traces were classified by their terminations;

1. both unknown
2. structure-unknown
3. rock-unknown
4. structure-structure
5. structure-rock
6. rock-rock

This process was undertaken manually by examining and classifying each trace. Figure 10.11a shows an isometric view of termination classified fact data.

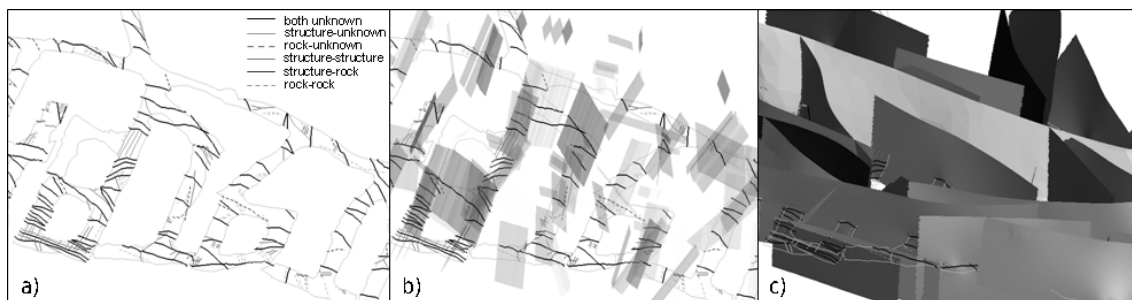


Figure 10.11 - Clipped isometric view showing a) classified fact data, b) "pseudo" fact glyphs and c) interpolated structures

10.3.6 Genetic Classification

The fact data were also classified on the genetic characteristics of each structure as identified by the geologists. This was done to ensure only similar styles of structure were

utilised in the interpretation. The main genetic structural modes were identified;

1. Shear/Major features; shears, faults and contacts
2. Compressional features; foliation
3. Tensile features; veins and joints
4. Mixed mode; shear veins, joints

More detailed classification can also be provided by sub-dividing each genetic group using additional discontinuity characteristics such as mineral infill, wall alteration, surface geometry, etc.

10.3.7 Orientation Grouping

To ensure realistic interpretation of structures, the data needed to be grouped by their orientation. Orientation analysis is first conducted on the fact data and the mean vectors of each set established. The fact data can then be queried and data selected where the unit normal vector lies within a tolerance angle of the downward or upward directed of the mean vector of the set.

10.3.8 Generation of fact glyphs

To further assist in interpretation, the dip and dip direction data were used to generate “pseudo” fact surfaces of each structure. This process involves generating a small 3-dimensional surface from each trace, with the size restricted in the strike direction by the mapped trace. The size in the dip direction was limited to 5m up and down dip (approximate maximum dimensions of excavations). These fact glyphs, represented as small 3-dimensional surfaces or planes, were then used to assist in the three-dimensional visualisation and interpretation of large-scale structures (Figure 10.11b). To further assist in interpretation, the fact glyphs can be colour coded to represent the various termination or genetic classification types.

10.3.9 Fact Data Selection and Interpolation

The interpolation process involved stepping through a clipped sectional or level view of the fact data and glyphs in three-dimensions and manually selecting fact data representing each interpreted structure. Each interpreted structure was assigned unique identification number. A structure is deemed continuous and interpreted as the same structure if it can be traced with fact data (based on glyph orientation, termination type and genetic mode) from level to level. The data set of traces for each interpreted structure was then interpolated using *RBF*'s and a 3-dimensional surface generated as a *TIN* with a minimum 5m triangulation resolution (Figure 10.11c).

10.3.10 Model Validation

To validate the existence of a modelled structure, its expected location somehow has to be verified. This is typically done using data independent of the modelling process. In practice, a modelled structure could be validated if it was predicted at some distance ahead of underground development and, with further mining, is intersected at its predicted location. Unfortunately, this opportunity is very rare. However, other forms of independent data, such as drill core logging can be used. It is proposed to utilise geological structure logging and discontinuity linear frequency data for validation purposes.

The drill core logging data are interrogated for the presence of logged structures in the vicinity of the intersection of the interpreted structure and the drill hole. If a structure is present the genetic type and orientation information are used to validate the interpreted structure. Any interpreted surface intercepting a drill hole where a corresponding logged structure has not been identified is termed invalid. In this case, the extent of the interpreted structure is trimmed to the half-distance to the nearest valid intercepts in other boreholes.

For oriented data, small “pseudo” fact glyphs can be made at positions down the drill hole where structures have been mapped to aid visual identification. Glyphs are represented as idealised circular disks with a set radius and colour coded by genetic type. Again, this data can be grouped via orientation. The interpreted structures were then validated against the drill hole glyphs. A semi-automated routine involves interrogating the distance between the logged structure and the intercept of the interpreted structure in the drill hole, as well as the angle between the unit normals. Distance and angular tolerance levels can then be used to valid the interpreted structure, typically 5m and 15° respectively. The valid intercept in the drill hole can be used as additional fact data and the structure is re-generated, if required.

Validation against oriented logging data is relatively straightforward, however the use of unoriented logging data is problematic. This is mainly due to non-specific nature of the orientation of logged structures in core. That is, the orientation of the logged structure is only represented by the alpha angle (i.e. minimum angle between local discontinuity plane and the drill hole core axis). The true orientation of the structure can therefore be any direction rotated around the borehole axis through alpha and any interpreted structure intersecting the borehole at this position running parallel to the alpha angle may be a possible candidate. A semi-automated computer programme routine was also developed to test for this condition. Firstly, an array of upward and downward directed unit normal vectors were constructed at the logged position normal to the alpha angle (see Figure 10.12). For each array, unit normal vectors were automatically constructed at a 10° radial increments.

The angle between the unit normal vector of the interpreted structure was then compared to the tolerance angle for each unit normal vector in both the upward and downward arrays.

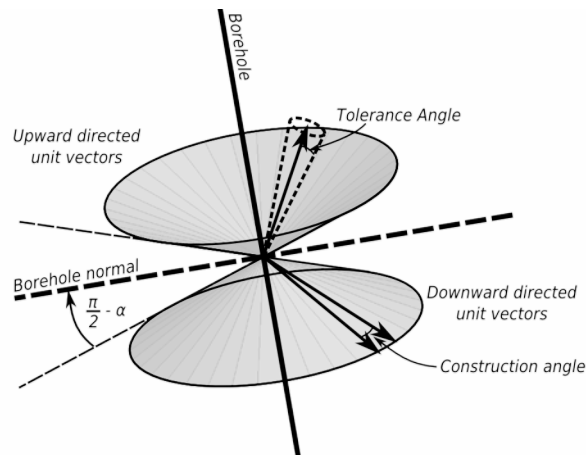


Figure 10.12 - Angular validation criteria for unoriented structural data

Unfortunately, the use of unoriented core data and this method of validation dramatically increases the probability of finding a structure that matches the validation criteria. For example, consider the surface area of the unit sphere as the complete random probability region, with a surface area of 12.57. For the oriented method, one unit normal generates a surface area on the unit sphere of 0.215 with a tolerance angle of 15°. For the unoriented method, one unit normal generates a surface area on the unit sphere of 3.25 for the same tolerance angle. This indicates that the probability of a completely random structure being validated (based on orientation alone) is around 1.7% using oriented data compared to 25.9% using unoriented data.

In some circumstances, the rock mass in the drill core is too badly broken for the geologists to record the orientation of structural features. In this case, discontinuity intensity data can also be used to validate interpreted structures. Once an interpreted structure has been postulated, the discontinuity intensity values in drill holes surrounding the structure are interrogated. A discontinuity linear intensity validation criteria of $>10\text{m}^{-1}$ was selected.

The use of discontinuity linear intensity data does have some limitations with respect to verification of the existence of structures. It must be remembered that the discontinuity linear intensity values are typically logged over 1m intervals, and in some circumstances over much larger intervals. A one metre, or greater, interval may lack sufficient resolution, especially for structures that may have a limited impact on local rock mass conditions. In addition, if the drill hole sampling directions are anisotropic, structures oriented sub-parallel to this direction will not be adequately sampled, impeding verification of interpreted structures.

10.3.11 Comparison with Traditional Digital Discontinuity Models

An example of the construction and validation of a deterministic discontinuity model using the proposed techniques is provided in Figure 10.13. The top section (Figure 10.13a) shows a perspective view of a traditional wireframe model of a fault surface, together with the fault intercept data sources, coloured in black (courtesy of Kanowna Belle Gold Mine). It can be seen that the surface is quite irregular, with substantial peaks/trough which influenced by using raw data as the triangulation nodes. In this model, *all* data points are assumed to be representative of the same geological feature. In addition, the surface extends well beyond assumed fault intercepts, implying a degree of continuity which may not be justified. Indeed, there is no indication of how valid the interpretation is between data points nor how far beyond outlying data points.

The lower half of Figure 10.13 shows an example model using the proposed implicit function based deterministic discontinuity modelling technique, together with valid data points (black) and invalid drill hole intercepts (red spheres). The surface coloured light purple represents an *RBF* fit to *all valid* data points. The darker purple surface represents the validated surface, which has been trimmed only to include valid intercepts (using the procedure above) and to a distance no more than 25m from at least two data points. This second criteria is based the demonstrated ability to confidently assess structural continuity between two mapping drives (i.e. 25m level interval). Using the proposed technique, models can be developed that provide realistic surface morphology, provide information on where the interpretation is valid, and where uncertainty exists in the model.

10.4 CONCLUSIONS

This chapter has described a number of novel modelling methods used to characterise the rock mass and its structure using implicit techniques. The choice of modelling approach is generally related to engineering objective and scale, analysis methods to be used and design methodology, and the level of complexity and detail required. Implicit function approaches provide the rock mechanics engineer with the ability to spatially model sparse and irregularly sampled data sets. Because of its implicit nature, isosurfaces can be generated at any value, and calculated at any point (e.g. on a structure, on an excavation surface, at numerical modelling grid points, at instrumentation locations, etc.). This makes their use flexible for a variety of design techniques. The use of implicit functions also allow for displaying of results at much greater resolutions than traditional geostatistical techniques, as they are not restricted by the size of blocks in block models. This aspect can reduce the issues with respect to complexity of site geology and scale.

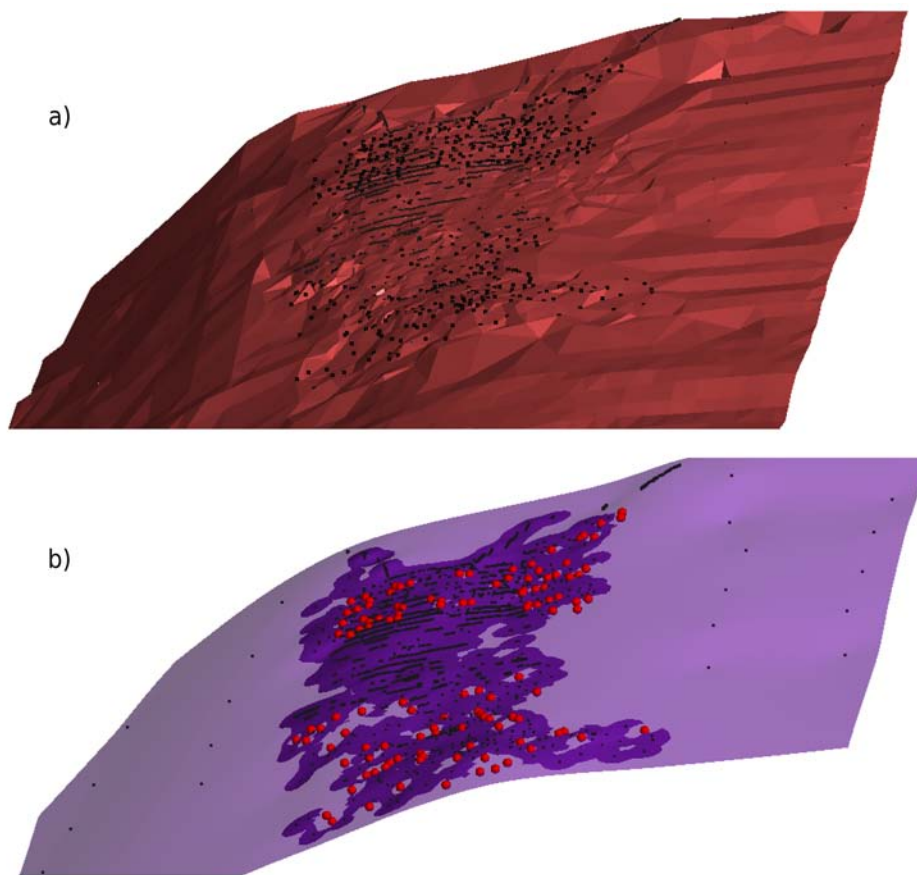


Figure 10.13 - Perspective view of models of Fitzroy Fault a) using original data and traditional modelling techniques and b) proposed implicit function based approach (see text for details)

10.4.1 Spatial Models of Discontinuity Intensity

This chapter has described some of the issues, together with some approaches and improvements, related to spatial modelling of discontinuity intensity data using implicit functions. In terms of developing meaningful and accurate spatial models of discontinuity intensity from one-dimensional data it is essential that the influence of sampling and rock mass isotropy be considered. When developing a spatial model from intensity data it is recommended these aspects be considered (shown in Table 10.2).

Notwithstanding these issues, even for a spatial model developed from an entirely anisotropically sampled data set, extreme spatial changes in the one-dimensional intensity still represent significant changes in the rock mass structure, and therefore identifying where they occur can provide useful information to the design engineer. However, it must be remembered that it is unknown whether this spatial change is due to a change in either anisotropy, discontinuity size or density.

Table 10.2 - Summary of the influence of sampling and rock mass anisotropy on spatial models of discontinuity intensity

Sampling Orientation	Rock mass	Spatial Modelling Considerations
Isotropic	Isotropic	Assumption of the isotropic representation of the 3-dimensional discontinuity locus may be valid. Isotropically sampled rock mass will potentially provide an accurate isotropic representation of discontinuity intensity. Validity of the assumption of an isotropic rock mass may be tested; addition or removal of samples with different orientations within a test cell should <u>not</u> greatly influence the mean.
Isotropic	Anisotropic	Assumption of the isotropic representation of the 3-dimensional discontinuity locus is <u>not</u> valid. Isotropically sampled rock mass may potentially provide sufficient information to enable a tensor representation of discontinuity intensity, in some areas. Rock mass anisotropy may be tested; addition or removal of samples with different orientations within a test cell <u>should</u> influence the mean.
Anisotropic	Isotropic	Assumption of the isotropic representation of the 3-dimensional discontinuity locus may be valid, however, in sufficient sampling directions to test for rock mass isotropy. Use of corrected one-dimensional data may improve accuracy of isotropic model.
Anisotropic	Anisotropic	In sufficient sampling directions to test for rock mass anisotropy.

10.4.2 Deterministic Discontinuity Modelling Framework

A detailed methodology for constructing 3-dimensional deterministic discontinuity models has also been developed. The proposed implicit function approach to discontinuity modelling has many advantages over traditional manual wire-frame modelling techniques. Firstly, the proposed approach removes some of the biases and subjectivity caused by manual interpretation. The use of implicit functions make it possible to capture the subtle (real) surface profiles of structures, yet also has the ability to deal with noisy data, if required.

As we have seen, the validation procedure is an important feature of the methodology as it allows development of models that include information on where the interpretation is valid and where uncertainty exists in the model. Another feature of the proposed technique is that the validation rules can enable construction of interpretive structural models to various levels of confidence.

Recently in the mining industry, we have witnessed an increase in capture of digital discontinuity data, such as photogrammetric and computer based mapping systems. The

proposed methodology, in conjunction with the rock mass characterisation framework, enables rapid construction of deterministic discontinuity models. Because of its semi-automated approach structures can also be regenerated quickly and regularly with the inclusion of more data, providing engineers and geologists with up-to-date detailed models.

The deterministic modelling approach also provides the rock engineer with an important tool for rock mass modelling and excavation design. The spatial discontinuity intensity models and the deterministic discontinuity models can be combined to assess the influence of large-scale structure on local rock mass conditions. For example, it can provide the engineer with a tool to predict anticipated rock mass conditions based on the presence of a certain style of fault. Accurate models of large-scale discontinuities are also important in domain definition or for optimising domain boundaries. Because of their implicit basis, boundaries can be quickly shifted. Alternatively, the deterministic models can be used to select data. For example, distance fields can be used to rapidly query data nearby or on a certain structure. The highly detailed deterministic discontinuity models can also be easily imported into numerical modelling packages, such as linear elastic or non-linear continuum codes, which may provide more detailed and accurate understanding of strain accommodation and its influence on rock mass behaviour.

Practical application of 3-dimensional spatial models of 1- and 2-dimensional discontinuity intensity data and deterministic discontinuity modelling techniques are demonstrated in Chapters 12 and 13.

CHAPTER 11 - AN INTEGRATED APPROACH TO THE GEOTECHNICAL DESIGN OF SPANS IN OPEN STOPE MINING

11.1 INTRODUCTION

In the planning and design of underground mines, company strategy and business plans are the main drivers for advancing a particular project. In this regard, management define the business objectives, and to some degree, the functional requirements and possible constraints on mine design. Given the inherent uncertainty associated with rock engineering, there is always a risk that the proposed design may not perform as intended, with associated economic and safety implications. Management are therefore responsible for formulating policies relating to acceptable business risks, which then need to be addressed in the design process. It is thereafter the responsibility of the design engineer to develop a design that attempts to accommodate these objectives and constraints, within the specified performance criteria.

Due to the unique project-specific rock mass conditions, orebody characteristics and geometry, as well as the practical and economic constraints of the day, the open stope design process will inherently generate a unique design. With that, there is the fundamental realisation that there will be no accurate method to pre-determine the reliability of the design (i.e. based on similar rock masses and mining undertaken elsewhere). Design reliability can only truly be assessed by evaluating how well it has achieved its intended performance criteria, during or after mining. The objectives of the design engineer will therefore be to ***initially aim to generate a design to the required level of reliability*** at early stages of project development. If, during initial construction, the generated design does not reliably provide the required performance then it maybe necessary to ***optimise and improve reliability of the design*** or implement mitigation strategies to manage the risk of potential poor performance.

11.2 DESIGN OPTIMISATION THROUGH AN INTEGRATED APPROACH

The key philosophy behind design optimisation is the continual reduction in uncertainty in collected data, analysis and design methods used with a view to ***improving the overall reliability of the design***. That is, improving the probability of success in achieving the required performance criteria. A stope span design optimisation approach is proposed which attempts to ensure that the appropriate methodologies in data collection, data analysis, rock

mass model formulation and stope design are utilised at relevant project stages in order to minimise uncertainty and maximise design reliability. The design optimisation approach recognises that the appropriateness of a particular design methodology is highly dependant on the availability of an appropriate rock mass model, which is in turn dependant on the availability of quality rock mass data. With respect to the design of spans in open stope mining, the key aims of the proposed integrated approach are to;

- Assess the suitability of data for analysis
- If data is unsuitable, assess the most appropriate data collection strategy
- Assess the most appropriate approach to rock mass modelling
- Assess the most appropriate design methodologies
- Assess the reliability of the design criteria and quantify the potential economic impact of the design on the project

The proposed approach also recognises that optimisation requires continual integration of state-of-the-art techniques. During development of this thesis, a number of improvements have been proposed in key areas of the rock engineering design process which can be incorporated into the integrated approach, including;

- A rock mass data model that facilitates the ongoing rock mass characterisation process.
- Spatial rock mass and deterministic discontinuity modelling techniques to improve the understanding of the spatial variability of rock mass parameters, inter-relationships between rock mass characteristics and their role in design. Importantly, this enables the understanding of the influence of large-scale structures on rock mass characteristics and excavation performance.
- Improved geometrical assessments of stope performance that maximise the use of stope performance data.

To supplement these techniques a back analysis frame work is also proposed to assist in improving design reliability. A key component of the back analysis framework was the development of a spatial model which integrates rock mass characterisation models, performance assessment data and the results from numerical modelling. With respect to numerical model, a number of improvements to linear elastic back analysis are also proposed.

An overview of the integrated approach is outlined in Figure 11.1. The diagram outlines the interaction of a number of rock engineering design components used for the initial design

(to the left of the diagram) to detailed and ongoing design and operation of open stopes (depicted on the far right). A suggested range of data, rock mass model and design reliability target levels have also been proposed for each stage of project development. The diagram can be used in conjunction with a general rock engineering span design flowchart provided in Figure 11.2. This figure outlines the general steps involved in developing a robust stope design. The process shown in Figure 11.2 has been divided into numbered sections which correspond to the main components shown in Figure 11.1. The following sections describe in more detail the various components of the proposed integrated approach.

11.3 PROJECT DEVELOPMENT STAGE AND OBJECTIVES

The top section of Figure 11.1 briefly outlines some of the major objectives to be achieved during the various stages of project development of an open stope mining operation. At the Conceptual stage, the objectives of design are to assess the most appropriate mining method, given the general orebody geometry and rock mass characteristics. At the Pre-feasibility stage, the mining method has generally been selected, and likely stope dimensions and mining block configurations will need to be established. Here, the use of empirical methods are generally unavoidable, simply as there are insufficient data to justify more sophisticated methods.

At the Feasibility phase, sufficient data should exist to enable simple analytical methods (which are appropriate for the rock mass model and identified anticipated failure modes) and also to utilise basic numerical methods. Main objectives include setting sub-level intervals (usually determined by equipment selection and drilling accuracy) and along strike pillar placements. At this stage the global sequence is generally determined and detailed stope design may commence. Methods that are able to account for spatial variability in material properties are desirable in order to optimise the design for the various regions of orebody.

During early construction, the first few stopes will provide invaluable data on stope span performance against initial predictions. Maximum effort should be placed on back analyses and confirming the reliability of the initial design criteria during these stages. Continuing with design parameters that are either over-conservative or over-aggressive will have a significant impact on future project viability. During the early construction phase sufficient data usually exists to develop more detailed mining area stope sequences.

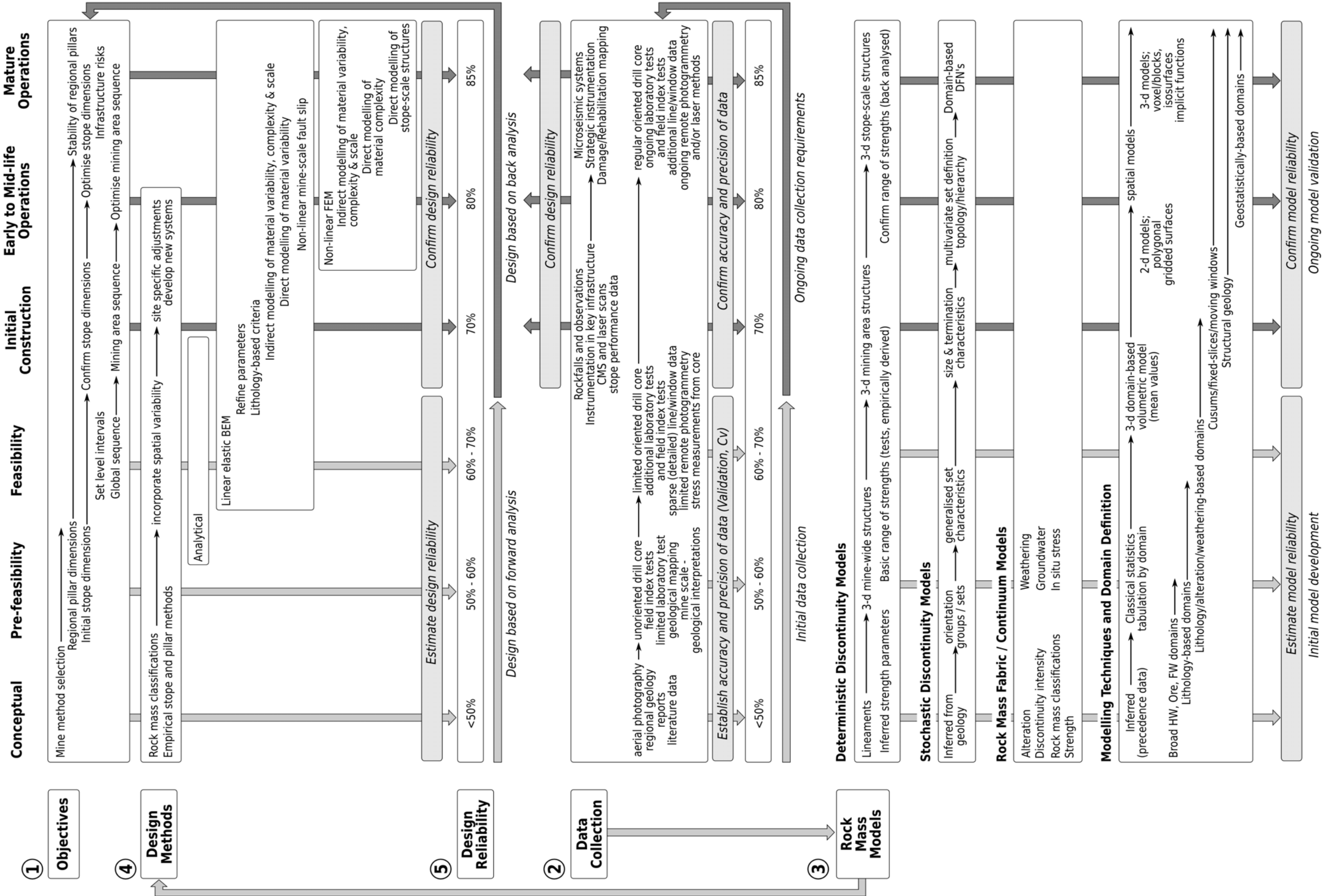


Figure 11.1 - Interaction and progression of design objectives, design methods, rock mass models and data collection with project development

The discussion above demonstrates that a staged approach to the level of complexity and sophistication of design methods is generally appropriate. This is done to ensure that design methodologies are selected which are able to reliably capture the complexity of rock mass interactions and observed behaviour, and to provide designs with levels of reliability commensurate with stage of project development.

11.4 DATA COLLECTION

The centre section of Figure 11.1 outlines the levels of detail in rock mass characterisation and response data collection as an open stope mining project develops. The principal aims of a data collection programme for open stope mining should be to ensure that;

- There are sufficient data density around proposed stope spans
- The required data types are available for the analysis techniques proposed at each stage of development
- Data is of sufficient quality to reliably undertake span design

If existing data is insufficient, appropriate sampling strategies need to be adopted, taking into consideration complexity of rock mass domains and data collection methods employed. The anticipated rock mass data collection requirements are also a function of the level or stage of project development. This is highlighted by Haile (2004), as shown in Table 2.2.

At the Conceptual stage rock mass data are initially concentrated around exploratory holes, becoming more concentrated around defined orebodies, however the quantity and type of rock mass data may still be very limited. At the Feasibility phase, it is envisaged that there will be rock mass data of sufficient quantity and quality to reliably ascertain the mean and dispersion of key rock mass parameters in the major rock types identified.

Early construction will allow direct access to the rock mass to verify variability in various rock mass parameters, yet also allow collection of additional rock mass parameters that could not be collected in early stages (for example, discontinuity persistence and termination characteristics). Ongoing data collection programmes aim to improve data quantity, density and spatial distribution, allowing for more sophisticated rock mass models to be built. As the project develops, additional rock mass data should be collected to improve the spatial distribution of samples that will enable reliable spatial models to be developed and/or to act as independent samples to validate existing models. Collection of additional data may also be required to expand the data set to include newer areas of mine development.

As projects moves past initial construction, the opportunity exists to capture excavation performance data to enable assessments of design reliability (see section 11.7). These data become invaluable for the optimisation process which requires verification and refinement of input parameters. In addition, rock mass response observations and rock mass data should be continually collected during mining in order to derive any additional required input parameters (i.e. for use in more sophisticated design methodologies) and to minimise uncertainty in their estimation.

11.4.1 Data Suitability and Reliability

One of the key aims of the integrated approach is to ensure that rock mass data is suitable for analysis needs. At any stage of the project, data firstly needs to be collated and assigned to the preliminary or established domains. Preliminary domains are typically based on geological characteristics, such as lithology, weathering and alteration. More detail on the domain definition process is provided in section 11.5.4.

The first step in assessing data suitability is to check whether it is valid (see section 3.4.1). The next phase is to undertake basic data analysis to establish basic statistical moments to evaluate data homogeneity, isotropy and reliability. As noted in Chapter 3, data reliability can generally be improved by ensuring that any biases are removed prior to analysis. Importantly, data need to be checked to ensure that all required input parameters for the selected analysis or design methodology are available in each design sector. The rock mass characterisation data dependency diagram (Figure 9.1) can be used as a tool to initially establish the required basic data types.

Data also need to be assess in terms of spatial distribution and variability. A visual assessment of data points in three-dimensions, relative to the location of proposed stopes, should be conducted in each domain. Where samples or data are clustered or poorly represented within a domain, additional sampling locations may need to be considered. After basic data analysis, the coefficient of variation of each parameter should be checked in each domain. Guidelines for the range of coefficient of variation for each stage of development is presented in Figure 11.1. If the coefficient of variation is outside of this range in any domain, then collection of additional data should be considered. Notwithstanding this, the variability of input parameters generally needs to be kept within certain tolerable limits in order to provide a certain design reliability. A number of methods for assessing the impact of data variability on the design reliability are provided in section 11.7.

11.4.2 Data Collection Programmes

If it is found that the existing data is not suitable (i.e. missing or incorrect data, clustered or sparsely populated, insufficient precision, or contains excessive biases) then additional data need to be collected. A number of different aspects need to be considered in developing an appropriate data collection programme that minimises uncertainty and improves reliability (see Chapter 3). A brief summary of some aspects are provided below;

- **Data collection methods:** Once the required basic data types have been established, it will be necessary to decide on the most reliable data collection methods to be employed. This can be assessed using the rock mass characterisation data dependency diagram (Figure 9.1), in conjunction with Figure 3.4. The limitations of each rock mass sampling scheme (i.e. data types, subjective versus objective, quantitative versus qualitative, etc.) need to be assessed relative to the required objectives and level of reliability. The relative amount/proportions of each method will also need to be optimised.
- **Minimising biases and uncertainty:** The location and orientation of sampling schemes need to be optimised such that sampling biases (both discontinuities and rock fabric testing) are minimised; e.g. ensuring that a sufficient number of drill hole orientations are planned to minimise blind zones, at least 2 scanline mapping orientations per domain, truncation and censoring limits recorded, etc. A more detailed account of considerations in the planning and execution of rock mass characterisation programmes is provided in Appendix A. Locations and orientations of holes should also be planned to minimise the possibility of encountering significant 'unknown' geological features in key areas (i.e. minimise Type 1 uncertainties).
- **Maximise volumetric coverage:** Both reliability and volumetric coverage of rock mass characterisation can be maximised by utilising a number of test methods (e.g. Field index test, Schmidt Hammer tests, Point Load index tests and laboratory tests) and developing reliable correlations between indices.
- **Optimise the number of samples:** The cost of additional data must be weighed against the likely increase in reliability. A number of recommendations with regard to the length of sampling lines/windows and amount of discontinuities to be collected is also provided in Appendix A. Notwithstanding this, the amount, and hence precision, of data should be related to the required level of reliability (see below).

Where there is no opportunity to collect further data (i.e. due to financial or time constraints) then there is a risk that the design will not meet its required level of reliability and the poses a significant risk to project viability. This risk needs to be well documented and communicated to management.

Reliability-based Approach To Data Collection

If the general relationship between the number of samples and resulting precision can be ascertained, then the number of additional samples to achieve a minimum level of reliability can be used to influence the data collection programme (section 3.4.4). This approach can be applied to any rock mass parameter where the underlying distribution is known or assumed.

11.4.3 Rock Mass Characterisation Framework

The Rock Mass Data Framework (presented in Chapter 9) can be used to assist in data collection, management and basic data analysis requirements as outlined in Figure 11.2. In summary, use of the model can assist in the following areas;

- Allow integration of rock mass data from a variety of sampling schemes (subjective and objective), such as; drill core logging, scanline and window mapping, geological mapping and digital photogrammetry
- Organise and store data in an accessible digital format that enables sharing of information
- Undertake basic data validation
- Calculation of statistical moments of variables based on domain assignment and ascertain data reliability
- Extraction and preparation of rock mass data from various data sources based on a number of queries
- Allows for spatial data analysis and complex multivariate analysis techniques
- Correct statistical treatment of biases and analysis of geometric discontinuity parameters (i.e. spacing, persistence and orientation) which is directly based on the adopted sampling technique.

11.5 ROCK MASS MODELS

The previous chapters have shown that there are many approaches to modelling the rock mass from simple tabulation of statistical analysis of rock mass parameters to sophisticated 3-dimensional spatial models. The following sections describe existing and suggested approaches to rock mass modelling as projects develop, along with some methods to assess model reliability, as outlined in the lower section of Figure 11.1.

11.5.1 Deterministic Discontinuity Models

At conceptual and pre-feasibility stages, information on large-scale discontinuities is

generally restricted to regional geological features, with data taken from regional geology reports, or from large-scale aerial or geophysical/remote sensing data sets. Models of the structures will generally consist of plan views, showing known or inferred location and continuities. Orientations are either inferred or qualitative, e.g.; shallow, moderate or steeply dipping. Other rock engineering features, such as strength are not known and are generally inferred. As data density increases with project development, the ability to identify smaller scale structures increases, such that 3-d models of mine-wide to mining-area scale structures can be developed, along with their geometry and rock engineering attributes. The deterministic discontinuity technique (presented in section 10.3) is particularly well suited for operations where subjective and objective discontinuity mapping data exist. At mature operations where microseismicity or mine wide deformations are controlled by faults, additional information may be incorporated (either by measurement or back analysis), such as; surface geometry, strength, stiffness and deformation properties and/or characteristics of local asperities.

11.5.2 Stochastic Discontinuity Models

As seen in section 8.6, there are many approaches to modelling smaller scale discontinuities, however, the approach is principally determined by the availability of data at the relevant stages of project development;

- A conceptual level, properties of small-scale discontinuities inferred from the rock mass structure based similar geological environments
- At pre-feasibility to feasibility, data from drilling and reconnaissance mapping provide basic orientation groups in various rock types (i.e. set definition), with statistical models of spacing/intensities, small-scale profiles and surface conditions
- Data from larger exposures enable domain based stochastic models of discontinuity size, and rock mass structural hierarchy using termination data
- Development of joint network models of *DFN*'s possible where detailed discontinuity mapping data exist

11.5.3 Rock Fabric / Continuum Models

Figure 11.1 highlights a number of models of different aspects of the rock fabric / continuum are required in the design process, such as; rock fabric strength, degree of weathering and alteration, discontinuity intensity (as developed in 10.2), and rock mass classification ratings and rock mass strength estimations (Chapter 4). A variety of model types can be developed using the methods outlined in Chapter 8.

11.5.4 Rock Mass Modelling Techniques and Domain Definition

The lower section of Figure 11.1 outlines some typical rock mass modelling methods at various stages of project development, along with a number of approaches for domain definition (see section 8.7).

Modelling Techniques

One of the simplest methods is to utilise classical statistics, by tabulating various rock mass rock mass properties for each domain, with domain boundaries represented on maps and plans. More sophisticated models represent domain boundaries as 3-dimensional volumes, with the statistical moments calculated for each rock mass parameter (or discontinuity parameter for each set) for data located within these volumes or domains. Lastly, the spatial variability of parameters can be represented within these volumes using some of the techniques outlined in section 8.5.

Domain Definition

With regard to the definition of domain boundaries, the following questions may need to be considered;

- How do we construct domains that best represent spatially homogeneous regions?
- Do they effectively minimise parameter variability?
- Can domain boundaries be optimised?
- Is it possible to sub-divide and categorise the domains based on data density? (spacing between holes/sections, no. samples per m³, exposure validation)

In order to answer these questions, a generalised procedure for domain definition (using the techniques presented in section 8.7) is proposed below;

1. Select initial domain boundaries
2. Collate data within boundaries
3. Select parameter of interest
4. Calculate mean, standard deviation and coefficient of variation
5. Change domain boundary, re-do steps above
6. Assess changes in mean and standard deviation or coefficient of variation
7. Accept or reject proposed change to domain boundary

11.5.5 Assessing Model Suitability and Reliability

The approach taken to developing a rock mass model is dependent on;

- engineering objective and scale
- proposed design methodology
- complexity and detail required
- quality and quantity of data available

In order to assess the most appropriate approach to rock mass modelling a number of questions need to be addressed;

- Is the adopted approach valid, given the amount and distribution of data?
- Does the model adequately capture all parameters to assess rock mass interactions?
- Can all required rock mass input parameters be adequately represented in each domain?

As we have seen in the previous chapters, there are a multitude of rock mass modelling approaches, each with various capabilities, limitations and advantages. It may be found that a single mine rock mass model cannot provide the required solution. In this case, an integrated or hybrid approach may be required, where different models are used at a number of scales and for various purposes.

Model reliability can usually be assessed by how well it spatially represents the conditions in the field. In this regard, the accuracy of any developed models can be established by validation in the field (through further mapping) or using alternative data sources. It is also recommended that the techniques described in Chapter 8 be used to gauge the reliability of spatial models, for example; cross-validation and Q-Q plots, or uncertainty and isoprobability maps for models developed using kriging and conditional simulation.

11.6 DESIGN METHODS

The reviews undertaken in previous chapters suggest that the most appropriate design methodology is largely a function of;

- the level of detail of the study, usually related to project development stage,
- specific objectives of the engineering design,
- level of reliability or tolerance required,
- quality and quantity of input data,
- spatial representation and complexity of conceptual rock mass models,

- level of understanding of the engineering problem.

The first two aspects have been discussed previously (section 11.3). The level of reliability or tolerance required by the design is generally understood by the design engineer, given the level of study, project objectives and management requirements. However, assessing the reliability provided by a particular design methodology, given the input data, is more problematic. In light of this, a procedure for assessing the reliability of the design methods is proposed in section 11.7. The appropriateness of one design methodology over another also depends on the ability of the method to reliably capture rock mass interactions and anticipated rock mass response mechanisms. Empirical methods do not explicitly capture rock mass failure modes, and therefore are more appropriate where rock mass interactions cannot be thoroughly understood, that is, at early stages of project development. Where there is a more thorough understanding of in situ and induced rock stresses, rock mass strength and rock mass structure, then assessments can be made on whether failure will be principally controlled by rock mass failure or structurally controlled. The rock mass model therefore is a crucial component in guiding the design engineer in identifying anticipated rock mass responses.

The staged approach is required as selection of the most appropriate method is based on the knowledge of the principal failure mechanisms. Initially empirical methods are more appropriate as they do not rely on a detailed understanding of failure mechanisms. Analytical methods will become preferred as simplistic mechanisms become reasonably understood. Finally, methods capable of incorporating complexity, such as numerical modelling, will be more appropriate for detailed and ongoing design. Figure 11.1 also indicates that it may be advantageous to conduct a number of design methodologies in parallel to account for uncertainty in potential rock response mechanisms.

11.6.1 Empirical Methods

Preliminary design of spans and pillars, from Conceptual to Pre-feasibility, is generally done using empirical methods. The use of empirical methods may also be extended into initial construction, with refinement possible using stope performance data. However, the design engineer must be cognisant that empirical methods do not represent a rigorous design methodology (Chapter 4). Notwithstanding this, a number of strategies are proposed in order to improve reliability and optimise the design for various regions of the mine;

- Mining sector rock mass properties – Rudimentary use of empirical methods involves assessment of bulk rock mass properties and derivation of respective span geometries for each mining sector (e.g. hangingwall, footwall, ore).
- Incorporating spatial variability – The spatial variability of empirical parameters can

be used to optimise and improve design reliability in various regions of the mine. In this regard, geostatistical or non-geostatistical models (section 8.5) can be used to spatially model both input and design parameter variability (Cepuritis, 2004; Villaescusa et al., 2003a).

- Potential for modifications and site specific adjustments - It may be found that parameter weightings of existing techniques do not provide optimal results under all conditions. In this case, mechanisms for making adjustments should be explored, including those outlined in Chapter 4.
- Development of new or hybrid systems - Development of new empirical systems, via formulation of alternate parameters and/or weightings, may provide improved reliability in predicting rock mass response. Hybrid methods - those that incorporate the results of numerical modelling (Villaescusa et al., 1997) or analytical methods, should also be considered to improve efficacy of empirical based approaches.

In development of new or hybrid systems, careful consideration must be given to selection and inclusion of each parameter, how it interacts with other parameters and subsequent assignment of the relative influence of each parameter. When considering the design (or even use) of an empirical method some basic requirements need to be assessed;

- **Consider the specific engineering objective:** The system must be designed in such a way that it maximises the understanding of the rock mass behaviour for the engineering objective and to the level of study/detail required. One must consider the dangers of using a rock mass classification system that was originally intended for another engineering application where the design objectives are dissimilar.
- **Must include all the required “parameters” that influence Engineering Objective:** Consider the scale, boundary conditions, potential range of geological conditions, rock mass interactions, behaviour and response mechanisms.
- **Relative “influence” of each parameter justifiable:** Critically assess each parameter and provide sound justification for its “weighting”. The use of multivariate statistics applied in a multi-dimensional space may need to be considered to optimise the usefulness of the parameter data. Recognise that the parameter “weighting” may also need to be adjusted based on changing conditions and interactions with other parameters. State all assumptions, so the user is informed of the conditions for its formulation.
- **Require sufficient case histories for specific engineering objective in the range of anticipated conditions:** Ensure that the method is employed only within the range of the case history database and caution that, if applied outside the

experience base, the reliability will be unknown.

- **Demonstrated success in predicting an engineering outcome within tolerable limits:** Accuracy and precision in predicting outcome is ascertained and potential users are acutely aware of any limitations or conditions. In this regard, statistical and/or likelihood methods **are strongly encouraged** as this allows mine operators to choose design curves based on acceptable risk and to estimate or verify design reliability.

11.6.2 Analytical Methods

Design analysis may involve the use of analytical models, however, they require very specific and well defined, yet simplistic, modes of failure (i.e. buckling, key block, etc.), with a number of basic assumptions. Sufficient rock mass data are required to enable identification of the various failure modes, and therefore, they are generally appropriate for at least pre-feasibility level studies. In addition, their use may be restricted to a range of rock mass responses which are dependant on certain geological environments, level of complexity and scale.

11.6.3 Numerical Methods

The principal objective of numerical modelling in span design is to derive likely strains, displacements and extent of damaged/unstable rock mass around proposed excavation boundaries. In the case where, due to practical or operational constraints, spans cannot be designed to perform reliably unsupported then outputs from numerical modelling can also be used to assist in the design of rock reinforcement. As mentioned in Chapter 7, there are a number of numerical methods available, however, their use in regular open stope design is often limited by a number of factors. A staged approach is recommended in the use of more sophisticated numerical modelling techniques, whilst also being cognisant of the additional effort required (Wiles, 2006);

- Refine Parameters; refine input or geometric parameters in linear elastic models, conduct sensitivity analyses on input parameters, such as magnitudes and directions of the in situ stress regime, refine pillar and excavation geometries.
- Lithology-based criteria; developing simple stress-based criteria for each lithology. This involves using a simple single material property linear elastic model and defining stress-based criteria for each lithology by collating back analysis data on a unit-by-unit basis.
- Directly model material variability; Here, geological zones with different material properties are directly incorporated into the linear elastic model in forward analysis.
- Directly model material complexity; more complex material models (e.g. non-linear

modelling) that include inelastic fault slip or methods that incorporate additional mechanisms. Models that incorporate inelastic or time-dependant materials will require substantial effort in model construction and calibration. For fault slip models, considerable effort is also required to define reliable location and orientation for each structure.

11.6.4 Integrating Rock Mass Models and Numerical Codes

As the level of complexity and sophistication of numerical models increases, rock mass characterisation models should be used to define material zones (and material properties) and displacement discontinuities in *BEM/FEM* codes.

Direct Incorporation Of Material Variability

Incorporating material variability into numerical modelling can be done with various degrees of complexity or sophistication. The basic approach is to define a number of distinct geological zones (or rock mass domains – see section 8.7) and to incorporate their geometry along with their mean input material property parameters. In this regard, the deterministic discontinuity modelling approach (see Chapter 10) can be used to generate detailed boundaries for said geological zones. Incorporating spatial variability of material properties into numerical models is perhaps the most sophisticated use of rock mass models. It has been shown that geostatistical models (e.g. block models) of rock mass classifications, and subsequent estimated rock mass strengths, can be used as direct input into numerical modelling (Stavropoulou et al., 2007) using *FLAC^{3D}* (Itasca Consulting Group Inc, 2002). Similar approaches have been in use in civil geotechnical engineering design, where input parameters are represented as spatial random fields in 2-dimensional *FEM* analyses (Griffiths and Fenton, 1993). Unfortunately, the ability to directly capture spatial variability in all commercially available codes is limited.

Direct Incorporation Of Discontinuities

The ability to incorporate several large, mine-scale discontinuities into 3-dimensional *FEM/BEM* numerical codes has been available for many years. This requires the accurate geometrical representation of large scale features and estimates of their engineering properties. The deterministic discontinuity modelling approach (see Chapter 10) provides a means to provide accurate and reliable models of large-scale discontinuities for direct inclusion into numerical models. As noted in Chapter 7, Elmo and Stead (2010) directly incorporate smaller scale discontinuities (using *DFN* models) into a 2-dimensional hybrid finite element/discrete element code to model pillar behaviour. It must be noted that, as each *DFN* is a stochastic realisation, the results from each numerical modelling run will be unique to the incorporated discontinuity pattern. *DFN* modelling has also been used (Rafiee

and Vinches, 2008) to provide input for 3-dimensional distinct element codes, such as *UDEC* (Itasca Consulting Group Inc, 1984).

The use of *DFN*'s in numerical modelling may be justifiable in understanding the response of critical infrastructure where smaller scale discontinuities are anticipated to play a crucial role (i.e. primary instability mechanism) and where sufficiently detailed discontinuity mapping data exist. However, the inclusion of a multitude of smaller excavation-scale discontinuities in mine-scale models is still problematic, mainly due to;

- The sheer number of generated discontinuities are still beyond software and hardware capabilities
- Inability to derive detailed joint network models that model discontinuity property variability which are spatially accurate for the whole mine
- Sufficiently detailed discontinuity data may only be available for a small number of locations

Unfortunately, these issues severely limit the practical incorporation of small scale discontinuities (via *DFN* models) in linear elastic methods for mine-wide span design. Another issue with numerical modelling codes is that some features that influence rock mass response, such as blast damage, cannot be directly incorporated into the numerical model. A number of techniques are proposed to attempt to overcome some of these issues (see 11.8) when using 3-dimensional linear elastic codes for back analysis.

11.7 DESIGN RELIABILITY

An important objective of the integrated approach to open stope span design is to assess the level of reliability of derived design parameters and whether they are appropriate for the stage of project development. This concept is shown in Figure 11.1, along with example ranges of design reliability target levels for each stage of project development. The example reliability target levels are not based on any case study data and are presented for demonstration purposes only. Determination of what is considered an acceptable level of reliability can only be done once all consequences of failure and associated risks have been determined and whether meet company guidelines on acceptable risk. Notwithstanding this, the design engineer should be able to demonstrate the level of reliability in his/her design.

Fundamentally, design reliability relates to the probability of the excavation succeeding in fulfilling its intended function during its duty life. Its intended function are generally based on a set of performance criteria, with a mechanism to predict conditions of instability (i.e. instability criteria) or undesirable rock mass behaviour (i.e. performance function), which in

open stope span design, is usually controlled by aspects of the design variable such as stope geometry and sequence. Some common performance assessment criteria, instability criteria and design variables used in open stope span design are outlined in Table 11.1.

Table 11.1 - Example open stope span design criteria

Performance Assessment Criteria	Instability Criteria or Performance Function	Design Variables
Qualitative; <ul style="list-style-type: none"> • Stable, Unstable, Failed 	Empirical Parameters; <ul style="list-style-type: none"> • Q, RMR, N, N' 	Size; <ul style="list-style-type: none"> • Critical span
Quantitative; <ul style="list-style-type: none"> • $ELOS$, % dilution • circularity, extensivity, hemisphericity, relative volume • Direct volume comparisons • Measurements of rock mass strain and displacements 	Critical State; <ul style="list-style-type: none"> • stress threshold • strain threshold • displacement • displacement rate 	<ul style="list-style-type: none"> • Hydraulic radius • Radius factor Orientation Shape Sequencing

As mentioned in Chapter 2, some design methodologies may involve simplistic equations, whilst others involve complex computational processes, therefore approximations may be necessary in all or some steps of the analysis and design. A general approach to establishing design reliability in forward analysis is provided below (Baecher and Christian, 2003);

1. **Establish an analytical model.** There must be some way to compute the margin of safety, factor of safety or other measure of performance. There may be error, uncertainty or bias in the analytical model, which need to be accounted for in the reliability analysis.
2. **Estimate statistical descriptions of input parameters.** The parameters include not only the properties of materials, but also loads and geometries, described by means, variances and covariances. Spatial correlation parameters and skewness may be included as well. The forms of distribution of parameters may be important as well.
3. **Calculate statistical moments of the performance function.** Calculating the mean and variance of the performance function. In some simple analytical models this can be done exactly, however, other methods may require approximations.
4. **Calculate the reliability index and probability of failure.** If the performance function has a well defined probabilistic description, such as normal distribution, this is a simple calculation. In many cases, the distribution is not known, or the intersection of the performance function with the probabilistic description of the parameters is not simple. In these cases the calculation of the probability of failure is

likely to involve further approximations.

As noted previously, different analysis methods should produce different means and variances in the *performance function*, and thus different *probabilities of failure* and design reliability. **A reliability-based design approach provides a quantitative method for comparison of results from a number of methods.** This enables the engineer to establish the relative reliability of each design method which can be used select the most appropriate methodology. The exact approach taken to determine design reliability will be dependent on the design methodology and whether there are data available for design verification (i.e. back analysis data). The following sections describe a number of proposed methods that can be used to estimate design reliability for initial forward analysis (pre-construction) as well as those based on back analysis.

11.7.1 Estimates of Open Stope Design Reliability for Initial Forward Analysis

In the initial design of stopes, it is generally assumed that the selected design methodology adequately captures the anticipated rock mass interactions controlling behaviour. In this case, reliability of the derived design variables (and design performance) will be controlled by the uncertainty in the methodology input variables.

Empirical Methods

The uncertainty and the relative poor precision associated with design criteria developed using existing empirical stope design methods has been described earlier in Chapter 4. Currently, the most effective way of quantifying reliability of empirically derived design parameters is to assess the predictive capability of the empirical database using probabilistic and likelihood methods (Mawdesley et al., 2001; Suorineni et al., 2001). Mean input parameters can be used to assess the average likelihood of “stable”, “unstable” or “failed” stopes, given the chosen span and empirical performance function (e.g. *RMR*, *Q*, *N'*, etc.). It is recommended that this approach also be used for assessing design reliability using site-specific developed empirical methods.

Analytical And Numerical Methods

Where an analytical solution exists to define the limit state of the *performance function*, a number of methods are available to estimate the design reliability or probability of failure. Where the mean and variance of capacity and demand inputs are known, classical reliability-based methods can be implemented, such as;

- First Order Second Moment (*FOSM*) method (Dettinger and Wilson, 1981)
- First Order Reliability Method (*FORM*) (Hasofer and Lind, 1974)

Other methods that are routinely undertaken in rock engineering for relatively simple analytical analyses and numerical modelling based on input parameter variability include;

- Point Estimation Method (*PEM*) (Rosenblueth, 1975)
- Alternative Point Estimation Method (*APEM*) (Harr, 1989)
- Stochastic Simulation Methods (e.g. Monte Carlo and Latin Hypercube)

11.7.2 Confirming Design Reliability Based on Back Analysis

A significant focus of the thesis is the importance of ongoing back analysis. The main objective of back analysis is to provide reliable instability criteria or performance functions that can be correlated to past performance and used as a predictor to future stope performance. The following sections describe how back analysis can be used to develop instability criteria for use in optimising forward analysis and design, as well as how it can be used to establish design reliability. A more detailed back-analysis framework is also proposed that utilises an integrated approach to optimise instability criteria for ongoing design in operational mines (see section 11.8).

Site Specific Back Analysis Based On Existing Empirical Techniques

At early stages of mine development, early back analysis may look at verifying the reliability of existing empirical methods, such as Mathew's or Potvin's stability graph methods (Mathews et al., 1981; Potvin and Hudyma, 1989). Logistic regression or Bayesian likelihood discriminant analysis (Mawdesley et al., 2001; Suorineni et al., 2001) are still probably the optimal methods for assessing design reliability using purely qualitative performance assessments.

Back Analysis Of Quantitative Performance Assessment Criteria

Initial confirmation of design reliability can be made by back analysing quantitative performance assessment criteria, such as, depth of failure or *ELOS* against design variables such as span width, hydraulic radius or radius factor. By analysing stope performance data the likelihood of obtaining a certain amount of dilution for a given span dimension can be ascertained. Unfortunately, classical statistical approaches (where one assumes a population distribution) may not be viable, due to small sample sizes, significant variability or no apparent fit to standard models. For example, Figure 11.3a shows stope performance from the data from the Mt Marion Gold Mine (Villaescusa, 2010). Although there is a general trend, it is difficult to ascertain meaningful correlations through linear regression. In this case, it is proposed that non-parametric (distribution-free) statistical approaches may be warranted to estimate probability density functions;

- Data is first separated into a number of bands based on the dependent design variable or performance function.
- The percentage of the data within each band over a certain threshold of the performance assessment criteria is then calculated.
- The results are then plotted as a relative frequency histogram or line, or the probability density is estimated using kernel density estimators.

Figure 11.3b shows the example data represented as probabilities of depth of failure versus hydraulic radius. In this way, the probability of depth of failure exceeding 1m, 2m and 3m for, say, a hydraulic radius of 8m can be estimated as 80%, 53% and 26%, respectively.

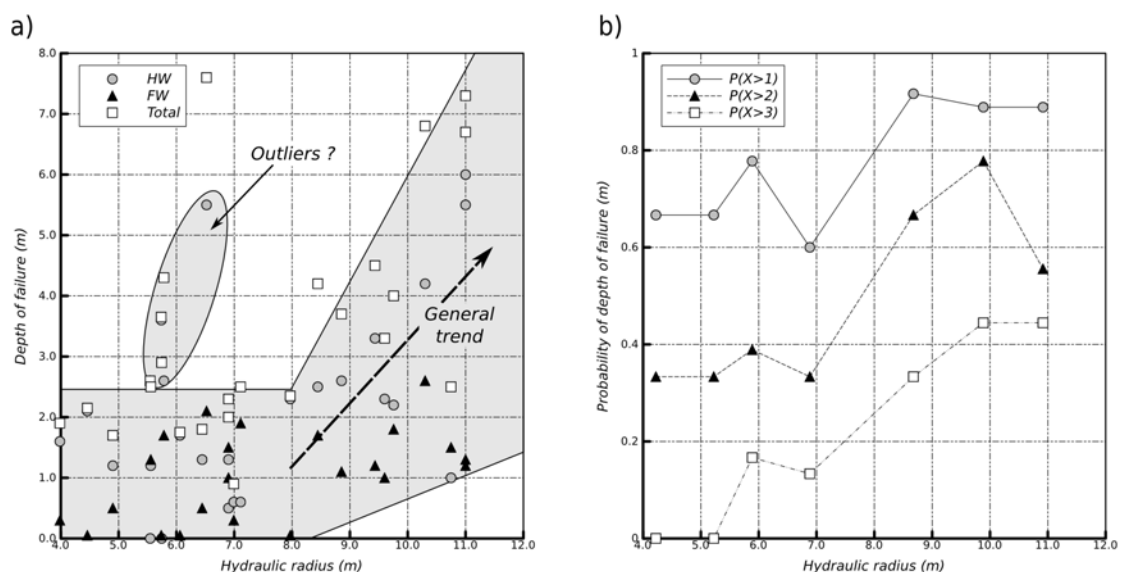


Figure 11.3 - Plot of a) depth of failure versus hydraulic radius for Mt Marion data (Villaescusa, 2010) and b) probability of depth of failure versus hydraulic radius for 1m, 2m and 3m

Reliability Of Linear Elastic Instability Criteria

It is proposed that the reliability of instability criteria based on linear elastic modelling be quantified based on the method proposed by Wiles (2006) (see section 7.6). The method can be applied to alternate candidate instability criteria with their corresponding C_v compared. This can be used as an effective tool to compare the reliability of various instability criteria options.

Direct Volumetric Comparisons

Numerical modelling techniques offer the advantage in that the geometrical aspects of the stope design are intrinsically captured in the method. The design engineer may elect to assess or present results from various models, or design alternatives, by comparing one or more stope geometry aspects, layouts or sequence options. Isosurfacing (i.e. 3-d

contouring) of numerical modelling outputs at critical values of the instability criteria, such as critical strain or stress, can indicate the predicted performance geometry (e.g. over-break). Design reliability can therefore be assessed by comparing the predicted over-break versus the actual over-break geometries;

- Location - does the predicted over-break match where actual observed over-break has occurred on the stope surface or, on a larger scale, across the mining block?
- Size - are the relative volumes of predicted versus actual similar?
- Shape - does the predicted criteria have similar shape characteristics to observed over-break shapes?
- Orientation - does the predicted criteria have similar trends to observed over-break?

Although these questions are fundamental in assessing design reliability, the difficulty lies in *quantitatively* comparing all geometric aspects. A number of novel methods to quantitatively define size and shape of over-break have been proposed in Chapter 6. These quantifiable measures can be used in volumetric comparisons of predicted versus actual over-break.

Normalised Isotropic Distance Variation

Although the methods proposed in Chapter 6 can assist in quantitatively defining size and shape of over-break, comparison of location and orientation of over-break are still probably best evaluated using qualitative/visual techniques. Notwithstanding this, it is proposed to utilise the variation in isotropic distance between two surfaces in order to obtain a measure of the spatial difference between two volumes in order to visualise *where* predicted volume and actual volumes differ. This may be of assistance in identifying site-specific rock mass or implementation conditions that contributed to the different response in different areas of the mine. If it is necessary to compare isotropic distances between different stope volumes/sizes then isotropic distances may need to be translated into a normalised mean and standard deviation. In this case, it is proposed that the critical span be used to normalise the data, such that the relative reliability of predictions can be compared between stope surfaces of different scales.

11.8 AN INTEGRATED BACK ANALYSIS FRAMEWORK

Back analysis is a fundamental requirement in confirming the reliability of the predictive capability of any design methodology. However, as noted in Chapter 7, the uniqueness of the solution in back analysis cannot be confirmed. That is, the same observed response may potentially be predicted using a variety of failure models (i.e. continuum or discontinuum) and from a range of input parameters. The following sections describe a framework that attempts to integrate different rock mass characterisation models, numerical modelling and

stope performance data to assist in improving the overall excavation design process for operational open stope mines. The back analysis framework particularly emphasises linear elastic techniques, principally because more sophisticated techniques (i.e. non-linear finite element or discrete element discontinuum methods) are generally not practical for routine stope span optimisation by mine operations personnel. This is mainly due to complex and time consuming model set-up, additional input parameter requirements and long run times.

11.8.1 Integrated Spatial Model and Relational Databases

In order to continually improve the understanding of rock mass and its response to mining, all rock mass data and data pertaining to back analysis and design need to be integrated into a single (update-able) spatial model. In order to achieve this, an integrated 3-dimensional spatial model was developed using a novel application of implicit functions. Additional data that can not be represented spatially (i.e. production figures, dates, etc.) were also integrated by development of a number of linked relational databases. The following sections describe the various data types and models developed as part of the integrated back analysis framework.

Rock Mass Characterisation Data And Models

Rock mass spatial models and data values from the rock mass characterisation data model (as described in Chapter 8, 9 and 10) can be incorporated, such as;

- Rock fabric point data (intact strength, weathering, alteration) and spatial models
- Discontinuity characteristics for selected sets
- Discontinuity intensity models (1-dimensional and 2-dimensional)
- Deterministic discontinuity models;
 - small scale discontinuities represented as convex planar disks, parallelograms or 3-dimensional surfaces (pseudo-fact glyphs)
 - Large-scale discontinuities, lithological and other boundaries as implicit functions or 3-dimensional surfaces

Combining this data into one model allows for the understanding of the role and influence of large scale structures on rock mass properties and to develop spatial relationships and correlations between various rock mass parameters.

Numerical Modelling Data

All numerical modelling parameter outputs (e.g. stresses, strains, displacements) can be imported into the integrated spatial model, as results are usually defined at specific points or

on a regular grid. A basic requirement for effective use of numerical modelling results in the integrated model is to tie in excavation geometry (planned and actual performance) with the modelling sequence number. This sequence number can then be related to dates and timing of key stoping activities, such that it is matched to blasting, extraction, filling, as well as correlating it to observations of performance and monitoring data.

Stope Performance Data

A purpose designed stope performance database has been developed to store geometric performance criteria, along with *CMS* derived physicals and qualitative stope performance information. The database has similar characteristics to other databases used in empirical studies (Clark and Pakalnis, 1997), containing fields for quantitative and qualitative information in the following areas;

- Stope details and design (e.g. stope name, location, key dates, planned and actual physicals, sequence number, design and *CMS* files)
- Stope surface details (e.g. geometry of stope surfaces, performance criteria)
- Rock mass and boundary condition data
- Drilling and blast details
- Rock reinforcement data
- Ore extraction and back filling data.

This data can be represented spatially as attributes attached to either the design or *CMS* geometries for individual stopes or stope surfaces. The qualitative information from the stope performance reviews provides an important role in design optimisation (Villaescusa, 2004). Analysis of these data may indicate additional contributing influences on stope performance that are not directly incorporated into the existing design methodology and/or where design methodologies may need to be modified. For example;

- It may be observed that cut-off slot layout and ring firing direction play an important role in stope performance, particularly in relation progressive exposure of large-scale discontinuities. Therefore, evaluation of the location and orientation of interpreted large-scale structures should become an integral part of stope layout and the drill and blast design.
- Anecdotal evidence from the reviews may suggest that rock mass response is dominated by movement along faults, rather than yielding and failure through the rock mass. In this circumstance, linear elastic boundary element methods with non-linear fault slip may be appropriate. This also aids the design engineer to further direct data collection, rock mass modelling and monitoring efforts such that appropriate model geometry, input parameters and calibration data can be defined.

Observations And Monitoring

Observations and monitoring data related to rock mass response and excavation performance are of vital importance in the design optimisation process. In order for effective use of this data, the location and timing of the observation or monitoring data are stored in a way that it can be compared to back analysis results and any derived design or prediction criteria.

Integrated Spatial Model Represented As Implicit Functions

Figure 11.4 shows an isometric view of a number of parameters modelled as implicit functions (using *RBF*'s) for a particular area of a mine, including; deterministic discontinuity models, isosurfaces from 1-dimensional discontinuity intensity data, stope design geometry, *CMS* model (colour contoured by depth of over-break) and the results from linear elastic modelling showing maximum shear stress (15MPa isosurface selected). The representation of the spatial model as a series of implicit functions has a number of advantages when trying to understand relationships between parameters and for back analysis purposes (see section 11.8.3).

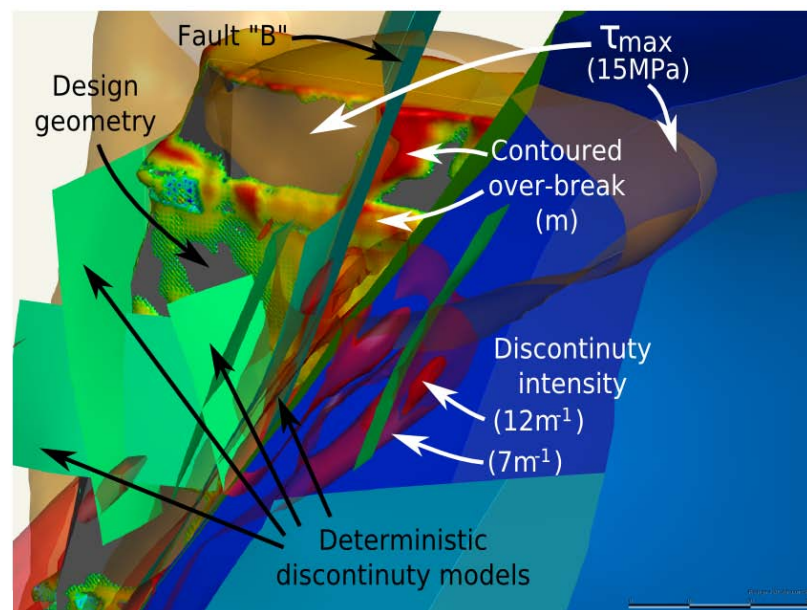


Figure 11.4 - Isometric view showing some components of the integrated spatial model

11.8.2 Proposed Techniques for Improved Linear Elastic Back Analysis in Open Stope Design

The previous chapters have shown that there are many limitations using a linear elastic continuum model in back analysing open stope performance. However, it is considered that a number of improvements can be made to increase the reliability of back analysis solutions. Based on some of the limitations discussed in the previous chapters and issues discussed

above, the following guidelines are proposed to improve the efficacy of linear elastic back analyses;

1. Divide the rock mass into domains and assign a best estimate of the rock mass strength and deformation properties to each domain utilising empirical techniques. It is necessary to ensure that data points from different rock mass domains are separated. That is, site-specific damage and strength curves (i.e. instability criteria) are to be developed for individual rock mass domains. Data is also to be separated into cable reinforced and unreinforced data sets.
2. All attempts should be made to account for different strength envelopes and rock mass responses based on stress path to failure. For each mining step, each stress analysis point (i.e. grid point or *CMS* excavation surface point) is tracked in terms of the change in principal stress magnitudes. A classification of stress path can be used. An example of such a classification is proposed in Figure 11.5. In addition, it may be useful to classify data points for pillars, abutments or those on or near excavation surfaces. This may be established for each data point by calculating the minimum isotropic distance to an excavation surface.
3. Initially develop site-specific rock mass damage and strength criteria where the rock mass has not previously undergone significant rock mass damage (i.e. from excavation surfaces on 'Primary' stopes). This will potentially reduce variability and improve accuracy of criteria.
4. Develop a catalogue of rock mass responses and observable damage, similar to those proposed by Beck and Duplancic (2005), such as changes in; fracture density, ground support requirements or rehabilitation, blast-hole condition, depth of over-break, pillar damage (see Figure 11.6) micro-seismic activity, etc. (Roberts et al., 1998). These phenomena can then be linked to stress induced damage levels and stress paths.

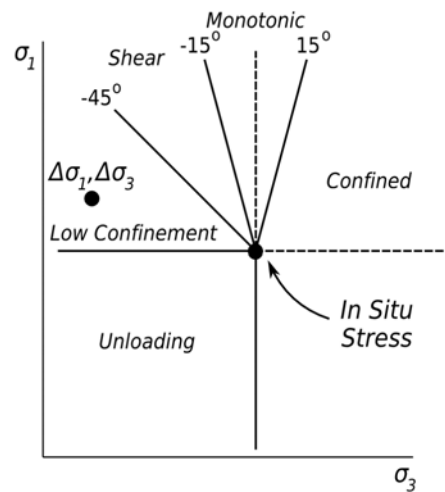


Figure 11.5 - Example stress path classification for excavations steps in linear elastic modelling

Pillar rating	Pillar condition	
1	No indication of stress-induced fracturing. Intact pillar.	
2	Spalling on pillar corners, minor spalling of pillar walls. Fractures oriented subparallel to walls and are short relative to pillar height.	
3	Increased corner spalling. Fractures on pillar walls more numerous and continuous. Fractures oriented subparallel to pillar walls, and lengths are less than half pillar height.	
4	Continuous, subparallel, open fractures along pillar walls. Early development of diagonal fractures (start of hourglassing). Fracture lengths are greater than half pillar height.	
5	Continuous, subparallel, open fractures along pillar walls. Well-developed diagonal fractures (classic hourglassing). Fracture lengths are greater than half pillar height.	
6	Failed pillar, may have residual load-carrying capacity and be providing local support to stope back. Extreme hourglass shape or major blocks fallen.	

Figure 11.6 - Example of pillar rock mass damage rating (after Roberts et al, 1998)

- The influence of scale and applicability of an “equivalent continuum” model needs to be continually evaluated. In this regard, the relationship between rock mass structure and the excavation geometry needs to be reviewed. It is recommended that discontinuity intensity data for each excavation surface is used as a qualitative assessment to the appropriateness or reliability of an “equivalent continuum” approach. It is proposed to utilise and assessment of discontinuity linear frequency and critical span for the excavation surface under consideration. Based on comments by Hoek (1988) and results from Elmo and Stead (2010) and Board (1989)

(see Chapter 7), a suggested qualitative assessment is provided in Table 11.2, however, it is recommended that site specific quantitative criteria are developed based on the results of back analysis. It is suggested that the reliability method, as proposed by Wiles (2006) in section 7.6, be used for developing and defining site-specific categories. Evaluation of discontinuity intensity can be made using techniques described in section 10.2.

6. If isotropic models have been selected, then it is recommended that the isotropy of the rock mass is continually evaluated. In this regard, methods outlined in Chapter 10 and Appendix A should be used to test for isotropy. If isotropy cannot be guaranteed, then serious consideration should be given to utilising anisotropic models.

Table 11.2 - Proposed qualitative assessment of the appropriateness of continuum models based on discontinuity linear frequency and critical span

Discontinuity linear frequency * Critical span ($\lambda_t * S_c$)	Appropriateness of Equivalent Continuum Models
<1	Intact/Massive behaviour
1 - 7	Inappropriate - High variability
7 - 10	Apply with caution
>10	Appropriate

The aim of the proposed technique is to improve the reliability of linear elastic critical stress-based failure criteria, by recognising the type of rock mass response and attempt to include the influence of rock mass variability, stress path and scale.

11.8.3 Back Analysis Process

The proposed back analysis process requires interrogation of the integrated spatial model as well as the stope performance, observational and rock mass characterisation databases. This is done in order to understand relationships between the rock mass, stope design and its observed response. An overview of the proposed interrogation process for back analysis is outlined in Figure 11.7. To implement this proposed approach, a number of activities need to be conducted to provide the necessary inputs, including; rock mass modelling, definition of the existing stope design parameters and geometries used, recording of stope production details, planned and actual stope and development geometries, and numerical modelling. The inputs are shown on the left-hand side of the diagram. The components in Figure 11.7 shown with stylised 3-dimensional boxes indicate parameters that can be represented as implicit functions (as *RBF*'s - see section 8.5.6), from which 3-dimensional spatial queries or *volumetric queries* can be created (see below). Dashed lines indicate data which cannot be represented as an implicit function, however, data may be spatially and/or temporally

incorporated into the interrogation process.

Hypothesis Testing Using Implicit Functions And Volumetric Queries

Traditional geographical information systems (*GIS*) were primarily developed for geographical and land use applications and as such are represented in 2-dimensions. The advantage with *GIS* is that the spatial relationship between objects (topology) enables querying of geometrical objects and their associated attributes. However, for the time being, full 3-dimensional *GIS* is still not fully evolved to where it can be used with efficacy in querying 3-dimensional shapes, their attributes and inter-relationships.

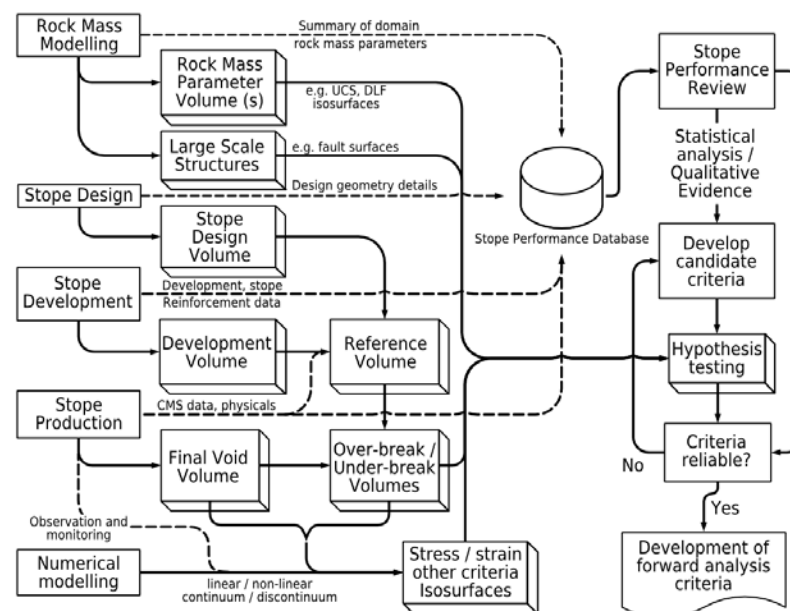


Figure 11.7 - Framework for back analysis of slope performance utilising numerical modelling, volumetric queries and slope performance databases

One particular advantage of using implicit function modelling techniques is that parameter values can be estimated at any value within the rock mass volume and a resulting surface generated (i.e. “isosurface”). In addition, parameter values can be estimated at any position within the spatial model. Because of this mathematical basis, boolean logic can also be applied to implicit functions (based on *RBF*'s - see section 8.5.6). The implicit functions for all parameters in any spatial model can therefore be treated as the universal set and volumetric queries generated based on set logic operators such as; \cap (intersection - boolean logic “OR”) and \cup (union - boolean logic “AND”), and can be combined with comparison operators such as; “equal to”, “greater than”, “greater than or equal to”, “less than” and “less than or equal to”. This approach provides a means to query the rock mass region to find a surface or volume that matches any set of queries based on any number of parameters. This provides

the rock engineer with a powerful tool to develop a better understanding of rock mass parameter interactions and their influence on rock mass behaviour. Volumetric queries can then be used to understand interrelationships between the various numerical modelling output parameters, stope performance geometries and rock mass parameters. The volumetric querying method allows the same queries to be made with different mining steps and multiple modelling runs (i.e. changing geometries, parameters and sequences).

Update-able Model

A unique feature of the integrated back analysis approach is the ability to update the database as new or updated data becomes available. This also requires that correlations and bias corrections in the rock mass data model have been undertaken. Once data are updated the integrated spatial model can be updated; new implicit functions generated, new domains created, volumetric queries updated with the new implicit functions. This characteristic is especially important for rock mass behaviour and monitoring data with respect to ongoing calibration of numerical models.

11.8.4 Candidate Instability Criteria

The objective of the back analysis process is to select an instability criteria that *most reliably* captures the the observed performance. Observed performance can be assessed using *CMS* surveys, observations or monitoring data. Where instrumentation data are not available one has to rely solely *CMS* data and observations, which is commonly the case in most open stoping mines. In this case, over-break geometries, represented as implicit functions, can be used to develop correlations with the results of numerical modelling. Over-break geometries can be used to locate numerical modelling points that fall on, inside or at a specific distance from a *CMS* profile. The 3-dimensional geometry information can also be used to develop the 2- and 3-dimensional shape descriptors for statistical performance comparisons. Numerical modelling results can now be compared with quantitative descriptions of geometry. Analysis of stope performance reviews also assists in identifying certain rock mass conditions or other factors that affect stope performance (i.e. which cannot be incorporated into numerical models).

In order to improve reliability, it is proposed to utilise integrated spatial model and volumetric query technique to **indirectly** accommodate issues of structural complexity and scale, and other features that cannot be directly incorporated into numerical models (see section 11.6.4). For example, in areas of structural complexity, highly fractured rock masses under low confinement may be more prone to unravelling. In this case, volumetric queries can highlight these areas and rock mass responses can be compared. Alternatively, although large-scale discontinuities may not have been directly incorporated into initial numerical

model, volumetric queries can be used to interrogate and discriminate rock mass response data close to large-scale structures. In this way, their influence on rock mass response can be assessed indirectly by comparing it against the response of rock masses away from large-scale structures.

Example Candidate Criteria

Volumetric queries can be generated to select regions of the rock mass using a number of complex combinations. For example, based on the data presented in Figure 11.4 above, it is possible to select a volume of the rock mass around the excavation based on linear elastic stress-based criteria, rock mass quality and distance to a prospective geological structure. In this example, a query was constructed using the following criteria;

- Maximum shear stresses greater than 15MPa,
- Distance less than 10m from “Fault B”, and
- Discontinuity linear intensity greater than 7m^{-1}

The resulting volume is shown in Figure 11.8 and provides a very good correlation between the query volume and the location of over-break experienced during mining. Although “Fault B” represents a major structure that transects the entire stope, Figure 11.8b also highlights that its presence alone is not an indication that over-break will occur and that other factors are required for over-break to occur. Any number of alternate candidate instability criteria can then be developed, with the reliability of each criteria established using methods described in section 11.7.2, and selecting the most reliable criteria for further evaluation and forward design.

11.9 QUANTIFYING THE POTENTIAL ECONOMIC IMPACT OF THE DESIGN ON THE PROJECT

Once the reliability of controlling instability criteria or design has been established and accepted, future design geometries and sequence options can then be evaluated and compared for their relative merits, predicted rock mass response and performance. This needs an integrated appraisal considering all operational and financial aspects of the project. Notwithstanding this, the major factor influencing the choice of design options will be anticipated performance and their economic consequences. In order to determine the advantages of one design geometry/sequence option over another, a prediction of the economic impact of each option need to be estimated;

- The range of predicted over-break volumes and their likelihood (i.e. expected volume of over-break) needs to be evaluated. For example, for simple critical-stress based criteria, this would involve determining the shape of the critical stress-based

isosurfaces (hence volume) and their probability of occurrence based on confidence levels (Wiles, 2006). A similar approach can be taken using alternate criteria in more sophisticated models.

- Economic value of the expected volume over-break can then be determined. Predicted over-break volumes can be imported into grade models and economic value of the additional unplanned volume determined (i.e. grade and tonnes). Alternatively, over-break can be assumed to carry zero grade. In this case, the direct cost to operations is additional mining (load, haul and fill) and milling costs.
- The indirect economic impact of over-break and damage are much harder to define;
 - blocked draw-points, secondary breakage and damaged brows
 - re-drilling of blast holes
 - additional rehabilitation costs
 - leaving pillars (ore loss)
 - additional rises or cut-off slots
 - associated lost opportunities with short term diversion of resources
 - damage to permanent development access and infrastructure
- Empirical databases of past indirect consequences of over-break may be used to assess likely impacts to operations and indirect costs.

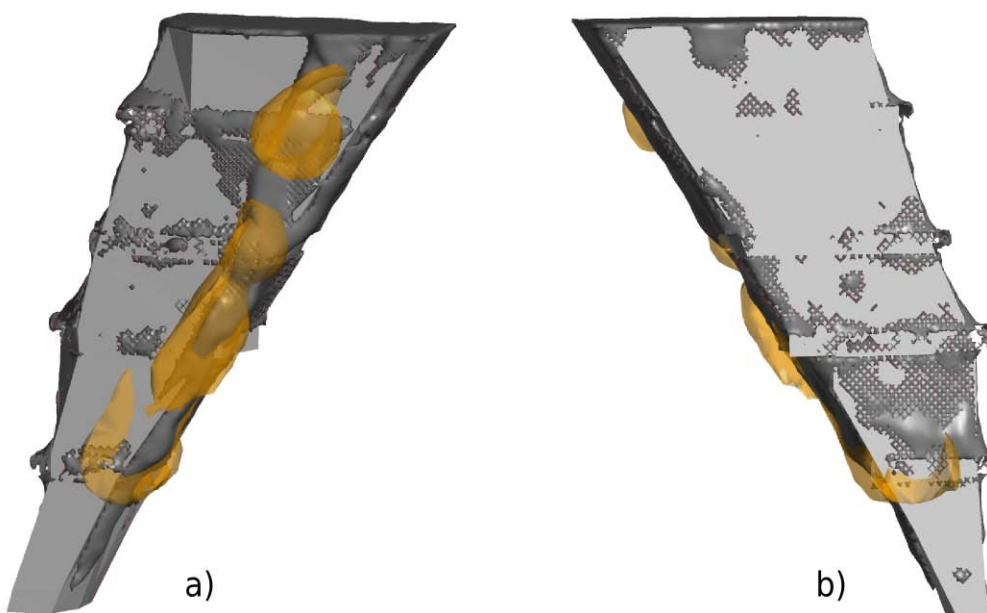


Figure 11.8 - Results of intersection of multiple candidate criteria (gold) for stope AP02 looking a) west and b) east, compared against CMS profile (dark grey).

After the reliability of the selected design parameters, and their respective potential economic impact, have been assessed then a quantitative-risk based design approach can be adopted to assess various design alternatives (Lilly, 2000; Lilly and Villaescusa, 2001).

11.10 CONCLUSIONS

An integrated design optimisation approach has been presented that attempts to ensure that the most appropriate design methods, rock mass models, data collection strategies and analysis techniques are utilised at the relevant stages of project development. This chapter also proposes a framework that attempts to integrate different rock mass characterisation models, numerical modelling and stope performance data, to improve the predictive capability of back analysis methods.

11.10.1 Continual Reduction in Uncertainty

The key philosophy behind the integrated design approach is the continual reduction in uncertainty in collected data, analysis and design methods used with a view to improving the overall reliability of the design. The approach presented attempts to achieve this by ascertaining and improving reliability in all facets of the rock engineering process;

- reduction of biases in data collected by appropriate planning of sampling methods and locations (section 11.4.2)
- reduction of bias and improved precision by correct application of data analysis methods (section 11.4.1)
- maximise volumetric coverage by optimising the percentages and types of data collection and test methods and to develop relationships between parameters (section 11.4.1)
- optimise domain boundaries to improve statistical homogeneity, optimise approaches to rock mass modelling, and establish reliability of rock mass models (section 11.5)
- adopting a staged approach to the selection of the most appropriate design methods based on the level of understanding of rock-excavation interactions (section 11.6)
- utilise methods to assess design reliability based on; performance criteria, instability criteria, direct volumetric comparisons (using novel scale independent geometric descriptors) and normalised isotropic distance (section 11.7).
- Assessing the economic impact of design reliability (section 11.9) to determine adequacy of the design. This can also be used as a tool to determine best alternatives between design approaches, or whether additional data need to be collected.

11.10.2 Improvements to Existing Techniques

The proposed approach also recognises that, in order to optimise the design process, it is also necessary to integrate state-of-the-art techniques in data collection, analysis, modelling and engineering analysis and design at the appropriate stage of project development. To assist in supporting the integrated approach, a number of new developments have improvements have been developed in key areas of the rock engineering design process;

- A rock mass data model has been developed that assists in facilitating the ongoing rock mass characterisation process. The data dependency diagrams assist in identifying the appropriate rock mass sampling methods to collect various data and develop various rock mass models. The data model is capable of integrating rock mass data from various sources, which promotes sharing of data and avoids duplication of data collection efforts. The data model is able to query rock mass data, define relationships between data types, apply bias corrections, and perform basic analysis for use in subsequent detailed analysis and rock mass modelling.
- An implicit based approach to spatial rock mass and deterministic discontinuity modelling can be employed to improve understanding of the spatial variability of rock mass parameters, inter-relationships between rock mass characteristics on their role in design. For example, understanding the influence of large-scale structures on rock mass characteristics and excavation performance.
- Improved scale independent geometrical assessments of stope performance have been proposed that maximise the use of stope performance data.
- An integrated back analysis framework has been presented that is able to account for structural complexity, scale and features that cannot be directly incorporated into linear elastic numerical modelling codes.
- With regard to linear elastic back analyses, an number of improvements have been proposed, as well as a suggested method to assess appropriateness of continuum models based on discontinuity intensity and critical span.

11.10.3 Practical Applications

Two case study mine sites have been selected to demonstrate certain aspects of the proposed framework. As practical application of the entire framework is limited by the existing data collection and monitoring programmes, as well as stage of project development of the selected case study mines, it is not possible to demonstrate all possible applications of the framework. In the following chapters a number of applications of the framework will be demonstrated;

1. The use of implicit function based rock mass modelling techniques to investigate and

- provide an improved understanding of the role of large-scale discontinuities on local rock mass conditions (sections 12.5, 13.4 and 13.6).
2. The use of implicit function based rock mass modelling techniques to generate high resolution rock mass models from sparse data and how their use can potentially assist in identifying previously unknown large-scale geological structures, minimising Type 1 uncertainties (section 12.4).
 3. The use of implicit function based rock mass modelling techniques to maximise volumetric coverage by developing relationships between parameters (section 12.3.7).
 4. Demonstration of integrating high resolution rock mass models with geometrical back analysis in the development of a site-specific back analysis and quantitative risk-based design methodology (section 12.6).
 5. The use of rock mass modelling techniques to; optimise domain boundaries and improve rock mass model reliability, and investigate spatial variation of rock mass characteristics along large-scale discontinuities (sections 13.5 and 13.6).
 6. The use of the back analysis framework and volumetric querying to improve the reliability of design instability criteria using traditional linear elastic modelling techniques (section 13.7).
 7. The use of the integrated model to enable a back analysis - forward analysis approach to open stope design using advanced non-linear numerical modelling with direct incorporation of a highly detailed deterministic discontinuity model. This exercise demonstrates the development of instability criteria based on plastic strain and velocity. The exercise also demonstrates the application of techniques to quantify the predictive capability or reliability of instability criteria (section 13.8).

CHAPTER 12 - CASE STUDY: BHP BILLITON CANNINGTON MINE

12.1 INTRODUCTION

The geology of the Cannington deposit is characterised by complex geometry and structural history, which has a significant influence on rock mass response to mining. A sound understanding of the geology and its impact on potential rock mass response are critical to mine design at the Cannington Mine. A number of aspects of the integrated approach to open stope design developed in this thesis will be demonstrated using data from the Cannington lead-silver-zinc underground operations. This chapter firstly provides a brief description of the structural geology of Cannington and the key geological features that influence rock mass response to mining. A number of the proposed rock mass modelling techniques will be demonstrated and used to develop a spatial rock mass model of a number of rock mass parameters for the Cannington Mine. The chapter will also demonstrate how the implicit function based rock mass modelling techniques have led to an improved understanding of geology, by assisting in the identification and modelling of a previously unidentified major mine-scale structure. The spatial rock mass models have also been used to develop an understanding of the influence of large-scale structures on rock mass characteristics. Finally, the chapter concludes with a demonstration of how integrated spatial rock mass models and stope performance data can be used to develop reliable site-specific empirical design tools.

12.1.1 Cannington Mine

The BHP Billiton Cannington Mine is a large underground lead-zinc-silver mine located in north western Queensland, approximately 240km south east of the major mining centre of Mt Isa. Cannington is the largest single producer of silver world-wide, producing approximately 6% of the world's primary silver production and about 7% of the world's primary lead output (Jeffrey, 2002), with an annual ore production of approximately 2.9Mtpa.

Underground mine access is via a 5.2km decline, with a 650m long, 5.6m diameter primary haulage shaft. The stoping activities are undertaken in a series of geologically distinct ore-bodies, which display a range of rock types and rock mass conditions. Rock engineering considerations have become one of the key design criteria during stope and mining block design. Sub-level open stoping (*SLOS*) is the primary production method, with a small amount of bench stoping being used in the narrower sections of the ore-bodies. Sub-level open stopes are mined in a combination of primary-secondary and pillar-less retreat

sequences on multiple mining fronts. All stope voids are backfilled predominantly with de-limed cemented paste fill, however, uncemented rock fill is used in stopes where fill will not be exposed by future mining.

12.2 GEOLOGY

The response of rock mass to mining at Cannington tends to be dominated by deformation along a number of late-stage brittle faults. Depending on the spacing, location and orientation of faults with respect to the local stress field and excavations, rock mass response can be manifested by shearing and/or dilation on fault surfaces, as well as shear failure of the rock mass between faults. The following sections attempt to provide a basic model of the regional and local folding and faulting, lithology and jointing in order to understand potential rock mass behaviour and response to mining.

12.2.1 Regional Geology

The Cannington Ag-Pb-Zn deposit is situated off the south-east corner of the Mt Isa Inlier, Queensland, Australia (Figure 12.1). More specifically, Cannington is located in the Eastern Fold Belt, which is characterised by sequences of variably deformed and metamorphosed Early to Middle Proterozoic sedimentary, volcanic and intrusive rocks. The structural geology of the region has been dominated by two major events; an early basement deformation and metamorphism cycle termed the Barramundi Orogeny (1.9-1.87 Ga) and a later multi-phase cycle (1.87 - 1.62 Ga) (Blake, 1987). The later multi-phase cycle can be sub-divided into 3 phases

- Sequence 1 (1.87 - 1.85 Ga); comprising mainly of felsic volcanism intruded by large granitic batholiths
- Sequence 2 (1.79 - 1.72 Ga); deposition of mixed shallow water sediments, bimodal volcanism, and metamorphism.
- Sequence 3 (1.68 - 1.62 Ga); deposition of fine-grained clastic sediments and carbonates, with only minor volcanics.

The final sequence was following by the Isan Orogeny (1.62 - 1.52 Ga) resulting in thrusting and nappe-style folding in upper layers as a result of north-south shortening, followed by a more dominant phase of extensive and deeper east-west shortening (Blake and Stewart, 1992) resulted in the dominant north - south structural grain of the inlier. This was manifested in the Eastern Fold Belt by the development of upright north-south folding, steep-dipping foliations, and the development of steep east-dipping reverse faults.

The Mt Isa inlier is also characterised by a series of late-stage cross-cutting strike-slip faults

that display dextral displacement. The strike-slip fault system does not form a conjugate fault pattern, but rather the angles between master and second-order faults, and second-order and third-order faults is approximately 30° , suggesting subsidiary faults represent riedel shears (Betts et al., 2006).

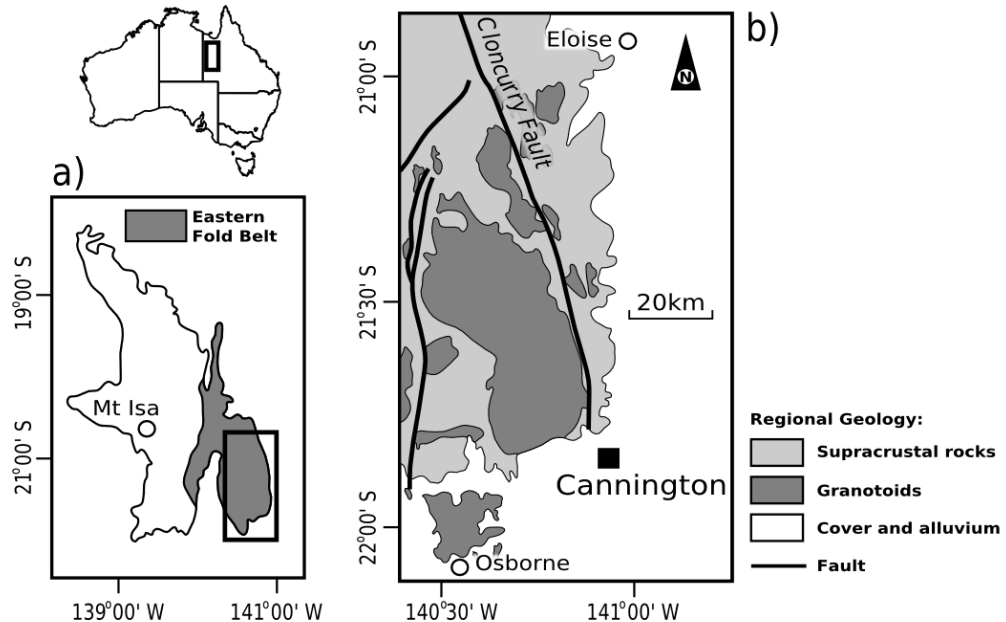


Figure 12.1 - Location of a) the Eastern Fold Belt of the Mt Isa inlier, b) Cannington Mine with regional geology (Chapman and Williams, 1998)

12.2.2 Mine Geology

The Proterozoic sequence hosting the Cannington deposit is unconformably overlain by 10 to 60m of horizontally bedded Cretaceous sediments. The deposit is hosted by migmatitic quartzofeldspathic gneiss that displays well-developed differential banding comprising biotite-rich (\pm sillimanite, muscovite, garnet) and quartz K-feldspar plagioclase-rich bands. The gneiss is considered to be part of the Maronan Supergroup, consisting of 1.68–1.66 Ga (Giles, 2000) immature siliciclastics and metabasic volcanic rocks. Quartzite units up to 1.5m thick are commonly intercalated with the gneiss. These rocks grade into unusually garnet-rich, interbanded sillimanite-garnet schists and garnetiferous quartzites that envelope the deposit up to 250m. Coarse grained pegmatites (up to 70% K feldspar, plagioclase and quartz, minor biotite and accessory garnet) are locally abundant in the gneissic rocks and range up to tens of metres in thickness. Amphibolites occur throughout the area and are generally concordant to the gneissic rocks (Bodon, 1998). A cross section showing local geology is shown in Figure 12.2.

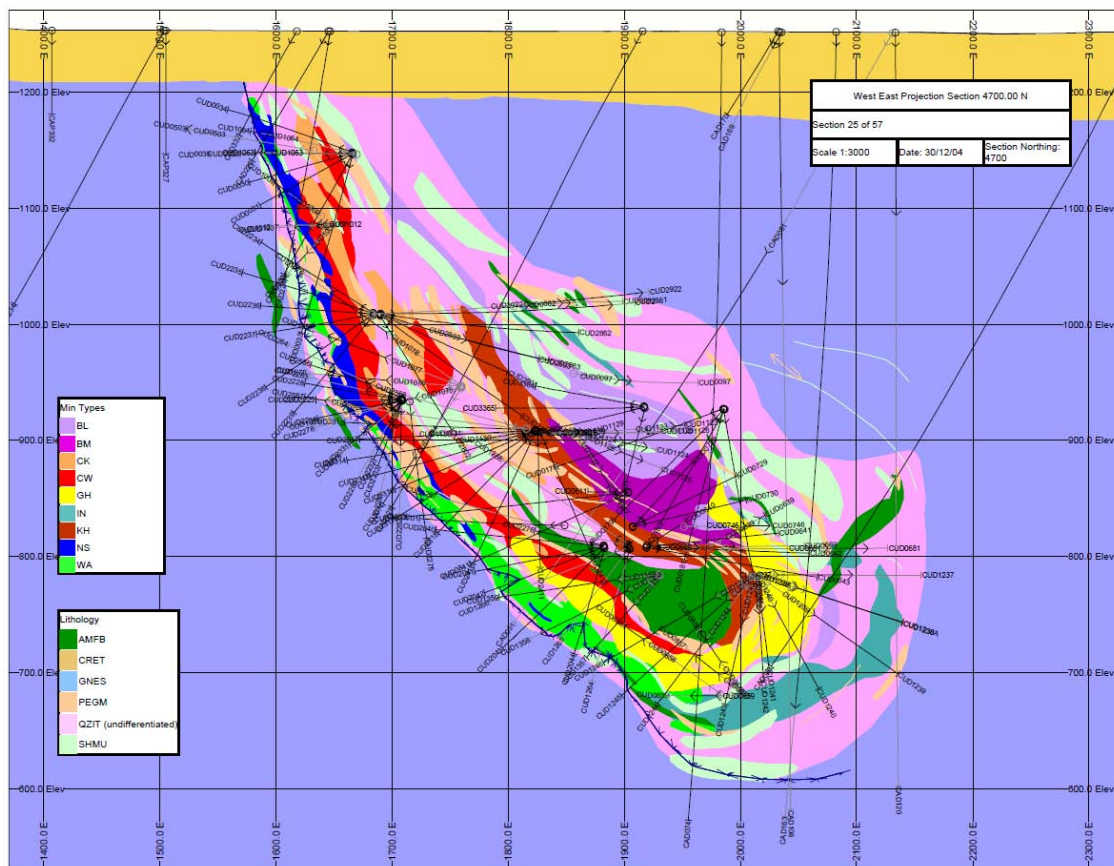


Figure 12.2 - Cross section at 4700mN showing local mine geology and mineralisation (courtesy BHP Billiton Cannington Mine)

The local mine geology is dominated by apparent synform folding around a lenticular amphibolite (termed the Core Amphibolite), however, recent interpretations suggest that the Core Amphibolite may be a shear related mega-boudin (Roache, 2004). At least four deformational phase have been recognised at Cannington (Gray, 1992);

- D1 - regional NW directed thrusting event, producing a local schistosity and rare minor rootless fold hinges in foliated rocks
- D2 - the major structural event recorded at Cannington and represented by tight to isoclinal north-south aligned folded structures with a well-developed axial surface schistosity. D2 folding in the Southern Zone is more intensely developed than in the northern zone.
- D3 - open folds with minor crenulation of D2 schistosity and a lack of axial foliation
- D4 - late-stage brittle structures.

Rock Mass Response

The properties of the local mine lithologies have been shown to impact on the rock mass response to mining. A qualitative ranking of the major lithology types and their impact on

rock mass response is provided below;

- Good; Massive quartzites, amphibolites, ore types and pegmatites
- Fair to Poor; Intercalated and foliated quartzites and schists
- Poor to very poor; Foliated gneiss and sillimanite-muscovite schists

In general the stoping conditions at Cannington are characterised by a higher quality ore material forming the stope side walls along the strike of the ore-body, and a poor quality sillimanite-muscovite schist and quartzites forming the stope hangingwall and in places the stope crowns (Streeton, 2000). In particular, the presence of lenses of gneiss and sillimanite-muscovite schist close to excavation boundaries generally provides the poorest rock mass response to mining. Other factors also influence local rock mass conditions and response such as intensity of foliation, mineral type and degree of alteration, proximity to sheared intrusive contacts and late stage brittle faulting.

Brittle Faults

The brittle faults at Cannington are described by (Gray, 1992) and (McCarthy, 1996). In order of significance, these faults comprise of major NNW trending east dipping Trepell and Hamilton Faults, the N trending, E dipping Broilga Fault zone, and the pervasive NE trending 'Bird' faults (Figure 12.3).

The Trepell and Hamilton faults are characterised by badly broken ground, 10-15m wide clay-chlorite gouge, with fractured zones that are up to 100m wide (along the Trepell fault). The Trepell fault divides the Cannington deposit into discrete Northern and Southern zones, which show differences in structural style, relative proportions of mineralization types, and economic grades. The Trepell fault and Hamilton Fault display oblique sinistral-reverse sense of movement (top-to-north west), imparting a 300m left-lateral separation to the Core Amphibolite (Giles, 2000).

The ore-body also appears to be cut by a set of north-south trending brittle structures along the eastern edge of the deposit, termed the Broilga fault zone. These faults generally dip steeply to the East and are characterised by brittle chlorite coated slickensided fractures. These faults appear to have been right-laterally off-set by a latter series of faults. The latter series of faults dominate the Southern zone which cut and offset the geologic sequence. These faults are a series of pervasive upright, east-north-east trending faults that show predominantly dextral reverse displacement, and are termed the 'Bird' faults. These faults form complex pattern of en echelon anastomosing structures (Bodon, 1998). The structures are characterised by gouge zones and local cavities with silica carbonate infill. Offsets are in the order of 20 to 30m, and where the east-north-east trending faults overprint the Broilga

fault zone, mineralisation occurs as a series of high-grade, fault-bounded breccia pods. Spacing between faults is generally in the order of 10m to 50m, with some faults possessing multiple splays and fault surfaces, whilst others comprise of wider zones. It is considered that these are possibly conjugate to and temporally related to the Trepell and Hamilton faults and appear to be the final stage of mine scale brittle deformation (Gray, 1992).

These late stage brittle faults play a significant role in the response of the rock mass to mining, hence defining the location, geometry and properties are crucial for ongoing mine planning and management of rock mass behaviour. In contrast to this, mine-scale geologic structures that were formed during earlier ductile deformation, such as the footwall shear, tend to have less impact on rock mass response principally as these structures tend to be healed re-crystallised zones having significantly higher shear strength characteristics.

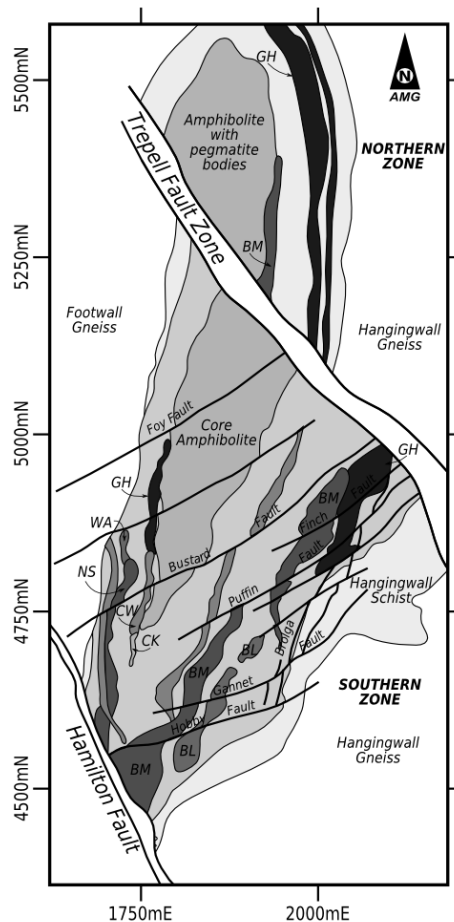


Figure 12.3 - Plan of interpreted geology at approximately 300mLV, showing the major brittle structures (after McCarthy, 1996)

Small Scale Discontinuities

Considering the higher temperatures associated with the D1 and D2 shearing and folding

events, it is considered that jointing at Cannington is primarily associated with faulting and folding related to lower temperature, later stage brittle deformation events, such as D4, or possibly D3. Table 12.1 summarises the jointing at Cannington by describing the sets, and their orientations, for each rock type (Power, 2004). Up to nine sets have been identified for the amphibolite and quartzites, with other rock types typically characterised by seven sets. It is considered that identification of such a large number of sets was due to the fact that orientation analyses were conducted by considering rock type only and no account was made for spatial variability or separation of data into structural domains. In order to provide meaningful orientation analysis and it is considered that data needs to be domained, using techniques previously described in Chapter 8. The use of these techniques is especially important in structurally complex ore-bodies such as Cannington.

Table 12.1 - Discontinuity sets at Cannington by rock type (after Power, 2004)

Set	GHB		HWL		PEG		SCH		AMP		QTZ	
	Dip	Brg										
1	64	346	70	350	80	312	60	85	70	340	80	330
2	72	317	70	270	68	340	55	275	10	40	69	20
3	63	270	80	230	76	55	70	10	80	30	16	0
4	79	216	70	190	69	122	60	215	35	60	85	151
5	63	82	45	90	37	149	70	155	75	80	70	169
6	66	34	70	10	34	265			65	155	58	222
7	74	168	70	310	77	204			70	210	79	222
8									30	270	81	250
9									80	305	56	298

Notes: GHB - Glenholme Breccia, HWL = Hanging wall Lead, PEG = Pegmatite
SCH = Schist, AMP = Amphibolite, QTZ = Quartzite

12.2.3 In Situ Stress

The in situ stress regime at Cannington has not been reliably determined to date due to the complexity of the geology and its interaction with mining. To date, 15 individual CSIRO HI-cell and 6 WASM AE stress measurements have been made. Windsor (2006) has attempted to reconcile the stress measurements placed within the context of continental and regional stress measurements, the regional and local structural geology and shear strength of large-scale geological structures. Based on this work the proposed in situ stress regime for Cannington is shown in Table 12.2.

Table 12.2 - In situ stress model for the Cannington Mine (Windsor, 2006)

Principal Stress	Magnitude	Trend*	Plunge
σ_1	= 0.060 x depth (m)	129°	14°
σ_2	= 0.046 x depth (m)	223°	08°
σ_3	= 0.027 x depth (m)	359°	80°

Notes: * trend with respect to Mine Grid which is equal to True North

12.3 MINE SCALE ROCK MASS MODEL

The previous sections have only briefly outlined the structural and geological complexity that characterises the Cannington deposit. The following section describes the development of a spatial model for the Cannington Mine. The model attempts to capture the spatial variability of various rock mass properties for mine design purposes by integrating the limited data sources available.

12.3.1 Previous Rock Mass Modelling

Initial attempts at modelling the rock mass conditions at Cannington (Luke and Edwards, 2004) involved constructing a block model in Datamine software of discontinuity linear intensity values, NGI-Q System (Barton et al, 1974) Q values and their component parameters (i.e. RQD , J_n , J_r , J_a and SRF). The main aim of this modelling was to assess whether the block modelling process, typically utilised in resource modelling could be successfully implemented using the high density, relatively high quality diamond drill core logging data and to see if the model produced a reasonable representation of the regional rock mass conditions at Cannington.

A brief summary of this modelling exercise follows. The block model generally covered the mine area south of the Trepell Fault, and was constructed with a minimum block size (daughter cells) of 8m x 12m x 8m in the X (mine grid east), Y (mine grid north) and Z (mine grid RL), respectively. Data and interpolation were constrained by major fault bounded domains, and then by lithological sub-domains. An isotropic inverse distance squared ($IDW2$) interpolation method was chosen to generate interpolated values within the block model. As some of the NGI-Q system parameters were not explicitly recorded in the drill core logging, namely J_w , SRF, J_a and J_r , some assumptions had to be made regarding the values of these parameters and their variability across the mine. The values for these parameters were set as constants, based on experience on local conditions, for the various domains.

Variography studies of geotechnical parameters during this study, and subsequent work

suggest that there is weak continuity for all parameters, with the most continuity typically aligned parallel to the strike of local stratigraphy (Binns, 2004). Binns (2004) extended the initial work by incorporation of an additional fault domain to constrain data and interpolation. The basis of the additional fault domains was the identification of a zone of intense fracturing mid-way between the Hamilton and Trepell faults. A geotechnical block model (March, 2007), was produced by Cannington geology staff. The model was based on the Datamine macros developed by Binns (2004), and was extended to include the drill hole data for the Northern Zone.

12.3.2 Resolution Issues in Stope Design

Although the block models did in fact provide a reasonable representation of the spatial variation of certain rock mass characteristics, there are a number of characteristics of block models that limit their usefulness in the rock engineering design process. Firstly, the spatial variability is represented in block models by changes in certain rock mass properties between individual cells or blocks. This means that there is a scale limit in the ability to observe discrete changes within a volume of rock, which depends entirely on the size of the blocks, or in effect, the model resolution (see Figure 12.4). The benefits of using of implicit functions become apparent, as values can be calculated at any resolution.

A second disadvantage of block models is that determining the exact value of a parameter on the surface of the excavation is not trivial. This complicated process would involve “cookie-cutting” the block model using the excavation geometry then selecting blocks or sub-blocks that line the void left by the excavation. The depth that these blocks extend into the rock mass is again related to block resolution and further complicated by geometry caused by alignment of the principal block model directions and the excavation. The use of implicit function based spatial modelling can alleviate this problem, by generating the parameter value at any point and at any distance from the excavation surface.

12.3.3 Scope of Current Modelling

The aim of the current modelling exercise was to generate an improved high resolution integrated rock mass model using implicit function modelling and *RBF* interpolation techniques. A secondary purpose was to generate a more up to date model, containing additional diamond drilling data that will include the Northern Zone of the Cannington mine. Another purpose of the modelling was to attempt to incorporate sparse intact rock strength data (e.g. laboratory *UCS* test results) to spatially model the variation of intact rock strength.

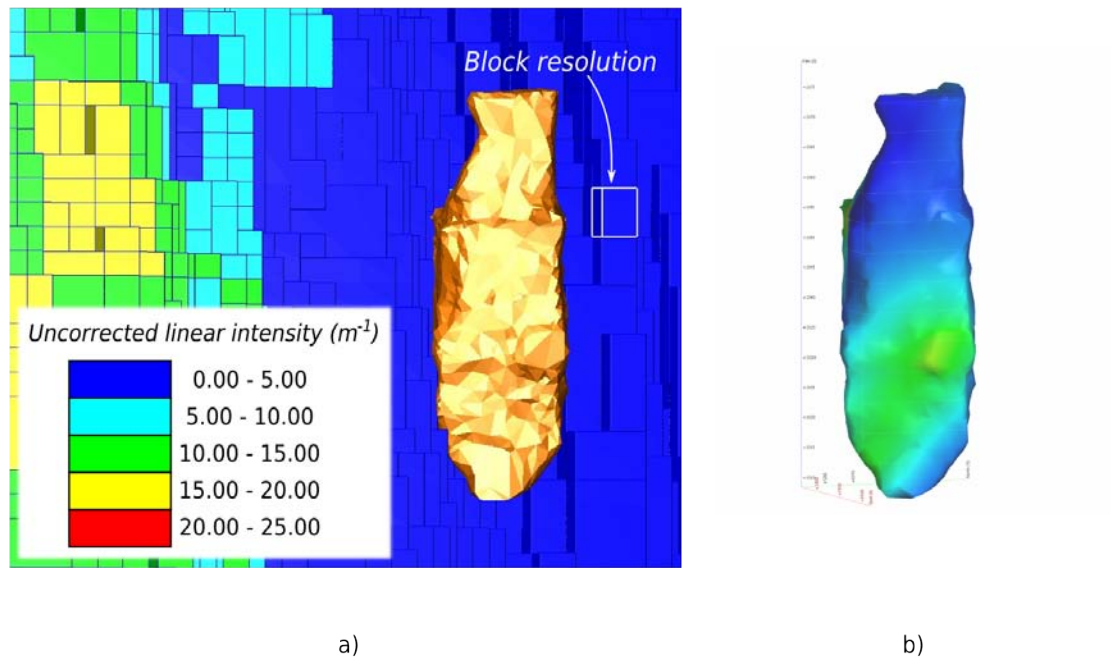


Figure 12.4 - Sectional view of stope 24jc6 showing discontinuity linear intensity values for a) existing Cannington block model and b) high resolution RBF surface interpolant

12.3.4 Data Sources

The data sources for the Cannington rock mass model were primarily taken from the diamond drill core logging. Additional data sources included the results from geomechanics laboratory testing, geological wire-frames of lithological and mineralogical boundaries, geotechnical window mapping, and geological drive mapping data.

Diamond Drill Core Logging

The Cannington diamond drill core logging database was utilised as the major data source for the construction of the geotechnical rock mass model. A number of parameter “tables” make up the diamond drill core database including; core recovery, alteration, position and description of faults, minor structure, lithology, mineralisation, geotechnical data.

The “Geotechnical” table was used as the primary data source and included the following parameters; *RQD*, Fractures per interval or *DLF* (typically calculated over a 1m interval), estimation of sets per interval, rock type. The data were then imported into the Rock Mass Data Model database for validation. The logged fractures per interval values were validated first. This involved ensuring there were no negative values within the data set. The discontinuities per interval values were then normalised to the logged interval, that is; (discontinuity count)/(length of interval). This value is equivalent to the uncorrected total

discontinuity linear intensity (λ_t).

Geomechanics Database

Geomechanical laboratory test results, compiled by Cannington geotechnical staff, were provided in a Microsoft Excel® spreadsheet (Rock testing data of Cannington - 19May04.xls). These data were reviewed, with the sample locations validated against the true drill hole names and sample depth intervals. The Uniaxial Compressive Strength (*UCS*) test results were reviewed, with tests which failed along an existing discontinuity marked and excluded from further analysis. The final *UCS* database consisted of 82 validated samples.

Wire-frames

Triangulated Irregular Network (*TIN*) wire-frames representing lithological boundaries that were used to select and constrain data for interpolation were obtained from the Cannington resource modelling server.

12.3.5 Unconfined Compressive Strength Modelling

Unconfined compressive strength (*UCS*) was assessed using the validated geomechanics test database. The *UCS* values for each rock type were statistically reviewed for the mean and likely ranges (see Table 12.3). This review indicated that some units had similar mean *UCS* values. It was therefore decided to amalgamate a number of lithological units to simplify the amount of *TIN* wire-frames for modelling purposes. In this case, the Cuckadoo and Nithsdale ore types were combined as one unit. The review also indicated that intact rock strength data are quite sparse for some ore types, especially the Glenholme Breccia, which comprises of around 28% of the volume of all ore types. No samples are available for the Invernarvon ore type, which makes up around 15% of ore types in the Central zone. From Table 12.3, it can also be seen that there is significant variability in some rock types, especially the sillimanite-muscovite schists, which based on the test data displays a coefficient of variation of around 70%. This C_v represents significant variability and level of data uncertainty may pose a significant risk to the mine in developing reliable models and developing subsequent design criteria, especially considering the stage of development of the mine.

Considering the complexity and size of the Cannington deposit, it is considered that there were an insufficient amount samples to interpolate intact rock strength from the samples directly. In order to capture the spatial variability, the geological and lithological *TIN*s were used as the basis for domaining and modelling intact rock strength. This firstly involved generating a common grid point model. The geology wire-frame *TIN*s were used sequentially to determine the lithology and ore type at each grid point. The spacing of the grid points had

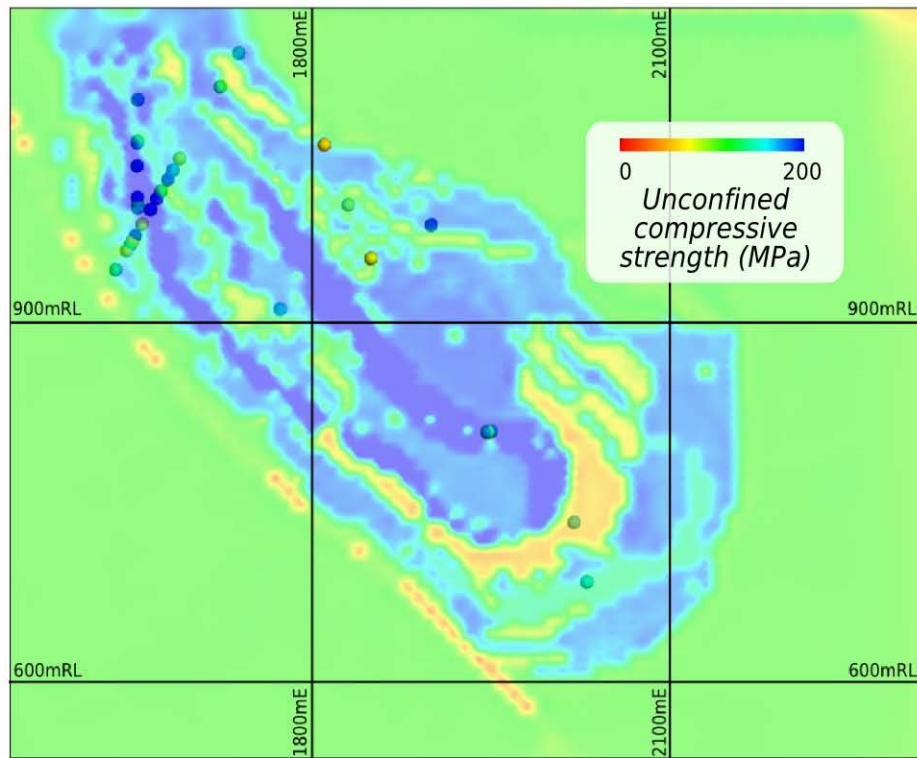
to be sufficiently close to capture the complex geology. The mean values in Table 12.3 were then used to assign a *UCS* value to each grid point based on the lithology and ore type. The *UCS* values were then modelled as an implicit function using an isotropic linear-model interpolation.

Table 12.3 - Summary of intact unconfined compressive strength by rock type at Cannington Mine

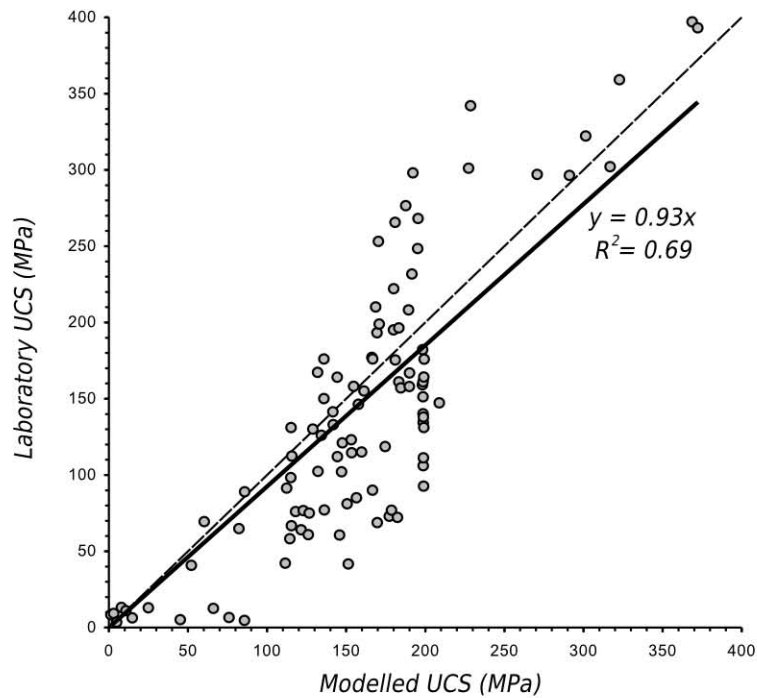
Rock/Ore Type	Major Lithology Code*	No. Samples	Mean (MPa)	Std. Dev.	C _v
Cretaceous mudstone	OMOB	6	9	3.4	0.39
Amphibolite	AMFB	7	195	86	0.44
Burnham and Broadbands (HW Pb)	HDMT	15	174	45.6	0.26
Cherty quartzite	QZCH	9	156	72.7	0.46
Cuckadoo (FW Zn)	QZCH	3	141	31	0.22
Garnetiferous quartzite	QZGA	9	171	60.2	0.35
Glenholme Breccia (HW Pb/Zn)	BREC	1	42	-	-
Gneiss	GNES	5	108	26.6	0.25
Kheri-Colwell mineralisation	PXAM	6	339	86.3	0.25
Nithsdale (FW Pb)	MTPX	2	145	19.8	0.14
Pegmatite	PEGM	9	118	31.7	0.27
Sillimanite-muscovite schist	SHMU	14	69	50.7	0.73

Notes: * - Ore types can be hosted in a number of rock types, hence the most dominant lithology is displayed here

Cross-validation can generally be used as a statistical exploratory tool to develop optimal variogram models (Davis, 1987). However, due to the nature of the modelling exercise and limited data set, detailed cross-validation of the derived *UCS* spatial model is not warranted in this case. Notwithstanding this, a simple visual comparison of the results of the modelling and *UCS* laboratory test data (shown as coloured spheres) is provided in Figure 12.5a. The modelled values show a reasonably good fit to the laboratory samples. This is also highlighted in Figure 12.5b. It can be seen, however, that the modelling tends to over-estimate *UCS* at lower values and under-estimate *UCS* at higher values, thus indicating an overall smoothing effect, which is to be expected, as modelling has been based on the mean laboratory test values for each lithology. Nevertheless, the modelling approach taken provides the design engineer with a reasonably accurate and detailed model capable of representing the spatial variability of intact *UCS* for a complex geological environment.



a)



b)

Figure 12.5 - Modelled UCS (MPa) values a) cross-section at 4700mN also showing valid UCS samples (spheres) and b) correlation between laboratory and modelled UCS values (dashed line represents equivalence)

12.3.6 Discontinuity Intensity Modelling

Spatial modelling of discontinuity linear intensity for the Cannington Mine involved utilising the validated diamond drill hole *DLF* logging data, consisting of approximately 650,000 x 1m composite samples. The data was firstly separated into 5 main zones;

- Cretaceous Zone
- North of Trepell Fault,
- South of Hamilton Fault,
- West of the “Footwall Shear”,
- Remainder falling into the “Central Zone”

This was done to ensure that interpolations were constructed for geologically distinct environments, with major mine-scale structures acting as hard boundaries to interpolations. Detailed variography of *DLF* data was not conducted for each zone. Instead, simplistic linear and spherical experimental semi-variogram models were used. The spherical models (range 30m, nugget values of 25% of maximum sill) were utilised to reduce nugget effects during interpolation. The range used in these models is comparable with the results of previous variography work on *DLF* data (Binns, 2004). Initial interpolation of *DLF* values within the Central Zone was done using the following anisotropic model;

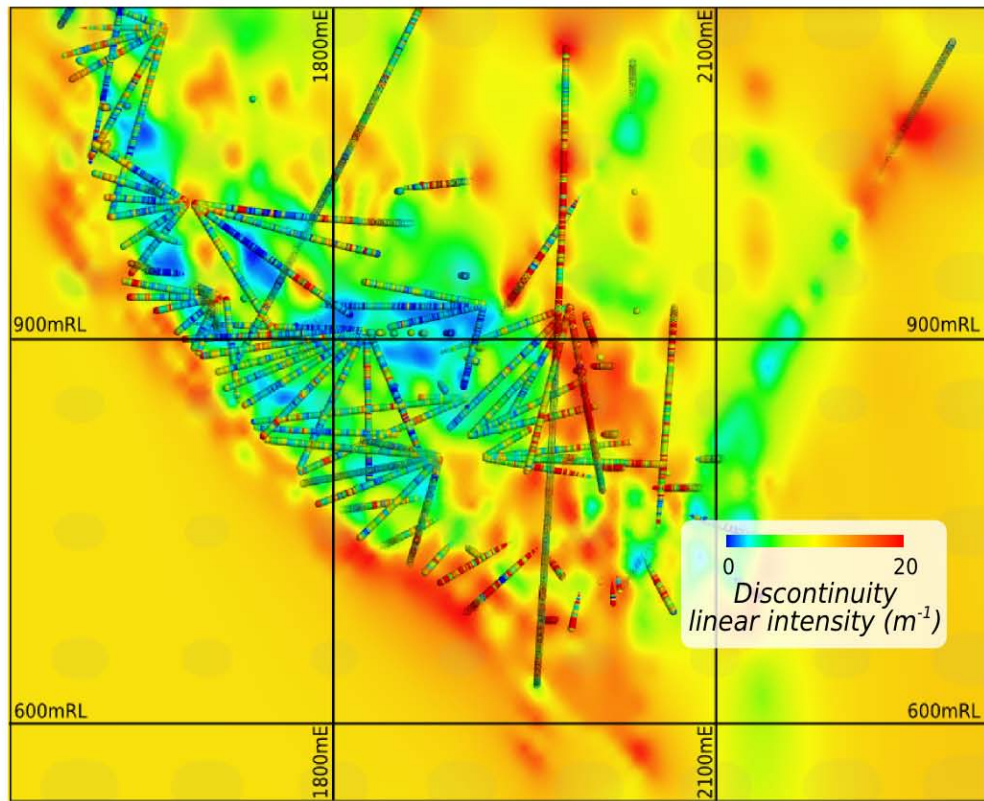
- Lithology Orientation (84° dip, 138° dip direction, 36° pitch, 3:2:1 anisotropy ratio)

The lithological interpolation orientation is similar to the weak stratigraphic trend observed by Binns (2004) in the original variography work. An example cross-section of the final *DLF* spatial model is shown in Figure 12.6a together with samples values.

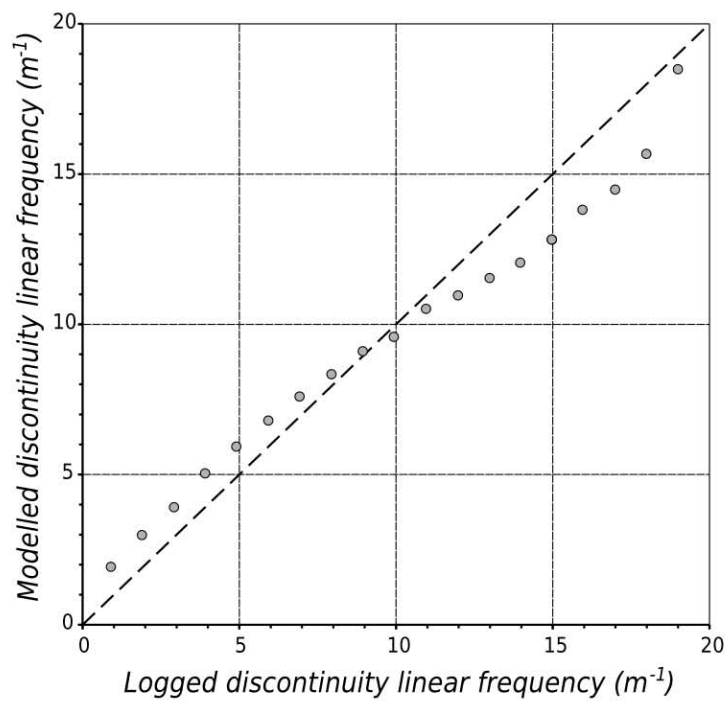
Model Validation

In order to evaluate the reliability of the model, *DLF* values were assessed using cross-validation techniques (see section 8.8). Due to the sheer volume of sample data, model reliability could not be ascertained utilising simple scatter plots. In this case, the modelled values were compared to the true logged sample values utilising a Quantile-Quantile plot (Q-Q plot).

A Q-Q plot for the logged and modelled *DLF* data is shown in Figure 12.6b. It can be seen that the modelling, in general has a very similar distribution to the logged values and provides a reasonably match to the logged data, however it can also be seen that the model over-estimates low *DLF* values and under-estimates high *DLF* values.



a)



b)

Figure 12.6 - Modelled DLF values a) cross-section at 4700mN also showing logged DLF samples (spheres) and b) Q-Q plot between logged and modelled DLF values

The model's maximum over-estimation is around 50% (at logged $DLF = 1m^{-1}$) and has a maximum under-estimation of around 17% (at logged $DLF = 17m^{-1}$), with a general overall over-estimation of DLF of around 3.6%. This phenomenon also suggests a slight smoothing of raw data values which may indicate that the range may be too large and/or insufficient nugget in the modelling parameters. Nevertheless, it is considered that the modelling method and parameters selected provide an accurate spatial model of discontinuity linear frequency.

12.3.7 Relationships between rock mass parameters

A review of the rock mass spatial models indicates an apparent spatial correlation exists between UCS and DLF (see Figure 12.7). That is, high values of UCS are manifested by low DLF values and *vice-versa*. In order to further investigate this observed phenomenon, laboratory UCS values were initially compared to the logged DLF over the section of core where the sample was taken to see if this correlation could be observed in the raw data (Figure 12.8a). It can be seen that there is a weak to moderately strong correlation between laboratory UCS and logged DLF , however there is a fair degree of scatter in the data. In addition, it is considered that the data set is quite biased as there are very few data points (i.e. laboratory samples) at higher DLF values. This bias is to be expected as laboratory samples are generally preferentially selected to be free from existing discontinuities and require a minimum sample length for testing (hence low DLF values).

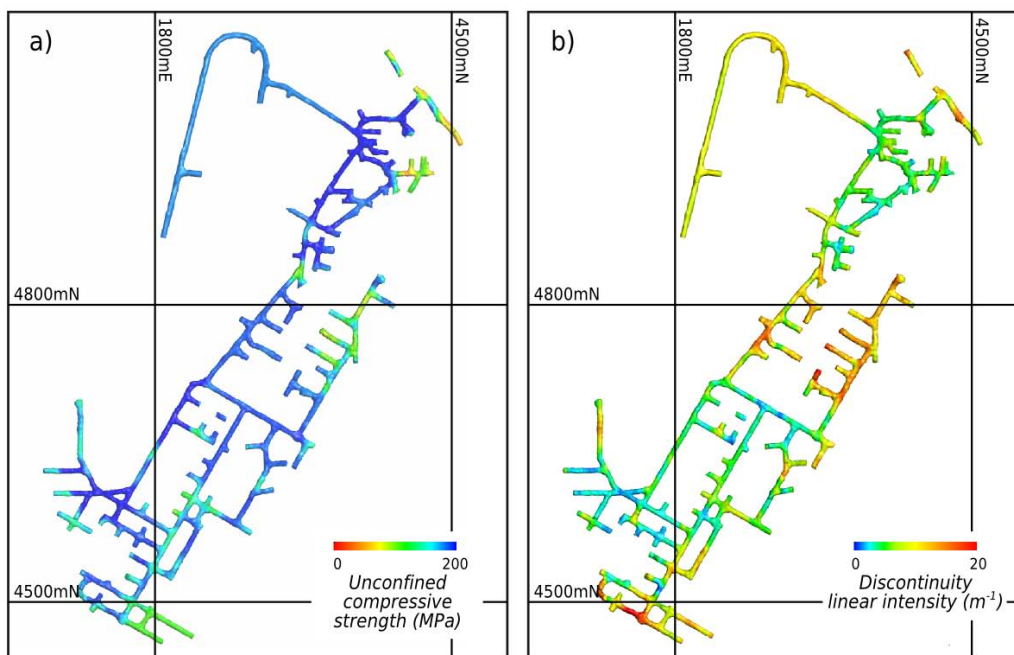


Figure 12.7 - Development at 350mLV showing interpolated a) UCS and b) DLF values for the Central Zone domain

In order to investigate this apparent relationship between modelled parameters, a grid of evenly spaced (15m) sampling points were created along the centreline of the 350mLV development access. Modelled parameters were then interpolated to these common points and compared (see Figure 12.8b). Although there is a good deal of scatter in the laboratory versus logged data, it appears that the spatial models provide a reasonably good reflection of this correlation, with the lower 95% confidence interval regression line matching the upper 95% confidence interval for the laboratory regression line. Comparison of the two regression line confidence intervals would indicate an approximate 90% confidence in having the same relationship for the two data sets. This level of confidence is quite encouraging considering the very limited *UCS* sample data and the different independent approaches taken to modelling each parameter.

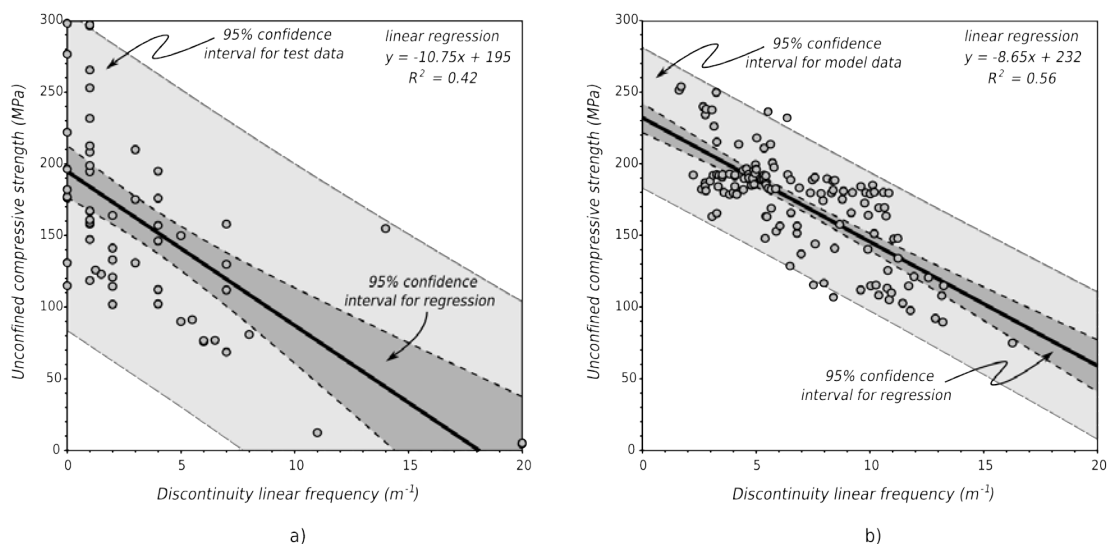


Figure 12.8 - Plot of a) *UCS* (MPa) for validated geomechanics laboratory data versus logged *DLF* (m^{-1}) at the sample position, and b) modelled *UCS* (MPa) versus modelled *DLF* (m^{-1}) for the integrated model data based on equally spaced (15m) sampling points along the 350mLV development

The outcomes of this exercise have a number of implications;

- Assuming that logged *DLF* contains a proportion of incorrectly recorded drill-induced breaks, then the relationship developed above (Figure 12.8a) may provide anecdotal evidence that the proportion of natural and drill induced breaks logged in drill core is inversely proportional to unconfined compressive strength.
- The apparent correlation between modelled *UCS* and modelled *DLF* can be used as a mechanism to indicate likely *UCS* values in areas where no *UCS* data exists.
- In this regard, the exercise above can be used to maximise the value of the higher density and more ubiquitous *DLF* data in order to define a spatial *UCS* model.
- It is considered that a similar approach can be utilised to develop more accurate

spatial models of *UCS* using high density (yet lower cost) intact rock strength data such as point load and Schmidt hammer index tests.

12.4 IDENTIFICATION OF LARGE-SCALE STRUCTURES FROM DISCONTINUITY INTENSITY MODELLING

This section outlines the interpretation and modelling of the “Squirrel Hills” fault zone at the Cannington mine. The interpretation and modelling was conducted utilising the discontinuity intensity spatial model, together with some limited digitised structural geology (from the geological backs fact mapping). The resulting structure is interpreted as being a significant mine-scale geological feature, over 400m in strike and 330m in dip.

12.4.1 Background

During a review of the discontinuity intensity model for the Central Zone domain, it was observed that a zone of high *DLF* occurs approximately half way between the Trepell and Hamilton Faults, with a similar orientation. This has been observed by previous workers (Binns, 2004) and since been dubbed the “Squirrel Hills” fault zone. Figure 12.9 shows interpolated discontinuity intensity values for the Central Zone at the 450mLV, showing the approximate position of the “Squirrel Hills” fault zone. It must be noted that the direction of maximum continuity in the interpolation shown in Figure 12.9 is approximately sub-perpendicular to the interpreted “Squirrel Hills” fault zone, thus providing strong evidence for presence of this feature. It was decided to test the hypothesis of the existence of such a structure by reviewing fact data in the vicinity of its anticipated position.

12.4.2 Geological Mapping

The fact mapping data were reviewed to see if the “Squirrel Hills” fault zone was manifested as a discrete geological structure or a wide zone of intense faulting. An initial review found that there was evidence for a discrete structure (i.e. fault) in most of the mapped areas of the mine, however, this evaluation was hindered by the quality/detail of mapping due to shotcrete or fibrecrete covering the backs and walls (usually down to grade line). In some locations where the “Squirrel Hills” fault zone was anticipated to intersect development, no mapping data were available. In addition, at the time of writing the majority of geological backs mapping data were only available in hard-copy (e.g. hand-drawn), hindering development of a comprehensive digital structural model.

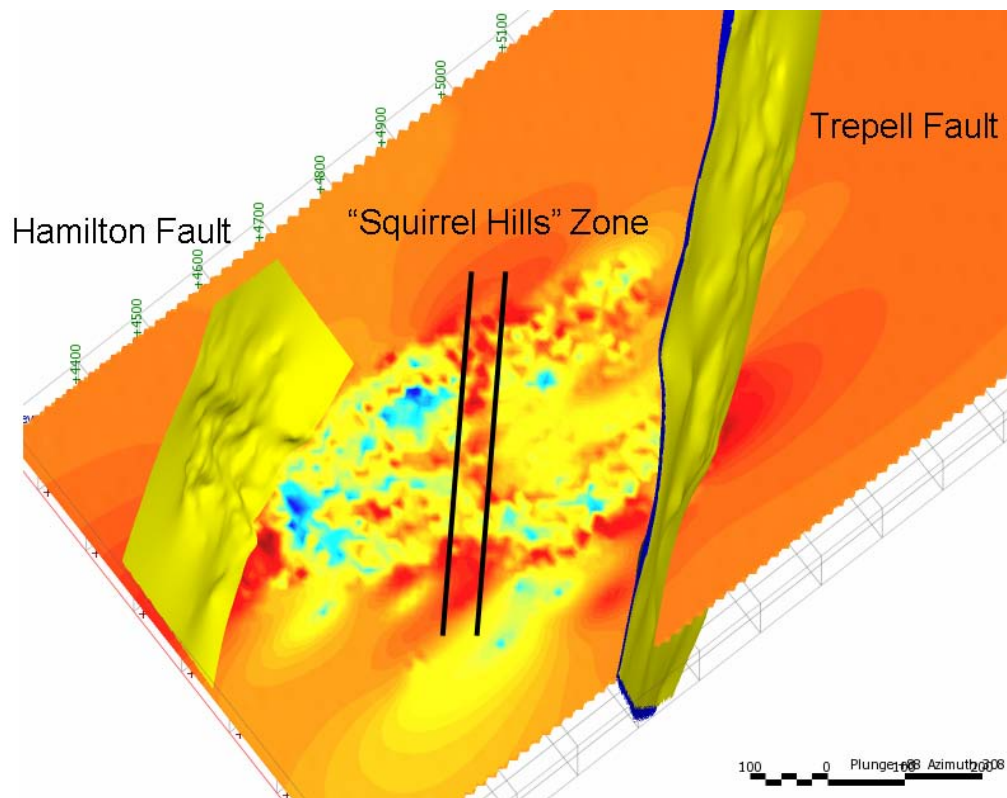


Figure 12.9: Isometric view of Trepell and Hamilton faults and discontinuity intensity modelled at 450mLV showing alignment of high intensity along the "Squirrel Hills" zone

12.4.3 Deterministic Modelling of the Squirrel Hills Fault Zone

To assist in modelling the "Squirrel Hills" fault zone, the hand drafted fact mapping around the expected position of the fault were digitised. The digitised mapping was geo-referenced by "draping" the 2-dimensional traces over the as-built development *TIN*'s to obtain full 3-dimensional trace of each structure (see Figure 12.10). Each structure was also annotated with;

- Dip
- Dip Direction
- Type of structure
- Infill type (e.g. rubble, breccia, gouge, etc.) - where available
- Width of infill - where applicable
- Comments (including sense of movement) - where available

A total of 2033 structures were digitised and annotated. Following geo-referencing, each structure was extrapolated 5m down dip and up dip to form a "pseudo" fact structure (see Figure 12.11). The trace of each interpreted intercept and the local dip/dip direction were then interpolated using techniques described in Chapter 8.

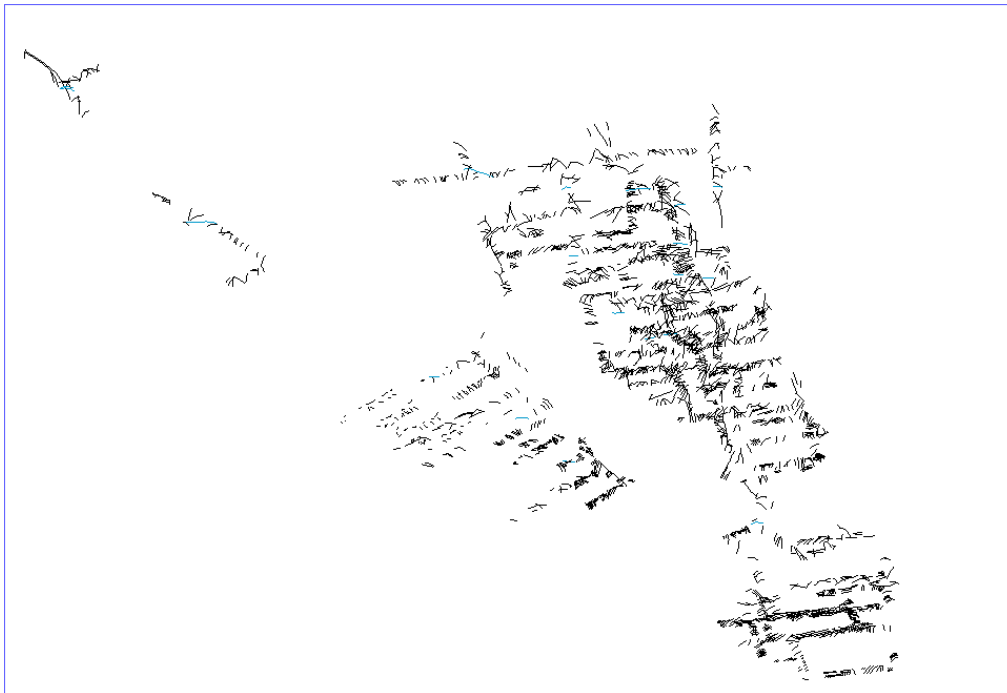


Figure 12.10 - Perspective (looking north east) of digitised fact mapping in vicinity of interpreted "Squirrel Hills" fault zone



Figure 12.11 - Perspective (looking north east) of three-dimensional "pseudo" fact models of digitised geology

12.4.4 Establishing Model Reliability

As outlined in section 8.8, comparison of the predictive model with actual measurements

needs to be done in order to ascertain the validity, accuracy and precision of the model. An assessment of the reliability of the developed 3-dimensional model is provided below.

Orientation Assessment

The orientation of the model was compared to the individual mapped intercepts, which are shown in Figure 12.12, (as poles to planes on a lower hemisphere equal angle stereographic projection). All directions are relative to mine grid. The plane of best fit of the interpreted modelled structure is $89^{\circ}/048^{\circ}$ which is in general agreement with the alignment of mapped intercepts, and falls within the 95% confidence interval.

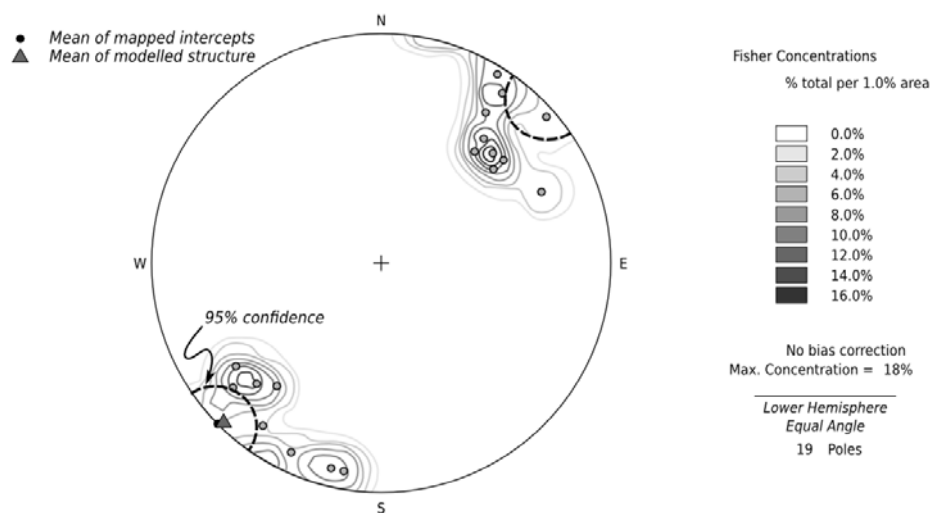


Figure 12.12 - Lower hemisphere stereographic projection of poles to planes for identified mapped intercepts of the Squirrel Hills structure

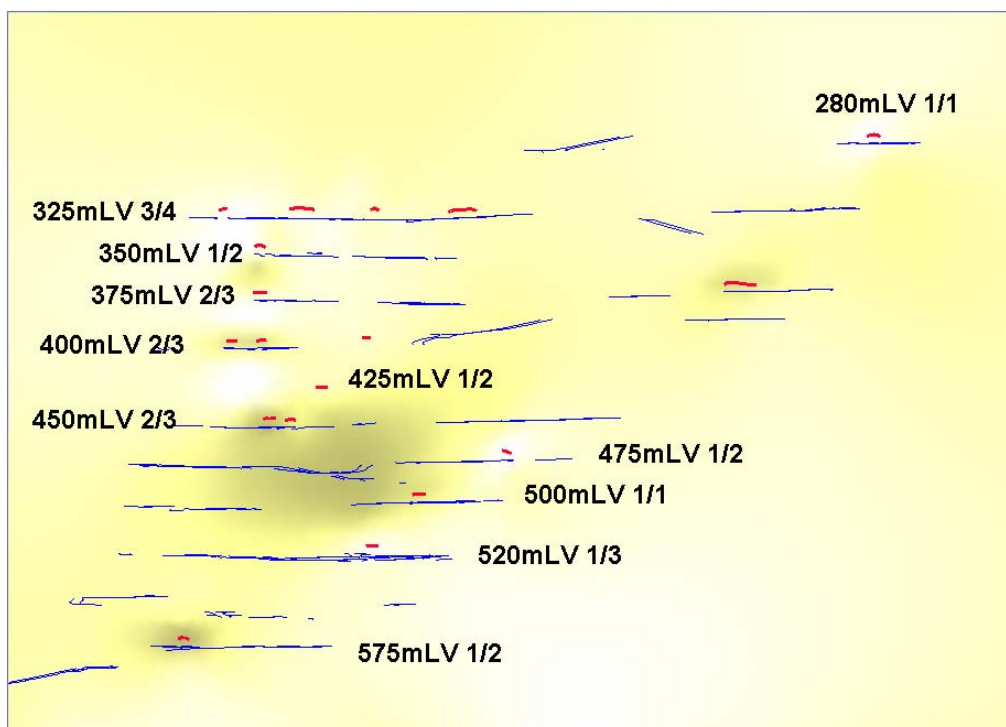
Mapping Validation

A brief summary of the levels and number of identified fault intercepts is shown in Table 12.4. The term “identified intercepts” relates to a mapped major fault or shear structure in the anticipated position and orientation of the overall trend of the “Squirrel Hills” fault zone. The term “Anticipated Intercepts” describes where the “Squirrel Hills” fault zone is anticipated to intersect development, and there was mapping conducted in the general area. This is depicted graphically in Figure 12.13.

The review of the mapping data suggests that in approximately 70% of cases where mapping data were present, an individual major structure is located in the anticipated position and orientation of the “Squirrel Hills” fault zone. The “Squirrel Hills” fault zone appears to be manifested as a distinct individual major fault/shear in the eastern and western areas of the Central Zone (i.e. near the footwall stopes and near the eastern side of the ST67 stope block).

Table 12.4 - Identified development intercepts of the "Squirrel Hills" fault zone from geological fact mapping

Mine Level	Identified Intercepts	Anticipated Intercepts
280mLV	1	1
325mLV	3	4
350mLV	1	2
375mLV	2	3
400mLV	2	3
425mLV	1	2
450mLV	2	3
475mLV	1	2
500mLV	1	1
520mLV	1	3
575mLV	1	2

**Figure 12.13 - Long section of interpreted "Squirrel Hills" fault zone (looking perpendicular to the south west), showing identified intercepts (red) for each level**

It was noted that where an anticipated structure was not present in the mapping data, some of these areas were obscured by shotcrete or fibrecrete, hence the structure may have possibly been over-looked during mapping. However, in some areas where shotcrete/fibrecrete did not obfuscate mapping of structures, a distinct individual structure matching the predicted position and orientation of the "Squirrel Hills" fault zone could not be identified. These areas seemed to be concentrated around the western side of the ST67

stope block, where an increase in the intensity of “Bird” faults may have off-set the predicted position. It was observed that, on one occasion, the interpreted “Squirrel Hills” structure was off-set by sinistral movement along a Bird parallel structure. The degree of such off-setting would be best established by interpretation of Bird structures and the relative sense of movements within this zone. Below 400mLV, there appears to be an overall sinistral “warping” of the strike of the interpreted structure, which could be indicative of off-setting by “Bird” structures through this area. However, this sense of movement is in contradiction to the majority of observed offsets caused by “Bird” faults elsewhere.

12.4.5 Summary

This application of rock mass spatial modelling techniques has demonstrated the value of integrating discontinuity intensity models with deterministic discontinuity modelling. Specifically, this exercise established the existence, and reliability (70% confidence in location and >95% confidence in orientation), of a significant, yet previously unknown, mine-scale structure. Confidence in the existence of this structure could be improved by undertaking the following tasks;

- Conduct new mapping to verify the existence of the “Squirrel Hills” structure in development where currently no mapping exists,
- Check mapping in areas where the anticipated intercept was not located. These areas tend to be located within a corridor along the western edge of the ST67 stopping block. It is highly likely that the “Squirrel Hills” is off-set by a group of “Bird” structures within this zone. The position of the interpreted structure, together with areas requiring further mapping are shown in Appendix C.
- Review of surface topographical maps for indicative trend/surface expression of structure (i.e. stream/creek).
- Review of aeromagnetic/gravity surveys.

12.5 TWO-DIMENSIONAL DISCONTINUITY INTENSITY MODEL

An exercise was conducted to establish the validity of the discontinuity linear intensity models (based on drill holes) using window mapping data. Details of the window mapping data are provided in Appendix D. To facilitate this, an areal discontinuity intensity model was generated from the window mapping data using the methodology described in Chapter 8. The model was restricted to an area of the North Block of the mine, close to the Trepell Fault. Data consisted of approximately 130m of drive mapping from 6 different locations. It is considered that sampling bias was minimised by collecting data from two orthogonal directions, with isotropic discontinuity orientations (see Chapter 8). Data from one mapping site are shown together with calculated corrected discontinuity areal intensity is shown in

Figure 12.14.

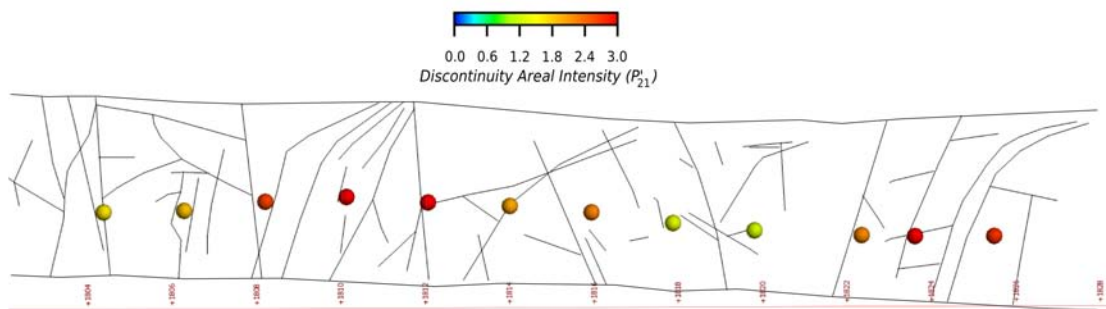


Figure 12.14 - Sectional view of north east wall of drive C8WX3 showing window mapping traces and calculated discontinuity areal intensity values

The validation process involved interpolating linear intensity (from drill core data) onto the corresponding points of calculated areal intensity (from window mapping data). In this way a direct comparison of both models in 3-dimensions could be established. Any spatial variation in linear intensity can be compared with the results from the areal intensity model.

During analysis of the areal intensity model, there appeared to be a spatial trend to the data which was apparently linked to the proximity of the Trepell Fault. In order to investigate this, the isotropic distance to the Trepell fault was calculated for each areal intensity data point and compared to the areal intensity values. The results of this analysis are shown in Figure 12.15. It can be seen that there is a clear correlation of increasing areal intensity with decreasing distance to the fault surface.

A similar investigation was conducted on the linear intensity model developed from drill core data. The linear intensity model values (calculated at the same points to the areal intensity model) also showed a very similar correlation with distance to the Trepell Fault (Figure 12.16a). The linear and areal intensity values from both models were directly compared and displayed a very good correlation (Figure 12.16b), with a proportionality constant of around 1.36. It is considered that this correlation coefficient may be improved by utilising corrected linear discontinuity data, unfortunately, alpha angles were not recorded during drill core logging. Notwithstanding this, the proportionality constant is close to unity indicating a relatively high dispersion of the discontinuity orientations (i.e. anisotropic conditions), which has previously been confirmed from orientation analysis (see Chapter 8).

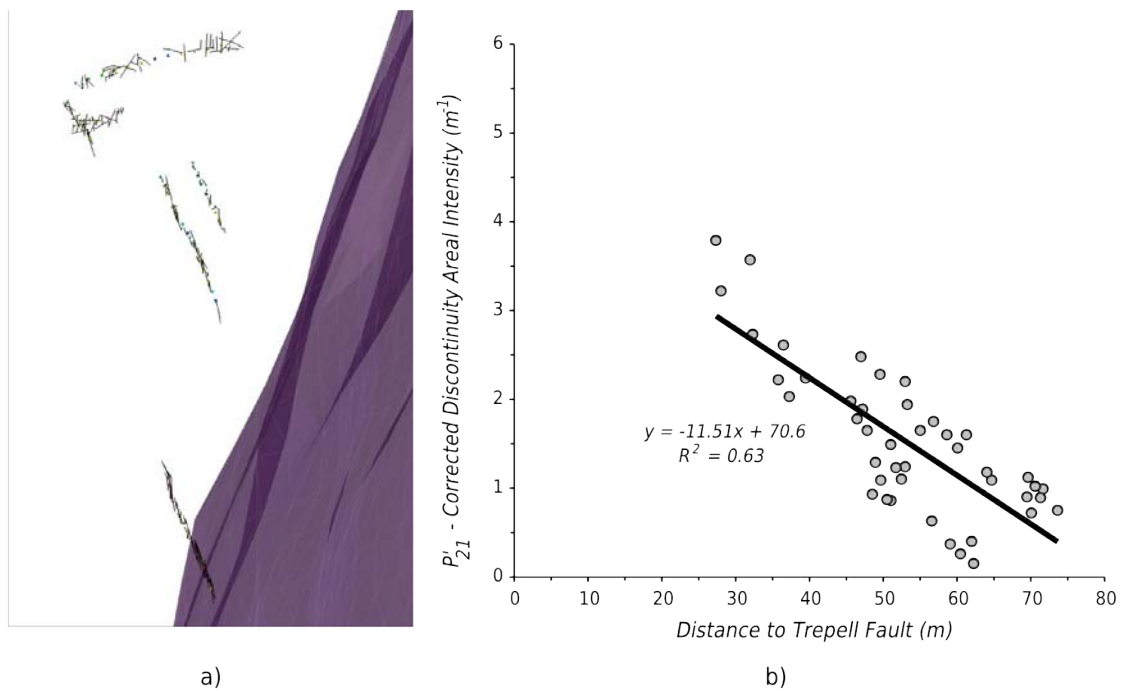


Figure 12.15 - a) Isometric view of mapped traces around stope 20ec8HL and Trepell Fault b) relationship between distance to Trepell Fault and increase in corrected areal intensity (P'_{21})

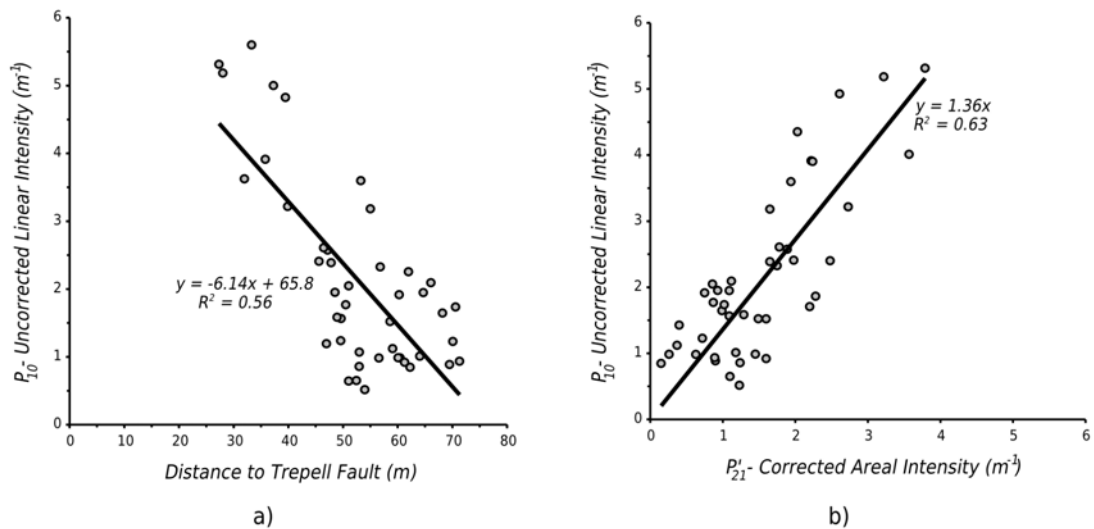


Figure 12.16 - Relationship between a) uncorrected linear intensity and distance to Trepell Fault b) proportionality relationship between areal and linear intensity

It is considered that the results of this analysis are significant in that data from two completely independent sources (i.e. window mapping versus unoriented drill core logging) confirm the same spatial variability in discontinuity intensity. The study also indicates that it is possible to maximise the value of unoriented drill core intensity data in isotropic rock masses. However, rock mass isotropy has to be confirmed, which in this case, can only be

effectively guaranteed from comprehensive analysis of mapping data using the techniques described in Chapter 10.

12.6 EMPIRICAL AND GEOMETRICAL BACK ANALYSIS OF STOPE PERFORMANCE

Back analysis of a number of stopes at Cannington was undertaken to see if any relationships could be developed that linked observed stope performance to stope geometry or certain rock mass characteristics. Initial geometrical back analysis work was conducted by Coles (2007). The work was aimed at trying to develop relationships based purely on geometry of the stopes and stope performance. That is, given the assumption that rock mass and boundary conditions are equal for all stopes, it is not unreasonable to expect that an increase in the size of stope should see a corresponding reduction in performance. Geometrical parameters considered included hydraulic radius, critical span and radius factor. Performance was assessed using depth of over-break and under-break. Unfortunately, no clear relationships could be developed indicating that geometry alone cannot be used as a predictor of stope performance and that rock mass and boundary conditions do indeed have a significant impact on stope performance (Coles, 2007). In order to investigate the influence of rock mass and boundary conditions on stope performance, this work also included an evaluation of the modified stability graph (Potvin, 1988) and is shown in Figure 12.17.

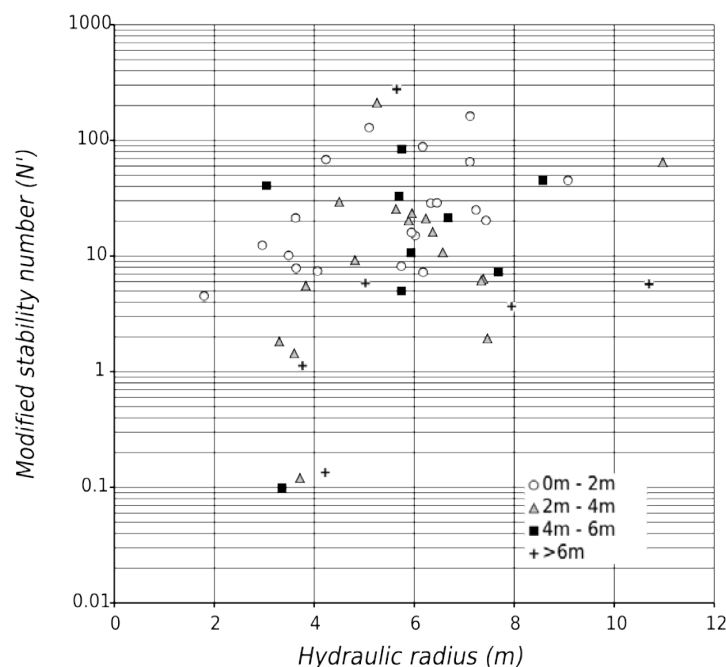


Figure 12.17 - Plot of modified stability number (N') versus hydraulic radius, classified by depth of over-break (after Coles, 2007)

Based on the methodology, one would expect high depths of over-break at high *HR* values

and low N' values. Conversely, low depths of over-break are expected at low HR values and high N' values. The data suggests that low and high depths of over-break do not tend to follow any particular trend. In this case, the results indicate that the modified stability graph method, as applied at the Cannington Mine, provides extremely poor reliability in predicting stope performance.

12.6.1 Scale independent empirical back analysis

Stope performance was re-assessed using the scale independent measures proposed earlier in the thesis (see Chapter 6). This enables stope performance data from stopes of vastly differing dimensions to be combined and included in analyses. Geometrical performance was quantified using the *Relative volume* (equation 6.14) of over-break, allowing performance to be assessed objectively. Stope performance data used in the back analysis exercise is shown in Appendix E. In this instance, "poor" performance is manifested by stopes that are observed to have a *Relative volume of over-break* greater than of 0.1.

Simple empirical back analysis were then conducted using *Relative volume of over-break* as compared to various rock mass parameters. Reliability of the back analyses was established using the recommended techniques for assessing quantitative performance criteria as outlined in section 11.7.2. The main rock mass parameters from the spatial models (i.e. UCS and DLF) have been integrated into the analysis as the performance functions. This has been achieved by evaluating the spatial distribution of rock mass parameters over the selected stope surfaces (see Figure 12.18). It can be seen that, in most cases, there is significant variability of rock mass parameters, even over small stope surfaces. Unfortunately, there is no simple mechanism to account for this spatial variability in simple empirical back analyses where performance has been assessed over the whole stope surface. Nevertheless, the mean values were calculated for each stope surface; this involved evenly discretising each stope surface (typically 2.5m spacing), evaluating the rock mass parameter at each discretised point and obtaining the mean for the stope surface.

Limitations And Sources Of Uncertainty

The following back analysis study was conducted utilising data from only 24 stopes from 4 different mining areas and only two rock mass parameters. Accordingly, not all parameters influencing stope performance have been accounted for (i.e. stress and previous rock mass damage, blast-induced damage, rock reinforcement, influence of large scale structures, stope surface orientation with respect to orientation of predominant structures, etc.). Some of these unaccounted factors will exacerbated poor performance (e.g. blast damage), whilst others will improve performance (e.g. rock reinforcement).

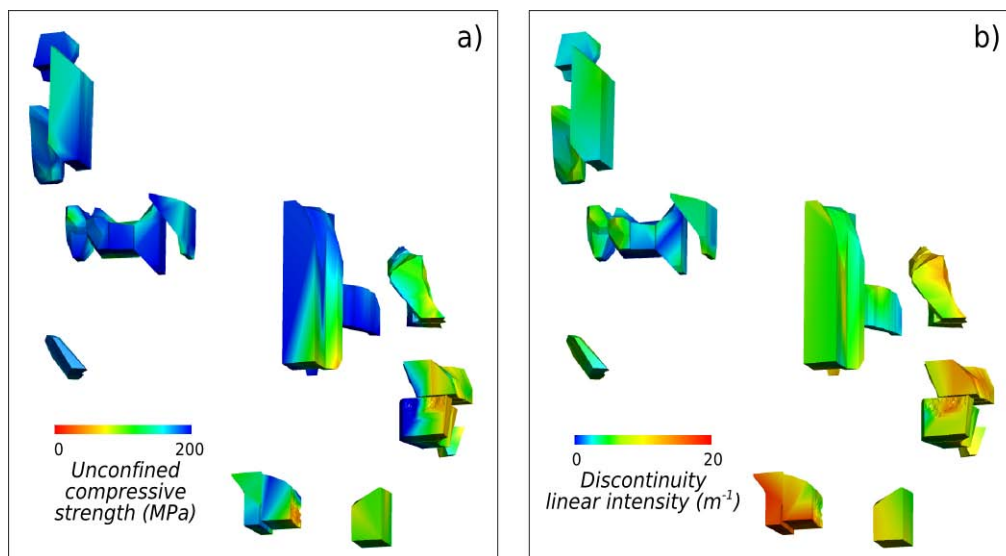


Figure 12.18 - Isometric view of a) modelled UCS and b) DLF on selected back analysed stopes

As the relative contribution of each of these factors on stope performance is unknown (and cannot be accounted for), it is acknowledged that any relationships developed from the selected rock mass parameters are anticipated to be biased and contain a fair degree of imprecision. In addition, errors in initial survey layout (i.e. for drill and blast set-up), design implementation and final CMS data will also effect results. These latter errors are also difficult to account for.

Unconfined Compressive Strength

Firstly, the influence of UCS on stope performance was investigated. For each stope surface, the *Relative volume* of over-break was plotted against UCS (see Figure 12.19a). It can be seen that there generally tends to be an increase in the number of “poor” performing stopes were the UCS values are between approximately 75MPa and 200MPa. It is also interesting to note that there are stopes that show very good performance, even at low UCS rock strengths.

In order to manage the scatter in results (due to the issues mentioned previously) and to provide a clearer relationship, the performance data were analysed using the non-parametric quantitative methods proposed in section 11.7.2. Data were firstly grouped and expressed as the percentage of “poor” performing stopes within 20MPa UCS bands (see Figure 12.19b). In this case, it can be seen that there is a very high percentage of poor performing stopes where the UCS is between 80MPa and 140MPa, with the poorest performing stopes displaying UCS values around 100MPa. Generally, performance improves where UCS values exceed 140MPa.

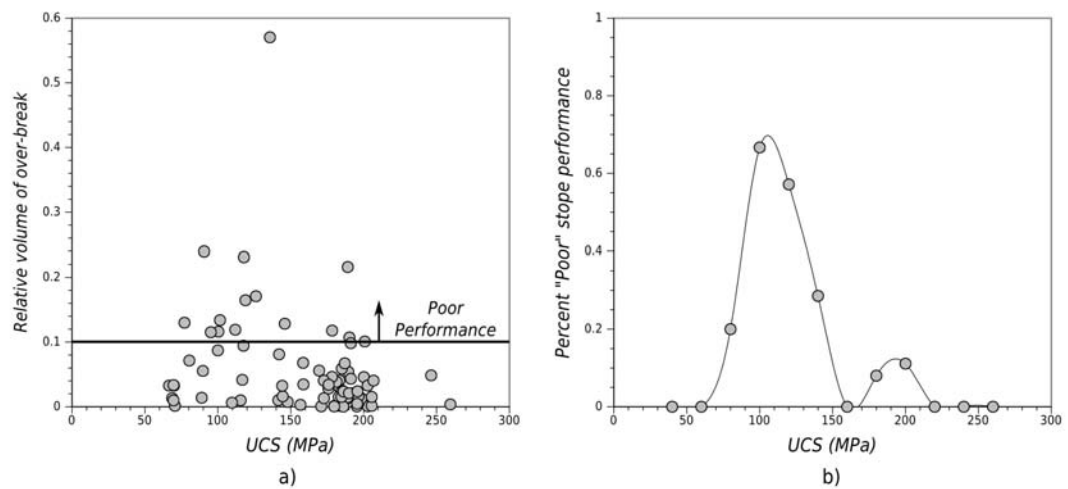


Figure 12.19 - Plot of a) Relative volume versus UCS (MPa) and b) Percentage of "Poor" stope performance versus UCS (MPa)

Discontinuity Linear Frequency

In a simplistic attempt to account for scale, *DLF* values were normalised with respect to the scale of the excavation. In this case, the critical span (S_c) for each stope surface was ascertained and multiplied by the *DLF* values to define a crude measure of the average number of discontinuities crossing the span (i.e. discontinuities per span). Figure 12.20a shows *Relative volume* of over-break versus the average number of discontinuities per span.

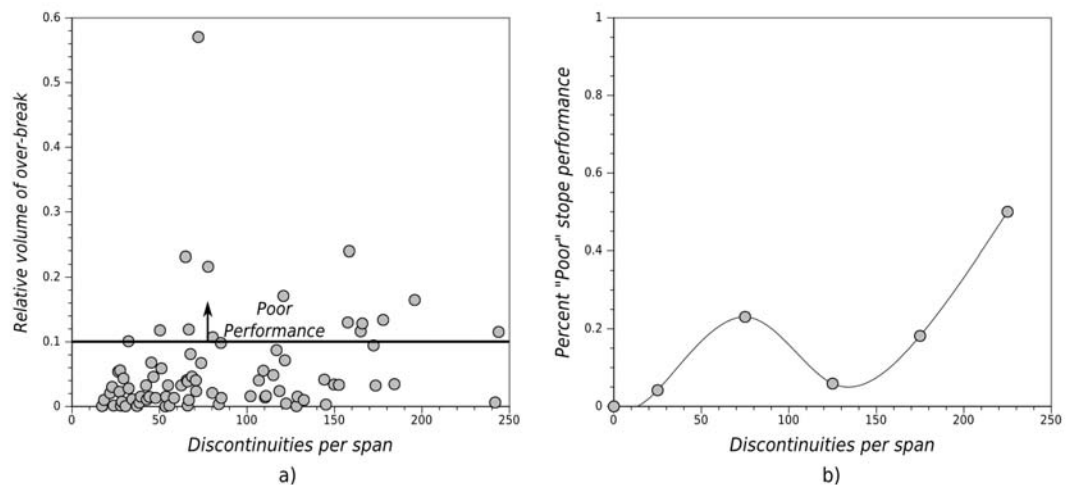


Figure 12.20 - Plot of a) Relative volume versus discontinuities per span and b) Percentage of "Poor" stope performance versus discontinuities per span

It can be seen that there does not seem to be any trend to the percentage of "poor" performing stopes with respect to discontinuities per span. In order to assess if there was an increase in the percentage of poor performing stopes with increasing number of discontinuities per span, the data were grouped in bands of 50 discontinuities per span. Figure 12.20b shows that there is an initial slight increase, then a relatively constant

proportion of “poor” performing stopes, then a further slight increase only after 175 discontinuities per span. This value can be considered as representing extremely fractured rock mass conditions with respect to the scale of the excavation.

Influence Of Scale

A final analysis considered the combined influence of both *UCS* and *DLF*. In order to account for the influence of scale, the span was divided by *UCS* and the resulting value multiplied by the average *DLF* (see Figure 12.21a). From Figure 12.21b, there appears to be an apparent increasing trend in the percentage of “poor” performing stopes with respect to the combined influence of discontinuities per span and *UCS*. Use of the combined parameters seems to provide a better relationship with stope performance than individual parameters alone, however, the reliability of the relationship is potentially hindered by the limited number of data points. Reliability could potentially also be improved by trialling a number of equations for the combined parameters. Notwithstanding this, the approach taken could be used to provide a basic stochastic approach to predicting stope performance.

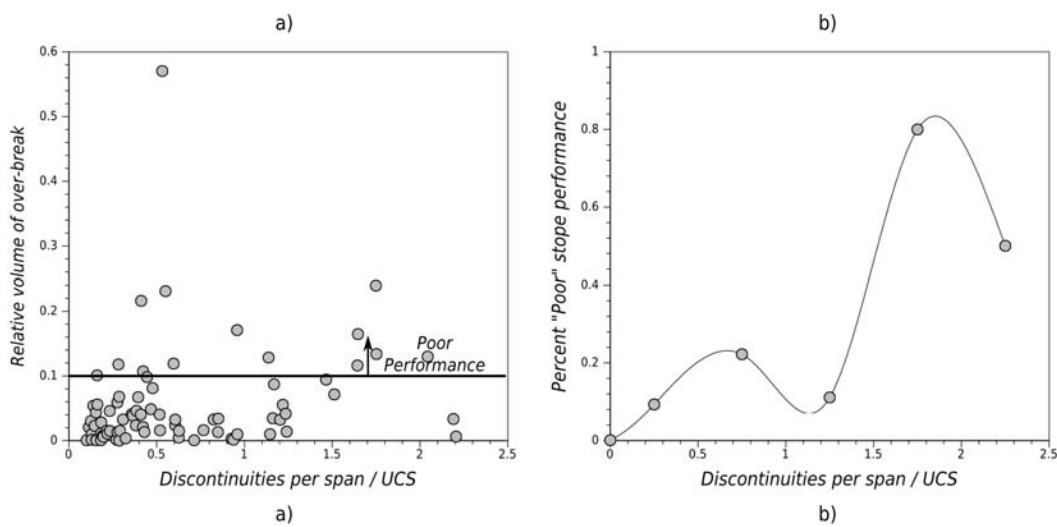


Figure 12.21 - Plot of a) Relative volume versus discontinuities per span divided by UCS and b) Percentage of “Poor” stope performance versus discontinuities per span divided by UCS

12.6.2 Forward analysis

Regression of various parameters against the percentage of “poor” stope performance can be used as an empirical tool for forward prediction. Figure 12.22a displays an exponential probabilistic model for over-break stope performance based on the back analysis using the combined parameters. It appears that this model tends to over estimate the percentage of “poor” performing stopes at higher parameter values and under-estimate the percentage of “poor” performing stopes at low parameter values. In this case, a simple linear regression model may be more appropriate (see Figure 12.22b). Confidence intervals can also be of value to indicate model reliability.

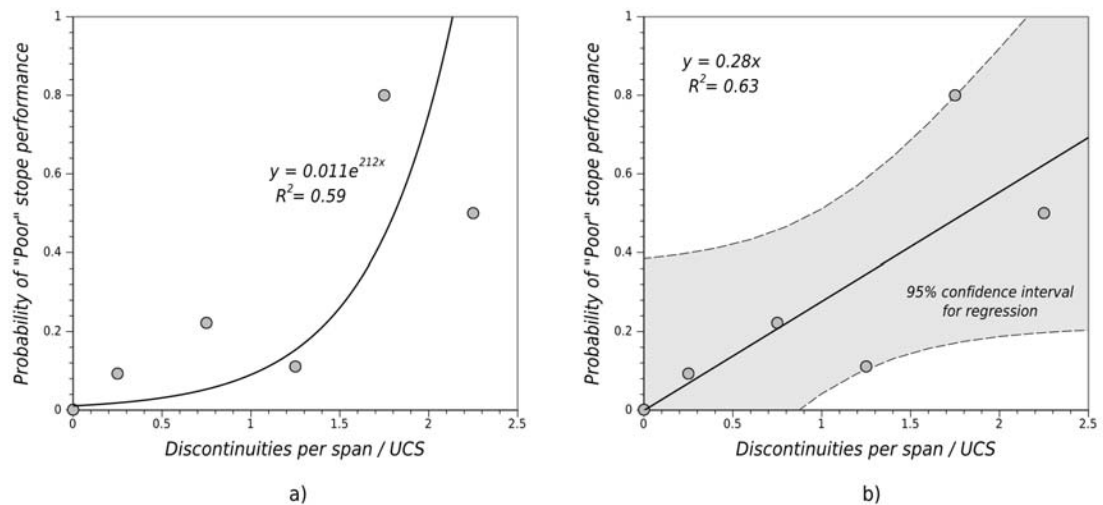


Figure 12.22 - Probabilistic models of over-break stope performance a) exponential model, and b) linear model

The simple back analyses conducted above, based on the selected individual and combined parameters, show that results are effected by a degree of scatter, or apparent unpredictability. This is not unexpected, considering that not all parameters influencing stope performance have been included. Notwithstanding this, it is suspected that the primary cause for this scatter in predicting "poor" stope performance (due to over-break) is by the inclusion of stopes that display a significant percentage of under-break, which has biased the data set. The under-break could be "apparent" due to errors such as; implementation/operational difficulties (i.e. the planned design could not be achieved), or errors in the provided *CMS* and design geometries. If the under-break is not "apparent", then the resulting under-break could be due to ineffectual drill and blasting or, alternatively, rock mass parameters have influenced performance. In order to investigate the possibility of the latter, the stope performance data were segregated based on the ratio of the amount of over-break to under-break for each stope surface. In this way, the influence of rock mass characteristics on the predominance of over-break or under-break can be investigated.

Figure 12.23a shows a comparison of cumulative distributions of *UCS* for predominantly "under-broken" stopes and predominantly "over-broken" stopes. It can be seen that "under-broken" stopes generally display higher *UCS* values. This is more apparent in the Q-Q plot shown in Figure 12.23b, where only the first 10th-percentile shows lower *UCS* values for "under-broken" stopes. Analysis of all quantiles indicates that the *UCS* is, on average, 12.9% higher for "under-broken" stopes than "over-broken" stopes. A similar, yet more pronounced relationship is seen with the number of discontinuities per span (see Figure 12.24). Here, "under-broken" stopes generally display much lower discontinuities per span than "over-broken" stopes, with "under-broken" stopes having an overall average of 33.8% lower discontinuities per span than "over-broken" stopes. This provides a strong indication that

the number of discontinuities per span has a significant influence on under-break.

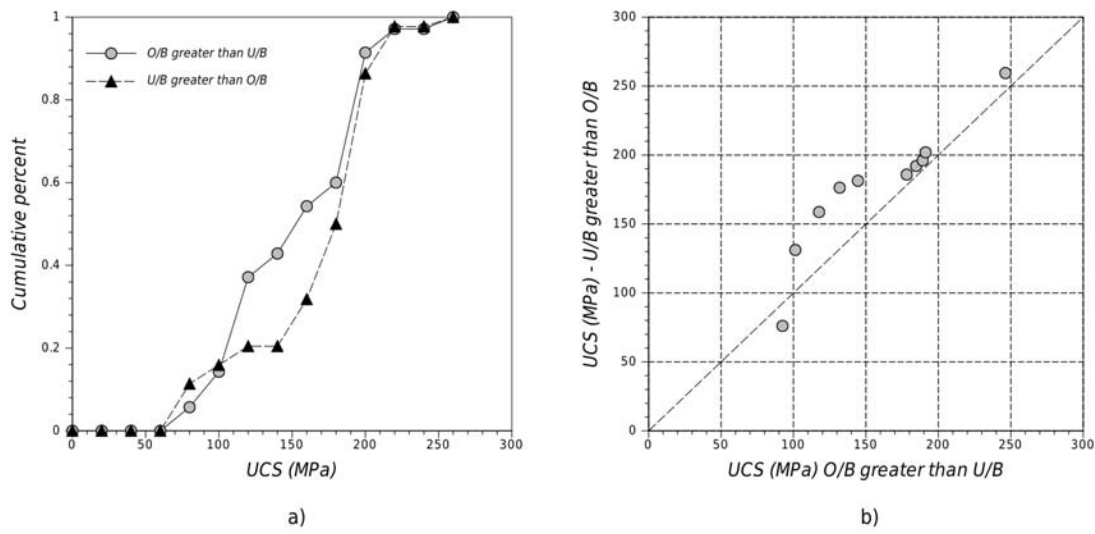


Figure 12.23 - Comparison of UCS for "under-broken" and "over-broken" stopes, showing a) cumulative distribution and b) Q-Q plot

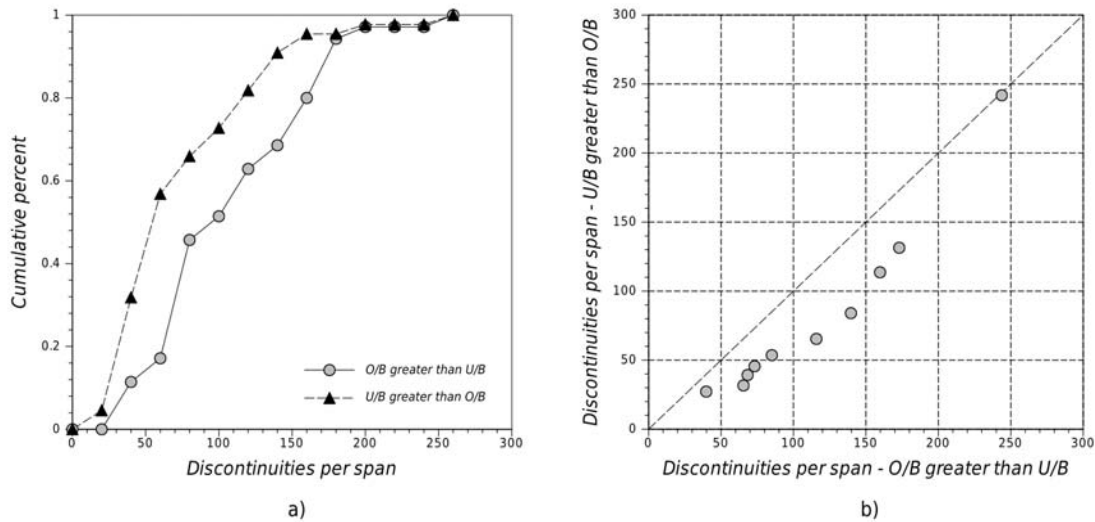


Figure 12.24 - Comparison of discontinuities per span for "under-broken" and "over-broken" stopes, showing a) cumulative distribution and b) Q-Q plot

In light of this observation, the data set was re-evaluated with new probabilistic models of "poor" performance due to over-break by only considering stopes surfaces which displayed a predominance of over-break. The updated probabilistic models for UCS, discontinuities per span and combined parameters are shown in Figure 12.25. Significance values for each model are provided in Table 12.5. As the p-values are much less than 0.05 in all cases, there is a significant relationship between the variables in the linear regression models.

Table 12.5 - Significance statistics for the probabilistic linear regression models of over-break

Model	R ²	F-statistic	D.F.	P-value
Discontinuities per span / UCS	0.77	13.78	4	0.021
UCS	0.74	16.72	6	0.006
Discontinuities per span	0.72	17.67	7	0.004

A similar procedure can be applied to generate probabilistic models for under-break. A probabilistic model for slope performance of both over-break and under-break is presented in Figure 12.26a. The probabilistic model can be integrated with the spatial rock mass models and used to evaluate probability of “poor” performance over proposed slope shapes. Figure 12.27 shows predicted probability of “poor” slope performance due to over-break on design geometries together with final *CMS* geometries.

The probabilistic model is generally in agreement with actual performance, with the majority of over-break occurring where predicted “poor” performance is highest (Figure 12.27a and Figure 12.27c) and only minor over-break where predicted “poor” performance was lowest (Figure 12.27b and Figure 12.27d).

12.6.3 Risk-based Design

Assuming that all unaccounted for parameters and mining practices essentially remain constant, then the proposed probabilistic models can be used as a forward design tool to estimate the likelihood of “poor” slope performance based on critical span, *UCS* and *DLF*. The following section describes the application of the quantitative risk-based design approach outlined in section 11.9.

Consider a proposed slope surface where the height is fixed at 25m and the critical span is approximately 20m. From the spatial rock mass models an average *UCS* of around 140MPa and an average *DLF* of around 7m⁻¹ has been determined at the proposed slope surface location. This provides a combined parameter value of 1.0. Figure 12.26 indicates that slope surface performance will likely result in a 45% probability of “poor” slope performance due to over-break (i.e. $P[\text{Relative volume} > 0.1]=0.45$), with a 95% confidence that there will be no more than 73% chance of “poor” performance, yet at least a 20% chance of “poor” performance. The model also predicts that there will be a probability of 8% of “poor” performance due to under-break, with a 95% confidence that there will be between 1% and 26% probability of “poor” performance due to under-break.

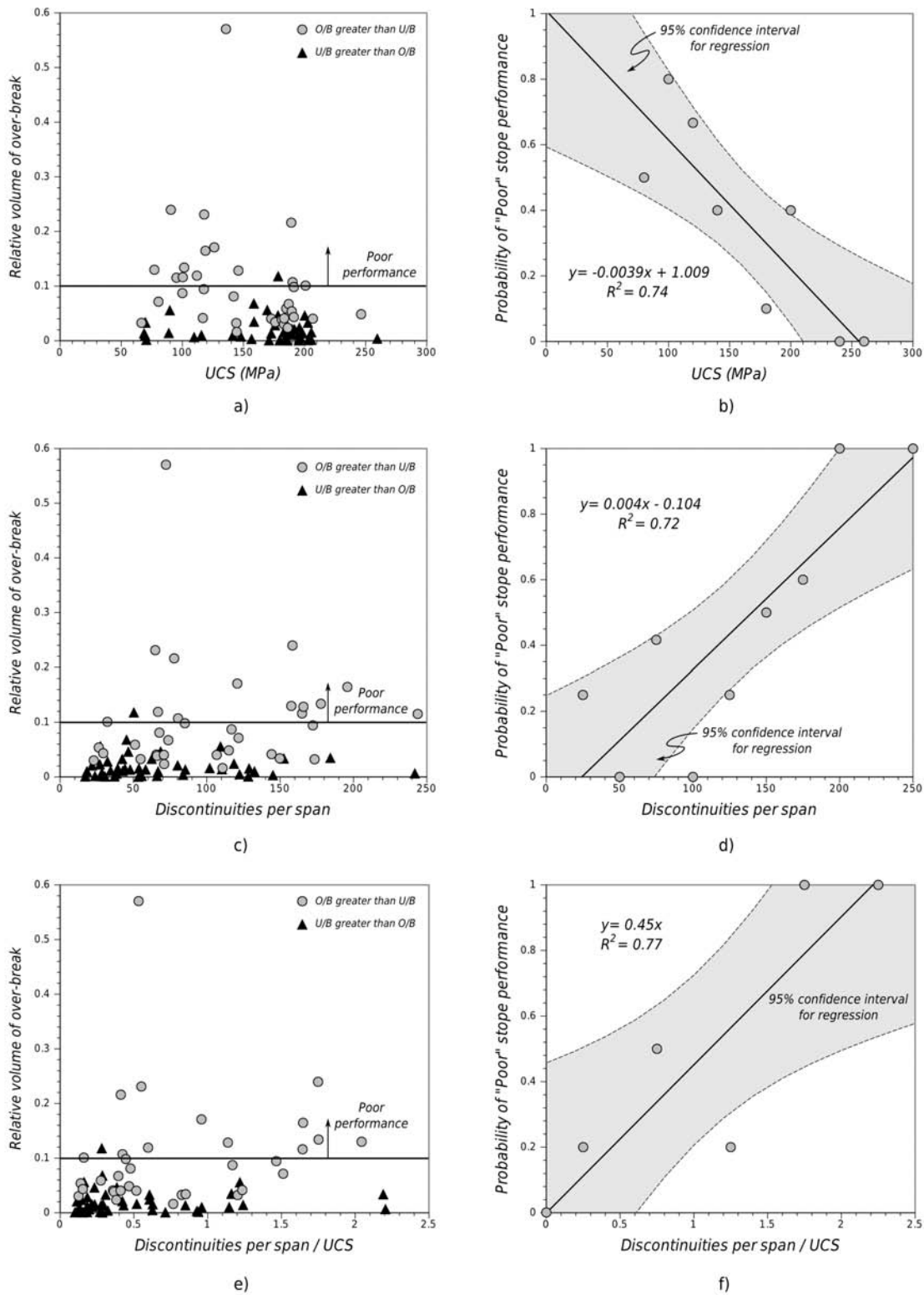


Figure 12.25 - Relative volume versus a) UCS, b) discontinuities per span and c) discontinuities per span divided by UCS with data segregated into predominantly "under-broken" and "over-broken" stopes, with empirical probabilistic models for performance prediction based on predominantly "over-broken" stopes for b) UCS, d) discontinuities per span and f) discontinuities per span divided by UCS

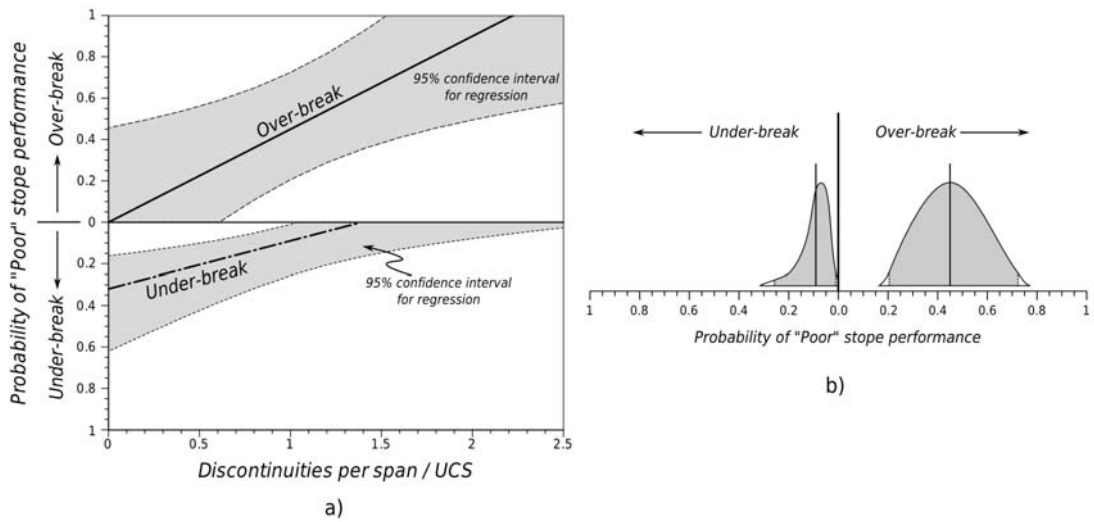


Figure 12.26 - a) combined probabilistic model of stope performance for over-break and under-break, and b) distribution of probability for example in text

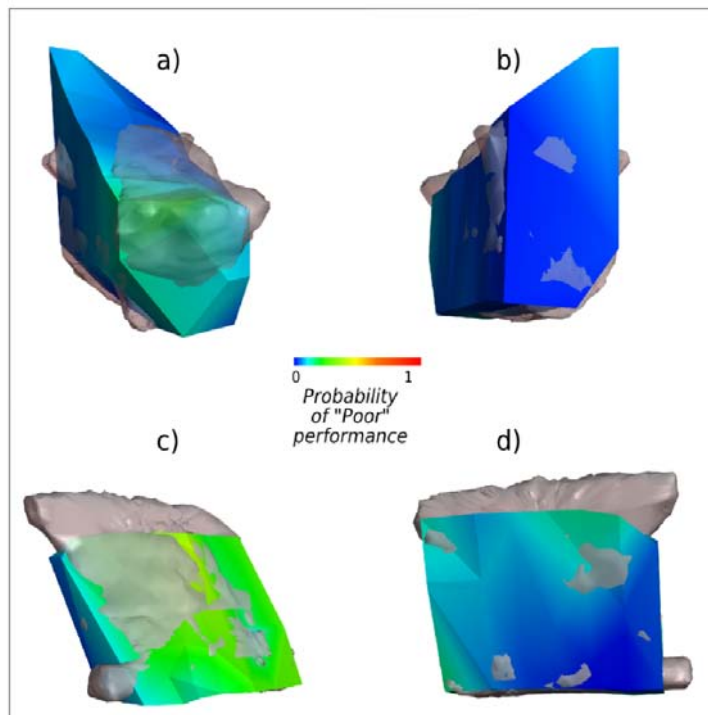


Figure 12.27 - Isometric view of stope 22h.c6HL looking a) north east and b) south west, and stope 47b.70FZ looking c) north west and d) east contoured by predicted probability of "poor" performance due to over-break together with CMS geometries

Whilst there should be a reduction in anticipated over-break by reducing the combined parameter value (i.e. selecting smaller span dimensions for constant rock mass parameters), an increase in the likelihood of under-break is also anticipated. Selection and optimisation of the most appropriate span dimension therefore will need to take into account the combined economic consequences of *both* over-break and under-break. An estimate of the volume and grade of over-break/under-break is generally required to establish economic consequences. The grade of the anticipated over-break or under-break material will depend on stope location and local grade distribution. Unfortunately, as has been demonstrated, the proposed empirical probabilistic method lacks sufficient accuracy to predict the precise value of *Relative volume* of either over-break or under-break with increasing span.

However, assuming that the selected critical *Relative volume* value has been economically justified to indicate the definition of “poor” performance, it can be used to ascertain the various volumes of over-break or under-break at a variety of scales. By rearrangement of equations 8.31 and 8.32, the volume of over-break or under-break can be estimated by;

$$Volume = \frac{Relative\ Volume * A_s^{3/2}}{3} \quad (12.1)$$

where A_s is the surface area of the stope surface under consideration. The probabilistic models can be used to ascertain the lower, mean and upper bound probabilities of this volume being exceeded for any given span. For example, if there is a 50% chance of “poor” stope performance, this equates to a 50% chance of exceeding the estimated volume of over-break or under-break. Multiplying the probabilities by the estimated volume provides the expected volume of over-break or under-break. This needs to be conducted for each stope surface at the selected span dimension. The expected volume of over-break and under-break for each stope surface can then be used to determine the economic consequences of the selected dimensions. The probabilistic back analysis can therefore be used in quantitative risk-based design similar to existing methods (Lilly, 2000; Lilly and Villaescusa, 2001). That is, the optimal span dimensions are those that reduce the **total cost**.

For example, given the input parameters provided in Table 12.6 for a theoretical *SLOS* operation, it is possible to determine the expected economic consequences of over-break and under-break in terms of cost per tonne with increasing span. For this exercise a number of simplistic assumptions were made;

- Only hangingwalls and footwalls contribute to over-break and under-break.
- Under-break is never recovered by subsequent stoping.

- The percentages of over-break loaded and hauled to surface, as well as milled, have been estimated as well as their associated costs.
- Due to the difficulty in establishing consequential costs (such as; secondary blasting, associated rehabilitation, re-scheduling, etc.) they have been ignored, however these can represent significant additional costs.

Table 12.6 - Input parameters for example economic assessment

Input Parameter	Value
Critical <i>Relative volume</i>	0.1
Ore width	7.5m
Stope height	25m
Over-break cost per tonne	\$18/t
Over-break milling cost	\$80/t
Average density	2.65t/m ³
Average grade of under-break	8.0g/t
Average grade of over-break	0.0g/t
SLOS cost per tonne	\$20/t
Vertical development per metre	\$1200/m

Figure 12.28a displays the additional unit costs (\$/tonne) attributed to over-break and under-break together with the base mining cost. Mining costs generally decrease with increasing span, mainly due to the reduced need for vertical development per tonne mined. Figure 12.28b shows the combined total unit cost versus span, together with lower and upper bounds based on the 95% confidence intervals from the probabilistic models. It can be seen that, based on the mean value, the “optimum” span is around 30m. This also corresponds to the span value where the mean likelihood of under-break is 0%. This indicates the importance of the economic consequences of under-break (i.e. ore loss) in stope design.

Summary

A simplistic scale-independent back analysis method has been developed to demonstrate the value of integrating spatial models and empirical stope performance data. The proposed empirical back analysis approach was undertaken on a limited number of stopes (24), from 4 distinct mining areas, and indicates how the approach can be used to optimise stope design at early stages of mine production.

Although the example back analysis results lacked sufficient precision to predict the actual severity of “poor” performance (i.e. exact *Relative volume*), it has demonstrated an ability to identify an increase in the probability of “poor” performing stopes, based on a limited

number of key rock mass parameters (i.e. *UCS* and *DLF*). This is significant considering that not all parameters influencing stope performance have been explicitly accounted for in the back analysis. The example methodology presented can also be used to assist in determining the “relative weighting” of each parameter in development of a site specific empirical design method, based on the proposed guidelines presented in Chapter 4.

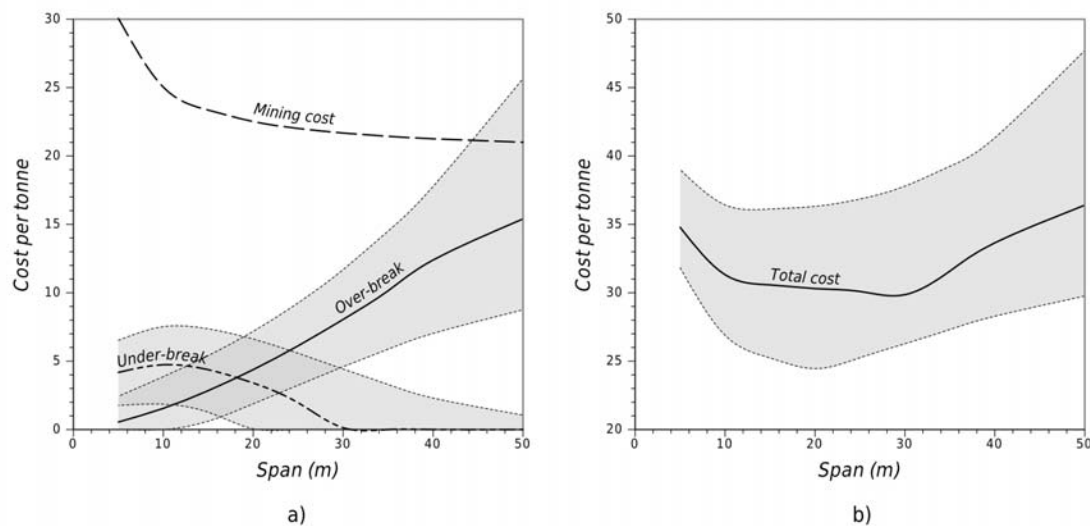


Figure 12.28 - Plot of cost per tonne for a) over-break, under-break and mining costs, with b) total cost against stope span, together with lower and upper bounds based on 95% confidence intervals for the probabilistic models

The proposed approach also demonstrated the use of confidence intervals about regressions to provide a measure of reliability in predictive models and economic consequences of selected stope design parameters. The approach also highlighted the importance of discriminating stopes that show a predominance of either under-break, or *vice-versa*, to improve predictive reliability. Other techniques to improve reliability could be to discriminate data by the degree of variability (i.e. coefficient of variation) of rock mass parameters across the stope surface, which then may assist in indicating a predominance of over-break or under-break. Further improvements could be made by investigating differences in stope wall orientation, drill and blast parameters, rock reinforcement schemes and incorporation of the results from numerical modelling. Unfortunately, due to data availability, this could not be achieved for this case study.

12.6.4 Assessment of Existing Empirical Methods

In order to assess whether the technique has provided any improvements over the existing Modified Stability Graph method, it was necessary to modify the data presented in Figure 12.17. In this case, the depth of failure was first converted to *Relative volume* and the same criteria for unacceptable performance applied (e.g. *Relative volume* > 0.1). Unacceptable performance was denoted as “unstable” and acceptable performance denoted as “stable”.

Logistic regression techniques (Mawdesley et al., 2001) were then applied to the data to provide the maximum likelihood discriminant between “stable” and “unstable” classes (see Appendix E). Figure 12.29 indicates a fair degree of scatter is present using the Modified Stability Graph method. The predictive capability can be gauged by the percentage of classified points relative to the optimally derived stability line. Table 12.7 shows the sensitivity and specificity of the logistic regression model. Sensitivity is defined as the percentage of stable points that report correctly to the stable zone, whilst specificity is defined as the number of points that report correctly to the unstable zone. Whilst the specificity is generally good, the low sensitivity, given the amount of stable points, shows a very poor predictive capability. For example, Table 12.7 indicates that 69.5% of all points in the Unstable zone are actually “stable”. This is reflected in log-likelihood ratio test (see Appendix E), that indicates there is no overall significant relationship between the dependent variable “stability” and the independent variables HR and N' . In this case, the empirical probabilistic technique using UCS and DLF provides a simple, yet more effective, method for predicting stope performance than the Modified Stability Graph method, in that;

- they have better predictive capability
- are capable of showing spatial variability of anticipated performance on stope surfaces
- risk is quantifiable and the likelihood and volumes of over-break can be used in risk-based design approaches

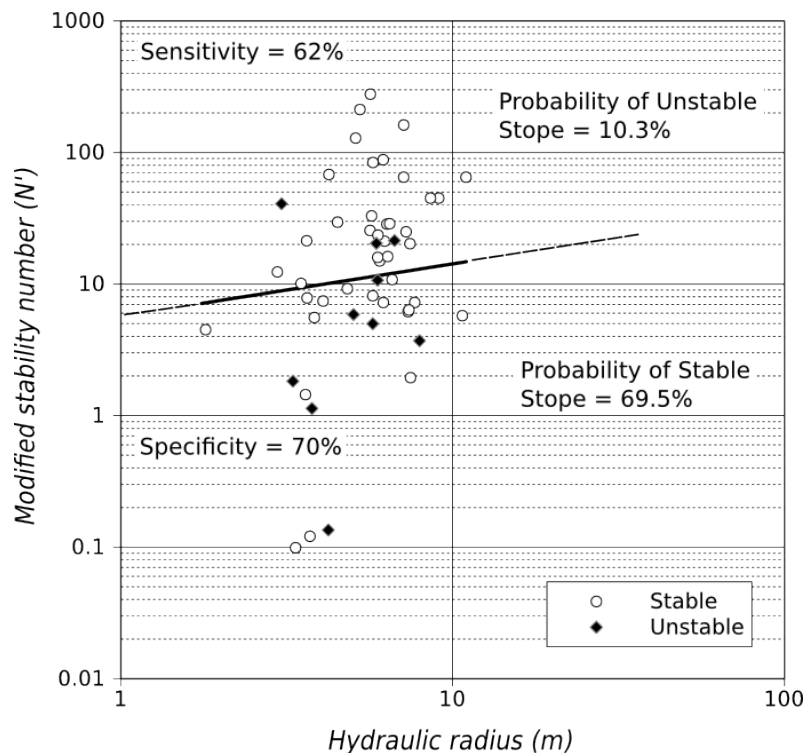


Figure 12.29 - Cannington stability graph data with the stability zone defined by logistic regression

Table 12.7 - Sensitivity and Specificity of the Cannington Logistic Regression Model

Parameter	Value
Sensitivity (% of stable cases reporting correctly to the stable zone)	61.9%
Specificity (% of unstable cases reporting correctly to the unstable zone)	70.0%
Percentage of stable points from all points below the logistic regression line	69.5%
Percentage of unstable points from all points above the logistic regression line	10.3%

12.7 CONCLUSIONS

This case study has shown how the site geology and its history play an important role in rock engineering design. At Cannington, key geological features, such as rock fabrics effected by retrograde metamorphism and late stage brittle geological structures, have a significant influence on the response of the rock mass to mining. Previous attempts at spatial modelling of rock mass properties for mine design purposes have proven relatively unsuccessful, primarily due to lack of sufficient detail at the stope scale (due to block resolution) and use of ineffective measures of discontinuity intensity, such as *RQD*. Block resolution issues and interpolation methods previously employed were unable to sufficiently capture the variable

nature of rock mass and complex structural geology of the Cannington deposit.

This case study has shown how the proposed implicit function based discontinuity intensity and deterministic discontinuity modelling techniques have been used to generate high resolution rock mass models from sparse data and have identified and modelled a previously unidentified large-scale geological structure. Significantly, the approach has enabled reduction in Type 1 uncertainty and also demonstrated techniques for establishing the reliability of the modelled structures. Finally, the combined use of the models has allowed for an understanding of inter-relationships between rock mass parameters, namely discontinuity intensity and UCS.

The example applications have highlighted the importance of rock mass models on understanding the role of large-scale structures on local rock mass characteristics. Significantly, it has been demonstrated that two distinct discontinuity intensity models (i.e. linear intensity and areal intensity), based on independent data, confirmed the spatial dependence of rock mass conditions on the proximity of large-scale structures.

The case study has also demonstrated the integration of stope performance back analysis data and spatial rock mass models in empirical design. The back analysis exercise briefly demonstrated some of the recommended techniques for development of a site-specific empirical design tool (see section 11.6.1). For example, a simplistic method to assess the relative influence of a number of rock mass parameters on stope performance was demonstrated. It is recommended that a similar multivariate approach could be taken to indicate the relative influence of additional contributing factors, such as stress and previous rock mass damage, blast-induced damage, rock reinforcement, influence of large scale structures and stope surface orientation.

Finally, the exercise demonstrated how the results of the back analysis can be combined with economic assessments of over-break and under-break to develop a quantitative risk-based approach to empirical stope design. This provides the design engineer to develop and understand the economic impact of design alternatives.

CHAPTER 13 - CASE STUDY: KANOWNA BELLE GOLD MINE

13.1 INTRODUCTION

This chapter describes the application of certain aspects of the integrated approach to open stope design at the Kanowna Belle Gold Mine. The chapter firstly describes the regional, local and mine geology with respect to the major structural features and their potential influence on rock mass conditions and response to mining. The chapter also describes application of some of the rock mass modelling techniques, including; the use of structural geology to assist in definition and optimisation of rock mass domains to improve model reliability and a demonstration of the deterministic discontinuity modelling technique. The chapter also demonstrates how combined use of the spatial rock mass models and deterministic discontinuity models can be used to provide a detailed understanding of the spatial variability of rock mass conditions along major mine scale structures.

The chapter also provides an example of an integrated approach to back analysis (section 11.8), firstly by looking at linear elastic back analysis where the rock mass modelling components (discontinuity linear intensity and deterministic discontinuity models) have been indirectly incorporated. This example highlights the influence of large-scale structures on rock mass characteristics and excavation performance. The exercise also demonstrates some of the proposed improvements to linear elastic back analysis techniques suggested in section 11.8.2. Finally, the chapter concludes with another example of an integrated approach to back analysis, this time using non-linear modelling with direct incorporation of highly detailed deterministic discontinuity models.

13.2 KANOWNA BELLE GOLD MINE UNDERGROUND OPERATIONS

Underground operations at Kanowna Belle Gold Mine (KBGM) are situated beneath the Kanowna Belle Open Pit, with large-scale long hole operations commencing in 1998. Current production stopes at Kanowna Belle are being mined at depths in excess of 1200m in challenging conditions, which will only increase as operations continue to head deeper. The Block A stopes of Kanowna Belle consist of large primary-secondary sub-level open stopes, mined directly beneath an existing open pit to depths of around 400m below surface. Mining was under-taken using using transverse longhole open stopes, in a primary/secondary extraction sequence in conjunction with cemented fill. The stopes are two lift high (60m), and 15m and 20m along strike for the primary and secondary stopes respectively. The stopes have widths varying from 10m to 35m and are all filled with paste fill. Cable reinforcement was mainly restricted to “rib-roc” type patterns, installed from sub-levels into

the hangingwalls.

Block C stopes are generally much smaller than Block A stopes, with stopes heights ranging from 35m to 100m, lengths from 15m to 20m with stope widths generally around 20m. These stopes were initially mined in a 1-3-5 sequence, the sequence then switched to a centre-out pyramidal sequence to control stress-related production issues and dilution (Villaescusa et al., 2003a). Mining for Block D and Block E currently is undertaken using small single-lift stopes (maximum of 35m height) in a bottom-up continuous pyramidal sequence with pastefill. In thicker zones of Block D, the orebody is mined in 2-3 panel stopes from the hangingwall to the footwall.

13.3 GEOLOGY

The response of rock mass to mining at Kanowna Belle is highly influenced by a dominant major fault (Fitzroy Fault) oriented sub-parallel to the orebody, as well as a series of sub-parallel subsidiary faults. Another series of “bedding” parallel structures, also influence the rock mass response, and are thought to play an important role in mine seismicity. The following sections describe the regional and local geology of the Kanowna Belle deposit.

13.3.1 Regional Geology

The regional geology of the Kanowna Belle Gold Mine has been described by numerous authors. A brief description of the tectonic, stratigraphic, and structural setting is important as it provides us with an improved understanding of the formation of the mine-scale rock mass structures, and their potential influence on the spatial variation of rock structure characteristics.

A compilation of the regional geology from craton to regional scale is provided in Figure 13.1. The Kanowna Belle Gold Mine sits in the Norseman-Wiluna belt of the Easter Goldfields Province (Figure 13.1b) of the Yilgarn Craton in Western Australia (Figure 13.1a). More specifically, the mine is located in the Boorara Domain of the Kalgoorlie Terrane. The basal stratigraphy of the Kalgoorlie Terrane is made up of three main units; a lower basalt unit, a komatiitic unit and an upper basaltic unit (Swager, 1997). Collectively, these units are known as the Kambalda Group. Overlying the Kambalda Group is a complex volcanoclastic succession of units known as the Black Flag Group (BFG) (Swager et al., 1990).

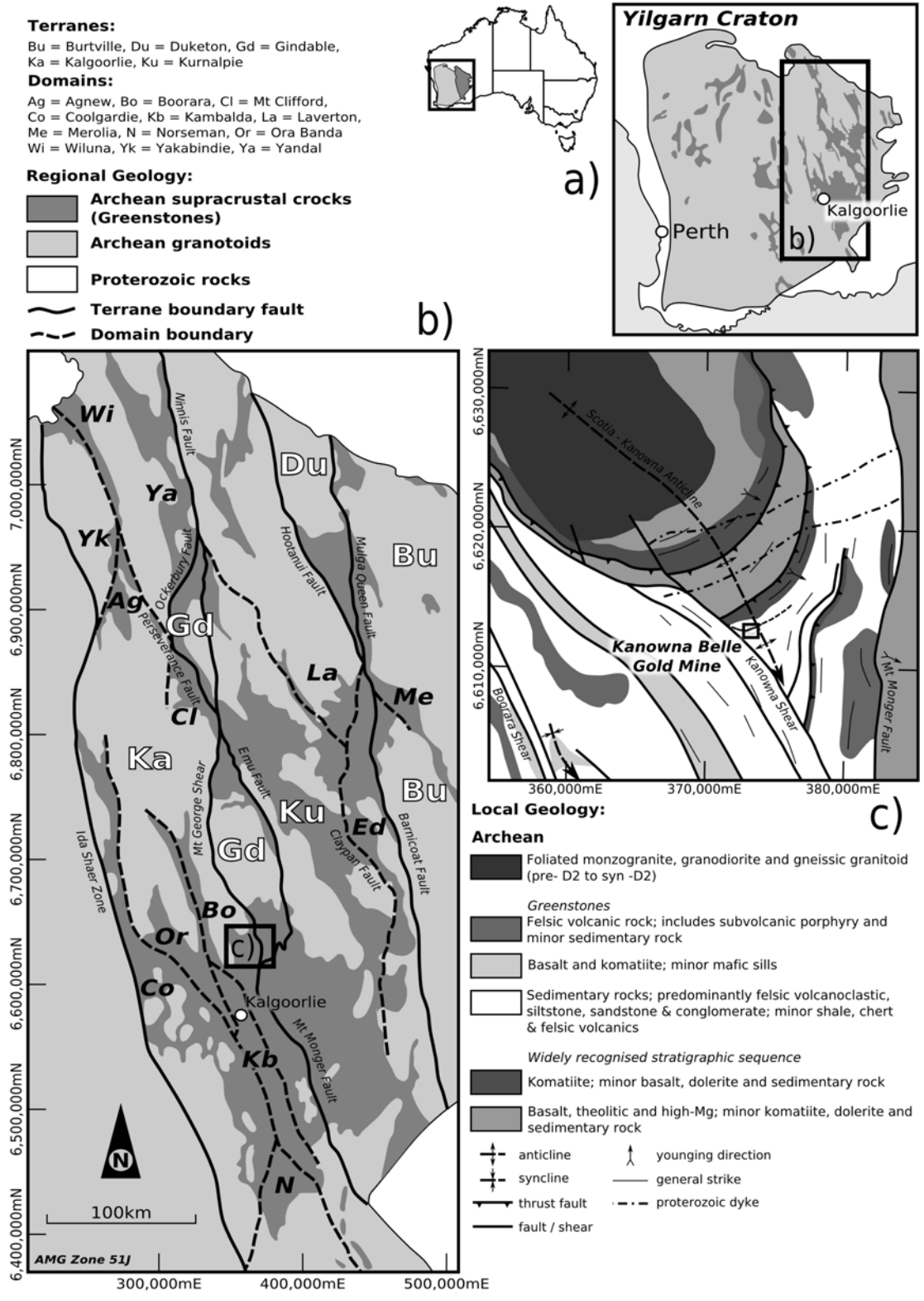


Figure 13.1 - Summary location showing a) the Yilgarn Craton of Western Australia, b) regional geology of the Norseman-Wiluna belt, and c) the local geology around the Kanowna Belle Gold Mine. (modified after Gee and Swager, 2008 and Ross et al, 2004)

Four major deformation events have been identified in the Kalgoorlie Terrane. These are; D1 recumbent folding and thrusting, D2 transpressional deformation with large-scale up folding, D3 transcurrent faulting with associated en echelon folds and D4 continuation of regional shortening (Ross et al., 2004). The D1 thrusting has been interpreted as a south to north shortening event, creating large-scale sequence repetition. The regional WNW-ENE D2 shortening was responsible for major upright, doubly plunging, NNW trending folds and faults, with regional upright foliation. The D3 event represents continued regional shortening during a sinistral transpressional regime (Swager et al., 1990). D4 comprises of a later shortening event (comparable to D3 sinistral transpression) comprising of reverse and oblique dextral faults. The dominant structural features of the local geology around the Kanowna Belle Gold Mine (Figure 13.1c) is the D1 related arcuate thrust faults and associated repetition of the komatiite unit and the D2 related Scotia-Kanowna anticline and NNW trending faults.

13.3.2 Generalised Mine Geology

The geology discussed at the mine scale is described with reference to a local mine coordinate system which is oriented 35° west of True North. The geometry of the Kanowna Belle deposit is shown in plan and section in Figure 13.2. The Kanowna Belle deposit is hosted by sedimentary volcanoclastic and conglomeratic rocks, which are separated into hangingwall and footwall sequences by a major, steeply south dipping zone of structural disruption termed the Fitzroy Structural Zone.

The hangingwall sequence is composed of felsic, syn-eruptive to reworked volcanoclastic siltstones and pebble conglomerates intruded by syn-depositional basaltic and andesitic dykes. The Grave Dam Grit is the most voluminous unit comprising of matrix supported felsic conglomerate. Underlying the Grave Dam Grit is the QED Rudite, which consists of a matrix supported felsic volcanic and volcanoclastic-dominated conglomerate. Both units are massive and probably upright (Archibald et al., 1999).

The footwall consists of thickly bedded heterolithic volcanogenic clast supported conglomerates, separated by thin lenses of arkosic/felsic matrix supported grit and sandstone (Golden Valley Conglomerate and Cemetery Sandstone, respectively). Locally, three lenses of the Cemetery Sandstone have been termed “felsic units” by the mine, named from west to east; Isabella, Larkin and Moore. The orientation of the contacts of these units is sub-parallel to regional D2 structures, such as the Kanowna Shear (see Figure 13.1c).

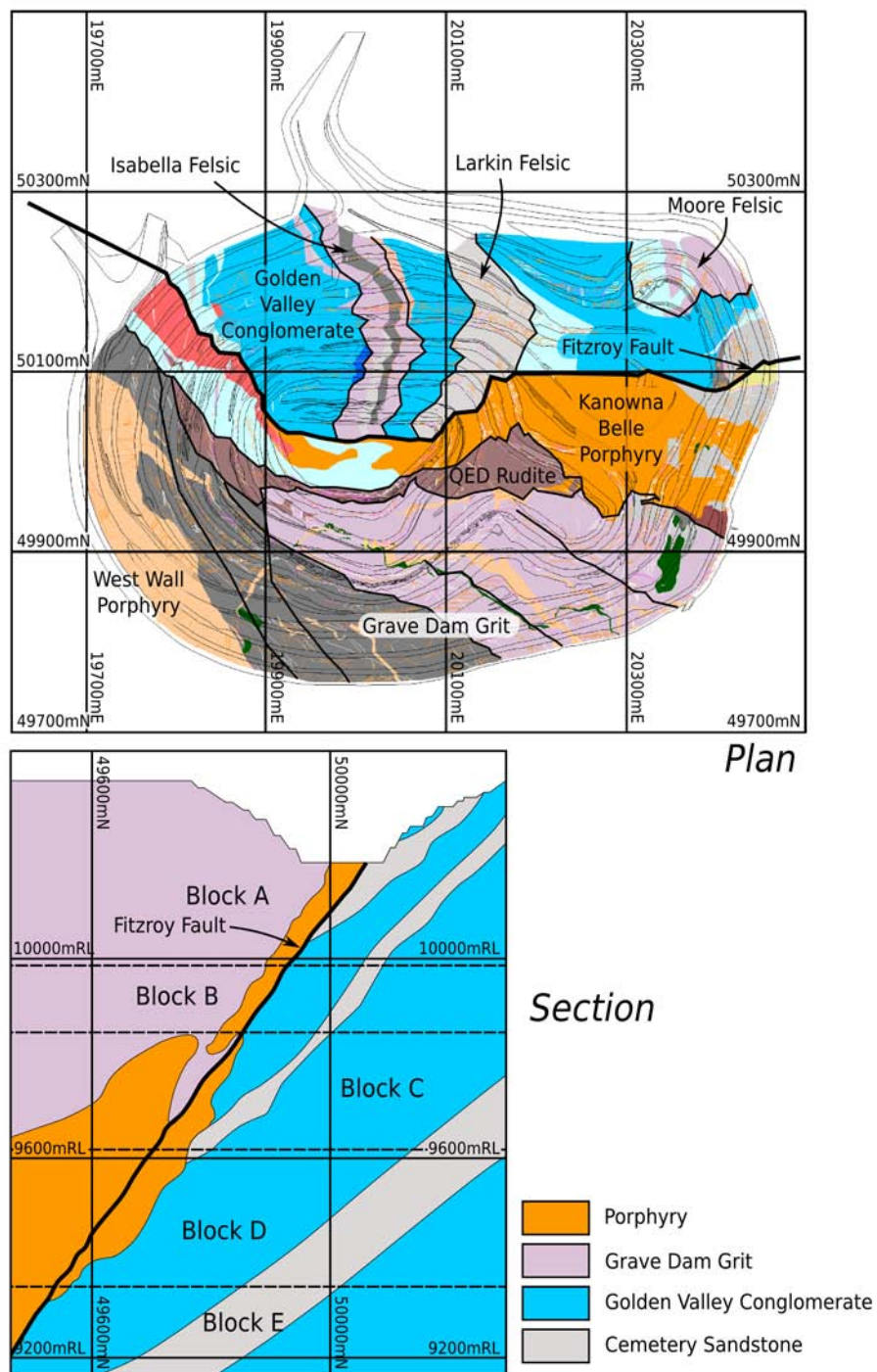


Figure 13.2 - Local mine geology in plan (top) and section (bottom)

Between the hangingwall and footwall sequences is a thin structurally emplaced komatiitic wedge, interpreted as being part of the Kambalda Group. This indicates significant structural interlayering of the stratigraphy.

The Fitzroy Structural Zone (up to 10m wide) has localised emplacement of the Kanowna Belle porphyry, which hosts at least 70% of known mineralisation. The Kanowna Belle

orebody is comprised of several ore shoots, including the large Lowes Shoot, and several smaller lodes including Troy, Hilder, Hangingwall and Footwall shoots controlled by sets of structures of various orientations oblique to Lowes. Lowes contains some 80% of known gold mineralisation (Beckett et al., 1998), and dips to the south (mine grid) and plunges steeply to the south east. The Lowes Shoot has a strike length of 500m, width of 5m to 50m, and down-plunge extent greater than 1250m. The overall steep south east plunge is interpreted to reflect the intersection of D1 and D2 structures. The intersection of these two structures is an important feature of the geology in terms of mineralisation and rock mass conditions. The Kanowna Belle orebody is dominated by the presence of the Fitzroy Fault, which is located to the footwall of the Fitzroy Structural Zone. The position of this structure relative to the mining hangingwall and footwall changes with depth and has a significant impact on the variability of ground conditions.

13.3.3 In Situ Stress

The in situ stress at Kanowna Belle has been estimated using the conventional CSIRO Hollow Inclusion (HI cell) methodology, undertaken at a variety of locations and depths within the mine. A summary of the in-situ stress conditions for Kanowna Belle Gold Mine (Villaescusa et al, 2003) is shown in Table 13.1.

Table 13.1 - In situ stress model for Kanowna Belle Gold Mine

Principal Stress	Magnitude	Trend*	Plunge
σ_1	= 0.079 x depth (m) + 0.12	299°	01°
σ_2	= 0.038 x depth (m) + 5.5	212°	14°
σ_3	= 0.034 x depth (m) - 3.7	034°	75°

Notes: * trend with respect to Mine Grid which is 35° west of True North

13.4 DETERMINISTIC DISCONTINUITY MODELLING

Objectives of this exercise was to define a deterministic discontinuity model that was sufficiently detailed at the stope-scale. This would enable modelled structures to be explicitly incorporated into numerical modelling (see Section 13.8).

13.4.1 Geological Fact Data

Large-scale structures were interpreted from geological mapping undertaken on mine levels and declines throughout the underground mine. The mapping data in the upper areas of the mine were augmented by inclusion of trace maps from open pit geological mapping. The underground geological mapping, conducted by KBGM mine staff, was conducted mainly on backs, with the 3-dimensional trace of each geological structure subsequently determined. The data were validated to remove any duplicate digitised traces, and ensure all dip and dip

directions were within valid ranges. In addition to orientation, digital traces were annotated with structure type (i.e. fault, shear, mineralised or non-mineralised vein, contact, etc.) and termination classifications.

13.4.2 Interpretation

Deterministic discontinuity models of stope-scale structures were developed and validated using the methods proposed in Chapter 10. Figure 13.3 shows a partial view of the final model.

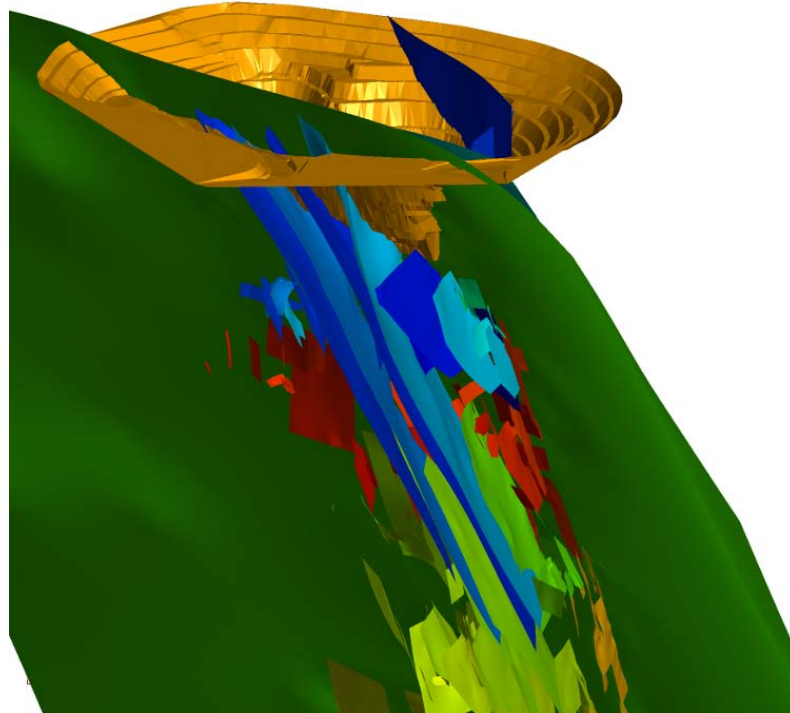


Figure 13.3 - Isometric view (looking south east) showing deterministic discontinuity models with the Kanowna Belle Open Pit for reference

13.4.3 Model Validation

On completion of modelling and validation, the orientation and size distributions of the modelled structures were reviewed. For the orientation analysis, data from each domain (see Section 13.5) were extracted and compared to modelled structures within each of the respective domains. An example of this comparison is shown in Figure 13.4. All directions are relative to mine grid. Here, fact data for small scale structures (e.g. from scan line and window mapping), large-scale structures (e.g. geological backs mapping) and model orientations in Blocks D and E were compared.

From Figure 13.4b and Figure 13.4c, it can be seen that there is excellent agreement

between the orientation of large-scale fact data and the orientation of interpreted structures. The orientations of the interpreted structures were also independently compared to geotechnical scan line mapping data (which were not utilised in the interpretation and modelling). Again, there is very good agreement between the two sets of data.

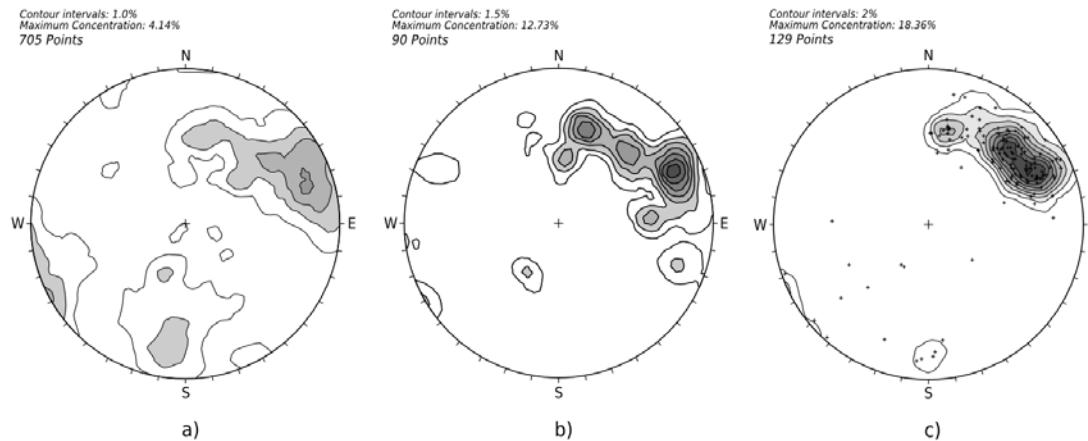


Figure 13.4: Lower hemisphere equal area stereographic projections comparing a) small scale structural orientations, b) geological fact mapping scale orientations and c) orientations of modelling structures for Block D and E

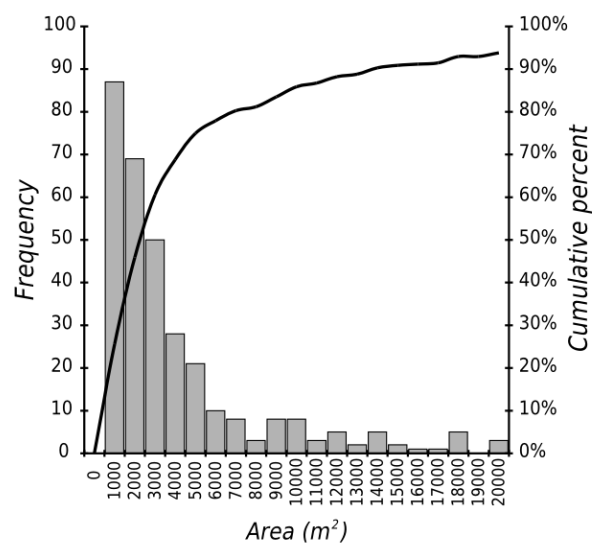


Figure 13.5 - Size distribution of deterministic discontinuity models

It can be seen from Figure 13.4, that there is a significant degree of anisotropy in the modelled structures. This orientation is approximately sub-parallel to the main Felsic contacts, principally the Isabella and Larkin units. Figure 13.4 also demonstrates the scale invariant nature of discontinuity orientations at Kanowna Belle. The size of the modelled discontinuities were also reviewed, with a histogram and cumulative size distribution shown in Figure 13.5. It can be seen that the modelled structures mimic expected truncated exponential or log-normal discontinuity size distributions. It should be noted that six of the largest structures (the hangingwall and footwall contacts of the Moore, Isabella and Larkin

felsic units) which make up the 95 to 100 percentile are not shown in this graph. Due to its overwhelming size, the Fitzroy Fault was excluded from this analysis. This analysis shows that the deterministic modelling technique employed did not overly bias the creation of larger structures and the results are generally representative of naturally occurring discontinuity size distributions.

13.4.4 Summary

During the interpretation and modelling exercise, a number of discrepancies were noted with the fact mapping, namely inconsistent dip and dip direction readings relative to the traces of digitised structures. The interpretations were severely hampered by the lack of orientation data on mapped structural traces, especially in lower parts of the mine. The primary cause of the lack of structural data in lower levels is the extensive use of in-cycle shotcreting of development headings in lower parts of the mine for ground control purposes. This will become an ever-present issue as mining continues to greater depths. As complete 'oriented' fact mapping data set is invaluable for interpretation work, alternative data collection methods that capture this data are required prior to shotcreting (such a digital photogrammetric techniques). Notwithstanding some of the data quality issues related to the lower portions of the mine, the resulting deterministic discontinuity model represents an extremely detailed structural model at the 'stope-scale'.

13.5 IMPROVED ROCK MASS DOMAINING USING LARGE-SCALE DISCONTINUITIES

Previous chapters have highlighted the importance of morphological changes of large scale-structures and their influence on local rock mass conditions. Chapter 8 also describes approaches that utilise structural geology analysis to assist in identifying these changes with a view to establishing domain boundaries.

The Conolly diagram approach (Conolly, 1936) can be used to identify zones of inflection on large-scale structures. These zones of inflection can generate areas of local rock mass dilational and rotational distortion. This approach has been used by others to identify changes in rock mass properties related to preferential ore mineralisation (Harris, 2001). The method involves constructing a plane of best fit at some distance from the structure under investigation and then constructing contours of distance to the plane of best fit. The position of the plane of best fit is limited importance, however, changes in relative deviation distance to this plane can assist in identifying inflections and warps, with closely packed contours indicating steep gradient changes. An example long section plot of a Conolly diagram for the Fitzroy Fault is shown in Figure 13.6.

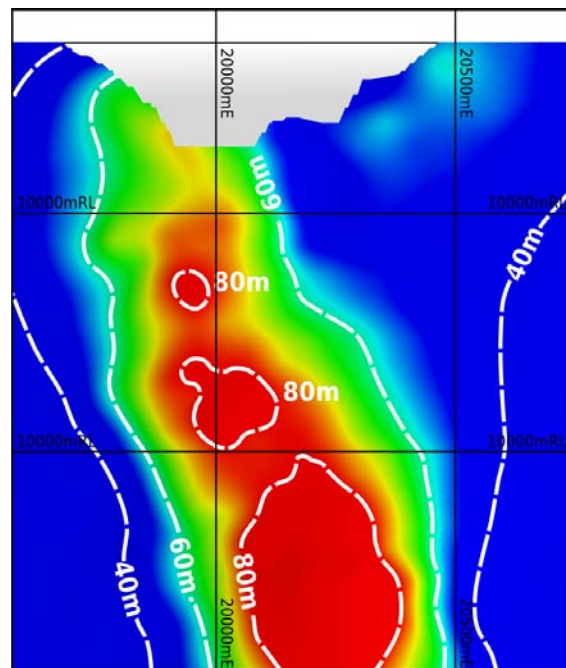


**Figure 13.6 - Conolly diagram of the Fitzroy Fault
(long section looking north)**

It can be seen that there is a structural trend plunging steeply to the east. Upon further inspection, this trend marks an inflection zone along the fault. The boundaries of this inflection zone are not readily apparent, yet are located where the gradient changes abruptly from background values. In this case, the eastern and western edges of the 60m contour interval were arbitrarily used to construct axial planes to the inflection. This was done by generating implicit functions to the lines of intersection at the 60m contour interval. A schematic plan showing the resulting structures is shown in Figure 13.8. The localised inflection and apparent dislocation appears to be consistent with a sinistral D3 transpressional regime, or the later D4 continued sinistral transpression (Swager et al, 1990).

13.5.1 Orientation Analysis

The placement of domain boundaries to delineate zone of structural homogeneity tends to rely on an evaluation of the structural geology, using major structures (e.g. faults, axial fold plains, monoclines, etc.) as boundaries. This subjective process can produce excellent results, yet requires a fair degree of skill and interpretation. The domaining technique using the method of slices outlined in Chapter 8 can also be used to delineate structural homogeneity. A brief exercise was undertaken by plotting the dip and dip direction of the dominant set (Set 1 in Figure 13.9) versus coordinate axis (Figure 13.7).

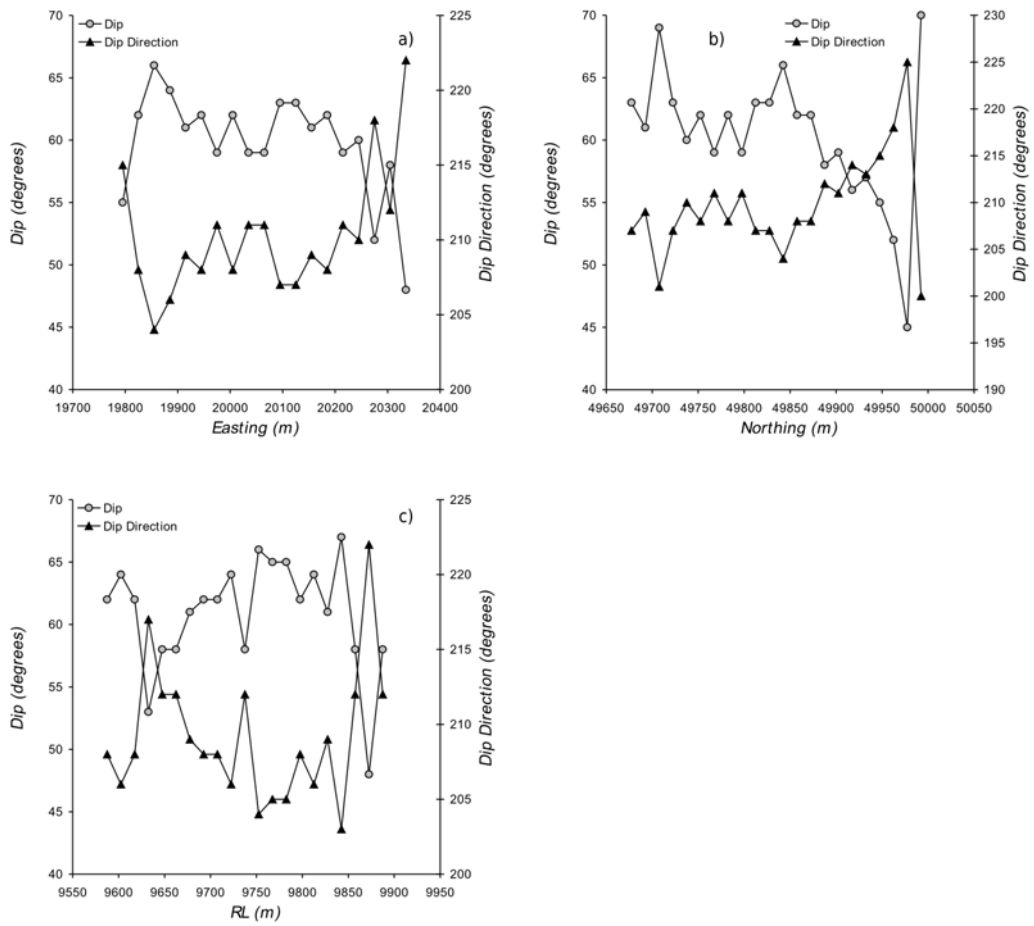


Figure 13.7 - Plots of dip and dip direction versus coordinate axis for Set 1 a) Easting , b) Northing and RL

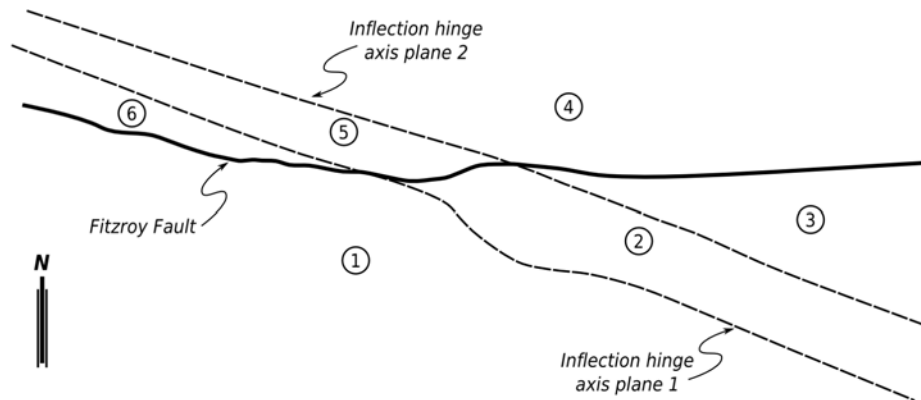


Figure 13.8 - Schematic plan showing delineation of structural domains based on inflection of the Fitzroy Fault

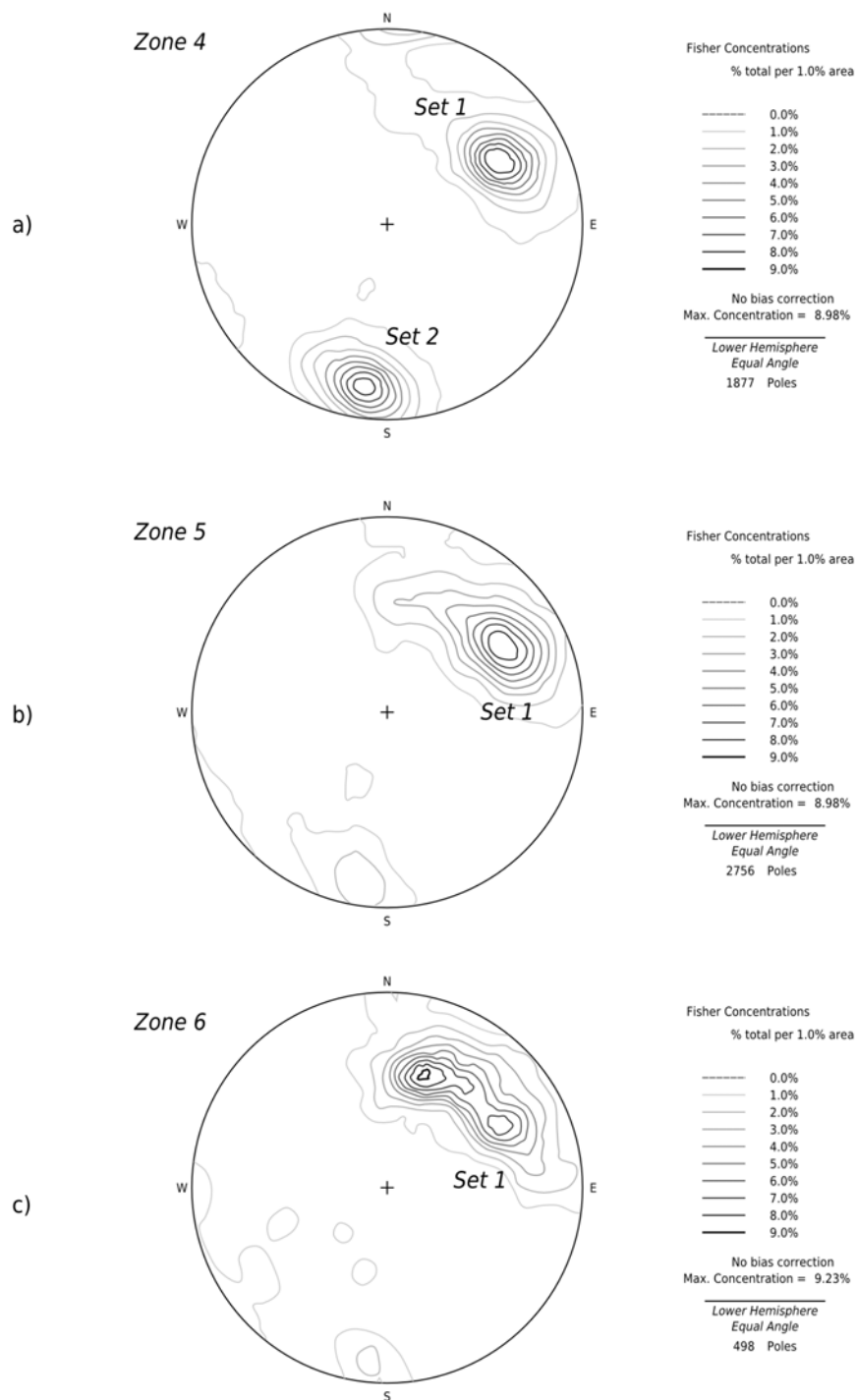


Figure 13.9 - Stereographic projections for structural domains a) Zone 4, b) Zone 5 and c) Zone 6 together with the axial plane and its pole

It can be seen that dip and dip direction are generally consistent in Easting through the centre of the deposit, with changes at the extremities. Orientation is generally consistent with Northing, however, becomes shallower in the northern parts with dip direction swing to the west. Dip and dip direction are both quite variable with depth. Delineation of structural homogeneity may be possible with Northing and Easting, however, is quite problematic with

RL. This indicates that alignment of the coordinate system with geological features which control structural homogeneity rarely coincide. This conclusion is similar to Martin and Tannant's (2004) work who also found poor correlations of structural changes with changes along coordinate axes, yet were able to find an optimal approach by modifying the slices into radial arcs, which would appear to be more appropriate for kimberlite intrusions.

It was therefore postulated that the identified inflection zone should have some impact on local rock mass conditions. In order to test this hypothesis, the boundaries of the inflection zone were used as preliminary structural domains (see Figure 13.8). Geological backs mapping data were then spatially grouped by the domains shown in Figure 13.8. For brevity, only analysis of domains 4, 5 and 6 are described here. Figure 13.9 shows contoured lower hemisphere equal angle stereographic projections of poles to all data for these zones. All directions are with respect to Mine Grid.

It can be seen that, at the drive scale, the rock mass appears to be dominated by one major discontinuity set (Set 1) in all preliminary domains. In addition, a secondary discontinuity set (Set 2) is apparent in Zone 4. From Figure 13.9 a general clockwise rotation of the dominant discontinuity orientation (Set 1) is observed moving from a general west to east direction (i.e. Zone 6 to Zone 4). In addition, there is a marked increase in the intensity of the second most dominant discontinuity orientation (Set 2) from Zone 6 to Zone 4. A conceptual model outlining these observations is provided in Figure 13.10. It can also be seen in Figure 13.9c that there appears to be a wide dispersion of Set 1 in Zone 6, in fact, two major orientations are apparent. It is considered that the domain boundary based on inflexion axial plane 1 may have been incorrectly placed.

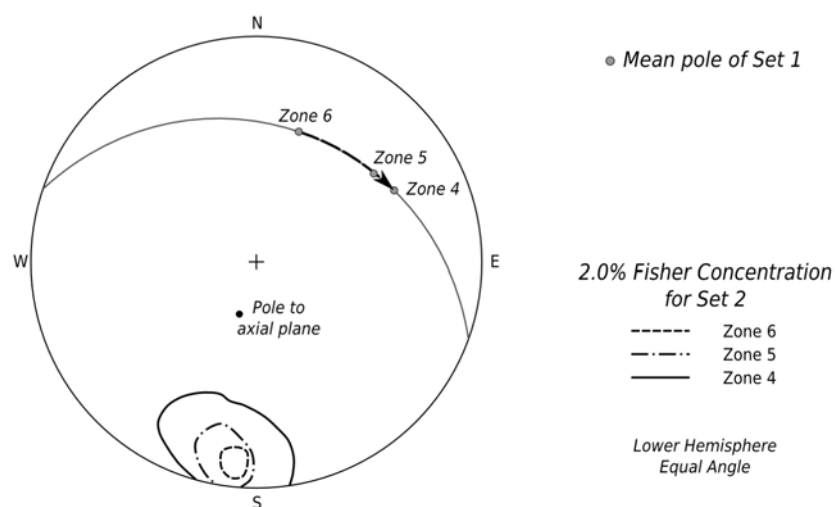
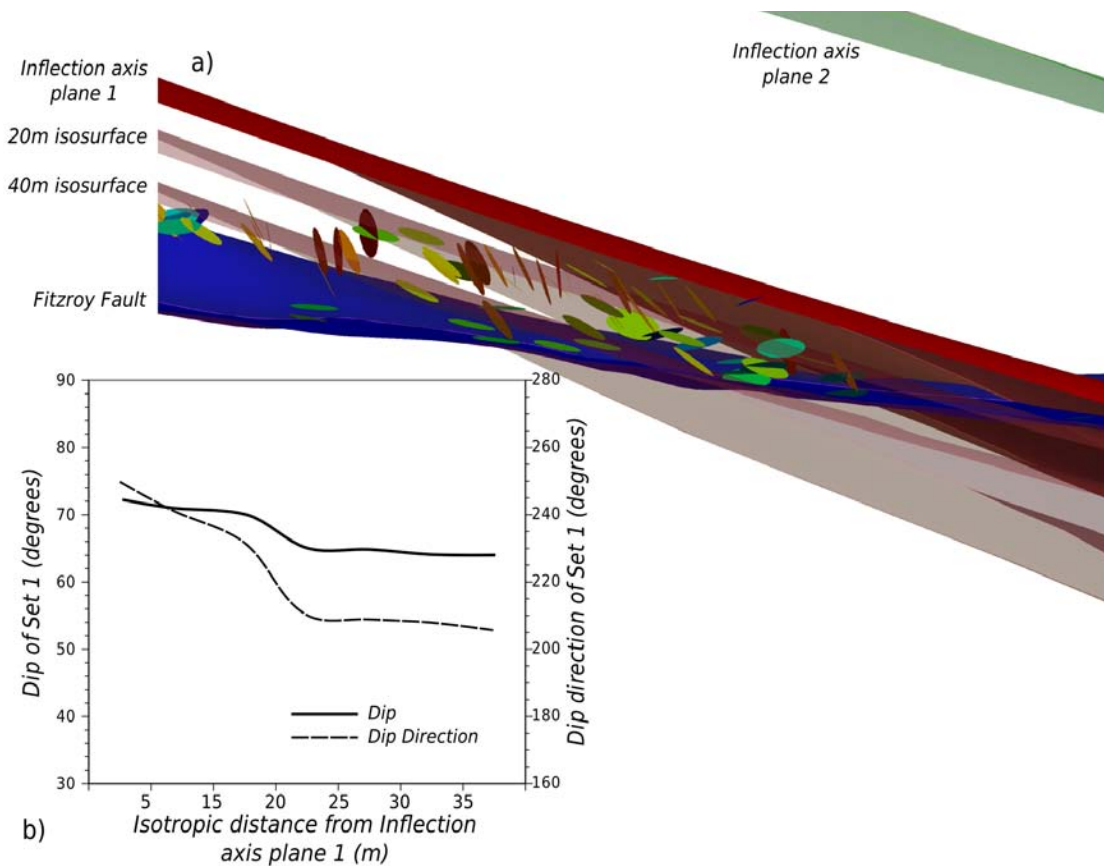


Figure 13.10 - Conceptual structural model showing clockwise rotation of mean poles of Set 1 across structural domains along the axial plane, with a corresponding increase in intensity of Set 2

In order to investigate this possibility, and to improve the reliability of defined sets, it was decided to optimise the domain boundaries using the proposed techniques outlined in 11.5.4. The advantage of modelling the structures using implicit functions is that the shape can be maintained and a series of isosurfaces can be created at various distances from its original position via distance fields. Structural data within fixed distance bands were then analysed. The change in the mean dip and dip direction for the set were then compared (see Figure 13.11). It can be seen that there is a distinct change in the dip direction at approximately 20m. There also is a small, yet discernible change in the dip angle at this position. Indeed, shifting the boundary to this position sees the disappearance of the more westerly dipping pole concentration for Zone 6 (c.f Figure 13.12a and b). In addition, there has been a significant decrease in dispersion (i.e. increase in reliability) for Set 1, with a 69% and a 53% increase in Fisher's *K*-constant for zones 6 and 5, respectively. This exercise demonstrates the combined use of a number of domaining methods to generate reliable structural homogeneous zones. This has only been achieved by development and use of an integrated spatial model.



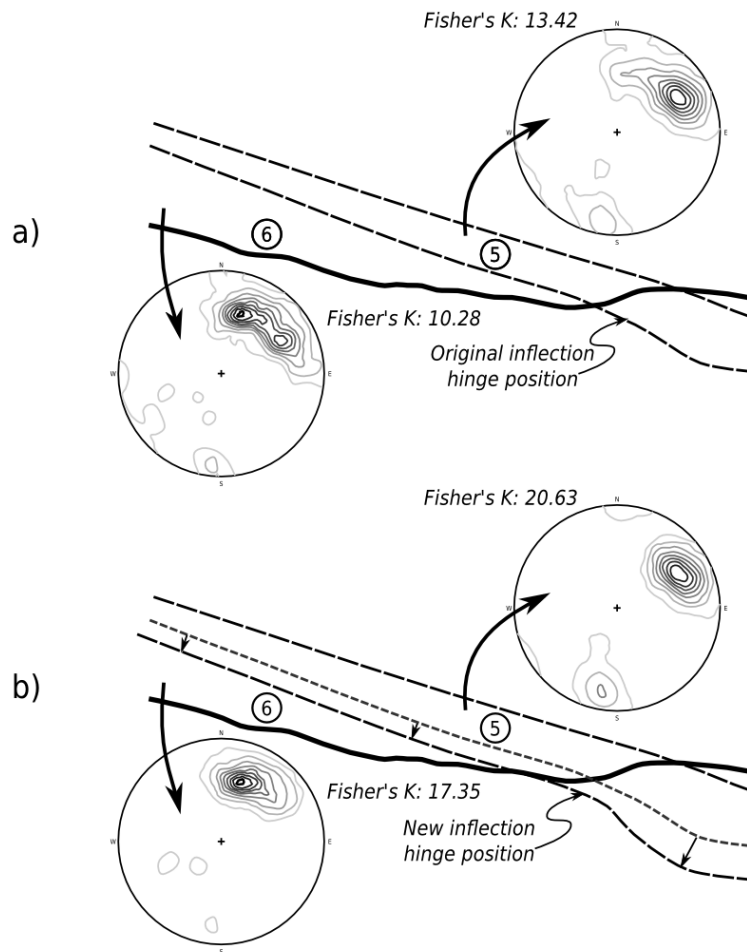


Figure 13.12 - a) original orientations and Fisher's K constants for Set 1 in zones 5 and 6, and b) updated orientations and Fisher's K constants with change of domain boundary

13.6 DISCONTINUITY INTENSITY MODEL

Data utilised in the modelling consisted over 2,230 drill holes (345,000m total) from the Kanowna Belle geological database. The data were further augmented by the inclusion of 1,170m of scan line data. Uncorrected discontinuity linear intensity or frequency (*DLF*) data (309,000 data points) were first validated using methods described in Appendix A. Notwithstanding this, the predominant drilling direction is relatively uniform (directed approximately $50^{\circ}/005^{\circ}$ relative to mine grid) which suggests that fracture intensity values can be modelled as scalar values and that any changes in discontinuity linear intensity are zones of inhomogeneity rather than an orientation bias effect.

13.6.1 Domains and Interpolation Parameters

The data were then divided into the domains described in Section 13.5. For each domain a 3-dimensional variography analysis was conducted in order to find the principal continuity directions and ranges. These were then used to define the interpolation parameters. Initial

inspection of the diamond drill hole database suggests that Fitzroy Fault has the most control on the variability of fracture intensity values in the area of interest. Initial interpolation of fracture intensity was done using two main anisotropic models;

- Fitzroy (D1) Orientation (61.4° dip, 185.4° dip direction, 53.5° pitch, 4:3:1 anisotropy ratio)
- Felsic Intersection Orientation (82° dip, 242° dip direction, 67° pitch, 4:3:1 anisotropy ratio) - The Felsic Intersection Orientation is derived by the line of intersection between the mean dip and dip direction of the Felsic contacts (D2) and the mean dip and dip direction of the Fitzroy Fault (D1) (see Figure 13.13).

Models were then created for each domain combined into a single model for the whole mine. As alpha angles were not recorded during logging for discontinuity linear frequency, the resulting models are unfortunately based on uncorrected data.

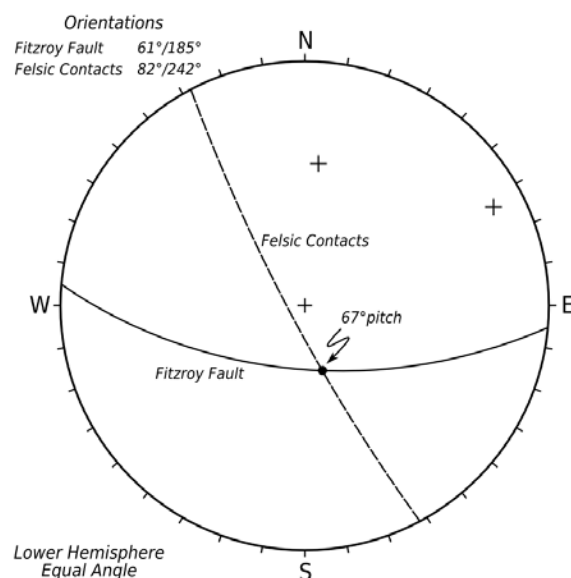


Figure 13.13 - Lower hemisphere equal angle projection showing intersection of Fitzroy Fault and Felsic Contacts, with pitch angle relative to Felsic Contact

In order to assess the influence on large-scale structures on rock mass conditions, *DLF* was plotted against distance to structures as shown in Figure 13.14. The selected data for this plot were restricted to the immediate area of mining in Block A. It can be seen from Figure 13.14 that there is a clear increase in *DLF* values with decreasing distance to a structure. This plot also shows that there are areas of the rock mass where structures have had limited impact on rock mass conditions, with no apparent increase in *DLF*, as indicated by the data points located in the lower left corner of Figure 13.14. This demonstrates the variable impact of large-scale discontinuities on local rock mass conditions. Conducting this type of analysis

can provide an important tool in order to rank structures by their relative influence on local rock mass conditions.

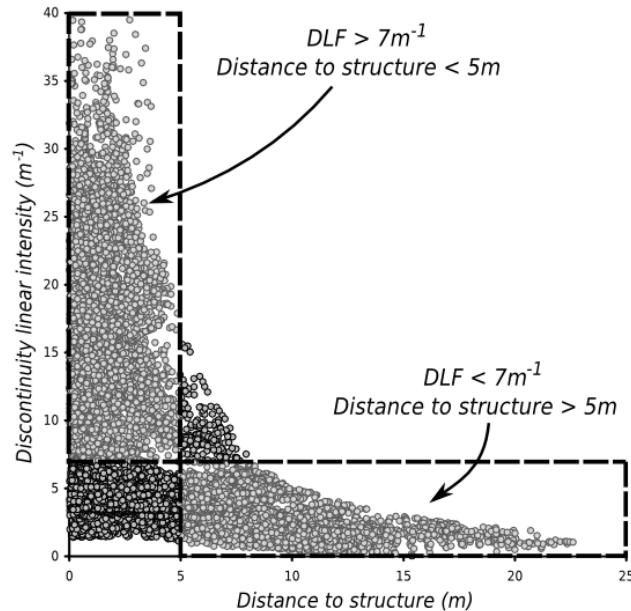


Figure 13.14: Plot of discontinuity linear frequency versus distance to a modelled structure for Block A rock mass showing discrimination zones used in linear elastic modelling

13.6.2 Variability of Rock Mass Characteristics on Large-Scale Discontinuities

The previous example briefly described how analysis of discontinuity intensity models and deterministic discontinuity models can be used to assess the influence of structures on local rock mass conditions. This section describes a similar approach to gain an understanding of the variability of local rock mass conditions **along** structures. In this exercise, an analysis was undertaken to understand the influence of one of the most significant large-scale discontinuities, the Fitzroy Fault, on local rock mass conditions along other modelled structures.

The discontinuity intensity model was used to interpolate intensity onto all deterministic discontinuity model surfaces. In this way, the local variability of *DLF* along structures can be observed. The lines of intersection of each structure with the Fitzroy Fault were determined (Figure 13.15). A series of equally spaced points were placed on the large-scale structures and the minimum isotropic distance from the lines of intersection were calculated. Figure 13.16 shows the characteristics of uncorrected *DLF* along modelled structure surfaces as a function of distance from their intersection with the Fitzroy Fault.

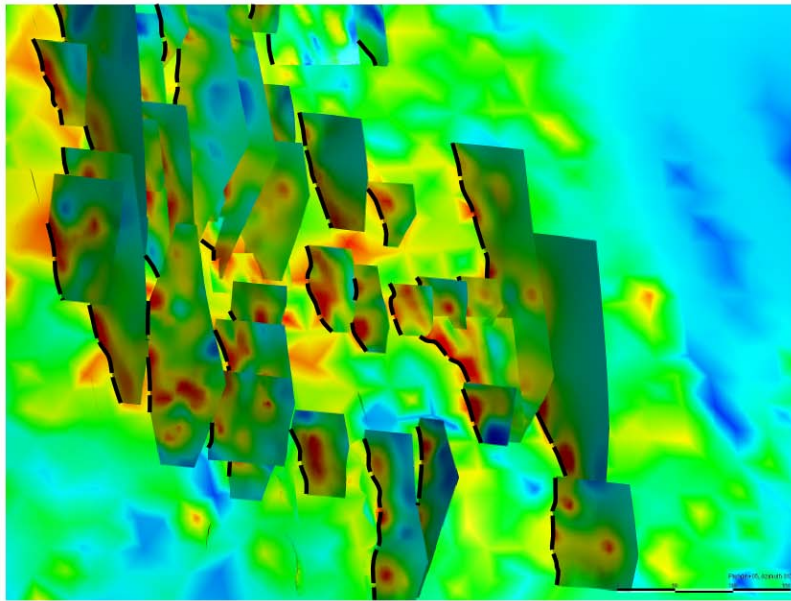


Figure 13.15 - Deterministic discontinuity models colour contoured by *DLF* showing lines of intersection with the Fitzroy Fault

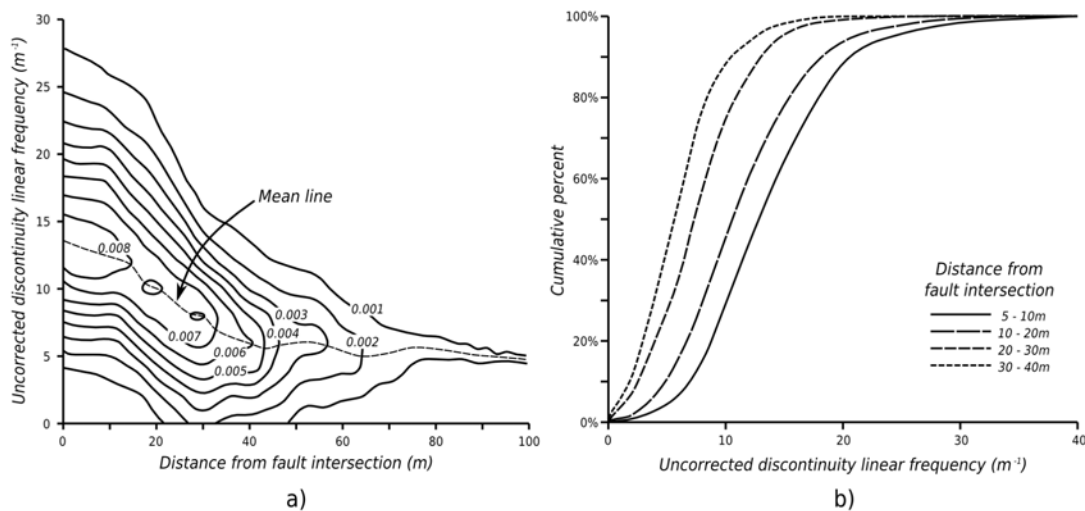


Figure 13.16 - Discontinuity linear frequency characteristics for modelled structures, showing a) bivariate kernel density estimation of modelled uncorrected discontinuity linear frequency versus intersection distance from the Fitzroy fault, b) example cumulative probability curves for various distances from the fault intersection

It can be seen that the mean *DLF* is highest closest to the intersection with the Fitzroy fault, and reduces approximately linearly away from the fault. The mean *DLF* then becomes approximately constant (around 6m^{-1}) at about 35-40m from the fault intersection. This figure is significantly higher than the general rock mass *DLF* at similar distances (c.f Figure 13.14).

Although the mean *DLF* is higher closer to intersection with the Fitzroy Fault, the variability is also higher. That is, the variability of discontinuity intensity seems to become less variable away from the fault intersection. The identification of highly variable rock mass conditions, especially in areas close to fault intersections, may have implications in the analysis of seismic response of large-scale structures.

13.6.3 Summary

The brief examples shown above illustrate some of the benefits of integrating rock mass modelling techniques to improve our understanding of the role of large-scale structures on the spatial variability of certain rock mass characteristics. The modelling techniques can be used to predict the likely rock mass conditions based on distance from a fault, or local rock mass conditions along a particular structure at a certain distance from its intersection with the Fitzroy fault.

13.7 LINEAR ELASTIC BACK ANALYSIS

The following sections describe a number of linear elastic back analysis exercises undertaken to demonstrate various aspects of the integrated back analysis framework (section 11.8). These exercises also highlight a number of improvements over standard approaches to linear elastic back analysis techniques, especially with regard to improving the reliability of derived instability criteria.

The numerical modelling exercises utilised the linear elastic boundary element code *Map3D* (Wiles, 1993). The main purpose of the numerical modelling was to identify the effects of induced stress on stope performance (i.e. principally over-break). The back analysis was conducted with a view to establishing a site specific linear elastic damage criteria (Chapter 7) that define the stress levels, or “damage levels”, corresponding to particular rock mass behaviour that directly affects stope performance.

The mine geometries used in the model were based on mine design shapes provided by Kanowna Belle Gold Mine. The shapes were further sub-divided to more accurately reflect the sub-level mining sequence. The geometry and stope sequence for Block A is shown in Figure 13.17. The modelling was restricted to initial mining in Block A and mainly focussed on primary stopes. It was assumed that there was minimal stress induced damage prior to stope excavation and that the stress path in the immediate vicinity of the stopes was attributable to the primary stope mining sequence.

13.7.1 Initial Modelling Parameters

In situ stresses from Section 13.3.3 were used as input parameters. Intact uniaxial compressive strength (*UCS*) values for the hangingwall, ore and footwall rock types in Block A were obtained from laboratory testing. The results show that the hangingwall has the highest intact rock strength (mean approx. 150MPa), with the footwall and the orebody showing mean intact rock strengths around 130MPa, however displaying higher variability. Rock mass quality for the Block A stopes was also assessed by utilising the *DLF* data from diamond drill hole logging. The *DLF* model confirmed that the main control on rock mass quality was large-scale discontinuities, principally the Fitzroy Fault. Rock mass quality was also assessed utilising the Geological Strength Index (*GSI*) (Hoek, 1994). A mean *GSI* of around 75 was estimated for rock masses remote from major discontinuities. Rock mass strength was initially estimated utilising the Hoek-Brown failure criteria (Hoek and Brown, 1998). From this, the mean unconfined rock mass strength was initially estimated to be around 20MPa.

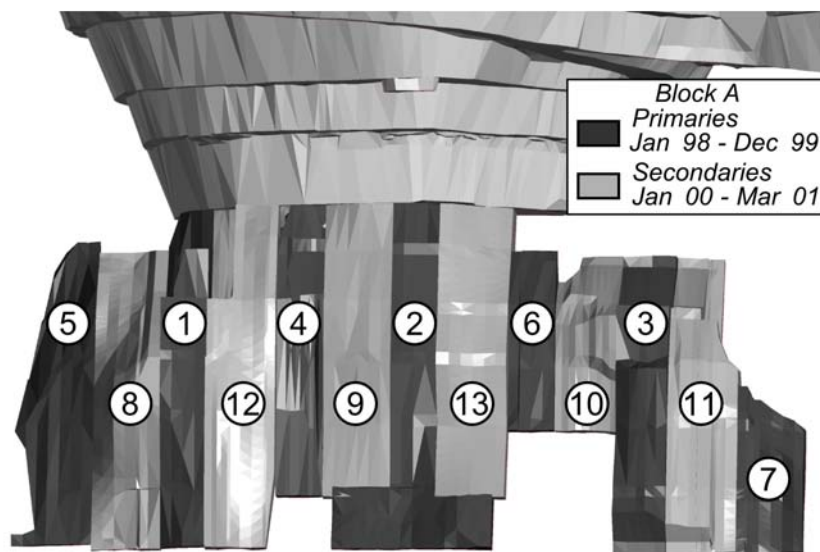


Figure 13.17 - Longitudinal view showing stope sequence for Block A

13.7.2 Assumptions

The principal assumption of the numerical modelling back analysis is that the *CMS* data points represent points in the rock mass where stress induced failure has occurred as a direct result of induced stresses exceeding the local rock mass strength, which in turn, is manifested as over-break at this location. Unfortunately, this assumption may lead to significant variability in back analysis results, as the *CMS* profile does not necessarily define the excavation damage zone (*EDZ*) or yield zone of rock mass. *CMS* points could actually represent “yielded” yet “un-removed” rock mass, where the local shape and span may arch and hold up yielded material. This also depends on the geometry (i.e. orientation, size and

shape) and intensity of existing and created discontinuities (Villaescusa et al, 2003). In this case, linear elastic modelling may over-estimate the stress state at failure. In addition, “yielding” of the rock mass may not be solely attributed to stress-induced rock mass damage, yet may be caused by other influences such as poor drill and blast practices.

13.7.3 Structures

One aspect of the proposed integrated back analysis framework is the ability to assess the influence of large-scale structures on rock mass response by **indirect** incorporation of discontinuities. In this case, the numerical model did not explicitly incorporate large-scale geological structures (i.e. as displacement discontinuities), however, the effects of large-scale structure and rock mass variability were studied by comparing results of numerical modelling *and* stope performance in areas of the rock mass known to be affected by large-scale structures. Regions of the rock mass were differentiated based on proximity to a modelled large-scale structure and local rock mass conditions using volumetric queries as described in Chapter 11.

13.7.4 Results

Results from numerical modelling (i.e. stresses, elastic strains and displacements) were evaluated on the raw *CMS* data points. Approximately 18,000 data points were used in the analysis and imported into the integrated spatial model. Only footwalls, hangingwalls and end walls were included in the data set (i.e. no backs). In order to improve reliability, the data set was filtered to exclude points where $DLF * \text{critical span} (\lambda_t * S_c)$ values were less than 10, as proposed in section 11.8.2. This resulted in the removal of only around 13% of data, points. This is primarily due to the very large stope spans in Block A.

The back analysis was conducted with a view to establishing a site specific linear elastic damage criteria (Chapter 7). Simple linear regression models (of σ_1 versus σ_3) were used to define critical stress-based criteria for all *CMS* data points (i.e. “failed” rock mass) as shown in Figure 13.18a, with the damage criteria parameters shown in Table 13.2. It can be seen that coefficient of variation for this relationship (all data) is greater than 0.38, which according to Wiles (2006), indicates a fairly poor level of reliability and that alternative models or approaches need to be contemplated.

In order to try to improve reliability and to study the effects of rock mass heterogeneity, the local *DLF* and distance to major structure were used to segregate *CMS* data points using volumetric queries (zones defined in Figure 13.14);

- points considered to be located in moderately jointed rock, and remote from

potential large scale discontinuities ($DLF < 7\text{m}^{-1}$ and distance to modelled structures $> 5\text{m}$), with modelling results shown in Figure 13.18b

- points representing very highly fractured rock mass, potentially influenced by large-scale structures ($DLF > 7\text{m}^{-1}$ and distance to modelled structures $< 5\text{m}$), with modelling results shown in Figure 13.18c

It can be seen that the amount of scatter in the data is greatly reduced for data representative of moderately jointed rock mass conditions (i.e. $DLF < 7\text{m}^{-1}$ and distance to modelled structures $> 5\text{m}$). Table 13.2 shows that the resulting criteria defined for moderately jointed rock mass conditions provides the most reliable model with a C_v below 30%.

Very highly jointed rock masses close to structures display more scatter, indicating higher degree of unpredictable performance, thus models created from this data should have lower reliabilities. Table 13.2 shows the stress-based model for highly jointed rock masses close to structure provided the least reliable criteria ($C_v > 45\%$). The results also show that the stress-based model for very highly jointed rock mass, although having an apparent higher rock mass UCS , has a much lower q gradient, indicating a weaker rock mass strength compared to the moderately jointed rock mass strength model.

The data sets were then further subdivided in to regions based on the stress path experienced, based on the classification described in section 11.8.2. Plots of σ_1 versus σ_3 were then contoured by depth of over-break to see if rock mass response was controlled by the stress-path (see Figure 13.19).

For moderately jointed rock masses (Figure 13.19a), the onset of increased over-break shows a good correlation with the estimated Hoek-Brown strength envelop. More significantly, depth of over-break increases with over stressing, and progressively increases as the loading path changes from monotonic loading, shear through to low confinement conditions. It can also be seen that there is a significant change in rock mass behaviour under unloading conditions, where increases in fall-off occurs, particularly close to the stope scale “rock mass” damage initiation criteria, which was found to be approximated by;

$$\sigma_1 = 0.33 \sigma_{cm} + 1.5 \sigma_3 \quad (13.1)$$

where σ_{cm} = unconfined rock mass strength. The value of σ_{cm} agrees well with the estimated rock mass compressive strength as described in section 13.7.1. This behaviour is similar to observed brittle rock mass failure mechanisms in smaller scale hard rock excavations under

low confinement conditions (Martin, 1997; Martin and Maybee, 2000).

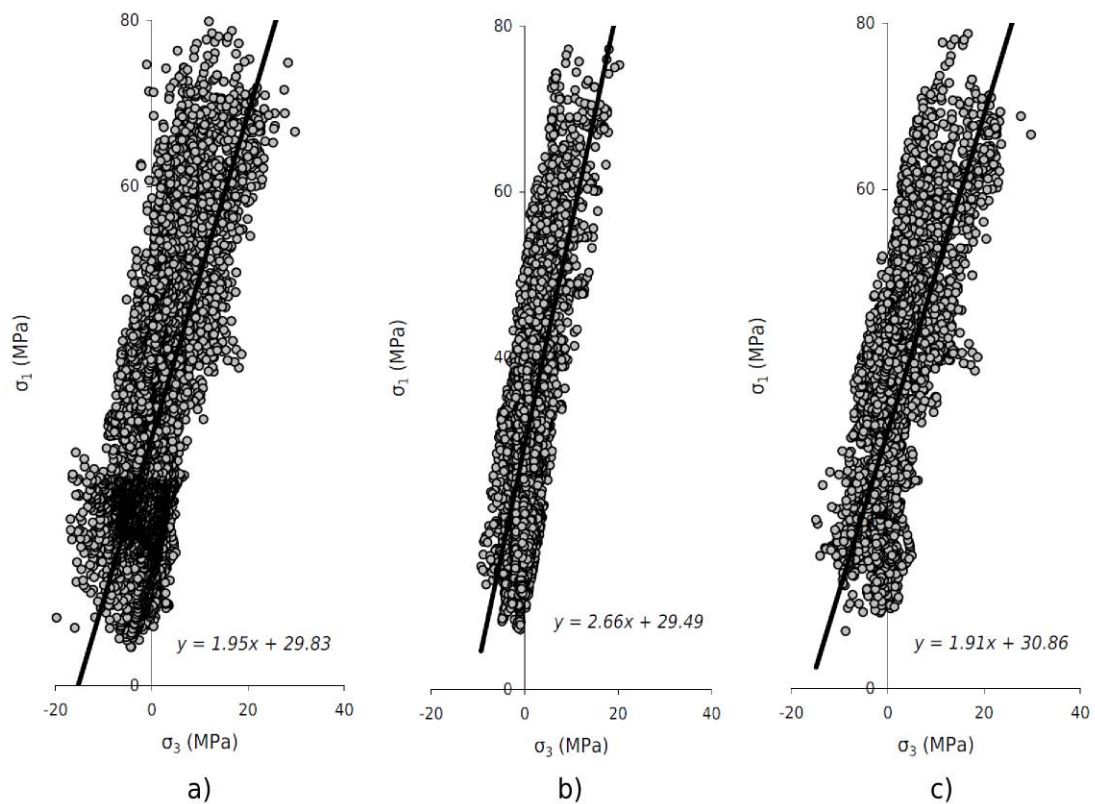


Figure 13.18 - Linear elastic critical stress-based criteria for a) all data, b) $DLF < 7m^{-1}$ and greater than 5m to a structure, c) $DLF > 7m^{-1}$ and less than 5m to a structure

Table 13.2 - Summary of linear elastic critical stress-based criteria

Model	n	σ_{cm} (MPa)	q	Std. Dev.	C_v
All data (standard method)	17780	29.8	1.95	10.78	0.38
$DLF < 7m^{-1}$, $> 5m$ to a structure	7470	29.5	2.66	8.77	0.27
$DLF > 7m^{-1}$, $< 5m$ to a structure	6007	30.9	1.91	11.38	0.46

For very highly fractured rock masses close to large-scale structures (Figure 13.19b), the maximum depth of over-break is similar to Figure 13.19a, however, the over-break generally occurs at lower stress levels, and the extent of over-break occurs over a wider range of stress conditions. It is interesting to note that over-break occurs at similar stress levels in the “unloading” region, however the observed depths of over-break are generally lower. The main increase in over-break for very highly fractured rock masses appears to begin at a constant stress level of around $\sigma_1 - \sigma_3 = 25\text{MPa}$ (at moderate levels of confinement, where $\sigma_3 > 2.5\text{MPa}$). In addition, there appears to be another increase in over-break at around $\sigma_1 - \sigma_3 = 42\text{MPa}$. A review of the relationship between the orientation of the large-scale structures and the stope surfaces indicates that the majority of over-break located immediately the

above the first stress level ($\sigma_1 - \sigma_3 = 25\text{MPa}$) occurs where the major structural orientation (large-scale) is largely sub-parallel to the stope surface. The second zone of increased over-break ($\sigma_1 - \sigma_3 = 42\text{MPa}$) appears to coincide with major structural orientations that are sub-perpendicular to the stope wall surfaces. This may indicate that over-break here is characterised by failure of small zones of poor rock mass quality at moderately low shear stresses (compared to moderately jointed rock). Figure 13.19b indicates that stopes with poor rock mass conditions and/or are in close proximity to a large-scale structure, generally are observed to have more wide-spread over-break characteristics. The actual shape and extent of over-break will of course, be dependent on orientation of both the surface and structure, proximity to surface, position of intersection and strength characteristics of the structure and local rock mass conditions.

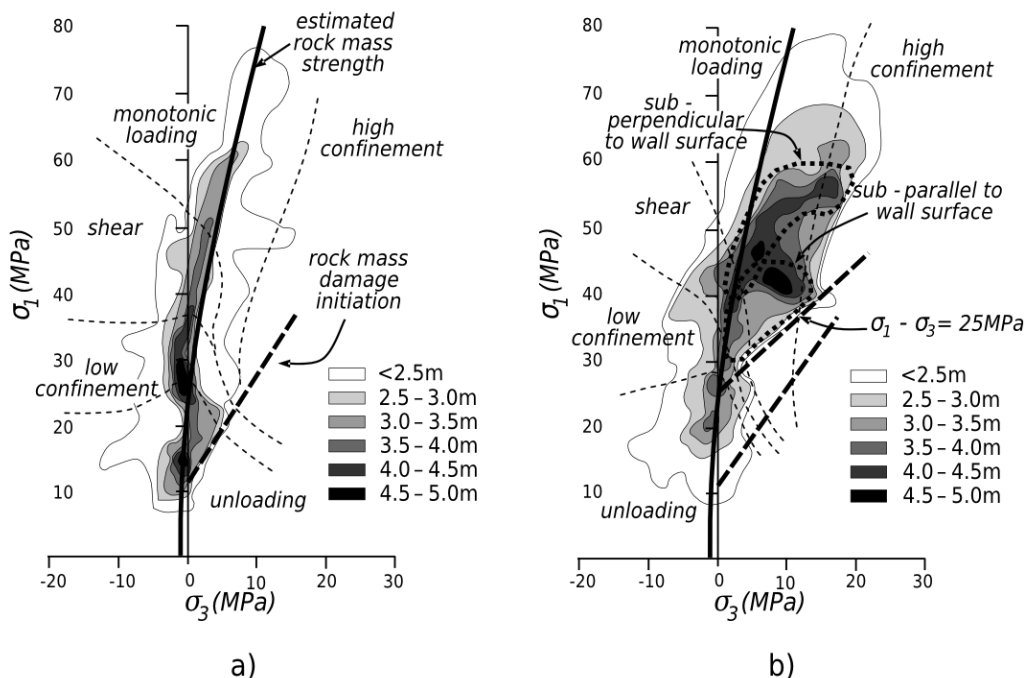


Figure 13.19 - Plot of σ_1 versus σ_3 for a) moderately jointed rock and b) very highly jointed rock <5m from structure, showing contours of over-break and loading conditions (thin dashed lines), theoretical Hoek-Brown rock mass strength (thick solid line) and estimated rock mass damage initiation criteria (thick dashed line)

13.7.5 Summary

The use of the integrate back analysis framework was applied to a linear elastic modelling exercise. The proposed approach demonstrated how the influence of large-scale structures can still be evaluated without their explicit and direct incorporation into linear elastic models. Significantly, the back analysis method employed showed that;

- Stress damage levels and stress-path can be used to ascertain an increase in the depth of over-break depending on *DLF* and distance-to-structure characteristics,

- Large-scale structures and surrounding poor rock mass conditions contributed to the majority of over-break,
- For both moderately jointed and very highly fractured rock masses, the spatial distribution of over-break below 2.5m is highly variable, and occurs over a very wide range of stress levels. It can potentially be attributable to small scale structural failures, blast induced damage and local fall-off around development.

The conclusions above have only been made possible by separating performance data based on proximity to structures and degree of rock mass fracturing, stress-damage levels, and stress-paths using the volumetric querying techniques. The exercise has also shown how the integrated approach can be used to derive linear elastic stress-based design criteria with greater reliability than existing approaches. It has also demonstrated under what conditions design criteria may potentially be unacceptable, thus highlighting where uncertainty lies in the design.

13.8 NON-LINEAR NUMERICAL MODELLING AND BACK ANALYSIS

The following sections describe advancements on the linear elastic approach using a non-linear finite element methods to study post-peak rock mass behaviour and to study the influence of large-scale discontinuities by direct incorporation into the numerical model. From this numerical modelling work, a number of slope instability criteria have been developed, based on stochastic analysis of existing performance. These instability criteria can be used as a forward prediction and design tool. A new method for assessing numerical model reliability is also presented. An important aspect of the integrated approach is the ability to determine design reliability. In this regard, a novel method to evaluate the predictive capability and reliability of the instability criteria is presented.

13.8.1 Modelling package

The modelling was undertaken using *Abaqus Explicit*, which is a general purpose, 3-D, non-linear, continuum or discontinuum finite element analysis product. *Abaqus* is designed specifically for analysis of problems where there is potential for significant plasticity, high levels of deformation and large numbers of material discontinuities. The package is utilised extensively in the automotive, aerospace and consumer electronics industries to assess structural integrity to static and dynamic loading. *Abaqus* was selected for the modelling due to the discontinuum and large strain abilities of the package and the large model size needed to represent the detailed mining geometry and large scale structures. Due to limited computing and technical resources at the University, the modelling was contracted to Beck Arndt Engineering.

13.8.2 Constitutive Model

Both continuum and discontinuum components of the numerical model were modelled using the Levkovitch Reusch (*LR2*) material model (Levkovitch et al., 2010), as described in Chapter 7. The main feature of the *LR2* constitutive model is that continuum parts are modelled as strain softening dilatant materials. Discontinuum components can be modelled as traction-separation based cohesive elements, which are allowed to dislocate, dilate and degrade. The main benefit of the implementation of *LR2* in *Abaqus* is that the mechanics and kinematics of the contacts between solid continuous parts bound by cohesive elements is very well resolved and robustly solved.

13.8.3 Modelling Approach

Numerical modelling was undertaken in a number of phases, utilising a number of models. Firstly, a large-scale global model was constructed incorporating all stope geometries – as mined (Block A to D) and planned (Block E), the open pit, decline and access development and mine-scale structures. Smaller, more detailed sub-models were then constructed in key areas, with strain outputs and tractions of the global models used as the boundary conditions for the sub-models. Modelling was specifically targeted at understanding rock mass response and influence of stope-scale structures on hangingwall stope performance.

13.8.4 Rock Mass Domains

The geometries of 6 different lithologically-based rock mass domains were directly incorporated into all models, each with separately derived rock mass parameters using the Generalised Hoek-Brown criterion (Hoek and Brown, 1997) and are shown in Table 13.3.

Table 13.3 - Non-linear rock mass modelling parameters

Unit*	m_i	m_b		s		a	Dilation	E_{rm} (GPa)
		Peak	Residual	Peak	Residual			
FWD	15	2.52	1.07	0.04	0.002	0.505	0.16	8.06
HWD	17	2.85	1.21	0.04	0.002	0.510	0.18	7.42
FEL	22	3.69	1.57	0.04	0.002	0.510	0.23	5.83
ORE	24	4.02	1.71	0.04	0.002	0.510	0.25	4.8
FWP	21	3.52	1.49	0.04	0.002	0.510	0.22	7.35
HWP	17	2.85	1.21	0.04	0.002	0.510	0.18	7.07

Notes: * FWD – Golden Valley Conglomerate, HWD – Grave Dam Grit, FEL – Cemetery Sandstone, ORE – Kanowna Porphyry, FWP – Footwall Porphyry, HWP – Hangingwall Porphyry

13.8.5 Excavation Steps

The extraction sequence is represented in the global model in approximately quarterly steps, while block scale models are extracted in steps no larger than a stope at a time. Selected stopes were extracted then filled sequentially. The large number of extraction steps is

necessary to ensure that the stress path throughout the entire area of interest is captured. For the sub-models, each stope was extracted with a minimum of three firings, usually consisting of; a) full height cut-off slot development (approximately 10% of final void), b) void creation (approximately 30-40% of final void) and c) final stope mass firing (remainder of stope void). Block A stopes usually involved a larger number of intricate firings.

13.8.6 Stope-scale structural model

The stope scale structural model (Section 13.4) geometry was imported into the numerical modelling code. The geometry consisted of 395 discrete separate structures, consisting of 188,727 vertices, 312,585 triangles and a total surface area of 6,181,700m². Each structure was further discretised where required (i.e. close to excavation boundaries). Stope scale structure surface elements were then modelled as cohesive elements.

The inclusion of such a detailed and extensive structural model is significant. Together with the capabilities of the numerical modelling code and approach taken, the model is able to represent the physics and interactions between stope-scale structure, excavations and the continuum rock mass components. This allows for efficient computation of displacements, damage and deformation to the required level of detail across larger numbers of stopes in a number of mining blocks. Importantly, the detailed nature of 'stope-scale' structural model negates some of the scale effects that reduce reliability of equivalent continuum models.

13.8.7 Modelling Output

A grid of 'results points' was constructed enabling calculation of various model parameters at each mining step at varying distances into the hangingwall rock mass. The points were generally located at approximately 1m intervals into the hangingwall, in an approximate 5m x 5m pattern across the hangingwall stope surfaces. Figure 13.20 shows the general arrangement of results points for Block C stopes. For each result point and mining step, the output parameters were entered into a purpose built database. In addition to the modelling results, other details for each result point were also captured and entered into the database, such as stope name, true distance to the hangingwall surface, distance to the nearest large scale structure in the hangingwall and its final stability condition. The final stability condition was assigned by determining whether the point lies within the final *CMS* void and beyond the planned geometry (i.e. over-break) and therefore assigned 'unstable' or whether it is located outside the *CMS* volume, within the 'stable' rock mass.

The resulting database consisted of 40,455 data points. The data was trimmed to exclude any points for stopes where no *CMS* surveys were taken and points that did not lie within the

projected surface area of a stope hangingwall. The trimmed data set for analysis consisted of 33,060 points, which still represents a significant amount of modelling data.

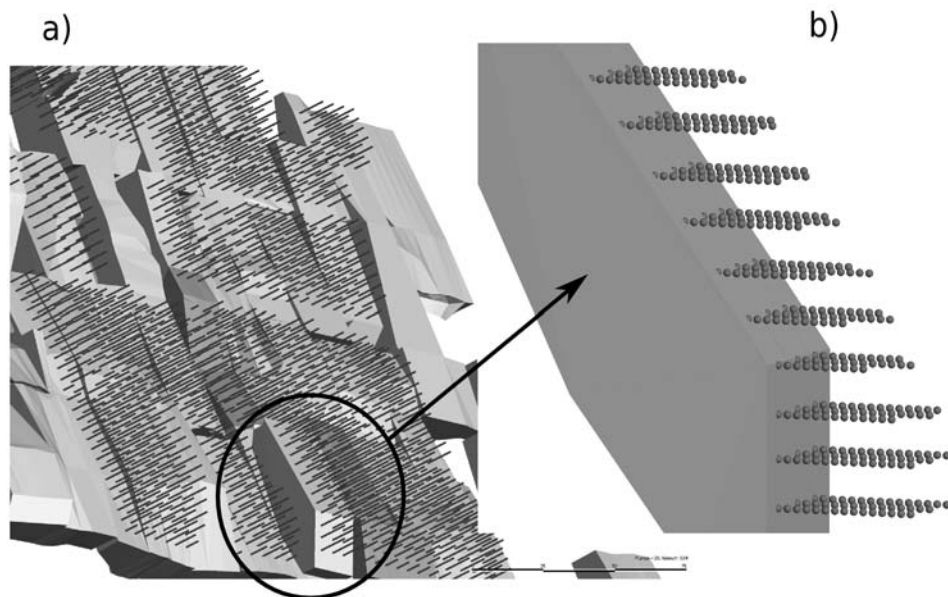


Figure 13.20 - Arrangement and distribution of results points for a) Block C stopes, showing b) detail for stope CD0062

13.8.8 Stochastic Analysis of Instability

Instability is generally defined by the unacceptable displacement of the rock mass into the excavation, thereby shortening the intended service life of the excavation or invalidating the intended function of the excavation. The criteria for instability are generally defined by a certain critical limit of displacement or velocity, or in the case of open stoping, a certain volume of rock mass. These criteria occur within a certain time frame, typically prior to complete removal of ore and stope filling. These criteria can be measured, albeit with various degrees of accuracy and precision, using instrumentation, such as extensometers, or laser cavity surveys. Unfortunately, other criteria for stability, such as plastic strain, cannot be readily measured quantitatively during operations, however can be qualitatively assessed as visual rock mass damage (Beck and Duplancic, 2005; Esterhuizen et al., 2006; Krauland and Soder, 1987; Lane et al., 1999). Numerical modelling provides a means to quantitatively estimate the levels of strain, displacement and velocity accumulated during mining and can be used to forecast excavation performance (Reusch et al., 2008).

The critical limits of instability were assessed from the numerical modelling primarily using velocity and plastic strain values calculated during stope extraction. Velocity is the change in displacement over time. With regards to the modelling results, here velocity refers to the magnitude of the computed resultant displacement vector between mining steps, expressed

as metres per step (i.e. m/step). Example velocity and plastic strain output is shown in Figure 13.21.

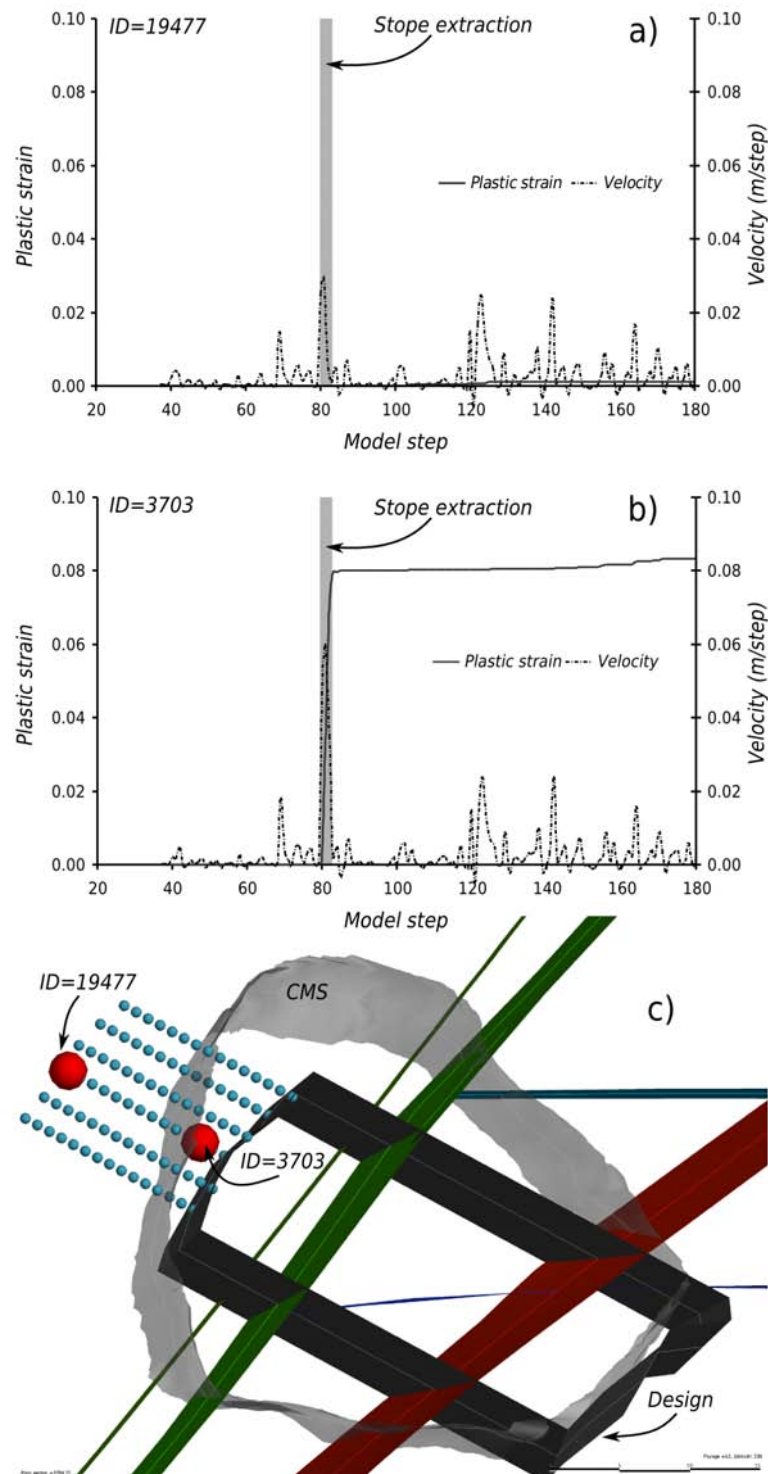


Figure 13.21 - Example data for stope CP0074 showing plastic strain and maximum velocity values versus mining step for a) a stable point and b) an unstable point, with locations shown in c) an isometric view of a 10m horizontal slice (mid-span) showing stope design, CMS, hangingwall data points and some stope scale structures (looking south west)

Velocity can be considered an upper bound criteria for instability, as **all points** with high velocity should theoretically be considered unstable. That is, rock without damage that has a high velocity must be unstable (e.g. moving rock mass bounded by structure). It must be understood that, due to the low occurrence of discontinuity connectivity of the modelled stope scale structures, only a very small percentage of the rock mass will be represented by fully formed rock blocks. Notwithstanding this, rotation and translation of sections of the rock mass adjacent to structure and close to the excavation can still occur, leading to relatively high velocity values in the model. Plastic strain or damage can be considered a lower bound criteria for instability, as material may be damaged, but may still be stable if the velocity is low. An unstable point in the rock mass can therefore have a number of combinations of velocity and plastic strain, as illustrated in Table 13.4. In terms of prediction of rock mass failure using these two variables, they are not mutually exclusive. In addition, plotting plastic strain versus velocity indicates that these variables are independent, with the covariance (Cov) and correlation coefficient (*r*) effectively zero (see Figure 13.22).

Table 13.4 - Anticipated stability and bounds to instability criteria for velocity and plastic strain

Velocity	Plastic strain	Anticipated Stability	Instability Criteria
High	High	Very Unstable	Upper bound
High	Low	Very Unstable	
Low	High	Unstable	Lower bound
Low	Low	Very stable	N/A

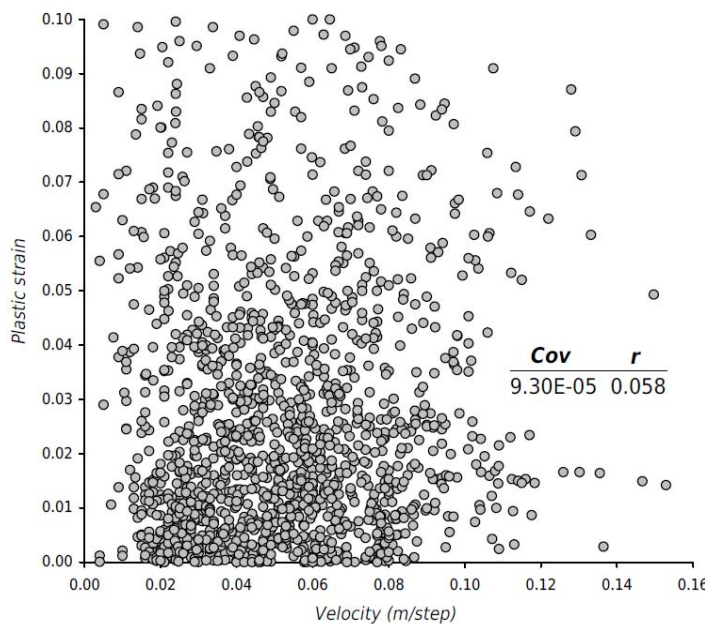


Figure 13.22 - Plastic strain versus maximum velocity during mining for unstable points indicating data independence

Figure 13.22 shows that there are very few 'unstable' data points with minor to moderate

levels of damage (e.g. plastic strain < 1%) and where the velocity is low, as expected. 'Unstable' points plotting in this region are thought to be due processes not explicitly incorporated into the model, such as dynamic effects (e.g. blast induced damage) or local small scale structure.

Limitations And Bias

Velocity values in the model are affected by the kinematic stability of rock-blocks, which in turn is dependant on; the proximity to excavation and the location, number, orientation and arrangement of cohesive elements (i.e. stope-scale structures) with respect to the excavation surface.

Plastic strain values within the model are also affected by the proximity to excavation boundary and cohesive elements. High plastic strain values can be effectively compartmentalised by stope-scale discontinuities. The degree of compartmentalisation is controlled by the geometry, specifically the location and orientation, of stope-scale geological structures with respect to the excavation surface. This can lead to highly damaged and yielded material located remote from the excavation surface, bounded by structure, however constrained kinematically by unyielded material closer to the excavation (see Figure 13.23).

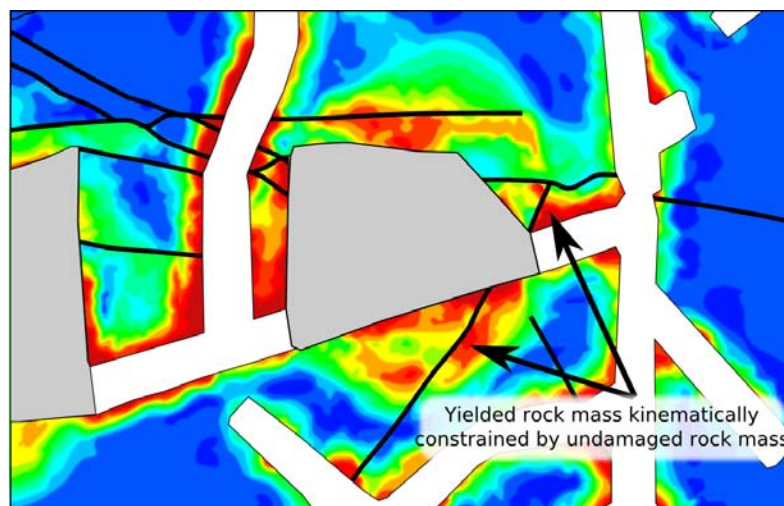


Figure 13.23 - Plan at 10006mRL showing influence of structure on contours of plastic strain

It must be kept in mind that the data set is inherently biased towards 'stable' classifications, due to;

- Incomplete CMS data under representing 'unstable' rock mass (such as occlusion and ore remaining in stopes). Data for Block A stopes is particularly biased by incomplete CMS data (see Figure 13.24).

- The *CMS* profile does not necessarily represent the excavation damage zone (*EDZ*) (Hajiabdolmajid and Kaiser, 2003), as such yielded material (i.e. damaged 'unstable' rock mass) which has arched will be classified as 'stable'.
- Yielded material may be effectively supported by hangingwall cable bolts.

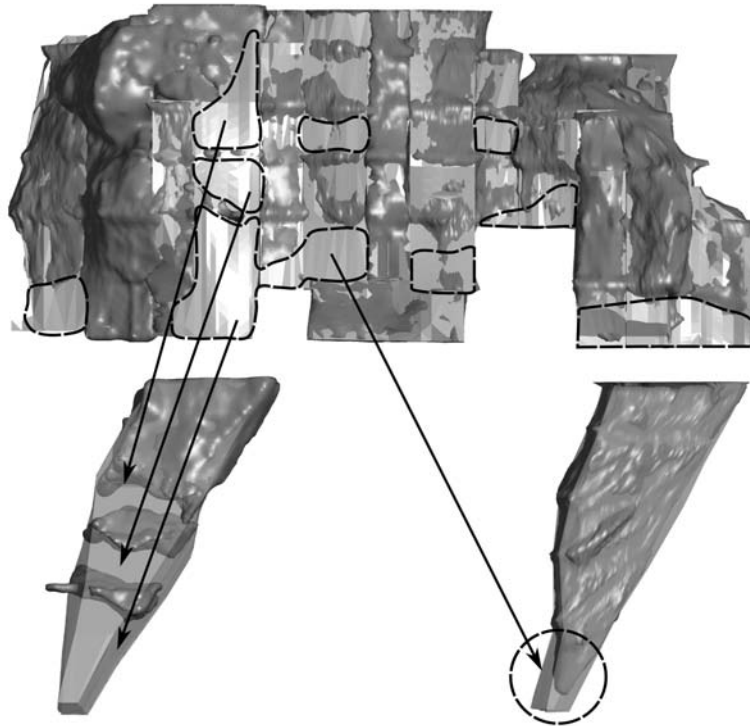


Figure 13.24 - Long section and selected sections of Block A stopes showing zones of incomplete representation of the final excavation from *CMS* data

13.8.9 Results of Stochastic Analysis

Since there is no direct correlation between plastic strain and velocity, logistic regression techniques are unlikely to produce reliable instability criteria. In this case, quantitative performance techniques were utilised. The maximum levels of plastic strain and velocity during stope extraction, were compared to the frequency with which they correspond to stable and unstable points. This was expressed as the percentage of the number of 'unstable' points within a velocity or plastic strain range compared to the total number of points within that velocity or plastic strain range. The percentage of unstable points for the selected interval range could therefore be considered an empirical 'probability of instability' as it is calibrated on the actual mining geometry, sequence and performance.

Velocity Only

The relationship between maximum velocity during stope extraction (regardless of plastic

strain) and the percentage of 'unstable' points is shown in Figure 13.25. The relationship shows an increase in the likelihood of instability with increasing velocity, however the relationship becomes erratic at higher velocities. This is primarily due to the lack of data at these higher velocity values, as indicated by relative frequency of unstable points and is also a function of the nature of the modelling method utilised.

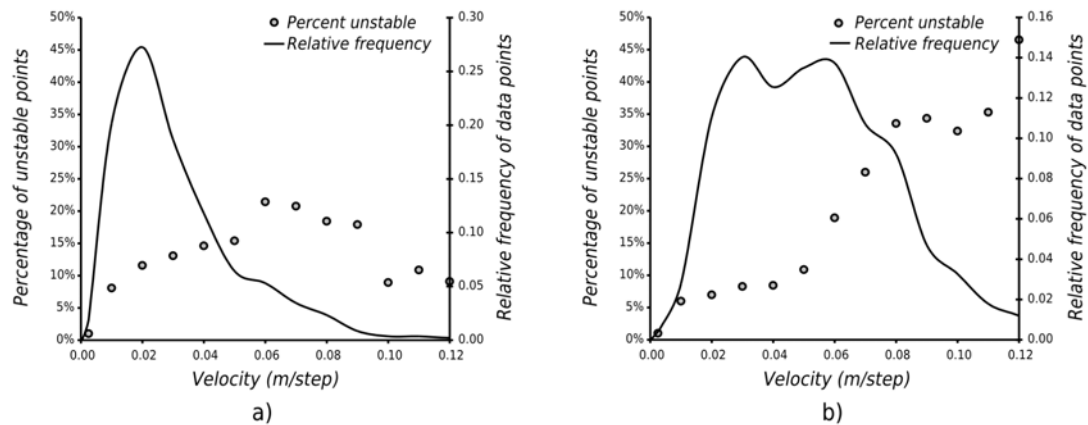


Figure 13.25 - Percentage of unstable points (left-hand y-axis) versus velocity for a) Block A and b) Block C stopes, with relative frequency of unstable data points (right-hand y-axis)

From Figure 13.25, it can be seen that over-break for Block A stopes generally occurs at lower velocity levels than Block C stopes. This suggests that the maximum velocity during mining increases with depth, and that with deeper mining, the rock mass between structures, either damaged or undamaged, is increasingly displaced with each mining step.

The overall low percentage of unstable points in Block A stopes, is thought to be mainly due bias from incomplete *CMS* data (see Figure 13.24). Block A stopes were the first to be mined at Kanowna Belle, during which procedures for *CMS* data collection were still being developed. This situation led to a number of stopes being surveyed when ore remained in the stope and/or during mid-stope extraction. In light of this, it is proposed to develop an instability criteria, based on velocity, using Block C data as shown in Figure 13.26. The proposed instability criteria shows an exponential relationship with a high correlation coefficient.

The relationship indicates that at velocities of >100mm per step in the model, there was a 0.50 correspondence with observed fall-off. In other words, if the model predicts a velocity of 100mm/step for any element, cell or node in the model, there is a 50% chance that element would report as over-break.

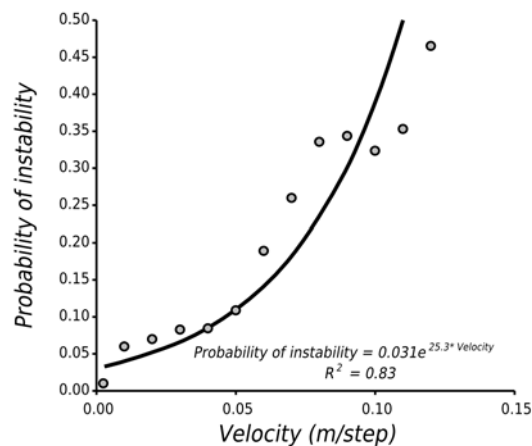


Figure 13.26 - Instability criteria based on velocity only

Plastic Strain Only

The relationship between plastic strain during stope extraction (regardless of velocity) and the percentage of 'unstable' points is shown in Figure 13.27. It must be noted that plastic strain values beyond 0.2 plastic strain (i.e. 20%) represent extremely damaged and comminuted rock mass and their inclusion adds little value to the analysis. As such, data beyond this value were deliberately truncated. The data suggests there is a reasonably good correlation between plastic strain and over-break instability, for both mining areas, up to around 3%. The relation between plastic strain and instability continues to correlate well beyond 3% plastic strain for Block C stopes, however, the relationship is poor after this value for Block A stopes.

It is considered that the poor relationship for Block A stopes after 3% plastic strain is again due to the bias towards 'stable' data points caused by incomplete *CMS* data. The data presented in Figure 13.27a could also suggest that highly yielded and severely damaged rock mass in Block A tends not to report as over-break. This could indicate that a high proportion of this yielded material is located in the floors and lower abutments, or 'arches' and is 'self-supporting', or is effectively supported by installed cable reinforcement elsewhere. Indeed, Figure 13.28 shows that the majority of 'stable' points are located in the lower sections of Block A stopes. These areas are also biased due to incomplete *CMS* data (c.f. Figure 13.24).

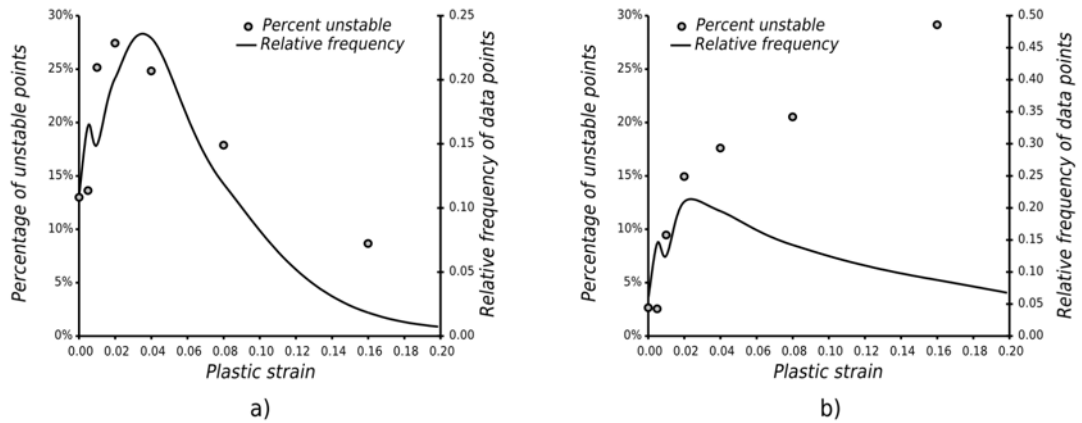


Figure 13.27 - Percentage of unstable points (left-hand y-axis) versus plastic strain for a) Block A and b) Block C stopes, with relative frequency of unstable data points (right-hand y-axis)

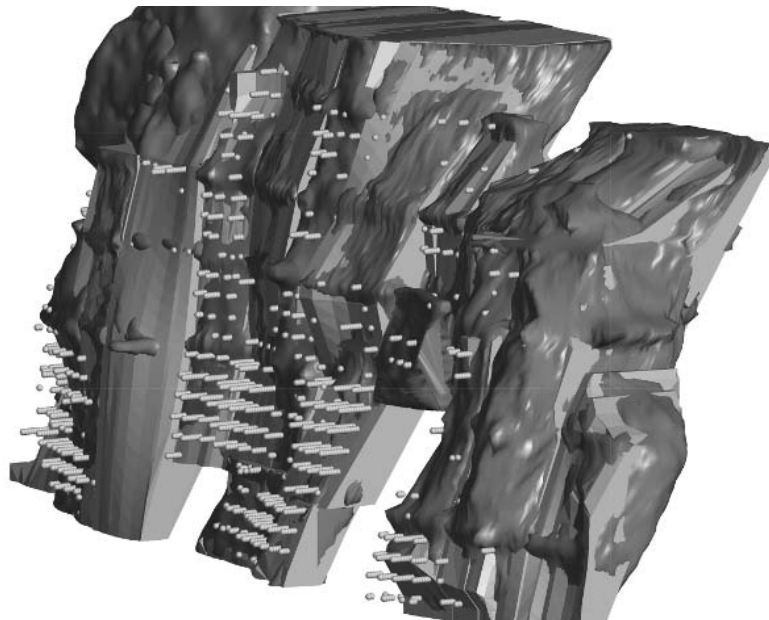


Figure 13.28 - Location of 'stable' data points in Block A where plastic strain > 0.03

Figure 13.27a also shows that appreciable levels of instability ($\approx 12\%$) occurs in Block A at little or no plastic strain. This could suggest that instability here is due to structural kinematic failures (i.e. undamaged rock) or other processes, such as blast induced rock mass damage. From Figure 13.27b it can be seen that plastic strain provides a good predictor of over-break instability for Block C stopes. The relationship indicates that the level of instability does not dramatically increase with increasing strain (c.f. velocity only), yet plateaus at higher strain levels. Importantly, the modelling suggests that instability due solely to plastic strain only accounts for a maximum of around 25-30% of observed instabilities. This highlights the importance of large scale structure and its role in instability and its influence on the strain field itself.

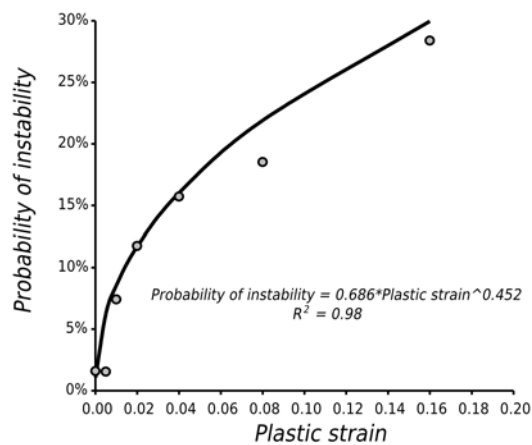


Figure 13.29 - Instability criteria based on plastic strain only

Due to the bias issues associated with Block A data, the plastic strain instability criterion was also developed using the Block C data (Figure 13.29). The criterion is a reasonable predictor of over-all instability, with a peak probability of fall off of 0.15-0.2 at more than 5% plastic strain, which corresponds to extremely comminuted material, or crushed rock (Beck and Duplancic, 2005). Rock masses with this corresponding level of plastic strain would almost certainly unravel if unconfined and exposed on a hangingwall. The reason why not all material with a plastic strain >5% is unstable, is that some of this material is located deep in the hangingwall adjacent to structures, with unyielded, kinematically restrained material in front (see Figure 13.23). In addition, yielded material which is located in the walls and abutments close to the floors of the stopes may not be kinematically able to report as over-break.

13.8.10 Instability Criteria as a Predictor and Design Tool

The correlations of instability with velocity and plastic strain are encouraging in terms of predictors of future instability, and hence appear attractive as design tools. In this regard, levels of instability can be predicted for a variety of stope geometries, layouts and sequences by forward numerical analysis. Simplistically, points in the forward analysis that display large velocities are predicted to have a very high likelihood of being associated with instability. Points showing high levels of plastic strain, low levels of confinement and are exposed at a hangingwall, are expected as having a moderate chance of reporting as fall-off. The plastic strain criterion is a useful lower bound on over-break, but requires additional interpretation to identify exposed damage and over-break potential.

In this thesis, velocity and plastic strain parameters have been investigated individually as potential instability criteria. Instability criteria can also be developed based on combinations of velocity, plastic strain or other parameters, or components of parameters. The challenge is to select the parameters or components that produce the most effective instability criteria for specific conditions. Figure 13.30a shows an example use of the velocity instability criteria as a prediction tool. Here contours of predicted maximum velocity (during mining) for the hangingwall are shown together with the modelled stope shape, together with the actual CMS profile for reference. From Figure 13.30a, there is very good agreement between the predicted maximum velocity of around 0.03m/step and the resulting over-break geometry. Figure 13.30 also shows modelled plastic strain.

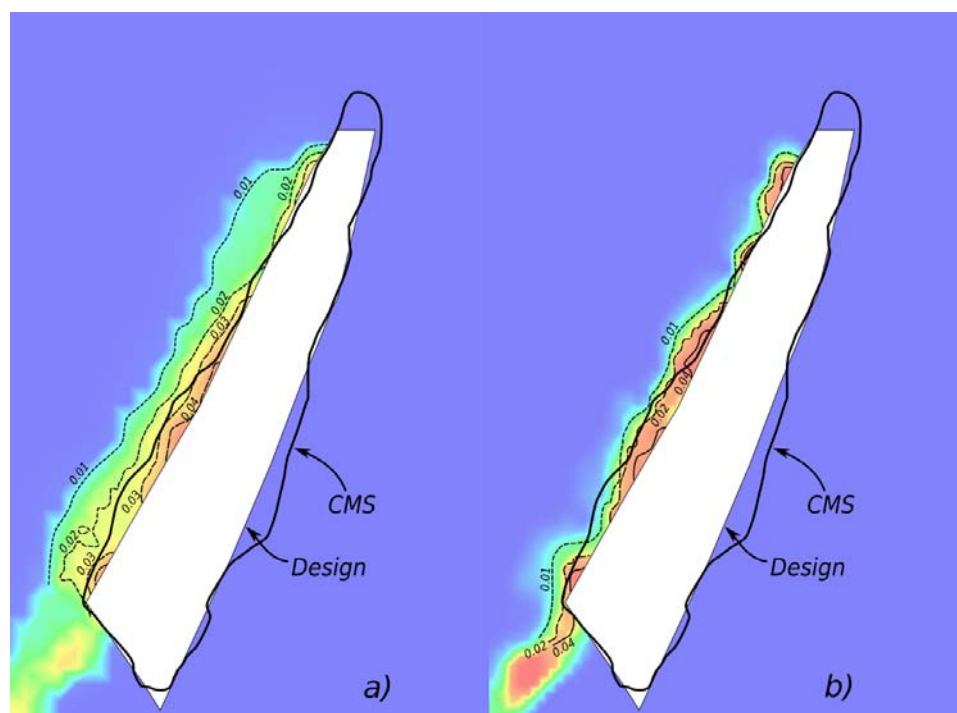


Figure 13.30 - Cross-section at 20032mE showing design and CMS geometries together with modelled a) velocity (m/step), b) plastic strain for the hangingwall.

The probability of instability can therefore be estimated for the desired level of velocity, plastic strain or alternate instability criteria as required. Figure 13.31 shows the estimated probability of hangingwall instability, during mining, using the velocity instability criteria. It must be noted that the probabilities on the long section are only appropriate for a particular mining sequence. In this case Figure 13.31 represents the actual mined sequence, which accounts for the apparent disjointed contour pattern. The predicted probability of instability can then be compared to actual performance using the techniques outlined in the following sections.

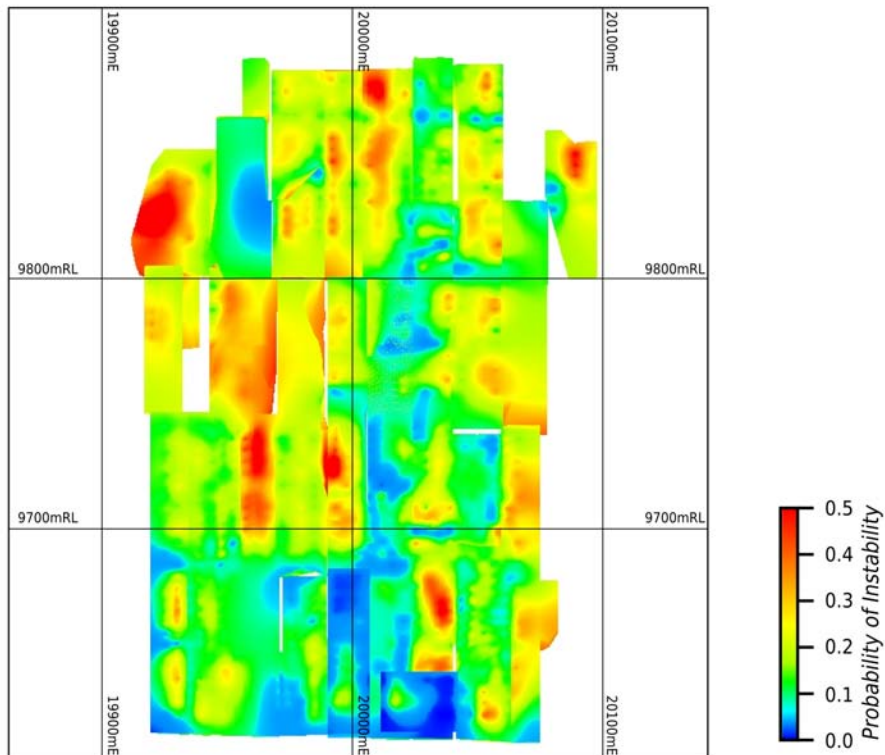


Figure 13.31 - Long section of Block C stopes showing probability of hangingwall instability, estimated from the velocity instability criteria.

Volume Of Instability

The 3-dimensional contours (i.e. isosurfaces) of the selected instability criteria can be used to estimate the expected volume of failure for a stope of a certain size in the given mining sequence (Figure 13.32). The volumes and respective probabilities of instability can be interpolated to derive a probability density function (Figure 13.33). Resulting probability density functions can be used to compare anticipated relative performance between stopes. Examples for two selected Block C stopes are shown in Figure 13.34 (In this case, x and y axes have been swapped for easier interpretation). It is suggested that alternate point estimation method (*APEM*) (Harr, 1989) be used to account for material property variability in the model and to define the confidence intervals around the volume of failure curves (Reusch et al., 2008). Incorporated with volumes of failure and cost of over-break, the long section provided in Figure 13.31 can assist planners to identify **where** higher risk stopes will appear in the mining sequence, in both time and location.

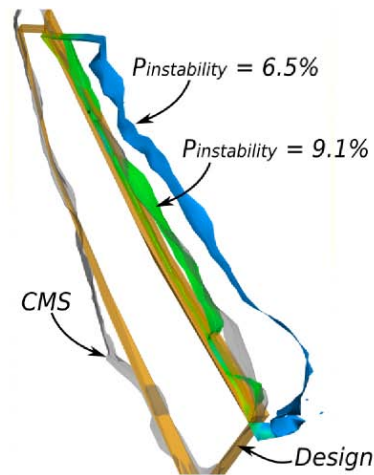


Figure 13.32 - Isometric section of stope CP0380 showing isosurfaces of probabilities of hangingwall instability based on velocity criteria.

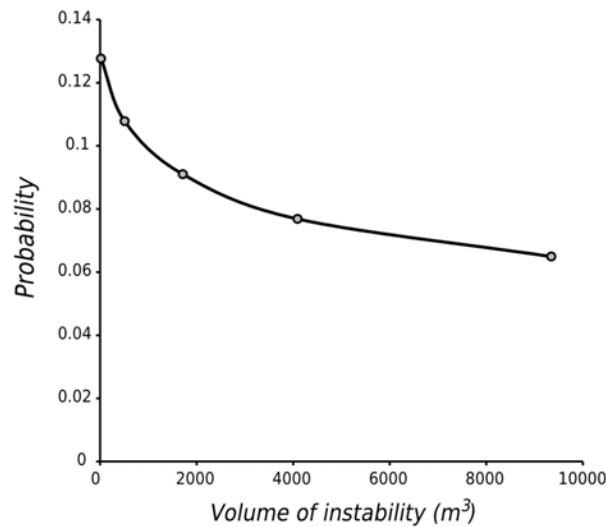


Figure 13.33 - Probability density function for volume of instability for stope CP0380

Expected Volume Of Instability

For a given modelled stope geometry and sequence, the expected volume of instability can therefore be obtained by multiplying the volume of the isosurface by the cumulative distribution function of probability of instability;

$$E[Vol] = \int_{T_c}^{T_0} f(t) dt * V(t) \quad (13.2)$$

where $f(t)$ is the probability density function for instability at value t and $V(t)$ is the corresponding isosurface volume for that probability. From Figure 13.26, it can be seen that the fitted curve to the velocity instability criteria does not pass through the origin (i.e. there is a small probability of instability at zero velocity). In order to avoid generating isosurfaces

with infinite volumes, albeit very small probabilities of instability, it is necessary to either force the instability criteria through the origin, or to select a cut-off probability (indirectly by its associated maximum volume of instability). Here, T_c refers to the minimum probability cut-off (at a selected maximum volume). For the analysis, a minimum probability of instability of 5% was selected for T_c . Parameter T_o refers to the maximum probability of instability, that is, where the predicted volume of instability is effectively zero. The expected volume of instability can then be estimated using the trapezoidal rule for integration. The probability density function of volume of instability for back analysed Block C stopes is provided in Appendix F.

Reliability Of Forward Analysis Criteria

The expected volume of failure can be used to as a forward analysis performance indicator for comparing different stope geometries or sequences and also as tool to assist in model calibration and assess model reliability. From Figure 13.34, it can be seen that stope CP0380 is expected to perform better than stope C9380, with maximum probabilities of instability of 14% and 42%, respectively at V_o . However, actual performance shows that indicates C9380 performed better than CP0380. Model reliability can also be ascertained by comparing actual versus expected volume of instability for individual stopes. Figure 13.34 shows that stope CP0380 actually performed worse than anticipated, in this case, the model under-predicted instability. Figure 13.34 also shows that the model over-predicted instability for stope C9380, with the degree of over-prediction higher than the prediction difference for stope CP0380. In this case, it could be argued the model is more reliable in the region for stope CP0380.

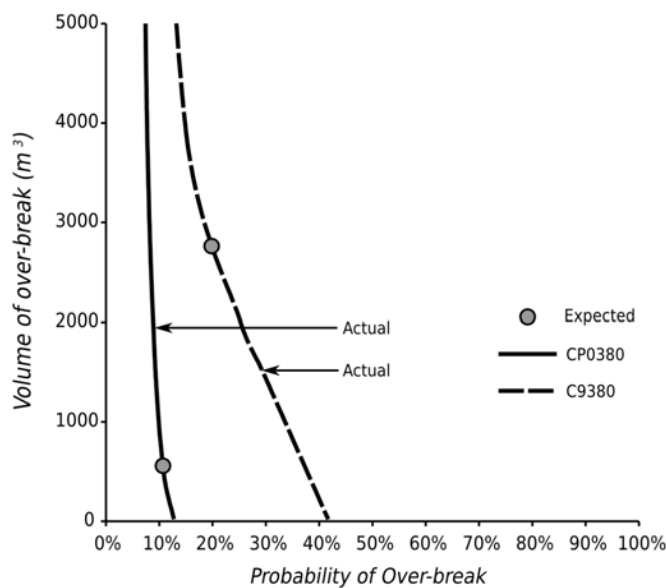


Figure 13.34 - Plot of predicted volume of instability versus probability of instability for stopes CP0380 and C9380, showing actual and expected volumes of instability

The reliability of the predictive capability of the instability criteria based on velocity was then assessed using the techniques proposed in section 11.7.2, by direct volumetric comparison of actual versus predicted over-break. In order to provide scale independent assessments, relative volume of over-break was used as the performance assessment criteria. Figure 13.35a shows the actual relative volume of back analysed stopes against the relative volume of the predicted, or expected volume, of over-break. It can be seen that there is a general positive correlation between the actual and predicted, however, there are some cases where there are extreme differences between expected and actual over-break. In order to quantify the degree of over- and under-prediction, the percentage increase or decrease in expected relative volume over the actual relative volume was assessed (i.e. over-prediction and under-prediction, respectively) for each stope. The results were then plotted as a cumulative percentage graph shown in Figure 13.35b. It can be seen that, on average, the instability criteria based on velocity only over-predicts over-break by around 23%. This is in some ways expected, as the influence of rock reinforcement has not been explicitly taken into consideration by the modelling. The quantification technique presented shows that over-break can be predicted with reasonable accuracy (within $\pm 30\%$) in only around 40% of cases. It should also be noted that Figure 13.35b was heavily influenced by data from two stopes (plotted in the bottom middle portion of Figure 13.35a) where the over-prediction was more than 100%. Removal of these two case studies would significantly improve the overall predictive capability using the selected instability criteria.

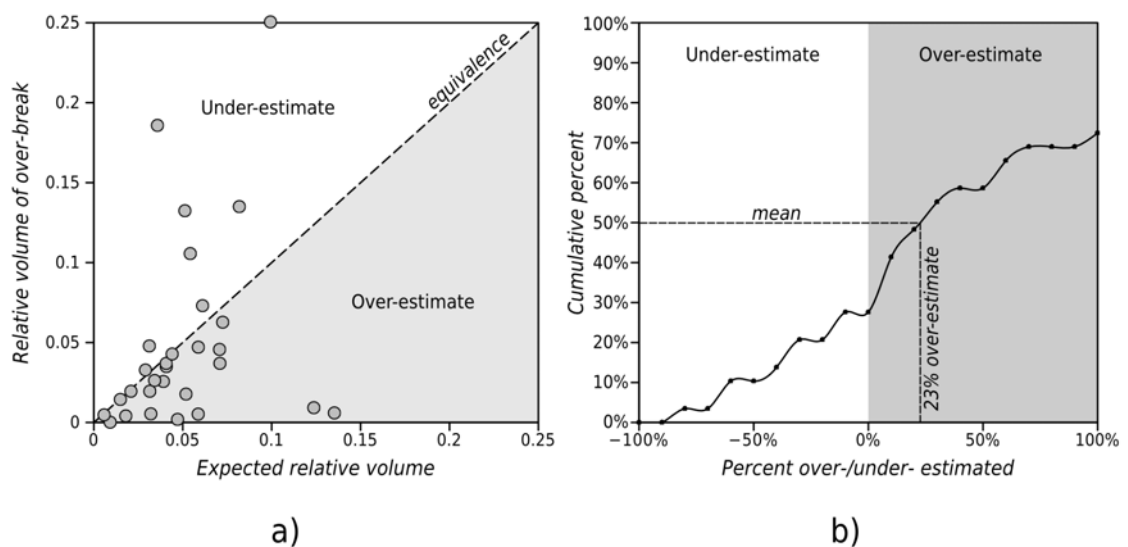


Figure 13.35 - Plot of a) Actual relative volume versus expected (predicted) relative volume, and b) cumulative percent of over-/under- estimations based on relative volume

The results of the reliability quantification can also be plotted spatially to determine *where* performance has been over- or under- predicted (Figure 13.36). This provides the design engineer with the location of stopes in order to investigate additional factors which may have contributed to poorer than anticipated performance (i.e. under-estimates of instability),

such as poor implementation, poorer rock mass or unknown geological conditions. Conversely, over-predicted instability can highlight optimal implementation practices and rock reinforcement performance, or alternatively potential under-break and ore loss.

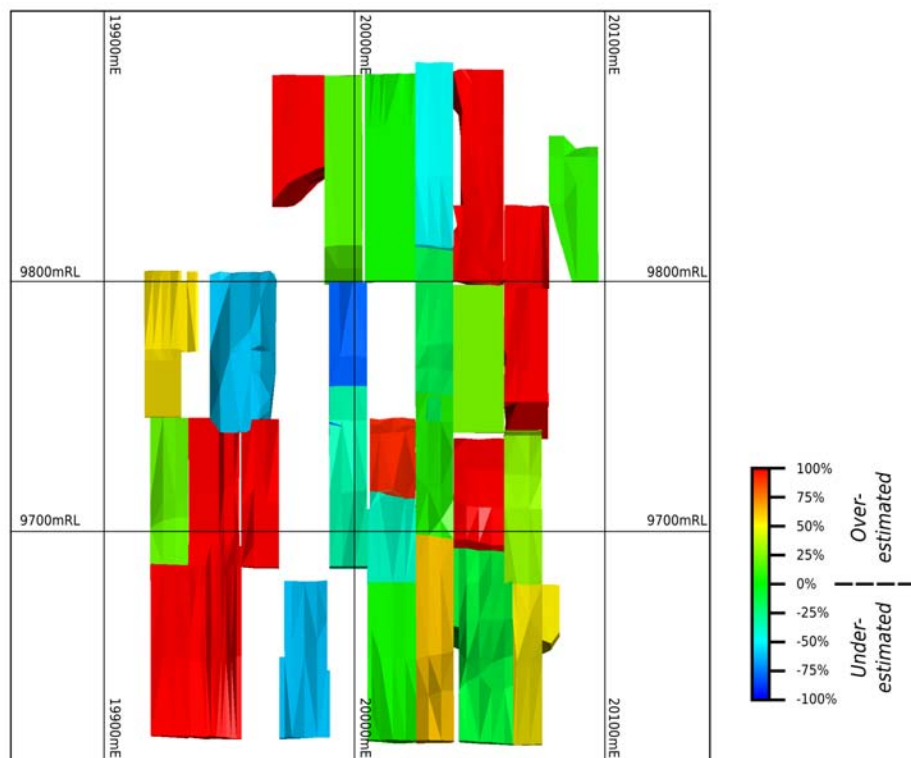


Figure 13.36 - Long section of Block C stopes showing percentages of over- and under-estimation of instability based on velocity instability criteria.

13.8.11 Discussion

The combination of the capabilities of 3-dimensional non-linear numerical code and *LR2* constitutive parameters enables stope geometries and sequences, multi-scale explicit deterministic discontinuities, and resulting instability mechanisms to be directly captured in the modelling. The modelling exercise was significant in that an intense array of stope-scale structures were directly incorporated to explicitly model discontinuous behaviour at the stope scale. The results of the modelling not only identified the importance of stope-scale structure on discontinuous behaviour, yet also its role and influence on the strain field as well.

In this example, only plastic strain and velocity were used to develop instability criteria, yet other parameters and combinations of parameters (e.g. level of confinement, volumetric versus shear strain, etc.) and their contribution to instability should be investigated. Importantly, the velocity instability criterion developed was only made possible by the inclusion of the detailed stope-scale structure model. It is therefore imperative that mines

develop accurate stope-scale models for detailed planning and design studies that utilise numerical modelling techniques.

The non-linear modelling exercise also demonstrated the value in combining the proposed design reliability techniques and geometric performance measures (sections 11.7.2 and 6.8, respectively) to quantify the predictive capability of selected instability criteria. This approach can be used to compare and quantify the reliability of different instability criteria and, importantly, show *where* differences exist.

13.9 CONCLUSIONS

The chapter has demonstrated a number of practical applications of the integrated approach to open stope design as applied at Kanowna Belle Gold Mine. This chapter has shown how a sound understanding and integration the structural geology is required in order to develop realistic rock mass models by assisting in; definition of rock mass domains, development of interpolation parameters, constraining interpolations and validation of deterministic discontinuity models. The chapter also demonstrated a practical application of the proposed deterministic discontinuity modelling technique in order to develop a highly detailed stope-scale discontinuity model. The combined deterministic discontinuity and spatial rock mass models were then used to assess the variability of rock mass conditions along stope-scale structure, and to indicate the influence of large scale structures on local rock mass conditions. Similar behaviour was also observed at the Cannington Mine (Chapter 12).

From a rock engineering design perspective, the example back analysis exercises have demonstrated the value of integrating rock mass characterisation models with numerical modelling and performance data to develop improved and more reliable design approach whilst still using linear elastic back analysis techniques. It has also been shown that non-linear numerical modelling can allow for more complex material behaviour to be incorporated into the back analysis. It is considered that the non-linear modelling approach taken represents a significant advance in capturing rock mass response mechanisms, particularly at the stope scale. This has only been achieved by the direct incorporation of such a highly detailed stope-scale deterministic discontinuity model.

Both numerical modelling exercises presented in this chapter demonstrate that substantial improvements in the detail and reliability of instability criteria that can be achieved over traditional empirically based design methodologies, which rely on 'stability' classifications, or at best, scale-dependent *ELOS* estimations that provide little or no geometric information on

over-break. The approach taken in this thesis enables prediction of volumes, shapes and likelihood of over-break on a mining block scale, as well as indicating where it will occur for a given mining geometry and sequence. Importantly, the predictive capability or reliability of the instability criteria can be quantified. Expected volumes of failure and associated costs can be quantified for a number of mine geometries and sequences and then be incorporated into quantitative risk-based design methodologies similar to those demonstrated in Chapter 12. It is therefore considered that the techniques demonstrated in this thesis provides the design engineer with an invaluable planning and design tool.

CHAPTER 14 - CONCLUSIONS

14.1 AN INTEGRATED APPROACH TO THE GEOTECHNICAL DESIGN OF OPEN STOPES

In relation to the design of open stopes, optimal design is achieved through continual re-assessment, or retrospective analysis, of rock mass characterisation, geotechnical models, rock engineering design methodologies and stope performance. The primary reason for this established approach is due to the uncertain nature of the engineering properties of the rock mass and their influence on potential responses to mining.

This thesis proposes a framework that attempts to integrate different rock mass characterisation models, numerical modelling and stope performance data to assist in improving the overall excavation design process. A key philosophy behind the design optimisation process is the continual reduction in uncertainty in collected data, analysis and design methods used with a view to improving the overall reliability of the design. The proposed approach attempts to ensure that the appropriate methodologies in data collection, data analysis, rock mass model formulation and stope design are utilised at relevant project stages in order to minimise uncertainty and maximise design reliability. The design optimisation approach recognises that the appropriateness of a particular design methodology is highly dependant on the availability of an appropriate rock mass model, which is in turn dependant on the availability of quality rock mass data.

14.2 MAIN FINDINGS AND ACHIEVEMENTS OF RESEARCH

With respect to the design of spans in open stope mining, the key aims of the proposed integrated approach were to develop guidelines to;

- Assess the suitability of data for analysis
- If data is unsuitable, assess the most appropriate data collection strategy
- Assess the most appropriate approach to rock mass modelling
- Assess the most appropriate design methodologies
- Assess the reliability of the design criteria and quantify the potential economic impact of the design on the project

In this regard, the key objectives of this thesis were to investigate and develop an integrated system of improved techniques for use in the design of open stope mines, principally in the areas of;

- Rock mass data collection and management
- Rock mass characterisation and rock mass modelling techniques
- Collection and analysis of stope performance data and its integration into the mine-design process
- Selection of appropriate and reliable open stope mine design techniques

Some specific achievements of the research in relation to these aims and objectives are described below.

During the development of the thesis, it was recognised that rock mass characterisation data can come from a variety of disparate sources, with each source offering different levels of data quantity and quality (degree of subjectivity, precision, accuracies and biases issues). In light of this, a rock mass data model has been developed that is capable of storing data from a variety of rock mass characterisation data collection methods. The data model is able to store data from objective data collection techniques such as; drill core logging, scanline mapping, window mapping, results from digital photogrammetry and laser scanning, as well as data from subjective data collection techniques such as geological face and backs mapping. The data model allows for standard methods for correct statistical treatment of biases based on the adopted sampling technique, as well as statistical analysis of geometric discontinuity parameters (i.e. spacing, persistence and orientation) to improve both accuracy and precision of data. The rock mass data model allows for systematic organisation of data to enable spatial data analysis, complex multivariate analysis techniques and development of a variety of rock mass characterisation models.

The study has highlighted that there are many approaches to rock mass modelling, from simplistic statistical tabulation of rock mass characteristics to stochastic-geometric discontinuity network models and spatial models of various rock mass parameters. The approach taken to developing a rock mass model requires consideration of the engineering objectives, level of project development, and design methodologies and analyses to be employed. This will then dictate the scale, complexity, and detail required of the model. The present study has shown, through the rock mass characterisation framework, that the quality, quantity and distribution of the underlying data has a significant impact on our understanding of the potential rock mass behaviour and the reliability of rock mass models and subsequent analyses. The rock mass characterisation framework and digital rock mass data model provide invaluable tools for the planning and execution of ongoing rock mass characterisation programmes.

An important objective of this thesis was to investigate the development of models that account for the spatial variability of rock mass parameters, such that stope design can be optimised in various regions of the mine according to local conditions. Geostatistical models have been shown to provide insights into the spatial variability of rock mass properties for engineering design, however there still are a number of aspects that hinders their full and comprehensive inclusion into rock mechanics applications. These include; stationarity assumptions, strict data requirements in terms of sample sizes, spacing and data distribution for multi-directional variography studies and block model resolution issues. In order to overcome some of these issues the thesis demonstrated a novel application of implicit function-based techniques (using *RBF*'s) for the spatial modelling of engineering rock mass parameters. The Implicit function modelling approach alleviates some of the resolution issues associated with block modelling techniques, and is particularly well suited to the modelling of irregularly sampled and sparse data sets.

The study has shown that, whilst spatial modelling of the majority of rock engineering rock mass parameters can be conducted in a similar fashion to traditional geological modelling, spatial modelling of discontinuity intensity is complicated by sampling directions and rock mass structure. Guidelines have been developed to evaluate the validity of spatial modelling of discontinuity intensity, based on the degree of anisotropy of the rock mass and sampling directions. Another contribution of the thesis was the development of the spherical variance test cell method to test for sampling anisotropy.

A detailed review was undertaken of existing rock mass classifications methods in relation to the design of open stopes. The review highlighted that rock mass classifications systems include interpretation and simplification of only some of the engineering geology, rock mechanics and rock engineering parameters. In this respect, they are unable to completely capture the complex rock mass interactions and behaviour under all geological regimes and boundary conditions, which may involve any number of failure mechanisms. Importantly, the study recognised the inappropriateness of *RQD* as a measure of discontinuity intensity as the excavation scale increases, and that other measures of discontinuity intensity, such as discontinuity linear frequency, are more appropriate for open stope design as they can be used irrespective of the scale of the excavation.

One of the important conclusions made during this thesis is that existing rock mass classification and empirical design methodologies represent non-rigorous design approaches and should be restricted to preliminary designs. Notwithstanding this, the thesis recommends that site specific empirical methods can be developed and used in the initial

construction stages in order to improve design reliability. In light of this, a number of guidelines have been proposed to assist in development of site-specific empirical design methods. A significant contribution of the thesis was the development of a number of methods to establish design reliability based on performance data. Practical application of the guidelines and design reliability methods was demonstrated on case study data.

The thesis also identified that existing measures of slope geometry and performance are unable to adequately capture comparisons of performance between slopes of differing shape and size. Indeed, it is difficult to determine whether a change in existing parameters are due to a change in “shape” or a change in “size” of either the over-break/under-break or the slope surface under investigation. During the course of this thesis new scale independent shape descriptors have been developed to enable quantification of the relative performance of slope surfaces, irrespective of their size. This important contribution allows inclusion of slope surfaces of vastly differing sizes to be included and compared in unbiased back analyses. This leads to an increase in the case history database than may otherwise be possible and lead to improved reliability in subsequent back analysis studies.

From the literature reviews and numerical modelling exercises, it is clear that large-scale discontinuities, such as faults, constitute one of the most important factors controlling slope performance. The rock mass characterisation case studies presented have also shown that large-scale structures can have a major influence on the spatial variability of rock mass parameters. An important contribution of this thesis has been the development of a deterministic discontinuity modelling technique that enables construction and validation of models of large-scale structures from a variety of rock mass characterisation data sources. The proposed implicit function approach removes some of the biases and subjectivity causes by manual interpretation, makes it possible to capture the subtle (real) surface profiles of structures, yet also has the ability to deal with noisy data, if required. The validation procedure is an important feature of the methodology as it allows development of models that include information not only on where the interpretation is valid yet where uncertainty exists in the model.

Importantly, the implicit function based approach, used in conjunction with the rock mass characterisation framework, can enable the rapid construction of deterministic discontinuity models. The semi-automated approach enables structures to be regenerated quickly with the inclusion of new data, providing engineers and geologists with up-to-date detailed models. Accurate models of large-scale discontinuities are also important in domain definition or for optimising domain boundaries. Because of their implicit basis, boundaries

can be quickly shifted. Alternatively, the deterministic models can be used to select data. For example, distance fields can be used to rapidly query data nearby or on a certain structure.

A number of improvements to linear elastic continuum based back analysis techniques have been proposed in order to improve the reliability of instability criteria. The proposed improvements also include methods to assess the appropriateness of continuum models based on discontinuity intensity and critical span.

A novel approach taken in the thesis employed the use of implicit functions to indirectly incorporate the effects of large scale structures and other parameters in numerical modelling and empirical design. The significance of the approach is that it is able to account for structural complexity, scale and features that cannot be directly incorporated into traditional design methods. The case study back analyses demonstrated the value of integrating rock mass characterisation models with numerical modelling and performance data to develop improved and more reliable instability criteria for use in design, even with the limitations associated with linear elastic modelling. Non-linear numerical modelling can allow for more complex material behaviour to be incorporated into the back analysis. It is considered that the non-linear modelling approach demonstrated in the thesis represents a significant advance in capturing rock mass response mechanisms, particularly at the stope scale. This approach has only been possible by the development and direct incorporation of the highly detailed stope-scale deterministic discontinuity model.

The thesis demonstrated how development of instability criteria can enable prediction of volumes, shapes and likelihood of over-break, as well as indicating where it will occur for a given mining geometry and sequence. The thesis also demonstrates the development of techniques to quantify the predictive capability or reliability of any potential instability criteria. It is considered that these developments provide the design engineer with an invaluable planning and design tool in order to assess expected volumes of failure and associated costs, for any particular mine geometry/sequence, and to quantify risks between design alternatives.

14.3 THESIS LIMITATIONS AND RECOMMENDATIONS FOR FUTURE WORK

The integrated approach presented has primarily concentrated on the rock engineering design of unreinforced open stope walls. The approach presented would greatly benefit from incorporation and detailed treatment of rock reinforcement and drill and blast design principles. Further work is also warranted on how the proposed rock engineering approach

can be integrated with other mine design activities and considerations, such that complete and reliable evaluations of design alternatives can be made.

It is considered that the deterministic discontinuity modelling technique developed in this thesis could be further improved by developing a hybrid approach, by incorporating the advantages of geological rule-based and stochastic-mechanistic methods. Stochastic-mechanistic methods enable development of a strict mine-scale structural geological framework, whilst rule-based-methods can improve local estimation accuracy of discontinuity systems. This could be especially important for sparsely sampled rock masses with limited excavation scale exposures (i.e. block cave mines). However, this approach still requires a minimum number of mapping exposures for highly detailed mapping and analysis to enable empirical rules to be developed.

Both stochastic-geometric and deterministic discontinuity models rely on discontinuity data collected from limited rock mass exposures. The case studies presented indicated that the widespread use of shotcrete in underground mine development can hinder access to the exposed rock mass for data collection purposes. It is considered that this will become a growing problem as mine development heads deeper into higher stressed rock masses and more challenging conditions where shotcrete and/or mesh is applied as a matter of course. It is imperative that routine collection of discontinuity data is integrated into the development cycle prior to application of shotcrete or mesh. A number of mines now routinely undertake digital photogrammetry prior to shotcrete application, however, it is yet to be seen whether they have taken full advantage of the data collected by developing more detailed and reliable rock structure models. Given these issues, and others highlighted in Appendix A, further research is warranted into the correct treatment of biases for remote methods, as well as improving resolution issues in order to capture surface characteristics, and facilities to record and capture discontinuity terminations, and structural hierarchy.

The work in the present study recognised that *CMS* profiles do not necessarily define the excavation damage zone (*EDZ*) or yield zone of rock mass and that their inclusion in back analysis studies can be a source of uncertainty. Unfortunately, the back analysis studies presented in the thesis relied heavily on *CMS* data, principally due to a lack of instrumentation and monitoring data. Reliability of derived instability criteria could have been significantly improved with the integration of instrumentation and monitoring data. Research on methods for routine integration of displacement and strain data in back analyses utilising non-linear numerical modelling is highly recommended.

The non-linear modelling exercise indicated that some areas of the model displayed low reliability in predicting performance. For example, 'unstable' volumes of rock mass were predicted as 'stable' by the non linear modelling (i.e. low strain and low velocity). It is important to identify these areas as they could be used as an investigative tool in order to understand possible explanations for discrepancies. Here, the cause may be due to features and processes not directly accounted for in the numerical model, such as; unidentified stope-scale structure, unexpected material property variability, or blast induced rock mass damage. Further research in this area is warranted. In addition, it is considered that integrated approach would benefit from the incorporation of quantitative blast damage models in order to improve reliability and predictive performance.

REFERENCES

- 3G Software and Measurement. (2008). Contact free acquisition and assessment of rock and terrain surfaces by metric 3D images. http://www.3gsm.at/eng/home_eng.asp?ID=1. (accessed , 2008).
- ADAM Technology. (2008). 3D Measurement Software and Solutions. <http://www.adamtech.com.au>. (accessed , 2008).
- Adu-Acheampong, A. (2003). Stability of open stopes intercepted by graphitic shears at Ashanti Goldfields Company Ltd., Obuasi Operations in Ghana. In , *In Proceedings of the 2003 SME Annual Meeting*, 6p.
- Archibald, N., Beckett, S and Seery, J. (1999). A Field Guide to the Geology of the Kanowna Belle Gold Mine Open Pit. Fractal Graphics, Perth. Unpublished Company Report.
- ASTM (1986). Standard test method of unconfined compressive strength of intact rock core specimens. D 2938. pp.390-391.
- Attewell, P. and Farmer, I. (1976). *Principles of engineering geology*. Chapman & Hall Ltd, London.
- Ayalew, L., Reik, G and Busch, W. (2002). Characterizing weathered rock masses - a geostatistical approach. *Int. J. Rock. Mech. Min. Sci.*, **39**, pp.105-114.
- Baczynski, N. (1980). *Rock Mass Characterisation and its Application to Assessment of Unsupported Underground Openings*, PhD Thesis. University of Melbourne, 248p.
- Baecher, G. and Christian, J. (2003). *Reliability and Statistics in Geotechnical Engineering*. John Wiley & Sons, Chichester, England.
- Baecher, G. and Lanney, N. (1978). Trace length biases in joint surveys. In Y. Kim (ed.), *Proceedings 19th US Symposium on Rock Mechanics*, University of Nevada, Reno, pp. 56-65.
- Baecher, G., Einstein, H and Lanney, N. (1977). Statistical description of rock properties and sampling. In , *Proceedings of the 18th U.S. Symposium on Rock Mechanics*, pp. 1-8.
- Barton, N. (1988). Rock Mass Classification and Tunnel Reinforcement Selection Using the Q-System. In L. Kirkaldie (ed.), *Rock Classification Systems for Engineering Purposes*. American Society for Testing and Materials, Philadelphia, pp.59-84.
- Barton, N., Lien, R and Lunde, J. (1974). Engineering Classification of rock masses for the design of tunnel support. *Rock Mech.*, **6**, pp.189-236.
- Barton, N., Løset, F, Lien, R and Lunde, J. (1980). Application of the Q-system in design decisions. In M. Bergman (ed.), *Subsurface space*, New York: Pergamon, pp. 553-561.
- Beck, D. and Duplancic, P. (2005). Forecasting Performance and Achieving Performance Indicators in High Stress and Seismically Active Mining Environments. In Y. Potvin and M. Hudyma (ed.), *Proceedings of the 6th International Symposium on Rockbursts and Seismicity in Mines, Perth, Australia, 9-11 March*, pp. 409-418.

- Beckett, T., Fahey, G, Sage, P and Wilson, G. (1998). Kanowna Belle Gold Deposit. In D. Berkman and D. Mackenzie (ed.), *Geology of Australian and Papua New Guinean Mineral Deposits*, Australiasian Institute of Mining and Metallurgy, Melbourne, pp. 201-206.
- Betts, P.G., Giles, D, Mark, G, Lister, G, Goleby, B and Ailleres, L. (2006). Synthesis of the proterozoic evolution of the Mt Isa Inlier. *Aust. J. Earth Sci.*, **53**, pp.187-211.
- Bieniawski, Z. (1973). Engineering Classification of Jointed Rock Masses. *Transactions of the South African Institute of Civil Engineering*, **15**, pp.335-344.
- Bieniawski, Z. (1974). Geomechanics classification of rock masses and its application to tunnelling, in Advances in Rock Mechanics. In , *Proceedings of the Third Congress of the International Society for Rock Mechanics*, National Academy of Sciences, Washington, pp. 27-32.
- Bieniawski, Z. (1978). Determining rock mass deformability – experience from case histories. *Int. J. Rock Mech. Min. Sci. Geomech. Abstr.*, **15**, pp.237-247.
- Bieniawski, Z. (1989). *Engineering Rock Mass Classifications*. Wiley, New York.
- Bieniawski, Z. (1993). Design Methodology for Rock Engineering: Principles and Practice.. In J. Hudson (ed.), *Comprehensive Rock Engineering*. Pergamon Press, pp779-793.
- Bingham, C. (1964). *Distributions on the sphere and on the projective plane*, PhD Thesis. Yale University, 93p.
- Binns, M. (2004). Cannington Geotechnical Model Improvements and Testing. Hatch Limited. Unpublished Internal Memorandum to BHP Cannington Mine. p17.
- Birch, J. (2006). Using 3DM Analyst Mine Mapping Suite for Rock Face Characterisation. Workshop on "Laser and Photogrammetric Methods for Rock Face Characterisation". In F. Tonon and J. Kottenstette (ed.), *41st U.S. Rock Mechanics Symposium. American Rock Mechanics Association. Colorado School of Mines, June 17-18*, pp. 13-32.
- Blake, D. (1987). Geology of the Mount Isa Inlier and environs, Queensland and Northern Territory. . Bureau of Mineral Resources Bulletin No. 225.
- Blake, D. and Stewart, A. (1992). Stratigraphic and tectonic framework, Mount Isa Inlier. In A. Stewart and D. Blake (ed.), *Detailed Studies of the Mount Isa Inlier*, Australian Geological Survey Organisation Bulletin No. 243, pp. 1-11.
- Board, M. (1989). Examination of the use of continuum versus discontinuum models for design and performance assessment for the Yucca Mountain site. Prepared for Division of High-Level Waste Management, Office of Nuclear Material Safety and Safeguards, US Nuclear Regulatory Commission. Unpublished report No. NUREG/CR--5426 TI89 016813. p83.
- Bodon, S. (1998). Paragenetic Relationships and Their Implications for Ore Genesis at the Cannington Ag-Pb-Zn Deposit, Mount Isa Inlier, Queensland, Australia. *Econ. Geol.*, **93**, pp.1463-1485.
- Bodonyi, J. (1970). Laboratory tests of certain rocks under axially symmetrical loading conditions. In , *Proceedings of the Second Congress of the International Society for Rock*

- Mechanics, Belgrade*, pp. 389-397.
- Bonnet, E., Bour, O, Odling, N, Davy, P, Main, I, Cowie, P and Berkowitz, B. (2001). Scaling of Fracture Systems in Geological Media. *Rev. Geophys.*, **39**, pp.347-383.
- Brady, B. and Brown, E. (2004). *Rock Mechanics for Underground Mining*. Kluwer Academic Publishers.
- Bridges, M. (1990). Identification and characterisation of sets of fractures and faults in rock. In Barton and Stephansson (ed.), *Proceedings of the International Symposium on Rock Joints*, Balkema, Rotterdam, pp. 19-26.
- Broch, E. and Franklin, J. (1972). The Point-Load Strength Test. *Int. J. Rock Mech. Min. Sci. Geomech. Abstr.*, **9**, pp.669-676.
- Brown, E. (1985). From theory to practice in rock engineering. *Trans. Inst. Min. Metall. (Sect A: Min. industry)*, **94**, pp.67-83.
- Brown, E. and Rosengren, K. (2000). Characterising the Mining Environment for Underground Mass Mining. In , *MassMin 2000*, Aus.I.M.M, Brisbane, Australia, pp. 17 - 27.
- Brzovic, A. and Villaescusa, E. (2007). Rock mass characterization and assessment of block-forming geological discontinuities during caving of primary copper ore at the El Teniente mine, Chile. *Int. J. Rock. Mech. Min. Sci.*, **44**, pp.565-583.
- Bye, A. (2006). The strategic and tactical value of a 3D geotechnical model for mining optimization, Anglo Platinum, Sandsloot open pit. *J. S. Afr. Inst. Min. Metall.*, **106**, pp.97-104.
- Carr, J., Beatson, R, Cherrie, J, Mitchell, T, Fright, W, McCallum, B and Evans, T. (2001). Reconstruction and Representation of 3D Objects with Radial Basis Functions. In, *ACM SIGGRAPH '01, Los Angeles, CA*, Springer, pp. 67-76.
- Caumon, G., Collon-Drouaillet, P, Le Carlier de Veslud, C, Viseur, S and Sausse, J. (2009). Surface-Based 3D Modeling of Geological Structures. *Math. Geosci.*, **41**, pp.927-945.
- Cepuritis, P. (2004). Three-dimensional rock mass characterisation for the design of excavations and estimation of ground support requirements. In Villaescusa, V and Potvin, Y (ed.), *Ground Support in Mining and Underground Construction*, A.A. Balkema, Rotterdam, pp. 115-128.
- Chan, L. (1986). *Application of block theory and simulation techniques to optimum design of rock excavations*, PhD Thesis. University of California, Berkeley, LA, p.
- Chau, K. and Wong, R. (1996). Technical Note: Uniaxial Compressive Strength and Point Load Strength of Rocks. *Int. J. Rock Mech. Min. Sci. Geomech. Abstr.*, **33**, pp.183-188.
- Cividini, A. and Gioda, G. (1993). Numerical Back Analysis Techniques for Rock Engineering. In (ed.), *Assessment and Prevention of Failure Phenomenon in Rock Engineering*. Balkema, Rotterdam, pp11-21.
- Clark, L. and Pakalnis, R. (1997). An Empirical Design Approach for Estimating Unplanned Dilution from Open Stope Hangingwalls and Footwalls. In , *Proceedings of the 99th AGM - CIM*, Vancouver, pp. 25.

- Coggan, J., Stead, D and Eyre, J. (1998). Evaluation of techniques for quarry slope stability assessment. *Trans. Inst. Min. Metall. (Sect B: App. Earth Sc.)*, **107**, pp.B139-B147.
- Coles, D. (2007). *Performance of Open Stopes at BHP-Billiton Cannington Mine*, B.Eng. Thesis. Western Australian School of Mines, Curtin University of Technology, 161p.
- Conolly, H. (1936). A contour method of revealing some ore structures. *Econ. Geol.*, **31**, pp.259-271.
- Cox, D. and Miller, H. (1965). *The Theory of Stochastic Processes*. Methuen, London.
- Cruden, D. (1977). Describing the Size of Discontinuities. *Int. J. Rock Mech. Min. Sci. Geomech. Abstr.*, **14**, pp.133-137.
- Davis, B. (1987). Uses and Abuses of Cross-Validation in Geostatistics. *Math. Geol.*, **19**, pp.241-248.
- Davis, J. (2002). *Statistics and Data Analysis in Geology*. John Wiley & Sons.
- de Kemp, E. (2000). 3-D visualization of structural field data: examples from the Archean Caopatina Formation, Abitibi greenstone belt, Quebec, Canada. *Comput. Geosci.*, **26**, pp.509-530.
- Deere, D. (1964). Technical description of rock cores for engineering purposes. *Rock Mechanics and Engineering Geology*, **1**, pp.17-22.
- Dershowitz, W. (1984). *Rock joint systems*, PhD Thesis. MIT, Cambridge, MA, 987p.
- Dershowitz, W. and Einstein, H. (1988). Characterising Rock Joint Geometry with Joint System Models. *Rock Mech. Rock Eng.*, **21**, pp.21-51.
- Dershowitz, W. and Herda, H. (1992). Interpretation of Fracture Spacing and Intensity. In Tillerson and Wawersik (ed.), *33rd U.S. Symposium on Rock Mechanics*, Balkema, Rotterdam, pp. 757-766.
- Dettinger, M. and Wilson, L. (1981). First Order Analysis of Uncertainty in Numerical Models of Groundwater Flow Part 1. Mathematical Development. *Water Resour. Res.*, **17**, pp.149-161.
- Deutsch, C. (2002). *Geostatistical Reservoir Modeling*. Oxford University Press, New York.
- Diederichs, M. (1999). *Instability of Hard Rock Masses: The Role of Tensile Damage and Relaxation*, PhD Thesis. University of Waterloo, 617p.
- Diederichs, M. and Kaiser, P. (1999a). Stability of large excavations in laminated hard rock masses: the voussoir analogue revisited. *Int. J. Rock. Mech. Min. Sci.*, **36**, pp.97-117.
- Diederichs, M. and Kaiser, P. (1999b). Tensile strength and abutment relaxation as failure control mechanisms in underground excavations. *Int. J. Rock. Mech. Min. Sci.*, **36**, pp.69-96.
- Diederichs, M., Kaiser, P and Eberhardt, E. (2004). Damage initiation and propagation in hard rock during tunnelling and the influence of near-face stress rotation. *Int. J. Rock. Mech. Min. Sci.*, **41**, pp.785-812.
- Drucker, D. and Prager, W. (1952). Solid mechanics and plastic analysis for limit design. *Quarterly of Applied Mathematics*, **10**, pp.157-165.

- Elbrond, J. (1994). Economic effects of ore losses and rock dilution. *CIM Bulletin*, **87**, pp.131-134.
- Escuder Viruete, J., Carbonell, R, Jurado, M, Marti, D and Perez-Estuan, A. (2001). Two-dimensional modeling and prediction of the fracture system in the Albala Granitic Pluton, SW Iberian Massif, Spain. *J. Struct. Geol.*, **23**, pp.2011-2023.
- Esterhuizen, G., Iannacchione, A, Ellenberger, J and Dolinar, D. (2006). Pillar stability issues based on a survey of pillar performance in underground limestone mines. In, *Proc. 25th Int. Conf. on Ground Control in Mining*, , pp. 354-361.
- Fairhurst, C. (1964). On the validity of the 'Brazilian' test for brittle materials. *Int. J. Rock Mech. Min. Sci. Geomech. Abstr.*, **1**, pp.535-546.
- Fisher, R. (1953). Dispersion on a sphere. *Proceedings of the Royal Society of London*, **A217**, pp.295-305.
- Franklin, J. (1971). Triaxial strength of rock material. *Rock Mech.*, **3**, pp.86-98.
- Gaich, A., Fasching, A and Gruber, M. (1999). High Resolution Stereoscopic Imaging for Tunnel Construction. *Felsbau*, **17**, pp.15-21.
- Giles, D. (2000). *Tectonic setting of Broken Hill-type mineralisation: the Cannington perspective*, PhD Thesis. Monash University, Melbourne, 215p.
- Goodman, R. (1976). *Methods of Geological Engineering in Discontinuous Rock*. West: St Paul.
- Goodman, R. and Shi, G. (1985). *Block Theory and its Application to Rock Engineering*. Prentice-Hall, New Jersey.
- Gray, D. (1992). Structural report on the Cannington Pb-Zn-Ag deposit, Mount Isa Inlier. Unpublished Report to BHP Minerals.
- Griffith, A. (1921). The phenomena of rupture and flow in solids. *Philosophical Transactions of the Royal Society, London*, **A221**, pp.163-197.
- Griffiths, D. and Fenton, G. (1993). Seepage beneath water retaining structures founded on spatially random soil. *Geotechnique*, **43**, pp.577-587.
- Hagan, T. (1980). A Case for Terrestrial Photogrammetry in Deep-Mine Rock Structure Studies. *Int. J. Rock Mech. Min. Sci. Geomech. Abstr.*, **17**, pp.191-198.
- Haile, A. (2004). A reporting framework for geotechnical classification of mining projects. *AusIMM Bulletin*, **5**, pp.30-37.
- Hajiabdolmajid, V. and Kaiser, P. (2003). Brittleness of rock and stability assessment in hard rock tunneling. *Tunn. Undergr. Sp. Tech.*, **18**, pp.35-48.
- Hammah, R. and Curran, J. (1998). Fuzzy Cluster Algorithm for the Automatic Identification of Joint Sets. *Int. J. Rock. Mech. Min. Sci.*, **35**, pp.889-905.
- Harr, M. (1989). Probabilistic estimates for multivariate analyses. *App. Math. Modelling*, **13**, pp.313-318.
- Harries, N. (2001). *Rock Mass Characterisation for Cave Mine Engineering*, PhD Thesis. University of Queensland, 492p.

- Harris, P. (2001). Structural Applications of Datamine at Mt Marion Gold Mine. In , *The Sharp End of the Pick: Innovations in Mining Geology*, Kalgoorlie, Australia, 12p.
- Hasofer, A. and Lind, N. (1974). An exact and invariant first-order reliability format. *Journal of the Engineering Mechanics Division, ASCE*, **100(ME1)**, pp.111-121.
- Hawkins, A. (1998). Aspects of rock strength. *Bull. Eng. Geol. Environ.*, **57**, pp.17-30.
- Hernandez-Stefanoni, J. and Ponce-Hernandez, R. (2006). Mapping the spatial variability of plant diversity in a tropical forest: comparison of spatial interpolation methods. *Environmental Monitoring and Assessment*, **117**, pp.307-334.
- Hester, M. (1982). *Statistical simulation of fracture distributions in rock masses and its applications to the stability of rock slopes*, M.Sc. Thesis. University of Arizona, Tuscon.
- Hobbs, D. (1964). The strength and stress-strain characteristics of coal in uniaxial compression. *J. Geol.*, **72**, pp.214-231.
- Hoek, E. (1988). The Hoek-Brown Failure Criterion - a 1988 Update. In , *15th Canadian Rock Mechanics Symposium*, pp. 31-38.
- Hoek, E. (1992). When is a design in rock engineering acceptable? Müller Lecture. In, *Proceedings of the 7th International Congress on Rock Mechanics, Aachen, A.A. Balkema, Rotterdam*, pp. 1485-1497.
- Hoek, E. (1994). Strength of rock and rock masses. *ISRM News Journal*, **2**, pp.4-16.
- Hoek, E. and Brown, E. (1980). *Underground Excavations in Rock*. Institute of Mining and Metallurgy, London.
- Hoek, E. and Brown, E. (1997). Practical Estimates of Rock Mass Strength. *Int. J. Rock. Mech. Min. Sci.*, **34**, pp.1165-1186.
- Hoek, E., Kaiser, P and Bawden, W. (1995). *Support of Underground Excavations in Hard Rock*. A.A. Balkema, Rotterdam.
- Hoek, E., Wood, D and Shah, S. (1992). A modified Hoek-Brown criterion for jointed rock masses. In J. Hudson (ed.), *Proceedings of the ISRM Rock Characterisation Symposium: Eurock '92, Chester, UK, 14-17 September*, pp. 209-213.
- Hudson, J. and Cosgrove, J. (1997). Integrated structural geology and engineering rock mechanics approach to site characterization. *Int. J. Rock. Mech. Min. Sci.*, **34**, pp.577-591.
- Hudson, J. and Feng, X. (2007). Updated flowcharts for rock mechanics modelling and rock engineering design. *Int. J. Rock. Mech. Min. Sci.*, **44**, pp.174-195.
- Hudson, J. and Harrison, J. (1997). *Engineering Rock Mechanics: An Introduction to the Principles*. Pergamon Press: Oxford.
- Hudson, J. and Harrison, J. (2002). The Principles of Partitioning Rock masses into Structural Domains for Modelling and Engineering Purposes. In, *Proc. North American Rock Mechanics Symp*, Toronto, Canada.
- ISRM (1978). Suggested methods for the quantitative description of discontinuities in rock masses. *Int. J. Rock Mech. Min. Sci. Geomech. Abstr.*, **15**, pp.319-368.

- ISRM (1981). *Suggested methods for rock characterisation, testing and monitoring. Commission on testing methods, International Society for Rock Mechanics*. Pergamon Press.
- ISRM (1985). Suggested Method to Determine Point Load Strength. Commission on testing methods, International Society for Rock Mechanics. *Int. J. Rock Mech. Min. Sci. Geomech. Abstr.*, **22**, pp.51-60.
- Itasca Consulting Group Inc (1984). *UDEC - Universal Distinct Element Model*. Itasca, Minneapolis, Minnesota USA.
- Itasca Consulting Group Inc (1988). *3DEC - Three-Dimensional Distinct Element Model*. Itasca, Minneapolis, Minnesota USA.
- Itasca Consulting Group Inc (2002). *FLAC3D - Fast Lagrangian analysis of continua in 3 dimensions: user's guide*. Itasca, Minneapolis, Minnesota USA.
- Jarosz, A. and Shepherd, L. (2000). Open Stope Cavity Monitoring for the Control of Dilution and Ore Loss. In, *MPES2000*, pp. 63-66.
- Jeffrey, S. (2002). The Cannington Ag-Pb-Zn BHT deposit; a world class discovery with a silver lining. In V. Preiss (ed.), *Geoscience 2002: Expanding Horizons. Abstracts of the 16th Australian Geological Convention, Adelaide Convention Centre, Adelaide, SA, Australia, July 1-5*, pp. 265.
- Jimenez-Rodriguez, R. and Sitar, N. (2006). A spectral method for clustering of rock discontinuity sets. *Int. J. Rock. Mech. Min. Sci.*, **43**, pp.1052-1061.
- Jimenez, R. (2007). Technical Note: Fuzzy spectral clustering for identification of rock discontinuity sets. *Rock Mech. Rock Eng.*, **41**, pp.929-939.
- Jing, L. (2003). A review of techniques, advances and outstanding issues in numerical modelling for rock mechanics and rock engineering. *Int. J. Rock. Mech. Min. Sci.*, **40**, pp.283-354.
- JORC (2004). Australasian Code for Reporting of Exploration Results, Mineral Resources and Ore Reserves. Prepared by: The Joint Ore Reserves Committee of The Australasian Institute of Mining and Metallurgy, Australian Institute of Geoscientists and Minerals Council of Australia (JORC). . p31.
- Journel, A. and Huijbregts, C. (1978). *Mining Geostatistics*. Academic Press.
- Kalamaras, G. and Bieniawski, Z. (1995). A rock mass strength concept for coal seams incorporating the effects of time. In T. Fujii (ed.), *Proceedings 8th International Conference on Rock Mechanics*, A. A. Balkema, Rotterdam, pp. 295-302.
- Kalenchuk, K., Diederichs, M and McKinnon, S. (2006). Characterizing block geometry in jointed rockmasses. *Int. J. Rock. Mech. Min. Sci.*, **43**, pp.1212-1225.
- Kanatani, K. (1984). Distribution of Directional Data and Fabric Tensors. *Int. J. Eng. Sci.*, **22**, pp.149-164.
- Kendall, D. (1977). The Diffusion of Shape. *Advances in Applied Probability*, **9**, pp.428-430.
- Klose, C., Seo, S and Obermayer, K. (2005). A new clustering approach for partitioning

- directional data. *Int. J. Rock. Mech. Min. Sci.*, **42**, pp.315-321.
- Krauland, N. and Soder, P. (1987). Determining Pillar Strength From Pillar Failure Observations. *Engineering and Mining Journal*, **8**, pp.34-40.
- Krige, D. (1951). A statistical approach to some mine valuations problems at the Witwatersrand. *Journal of the Chemical, Metallurgical and Mining Society of South Africa*, **52**, pp.119-139.
- Kulatilake, P. and Wu, T. (1984a). Estimation of Mean Trace Length of Discontinuities. *Rock Mech. Rock Eng.*, **17**, pp.215-232.
- Kulatilake, P. and Wu, T. (1984b). Sampling Bias on Orientation of Discontinuities. *Rock Mech. Rock Eng.*, **17**, pp.243-253.
- Kulatilake, P., Wang, S and Stephansson, O. (1993). Effect of Finite Size Joints on the Deformability of Jointed Rock in Three Dimensions. *Int. J. Rock Mech. Min. Sci. Geomech. Abstr.*, **30**, pp.479-501.
- Kulatilake, P., Wathugala, D, Poulton, M and Stephansson, O. (1990). Analysis of structural homogeneity of rock masses. *Engineering Geology*, **29**, pp.195-211.
- La Pointe, P. (1993). Pattern analysis and simulation of joints for rock engineering. In J. Hudson (ed.), *Comprehensive Rock Engineering*. Pergamon Press, Oxford, pp215-239.
- Lane, W., Yanske, T and Roberts, D. (1999). Pillar Extraction and Rock Mechanics at the Doe Run Company in Missouri 1991 to 1999. In Amadei, Kranz, Scott and Smeallie (ed.), *Proceedings of the 37th US Rock Mechanics Symposium*, A.A. Balkema, Rotterdam, pp. 285-292.
- Lappalainen, P. and Pitkajarvi, J. (1996). Dilution control at Outokumpu mines. In , *Proceedings of Nickel 96, Kalgoorlie*, AusIMM, Carlton, Australia, pp. 25-29.
- Laslett, G. (1982). Censoring and Edge Effects in Areal and Line Transect Sampling of Rock Joint Traces. *Math. Geol.*, **14**, pp.125-140.
- Laubscher, D. (1977). Geomechanics Classification of Jointed Rock Masses - Mining Applications. *Trans. Inst. Min. Metall. (Sect A: Min. industry)*, **86**, pp.A1-A7.
- Laubscher, D. (1990). A geomechanics classification system for the rating of rock mass in mine design. *J. S. Afr. Inst. Min. Metall.*, **90**, pp.257-273.
- Laubscher, D. and Taylor, H. (1976). The importance of geomechanics classification of jointed rock masses in mining operations. In , *Proceedings of the Symposium on Exploration for Rock Engineering*, Johannesburg, pp. 119-128.
- Lauffer, H. (1958). Gebirgsklassifizierung für den Stollenbau. *Geologie und Bauwesen*, **74**, pp.46-51.
- Lee, J., Veneziano, D and Einstein, H. (1990). Hierarchical Fracture Trace Model. In Hustrulid and Johnstone (ed.), *Proceedings of the 31st U.S. Symposium on Rock Mechanics, Golden, Colorado*, Balkema, Rotterdam, pp. 261-268.
- Levkovitch, V., Reusch, F and Beck, D. (2010). Application of a non-linear confinement sensitive constitutive model to mine scale simulations subject to varying levels of

- confining stress. In J. Zhao, V. Labiouse, J. Dudt and J. Mathier (ed.), *Proceedings of the European Rock Mechanics Symposium, Lausanne, Switzerland, 15-18 June*, pp. 161-164.
- Li, J. (2004). *Critical strain of intact rock and rock masses*, PhD Thesis. Western Australian School of Mines, Curtin University of Technology, 186p.
- Li, J. and Heap, A. (2008). A review of spatial interpolation methods for environmental scientists. *Record* 2008/23. p137.
- Lichti, D. (2004). A Resolution Measure for Terrestrial Laser Scanners. In, *Proc. XXth ISPRS Congress*.
- Lilly, P. (1986). An empirical method of assessing rock mass blastability. In Davidson (ed.), *Large Open Pit Mining Conference, AusIMM, Victoria*, pp. 89-92.
- Lilly, P. (2000). The minimum total cost approach to optimum pit slope design. In Panagiotou & Michalakopoulos (ed.), *Mine Planning and Equipment Selection*. Balkema, Rotterdam, pp77-82.
- Lilly, P. and Villaescusa, E. (2001). Optimising Pit Slope Angles and Underground Stope Spans Using a Risk-Based Approach. In, *Strategic Mine Planning Conference, Aus.I.M.M, Perth, W.A*, pp. 71-74.
- Liu, Q., Brosch, F and Riedmüller, G. (2004). The significance and prediction of different rock mass characteristics for rock engineering. *Int. J. Rock. Mech. Min. Sci.*, **41**, pp.103-117.
- Lopez, P., Riss, J and Archambault, G. (2003). An experimental method to link morphological properties of rock fracture surfaces to their mechanical properties. *Int. J. Rock. Mech. Min. Sci.*, **40**, pp.947-954.
- Luke, D. and Edwards, A. (2004). Geotechnical block Modelling at BHP Billiton Cannington Mine. In Villaescusa, E and Potvin, Y (ed.), *Proceedings of the 5th International Symposium on Ground Support, Perth, Western Australia*, A.A. Balkema, Leiden, pp. 129-138.
- Maerz, N. and Zhou, W. (2005). Multivariate Clustering Analysis of the ECRB Cross Drift Discontinuities, Yucca Mountain Project. In, *Proc. 40th U.S. Symp on Rock Mechanics*, 10p.
- Maerz, N., Ibarra, J and Franklin, J. (1996). Overbreak and underbreak in underground openings. Part 1: Measurement using the light sectioning method and digital image processing. *Geotech. Geol. Eng.*, **14**, pp.307-323.
- Magee, D. (2005). *Geometric Back Analysis of CMS Stope Surveys at Kanowna Belle*, B.Eng. Thesis. Western Australian School of Mines, Curtin University of Technology, 65p.
- Malatesta, L. (2006). *Performance of Sub-Level Open Stopes at Kanowna Belle Gold Mine*, B.Eng. Thesis. Western Australian School of Mines, Curtin University of Technology, 114p.
- Marcotte, D. and Henry, E. (2002). Automatic joint set clustering using a mixture of bivariate normal distributions. *Int. J. Rock. Mech. Min. Sci.*, **39**, pp.323-334.
- Mardia, K. and Jupp, P. (1999). *Directional Statistics*. John Wiley & Sons, New York.
- Margulies, L., Lorentzen, T, Poulsen, H and Leffers, T. (2002). Strain tensor development in a

- single grain in the bulk of a polycrystal under loading. *Acta Materialia*, **50**, pp.1771-1779.
- Martin, C. (1997). The Effect of Cohesion Loss and Stress Path on Brittle Rock Strength. *Can. Geotech. J.*, **34**, pp.698-725.
- Martin, C. and Maybee, W. (2000). The strength of hard-rock pillars. *Int. J. Rock Mech. Min. Sci.*, **37**, pp.1239-1246.
- Martin, C., Kaiser, P and McCreath, D. (1999). Hoek-Brown parameters for predicting the depth of brittle failure around tunnels. *Canadian Geotechnical Journal*, **36**, pp.136-151.
- Martin, M. and Tannant, D. (2004). A technique for identifying structural domain boundaries at the EKATI Diamond Mine. *Engineering Geology*, **7**, pp.247-267.
- Massoud, H. (1987). *Modelisation de la petite fracturation pour les techniques de la geostatistique*, PhD Thesis. Ecole Nationale Superieure des Mines de Paris, 189p.
- Matheron, G. (1962). *Traité de géostatistique appliquée. Tome 1*. Editions Technip, Paris.
- Mathews, K., Hoek, E, Wyllie, D and Stewart, S. (1981). Prediction of stable excavations for mining at depth below 1000 metres in hard rock. CANMET Report DSS Serial No. OSQ80-00081, DSS File No. 17SQ.23440-0-9020, Ottawa: Dept. Energy, Mines and Resources. Unpublished Report. p39.
- Mathis, J. (1988). *Development and verification of a three-dimensional rock joint model*, PhD Thesis. Lulea University of Technology, 144p.
- Mauldon, M. (1994). Intersection Probabilities of Impersistent Joints. *Int. J. Rock Mech. Min. Sci. Geomech. Abstr.*, **31**, pp.107-115.
- Mauldon, M. (1998). Estimating Mean Fracture Trace Length and Density from Observations in Convex Windows. *Rock Mech. Rock Eng.*, **31**, pp.201-216.
- Mawdesley, C., Trueman, R and Whiten, W.J. (2001). Extending the Mathews stability graph for open-stope design. *Trans. Inst. Min. Metall. (Sect A: Min. industry)*, **110**, pp.A27-A39.
- McCarthy, C. (1996). *Alteration associated with late (D4) brittle faults, Cannington, NW Queensland*, B.Sc. Honours Thesis. University of Tasmania, Hobart, 107p.
- McMahon, B. (1985). Australian Geomechanics Society E.H. Davis Memorial Lecture: Geotechnical Design in the face of uncertainty. *Aust. Geomech.*, **10**, pp.7-19.
- Miller, F., Potvin, Y and Jacob, D. (1992). Laser measurement of open stope dilution. *CIM Bulletin*, **85**, pp.96-102.
- Miller, S. (1979). Geostatistical Analysis for Evaluating Spatial Dependence in Fracture Set Characteristics. In, *Proceedings of the 16th APCOM, University of Arizona, Tuscon*, , pp. 537-547.
- Miller, S. and Luark, R. (1993). Spatial Simulation of Rock Strength Properties Using a Markov-Bayes Method. *Int. J. Rock Mech. Min. Sci. Geomech. Abstr.*, **30**, pp.1631-1637.
- Milne, D., Pakalnis, R and Lunder, P. (1996). Approach to the quantification of hangingwall behaviour. *Trans. Inst. Min. Metall. (Sect A: Min. industry)*, **105**, pp.A69-A74.
- Milne, D., Pakalnis, R, Grant, D and Sharma, J. (2004). Interpreting hanging wall deformation

- in mines. *Int. J. Rock. Mech. Min. Sci.*, **41**, pp.1139-1151.
- Mitri, H., Edrissi, R and Henning, J. (1994). Finite element modelling of cable-bolted stopes in hard rock underground mines. I , *Proceedings of the SME Annual Meeting, Albuquerque, New Mexico*.
- Mogi, K. (2007). *Experimental Rock Mechanics*. Taylor & Francis, London, New York.
- Moody, J. and Hill, M. (1956). Wrench fault tectonics. *Geol. Soc. Amer. Bull.*, **67**, pp.1207-1246.
- Morin, B. (2006). Cutting Edge long Hole Open Stope Analysis at Perilya's Broken Hill Operations. *Second International Seminar on Strategic versus Tactical Approaches in Mining 2006*, Australian Centre for Geomechanics. pp. 1-17.
- Mostyn, G. and Douglas, K. (2000). Strength of Intact Rock and Rock Masses. In , *GeoEng 2000, International Conference on Geotechnical and Geological Engineering*, Melbourne, Australia, pp. 1398-1420.
- Murrell, S. (1965). The effect of triaxial stress systems on the strength of rock at atmospheric temperature. *Geophys. J. R. Astr. Soc.*, **10**, pp.231-281.
- Nicholson, G. and Bieniawski, Z. (1990). A nonlinear deformation modulus based on rock mass classification. *Int. J. Min. Geol. Eng.*, **8**, pp.181-202.
- Nickson, S. (1992). *Cable support guidelines for underground hard rock mine operations*, M.A.Sc. Thesis. Department of Mining and Mineral Processing, University of British Columbia, 223p.
- Nickson, S., Coulson, A and Hussey, J. (2000). Noranda's approach to evaluating a competent deposit for caving. In G. Chitombo (ed.), *Proceedings of MassMin 2000, Brisbane*, Australian Institute of Mining and Metallurgy, Melbourne, pp. 367-383.
- NIST/SEMATECH. (2009). e-Handbook of Statistical Methods. <http://www.itl.nist.gov/div898/handbook/>. (accessed , 2009).
- Obert, L. and Duvall, W. (1967). *Rock Mechanics and the Design of Rock Structures*. John Wiley and Sons, New York.
- Oda, M. (1982). Fabric tensor for discontinuous geological materials. *Soils and Foundations*, **22**, pp.96-108.
- Oda, M., Yamabe, T and Kamemura, K. (1986). A Crack Tensor and Its Relation to Wave Velocity Anisotropy in Jointed Rock Masses. *Int. J. Rock Mech. Min. Sci. Geomech. Abstr.*, **23**, pp.387-397.
- Oddie, M. and Pascoe, M. (2005). Stope Performance at Olympic Dam Mine. In , *Ninth Underground Operators Conference*, AusIMM, Perth, pp. 265-272.
- Ozturk, C. and Nasuf, E. (2002). Geostatistical assessment of rock zones for tunneling. *Tunn. Undergr. Sp. Tech.*, **17**, pp.275-285.
- Pakalnis, R. (1986). *Empirical stope design at Ruttan Mine*, PhD Thesis. University of British Columbia, 276p.
- Pakalnis, R. and Vongpaisal, S. (1993). Mine design an empirical approach. In Bawdin &

- Archibald (ed.), *Innovation in Mine Design for the 21st Century*. Balkema, Rotterdam, pp.455-467.
- Pakalnis, R., Poulin, R and Hadjigeorgiou, J. (1995). Quantifying the cost of dilution in underground mines. *Min. Eng.*, **December**, pp.1136-1141.
- Palmstrøm, A. and Broch, E. (2006). Use and misuse of rock mass classification systems with particular reference to the Q-system. *Tunn. Undergr. Sp. Tech.*, **21**, pp.575-593.
- Pascoe, M. and Oddie, M. (2003). Assessing Stope Overbreak at Olympic Dam. In B. Hebblewhite (ed.), *Proceedings 1st Australasian Ground Control in Mining Conference: Technology and Practice*, UNSW Press, Sydney, pp. 71-79.
- Patching, T. and Coates, D. (1968). A recommended rock classification for rock mechanics purposes. *CIM Bulletin*, **October**, pp.1195-1197.
- Pine, R. and Harrison, J. (2003). Rock mass properties for engineering design. *Quart. J. Eng. Geol. Hydrogeol.*, **36**, pp.5-16.
- Piteau, D. (1973). Characterizing and extrapolating rock joint properties in engineering practice. *Rock Mech.*, **2**, pp.5-31.
- Ponierwierski, J. (2005). Effect of stope size on sustainable steady-state production rates in a sub-level open stoping system. *Trans. Inst. Min. Metall. (Sect A: Min. industry)*, **114**, pp.A241-A250.
- Poropat, G. (2005). Remote 3D Mapping of Rock Mass Structure. Workshop on "Laser and Photogrammetric Methods for Rock Face Characterisation". In F. Tonon and J. Kottenstette (ed.), *41st U.S. Rock Mechanics Symposium. American Rock Mechanics Association. Colorado School of Mines, June 17-18.*, , pp. 63-75.
- Poropat, G., Elmouttie, M and Walford, D. (2007). Joint set definition using topology based structure mapping. In, *Proceedings of the 1st Canada-US Rock Mechanics Symposium, Vancouver, Canada, 27-31 May*, pp. 107-111.
- Potvin, Y. (1988). *Empirical open stope design in Canada*, PhD Thesis. University of British Columbia, 343p.
- Potvin, Y. and Hudyma, M. (1989). Design guidelines for open stope support. *CIM Bulletin*, **82**, pp.53-62.
- Potvin, Y. and Milne, D. (1992). Empirical cable bolt support design. In P. Kaiser and D. McCreath (ed.), *Rock Support in Mining and Underground Construction*, A.A. Balkema, Rotterdam, pp. 269-275.
- Power, G. (2004). Discontinuity Systems. BHP Billiton Cannington Mine. Internal memorandum.
- Price, N. (1966). *Fault and Joint Development in Brittle and Semi-Brittle Rock*. Pergamon, Oxford.
- Price, N. and Cosgrove, J. (1990). *Analysis of Geological Structures*. Cambridge University Press: Cambridge.
- Priest, S. (1993). *Discontinuity Analysis for Rock Engineering*. Chapman & Hall, London.

- Priest, S. and Hudson, J. (1976). Discontinuity spacing in rock. *Int. J. Rock Mech. Min. Sci. Geomech. Abstr.*, **13**, pp. 135-148.
- Priest, S. and Hudson, J. (1981). Estimation of Discontinuity Spacing and Trace Length Using Scanline Surveys. *Int. J. Rock Mech. Min. Sci. Geomech. Abstr.*, **18**, pp. 183-197.
- Priest, S. and Samaniego, J. (1988). Face Stability Analysis in Fractured Rock by the Statistical Simulation of Rigid Block Failure. In, *Proceedings of the 5th Australia-New Zealand Conference on Geomechanics*, pp. 398-403.
- Pusch, R. (1994). *Waste Disposal in Rock*. Elsevier Publishing Company.
- Rafiee, A. and Vinches, M. (2008). Application of geostatistical characteristics of rock mass fracture systems in 3D model generation. *Int. J. Rock. Mech. Min. Sci.*, **45**, pp.644-652.
- Ramamurthy, T., Rao, G and Rao, K. (1985). A strength criterion for rocks. In, *Indian Geotechnical Conference*, pp. 59-64.
- Read, S., Richards, L and Cook, G. (2003). Rock mass defect patterns and the Hoek-Brown failure criterion. In, *Proc 10th ISRM International Congress on Rock Mechanics*, pp. 947-954.
- Reid, T. and Harrison, J. (2000). A semi-automated methodology for discontinuity trace detection in digital images of rock mass exposures. *Int. J. Rock. Mech. Min. Sci.*, **37**, pp.1073-1089.
- Reusch, F., Beck, D and Tyler, D. (2008). Quantitative forecasting of sidewall stability and dilution in Sub-level caves. In, *Proceedings of MassMin2008, Luleå, Sweden, 9-11 June*, pp. 453-460.
- Riedel, W. (1929). Zur Mechanik geologischer Brucherscheinungen. *Zbl. Miner. Geol. Palaeont.*, pp.B354.
- Roache, T. (2004). Shear zone versus fold geometries at the Cannington Ag-Pb-Zn deposit: implications for the genesis of BHT deposits. *J. Struct. Geol.*, **26**, pp.1215-1230.
- Roberts, B. (2005). Cannington Stope Design Procedure. . Internal Unpublished Report. p19.
- Roberts, D., Lane, W and Yanske, T. (1998). Pillar extraction at the Doe Run Company 1991-1998. In M. Bloss (ed.), *Minefill '98. Proceedings of the Sixth International Symposium on Mining with Backfill*, AusIMM, Carlton, Australia, pp. 227-233.
- Rocscience Inc (1998). DIPS - Graphical and Statistical Analysis of Orientation Data, Toronto, Canada.
- Rocscience, I. (1990). Examine3D - A 3D computer-aided engineering analysis package for underground excavations in rock, Toronto, Canada.
- Rosenblueth, E. (1975). Point estimates for probability moments. *Proceedings of the National Academy of Science U.S.A.*, **72**, pp.3812-3814.
- Rosengren, K. (1970). Diamond drilling for structural purposes at Mount Isa. *Industrial Diamond Review*, **30**, pp.388-395.
- Ross, A., Barley, M, Brown, S, McNaughton, N, Ridley, J and Fletcher, I. (2004). Young porphyries, old zircons: new constraints on the timing of deformation and gold

- mineralisation in the Eastern Goldfields from SHRIMP U-Pb zircon dating at the Kanowna Belle Gold Mine, Western Australia. *Precambrian Res.*, **128**, pp.105-142.
- Rusu, C. and Rusu, V. (2006). Radial Basis Functions Versus Geostatistics in Spatial Interpolations. In M. Bramer (ed.), *IFIP International Federation for Information Processing*. Springer, Boston, pp119-128.
- Rzhevsky, V. and Novik, G. (1971). *The physics of rocks*. Mir Publication, Moscow.
- Sakurai, S. (1981). Direct strain evaluation technique in construction in underground openings. In *Proceedings of the 22nd U.S. Rock Mechanics Symposium*, pp. 278-282.
- Sakurai, S. (1997). Lessons Learnt from Field Measurements in Tunnelling. *Tunn. Undergr. Sp. Tech.*, **12**, pp.453-460.
- Santalo, L. (1976). Sobre la distribucion de los tamanos de corpusculos contenidos en un cuerpo a partir de la distribucion en sus secciones a proyecciones. *Trabajos de Estadistica*, **6**, pp.181-196.
- Savely, J. (1972). *Orientation and engineering properties of jointing in the Sierra pit, Arizona*, M.Sc. Thesis. University of Arizona, Tuscon.
- Scheidegger, A. (1965). On the statistics of the orientation of bedding planes, grain axes, and similar sedimentological data. U.S. Geol. Survey Prof. Paper 525-C. . p164-167.
- Scoble, M. and Moss, A. (1994). *Dilution in Underground Bulk Mining*. The Geological Society, London.
- Scott, C. and Power, G. (1998). Stope Stability Assessments. Cannington Mine. Unpublished Internal Memorandum. p5.
- Sen, Z. and Kazi, A. (1984). Discontinuity Spacing and RQD Estimates from Finite Length Scanlines. *Int. J. Rock Mech. Min. Sci. Geomech. Abstr.*, **21**, pp.203-212.
- Serafim, L. and Pereira, P. (1983). Consideration on the geomechanical classification of Bieniawski. In *Proceeding of the International Symposium of Engineering Geology and Underground Construction*, LNEC, Lisbon, pp. 1133-1142.
- Serra, J. (1982). *Image Analysis and Mathematical Morphology*. Academic Press, London.
- Shanley, R. and Mahtab, M. (1976). Delineation and Analysis of Clusters in Orientation Data. *Math. Geol.*, **8**, pp.9-22.
- Sharrock, G., Slade, N, Thin, I and Duplancic, P. (2002). The Prediction of Stress Induced Caving on a Mining Abutment. In *International Seminar on Deep and High Stress Mining*, , pp. 1-21.
- Sheorey, P. (1997). *Empirical Rock Failure Criteria*. A.A. Balkema, Rotterdam..
- Sheorey, P., Biewas, A and Choubey, V. (1989). An empirical failure criterion for rocks and jointed rock masses. *Eng. Geol.*, **26**, pp.141-159.
- Snow, D. (1965). *A parallel plate model of fracture permeability media*, PhD Thesis. University of California, Berkeley, LA.
- Sofianos, A. (1996). Analysis and design of an underground hard rock voussoir beam roof. *Int. J. Rock Mech. Min. Sci. Geomech. Abstr.*, **33**, pp.153-166.

- Starfield, A. and Cundall, P. (1988). Towards a Methodology for Rock Mechanics Modelling. *Int. J. Rock Mech. Min. Sci. Geomech. Abstr.*, **25**, pp.99-106.
- Stavropoulou, M., Exadaktylos, G and Saratsis, G. (2007). A Combined Three-Dimensional Geological-Geostatistical-Numerical Model of Underground Excavations in Rock. *Rock Mech. Rock Eng.*, **40**, pp.213-243.
- Stewart, P. (2005). *Minimising dilution in narrow-vein mines*, PhD Thesis. University of Queensland, Brisbane, 261p.
- Streeton, G. (2000). Geotechnical Aspects of Open Stope Design at BHP Cannington. In , *MassMin 2000*, AusIMM, pp. 747-753.
- Strouth, A. and Eberhardt, E. (2006). The use of LiDAR to overcome rock slope hazard data collection challenges at Afternoon Creek, Washington. Workshop on "Laser and Photogrammetric Methods for Rock Face Characterisation". In F. Tonon and J. Kottenstette (ed.), *41st U.S. Rock Mechanics Symposium. American Rock Mechanics Association. Colorado School of Mines, June 17-18*, pp. 109-120.
- Sturzenegger, M., Yan, M, Stead, D and Elmo, D. (2007). Application and limitations of ground-based laser scanning in rock slope characterization. In , *Proceedings of the 1st Canada-US Rock Mechanics Symposium, Vancouver, Canada, 27-31 May*, pp. 29-36.
- Sullivan, T., Duran, A and Eggers, M. (1992). The Use and Abuse of Oriented Core in Open Pit Mining. In , *Third Large Open Pit Mining Conference*, pp. 387-395.
- Suorineni, F. (1998). *Effects of faults on stress on open stope design*, PhD Thesis. University of Waterloo, Department of Earth Sciences, Waterloo, Canada, 344p.
- Suorineni, F., Kaiser, P and Tannant, D. (2001). Likelihood statistic for interpretation of the stability graph for open stope design. *Int. J. Rock. Mech. Min. Sci.*, **38**, pp.735-744.
- Swager, C. (1997). Tectono-stratigraphy of late Archaean greenstone terranes in the southern Eastern Goldfields, Western Australia. *Precambrian Res.*, **83**, pp.11-42.
- Swager, C., Griffin, T, Witt, W, Wyche, S, Ahmat, A, Hunter, W and McGoldrick, P. (1990). Geology of the Archean Kalgoorlie Terrane - An Explanatory Note. Geological Survey of Western Australia, Record 1990/12.
- Tauxe, L., Kylstra, N and Constable, C. (1991). Bootstrap Statistics for Paleomagnetic Data. *J Geophys Res*, **96**, pp.11723-11740.
- Terzaghi, K. (1946). Rock Defects and Loads on Tunnel Support. In R. Proctor and T. White (ed.), *Rock Tunnelling with Steel Supports*. Commercial Shearing Co., Youngstown, OH, pp15-99.
- Terzaghi, R. (1965). Sources of Error in joint surveys. *Géotechnique*, **15**, pp.287-304.
- Tresca, H. (1864). Memoire sur l'ecoulement des corps solides soumis a defortes pressions. *Comptes Rendus de l'Académie des Sciences, Paris*, **59**, pp.754.
- Trueman, R. (1988). *An evaluation of strata support techniques in dual life gateroads*, Ph.D. Thesis. University of Wales, Cardiff.
- Tsiambaos, G. and Sabatakakis, N. (2004). Considerations on strength of intact sedimentary

- rocks. *Eng. Geol.*, **72**, pp.261-273.
- Ullah, Z. (1997). *Applicability of the Mathews Stability Graph for Evaluating Stability of Open Stopes at the Mount Charlotte Mine*, M.Eng. Thesis. Western Australian School of Mines, Curtin University of Technology, 84p.
- Veneziano, D. (1978). *Probabilistic model of joints in rock*, PhD Thesis. MIT, Cambridge, MA.
- Villaescusa, E. (1991). *A Three Dimensional Model of Rock Jointing*, PhD Thesis. University of Queensland, 252p.
- Villaescusa, E. (1998). Geotechnical design for dilution control in underground mining. In Singhal (ed.), *Mine Planning and Equipment Selection 1998*, Balkema, Rotterdam, pp. 141-149.
- Villaescusa, E. (2004). Quantifying open stope performance. In, *MassMin2004*, pp. 96-104.
- Villaescusa, E. (2010). *Underground Rock Engineering*, Master of Mining Geomechanics Class Notes. Western Australian School of Mines, 255p.
- Villaescusa, E. and Brown, E. (1992). Maximum Likelihood Estimation of Joint Size from Trace Length Measurements. *Rock Mech. Rock Eng.*, **25**, pp.67-87.
- Villaescusa, E. and Cepuritis, P. (2005). The effects of large scale faults on narrow vein stope stability : A Case Study. In, *Proceedings of the 40th US Rock Mechanics Symposium*, 6p.
- Villaescusa, E. and Li, J. (2004). A review of empirical methods used to estimate rock mass compressive strength and deformability in the mining industry. In, *MassMin Chile*, pp. 59-68.
- Villaescusa, E., Cepuritis, P, Li, J, Heilig, J, Wiles, T and Lund, T. (2003a). Open Stope Design and Sequences at Great Depth at Kanowna Belle. Unpublished Research Report for Placer Dome Asia Pacific. p221.
- Villaescusa, E., Tyler, D and Scott, C. (1997). Predicting underground stability using a hangingwall stability rating. In Lee, HK, Yang, HS and Chung, SK (ed.), *Proc. 1st Asian Rock Mechanics Symposium, Environmental and Safety Concerns in Underground Construction*, Seoul, South Korea, pp. 171-176.
- Villaescusa, E., Windsor, C, Li, J, Baird, G and Seto, M. (2003b). Experimental Verification of AE In situ Stress Measurements. In, *Proceedings of the 3rd International Symposium on Rock Stress*, Kumamoto, Japan.
- von Mises, R. (1913). Mechanik der festen Koerper im plastisch deformablen Zustand, Göttingen Nachrichten. *Mathematisch-Physikalische Klasse*, **1**, pp.582-592.
- Warburton, P. (1980). A Stereological Interpretation of Joint Trace Data. *Int. J. Rock Mech. Min. Sci. Geomech. Abstr.*, **17**, pp.181-190.
- Warburton, P. (1983). Applications of a new computer model for reconstructing blocky rock geometry - analysing single block stability, and identifying keystones . In , *Proceedings of the 5th International Congress on Rock Mechanics*, ISRM, Melbourne, pp. F225-F230.
- Watters, R., Zimbelman, D, Bowman, S and Crowley, J. (2000). Rock Mass Strength Assessment and Significance to Edifice Stability, Mount Rainier and Mount Hood,

- Cascade Range Volcanoes. *Pure. App. Geophys.*, **157**, pp.957-976.
- Webster, R. and Oliver, M. (2001). *Geostatistics for Environmental Scientists*. John Wiley & Sons, Ltd, Chichester.
- Wiles, T. (1993). MAP3D User Manual. Mine Modelling Report, Copper Cliff, Ontario, Canada..
- Wiles, T. (2001). Map3D Course Notes. Masters of Geomechanics, Western Australian School of Mines. . Mine Modelling Pty Ltd. p124.
- Wiles, T. (2006). Reliability of numerical modelling predictions. *Int. J. Rock. Mech. Min. Sci.*, **43**, pp.454-472.
- Windsor, C. (1993). Measuring stress and deformation in rock masses. In Szwedzicki (ed.), *Geotechnical Instrumentation and Monitoring in Open Pit and Underground Mining*, Balkema, Rotterdam, pp. 33-52.
- Windsor, C. (1999). Systematic Design of Reinforcement and Support Schemes for Excavations in Jointed Rock. In Villaescusa, E, Windsor, CR and Thomson, AG (ed.), *Rock Support and Reinforcement Practice in Mining*, Balkema, Rotterdam, pp. 35-58.
- Windsor, C. (2006). Structural Geology, Stress and Strength at Cannington Mine. Unpublished Draft Report. BHP Billiton - Cannington Mine. p54.
- Windsor, C. and Thompson, A. (1992). SAFEX - A Design and Analysis Package for Rock Reinforcement. In, *Proceedings of the International Symposium on Rock Support, Sudbury, Canada*, Balkema, Rotterdam, pp. 17-23.
- Windsor, C. and Thompson, A. (1997). *A course on structural mapping and structural analysis*. Rock Technology Pty Ltd.
- Windsor, C., Thompson, A and Chitombo, G. (1995). Excavation Engineering - The Integration of Excavation Design, Blast Design and Reinforcement Design. In, *Explo'95 Conference*, Brisbane, Australia, pp. 101-109.
- Winsor, C.N. 1998. The Controls Exerted on Local Discontinuities by Regional Tectonic Influences, The Broken Hill Pasmaico Lead Lode Example. *Australian Geomechanics*, Vol. 33, No.1, pp. 82-90.
- Woodcock, N. (1977). Specification of fabric shapes using an eigenvalue method. *Geol. Soc. Amer. Bull.*, **88**, pp.1231-1236.
- Wu, H. and Pollard, D. (1995). An experimental study of the relationships between joint spacing and layer thickness. *Journal of Structural Geology*, **17**, pp.887-905.
- Young, D. (1987). Random Vectors and Spatial Analysis by Geostatistics for Geotechnical Applications. *Math. Geol.*, **19**, pp.467-479.
- Yow, J. (1987). Technical Note: Blind Zones in the Acquisition of Discontinuity Orientation Data. *Int. J. Rock Mech. Min. Sci. Geomech. Abstr.*, **24**, pp.317-318.
- Yudhbir, R., Lemanza, W and Prizl, F. (1983). An empirical failure criterion for rock masses. In, *Proceedings of the 5th International Society of Rock Mechanics*, Balkema, AA, Rotterdam, pp. B1-B8.
- Zhang, L. and Einstein, H. (1998). Estimating the Mean Trace Length of Rock Discontinuities.

Rock Mech. Rock Eng., **31**, pp.217-235.

Zhang, L. and Einstein, H. (2000). Estimating the intensity of rock discontinuities. *Int. J. Rock Mech. Min. Sci.*, **37**, pp.819-837.

Zhou, W. and Maerz, N. (2002). Implementation of multivariate clustering methods for characterizing discontinuities data from scanlines and oriented boreholes. *Comput. Geosci.*, **28**, pp.827-839.

Every reasonable effort has been made to acknowledge the owners of copyright material. I would be pleased to hear from any copyright owner who has been omitted or incorrectly acknowledged.

APPENDIX A - ROCK MASS DATA COLLECTION AND ANALYSIS METHODS

A.1 Diamond Drill Core Logging

A.2 Manual Mapping of Exposures

A.3 A review of Remote Discontinuity Mapping Techniques

A.4 Bias Corrections to *UCS* and Point Load Data

A.5 Analysis of Discontinuity Data

A.1 DIAMOND DRILL CORE LOGGING

Diamond drill core is perhaps the most common method for sampling the rock mass. Although there are limitations with sample size and orientation bias, diamond drill core allows for an extensive, and otherwise physically inaccessible, volume of rock mass to be sampled. The objective of diamond drilling for rock mechanics purposes is to obtain a continuous, correctly oriented sample in the most undisturbed form as possible (Brady and Brown, 2004).

Sampling Programmes

Drill core can be oriented to assist in the collection of orientation and other characteristics of discontinuities. However, the majority of diamond drilling in mining is principally designed to delineate and evaluate the orebody, from a geological perspective. The design of these programmes is usually set out to intersect and sample the orebody on an approximate equally spaced grid arrangement, with the holes usually aligned approximately normal to the orebody. This is done to obtain representative and “unbiased” assay samples for resource modelling. Unfortunately, having most drill holes aligned in the same direction will introduce a bias, effectively under-sampling discontinuity planes sub-parallel to the dominant drilling direction (Sullivan et al., 1992; Yow, 1987).

There are many factors that need to be considered when planning a rock mechanics specific diamond drilling programme. More detailed information on these aspects are provided by a number of authors; (Goodman, 1976; Nickson et al., 2000; Rosengren, 1970; Sullivan et al., 1992). It is important to note, however, that the size and type of diamond drilling can have an effect the ability to adequately characterise the rock mass. For example, in weaker rock masses, smaller diameter holes generally generate more fractured core than larger diameter holes. The use of triple-tube drilling is highly recommended in weaker rock masses, over conventional double tube drilling, to reduce the risk of core damage and core spinning inside the inner tubes.

Core Logging Techniques

There are a variety of ways in which drill core can be logged for engineering purposes, however, the type of data that can be collected from diamond drill core logging can be broadly categorised as either;

- **Interval Data** - This consists of attributes that can be characterised as being

uniform over a specific interval. Examples of such data include intact rock strength, weathering, alteration and drill core quality.

- **Point Data** – this data includes features in the rock mass that can be characterised at a specific single point, such as discontinuities, or samples for laboratory or field index tests.

Interval Logging

There are many styles of recording interval logging data, from graphical borehole logs to simple tabular formats (i.e. row and column layout), each with their advantages and disadvantages. Graphical borehole formats provide a comprehensive graphical overview of all the rock mass parameters and how they vary along the length of the borehole. In this respect, they allow for a rapid and simultaneous appreciation of all the various rock mass parameters. Conversely, tabular formats do not have the ability to provide this abundance of visual data. However, tabular formats are more amenable to incorporation in databases and for use in subsequent numerical or statistical analyses and modelling. The typical rock parameters that are recorded in interval logging include; weathering and alteration, field estimates of rock strength, drill core recovery, *RQD* (Deere, 1964), fracture frequency or discontinuity linear frequency.

Lithology

The physical and chemical properties of the rock fabric can have a significant influence on the engineering properties and behaviour. Lithology is the study and description of rocks, especially at the macroscopic level (hand specimen to outcrop scale), in terms of their colour, texture, and composition and is an integral part of understanding the geology of a project site. The lithological features of the rock fabric, such as mineralogy and grain size, are fundamental aspects in controlling their mechanical behaviour (Attewell and Farmer, 1976; Rzhnevsky and Novik, 1971). It must be emphasised that, although rock type alone cannot provide quantitative information about the engineering properties, it can provide qualitative information about its mechanical behaviour. In this context, rock type can be used to generalise the comparative mechanical behaviour between lithologies at a project site.

Weathering and Alteration

Weathering generally refers to the combined effects of chemical decomposition and mechanical disintegration of the rock mass. The nature and rate of weathering depends on climate, topography, rock type and time. The severity and distribution of weathering can be

effected by the proximity to the surface, meteoric groundwater processes, the presence of discontinuities and rock fabric porosity. Weathering tends to be more severe along discontinuities (ISRM, 1978) as they offer more rock fabric surface area and pathways into the rock mass. In general, the extent and severity of weathering of the rock mass as a whole should be described. It may also be beneficial to describe the extent and severity of weathering of discontinuities, even by sets or families of discontinuities, and the rock fabric separately. An example of a rock mass weathering classification scheme is provided in Table A.1. In addition, particular lithologies are effected by weathering processes in different ways than other lithologies. It may therefore be prudent to devise weathering classification schemes that cover the observed manifestation of weathering for these rock types.

Table A.1 - Example classification of rock mass weathering

Weathering Description	Code	Field Identification
Extremely weathered	EW	Rock substance affected by weathering to the extent that the rock exhibits soil properties - i.e. it can be remoulded, but the texture of the original rock is still evident
Highly weathered	HW	Rock substance affected by weathering to the extent that limonite staining or bleaching affects the whole of the rock substance and other signs of chemical and physical decomposition are evident. Porosity and strength may be increased or decreased compared to the fresh rock usually as a result of iron leaching or deposition. The colour and strength of the original rock substance is no longer recognisable.
Moderately weathered	MW	Rock substance affected by weathering to the extent that staining extends throughout the whole of the rock substance and the original colour of the fresh rock is no longer recognisable.
Slightly weathered	SW	Rock substance affected by weathering to the extent that partial staining or discolouration of the rock substance usually by limonite has taken place. The colour and texture of the fresh rock is recognisable.
Fresh	FR	Rock substance unaffected by weathering.

Alteration generally refers to the chemical alteration of the rock fabric either by decomposition or replacement of the original rock fabric minerals. Significantly, alteration minerals, such as phyllosilicates (e.g. chlorite, sericite and clay minerals), can have a detrimental effect on the rock engineering properties; decrease in rock fabric strength and elasticity, increase in swelling and/or slaking potential, as well as an increase in time-dependant strength degradation. It is therefore important to record the degree of severity of alteration during rock mass characterisation, including the type, form and abundance of alteration minerals present in the rock fabric and discontinuities.

Discontinuity Data

Discontinuities are logged individually as point data. When logging discontinuities, typical information consists of; distance down hole, type (e.g. join, bedding, etc.), alpha and beta angles (see Figure A.1), surface characteristics, infilling materials and their widths.

Drill Core Orientation Techniques

Drill core orientation involves placing a known reference line along the axis of the drill core which, and together with the knowledge of the hole's trajectory, can enable the orientation of discontinuities to be determined. A number of techniques are used in the Australian mining industry, each with variable reliability. The most common orientation techniques include (from least to most reliable);

- Arbitrary Reference Line - a continuous arbitrary reference line is used to record all orientations to a local coordinate system. Subsequent structural analysis can allow for rotation of data to the global reference system.
- Marker Line - This method is similar to the arbitrary reference line method, however, the reference line is aligned parallel to the intersection of a geological feature in the core with a known orientation.
- Spear and Pencil - Rudimentary tool to mark bottom of hole on core. Generally of low reliability, yet inexpensive.
- Van Ruth or Craelius Tool - downhole wireline tool that measures orientation and shape of core stub, or "stick-out" using sliding pins. The tool is weighted to consistently find bottom of hole. Drilling proceeds and once core is recovered the angle of core "stick-out" matched to orientation of the tool.
- Clay Impression - Rarely used in the mining industry, yet works in a similar fashion to Van Ruth or Craelius tool however used clay used instead of pins.

Once the 'bottom of hole' is established, using one of the methods described above, the core is pieced together and a reference line is then drawn long the core axis. All of the orientation methods above are highly dependent on the integrity of the core, and the ability to continue the orientation line from one drill core run to the next. Zones of broken or highly fractured core typically make it impossible to continue the orientation line across these zones. In addition, sections of the core may "spin" inside the inner tubes during the drilling process making it impossible to align and match up core. These issues are affected by the drilling method, rock mass conditions, driller skill and diligence, and adequate equipment and maintenance.

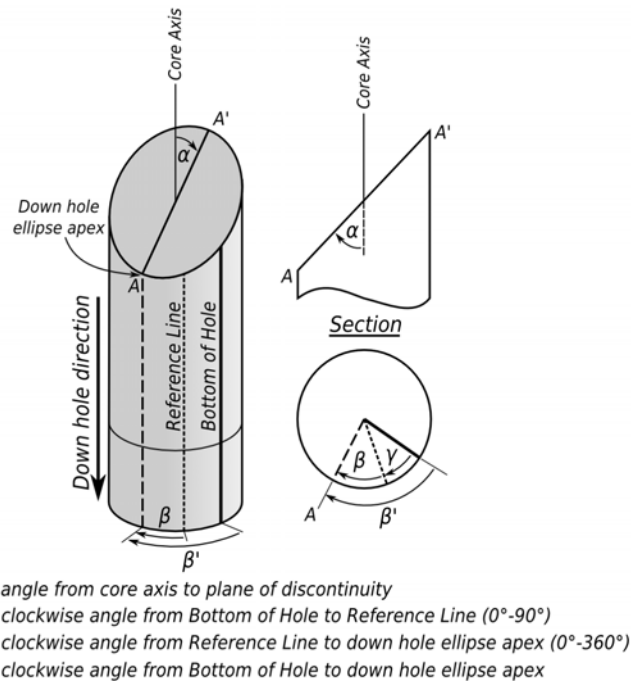


Figure A.1 - Recommended discontinuity orientation measurements for core

Alternative In-hole Tool Methods

Discontinuity orientation can also be established from the walls of the drillhole, rather than the drill core. This has an advantage over the cored techniques, in that there is almost no disturbance of the rock mass in the borehole walls, therefore orientation reliability is greatly improved. These techniques can be especially useful for cored holes that were not oriented.

- Optical Imaging - involve using optical focussed video cameras, taking continuous video images.
- Digital Scanning - utilise rotating mirror devices, combined with high resolution photoelectric transformers, such as rotating line scanner charge coupled devices (CCD), to take a full colour continuous image of the borehole wall.
- Impression Packers - similar to a hydraulic or pneumatic packer, containing a pressure sensitive film beneath the outer membrane, with the packer inflated against the borehole wall and an image of a section of the wall taken.
- Acoustic or Sonic Wave - the technology principally relies on sonic wave travel time and wave attenuation to obtain an acoustic image of the borehole wall.

All these techniques, do however, rely on specific operating conditions, such as smooth borehole walls (e.g. diamond drilled) and some require clear borehole fluids. This may precluded their use under certain conditions.

A.2 MANUAL MAPPING OF EXPOSURES

Typically in mining, whether it be open pit or underground mining, the *orientation* of exposures available for mapping are usually predetermined, such as pit walls, cross-cut and ore drives. In addition, there may only be limited access to the rock mass biasing *where* measurements can take place. The method of excavation (e.g. rock cutting versus drill and blast methods) may also introduce additional biases by removing rock mass containing smaller discontinuities (see Figure A.2). This process results in a 'stereological thick' section potentially invalidating statistical assumptions used in stereological analysis techniques (Harries, 2001; Mathis, 1988).

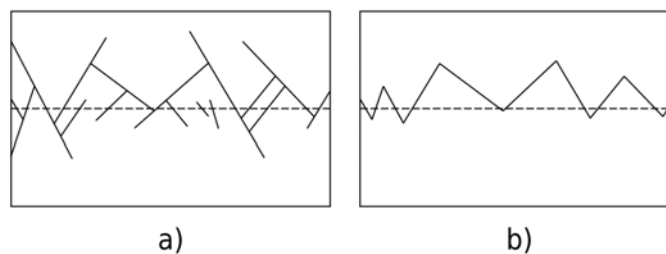


Figure A.2 - Problems associated with stereological thick sections a) all discontinuities intersecting a designed wall, b) resultant wall profile after excavation (Harries, 2001)

Spot Mapping

Spot mapping can be described as a reconnaissance mapping method, whereby geological features are mapped on an ad-hoc, subjective basis, either because of limited outcrops or level of study does not require detailed systematic mapping. Generally, the location of individual measurements are not recorded, with only an approximate locality for the mapping provided. In addition, the orientation of the sampled exposure is seldom recorded, and therefore the degree of orientation bias cannot be established nor accounted for.

Line Mapping

Line mapping involves describing all the geological features that intersect a line of a known location and orientation on a rock mass exposure (Attewell and Farmer, 1976; Priest and Hudson, 1976). Typically, all features that intersect the line are recorded in a systematic and objective manner. Typically, line mapping is used to record discontinuity data, however, they also can be used to record rock fabric characteristics, such as strength, weathering and alteration. Discontinuity attributes are recorded similar to core logging, however, additional information such as trace lengths, terminations, larger scale surface characteristics and true dip and dip direction are recorded.

Horizontal line mapping is generally located around 1.5m from the floor. The start and end points are marked on the excavation surface, with the positions recorded in the local mine coordinate system. The length and orientation of the line is also recorded. Rock mass exposures may have irregular lower limits or upper limits (i.e. undulating floors or roofs). This has the potential to bias trace lengths. In order to minimise these biases, a regular sampling region is created. In order to correct for truncation bias, it is also necessary to decide and state the minimum discontinuity trace length that will be recorded. This information is **mandatory** if bias corrections are to be made. It must be noted that lines should be of sufficient length to adequately characterise a rock mass domain. Priest and Hudson (1976) suggests that between 1000 and 2000 discontinuities must be sampled to provide an adequate characterisation of a typical site. Additional measurements may be required where a site exhibits many different lithologies, highly variable discontinuity characteristics, or where a higher degree of confidence in engineering design is required. The number of discontinuity samples might be made up from line mapping of between 150 and 350 discontinuities, about 50% of which have at least one end visible, taken at between 5 and 15 sample locations, chosen to represent the main zones of geologic structure and lithology (i.e. domains). In complex lithological zone, where up to six discontinuity sets may be present, it is suggested that around 40 discontinuity samples per set are taken (Savelly, 1972; Villaescusa, 1991). It is extremely important to identify and separate measurements from different rock mass 'domains'. Line mapping should be conducted at three orthogonal orientations of equal length to eliminate directional bias.

Window Mapping

Window or cell mapping is an areal mapping technique that involves recording all discontinuities that are observed within a sampling region. The sampling region is typically rectangular in order to account for censoring, truncation and orientation bias (Kulatilake and Wu, 1984a; Kulatilake and Wu, 1984b), although circular sampling regions can make treatment of biases more simplistic (Mauldon, 1998). Rock mass data within the area to be sampled are typically recorded as a scaled sketch or drawing, represented in plan or section. To assist in accurately representing the location and scale of features, a drawing grid is typically used as a reference. Individual discontinuities can be distinguished by assigning a unique identification number in the sketch, with the attributes recorded on a separate data sheet. It must be noted, however, that not all features within the sampling region may be manually accessible. That is, only features located approximately 2m from the floor can be reached for physical examination and direct measurement, such as discontinuity orientation measurements by compass or surface profile measurements. Attributes for discontinuities outside this region may therefore need to be estimated visually from some distance, hence

their reliability may be lower.

In order to ensure adequate characterisation of a site, the side length of the window mapping should be large enough to contain between 30 and 100 discontinuities. It is also recommended that two similar sized windows should be taken, at orthogonal directions (Priest, 1993). Window mapping is generally more suitable than line mapping under following conditions;

- Semi-homogeneous, moderately to heavily jointed rock masses
- Limited amounts of multi-directional access available

The main advantage of window mapping over line mapping is that it provides a reasonably comprehensive data over a much smaller area. In addition, the actual location of discontinuities can be established, such that they can also be treated deterministically. This may involve digitising line segments (e.g. discontinuities) and polygons (e.g. fabric data) and subsequently geo-referencing this geometrical information to the local mine coordinate system. Window mapping is still time consuming, and requires dedicated personnel to collect data accurately. Importantly, sampling biases need to be understood by personnel collecting data.

Geological Mapping Techniques

Geological mapping is routinely undertaken by geologists during mine development. The main purpose of this mapping is to assist in improving the understanding of the general mine geology, to understand the geological controls on economic mineralisation. Typical sampling regimes for routine underground mine geological mapping predominantly consist of two formats; face mapping (vertical faces) and backs (roof) mapping.

Geological mapping techniques may appear to have limited usefulness in rock mass characterisation for rock mechanics purposes, mainly as these sampling methods are highly subjective and unsystematic techniques. In addition, the treatment and correction of biases is often difficult. In light of the above general comments, the use of “geological mapping” data for construction of stochastic models of geotechnical or “rock mechanics” parameters could be considered of limited value. However, geological data generally has an advantage over traditional geotechnical data collection methodologies, mainly due to the data density and coverage over the mine. It is considered that geological mapping data still provides a very important role in rock mechanics. It can be used in the delineation and definition of rock mass domain boundaries, and in the development of “deterministic” models and subsequent analysis techniques.

A.3 A REVIEW OF REMOTE DISCONTINUITY MAPPING TECHNIQUES

The following sections briefly outline remote rock mass characterisation data collection techniques commonly used in the mining industry, along with some issues in their use.

Stereoscopic Techniques

The most predominant stereoscopic methods utilised in the mining industry for rock mass data collection employ photogrammetric techniques. Photogrammetry is the technique of registering topographical features of a corresponding pair of stereographic images, and referencing them to a local cartesian coordinate mapping system (Hagan, 1980). The main advantages of image-based data collection techniques include (Gaich et al., 1999);

- Objectivity of images
- Reduction of time required for field surveys
- Data acquisition in inaccessible areas
- Acquisition of statistically sufficient quantity of data
- Processing and detailed evaluation of data in the office without time constraints
- Permanent record for review purposes

Digital photogrammetry is particularly wide-spread in the mining industry, with a number of systems in use including; Sirovision (Poropat, 2005), JointMetrix3D (3G Software and Measurement, 2008), and 3DM Analyst (ADAM Technology, 2008). These systems generally consist of three main parts;

- Photogrammetric data collection; image capture, placement of survey control or ranging targets (if applicable), surveying of targets and/or camera locations.
- Relative or absolute digital image registration and geo-referencing, generation of X, Y, Z point cloud from image pixels, 3-dimensional surface construction using triangulated networks and image draping over the constructed 3-dimensional model
- Post-processing using software for analysis of discontinuity planes and traces

Once a 3-dimensional surface model has been constructed, analysis software allows for the manual interpretation and digitising of discontinuity planes (e.g. polygonal boundaries) and traces. Once digitised, geometric characteristics such as spacing, trace length and orientation distributions can be ascertained.

Laser Scanning Techniques

These techniques rely on the detection of laser illumination of rock mass surfaces and include devices such as *CMS* and laser scanning instruments. The illuminated point can then be resolved into 3-dimensional coordinates from distance and angular measurements. Laser techniques can produce a dense 'point-cloud', with data points for a typical scan resulting in millions of points. These points can be used directly to ascertain the position and orientation of discontinuities through planes of best fit (Sturzenegger et al., 2007), however, typically a triangulated mesh is initially developed to represent the rock mass exposure. Similar post-processing and digitising techniques to digital photogrammetry can be used to analyse rock discontinuity data.

Survey Control

Currently most methods still involve substantial time and resources to set up and tie-in the imaging/scanning devices to the local coordinate system and to capture the data within the underground production cycle.

Environmental Conditions

Atmospheric and excavation surface conditions have a significant impact on the viability of indirect methods. Environmental conditions include; rock mass colour/texture/reflectivity, airborne or surface moisture and dust. Poor environmental conditions can be particularly pronounced in underground operations where shotcrete is used as an integral part of the mining cycle and can effect both photogrammetry and laser methods.

Obtaining consistent lighting conditions for photography may also be problematic, where shadows can influence the effectiveness of photogrammetry. For underground applications, light sources are currently acceptable for small scale excavations (such as ore development and declines), however, it is still impractical to illuminate and use photogrammetric techniques in large open voids such as stopes. In such cases, laser-scanning techniques may be preferable.

Integration with the Mining Cycle

The use of shotcrete in the mining cycle also can limit the practical applicability of these methods. Where shotcrete is in systematic use, it is a fundamental requirement that the remote method is undertaken in a timely fashion and integrated into the development cycle (i.e. undertaken regularly and immediately after scaling and loading of the blasted face) as

rock mass data cannot be captured once exposures have been covered by shotcrete.

Resolution

The resolution of the digital cameras has increased dramatically in recent years, however, it still has a significant effect on the ability of the method to detect discontinuities. The resolution or size of pixels in the resulting image of a rock surface is a function of the resolution of the pixel sensor in the camera, focal length of the lens, distance of the camera to the target (Birch, 2006);

$$pixelsize_{ground} = \frac{distance}{f} pixelsize_{sensor} \quad (A.1)$$

where f is the focal length of the lens, $distance$ is the distance from the camera to the subject. For example, a Canon EOS 20D with a 28mm lens 174m from the target has a ground resolution of 4cm, compared to the JointMetrix3D system which has a ground spatial resolution of 1/5000 FoVm (e.g. 1 mm resolution for an excavation surface 5m away). The angular sampling density of laser points (for example, CMS instruments typically take one measurement per degree), the distance to the excavation surface, and the laser beam width will determine the resolution, or effective instantaneous field of view (*EIFOV*), of the laser survey (Lichti, 2004). The effective rock exposure resolution will impact on the ability to detect and define discontinuities. Indeed, the width of fine or low aperture discontinuities can potentially be below the effective rock exposure resolution of digital cameras and laser-based systems, and can contribute significantly to truncation bias. With respect to the evaluated photogrammetric and laser-scanning analysis software, no allowance has been made for determination and treatment of truncation bias. It is considered that this is a high priority area for improvement if these technologies are to be used to as rock mass characterisation tools. In addition to truncation issues, resolution also affects the ability to gather measures of small scale roughness.

Occlusion and Orientation Bias

Laser scanning techniques are particularly susceptible to occlusion and orientation bias. Occlusion bias is where discontinuity planes are aligned parallel to the line of sight to the laser, which can result in these discontinuities be occluded, or effectively “hidden” (Sturzenegger et al., 2007). Occlusion bias is therefore a form of orientation bias. It is important to minimise these effects by scanning the same rock mass exposure from a variety of positions and angles. This may be unavoidable in underground environment, particularly for large open stopes, where limited access options exist.

Statistical Treatment of Biases

Post-processing and analysis of digitised traces and planes is currently be done in a similar fashion to mapping or logging data (i.e. 1-dimensional and 2-dimensional data), however, there are a number of differences in the treatment of biases using remote 3-dimensional methods (Poropat, 2005). There are also concerns about the validity and usefulness of the statistical treatment of spacing collected by 3-dimensional methods. Examination of the Sirovision and JointMetrix3D analysis software systems, indicates that, due to the 3-dimensional nature of the data capture method, spacing measurements are calculated in a unique fashion. Here, traces are first projected onto a projection plane that is perpendicular to the mean trace dip and dip direction. Selected distances are then taken between the traces of discontinuities in the direction parallel to the mean normal vector for a particular discontinuity set (see Figure A.3).

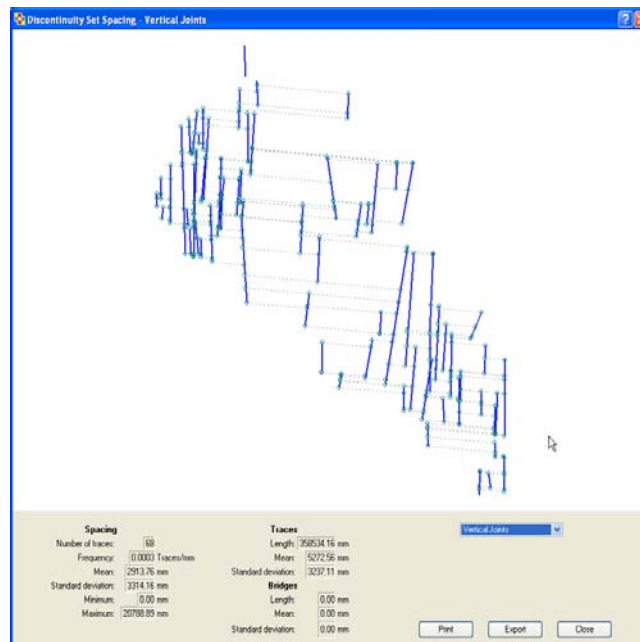


Figure A.3 - Example of spacing analysis in the JointMetrix3D analysis software (3G, 2008)

However, the distances measured between discontinuities are not taken with respect to regular spaced sampling lines, with the locations manipulated such that they intersect the nearest discontinuity. As traces are “projected” onto a projection plane prior to calculating spacing, there is an assumption of continuity. Another concern is that the sampling region, or reference boundary, is ill-defined and there is limited consideration for 'discontinuity free' areas around the periphery of the sampling region. In effect, all of the above aspects artificially bias the calculations towards closely spaced discontinuities. In addition, it is unclear how orientation bias and censoring bias have been treated in establishing mean orientations and trace lengths in the software.

Excavation Relief Bias

The principal of stereographic methods and laser techniques is to detect discontinuities from their 3-dimensional profile that they make on the excavation or outcrop surface. The excavation method, for example smooth wall blasting (i.e. use of pre-splits) versus poorly controlled blasting may result in a difference in the number and size of discontinuity surfaces exposed. Whilst excavation relief is fundamental for these methods to work, it paradoxically introduces bias and other factors that make stereological statistical approaches more difficult.

Automatic Discontinuity Detection

Recently, some researchers and software vendors are investigating semi-automatic to fully automatic discrimination of discontinuities from photogrammetric and laser scanning data, however, success has been limited (Poropat et al., 2007; Reid and Harrison, 2000). Light conditions can influence the success of correctly identifying joint traces or planes, and there is always the risk that automatic algorithms may select artificial features, such as blast induced fractures, excavator tool marks, and half-barrels from drilling and blasting. Without detailed physical examination of rock mass exposures, it is uncertain whether remote methods and associated computer algorithms will have the ability to satisfactorily distinguish between natural discontinuities and artificial features.

Discontinuity Shear Strength Attributes

Shear strength attributes of discontinuities, such as discontinuity mineral infill, rock fabric alteration, weathering and strength are still unable to be reliably captured by photogrammetric and laser techniques. Manual field observations are **still required to adequately characterise** the rock mass (Strouth and Eberhardt, 2006).

A.4 BIAS CORRECTIONS TO UCS AND POINT LOAD DATA

Uniaxial Compressive Strength

The uniaxial compressive strength (*UCS*) test is undertaken on cylindrical specimens of rock, typically diamond drill core samples. Typical samples sizes range from approximately 24mm in diameter up to 85mm in diameter (AX to PQ core size), with diameter to height ratios ranging from 2.0 to 3.0. In the case of samples with differing height:diameter ratios, it is recommended that test results are corrected (ASTM, 1986);

$$C = \frac{C_a}{0.88 + \left(\frac{0.24d}{h}\right)} \quad (\text{A.2})$$

where C is the corrected *UCS* values for a 2:1 height:diameter ratio, C_a is the *UCS* test result and d and h are the diameter and height of the test specimen, respectively. The strength value also *generally* decreases with increasing sample size (Hoek and Brown, 1980). In order to compare results from various core sizes they proposed the following correction factor;

$$\sigma_{C(50)} = \frac{\sigma_c}{\left(\frac{50}{d}\right)^{0.18}} \quad (\text{A.3})$$

where $\sigma_{C(50)}$ is the equivalent *UCS* for a 50mm diameter sample, d and σ_c are the diameter and uniaxial compressive strength for the specimen, respectively. It must be noted that this conversion factor may not be appropriate for all rock types and grain sizes, as the maximum strength may smaller than 50mm (Hawkins, 1998), with *UCS* values decreasing with either reducing or increasing sample diameter. The results of uniaxial compression tests are also highly dependant on the degree of anisotropy and the direction of testing with respect to the prevailing anisotropy or predominant planes of weakness.

Additional details about the specimen and test results should at least include;

- Lithology, weathering and alteration, angle of schistosity or foliation with respect to the loading axis. Where core is oriented alpha and beta angles (see Section XX) of fabric should be recorded.
- Unique sample identification number, location or borehole, along with the depth position in the hole. Along with the drill hole survey information, this effective orients and positions the sample with respect to the local mine coordinate system.
- Core size diameter and height of test specimen
- Pre- and post-test photographs, with post-failure sketch showing major failure

planes.

- Identification of failure modes.

Position and angle of failure shear plane and whether this can be identified as being a pre-existing discontinuity.

Point Load Test

The point load test was developed to provide a simpler, faster and less expensive option for assessing intact rock strength. The method involves placing rock samples between conical plattens and loading them to failure. A number of test configurations for drill core or small lump samples have been devised. The (ISRM, 1985) also includes testing arrangement for anisotropic rocks and descriptions of failure modes which assist in identifying valid or invalid tests. The uncorrected point load strength (I_s) can be calculated as follows;

$$I_s = \frac{P}{D_e^2} \quad (\text{A.4})$$

where D_e is the equivalent core diameter (or D for diametral tests on core) and P is the load (kN) at failure. In order to compare point load strengths from a variety of block sizes, it may be necessary to correct for scale. The (ISRM, 1985) recommends the following procedure to correct for size;

$$I_{s(50)} = I_s \left(\frac{D_e}{50} \right)^{0.45} \quad (\text{A.5})$$

(Broch and Franklin, 1972) suggested, based on a limited number of correlation tests, that the point load strength can be related to the uniaxial compressive strength as follows;

$$\sigma_c = (22 - 24) I_{s(50)} \quad (\text{A.6})$$

Extreme care should be used with the above relationship as conversion factors can vary from around 15 - 50 (ISRM, 1985), with other authors suggesting that this relationship is both rock type *and* strength dependant (Tsiambaos and Sabatakakis, 2004). In addition, simple conversion factors cannot be universally applied to anisotropic rocks (Chau and Wong, 1996), with conversion factors dependant on the degree of anisotropy. In order to ascertain the degree of anisotropy, the strength anisotropy index, $I_{a(50)}$, can be calculated (Brady and Brown, 2004), which is defined as the ratio of mean $I_{s(50)}$ measured perpendicular and parallel to anisotropy.

A.5 ANALYSIS OF DISCONTINUITY DATA

Discontinuity Surface and Infill characteristics

Data describing discontinuity surface and infill characteristics are typically analysed using classical quantitative statistics. It is important to understand the range and variability of surface and infill characteristics found and its impact on rock mass behaviour. For example, one of the prime causes of the difference in cave fragmentation between rock masses is the percentage of hard mineral infill in veins (Brzovic and Villaescusa, 2007). Therefore, in certain circumstances, rock mass behaviour may be strongly influenced by the mineralogical characteristics of discontinuities.

Discontinuity infill properties can vary widely from clean, unaltered surfaces with no aperture to wide, gouge filled faults with highly altered and fractured wall rock. This variety and the enumerable nature of some of this data (i.e. qualitative descriptions), hinders the direct application of classical statistics. Typically, one has to resort to classifying or categorising data prior to undertaking statistical analyses. Extreme care and consideration, must be given when devising “categories” for quantitative analysis of surface and infill characteristics. The choice of “category” may not allow sufficient resolution (i.e. too coarse) in the statistical analysis or may be unsuitable for a subsequent engineering design methodology, such as rock mass classifications.

Discontinuity scale also needs to be considered in any analysis as surface and infill characteristics can be quantitatively described at a variety of scales, from drill core to underground exposures, or described on a mine scale (e.g. surface characteristics of mine-wide faults). It is recommended that the mean and range (distribution type and standard deviation) are described for each discontinuity set, in each domain at the core scale, mapping scale and mine-scale.

Discontinuity surface characteristics, such as waviness or planarity, may display certain degrees of anisotropy. That is, waviness or roughness may be more prominent in one direction than another. In this case, means and ranges may need to be established with respect to dip, dip direction or relative to other directions which may represent maximum or minimum values of these characteristics.

Orientation

Orientation is probably the most important geometric characteristic, as it influences the way

discontinuities interact with each other and, importantly in terms of stability, with excavation faces (Priest, 1993). The main aim of orientation analysis is to identify the main orientations of sets of discontinuities and to determine their mean orientations and the amount of dispersion around these means. It is also useful to determine the proportion of joint orientations that lie outside of identified set orientations. A number of relatively recent computer programs are available for the plotting and analysis of discontinuity orientation data; SAFEX (Windsor and Thompson, 1992), CANDO (Priest, 1993) and DIPS (Rocscience Inc, 1998).

Treatment of Orientation Bias

Depending on the direction and method of sampling, discontinuities from one set may be preferentially sampled than other discontinuity orientations. It is good practice to sample in three orthogonal directions to minimise bias. However, it is also possible to account for bias, to some degree, by applying a weighting factor. Priest (1993) shows that the probability of intersecting a discontinuity with a scanline P_s is proportional to its area A and the acute angle between the discontinuity normal and the scanline direction δ_s ;

$$P_s \propto A \cos \delta_s \quad (\text{A.7})$$

Discontinuities with their normals at a high angle to the scan line will be under represented. In this case, a weighting w_s can be applied to scan line samples;

$$w_s = \frac{1}{\cos \delta_s} \quad (\text{A.8})$$

Where discontinuities are sampled by planar surfaces (e.g. window mapping), one needs to consider the acute angle between the discontinuity normal and the normal of the sampling face δ_f . The weighting w_p for planar samples in this case is shown below;

$$w_p = \frac{1}{\sin \delta_f} \quad (\text{A.9})$$

In the case of scan line data as the acute angle δ_s approaches 90° , the weighting tends to infinity. Similarly, with window mapping data, the weighting approaches infinity as the acute angle δ_f approaches 0° . In order to circumvent this, an upper limit to weighting is applied. A maximum weighting value of 10 has been suggested (Priest, 1993), which correlates to δ_s and δ_f of 84.3° and 5.7° , respectively.

Mean Discontinuity Set Orientation

Contoured data can then be used to identify and delineate discontinuity orientation sets. Contouring can be done on either the weighted or unweighted pole data. Delineation of sets

involves determining the boundary limits, or specifying which individual discontinuities belong to a specific set. Once delineated, the mean orientation can be established by using either a unweighted or weighted approach. The mean orientation using the unweighted approach involves establishing the direction of the normalised resultant vector, r_n , of all discontinuities in the set. The weighted approach is similar, yet a normalised weighting is applied to each i^{th} discontinuity (Priest, 1993);

$$w_{ni} = \frac{w_i N}{\sum_{i=1}^N w_i} \quad (\text{A.10})$$

where w_i is the individual weightings, and N is the total number of discontinuities.

Orientation Dispersion

Once means for discontinuity sets have been established, statistical methods can be used to estimate the dispersion of orientations about the mean. A number of models can be used to describe directional distribution, however, the most common is the Fisher distribution (Fisher, 1953). The Fisher distribution assumes that orientations are distributed symmetrically about a mean. A number of asymmetrical distributions have been used, such as the Bivariate Fisher and Bingham distributions, however Dershowitz and Einstein (1988) indicated that “none of the currently used distributions provided statistically acceptable fit” to field data from a variety of rock masses. Until more reliable distributions are found, the continued use of Fisher distribution is considered acceptable. The probability density function of the distribution of orientations about an angle θ is given by (Priest, 1993);

$$f(\theta) = \frac{K \sin \theta e^{K \cos \theta}}{e^K - e^{-K}} \quad (\text{A.11})$$

where K represents a controlling parameter of the shape of the distribution, or “degree of clustering”. An estimate of K can be derived for a sufficiently large number of samples (Fisher, 1953), denoted by k , as follows;

$$k = \frac{M-1}{M-|r_n|} \quad (\text{A.12})$$

where M is the number of sample unit vectors in the set and $|r_n|$ is the magnitude of the resultant vector.

Set Definition

Assigning discontinuities into sets is one of the most important tasks in rock mass characterisation, as it allows the rock engineer to assess the rock mass structure. This is

done by establishing the families of discontinuities based on mean orientations, the degree of dispersion (using statistical distributions) and assess the degree of isotropy. These aspects are important input into analysis and design. There are a number ways to delineate discontinuities into sets, ranging from simple visual assignation to complex clustering algorithms.

The simplest form of set definition is to subjectively assess the degree of clustering of poles on a hemispherical projection and place a delineation zone around the cluster. Discontinuity poles falling within the delineation zone can then be used to calculate means and dispersions. Popular discontinuity orientation analysis software, such as SAFEX (Windsor and Thompson, 1992) and DIPS (Rocscience Inc, 1998), allow the user to select “windows” around data points to delineate discontinuity sets. In this process, data are usually presented as poles to planes, overlain with contours. Contours can be generated for weighted or unweighted poles. Care should be taken when using weighted contour plots, especially where data includes one data set whose orientation runs sub-parallel to the sampling direction. In this case, plots of weighted contours may over bias these data. Although the use of this simple technique is popular in mining, in some circumstances, especially where a limited number of data are available, it is possible to visually assign far too many sets than the data set can realistically support (see Figure A.4a). On the other hand, where a large number of data points exist, the subjective nature of human pattern recognition can be useful in determining sets, especially where overlapping clusters exists (Bridges, 1990).

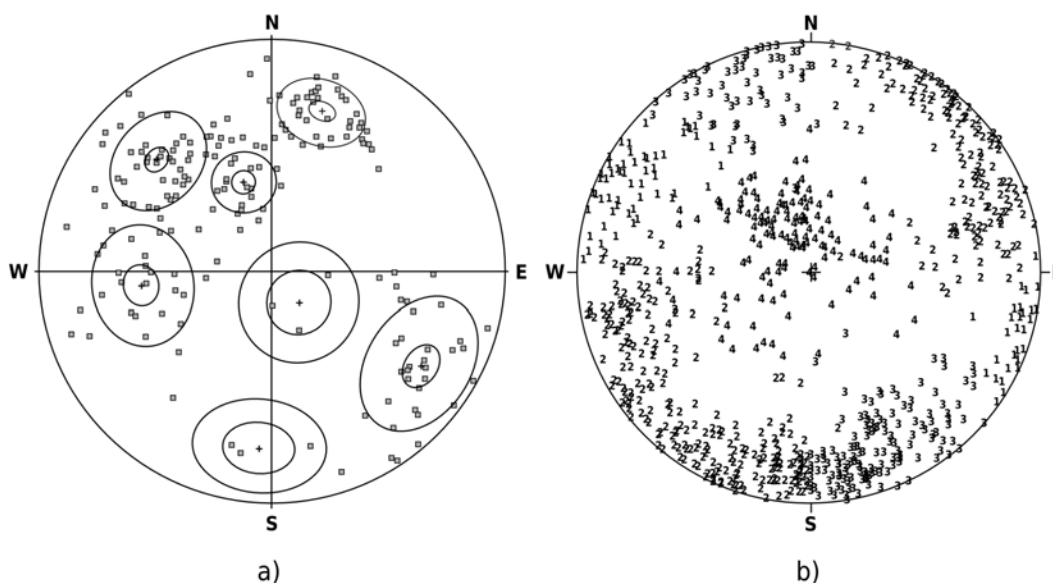


Figure A.4 - Example plot of a) set definition based on small data sets (Pötsch et al., 2007), and b) wide dispersion for four sets defined by clustering algorithm (Shanley and Mahtab, 1976, data from Kulatilake et al, 2004).

Once sets are defined, the degree of dispersion can be evaluated using Fisher's K constant, with low values indicating disperse orientations within the set and high values indicating more precise orientations. The probability density function (equation A.11) and Fisher's K constant can then be used to estimate the probability of a random orientation value being at an angle less than θ with the true orientation $P(<\theta)$ (Priest, 1993);

$$P(<\theta) \approx 1 - e^{K \cos \theta - 1} \quad (\text{A.13})$$

This allows for confidence in the grouping of orientation data (i.e. set) to be established by determining the angle from the mean orientation which could be considered "random".

Semi-Automated Computer Methods

A number of computer algorithms have been developed over the years to assist in the definition of sets. Some of these are shown in Table A.2. Early algorithms suffered from the fact that the number of sets had to be established *a priori* (Shanley and Mahtab, 1976). In addition, they assumed some sort of probabilistic structure to their orientation. Another drawback with some algorithms is that they assume that all discontinuities belong to a set. That is, discontinuities may not be "unassigned" or deemed "random". These factors can have significant ramifications for the mean and dispersion of the less well defined sets. As can be seen from Figure A.4b, the four sets shown almost span the entire projection, providing potentially "unrealistic" sets where set orientations range more than 90° in both dip and dip direction. In order to overcome this, some algorithms utilise probabilistic methods, such as a Poisson randomness test, to reject data from the set. Another method assigns discontinuity to a set via a fuzzy K-mean algorithm (Hammah and Curran, 1998). This uses an iterative process that seeks to partition the data into clusters by seeking out high density data, by looking at distance similarities between observations. The metric used for this distance similarity is the sine angle between unit normal vectors. The main advantage of this method is that the number of sets need not be known *a priori*. Early clustering algorithms also assigned discontinuities to one set only, providing a "hard" partitioning. The method provided by Hammah and Curran (1998) also allows for the likelihood, or "degree of membership", that a discontinuity belongs to a particular set. In this way, the boundaries between discontinuity sets can be described as "soft" or "fuzzy", with degree of membership for discontinuities ranging from 0 to 1.

Table A.2 - Summary of Discontinuity Set Definition Methods

Method	Distribution	Clustering Method	No. of sets <i>a priori</i>	Multi- variate	Set Classification
Manual	(Fisher, 1953)	Subjective interpretation manual	No	Possible	Hard
Shanley and Mahtab, 1976	(Bingham, 1964)	Modified one-level mode analysis	Yes	No	Hard
Dershowitz et al, 1996	Empirically derived	Iterative stochastic algorithm	Yes	Yes	Hard
(Hammah and Curran, 1998)	Distribution free	Fuzzy K-means	No	Yes	Soft
(Marcotte and Henry, 2002)	Bivariate Normal	Maximum likelihood and finite mixture distributions	No	No	Soft
(Zhou and Maerz, 2002)	Distribution free	Nearest neighbour, Fuzzy K-means, Fuzzy c-means, Vector quantization	No	Yes	Soft
(Klose et al., 2005)	Distribution free	Vector quantization	Yes	No	Hard
(Jimenez-Rodriguez and Sitar, 2006)	Distribution free	Spectral clustering algorithm in transformed space	No	No	Soft
(Jimenez, 2007)	Distribution free	Spectral clustering with fuzzy K-means	Yes	No	Soft

Algorithms can also be classified into whether they assess orientation alone, or whether they are able to assess orientation as well as other discontinuity characteristics during set definition. The latter types can be termed multivariate methods. Although orientation parameters are definable metrics in a multivariate analysis, the choice or magnitude of value used to represent other parameters, will have a significant influence on the results. For example, introducing surface characteristics one could use non-enumerable data such as roughness codes, or enumerable data that have asimilar data ranges, such as joint wall compressive strength (MPa) versus Schmidt Hammer Rebound number. The use and validity of these additional parameters in multivariate discontinuity analysis is still unclear.

Whilst recent developments in computer algorithms for set definition are encouraging, it still is to be seen whether a fully automated system can be developed that can take into account discontinuity set definition for all engineering objectives and requirements.

Assessment of Isotropy

Once the major discontinuity sets have been identified and their properties defined, the rock mass structure pattern can be characterised. This may involve assessing;

- the number of sets and relative intensities of each set,
- angular relationships between sets, that is, whether sets are oriented orthogonal or at acute angles to each other, and
- the degree of anisotropy.

The latter characteristic is especially important when trying to determine the applicability of certain design techniques. For example, the applicability of the Hoek-Brown failure criteria (see Chapter 4) is dependent on the rock mass structure being homogeneous and isotropic. It is therefore important to assess the isotropy of the rock mass. Read et al (2003) provide a simple assessment from stereographic contours plots to distinguish uniform (isotropic), random or regular discontinuity patterns using two indices ;

- the area within the 1% contour ($A_{1\%}$)
- the maximum concentration (C_{max})

Figure A.5 shows a recommended guide to classifying isotropy and structure of the rock mass. Care should be taken when utilising this method with limited data. Read et al (2003) suggest that the method only be applied with at least 200 data points. The definition of isotropic referred to in this method is based *solely* on orientations and not the degree of fracturing or intensity of each discontinuity set. It should also be noted that this approach is highly dependant on the counting methods used to generate contours.

Other methods for characterising the discontinuity orientation fabric involve assessing various parameters of the orientation tensor, namely the ratios between eigenvalues. The orientation tensor can be derived from the directional cosines of poles representing discontinuities (Scheidegger, 1965);

$$A_D = \frac{1}{n} \sum_{i=1}^n \begin{bmatrix} \sum l_i^2 & \sum l_i m_i & \sum l_i n_i \\ \sum m_i l_i & \sum m_i^2 & \sum m_i n_i \\ \sum n_i l_i & \sum n_i m_i & \sum n_i^2 \end{bmatrix} \quad (\text{A.14})$$

However, these methods of assessing structure characteristics through eigenvalues are generally applicable for unimodal clusters, axially symmetrical girdles of clusters or a combination of the two with orthorhombic symmetry (Woodcock, 1977). This limits their practical use for a wide range of discontinuity patterns that may be encountered.

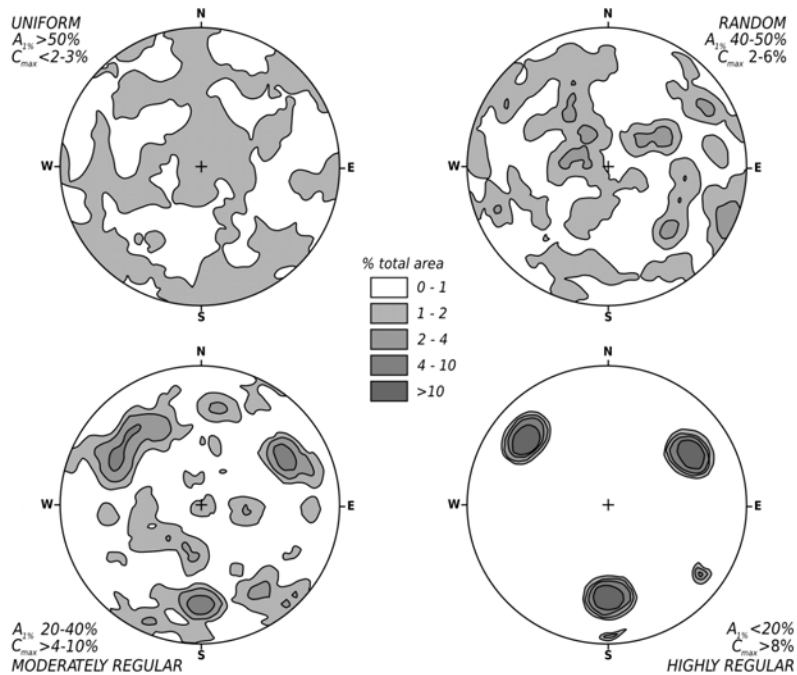


Figure A.5 - Classification of rock structure using contour areas from lower hemisphere equal area stereographic projections (after Read et al, 2003)

Discontinuity Density and Intensity

Discontinuity density and intensity are quantitative measures that describe the degree of fracturing of the rock mass. **Discontinuity density**, or volumetric frequency (λ_v), can be defined as **the average number of discontinuities centres per unit volume of rock mass** (m^{-3}). This measure is described as the most fundamental property of the rock mass (Priest, 1993), as it controls all other discontinuity properties. Volumetric frequency (λ_v) can be applied to all the discontinuities within the rock mass, or estimated for individual sets (λ_v^n). As it is practically impossible to completely dismantle the rock mass, define the boundaries of each discontinuity, and finally establish and count their centroids, other means need to be devised to **estimate** this fundamental intrinsic property.

Rather than locating all discontinuity centres, an estimate of discontinuity frequency can be derived from the total area of discontinuities per unit rock mass volume (m^{-1}). The **total area of discontinuities per unit volume** represents a measure of **discontinuity intensity**, which includes aspects of discontinuity size and shape, as well as the number of discontinuities.

Due to the limited exposed and sampled populations available, discontinuity density and intensity can only be **estimated** from areal or lineal measures. For example, areal frequency (λ_a) is the average number of discontinuity centre points intersected per unit area (m^{-2}) and

is influenced, or biased, by the angle between the discontinuity normal and the normal sampling plane and the position of the sampling plane relative to the discontinuity centre. An alternative measure, areal discontinuity intensity, is the total length of the discontinuity traces within a given area (m^{-1}). This measure attracts additional biases, due to the shape of the sampling area with respect to the orientation of discontinuity traces, and the ability to account for all trace lengths present within a sampling area.

Dershowitz and Herda (1992) provide a simple framework outlining the concepts of discontinuity **density** and **intensity** measures in one-, two- or three-dimensions. These measures can be applied to both the individual sets that make up the rock mass structure, or they can be applied without referring to specific sets or orientations. One-dimensional measures refer to measures applied along a sampling line, two-dimensional measures refer to measures applied over a sampling area, and three-dimensional measures refer to measures applied over a sampling volume. The following sections describe these measures and how they relate to the various definitions of discontinuity frequency and spacing. A summary of these measures is also provided in Figure A.6.

One-Dimensional Measures

A one-dimensional measure refers to a discontinuities intersected along a line. Spacing is a measure most commonly associated with one-dimensional sampling regimes. Three formal definitions of spacing are provided (Priest, 1993);

- **Total spacing** (S_t). This is the distance between a pair of immediately adjacent discontinuities measured along **a line of specific location and orientation** through the rock mass. The mean total spacing is given by;

$$\bar{S}_t = \frac{1}{n} \sum_{i=1}^n S_{ti} \quad (\text{A.15})$$

where n equals the sample size and S_{ti} is the i^{th} value of the total spacing.

- **Set Spacing** (S_s). This is the distance between a pair of immediately adjacent discontinuities from the same set, measured along **a line of specific location and orientation** through the rock mass. The mean set spacing is given by;

$$\bar{S}_s = \frac{1}{n} \sum_{i=1}^n S_{si} \quad (\text{A.16})$$

where n equals the sample size and S_{si} is the i^{th} value of the set spacing.

- **Normal Set Spacing** (S_n). This is the perpendicular distance between a pair of immediately adjacent discontinuities from the same set, measured **along a line of**

specific location and oriented parallel to the mean normal to the set. The mean normal set spacing is given by;

$$\bar{S}_n = \frac{1}{n} \sum_{i=1}^n S_{ni} \quad (\text{A.17})$$

where n equals the sample size and S_{ni} is the i^{th} value of the normal set spacing.

The set spacing can be related to the normal set spacing by;

$$S_n = S_s \cos \delta \quad (\text{A.18})$$

where δ is the acute angle between the discontinuity normal for the set and the sampling line. The actual definitions provided above are very important. They imply that the spacing values, and thus the mean calculations, are specific to the location and orientation of the sampling line. That is, the spacing values, or means of spacing values, from a sampling line oriented in one direction for a given rock mass will be different from those in another orientation and location. **Spacing is not an intrinsic discontinuity parameter**, yet is dependent on the geometrical arrangement of discontinuities (number per unit volume, size and shape, and orientation) and the chosen sampling regime.

Spacing may also be expressed as the inverse, that is the number of discontinuities per metre (ISRM, 1978). Commonly termed **discontinuity linear frequency** (λ), or **fracture frequency**, this measure can be made along a borehole or line mapping and can be considered a one-dimensional measure of discontinuity intensity. Similar definitions to those provided above can be applied for total (λ_t), set (λ_s) and normal set discontinuity linear frequency (λ_n).

Total discontinuity linear frequency (λ_t) along a borehole or scanline is a one-dimensional measure of discontinuity **density**, as it measures the **number** of discontinuities intersected per unit length and can be defined as;

$$P_{10} = \frac{1}{L} \sum_{i=1}^n x_i = \lambda_t \quad (\text{A.19})$$

where x_i is the i^{th} discontinuity intersected over a line of length L and has units m^{-1} . As this measure has units of m^{-1} , it can also be regarded as a measure of discontinuity **intensity**.

This measure can be related to **total spacing** (\bar{S}_t) by the following;

$$P_{10} = \frac{1}{\bar{S}_t} \quad (\text{A.20})$$

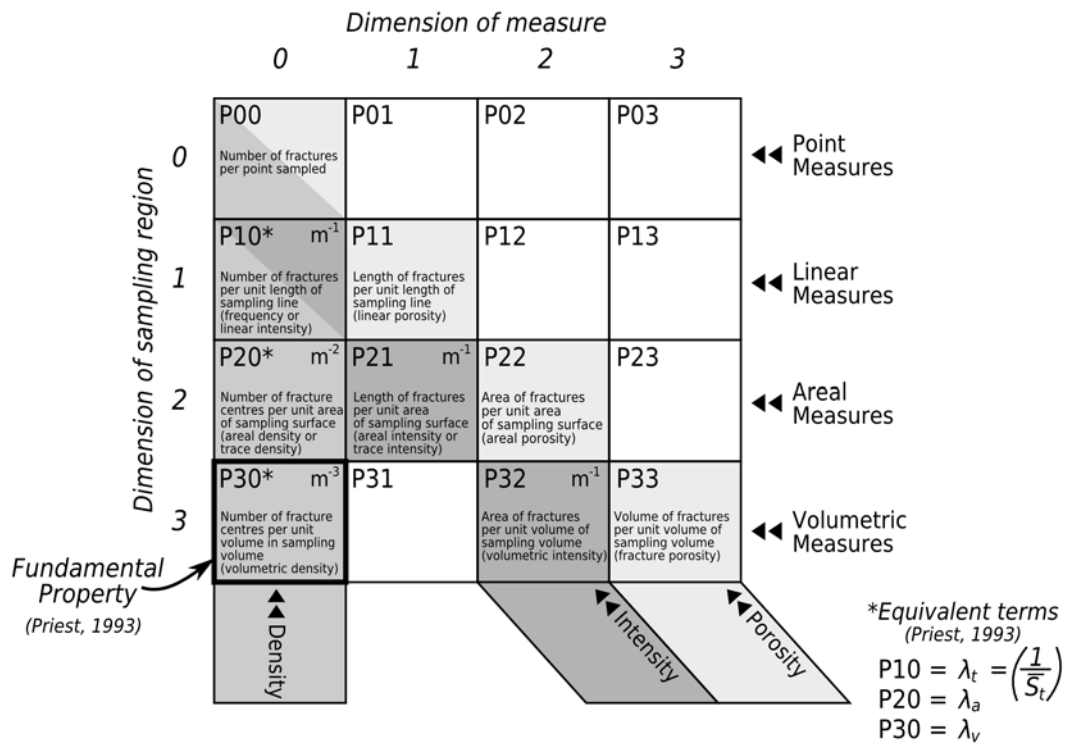


Figure A.6 - Matrix of rock mass fracture density and intensity measures (modified from Dershowitz and Herda, 1992)

The one-dimensional discontinuity **intensity** measure (P_{10}), as well as discontinuity linear frequency and spacing, are dependant on the direction of sampling with respect to the orientation of discontinuities. True discontinuity intensity (P'_{10}), or corrected total discontinuity linear frequency (λ'_t), for a line of a specific orientation can therefore be obtained by including the acute angle between the sampling line and the discontinuity normal;

$$P'_{10} = \frac{1}{L} \sum_{i=1}^n \frac{X_i}{\cos \delta_i} = \lambda'_t \tag{A.21}$$

where δ_i is the acute angle between the i^{th} discontinuity normal and the sampling line. The above measure can be applied to all discontinuities intersected, or to selected discontinuities from a particular set.

Dershowitz and Herda (1992) consider that these measures are independent of discontinuity size, and are therefore classified as **scale independent** measures. This can be illustrated in Figure A.7, where the values of these measures will remain the same if the discontinuity size is halved and the number of fractures is doubled. Although this measure is apparently independent of discontinuity size, it must be noted that the accuracy and precision of this measure is still dependant on the sample length. In addition, it is considered that the term “scale independent” is a misnomer, as the measure is specified in units related to length.

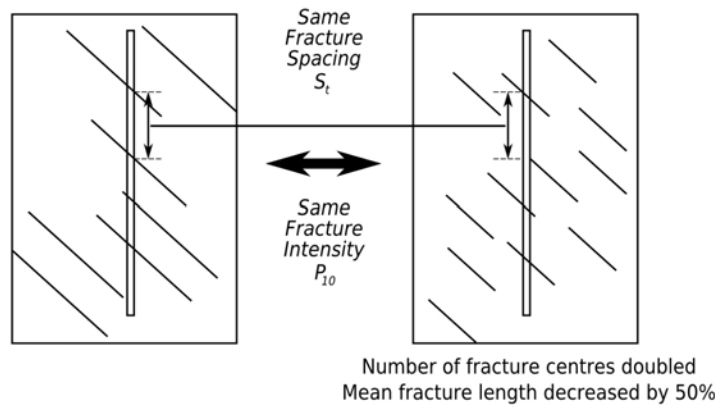


Figure A.7 - Illustration of scale independent discontinuity measure P_{10} (after Dershowitz and Herda, 1992)

In most core logging practices, discontinuity linear frequency is logged **without regard** to the angle between the discontinuity normal and the axis of the borehole. For anisotropic rock masses, this can have a significant impact on the accuracy of discontinuity linear frequency. In this case, λ_t and P_{10} values represent **biased estimates** of discontinuity linear frequency that are only valid in the direction of the drill hole (i.e. they represent vector quantities).

Two Dimensional Measures

Discontinuity **density** in two-dimensions is defined by measure P_{20} and can be described as the amount of discontinuity trace centres intersected in a sampling area. This measure is dependant on the discontinuity size relative to the size of the sampling area, and therefore can be considered a **scale dependant** measure. Two-dimensional discontinuity **intensity** can be described by the measure P_{21} , and is defined as the length of discontinuity traces intersected over a sampling area;

$$P_{21} = \frac{1}{A} \sum_{i=1}^n L_i \quad (\text{A.22})$$

where L_i is the length of the i^{th} discontinuity intersected over a sampling region with area A , with P_{21} having units m^{-1} . The two-dimensional intensity measure P_{21} is also considered scale independent as it directly incorporates discontinuity trace length. This measure can suffer from sampling area bias and as such the accuracy and precision of this measure is dependent on the shape and size of the sampling area. Typically, sampling areas are obtained by window mapping (i.e. rectangular shaped sampling planes). The shape and orientation of these windows with respect to the shape and orientation of discontinuity traces can introduce a number of sampling biases (Kulatilake and Wu, 1984a; Warburton, 1980). Importantly, the use of circular sampling windows can reduce orientation sampling bias (Mauldon, 1998). It must be noted that both the discontinuity **density** (P_{20}) and

discontinuity **intensity** (P_{21}) measures are dependant on the relative orientation of the discontinuities to the sampling plane. Corrected total discontinuity areal intensity (P'_{21}) for a plane of a specific orientation can therefore be obtained by including the acute angle between the normal of the sampling plane and the discontinuity normal;

$$P'_{21} = \frac{1}{A} \sum_{i=1}^n \frac{L_i}{\sin \delta_i} \quad (\text{A.23})$$

where δ_i is the acute angle between the i^{th} discontinuity normal and the normal of the sampling plane.

Three Dimensional Measures

Discontinuity **density** in three-dimensions is defined by measure P_{30} and can be described as the amount of discontinuity centres intersected within a sampling volume and is analogous with Priest's (1993) volumetric frequency (λ_v). Although this measure is a fundamental property of the rock mass structure, its measurement is dependant on the discontinuity size relative to the size of the sampling volume. It therefore can be considered a **scale dependant** measure.

Three-dimensional discontinuity **intensity** can be described by the measure P_{32} , and is defined as the surface area of discontinuities intersected within a sampling volume;

$$P_{32} = \frac{1}{V} \sum_{i=1}^n S_i \quad (\text{A.24})$$

where S_i is the surface area of the i^{th} discontinuity intersected over a sampling region with volume V , P_{32} with having units m^{-1} . The three-dimensional intensity measure P_{32} is **scale independent** as it directly incorporates discontinuity surface area.

Relationships Between Intensity Measures

The measures described above can be interrelated by accounting for the orientation biases of the scanline for linear intensity (P_{10}) and the sampling plane for areal intensity (P_{21}). Dershowitz and Herda (1992) consider that these simple relationships are valid, as long as there is no dependence of discontinuity size distribution with orientation. This would therefore indicate that the three-dimensional or volumetric discontinuity intensity measure (P_{32}) is the most useful measure, as it does not reflect any orientation effects and can be related to true spacing (\bar{S}_t) and linear intensity (P_{10}) without specification of discontinuity size (Dershowitz and Herda, 1992). It has been suggested that volumetric intensity measure provides the most meaningful measure of the "degree of fracturing" of the rock mass

(Mauldon, 1994). It is therefore useful to find this fundamental parameter from the various one- and two-dimensional fracture intensity measures. Dershowitz and Herda (1992) suggested that the volumetric intensity measure (P_{32}) can be related to the linear intensity measure (P_{10}) as follows;

$$P_{32} = C_{P3} \times P_{10} \quad (\text{A.25})$$

where C_{P3} is a proportionality constant dependent upon the distribution of the orientation of discontinuities (i.e. Fisher's constant, K) relative to the sampling line. Similarly, the areal intensity (P_{21}) can be related to linear intensity (P_{10});

$$P_{21} = C_{P2} \times P_{10} \quad (\text{A.26})$$

Dershowitz and Herda (1992) found, through modelling and testing of joint network models, that values of C_{P3} and C_{P2} vary between 1.0 and 5.0 and depend on the dispersion of the discontinuity orientations. Although the authors indicate the scale independent nature of the intensity measures P_{10} , P_{21} and P_{32} , it must be noted that, in order to minimise imprecision and inaccuracy, all intensity measures must be determined over sampling dimensions that are sufficient to adequately capture the minimum representative elemental volume (*REV*).

The proportionality constants investigated by Dershowitz and Herda (1992) assumed that all discontinuity shapes can be represented by circular planar discs. Any interdependence of discontinuity shape with orientation would also affect the proportionality constants. Where sampling scales between sampling dimensions are considerable (i.e. several orders of magnitude), the proportionality constants can only be applied where the discontinuity size distribution follows a scale independent distribution (such as a power law). This type of size distribution can result in discontinuity patterns of a self-similar or fractal nature. It must be noted that natural occurring discontinuity patterns only display self-similar characteristics over a certain range of scales (Bonnet et al., 2001).

In addition, the proportionality constants are only applicable if discontinuity size distributions are **orientation independent**, which only occur in some natural rock masses. If the discontinuity size distributions vary with orientation, then the proportionality constants for one and two dimensional intensity measures will be different depending on the sampling orientation. However, if the sampling directions are kept constant, then proportionality constants can potentially be derived for those specific orientations. The main factors influencing the applicability of proportionality constants are;

- Orientation dispersion
- Orientation dependent discontinuity size distributions

- Orientation dependent discontinuity shape
- Sampling scale bandwidth
- Truncation bias
- Scale dependant discontinuity size distributions (i.e. log-normal versus power)

Analysis of Discontinuity Linear Frequency and Spacing Data

Statistical analysis of discontinuity linear frequency and spacing data is mainly concerned with defining the mean and likely distribution of values. Although the mean provides useful information about the average discontinuity spacing (or degree of intensity), the full distribution can provide information about the likelihood or probability of obtaining smaller values over larger values, or vice versa. It also enables comparisons to be made between sample populations of spacing and linear frequency.

Prior to calculation of the mean, spacing values need to be corrected for bias, or the mean normal set spacing determined. The mean normal set spacing is given by;

$$\bar{S}_n = \frac{1}{n} \sum_{i=1}^n S_{ni} \quad (\text{A.27})$$

where n equals the sample size and S_{ni} is the i^{th} value of the normal set spacing. The estimate of the standard deviation for the normal set spacing is given by;

$$\sigma = \sqrt{\frac{1}{n-1} \sum_{i=1}^n (S_{ni} - \bar{S}_n)^2} \quad (\text{A.28})$$

The mean and standard deviation of corrected discontinuity linear frequency values can be determined in a similar fashion;

$$\bar{\lambda}'_t = \frac{1}{n} \sum_{i=1}^n \lambda'_{ti} \quad (\text{A.29})$$

where n equals the sample size and λ'_{ti} is the i^{th} value of the corrected discontinuity linear frequency. The estimate of the standard deviation for the corrected discontinuity linear frequency is given by;

$$\sigma = \sqrt{\frac{1}{n-1} \sum_{i=1}^n (\lambda'_{ti} - \bar{\lambda}'_t)^2} \quad (\text{A.30})$$

The arithmetic mean can be calculated for all discontinuities sampled in a scanline, or can be applied only to individual discontinuities within a set. The latter is more useful as it provides estimates of the relative intensity of individual sets within the rock mass.

Discontinuity Intensity with Orientation

The intensity measures provided above can be applied to individual sets within the joint network system, or alternatively, without regard to orientation or specific sets (i.e. implying isotropy). Another analysis method for characterising discontinuity frequency or spacing is to establish its variation with direction. By knowing the mean normal discontinuity linear frequency for each discontinuity set within the rock mass, it is possible to calculate the discontinuity frequency in any direction. The following method assumes that the rock mass consists only of a known number of discontinuity sets (i.e. no “random” joints), each with **parallel** discontinuities. Furthermore, the method assumes that the mean normal discontinuity linear frequencies do not vary significantly over the sampled region, that is, the method is only applicable for relatively homogeneous rock masses. The discontinuity frequency along a line of known direction is (Priest, 1993);

$$\vec{\lambda} = \sum_{i=1}^D \lambda_i \cos \delta_i \left(\frac{-\pi}{2} \leq \delta_i \leq \frac{\pi}{2} \right) \quad (\text{A.31})$$

where D is the number of parallel discontinuity sets, δ_i is the acute angle between the wanted sampling direction and the i^{th} set, and λ_i is the frequency along the normal to the i^{th} discontinuity set. Alternatively, equation A.31 can be represented as follows;

$$\vec{\lambda} = m_x s_x + m_y s_y + m_z s_z \quad (\text{A.32})$$

where s_x , s_y , s_z are the directional cosines of the sampling line, and m_x , m_y , m_z are given below;

$$m_x = \sum_{i=1}^D \lambda_i u_x \quad (\text{A.33})$$

$$m_y = \sum_{i=1}^D \lambda_i u_y \quad (\text{A.34})$$

$$m_z = \sum_{i=1}^D \lambda_i u_z \quad (\text{A.35})$$

where u_x , u_y and u_z are the directional cosines of the discontinuity unit normal vectors for the i^{th} set of D discontinuity sets. The equations above can be used to generate a directional discontinuity frequency diagram. The diagram is created by selecting sampling lines in a number of directions in fine increments, say 5° to 10° , calculating the resultant discontinuity frequency. A number of directional discontinuity diagrams are presented in Figure A.8. Figure A.8a shows a 3-dimensional surface plot on cartesian coordinate axes, displaying the variation of discontinuity frequency (z-axis) with trend (x-axis) and plunge (y-axis). Figure A.8b displays the directional frequency diagram represented on a lower hemisphere equal

area projection. Figure A.8c through to Figure A.8e shows a number of views of a 3-dimensional frequency locus diagram. Here, the distance from the origin denotes the frequency. The 3-dimensional locus diagram can be sectioned at any orientation to display the variation of discontinuity frequency projected on a plane. It is also possible to establish the maximum and minimum discontinuity frequencies and their directions. The derivation for local and global frequency minima and maxima directions is provided by Priest (1993). It is interesting to note that the global maximum and global minimum frequency values are not necessarily orthogonal to each other. In Figure A.8b, the global maximum and minimum directions are approximately 75° apart.

Discontinuity Intensity Tensor

Another method of describing the intensity of discontinuities and its distribution with direction is to represent it by a discontinuity intensity tensor. Discontinuity tensors have been developed for a variety of purposes, mainly to quantify discontinuity geometry. Discontinuity intensity tensor have been useful in trying to describe the variation of rock mass properties, such as wave velocity, deformability and strength with direction (Kulatilake et al., 1993; Oda et al., 1986). A second order tensor can be used to describe the discontinuity fabric, including size, orientation and density as follows (Oda, 1982);

$$F_{ij} = \frac{1}{V} \sum_{k=1}^{m^V} 2s^k r^k n_i^k n_j^k \quad (\text{A.36})$$

where s^k denotes the discontinuity surface area of the k^{th} discontinuity, V is the volume of rock mass considered, m^V is the number of discontinuities (i.e. the number of discontinuity centroids) in volume V , n_i^k and n_j^k ($i, j = x, y, z$) are components of the unit normal vector of the k^{th} discontinuity with respect to the orthogonal reference axes i and j ($i, j = x, y, z$). The surface area (s) is assumed to equal πr^2 , since each discontinuity is an idealised disc with radius r . It is assumed that each discontinuity contributes to the discontinuity intensity tensor in proportion to the cubic radius (hence $s2r = \pi r^3$). With this formulation, small radii discontinuities can be safely ignored without introducing serious error. However, it may be more appropriate to simply substitute the terms $2s^k r^k$ with S^k , which represents the entire surface area of the k^{th} discontinuity regardless of shape (Zhang and Einstein, 2000). The discontinuity intensity tensor can be described in matrix notation as follows;

$$F_{ij} = \begin{bmatrix} F_{xx} & F_{xy} & F_{xz} \\ F_{yx} & F_{yy} & F_{yz} \\ F_{zx} & F_{zy} & F_{zz} \end{bmatrix} \quad (\text{A.37})$$

The application of the discontinuity intensity tensor is limited by our ability to practically ascertain the size, and therefore area, of all discontinuities within a volume of rock mass. However, the tensor can be estimated by firstly assuming that discontinuity size and

orientation distributions are statistically independent of each other. In this case, the discontinuity intensity tensor of each discontinuity set can be determined from the mean linear intensity, and through summation, the rock mass discontinuity intensity can be established;

$$F_{ij} = \sum_{k=1}^N F_{ij}^{(k)} \quad (\text{A.38})$$

where N is the total number of k discontinuity sets. Oda et al (1986) describes that the first invariant (F_0) of F_{ij} , which is a scalar value, can be used as a measure of discontinuity intensity (termed the 'isotropic index'). As pointed out by Zhang and Einstein (2000), this can be directly related to the volumetric intensity measure (P_{32}). The discontinuity intensity tensor can also be used to establish an 'anisotropy index' (A^F) from analysis of tensor invariants (Oda et al, 1986; Kulatilake et al, 1993);

$$A^F = \frac{\left[(F_1 - F_2)^2 + (F_2 - F_3)^2 + (F_3 - F_1)^2 \right]^{1/2}}{F_1 + F_2 + F_3} \quad (\text{A.39})$$

where F_1 , F_2 and F_3 are the principal values of F_{ij} . The main drawback of representing the variation of discontinuity intensity as second order tensors is that the principal components are orthogonal to each other. However, the maximum and minimum discontinuity intensity directions are not necessarily orthogonal to each other (Hudson and Harrison, 1997). In this case, second order tensors are an approximation of the true variation of discontinuity intensity with orientation. The use of higher order tensors can overcome this limitation (Kanatani, 1984), however their additional complexity make them inconvenient and impractical. Notwithstanding this, the use of the isotropy (F_0) and anisotropy (A^F) indices provide useful measures for comparing the volumetric discontinuity intensity and relative anisotropy between rock masses.

Discontinuity Persistence Analysis

As mentioned previously, discontinuity size is one of the most difficult parameters to ascertain. However, an analysis of persistence or trace length values provides a 2-dimensional estimate or measure of discontinuity size. The mean trace length is often used as a measure of persistence, however, the accuracy and precision of this value is also influenced by sampling. Significantly, all forms of discontinuity bias will effect the accuracy of the mean value. It is necessary to account for these forms of bias in any analysis of mean trace length. Methods for determining mean trace lengths have been developed by a number of authors, however, they are dependent on a number of assumptions and restricted to certain sampling regimes.

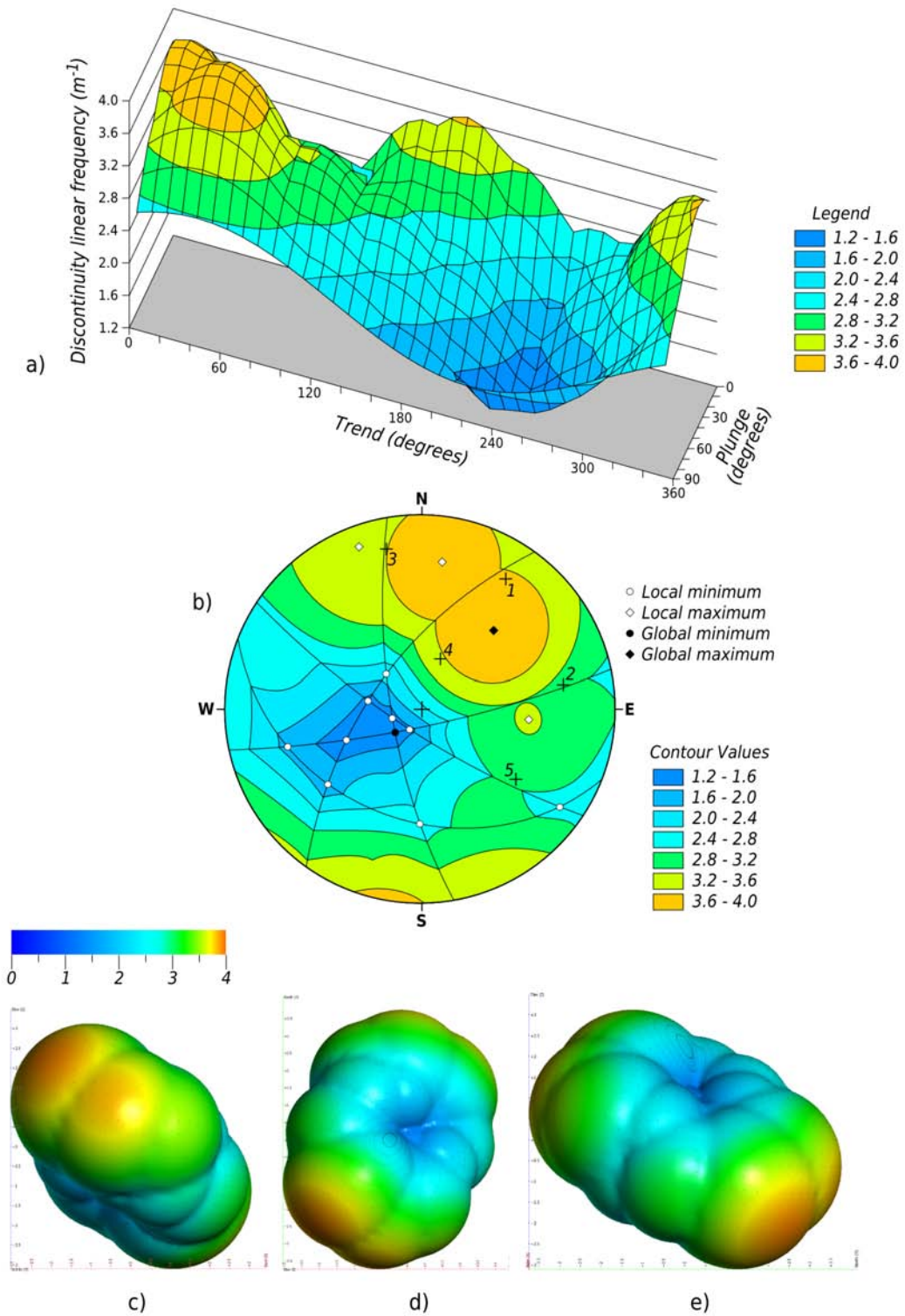


Figure A.8 - Variation of discontinuity frequency with direction a) on a perspective 3-dimensional surface plot, b) on a lower hemisphere equal area stereographic projection and as a 3-dimensional locus diagram looking c) north, d) down and e) west (data used to generate diagrams taken from Harries, 2001)

The methods generally fall into two main categories; those that assume an underlying trace length distribution (i.e. statistical models) and those that do not (i.e. distribution independent). The underlying form of distribution for trace lengths is a matter of debate, however, log-normal and negative exponential distributions are commonly considered (Baecher and Lanney, 1978). Distribution dependent methods suffer from a number of drawbacks; the underlying trace length distribution has to be determined empirically, or it has to be assumed. However, it is almost impossible to practically determine the appropriateness of one distribution over another due to sampling biases and insufficient exposure populations.

Warburton (1980) was one of the first researchers to apply a stereological approach to estimate discontinuity size. He developed a simple statistical model of discontinuities, which assumes a Poisson process for their spatial distribution and assumes that they are parallel convex circular discs. That is, only discontinuities from the same set are analysed at a time. From this model, a method was developed to determine mean trace lengths from area and scan line sampling, including the effects of truncation bias. In addition, the statistical model makes it possible to define an analytical distribution of discontinuity size. Unfortunately, this work did not address the effects of censoring bias.

One method to estimate parameters of the underlying trace length distribution considers correction of censoring biases in areal and line mapping (Laslett, 1982). The technique utilises a maximum likelihood estimator from observed censored trace lengths. If the underlying distribution is known, then the corrected mean trace length can be estimated. For scan line data, the estimated mean trace length is as follows;

$$\hat{\mu}_L = \frac{1}{\lambda} = \frac{\sum_{i=1}^n X_i - \sum_{j=1}^m Y_j - \sum_{k=1}^p Z_k}{(2n+m)} \quad (\text{A.40})$$

where $\hat{\mu}_L$ is the maximum likelihood estimate of the negative exponentially distributed mean trace length, and X_i , Y_j , Z_k and n , m , p are the lengths and number of traces with both ends observed, one end observed, and no ends observed, respectively. Villaescusa (1991) was able to combine the approaches of Warburton (1980) and Laslett (1982) to estimate distribution size from scan lines, whilst also accounting for censoring effects.

Mauldon (1998) provides a number of distribution independent end-point estimators for determining mean trace length for rectangular, circular and irregularly shaped sampling windows. The mean trace length can be estimated from circular sampling windows as

follows;

$$\hat{\mu} = \frac{\pi R}{2} \left(\frac{m+p-n}{m-p+n} \right) \quad (\text{A.41})$$

where R is the radius of the circular sampling window, definitions of m , n , p are as per equation A.40. It is important to note, however, that the method fails if ((Zhang and Einstein, 1998);

- $p = m$, then $\hat{\mu} \rightarrow \infty$, as all discontinuities transect the sampling window. In this case, larger sampling windows are required. However, due to the size limitations of most underground excavations, in general this is not practical.
- $n = m$, then $\hat{\mu} = 0$. In this case, the mean length cannot be determined as both ends (i.e. the point estimators) are located inside the sampling window. In this case, a maximum likelihood method can be used to obtain the corrected trace length distribution (Laslett, 1982; Villaescusa and Brown, 1992).

An important aspect of this work was the recognition the mean trace length determinations using end-point estimators from circular sampling windows are independent of both the underlying discontinuity trace length and orientation distributions.

Termination

In order to assist in the determination of persistence, the ISRM (ISRM, 1978), recommend that the termination characteristics of the traces of discontinuities are recorded during line or window mapping exercises. In this case, termination of a trace can be describes as being either;

- terminating in rock (r)
- terminating against another discontinuity (d), or
- unobserved extending beyond the excavation (x)

These classifications can then be utilised to estimate the degree of persistence, for example discontinuities with high (x) scores typically have high persistence, with those with high (r) scores will have low persistence. In addition, termination type may provide information about discontinuity shape, as those that have both ends terminating against two parallel discontinuities will be rectilinear.

The ISRM (ISRM, 1978) also suggest a termination index to rate the persistence of discontinuities for the rock mass;

$$T_r = \frac{100N_r}{N_r + N_x + N_d} \quad (\text{A.42})$$

where N_r is the number of discontinuity terminations ending in rock, N_x is the number of unobserved discontinuity terminations, N_d is the number of discontinuity terminations against another discontinuity. It must be noted that the measure provided in equation A.42 is for semi-trace length data, that is, applying termination characteristics to the traces observable only on one side of the sampling line. The termination index for full trace length data, that is applying termination classification to both ends of the discontinuity trace, is provided as follows;

$$T_r = \frac{100N_r}{2(N_r + N_x + N_d)} \quad (\text{A.43})$$

These measures can be applied to the rock mass to determine variations in persistence, with a high T_r indicating that a rock mass has many intact rock bridges, and a rock mass with a low T_r indicating “blocky” rock mass conditions. The termination index can also be applied to individual sets in order to differentiate persistent and non-persistent sets. (Lee et al., 1990) present a method for modelling rock joints in two-dimensions which includes an assessment of the termination style used to characterise discontinuity hierarchy. The assessment includes how joints terminate against each other, either as T-intersections or X-intersections. The probability of each termination type can then be derived empirically (Lee et al., 1990). Another termination measure can account for fractures crossing one another, by utilising a modified termination index (Harries, 2001);

$$P_t^s = \frac{\sum_{i=1}^n T_i}{\sum_{i=1}^n (T_i + X_i)} \quad (\text{A.44})$$

where P_t^s is the probability of termination for the given discontinuity set s , n is the number of fractures in the given discontinuity set s , T_i is the number of T-intersections seen for each discontinuity in the set (0,1,2) and X_i is the number of X intersections seen for each discontinuity in the set (0,1,2...∞). The probability of a discontinuity crossing the pre-existing discontinuity is therefore;

$$P_x^s = 1 - P_t^s \quad (\text{A.45})$$

where P_x^s is the probability of a discontinuity crossing (i.e. X-intersection) for the given discontinuity set s .

Drillhole Discontinuity Linear Frequency and RQD

RQD and discontinuity linear frequency (fracture frequency) values from drill core can

provide significant volumetric coverage to characterise a project site. However, prior to undertaking analyses on this data it may be beneficial to check and validate the data for logging errors. One way of doing this is to compare *RQD* and fracture frequency logged over the same intervals. Figure A.9 shows a logging data from a selection of drill holes at the Kanowna Belle Gold Mine (Villaescusa et al., 2003a). It can be seen that low *RQD* values co-exist with low fracture frequency values, and conversely, high *RQD* values with high fracture frequency values. The latter may indicate that “healed” discontinuities have been logged/recorded in the linear frequency measure, yet have not been included in the *RQD* calculation.

It can also be seen from Figure A.9 that the majority of data points above an *RQD* of around 40 lie between relationships provided by a number of authors. It is also interesting to note that the linear relationships intercept the x-axis between 20 and 40 discontinuities per metre, suggesting an upper limit of linear frequency of around 40m^{-1} corresponding to an *RQD* of 0.

Without additional information about logging procedures and from individuals logging the core, the cause of these errors is indeterminable. However, it is thought that if *RQD* is calculated “on-the-fly” by technicians during logging, errors may occur. It may be reasonable to expect that fracture frequency is a much easier parameter to log and verify, and that potential errors could be picked up immediately. Regardless of the cause of these errors, major discrepancies between *RQD* and discontinuity linear frequency are of great concern. It is therefore considered that the practice of checking *RQD* versus linear frequency as a matter of routine during logging is **an essential quality control procedure**. Where the cause of the error is indeterminable, it may be necessary to assume that discontinuity linear frequency values are less erroneous than *RQD* values. In this case, *RQD* can potentially be “corrected” by imposing some form of assumed relationship between discontinuity linear frequency and *RQD*. Lower and upper bounds to this relationship could be used as modification “cut-offs”. Figure A.10 shows such an example, where the linear frequency values are firstly limited to a maximum of 40m^{-1} . The *RQD* value for the data pair is then modified if it falls outside of the upper and lower limits;

- lower limit; $RQD = -2.5(\text{linear frequency}) + 70$
- upper limit; $RQD = -2.5(\text{linear frequency}) + 120$ (truncated at a maximum value of $RQD = 100$)

The validity of such an approach is questionable, yet may be unavoidable if *RQD* values are required in further engineering design processes.

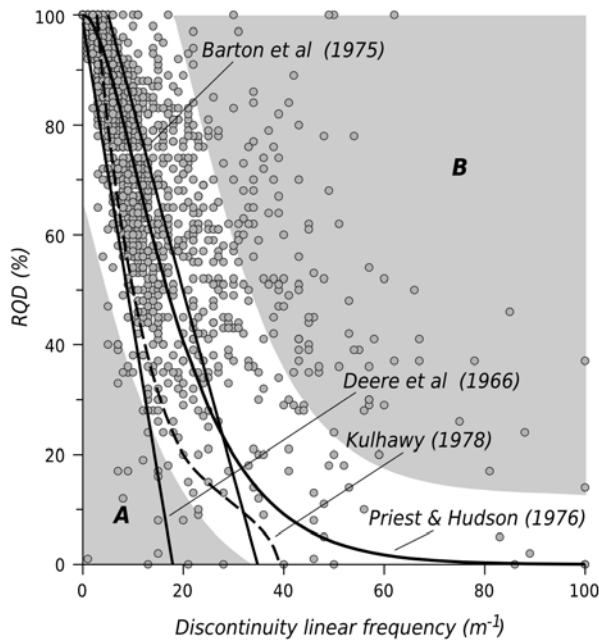


Figure A.9 - Example Kanowna Belle borehole data (Villaescusa et al, 2003) with RQD plotted against discontinuity linear frequency (m⁻¹), together some published relationships. Shaded regions indicate potentially erroneous data, where low RQD exists with low fracture frequency values, and high RQD exists with high fracture frequency values (labelled "A" and "B", respectively).

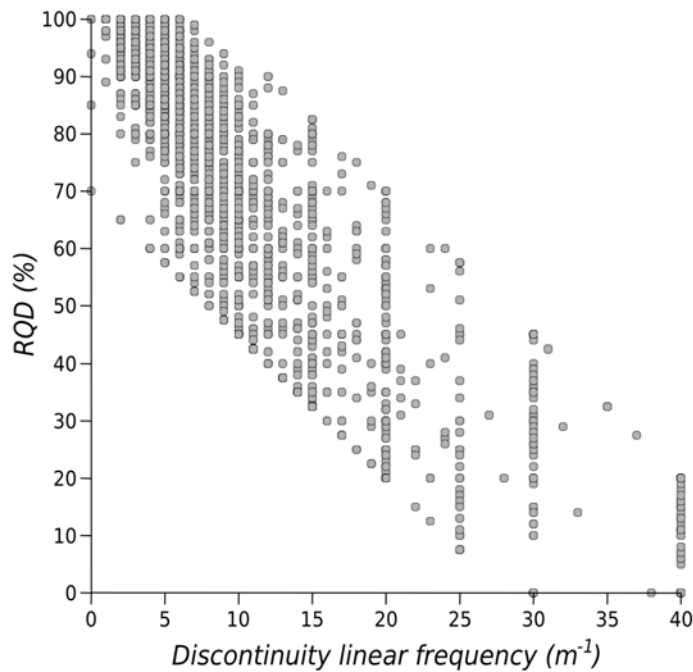


Figure A.10 - Example of "corrected" RQD values against fracture frequency data by applying lower and upper bound cut-offs to a linear relationship

APPENDIX B - COMPARISON OF EMPIRICAL METHODS IN OPEN STOPE DESIGN

Table B.1 - Empirical stope design methodologies extended from the NGI Q-system

(next 3 pages)

Reference	Case History Information	Performance Assessment Classifications	Design Zones	Design Line Determination Method
Mathews et al (1981)	Country: Canada (2), Australian (1) Mines: 3 Mining Method: Principally LHOS Case Histories: 50 supported/unsupported Additional: defines term "shape factor". Case histories "supplemented" with ranges of NGI-Q. All cases histories less than 650m below surface.	Stable: The excavation will stand unsupported with occasional localised ground support to control slabbing. Unstable: The excavation will experience localised caving but tend to form a stable arch. Cable bolts and modification of the extraction sequence are suggested as ways to make open stoping feasible in this region. Caved: The excavation will not stabilise until the void is full.	Stable Zone: Cable bolts and modification of the extraction sequence are suggested as ways to make open stoping feasible in this region. Potentially Unstable Zone: Potentially Caving Zone:	Visually assigned
Potvin (1988)	Country: Canada Mines: 34 Mining Method: Principally LHOS Case Histories: 175 unsupported, 66 supported, 84 main database, 92 complimentary Additional: defines term "Hydraulic Radius", re-calibration of factors A, B, C	Stable: "low" amounts of dilution Unstable: Experienced dilution and ground-falls causing operational problems. Unravelling between cables. Caved: Not adequately defined, however offers "Severe ground control problems, Support system failure"	Stable Zone: Transition Zone: Caved Zone:	Unsupported curves. Visual assigned
Nickson (1992)	Country: Canada / NW USA Mines: 12 Mining Method: LHOS, Cut and Fill, VCR, Room and Pillar Case Histories: 13 unsupported, 46 supported Additional: Supplemented Potvin's (1988) database	Stable: Observed or reported to be within the designed excavation limits, or contributed "low" amounts of dilution Unstable: Experienced dilution and ground-falls causing operational problems, Unravelling between cables Caved: Observed or reported to be well beyond the design limits, due to ground fall or excessive dilution. Support system failure	Stable Zone: Unsupported Transition Zone: Stable with Support Zone: Supported Transition Zone: Caved Zone:	Statistical discriminant analysis using Mahalanobis Distance for; unsupported used to define "unsupported" transition/caved design line. supported to define "supported" stable/transition design line. Other design lines visually assigned.
Pakalnis and Vongpaisal (1993)	Country: Canada Mines: 1 Case Histories: 172 Additional: Entry Method, Backs only	Stable: There have been no uncontrolled falls of ground. If instrumentation is available, no movement of the back has been observed. There are no extraordinary support measures implemented. Potentially Unstable: The opening may exhibit fault/shears having orientations that form potential wedges in the back. Extra ground support may have been installed to prevent potential falls of ground. Instrumentation installed in the back has recorded continuing back movement. Unstable: uncontrolled fall of ground has occurred. Stope caved	Stable: Potentially Unstable: Unstable:	Statistically derived using discriminant analysis
	Country: Canada Mines: 1 Mining Method: LHOS Case Histories: 133 Additional: Isolated, rib and en echelon stopes	Dilution based (%)	Dilution lines: at 0%, 5%, 10%, 15%, 20% for various stope configurations	Statistical regression

Reference	Case History Information	Performance Assessment Classifications	Design Zones	Design Line Determination Method
Stewart and Forsyth (1995)	<p>Country: Canada / NW USA</p> <p>Mines:</p> <p>Mining Method:</p> <p>Case Histories: No new data</p> <p>Additional: mainly a review of Potvin's (1988) method, with critique of his proposed modified factors. Stewart and Forsyth recommend Mathews et al (1981) original A, B, C factors</p>	<p>Stable: Same as Mathews et al (1981)?</p> <p>Unstable: Same as Mathews et al (1981)?</p> <p>Major Failure: Cases where the extent of back or wall failure is greater than about 50% of the smaller dimension of the opening</p>	<p>Potentially Stable Zone: essentially self-supporting. Pattern rock bolting or localised or spot bolting. Dilution should be minimal, estimated at less than 10%</p> <p>Potentially Unstable Zone: Should require extensive and heavy support. Large and probably unacceptable failure and excessive dilution may result if not supported, dilution in excess of 30%</p> <p>Potential Major Collapse: Will require extensive and heavy support. If not supported may lead to unacceptable failure, ore loss with dilution estimated greater than 30%</p> <p>Potentially Caving Zone: Probably unsupported, will fail and continue to fail until void is filled, or until breakthrough.</p>	Visually assigned
Clark and Pakalnis (1997)	<p>Country: Canada</p> <p>Mines: 6</p> <p>Mining Method: LHOS</p> <p>Case Histories: 79 unsupported, 18 supported</p> <p>Additional: FW/HW surfaces, point anchor support</p>	ELOS based (i.e. ELOS calculated for each data point)	<p>Blast damage: (ELOS <0.5m)</p> <p>Minor Sloughing: (ELOS = 0.5m to 1.0m)</p> <p>Moderate Sloughing: (ELOS = 1.0m to 2.0m)</p> <p>Severe Sloughing / Possible Wall Collapse: (ELOS >2.0m)</p>	Logistic regression and "engineering judgement"
Scott and Power (1998)	<p>Country: Australia</p> <p>Mines: 1</p> <p>Mining Method: LHOS</p> <p>Case Histories: 45 (9 stopes)</p> <p>Additional: Mixture of supported and unsupported stope walls analysed. Limited data set of "failed" cases</p>	<p>Stable: No or minimal fall-off, with support dilution estimated at less than 10%</p> <p>Unstable: Substantial amounts of fall-off, a stable unsupported configuration reached after 10 to 30% dilution</p> <p>Major Failure: Large amounts of wall fall-off, stable unsupported configuration reached after greater than 30% dilution</p> <p>Caving: Void forms uncontrollably until filled with fallen material</p> <p>Stable/caved: Wall performs as stable, but is supported by cable bolts to some degree</p>	<p>Potentially Stable Zone:</p> <p>Potentially Unstable Zone:</p> <p>Potentially Caving Zone:</p> <p>As per Stewart and Forsyth (1995)</p>	No change to design lines. Recommend that Potvin's (1988) Stable/Unstable line be used for design 'poorer' GHB stopes, whilst Stewart and Forsyth (1995) design lines be used elsewhere.
Trueman et al (2000)	<p>Country: Australia</p> <p>Mines: 1</p> <p>Mining Method: LHOS</p> <p>Case Histories: 180</p> <p>Additional: Mixture of supported and unsupported stope walls analysed. Includes larger stopes</p>	<p>Stable: where stope surfaces remain intact without support throughout mining activity</p> <p>Failure: where reasonable instability of an unsupported stope surface has occurred resulting in over-break Failure with support: where over-break occurred which was arrested by cable support</p> <p>Major Failure: where a large amount of over-break has occurred in an unsupported stope surface.</p>	<p>Stable Zone:</p> <p>Transition Zone:</p> <p>Failure Zone:</p>	Design Lines: "stable-transition" line chosen from Stewart and Forsyth's (1995) "Potentially stable" line, with the "transition- failure" line taken as from the base of Stewart and Forsyth's (1995) "potentially unstable" line.

Reference	Case History Information	Performance Assessment Classifications	Design Zones	Design Line Determination Method
Streeton, G.C. (2000)	Country: Australia Mines: 1 Mining Method: LHOS Case Histories: 100 (20 stopes) Additional: Mixture of supported and unsupported stope walls analysed, two main orebody types. Limited set of "failed" and "Major failure" cases.	Does not specify, however, assume that the categories are the same as Scott and Power (1998) as this work extends on the original case history database.	Cannington Stability Line: 92% of all cases above line, 97% of "stable" cases above line, 75% of "unstable" above line, 0% "major failure" above line	Design Line: developed by "fitting a curve to the data", however, methodology not provided.
(Mawdesley et al., 2001)	Country: Australia Mines: ?? Mining Method: LHOS Case Histories: 400 Additional: 180 case histories from Mt Charlotte, others not specified.	Stable: not specified Failed: not specified Major Failure: not specified Assumed as per Trueman et al (2000)	Isoprobability Contours: of Stable, Failed and Major Failure.	Design Lines: logistic regression of Stable, Failed and Major Failure data to provide isoprobability contours
Oddie and Pascoe (2005)	Country: Australia Mines: 1 Mining Method: LHOS Case Histories: 271 Additional: 28 backs point anchor support, Modified Factor A based on shear stress, volume of over-break not utilised, ELOS measured by ((indicative depth? of over-break x area of over-break) / surface area)	Stable: (little or no deterioration) - ELOS <0.75, dilution <10% Unstable: (limited failure) - ELOS 0.75 to 2.0 Failed: (unacceptable failure) - ELOS >2.0	Design Line: 80% of cases above line stable	Design Lines: Visually assigned, $N=0.03HR^3$

APPENDIX C - VALIDATION PLANS FOR THE SQUIRREL HILLS STRUCTURAL INTERPRETATION

C.1 Perspective views of mine levels (+/- 15m slice) showing digitised mapping, interpreted intercepts and interpreted/modelled "Squirrel Hills" structure (grey surface)

Key:

Red traces - indicate mapped structure verifying presence of the "Squirrel Hills Fault".

Circled green - indicate areas where manifestation of the "Squirrel Hills Fault" not observed, or partial obscured by shotcrete.

Circled purple - indicate areas of the anticipated intersection of "Squirrel Hills Fault" in development, yet no mapping data exist. Mapping required to verify its existence.

Green dashed lines - interpreted splay or relay structure associated with "Squirrel Hills Fault"

C.1 PLAN VIEWS OF CANNINGTON MINE LEVELS

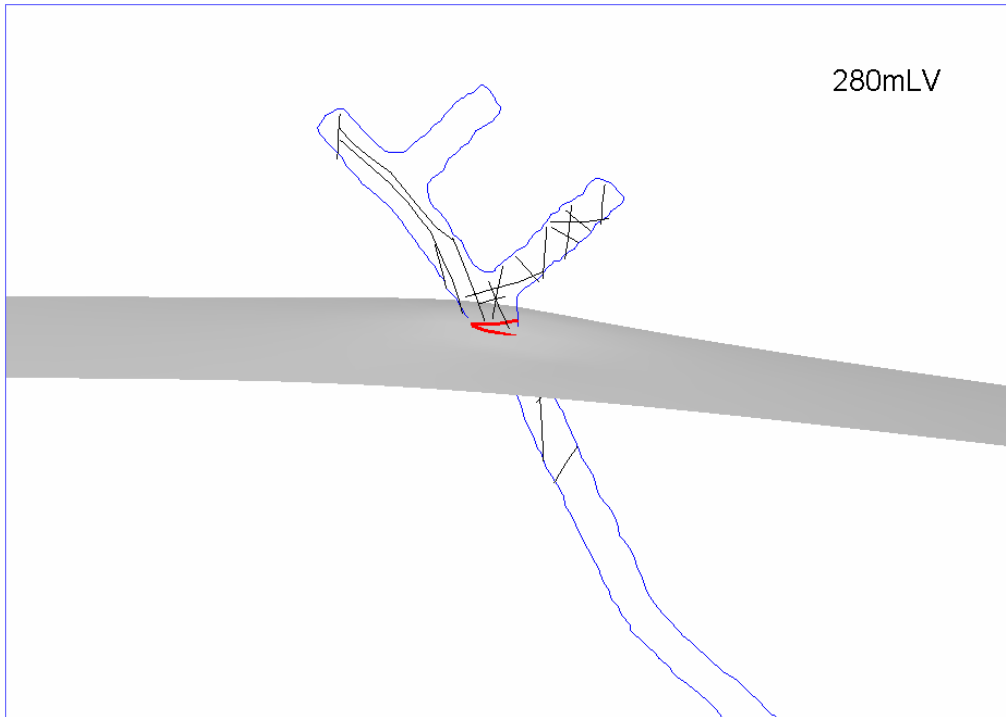


Figure C.1 - 280mLV

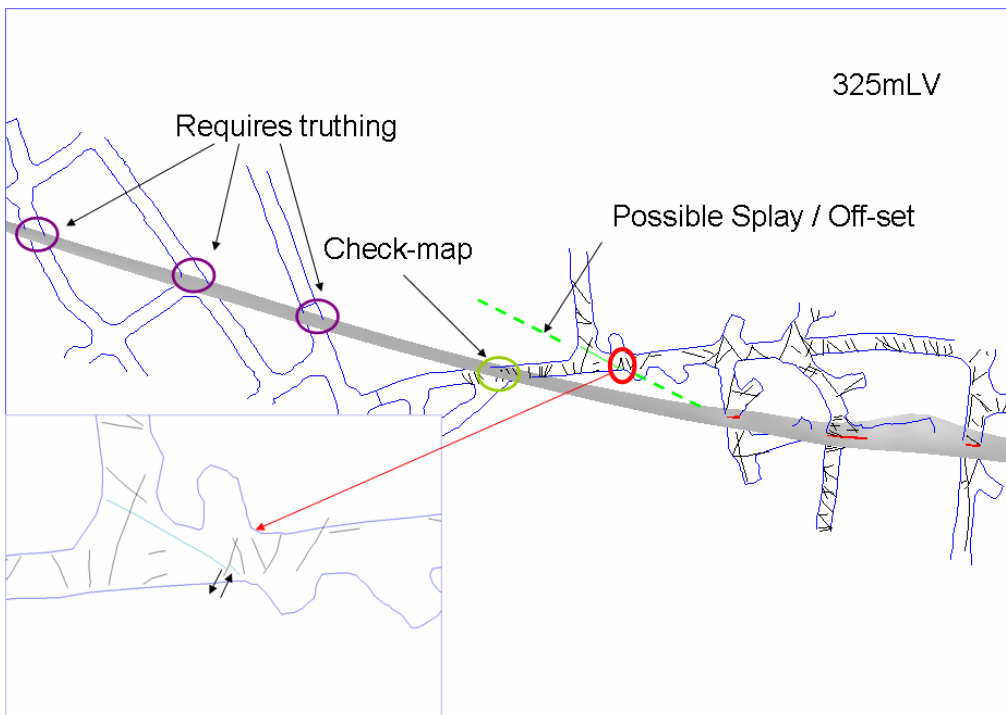


Figure C.2 - 325mLV

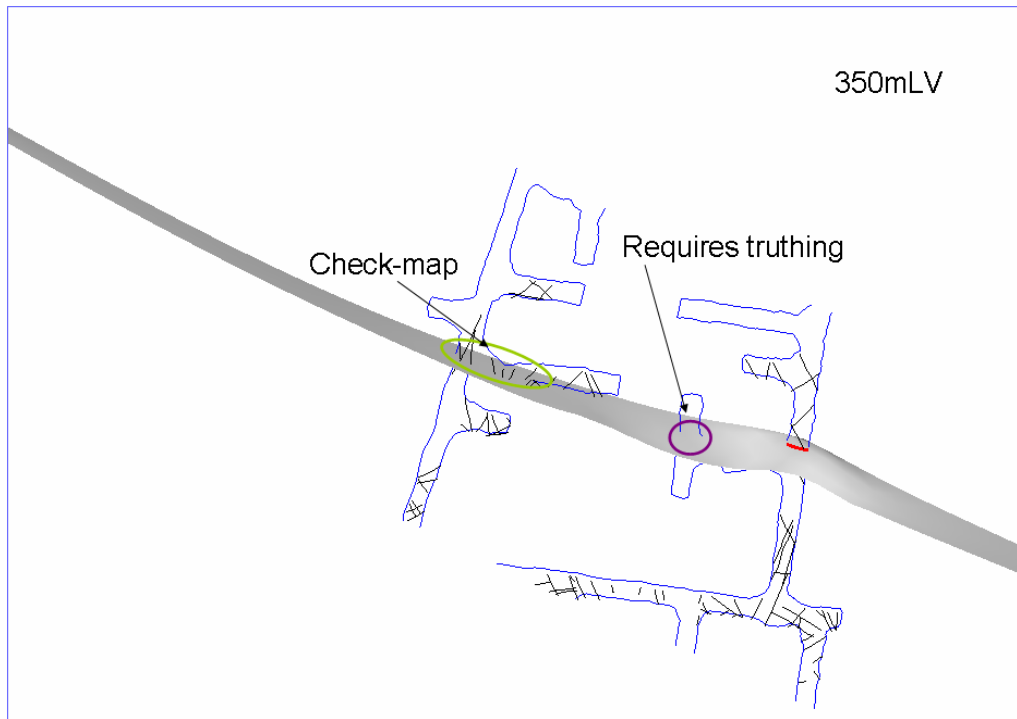


Figure C.3 - 350mLV

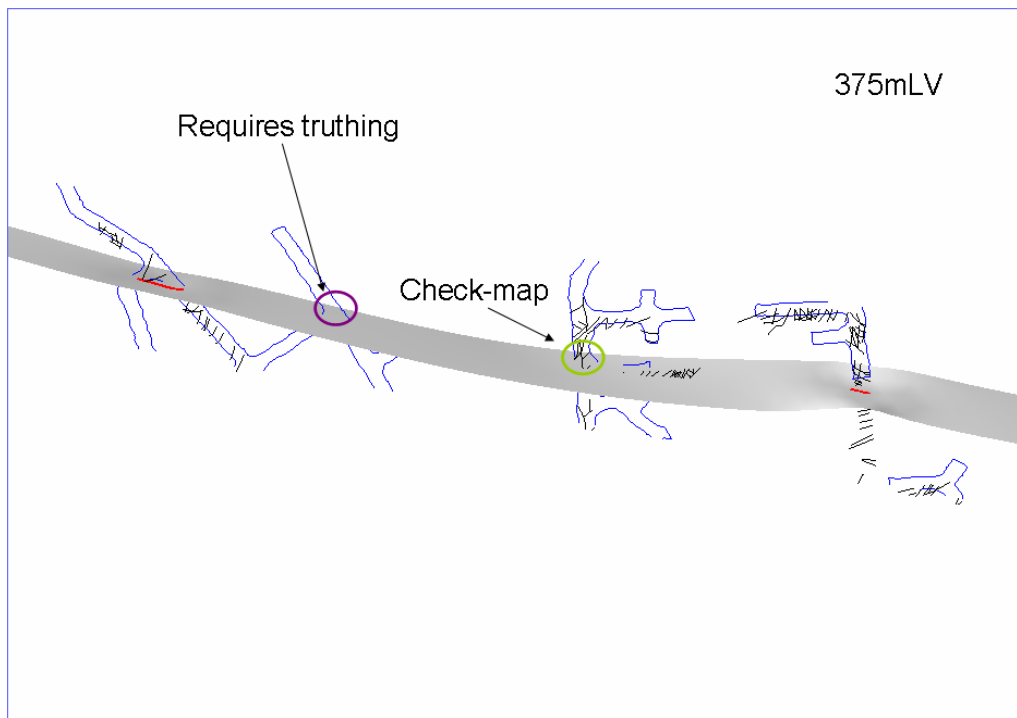


Figure C.4 - 375mLV

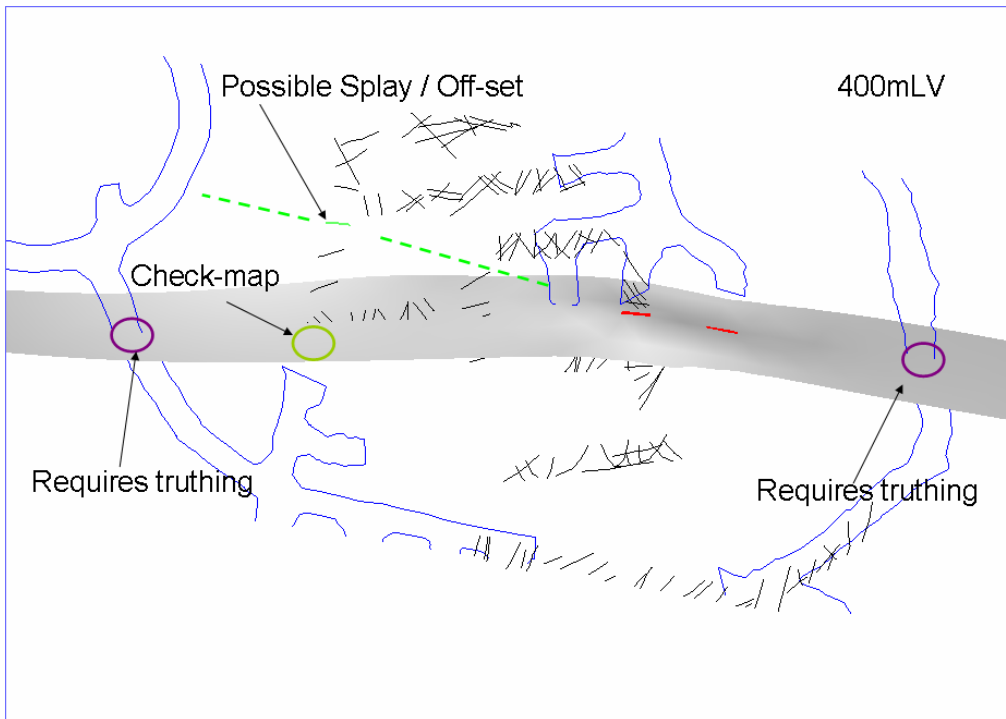


Figure C.5 - 400mLV

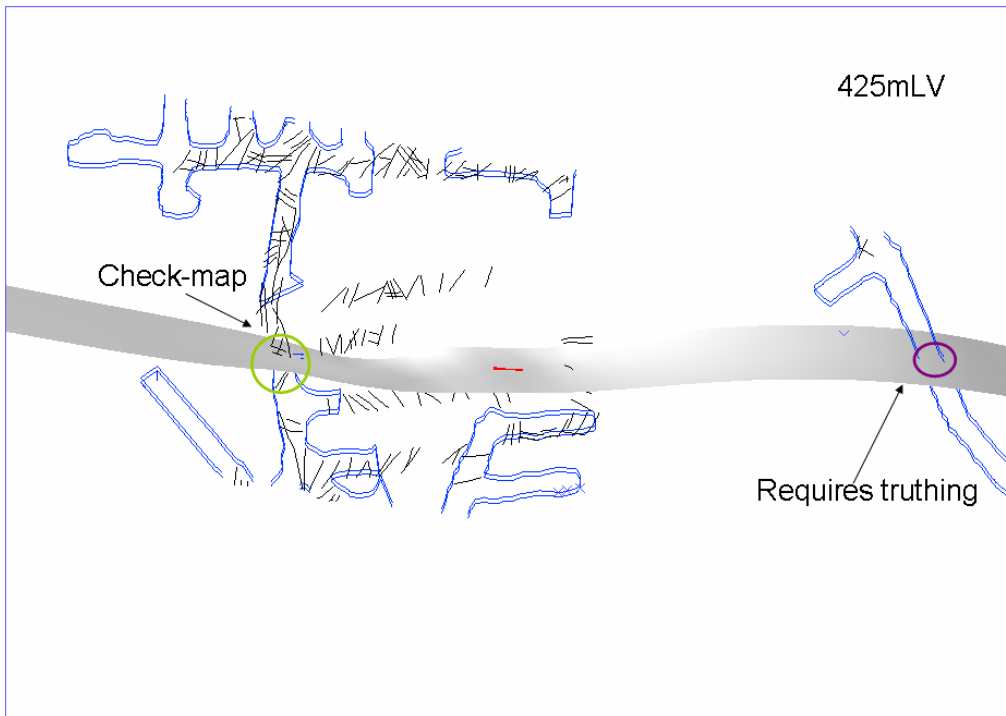


Figure C.6- 425mLV

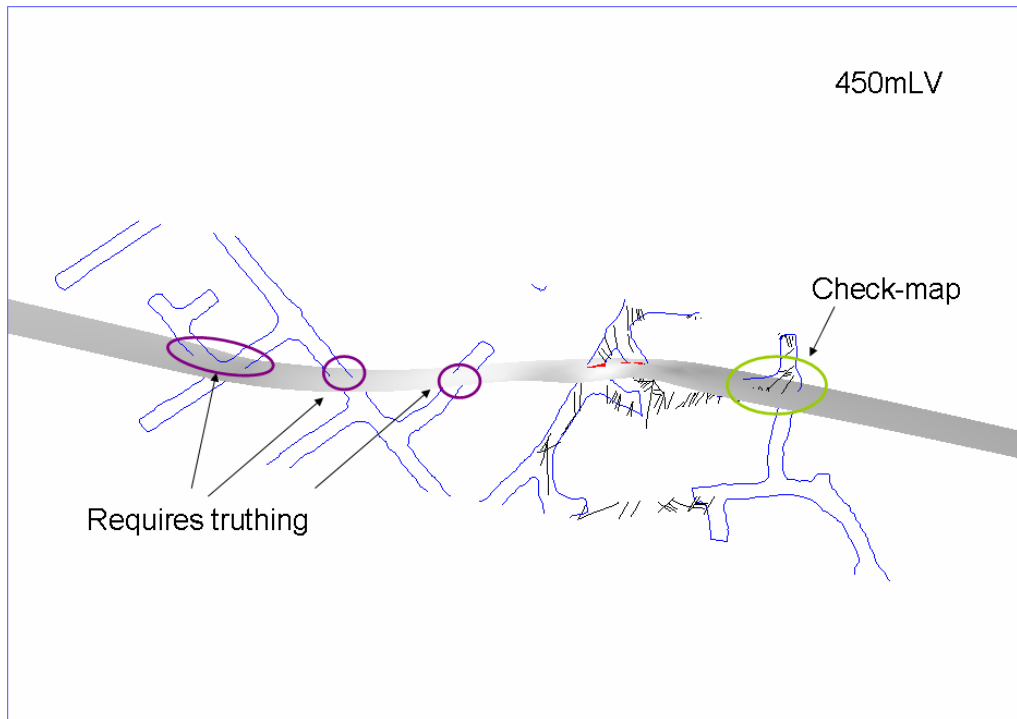


Figure C.7- 450mLV

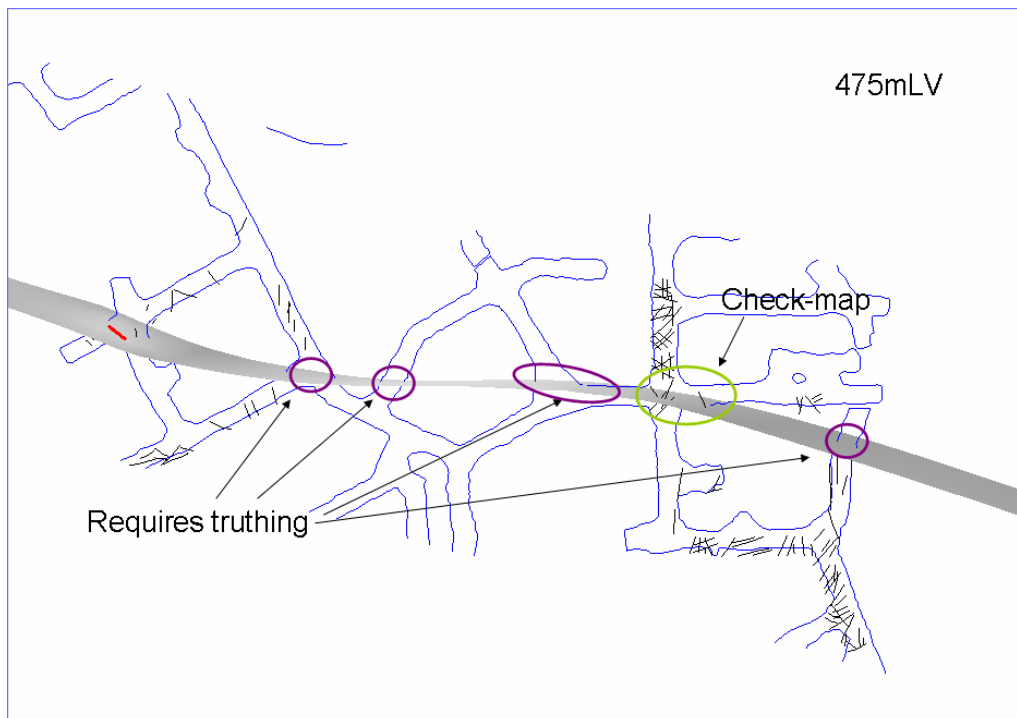


Figure C.8- 475mLV

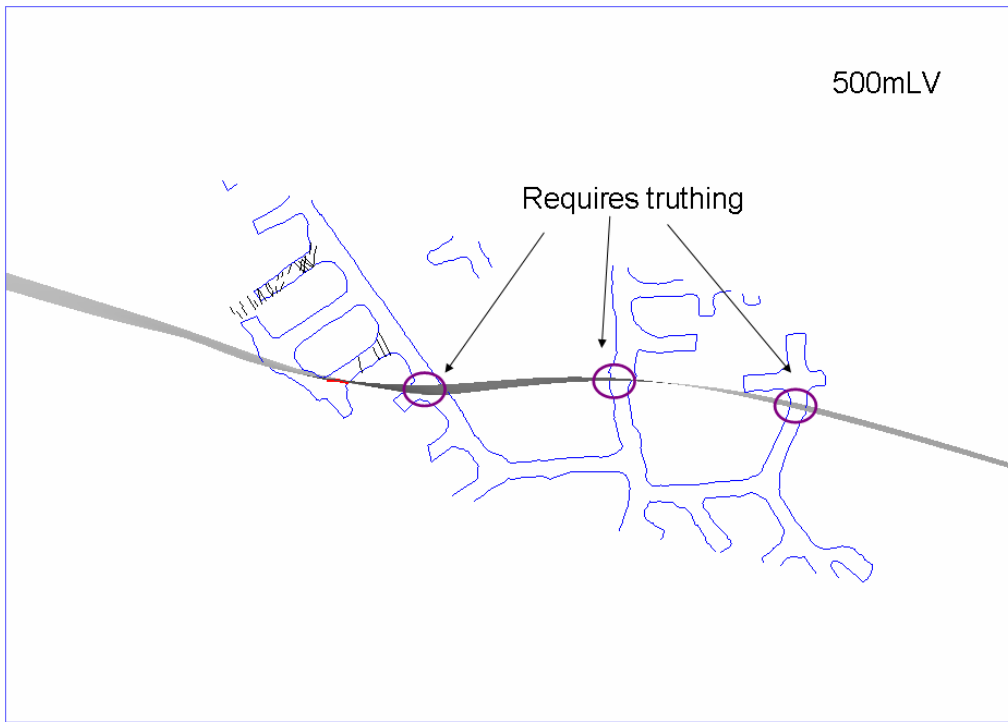


Figure C.9- 500mLV

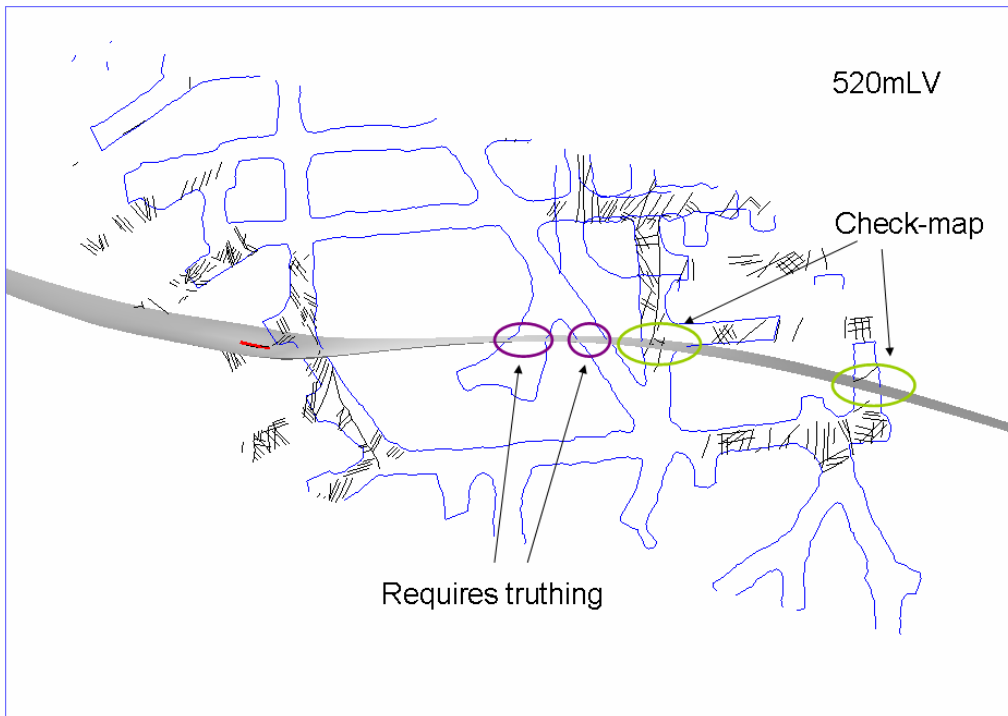


Figure C.10- 520mLV

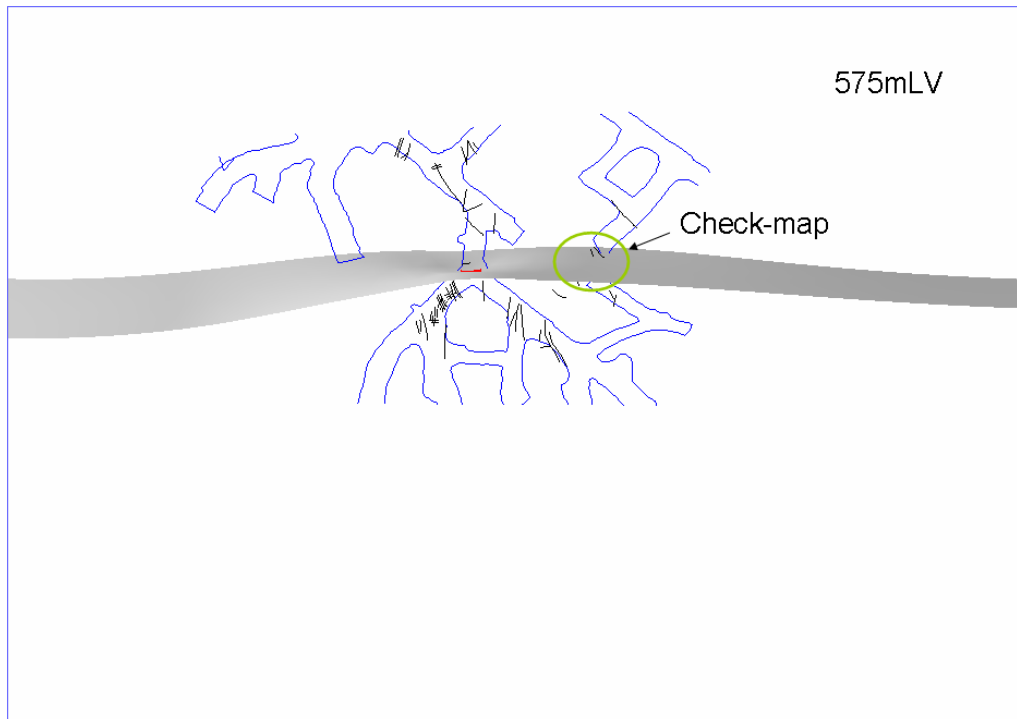


Figure C.11- 575mLV

APPENDIX D - CANNINGTON WINDOW MAPPING DATA

D.1 Window Mapping Data used for validating spatial discontinuity intensity models and assessments of rock mass isotropy (Chapter 10)

D.1 CANNINGTON NORTH BLOCK WINDOW MAPPING DATA

hole_id	id	depth_to	type	m_set	strength	wall_strength	number	est_spacing	trace_s	t1_s	t2_s	trace_d	t1_d	t2_d	continuity	wav_m	amp_m	wav_lg	amp_lg	profile	plan.	rough.	jrc	infill	width	dip	direction
C8XW_01	1	1.9	J	1	4	4	1	99	0.5	U	U	4.2	R	R	2.3154	650	13			3	3	3	3			45	156
C8XW_01	2	1.91	J	2	4	5	1	15	0.4	U	U	0.9	R	J	1.0707	150	40			3	5	3	6			88	74
C8XW_01	3	2.6	J	3	4	5	1	99	0.6	R	R	0.25	U	U	0.674	250	5			2	4	3	4			57	45
C8XW_01	4	4.3	J	4	4	4	1	1.7	0.1	U	U	0.35	R	R	0.7108	200	20			2	3	3				87	84
C8XW_01	5	4.7	J	5	2	5	1	99	0.1	U	U	0.45	R	J	0.5721	100	5			1	3	3	2			35	75
C8XW_01	6	4.9	J	2	5	5	1	3.2	0.4	U	U	0.25	R	R	0.5252	350	11			3	4	3	3			73	115
C8XW_01	7	4.91	L	6	4	5	1	99	2.1	J	R	0.3	U	U	0.712			1.35	0.07	5	4	3	3			40	204
C8XW_01	8	7.1	J	6	4	4	1	99	0.3	U	U	2.2	R	U	2.7667	900	30	1.75	0.1	3	5	3	5			65	50
C8XW_01	9	7.6	J	3	3	4	1	1.2	0.35	U	U	0.95	R	J	1.7379	400	4		58	3	5	2	5			63	45
C8XW_01	10	8.75	J	7	4	5	1	1.1	0.15	U	U	0.45	R	R	0.6505	600	10			2	3	3	3			75	160
C8XW_01	11	9.2	J	6	5	5	1	99	0.35	U	U	0.95	R	R	0.6843	400	5			2	3	4	8			14	200
C8XW_01	12	9.4	J	7	4	5	1	0.35	0.2	U	U	0.6	R	R	0.8571	370	17			3	3	3	5			65	142
C8XW_01	13	10.2	F	7	2	4	1	3.5	0.2	U	U	6	U	U	4.1117	999	80			2	1	2	2	Bx	10	67	140
C8XW_01	14	10.8	J	3	3	4	1	2.5	0.4	U	R	0.8	U	U	1.4182	400	6			3	3	3				66	45
C8XW_01	15	12.1	J	7	4	5	1	99	0.5	U	U	0.7	R	J	0.5794	600	10			3	2	4				75	152
C8XW_01	16	12.2	J	3	4	5	1	99	0.4	U	U	2.1	R	R	2.007	555	5	19	0.05	2	4	3				76	46
C8XW_01	17	12.5	J	8	5	5	1	99	0.4	R	R	0.9	U	U	0.7431	300	3			1	3	3	3			64	212
C8XW_01	18	13.2	F	7	3	4	1	99	0.2	U	U	99	U	U	3.9174	700	20			2	2	2		Bk	20	78	123
C8XW_01	19	13.3	J	7	4	5	1	0.35	0.1	U	U	0.35	R	R	0.4951	10	2			1	1	3	1			89	301
C8XW_01	20	13.8	J	2	5	5	1	99	0.2	U	U	0.95	R	R	1.2943	650	10			3	4	3	5			89	77
C8XW_01	21	15.8	J	3	4	5	1	99	0.35	U	U	0.65	J	R	0.8256	550	5			2	3	4	6			55	66
C8XW_01	22	16	J	9	3	4	1	99	2	U	U	0.8	U	U	2.8366	700	14			5	3	4	7			74	36
C8XW_02	1	2.4	J	7	4	5	1	5	0.95	R	R	0.1	U	U	1.2952	65	2			4	2	2	3			32	202
C8XW_02	2	2.41	J	5	4	5	1	4.7	0.1	U	U	0.3	R	R	0.6428	250	1			1	2	2	2			89	259
C8XW_02	3	4	J	4	4	5	1	0.25	0.25	U	U	1.2	J	U	2.122	400	2			4	4	3	5			74	337
C8XW_02	4	4.05	V	1	5	5	1	4.8	0.05	U	U	2.9	R	R	3.6244	250	3	2.5	0.1	2	3	3	7	Qz	20	52	170
C8XW_02	5	4.2	J	4	4	5	1	3.5	0.2	U	U	0.6	J	R	1.4518	220	1			1	4	3	4			72	343
C8XW_02	6	4.5	J	3	4	5	1	0.95	1.1	J	R	1	U	U	0.8786	100	2			2	3	3	8			43	194
C8XW_02	7	5.6	J	3	4	5	1	5	1.3	R	J	0.2	U	U	1.2822	90	2			2	3	2	3	Ch		44	203
C8XW_02	8	6.8	J	2	3	5	1	4.7	0.05	U	U	5.1	R	U	6.5636	150	3	0.9	0.02	2	3	3	5	Cb	2	46	267
C8XW_02	9	7.8	J	1	3	5	1	5	0.1	U	U	1.1	R	J	0.9752	250	2			2	2	2	1			74	148
C8XW_02	10	8.8	J	8	4	5	1	0.45	0.35	U	U	1.05	R	U	1.727	600	1			1	4	2	3			88	235
C8XW_02	11	9.9	J	4	5	5	1	8.3	0.3	U	V	1	R	R	1.6348	900	1			1	2	2	2	As		82	336
C8XW_02	12	10	J	2	4	5	1	1.2	5	U	U	3.6	J	U	3.6179	160	4	1.8	0.05	3	3	3	8	Cb	1	24	288
C8XW_02	13	10.35	J	8	4	5	1	2.7	0.9	U	U	1.1	R	U	1.8149					2	4	4	6			86	35
C8XW_02	14	11.6	J	4	3	5	1	2.2	0.25	U	U	0.4	R	U	0.8644	150	2			1	2	3	3			89	355
C8XW_02	15	13.2	J	2	4	5	1	0.55	0.2	U	U	1.15	R	R	1.2077	170	3			2	3	2	5	Fe		39	272
C8XW_02	16	14.8	J	2	4	5	1	3.6	0.1	U	U	1.15	R	R	1.2477	200	2			1	3	2	3	Fe		42	264

hole_id	id	depth_to	type	m_set	strength	wall_strength	number	est_spacing	trace_s	t1_s	t2_s	trace_d	t1_d	t2_d	continuity	wav_m	amp_m	wav_lg	amp_lg	profile	plan.	rough.	jrc	infill	width	dip	direction
C8XW_02	17	16	J	2	4	5	1	0.25	0.05	U	U	2.9	R	R	2.2141	500	2	2.2	0.03	2	3	2	3	Cb		50	267
C8XW_02	18	16.3	J	8	4	5	1	7.8	0.35	U	U	0.95	R	R	1.2645	350	3			4	3	2	7	Ch		88	145
C8XW_02	19	17	J	5	4	5	1	99	1.9	R	J	0.5	U	U	1.8871	300	2	1.7	0.01	2	3	2	3	Ch		71	190
C8XW_02	20	17.9	J	4	4	4	1	3.9	0.35	R	U	0.25	U	U	0.795	300	1			1	4	2	2			82	218
C8XW_02	21	18	J	2	4	4	1	1.2	0.05	U	U	3.7	R	R	2.6617	450	3	1.7	0.05	3	2	3	3	Cb	1	50	265
C8XW_02	22	18.01	J	3	4	4	1	1.5	0.35	R	R	0.2	U	U	0.6873	250	1			1	4	3	3	Fe		57	207
C8XW_02	23	18.8	J	4	3	5	1	6	0.9	R	R	0.25	U	U	0.8042	900	1			1	4	2	4			80	203
C8XW_02	24	19.2	J	2	6	4	1	3.7	0.05	U	U	2.35	R	J	3.1097	220	15			2	3	3	5	Cb	2	62	247
C8XW_02	25	19.5	J	2	3	4	1	10.5	2.9	R	U	0.05	U	U	1.9798	900	10	1.3	0.02	3	3	3	5			54	200
C8XW_02	26	19.51	J	9	3	4	1	6.8	0.4	U	U	3.2	R	J	2.3192	95	2	1.92	0.17	3	3	3	7	Fe		60	60
C8XW_02	27	21	J	7	5	4	1	0.45	1.35	R	R	0.25	U	U	1.3593	150	3	2.6	0.02	2	3	3	6			53	7
C8XW_02	28	21.5	J	7	4	4	1	0.45	1.45	R	R	0.25	U	U	2.7895	170	3	1.15	0.02	3	3	2	5			60	10
C8XW_02	29	21.9	J	7	4	4	1	1.35	2.3	R	R	0.35	U	U	1.9272	165	4	2.2	0.03	2	3	3	3			62	9
C8XW_02	30	22.2	J	2	3	4	1	7	0.2	U	U	3.95	R	R	4.3258	110	3	1.25	0.01	1	2	3	3			37	198
C8XW_02	31	23.7	J	1	3	5	1	0.35	0.05	U	U	2.8	R	U	2.8215	900	2			1	2	2	2	Ch		70	190
C8XW_02	32	24.1	J		4	5	1	5	0.25	U	U	0.27	R	R	0.534					1	3	2	3	Fe		89	22
C8XW_02	33	24.6	L		5	5	1	5	1.3	U	U	1.55	J	R	1.3626	350	2	0.35	0.02	2	3	2	4			70	30
C8XW_02	34	27.8	J	8	4	4	1	4.5	0.25	U	U	0.4	R	R	0.7792	450	3			2	2	3	4	Fe		72	67
C8XW_02	35	29	J	2	3	4	1	5.5	0.1	U	V	2.6	R	U	3.6898	750	1	2	0.01	1	3	2	2			48	249
C8XW_03	1	1.2	J	8	3	5	1	5	0.95	F	U	0.3	U	U	1.6561	950	4	1.25	0.02	2	5	2	7			24	182
C8XW_03	2	1.21	J	2	4	5	1	5.5	1.25	U	U	3.2	J	U	2.6184	750	3	1.25	1	3	5	2	5			80	56
C8XW_03	3	2	F	1	2	4	1	0.35	7.5	U	U	6	U	U	5.8235	900	3			2	3	2	3	Cb	3	67	20
C8XW_03	4	2.5	F	1	2	4	1	2.6	7.5	U	U	6.5	U	U	5.9502	750	4	1.3	0.04	2	3	3	3	Bx	5	72	10
C8XW_03	5	2.51	J	8	4	5	1	0.45	0.35	J	R	0.25	U	U	1.1448					1	4	2	2			30	228
C8XW_03	6	3.9	J	8	4	5	1	0.3	0.55	J	J	0.2	U	U	1.0699	75	1			1	2	3	3			50	253
C8XW_03	7	4	J	8	4	5	1	1.45	1.35	J	R	0.05	U	U	1.9378	60	1			4	3	2	5	Ch		60	242
C8XW_03	8	4.1	J	1	3	5	1	1.2	0.35	U	U	3	R	R	4.2393	145	3	1.25	0.02	2	4	2	4	Ch	2	77	33
C8XW_03	9	4.11	J	8	4	5	1	0.25	1.2	J	R	0.35	U	U	1.3306	900	1	1.5	0.01	1	4	2	2	Ch	1	36	230
C8XW_03	10	5.2	J	2	4	5	1	2.2	0.05	U	U	0.8	J	R	0.9494	110	2			4	3	3	3			80	54
C8XW_03	11	6	F	1	2	5	1	5	2	U	U	8	U	U	4.3133	300	3	2.2	0.15	4	5	3	8	Bx	25	83	13
C8XW_03	12	7.2	J	2	3	5	1	1.5	0.65	J	U	1.35	J	U	1.6139	250	7	0.45	0.05	1	5	3	8			86	80
C8XW_03	13	7.98	J	1	4	5	1	0.35	0.55	J	U	0.35	U	U	0.7205	350	3			1	5	2	6			78	231
C8XW_03	14	8	J	8	4	5	1	2.1	1.6	U	U	0.25	U	U	1.1964	80	1			1	3	2	3	Fe		33	230
C8XW_03	15	8.05	J	1	3	5	1	0.95	3	U	R	1.5	U	U	2.9805	750	2	1.5	0.02	2	3	3	5			71	3
C8XW_03	16	8.2	J	8	3	5	1	5	0.55	R	J	0.25	U	J	0.6446	270	6			2	3	2	8			30	247
C8XW_03	17	9.1	J	2	3	5	1	1.6	0.8	U	U	4.2	U	U	4.1739	200	2	1.2	0.02	1	3	2	2	Ch		74	88
C8XW_03	18	9.11	J	2	4	5	1	0.85	0.25	U	U	0.55	U	R	0.5583	60	2			1	3	3	4			75	90
C8XW_03	19	9.12	J	5	4	5	1	5.5	1.7	R	U	0.45	U	U	1.9919	650	3			1	2	3	3			67	55
C8XW_03	20	9.35	J	9	5	5	1	1.25	0.25	U	J	0.75	J	R	1.0798	35	2			4	5	4	9			35	123
C8XW_03	21	9.75	J	9	4	5	1	5	0.25	R	R	0.2	U	U	0.3752	50	2			2	3	4	7			35	125
C8XW_03	22	10.45	J	9	5	5	1	5.9	0.25	U	U	0.55	R	R	0.7552	80	3			2	3	4	7			58	203

hole_id	id	depth_to	type	m_set	strength	wall_strength	number	est_spacing	trace_s	t1_s	t2_s	trace_d	t1_d	t2_d	continuity	wav_m	amp_m	wav_lg	amp_lg	profile	plan.	rough.	jrc	infill	width	dip	direction	
C8XW_03	23	10.9	J	8	4	4	1	5.5	0.05	U	U	0.45	R	R	0.4459	350	3			2	3	3	5			42	242	
C8XW_03	24	11	J	2	4	4	1		0.05	U	U	1.25	U	R	2.0216	270	3	2.5	0.15	3	3	3	6	Fe		77	74	
C8XW_03	25	11.65	J	1	4	5	1	5	0.45	U	U	0.55	R	U	0.6229	320	3			2	3	3	6			80	30	
C8XW_03	26	11.95	J	2	4	5	1	0.45	0.2	U	U	1.65	R	U	1.2127	120	2			1	3	2	3	Ch		70	98	
C8XW_03	27	12.75	J	2	4	4	1	0.25	0.1	U	U	4.8	R	U	3.7427	350	1	2.5	0.14	1	3	3	3	Fe		66	76	
C8XW_03	28	13	J	9	3	4	1	0.25	0.2	U	U	1.2	J	R	1.4628	370	6			2	3	3	6			27	175	
C8XW_03	29	13.5	F	1	2	5	1	4.1	99	U	U	6	U	U	5.7219	100	3	2	0.02	2	3	3	5	Ch	10	70	24	
C8XW_03	30	14.3	J	2	4	5	1	1.25	0.1	U	U	1.15	R	U	1.1064	250	1			1	3	2	3	Ch		72	87	
C8XW_03	31	14.6	J	3	3	5	1	5	5.6	U	J	1.2	U	U	5.4712	150	3	2.5	0.02	1	3	3	4	Fe	1	45	252	
C8XW_03	32	14.65	J	9	4	4	1	1.75	0.15	U	U	1.05	J	R	1.0499	65	2			2	3	4	7			26	136	
C8XW_03	33	16.2	J	4	4	5	1	2.3	0.45	U	U	5.5	U	U	4.207	950	3	2.3	0.04	2	3	3	5			89	6	
C8XW_03	34	16.3	J	2	4	5	1	0.45	0.25	J	U	1.35	J	R	1.5604	180	3	1.1	0.08	2	5	3	7			80	62	
C8XW_03	35	16.5	J	1	4	4	1	1.1	0.45	U	U	1.25	U	U	1.223	150	2			2	3	3	4	Ch		66	8	
C8XW_03	36	16.85	J	2	2	4	1	4.7	0.5	U	U	0.85	J	J	1.0803	210	4	0.7	0.02	2	5	4	8			80	49	
C8XW_03	37	17.2	J	1	3	5	1	0.4	0.35	U	U	2	U	R	1.7293	900	3	1.8	0.08	2	3	3	5			72	2	
C8XW_03	38	17.5	F	1	3	5	1	1.2	1	U	U	5.7	U	U	4.5521	200	3	4.5	0.1	2	5	3	7	Bk	3	73	357	
C8XW_03	39	17.55	J	1	3	5	1	0.3	0.25	U	U	1.6	U	R	2.0596	750	3	2	0.1	3	2	3	6			72	5	
C8XW_03	40	18.1	J	1	4	5	1	0.45	0.1	U	U	0.8	R	R	0.8472	200	2			1	4	4	7			76	6	
C8XW_03	41	18.21	J	2	4	5	1	0.35	0.4	J	U	0.75	R	J	0.8774	180	3			4	5	3	5			82	253	
C8XW_03	42	18.5	F	1	3	5	1	0.45	1.25	U	U	6	U	U	5.1001	700	10	3.5	0.1	3	4	3	7			72	7	
C8XW_03	43	19.2	F	1	3	5	1	1.7	3.5	U	U	6.5	U	F	5.5899	250	10	2.5	0.1	3	5	3	8	Bx	20	75	351	
C8XW_03	44	20.5	F	4	3	4	1	9	0.1	U	U	5.7	U	U	4.1192	999	6	3.2	0.2	3	3	2	4	Bx	100	88	307	
C8XW_03	45	21.3	J	5	3	4	1	1.5	0.35	U	U	1.25	R	R	2.4927	300	1	1.25	0.01	4	2	3	4			78	348	
C8XW_03	46	22	J	6	2	4	1	6	0.35	U	U	2.95	J	F	3.3071	220	5	6.5	0.3	3	3	3	8	Cb	2	42	95	
C8XW_03	47	22.05	J	8	3	5	1	2.2	0.95	J	J	0.2	U	U	0.9392	170	2			2	3	3	5	Fe		24	185	
C8XW_03	48	22.2	Sh	7	2	3	1	6.5	0.05	U	U	2	R	U	2.6346	340	15	1.8	0.14	3	3	2	4	Ch	5	80	78	
C8XW_03	49	22.4	J	5	3	5	1	0.5	1.25	U	U	1.15	U	U	1.7559	750	4			1	3	3	4			73	13	
C8XW_03	50	22.5	J	8	2	4	1	2.2		F	U	0.25	U	U	3.8499	200	3	2.5	0.1	2	2	2	4	Fe	1	25	186	
C8XW_03	51	22.7	J	10	2	4	1	6	0.25	R	J	0.3	U	U	0.6586	650	35			3	3	2	6	Ch	2	30	287	
C8XW_03	52	23	J	9	3	4	1	1.65	0.2	U	U	2.35	F	J	2.1574	120	2	2	0.12	3	3	2	4	Cb	1	32	344	
C8XW_03	53	23.6	J	8	2	4	1	2.6	0.65	R	J	0.25	U	U	0.8666	170	4			2	3	2	4	Cb	3	24	235	
C8XW_03	54	24.1	J	1	3	5	1	1.1	0.45	U	U	5.5	U	U	4.2017	250	2	1.75	0.15	2	4	3	5			83	342	
C8XW_03	55	24.5	J	2	3	4	1	1.8	0.35	U	U	2.67	U	R	3.7287					2	3	2	5	Ch		80	310	
C8XW_03	56	25.05	J	9	2	4	1	1.95	0.25	U	U	5.5	J	U	4.2669			2.25		3	3	4	7			75	330	
C8XW_03	57	25.5	J	1	3	5	1	2.1	0.4	U	U	3.5	U	R	2.4271	250	2	2.7	0.12	2	3	3	7			85	350	
C8XW_03	58	26	J	3	3	4	1	2.5	1.2	J	J	0.2	U	U	1.6218					1	4	4	6	Fe				
C8XW_03	59	26.1	J	1	3	4	1	0.4	0.2	U	U	2.1	R	J	1.0771					2	2	3	4	Fe				
C8XW_03	60	27.3	J	1	3	4	1		0.25	U	U	1.1	R	R	0.5641	370	3			2	2	2	3	Ch	1	89	153	
D0XW_01	1	1.6	J	3	4	5	1	99	1.2	R	R	0.25	U	U	1.5869	550	2			4	2	3	2			41	212	
D0XW_01	2	1.9	J	1	4	4	1	3.5	0.1	U	U	2.25	R	R	2.1018	770	5	2.2	0.17	3	3	2	6	Cb	2	70	105	
D0XW_01	3	2.7	V	5	2	5	1	0.15	0.05	U	U	3.5	U	R	4.9812	50	2	1.7	0.02	2	3	3	4	Cb	3	28	127	

hole_id	id	depth_to	type	m_set	strength	wall_strength	number	est_spacing	trace_s	t1_s	t2_s	trace_d	t1_d	t2_d	continuity	wav_m	amp_m	wav_lg	amp_lg	profile	plan.	rough.	jrc	infill	width	dip	direction
D0XW_01	4	3	J	5	3	5	1	0.35	0.05	U	U	0.75	J	V	0.4834	210	3			2	2	2	3	Ch		54	125
D0XW_01	5	3.7	J	3	4	5	1	1.5	1.05	R	J	0.2	U	U	1.5129	200	1	0.8	0.01	2	2	2	2	Fe		43	206
D0XW_01	6	4	J	2	3	5	1	2.4	0.05	U	U	2.8	R	F	2.8861	270	3	1.9	0.04	3	3	2	5	Ch		53	273
D0XW_01	7	5.5	F	1	3	4	1	99	0.1	U	U	6	U	U	4.8378	900	3	2.2	0.15	3	2	2	2	Bk	10	52	116
D0XW_01	8	5.75	J	6	4	4	1	7	0.03	U	U	1.3	F	R	1.6174	170	5	1.1	0.02	3	3	3	4			73	88
D0XW_01	9	6	J	3	3	5	1	99	1.4	F	R	0.05	U	U	1.5401	50	3	0.7	0.02	3	5	3	7	Fe		40	220
D0XW_01	10	7.8	F	4	2	4	1	99	0.1	U	U	6	U	U	4.0692	999	3	2.3	0.05	3	2	3	2	Bk	10	77	62
D0XW_01	11	9	J	3	5	5	1	6	0.35	R	R	0.1	U	U	0.4288	300	2			2	2	2	1			43	204
D0XW_01	12	9.3	J	6	4	5	1	6	0.3	U	U	1.5	J	J	1.0308	750	3			2	2	3	3			84	237
D0XW_01	13	9.6	J	7	4	5	1	7	0.3	U	U	1.1	R	J	0.7801	150	2			1	2	2	2			84	3
D0XW_01	14	10	J	2	1	5	1	2.5	0.25	U	U	2.3	R	R	2.1104	650	2	2	0.01	1	3	2	5			36	305
D0XW_01	15	10.05	J	2	4	5	1	0.15	0.05	U	U	2.5	R	U	3.8343	450	5	2.1	0.02	2	3	4	7	Ch		34	262
D0XW_01	16	10.1	J	8	4	5	1	7	1.2	R	U	0.3	U	U	1.6927	999	2			1	1	2	1	Ch		63	200
JGDS_01	1	0.6	J	2	1	5	1	0.3	0.1	U	U	4.5	R	U	4.404	230	3	2.6	0.07	2	5	3	8			37	243
JGDS_01	2	0.9	J	1	1	5	1	15.5	0.2	U	U	4.2	R	U	4.495	350	3	1.2	0.1	2	3	3	5			56	46
JGDS_01	3	0.91	J	3	3	5	1	1.35	0.1	U	U	1.25	R	U	1.3023	230	2	0.75	0.01	2	3	3	3			86	359
JGDS_01	4	1.2	J	4	4	5	1	99	2.1	U	J	0.2	U	U	2.3531	680	15			4	3	2	4			55	257
JGDS_01	5	2	J	3	4	5	1	0.35	0.25	U	U	3.2	U	U	4.0572	500	5	2.5	0.01	1	3	3	4	Fe		89	346
JGDS_01	6	2.5	J	3	4	5	1	0.25	0.2	U	U	2.2	R	R	2.7119	700	3	1.5	0.03	2	3	3	5			84	338
JGDS_01	7	3	J	4	4	5	1	1.6	1.4	J	R	0.1	U	U	1.6985	250	2	0.9	0.02	2	3	2	6			29	252
JGDS_01	8	3.3	J	3	4	4	1	1.1	0.05	U	U	1.6	U	R	1.8555	500	4			3	4	2	4			85	340
JGDS_01	9	3.7	J	4	5	5	1	99	0.1	U	U	1.1	J	J	1.1688	800	11			3	5	3	5			39	230
JGDS_01	10	3.95	J	1	4	5	1	99	0.2	U	U	1.25	J	J	1.1203	150	3			2	5	4	9			29	353
JGDS_01	11	4.3	J	3	4	5	1	6.3	0.2	U	U	6	U	U	4.313	300	3	2.7	0.03	2	4	3	6	Qz	2	83	346
JGDS_01	12	4.5	J	3	4	5	1	0.45	0.2	U	U	2.6	R	R	2.258	350	1			1	2	4	3	Fe		80	350
JGDS_01	13	5	J	3	4	5	1	0.25	0.05	U	U	1.2	U	R	1.3506					1	2	3	2			85	350
JGDS_01	14	6	J	10	4	5	1	99	2	U	U	1.1	U	R	2.0166	950	2	0.75	3	4	4	3	7			84	294
JGDS_01	15	7.5	J	10	2	5	1	99	3.5	U	U	6	U	U	3.6273	160	2	1.95	0.15	2	5	3	7			85	280
JGDS_01	16	8.9	J	2	4	4	1	1.25	0.05	U	U	2.2	R	U	3.1475	750	2	1.4	0.02	2	3	3	5			40	240
JGDS_01	17	13.4	J	2	4	5	1	2.7	0.1	U	U	2.4	R	J	2.757	900	2	0.9	0.02	3	2	2	2	Cb		38	215
JGDS_01	18	14.4	J	3	4	5	1	7	0.25	U	U	2.3	U	J	1.681	250	3	0.6		3	3	3				83	146
JGDS_01	19	14.7	J	3	4	5	1	7.5	0.1	U	U	2.6	U	J	2.0119	400	3	2.5	0.05	3	2	3	3			86	1
JGDS_01	20	15.2	J	4	3	4	1	1.2	0.2	U	U	1.25	J	J	1.3931	350	3	0.7	0.05	3	5	3	3	Ch	2	64	135
JGDS_01	21	15.3	J	2	3	4	1	10.5	0.35	U	U	2.3	J	R	1.8554	250	3	2.1	0.02	2	5	3	8			47	154
JGDS_01	22	16	F	7	2	4	1	99	0.2	U	U	6	U	U	4.4136	400	1	0.5	0.01	2	3	2	3	Bk	2	60	88
JGDS_01	23	17.8	J	7	4	5	1	99	2	J	J	0.2	U	U	1.58	270	1			2	2	3	3			36	330
JGDS_01	24	18	J	9	2	4	1	99	3.9	J	J	0.45	U	U	3.905	999	15	3.1	0.15	3	3	4	9			45	133
JGDS_01	25	18.25	J	8	5	5	1	3.75	0.1	U	U	1.25	R	R	1.4867	380	1	1.2	0.01	2	4	3	7			68	17
JGDS_01	26	18.5	J	5	4	5	1	99	1.9	R	R	0.2	U	U	1.8687	250	3	1.2	0.01	3	3	3	6			24	301
JGDS_01	27	18.7	J	5	4	5	1	1.4	1.3	J	R	0.35	U	U	1.7644	300	4	0.7	0.02	3	3	3	9			20	294
JGDS_01	28	18.9	J	3	3	5	1	0.45	0.1	U	U	1.1	R	R	1.2341	480	2			2	3	2	4			80	354

hole_id	id	depth_to	type	m_set	strength	wall_strength	number	est_spacing	trace_s	t1_s	t2_s	trace_d	t1_d	t2_d	continuity	wav_m	amp_m	wav_lg	amp_lg	profile	plan.	rough.	jrc	infill	width	dip	direction	
JGDS_01	29	19.2	J	3	4	5	1	7.6	0.25	U	U	1.3	R	U	0.9924	270	2			2	2	4	5			82	4	
JGDS_01	30	19.6	J	3	4	5	1	2.6	0.25	U	U	1.6	R	R	1.436	900	1	2.6	1	2	1	4	2	Cb	1	83	18	
JGDS_01	31	21.9	J	7	5	4	1	1.55	0.1	U	U	2.25	J	U	2.1764	250	1			2	2	4	4			59	198	
JGDS_01	32	22.2	J	8	3	5	1	99	0.2	U	U	0.45	R	R	0.7304	400	1			2	1	3	1	Fe		86	92	
JGDS_01	33	22.5	J	3	4	5	1	8	0.2	U	V	2.4	R	U	2.7623	350	2	1.2	0.01	4	2	2	6	Fe		87	180	
JGDS_01	34	23.1	J	6	4	5	1	8	1	U	U	2	R	R	1.6431	110	1			4	2	3	3			76	44	
JGDS_01	35	23.15	J	3	3	5	1	0.25	0.05	U	U	0.9	R	U	1.0333					2	3	3	2			87	355	
JGDS_01	36	23.3	J	7	3	5	1	0.1	0	U	U	0.5	R	U	0.9706	350	2			1	3	2	1			57	211	
JHDN_01	1	0.4	J	1	4	5	1	1.8	0.2	U	U	0.8	R	J	1.2416	100	3			2	4	2	5			79	20	
JHDN_01	2	1.3	J	1	5	5	1	0.45	0.2	U	U	1.4	U	R	2.556	850	5			3	3	2	3			68	77	
JHDN_01	3	1.4	J	2	4	5	1	0.7	1.9	U	R	0.25	U	U	2.4694	350	30			4	5	3	7			44	104	
JHDN_01	4	1.5	J	2	4	4	1	99	2.8	J	R	0.2	U	U	2.4889	350	2			2	2	3	2	Ca	1	33	144	
JHDN_01	5	1.6	J	1	5	5	1	0.22	0.15	U	U	0.6	R	J	0.5357	650	20			3	2	2	3			65	75	
JHDN_01	6	1.95	J	1	4	5	1	5	0.1	U	U	1.2	R	R	1.4429	250	10			2	3	2	3			65	75	
JHDN_01	7	2.3	F	3	3	5	1	1.3	0.2	U	U	99	U	R	3.7709	700	5			1	2	3	5			83	1	
JHDN_01	8	3	J	4	2	4	1	99	2.9	U	R	0.35	U	U	3.5355	700	5			2	3	4	7	Bk	3	53	280	
JHDN_01	9	3.05	J	3	1	5	1	0.48	0.35	U	U	0.4	R	J	0.5394	700	5			4	1	3	3					
JHDN_01	10	3.3	J	1	4	5	1	99	0.2	U	U	1.2	J	U	2.2837	250	5			2	5	3	3			66	47	
JHDN_01	11	3.5	J	3	3	5	1	0.05	0.2	U	U	0.5	R	R	0.5627	700	5			2	1	2	2					
JHDN_01	12	3.6	J	3	4	5	1	1.2	0.2	U	U	2.1	R	U	2.7457	250	5			1	2	3	2	Ch	1	89	36	
JHDN_01	13	4.5	J	1	1	4	1	99	0.2	U	U	2.5	R	R	2.0254	900	20			2	2	2	3	Ch	2	75	56	
JHDN_01	14	4.7	J	2	3	5	1	99	2.3	J	R	0.25	U	U	2.2108	800	20			3	3	3	7	Ch		68	95	
JHDN_01	15	4.8	J	1	4	6	1	2.5	0.2	U	U	1.4	R	J	1.8033	900	5			1	2	3	2			89	352	
JHDN_01	16	5.8	J	1	3	5	1	1.5	0.2	U	U	1.4	U	R	1.4903	101	20			2	2	3	3			84	5	
JHDN_01	17	6.2	J	5	3	5	1	99	0.2	U	U	3.1	R	U	4.221	900	10			1	2	2	2	Cb	1	42	212	
JHDN_01	18	6.6	J	6	1	4	1	99	0.4	U	U	2.7	R	U	3.4242	900	5			3	4	4	7	Fe	1	84	94	
JHDN_01	19	7.3	J	1	3	5	1	0.3	0.2	V	U	2.3	R	J	2.1559	101	10			2	3	3	4			86	6	
JHDN_01	20	7.5	J	1	3	5	1	0.45	0.2	U	U	1.3	R	R	0.8887	101	10			2	4	3	4			85	10	
JHDN_01	21	7.9	J	8	3	5	1	99	1.1	R	R	0.2	U	U	0.9817	700	3			2	5	3	7			53	166	
JHDN_01	22	8.35	J	7	3	4	1	5	0.2	U	U	1.5	R	R	1.8272	101	30			3	2	4	4			62	175	
JHDN_01	23	8.8	J	9	3	5	1	99	0.2	U	U	0.8	R	R	1.0354	400	10			3	5	3	8	Fe	1	72	295	

APPENDIX E - CANNINGTON EMPIRICAL BACK ANALYSIS DATA

E.1 Geometric Back Analysis Data – used in development of shape descriptors (Chapter 6)
and development of scale independent empirical instability criteria (Chapter 12)

E.2 Logistic Regression of Modified Stability Graph Data (Chapter 12)

List of abbreviations used in back analysis data tables

Field	Description	Field	Description
stope_name	stope name	depth_ub	maximum depth of under-break
surface	stope surface	depth_ave_ob	average depth of over-break
des_span_crit	surface design critical span	depth_ave_ub	average depth of under-break
des_area	surface design area	vol_ob	volume of over-break
des_perimeter	surface design perimeter	vol_ub	volume of under-break
des_dip	surface design dip	area_ob	area of over-break
des_dip_dirn	surface design dip direction	area_ub	area of under-break
des_hr	surface design hydraulic radius	c_ob	circularity of over-break
des_hr_c	surface design corrected hydraulic radius	c_ub	circularity of under-break
des_rf	surface design radius factor	x_ob	extensivity of over-break
elos	equivalent linear over-break sloughage	x_ub	extensivity of under-break
ello	equivalent linear lost ore	h_ob	hemi-sphericity of over-break
depth_ob	Maximum depth of over-break	h_ub	hemi-sphericity of under-break

E.1 GEOMETRIC BACK ANALYSIS DATA

stope_name	surface	des_span_crit	des_area	des_perimeter	des_dip	des_dip_dirn	des_hr
22g.c6HL	Crown	11.312	272.795	71.231	0	203	3.83
22g.c6HL	East	23.5	835.054	130.467	89	110	6.4
22g.c6HL	North	18.686	693.542	107.353	90	22	6.46
22g.c6HL	South	18.8	652.589	109.75	78	40	5.946
22g.c6HL	West	19.021	680.099	118.397	83	113	5.744
22h.c6HL	Crown	19	641.841	108.028	32	155	5.941
22h.c6HL	East	23	690.798	109.037	90	292	6.335
22h.c6HL	North	19.2	690.546	111.849	90	22	6.174
22h.c6HL	South	15	405.915	80.765	79	38	5.026
22h.c6HL	West	25	831.763	130.54	78	112	6.372
22i.c6HL	East	19.57	797.677	151.773	90	291	5.256
22i.c6HL	North	19.781	1043.475	146.594	90	202	7.118
22i.c6HL	West	24.23	855.51	150.119	90	291	5.699
24j.c6HL	East	19.969	1125.305	155.458	90	292	7.239
24j.c6HL	North	20.773	1051.19	147.647	90	202	7.12
24j.c6HL	South	20.519	898.598	156.218	85	189	5.752
24j.c6HL	West	19.967	1003.094	177.96	87	133	5.637
29c.54HL	Crown	16.297	313.28	69.61	0	341	4.5
29c.54HL	East	20.64	590.265	104.466	85	92	5.65
29c.54HL	North	15.244	345.177	81.461	76	23	4.237
29c.54HL	South	16.067	495.275	87.137	90	210	5.684
29c.54HL	West	22.3	487.528	95.6	89	301	5.1
31..60FL	East	25.292	1130.42	142.227	64	60	7.948
31..60FL	North	10.468	298.848	94.206	90	169	3.172
31..60FL	West	28.159	1015.019	138.283	75	68	7.34
31..71FL	Crown	9.482	295.4	96.847	4	359	3.05
31..71FL	East	36.867	2738.954	249.641	62	86	10.972
31..71FL	South	17.946	863.048	179.207	90	0	4.816
31..71FL	West	36.149	2670.415	249.667	68	71	10.696
32m.c8HG	Crown	24.63	253.117	69.503	0	68	3.642
32m.c8HG	East	24.5	2120.599	247.287	87	299	8.575
32m.c8HG	North	25	1464.794	234.963	81	197	6.234
32m.c8HG	South	18.8	1286.632	216.344	90	22	5.947
32m.c8HG	West	24.63	2118.174	233.298	90	112	9.079
37..85HG	Crown	11.021	298.535	72.152	46	233	4.138
37..85HG	East	15.611	842.865	143.054	68	102	5.892
37..85HG	South	16.566	781.283	129.478	90	13	6.034
37d.51HL	Crown	20.154	57.234	94.612	42	112	5.89
37d.51HL	East	20.413	1149.598	154.002	90	300	7.465
37d.51HL	North	19.861	1092.706	166.295	90	210	6.571
37d.51HL	South	19.932	1255.123	171.865	90	210	7.303
37d.51HL	West	20.35	1540.149	194.707	83	126	7.91
40a.78HL	Crown	12.9	286.898	74.312	1	18	3.861
40a.78HL	East	29.121	988.417	131.087	86	144	7.54
40a.78HL	South	5.785	152.736	66.365	90	30	2.301
40a.78HL	West	27.512	832.485	125.499	78	132	6.633
40e.60HL	Crown	19.89	505.247	90.467	17	119	5.585
40e.60HL	East	20.025	630.54	102.004	89	300	6.182
40e.60HL	North	17.5	380.028	108.85	90	29	3.491
40e.60HL	West	19.89	870.668	130.624	61	120	6.665
47..70HG	Crown	12	243.309	67.565	0	194	3.601
47..70HG	East	12.09	347.999	82.472	56	116	4.22
47..70HG	South	22.562	576.638	100.39	90	210	5.744
47..70HG	West	12.591	317.752	78.08	68	105	4.07
47..71HG	Crown	10.001	222.671	67.478	0	164	3.3
47..71HG	East	10.232	296.655	79.856	56	129	3.715
47..71HG	North	23.084	641.693	107.732	90	30	5.956
47..71HG	South	22.85	631.127	104.765	90	30	6.024

stope_name	surface	des_span_crit	des_area	des_perimeter	des_dip	des_dip_dirn	des_hr
47..71HG	West	10.196	270.529	74.513	63	125	3.631
47..72HG	Crown	10.254	313.717	83.295	0	113	3.766
47..72HG	East	10.002	262.956	78.234	68	146	3.361
47..72HG	North	23.995	769.32	115.19	90	210	6.679
47..72HG	West	10.245	261.272	74.826	66	123	3.492
47a.65hl	East	22.582	1904.412	247.787	86	298	7.686
47a.65hl	North	15.257	1443.765	233.539	89	210	6.182
47a.65hl	West	22.883	2255.278	241.169	90	119	9.351
47b.70FZ	East	27.636	903.777	122.411	51	100	7.383
47b.70FZ	North	8.289	216.997	73.226	90	0	2.963
47b.70FZ	South	5.59	108.947	60.508	90	180	1.801
47b.70FZ	West	24.504	869.31	116.784	56	90	7.44
50..69HG	Crown	19.505	620.944	100.336	0	52	6.189
50..69HG	East	20.401	504.746	93.281	83	281	5.411
50..69HG	North	24.1	666.066	103.914	90	29	6.41
50..69HG	West	19.505	487.421	91.203	90	285	5.344
50..70HG	Crown	21.663	548.693	96.985	1	32	5.657
50..70HG	East	20.956	545.307	95.466	74	298	5.712
50..70HG	North	21.66	535.731	93.497	90	209	5.73
50..70HG	West	21.568	537.212	93.373	89	132	5.753
55b.69KG	Crown	17.256	418.788	91.19	4	22	4.592
55b.69KG	North	15.149	401.001	95.691	84	36	4.191
55b.69KG	South	11.799	448.963	103.03	90	211	4.358
55b.69KG	West	30	1071.741	133.963	75	118	8
55c.69KG	Crown	19.5	441.217	85.08	26	80	5.186
55c.69KG	South	19.79	538.032	94.406	90	211	5.699
55c.69KG	West	20.002	561.618	97.164	90	120	5.78
55e.75KG	Crown	10.229	183.436	63.169	0	0	2.904
55e.75KG	East	20	694.643	109.686	90	120	6.333
55e.75KG	North	20.365	699.235	108.231	90	30	6.461

stope_name	surface	des_hr_c	des_rf	elos	ello	depth_ob	depth_ub	depth_ave_ob	depth_ave_ub
22g.c6HL	Crown	3.83	4.202	0.297	0.007	2.4	1.2	1.188	0.241
22g.c6HL	East	6.4	7.353	0.569	0.216	3.6	4	1.007	0.89
22g.c6HL	North	6.46	6.579	0.264	0.05	1.1	1	0.394	0.223
22g.c6HL	South	5.946	6.579	0.2	0.109	1.3	2.5	0.376	0.392
22g.c6HL	West	5.744	6.329	0.094	0.166	0.9	2.3	0.273	0.474
22h.c6HL	Crown	5.941	6.849	0.994	1.538	4.6	17.5	1.997	3.846
22h.c6HL	East	6.335	7.246	0.01	0.725	0.4	1.9	0.155	0.943
22h.c6HL	North	6.174	6.579	0.006	0.582	0.5	1.2	0.114	0.704
22h.c6HL	South	5.026	5.495	1.454	0.843	12.8	7.1	2.899	2.482
22h.c6HL	West	6.372	7.813	0.147	1.113	3	11.1	0.591	1.845
22i.c6HL	East	5.256	6.667	0.07	0.602	2.7	3.1	0.52	0.789
22i.c6HL	North	7.118	7.353	0.109	0.227	1.7	2.3	0.335	0.473
22i.c6HL	West	5.699	7.246	0.547	0.878	4.9	5.1	1.083	2.215
24j.c6HL	East	7.239	7.353	0.066	0.371	1	2	0.267	0.568
24j.c6HL	North	7.12	7.463	0.246	0.419	1.4	4	0.536	0.69
24j.c6HL	South	5.752	7.143	0.152	0.423	4.1	2.9	0.398	0.994
24j.c6HL	West	5.637	7.042	0.295	0.346	2.4	2.9	0.766	0.815
29c.54HL	Crown	4.5	4.95	0.255	0.006	2.8	0.6	0.991	0.118
29c.54HL	East	5.65	6.667	0.12	2.031	14.2	16.8	0.755	2.975
29c.54HL	North	4.237	4.717	0.003	1.706	0.1	1.6	0.2	2.123
29c.54HL	South	5.684	6.173	0.083	1.411	1	4	0.369	2.287
29c.54HL	West	5.1	5.882	0.338	1.101	1.9	6.3	0.73	2.797
31..60FL	East	7.948	8.929	1.197	0.202	13.7	7.8	1.738	1.824
31..60FL	North	3.172	3.759	0.392	0.806	1.7	5.2	0.884	1.53
31..60FL	West	7.34	8.475	0.032	1.308	3.7	6.7	0.742	1.595
31..71FL	Crown	3.05	3.165	0.579	0.071	5.1	2.4	1.244	0.384
31..71FL	East	10.972	11.628	0.707	0.483	3.7	7.6	1.25	1.789
31..71FL	South	4.816	6.098	0.964	0.334	3.6	7.5	1.188	1.822

stope_name	surface	des_hr_c	des_rf	elos	ello	depth_ob	depth_ub	depth_ave_ob	depth_ave_ub
22g.c6HL	Crown	3.83	4.202	0.297	0.007	2.4	1.2	1.188	0.241
31..71FL	West	10.696	12.5	0.595	1.215	9.5	11	1.777	2.374
32m.c8HG	Crown	3.642	3.788	0.174	0.04	1.9	1.8	0.932	0.286
32m.c8HG	East	8.575	9.259	0.204	1.075	5.3	6.9	0.775	1.887
32m.c8HG	North	6.234	8.197	0.124	0.524	2.2	14.9	0.301	1.294
32m.c8HG	South	5.947	6.667	0.389	0.461	4.2	1.5	0.977	0.699
32m.c8HG	West	9.079	9.615	0.022	0.594	0.7	2.2	0.205	0.722
37..85HG	Crown	4.138	4.673	0.097	0.362	13.4	5.6	0.475	1.043
37..85HG	East	5.892	6.173	1.296	0.992	6.3	8.8	2.332	3.254
37..85HG	South	6.034	6.849	0.388	0.317	4.8	3.6	0.918	0.673
37d.51HL	Crown	5.89	6.494	1.433	0.664	3	3.3	0.43	0.366
37d.51HL	East	7.465	7.576	0.76	0.187	3.5	1.8	1.395	0.683
37d.51HL	North	6.571	7.353	0.429	0.111	2.9	1.5	0.56	0.461
37d.51HL	South	7.303	7.576	0.477	0.199	3.8	3.7	1.062	0.603
37d.51HL	West	7.91	7.95	0.532	0.256	2.8	6.2	0.932	0.827
40a.78HL	Crown	3.861	4.425	0.119	0.178	2.4	3	0.708	0.867
40a.78HL	East	7.54	8.772	0.166	0.676	6.8	6.8	0.772	1.938
40a.78HL	South	2.301	2.252	0.085	0.216	0.6	5.1	0.214	0.713
40a.78HL	West	6.633	8.065	0.147	0.664	4	4.6	0.778	1.17
40e.60HL	Crown	5.585	6.25	0.346	1.144	3.8	7	0.902	2.46
40e.60HL	East	6.182	6.757	0.002	0.495	0.2	3.2	0.047	0.667
40e.60HL	North	3.491	4.464	0.005	1.197	0.2	5.5	0.142	1.561
40e.60HL	West	6.665	7.246	0.323	0.894	7.6	16.8	0.761	4.235
47..70HG	Crown	3.601	4.132	0.288	0.423	2.4	4	0.897	1.417
47..70HG	East	4.22	4.425	1.489	0.489	6.3	6	2.904	2.061
47..70HG	South	5.744	6.494	0.921	0.343	5.4	7.7	1.359	2.193
47..70HG	West	4.07	4.386	0.044	0.667	1.6	5.2	0.384	0.968
47..71HG	Crown	3.3	3.65	0.593	0.004	3.5	1.5	1.669	0.096
47..71HG	East	3.715	3.817	0.411	0.111	3.3	5.5	0.837	1.587
47..71HG	North	5.956	6.849	0.798	0.048	3.6	2.5	1.088	0.373
47..71HG	South	6.024	6.757	0.052	0.166	0.9	4.4	0.25	0.385
47..71HG	West	3.631	3.759	0.015	0.285	1.1	2.8	0.226	0.628
47..72HG	Crown	3.766	3.788	1.364	0.316	6.6	2	5.523	1.277
47..72HG	East	3.361	3.817	0.472	0.247	5.5	4.6	1.572	0.824
47..72HG	North	6.679	7.576	1.075	0.227	4.6	3	1.75	0.82
47..72HG	West	3.492	3.731	0.008	1.676	0.9	8.5	0.128	2.545
47a.65hl	East	7.686	8.475	0.35	0.371	4.5	9.5	0.812	1.029
47a.65hl	North	6.182	6.173	0.168	0.419	1.7	3.6	0.53	0.836
47a.65hl	West	9.351	9.091	0.072	0.53	1.3	2.9	0.409	0.801
47b.70FZ	East	7.383	8.333	0.341	0.215	2.7	0.7	0.827	0.513
47b.70FZ	North	2.963	3.067	0.065	0.207	0.7	2.4	0.194	0.514
47b.70FZ	South	1.801	1.992	0.005	0.358	0.2	2.3	0.307	0.528
47b.70FZ	West	7.44	8.197	0.006	0.51	0.3	1.7	0.085	0.642
50..69HG	Crown	6.189	6.579	1.066	0.013	5.9	1	2.209	0.237
50..69HG	East	5.411	6.25	0.25	0.753	2.2	7.8	0.652	1.598
50..69HG	North	6.41	7.246	0.279	0.141	1.5	1.6	0.517	0.467
50..69HG	West	5.344	6.098	0.027	0.624	0.9	3.8	0.167	0.91
50..70HG	Crown	5.657	6.494	1.334	0.013	6.5	0.8	2.598	0.255
50..70HG	East	5.712	6.494	1.012	0.343	5.9	6.9	1.878	1.335
50..70HG	North	5.73	6.41	0.125	0.101	0.8	1.3	0.256	0.334
50..70HG	West	5.753	6.579	0.374	0.225	2.1	5.1	0.892	0.927
55b.69KG	Crown	4.592	5.208	1.122	0.062	7	2.9	3.521	0.591
55b.69KG	North	4.191	4.854	0.584	0.197	6.3	3.6	0.894	0.848
55b.69KG	South	4.358	4.808	0.004	0.39	0.4	1	0.072	0.527
55b.69KG	West	8	9.091	0.916	0.241	4.4	5.1	1.567	0.926
55c.69KG	Crown	5.186	5.882	0.05	0.857	0.8	6.6	0.246	1.45
55c.69KG	South	5.699	6.41	0.546	0.074	3.5	1.4	0.915	0.297
55c.69KG	West	5.78	6.494	0.258	0.132	2.1	0.9	0.595	0.382
55e.75KG	Crown	2.904	3.472	0.365	0.038	2.5	0.6	1.499	0.398
55e.75KG	East	6.333	7.042	0.122	0.23	1.8	2.3	0.394	0.475
55e.75KG	North	6.461	6.944	0.087	0.426	1.8	3.1	0.325	0.704

stope_name	surface	vol_ob	vol_ub	area_ob	area_ub	per_ob	per_ub	c_ob	c_ub	x_ob	x_ub	h_ob	h_ub
22g.c6HL	Crown	81	2	68.2	8.3	46.4	24.1	0.398	0.18	0.25	0.03	0.382	0.222
22g.c6HL	East	475	180	471.8	202.3	143	143.8	0.29	0.123	0.565	0.242	0.123	0.166
22g.c6HL	North	183	35	463.9	157.1	120.4	165	0.402	0.073	0.669	0.227	0.049	0.047
22g.c6HL	South	132	71	350.9	181.2	134.1	195.3	0.245	0.06	0.538	0.278	0.053	0.077
22g.c6HL	West	64	113	234.5	238.4	145.7	251.6	0.139	0.047	0.345	0.351	0.047	0.082
22h.c6HL	Crown	638	987	319.5	256.6	73.7	130.9	0.739	0.188	0.498	0.4	0.297	0.638
22h.c6HL	East	7	501	45.1	531.1	44.3	179.1	0.289	0.208	0.065	0.769	0.061	0.109
22h.c6HL	North	4	402	35.1	571.3	38.5	161.1	0.298	0.277	0.051	0.827	0.051	0.078
22h.c6HL	South	590	342	203.5	137.8	60.5	79.8	0.699	0.272	0.501	0.339	0.54	0.562
22h.c6HL	West	122	926	206.5	502	148.8	265.1	0.117	0.09	0.248	0.604	0.109	0.219
22i.c6HL	East	56	480	107.7	608.5	96	198.5	0.147	0.194	0.135	0.763	0.133	0.085
22i.c6HL	North	114	237	340.3	501	153.1	276.1	0.182	0.083	0.326	0.48	0.048	0.056
22i.c6HL	West	468	751	432.2	339.1	119.5	170.7	0.38	0.146	0.505	0.396	0.138	0.32
24j.c6HL	East	74	417	277.1	734.3	169	318.3	0.122	0.091	0.246	0.653	0.043	0.056
24j.c6HL	North	259	440	483	637.5	140.7	259.3	0.307	0.119	0.459	0.606	0.065	0.073
24j.c6HL	South	137	380	344.4	382.4	199.2	261.3	0.109	0.07	0.383	0.426	0.057	0.135
24j.c6HL	West	296	347	386.3	425.8	195.5	251.8	0.127	0.084	0.385	0.424	0.104	0.105
29c.54HL	Crown	80	2	80.7	16.9	86.4	42.6	0.136	0.117	0.258	0.054	0.293	0.077
29c.54HL	East	71	1199	94.1	403	74.1	143.9	0.215	0.245	0.159	0.683	0.207	0.394
29c.54HL	North	1.2	589	6	277.4	18.8	84.2	0.213	0.492	0.017	0.804	0.217	0.339
29c.54HL	South	41	699	111.1	305.6	53.5	104.8	0.488	0.35	0.224	0.617	0.093	0.348
29c.54HL	West	165	537	225.9	192	75.6	109.9	0.497	0.2	0.463	0.394	0.129	0.537
31..60FL	East	1353	228	778.3	125	177.2	115.6	0.311	0.118	0.689	0.111	0.166	0.434
31..60FL	North	117	241	132.3	157.5	86.9	121.9	0.22	0.133	0.443	0.527	0.204	0.324
31..60FL	West	32	1328	43.1	832.6	67.8	144.1	0.118	0.504	0.042	0.82	0.301	0.147
31..71FL	Crown	171	21	137.5	54.7	110.7	84.3	0.141	0.097	0.465	0.185	0.282	0.138
31..71FL	East	1937	1324	1549.6	739.9	401.7	528.2	0.121	0.033	0.566	0.27	0.084	0.175
31..71FL	South	832	288	700.6	158.1	204.1	208.8	0.211	0.046	0.812	0.183	0.119	0.385
31..71FL	West	1590	3245	894.7	1367	467.1	3853.4	0.052	0.001	0.335	0.512	0.158	0.171
32m.c8HG	Crown	44	10	47.2	35	44.6	79.3	0.298	0.07	0.186	0.138	0.361	0.128
32m.c8HG	East	432	2279	557.1	1207.5	306.9	530.8	0.074	0.054	0.263	0.569	0.087	0.144
32m.c8HG	North	181	768	601.4	593.4	330.1	474.3	0.069	0.033	0.411	0.405	0.033	0.141
32m.c8HG	South	501	593	512.6	848.3	190.9	343.5	0.177	0.09	0.398	0.659	0.115	0.064
32m.c8HG	West	47	1259	229.7	1742.8	183.2	424.1	0.086	0.122	0.108	0.823	0.036	0.046
37..85HG	Crown	29	108	61	103.5	60.9	108.7	0.207	0.11	0.204	0.347	0.162	0.273
37..85HG	East	1092	836	468.2	256.9	120	188.9	0.409	0.09	0.555	0.305	0.287	0.54
37..85HG	South	303	248	330.2	368.3	138	229.4	0.218	0.088	0.423	0.471	0.134	0.093
37d.51HL	Crown	82	38	190.9	103.8	149.2	161.8	0.108	0.05	3.335	1.814	0.083	0.096
37d.51HL	East	874	215	626.5	314.7	142.6	181.3	0.387	0.12	0.545	0.274	0.148	0.102
37d.51HL	North	469	121	837.3	262.5	175.7	175.5	0.341	0.107	0.766	0.24	0.051	0.076
37d.51HL	South	599	250	563.9	414.7	203.6	328.6	0.171	0.048	0.449	0.33	0.119	0.079
37d.51HL	West	820	394	879.8	476.6	372.8	412.5	0.08	0.035	0.571	0.309	0.084	0.101
40a.78HL	Crown	34	51	48	58.8	59.1	98.9	0.173	0.076	0.167	0.205	0.272	0.301
40a.78HL	East	164	668	212.4	344.6	163.1	206	0.1	0.102	0.215	0.349	0.141	0.278
40a.78HL	South	13	33	60.8	46.3	50.2	61.2	0.303	0.155	0.398	0.303	0.073	0.278
40a.78HL	West	122	553	156.8	472.5	106	175.5	0.175	0.193	0.188	0.568	0.165	0.143
40e.60HL	Crown	175	578	194.1	235	68.7	123.3	0.517	0.194	0.384	0.465	0.172	0.427
40e.60HL	East	1	312	21.5	467.9	47.4	176.5	0.12	0.189	0.034	0.742	0.027	0.082
40e.60HL	North	2	455	14.1	291.4	22.2	124.7	0.36	0.235	0.037	0.767	0.1	0.243
40e.60HL	West	281	778	369.4	183.7	160.8	138.3	0.18	0.121	0.424	0.211	0.105	0.831
47..70HG	Crown	70	103	78	72.7	43.4	57.3	0.52	0.278	0.321	0.299	0.27	0.442
47..70HG	East	518	170	178.4	82.5	63.2	60.7	0.561	0.281	0.513	0.237	0.578	0.603
47..70HG	South	531	198	390.7	90.3	83.7	124	0.701	0.074	0.678	0.157	0.183	0.613
47..70HG	West	14	212	36.5	219.1	33.3	102.3	0.414	0.263	0.115	0.69	0.169	0.174
47..71HG	Crown	132	1	79.1	10.4	43.8	13.1	0.518	0.762	0.355	0.047	0.499	0.079
47..71HG	East	122	33	145.7	20.8	57.2	39.6	0.56	0.167	0.491	0.07	0.184	0.925
47..71HG	North	512	31	470.8	83.1	92.9	121.6	0.686	0.071	0.734	0.13	0.133	0.109
47..71HG	South	33	105	132	272.7	98.5	200.5	0.171	0.085	0.209	0.432	0.058	0.062
47..71HG	West	4	77	17.7	122.6	30.6	106.7	0.238	0.135	0.065	0.453	0.143	0.151

stope_name	surface	vol_ob	vol_ub	area_ob	area_ub	per_ob	per_ub	c_ob	c_ub	x_ob	x_ub	h_ob	h_ub
47..72HG	Crown	428	99	77.5	77.5	53	53	0.347	0.347	0.247	0.247	1.668	0.386
47..72HG	East	124	65	78.9	78.9	61.5	61.5	0.262	0.262	0.3	0.3	0.47	0.247
47..72HG	North	827	175	472.7	213.3	101.5	172.2	0.577	0.09	0.614	0.277	0.214	0.149
47..72HG	West	2	438	15.6	172.1	17.2	81.8	0.663	0.323	0.06	0.659	0.086	0.516
47a.65hl	East	666	707	819.7	686.8	343.9	352.8	0.087	0.069	0.43	0.361	0.075	0.104
47a.65hl	North	242	605	456.9	723.8	170.7	398.5	0.197	0.057	0.316	0.501	0.066	0.083
47a.65hl	West	162	1195	396.5	1492.4	234.3	459.9	0.091	0.089	0.176	0.662	0.055	0.055
47b.70FZ	East	308	194	372.5	378	193.4	228.5	0.125	0.091	0.412	0.418	0.114	0.07
47b.70FZ	North	14	45	72.1	87.5	55.4	104.1	0.295	0.101	0.332	0.403	0.061	0.146
47b.70FZ	South	0.5	39	1.627	73.8	15.5	58.1	0.085	0.275	0.015	0.677	0.641	0.164
47b.70FZ	West	5	443	59	690.5	79.4	177.5	0.118	0.275	0.068	0.794	0.029	0.065
50..69HG	Crown	662	8	299.7	33.7	127.5	72.8	0.232	0.08	0.483	0.054	0.339	0.109
50..69HG	East	126	380	193.3	237.8	104	177.4	0.225	0.095	0.383	0.471	0.125	0.276
50..69HG	North	186	94	360.1	201.3	133	199.7	0.256	0.063	0.541	0.302	0.072	0.088
50..69HG	West	13	304	77.8	334.2	83.7	156.7	0.14	0.171	0.16	0.686	0.05	0.132
50..70HG	Crown	732	7	281.8	27.4	121.1	46.1	0.241	0.162	0.514	0.05	0.411	0.13
50..70HG	East	552	187	293.9	140.1	105.6	148.4	0.331	0.08	0.539	0.257	0.291	0.3
50..70HG	North	67	54	261.6	161.8	109.1	168.3	0.276	0.072	0.488	0.302	0.042	0.07
50..70HG	West	201	121	225.4	130.5	79	115.6	0.454	0.123	0.42	0.243	0.158	0.216
55b.69KG	Crown	470	26	133.5	44	55.6	84.8	0.543	0.077	0.319	0.105	0.81	0.237
55b.69KG	North	234	79	261.7	93.2	124.7	119.7	0.211	0.082	0.653	0.232	0.147	0.233
55b.69KG	South	2	175	27.6	331.8	42.2	131.1	0.195	0.243	0.061	0.739	0.037	0.077
55b.69KG	West	982	258	626.7	278.5	118.6	185.3	0.56	0.102	0.585	0.26	0.166	0.148
55c.69KG	Crown	22	378	89.6	260.7	67.9	143.2	0.244	0.16	0.203	0.591	0.069	0.239
55c.69KG	South	294	40	321.2	134.9	105.3	182	0.364	0.051	0.597	0.251	0.136	0.068
55c.69KG	West	145	74	243.6	193.8	135.1	189.2	0.168	0.068	0.434	0.345	0.101	0.073
55e.75KG	Crown	67	7	44.7	17.6	37.5	29.1	0.399	0.261	0.244	0.096	0.596	0.252
55e.75KG	East	85	160	215.9	336.7	138.2	199.9	0.142	0.106	0.311	0.485	0.071	0.069
55e.75KG	North	61	298	187.8	423.5	133.5	255.8	0.132	0.081	0.269	0.606	0.063	0.091

E.2 LOGIT REGRESSION OF CANNINGTON MODIFIED STABILITY GRAPH DATA

Logit models are typically applied to yes/no outcomes (giving a binary model). The stability graph data were characterised as either stable (1) and unstable (0). The output of a linear regression can be suitable for probabilities by using a logit model as follows:

$$\text{logit } p = \log o = \log\left(\frac{p}{1-p}\right) = \beta_0 + \beta_1 x_1 + \beta_2 x_2 + \dots + \beta_k x_k \quad (\text{E.1})$$

where p is probability, o is odds and β is the logit estimate for variable x . The modified stability graph method can be represented by the following logit function;

$$\log\left(\frac{p}{1-p}\right) = \beta_0 + \beta_1 HR + \beta_2 N' \quad (\text{E.2})$$

Use of maximum likelihood methods provides the following statistics;

Coefficient	Estimate	Std. Error	z-value	Pr(> z)
β_0	0.083	1.132	0.073	0.942
β_1	0.120	0.207	0.576	0.565
β_2	0.038	0.029	1.319	0.187

The maximum likelihood statistic is used to define the inclination of the stability zone boundaries. A cumulative distribution curve is plotted for the logit probability values for the stable class (S), as shown in Figure E.1. The inverse cumulative distribution curve of the unstable class (U') is also plotted. The point of intersection of the stable line and the inverse unstable line is termed the crossover point. The crossover point on the cumulative distribution graph represents the logit probability value that will define the separation line that will have the least amount of error. From Figure E.1, the crossover logit value of 0.715 has been selected to define the "stability" line. The following table lists the significance statistics for logit regression model;

Obs	Max. Deriv .	Model L.R.	d.f.	P-value	C-index
52	1.201e-05	5.309e+00	2.00e+00	7.033e-02	6.917e-01
Dxy	Gamma	Tau-a	R ²	Brier	
3.833e-01	3.861e-01	1.2142e-01	1.5545e-01	1.435e-01	

The table shows the following elements: number of observations used in the fit, maximum absolute value of first derivative of log likelihood, model likelihood ratio χ^2 , degrees of freedom, P-value, C index (area under ROC curve), Somers' Dxy, Goodman-Kruskal γ , Kendall's τ_a rank correlations between predicted probabilities and observed response, the

Nagelkerke R^2 index, and the Brier score computed with respect to $Y >$ its lowest level. As the P-value of the G-test statistic (log-likelihood ratio) is greater than 0.05, we accept the null hypothesis that there is no overall significant relationship between the dependent variable “stability” and the independent variables HR and N' .

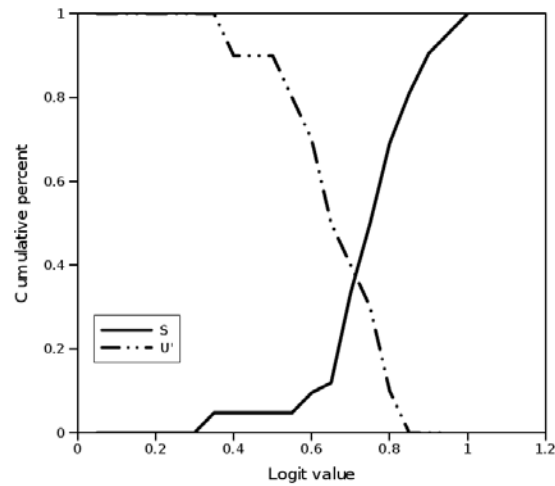


Figure E.1- Cumulative frequency of logit values for stable and inverse unstable

APPENDIX F - KANOWNA BELLE BACK ANALYSIS DATA

F.1 Geometric Back Analysis Data – used in development/demonstration of new shape descriptors (Chapter 6)

F.2 Probability density function graphs of expected volumes of over-break for back analysed stopes (Chapter 13)

List of abbreviations used in back analysis data tables

Field	Description	Field	Description
stope_name	stope name	depth_ub	maximum depth of under-break
surface	stope surface	depth_ave_ob	average depth of over-break
des_span_crit	surface design critical span	depth_ave_ub	average depth of under-break
des_area	surface design area	vol_ob	volume of over-break
des_perimeter	surface design perimeter	vol_ub	volume of under-break
des_dip	surface design dip	area_ob	area of over-break
des_dip_dirn	surface design dip direction	area_ub	area of under-break
des_hr	surface design hydraulic radius	c_ob	circularity of over-break
des_hr_c	surface design corrected hydraulic radius	c_ub	circularity of under-break
des_rf	surface design radius factor	x_ob	extensivity of over-break
elos	equivalent linear over-break sloughage	x_ub	extensivity of under-break
ello	equivalent linear lost ore	h_ob	hemi-sphericity of over-break
depth_ob	Maximum depth of over-break	h_ub	hemi-sphericity of under-break

F.1 KANOWNA BELLE GEOMETRIC BACK ANALYSIS DATA

stope_name	surface	des_span_crit	des_area	des_perimeter	des_dip	des_dip_dirn	des_hr
AB01-1	FW	71	2133.177	204.334	67	189	10.44
AB01-1	HW	71	2171.717	208.276	66	193	10.427
AP02	EW	33	4130.543	366.542	88	92	11.269
AP02	FW	20	3070.626	350.518	58	187	8.76
AP02	HW	20	2568.724	309.888	77	179	8.289
AP02	WW	41	4618.81	361.293	90	90	12.784
AP07	B	20.738	479.179	93.706	53	12	5.114
AP07	EW	29.19	1569.44	196.978	90	270	7.968
AP07	FW	20	1468.743	188.694	58	181	7.784
AP07	HW	20	1730.909	223.125	70	185	7.758
AP07	WW	29.19	1674.781	201.158	90	90	8.326
AP12	B	24.358	1740.757	211.562	22	163	8.228
AP12	EW	30.8	5074.068	380.401	90	270	13.339
AP12	FW	22	3814.717	381.22	57	163	10.007
AP12	HW	23.8	2549.782	292.674	74	176	8.712
AP12	WW	25	4069.378	381.055	90	90	10.679
AP18	B	35.719	918.609	128.622	34	90	7.142
AP18	EW	14.712	876.111	139.645	90	270	6.274
AP18	FW	29.441	2161.074	219.981	62	196	9.824
AP18	HW	29	1925.023	206.888	74	179	9.305
AP18	WW	23.444	2037.393	208.919	90	90	9.752
AP86	EW	13	2465.983	327.145	90	270	7.538
AP86	FW	26	4100.085	355.3	62	195	11.54
AP86	HW	28.37	4680.304	362.76	65	212	12.902
AP92	EW	36.12	2889.851	258.958	90	270	11.16
AP92	FW	19.8	2151.747	279.632	83	211	7.695
AP92	HW	19.8	2231.21	265.4	84	189	8.407
AP92	WW	38.5	3007.414	255.756	90	90	11.759
AP97	EW	38.57	3874.872	341.698	90	270	11.34
AP97	FW	19.5	2952.518	334.072	61	186	8.838
AP97	HW	19.5	2736.252	336.668	74	170	8.127
AP97	WW	43.47	4829.607	354.253	90	90	13.633
AS92	EW	23.416	2624.88	297.834	90	270	8.813
AS92	FW	20.7	2161.163	259.22	68	195	8.337
AS92	WW	27.54	2767.676	284.773	85	267	9.719
AT04	FW	30	4880.806	382.395	58	182	12.764
AT04	HW	30.337	4444.099	377.688	69	157	11.767
AT09	FW	26.989	2534.759	250.183	55	170	10.132
AT09	HW	27.188	2233.905	280.764	64	220	7.957
AT15	FW	30.901	3677.651	394.392	57	175	9.325
AT15	HW	30.901	3689.694	409.659	51	180	9.007
AT99	FW	29.782	4428.833	362.067	60	184	12.232
AT99	HW	29.767	4004.915	332.651	78	192	12.039
C0080	B	15	163.087	51.765	2	184	3.151
C0080	FW	15	1328.924	207.156	71	183	6.415
C0080	HW	15	1288.459	221.151	71	183	5.826
C0080	WW	27.46	752.873	117.11	90	270	6.429
C0574	B	13.05	261	66.1	0	0	3.949
C0574	FW	19.89	1329.394	174.708	67	166	7.609
C0574	HW	20	1424.72	182.472	56	180	7.808
C0580	EW	12.451	787	215.89	89	93	3.645
C0580	FW	20.136	1824.085	235.95	64	190	7.731
C0580	HW	20.46	1760.438	235.891	61	182	7.463
C0774	B	17.48	312.831	73.519	2	58	4.255
C0774	EW	24.08	2178.887	240.26	90	270	9.069
C0774	FW	17.48	1771.45	238.911	66	173	7.415
C0774	HW	17.546	1568.094	212.604	63	185	7.376
C0971	B	22.61	574.082	95.571	0	49	6.007

stope_name	surface	des_span_crit	des_area	des_perimeter	des_dip	des_dip_dirn	des_hr
C0971	FW	27.938	1025.893	133.598	59	202	7.679
C0971	HW	27.134	905.022	121.062	65	176	7.476
C0974	B	10.333	210.112	60.605	1	353	3.467
C0974	FW	22.074	1079.721	174.797	63	200	6.177
C0974	HW	19.943	1072.012	170.274	60	180	6.296
C0980	B	20.17	126.297	56.648	16	98	2.23
C0980	EW	20.92	933.158	152.384	90	90	6.124
C0980	FW	19.741	1007.245	156.318	69	184	6.444
C0980	HW	19.663	1131.928	168.568	56	180	6.715
C1068	B	12.89	263.945	71.49	8	168	3.692
C1068	EW	20.009	1000.316	183.364	74	255	5.455
C1068	FW	20.897	1001.716	178.179	62	197	5.622
C1068	HW	21.169	898.115	167.361	75	202	5.366
C1077	B	25.016	251.47	76.579	27	5	3.284
C1077	EW	13.773	394.364	98.791	81	262	3.992
C1077	FW	25.057	866.135	120.381	57	174	7.195
C1077	HW	25.189	836.235	119.983	59	183	6.97
C1080	B	24.111	179.896	63.978	0	181	2.812
C1080	EW	17	648.297	162.411	90	270	3.992
C1080	FW	24.105	1427.13	180.522	63	182	7.906
C1080	HW	24.111	1406.04	164.62	58	183	8.541
C1259	B	19.5	338.016	75.732	1	50	4.463
C1259	FW	19.5	1379.82	180.505	60	184	7.644
C1259	HW	20.059	1372.52	183.494	63	198	7.48
C1259	WW	21.531	1114.579	170.137	90	270	6.551
C1268	B	18.521	930.098	138.963	25	184	6.693
C1268	EW	32	1237.651	180.126	90	90	6.871
C1268	FW	18.527	1349.536	186.175	59	184	7.249
C1268	HW	18.513	780.368	121.41	90	3	6.428
C1459	B	19.682	148.278	57.511	9	12	2.578
C1459	EW	19.421	975.342	166.775	90	90	5.848
C1459	FW	19.635	1380.104	182.169	55	178	7.576
C1459	HW	19.693	1326.601	185.673	54	184	7.145
C1468	B	24.3	1166.66	148.808	27	194	7.84
C1468	EW	33.3	1112.115	173.048	90	90	6.427
C1468	FW	27.165	1811.44	203.375	58	188	8.907
C1468	HW	25	991.856	132	90	180	7.514
C8962	FW	20.1	1567.78	198.799	58	189	7.886
C8962	HW	20.726	1587.92	206.04	56	205	7.707
C8962	WW	30	1531.118	196.783	90	270	7.781
C9162	B	21.867	578.147	101.831	2	307	5.678
C9162	FW	22.079	1658.273	198.111	56	180	8.37
C9162	HW	23.581	1579.229	188.49	62	172	8.378
C9168	B		329.774	76.026	0	224	4.338
C9168	FW	21.379	1423.927	198.657	57	190	7.168
C9168	HW	20.034	1500.659	199.901	52	191	7.507
C9168	WW	19.626	1186.527	199.21	90	90	5.956
C9374	B	21.9	548.984	120.082	4	12	4.572
C9374	FW	21.9	1114.182	174.367	64	171	6.39
C9374	HW	14.5	847.127	158.377	84	182	5.349
C9374	WW	32.967	1529.69	174.55	90	270	8.764
C9568	FW	21	752.998	116.9	54	177	6.442
C9568	HW	20.09	731.072	116.794	57	190	6.259
C9571	FW	20.174	664.479	109.396	60	178	6.074
C9571	HW	20.93	731.975	113.433	53	189	6.453
C9674	B	21.83	547.978	104.475	1	264	5.245
C9674	EW	29.601	1619.569	214.442	86	104	7.552
C9674	FW	24.005	1847.858	193.627	59	178	9.543
C9674	HW	27.806	1468.772	185.412	62	191	7.922
C9674	WW	20.1	1148.635	173.512	90	270	6.62
C9874	B	18.027	596.335	102.775	1	246	5.802

stope_name	surface	des_span_crit	des_area	des_perimeter	des_dip	des_dip_dirn	des_hr
C9874	FW	17.961	1314.919	183.984	55	180	7.147
C9874	HW	17.988	965.772	164.228	65	181	5.881
C9883	B	16.31	311.297	69.769	0	37	4.462
C9883	FW	20.884	1093.825	147.488	68	187	7.416
C9883	HW	20.651	987.175	147.214	61	181	6.706
CD0062	B	9.9	150.35	50.92	14	2	2.953
CD0062	EW	19	1003.453	171.306	90	270	5.858
CD0062	HW	16.049	1169.428	183.976	63	177	6.356
CD0062	WW	21.085	1043.576	167.869	90	270	6.217
CD0262	B	19.161	196.9	74.452	0	0	2.645
CD0262	FW	19.246	708.963	108.11	78	183	6.558
CD0262	HW	26.893	710.787	107.31	77	180	6.624
CP0062	EW	33.216	2152.206	216.573	90	270	9.938
CP0062	FW	14.99	1294.053	203.334	53	175	6.364
CP0062	HW	15	1218.724	189.055	62	194	6.446
CP0062	WW	29.89	1716.8	213.407	90	90	8.045
CP0062_68	B	15	359.087	77.708	55	355	4.621
CP0062_68	EW	29.543	3660.993	355.915	90	270	10.286
CP0062_68	FW	14.98	2168.34	323.095	58	176	6.711
CP0062_68	HW	15.3	2476.805	360.527	60	188	6.87
CP0062_68	WW	30.568	3024.402	351.969	90	90	8.593
CP0074	B	15.018	464.492	97.247	2	50	4.776
CP0074	EW	33.943	1751.202	189.96	90	270	9.219
CP0074	FW	15.102	1004.175	179.398	60	188	5.597
CP0074	HW	15.015	957.759	158.89	64	178	6.028
CP0074	WW	32.517	1828.291	199.021	90	270	9.186
CP0362	EW	27.869	2282.247	227.943	90	90	10.012
CP0362	FW	15	1147.441	181.322	61	200	6.328
CP0362	HW	15	1519.601	230.981	56	193	6.579
CP0362	WW	30.107	2343.197	228.988	90	90	10.233
CP0362_68	B	14.96	325.882	72.752	58	22	4.479
CP0362_68	EW	27.869	3785.232	361.744	90	90	10.464
CP0362_68	FW	15	2135.836	319.273	62	200	6.69
CP0362_68	HW	14.99	2561.74	367.794	58	199	6.965
CP0362_68	WW	30.107	3678.221	364.171	90	90	10.1
CP0374	B	15.553	276.96	66.84	56	19	4.144
CP0374	EW	20.111	1119.013	179.531	90	90	6.233
CP0374	FW	15.74	1053.566	173.641	64	204	6.067
CP0374	HW	15.112	1209.502	189.278	60	192	6.39
CP0374	WW	20.983	1383.856	184.723	90	270	7.492
CP0380	B		38.503	34.822	89	358	1.106
CP0380	EW	12.482	1024.019	199.913	90	270	5.122
CP0380	FW		1365.801	214.118	69	183	6.379
CP0380	HW		1237.37	196.476	63	182	6.298
CP0380	WW	13.721	988.308	195.304	90	270	5.06
CP0762	B	14.67	292.131	71.858	2	38	4.065
CP0762	EW	12.38	754.866	193.488	86	273	3.901
CP0762	FW	22.484	1450.971	205.469	59	220	7.062
CP0762	HW	17.538	1127.118	195.837	54	185	5.755
CP0762	WW	21.08	1395.79	196.339	90	90	7.109
CP0768	B	14.98	575.978	128.54	24	188	4.481
CP0768	EW	25	1122.513	183.371	90	93	6.122
CP0768	FW	18.055	1272.091	183.495	59	215	6.933
CP0768	HW	15.067	1073.217	174.227	57	181	6.16
CP0768	WW	24.97	1783.162	199.79	90	270	8.925
CP9362	EW	17.649	1248.871	191.575	90	90	6.519
CP9362	FW	14.99	1213.028	193.584	61	164	6.266
CP9362	HW	14.98	1193.456	189.75	59	177	6.29
CP9362	WW	13.01	986.457	194.093	90	90	5.082
CP9362_68	B	15.864	205.963	58.705	1	99	3.508
CP9362_68	EW	27.355	2226.918	333.65	90	90	6.674

stope_name	surface	des_span_crit	des_area	des_perimeter	des_dip	des_dip_dirn	des_hr
CP9362_68	FW	15	2228.6	334.771	59	177	6.657
CP9362_68	HW	15	2254.258	332.211	58	180	6.786
CP9362_68	WW	30.107	2054.347	332.51	90	90	6.178
CP9662	B	14.998	288.864	68.454	2	53	4.22
CP9662	EW	22.511	1621.048	197.017	90	270	8.228
CP9662	FW	16.725	1134.964	187.113	65	180	6.066
CP9662	HW	14.992	1122.083	197.783	66	197	5.975
CP9662	WW	24.74	1464.011	184.091	90	270	7.953
CP9668	B	14.984	333.525	76.221	1	95	4.376
CP9668	EW	20.635	1127.186	187.362	90	90	6.016
CP9668	FW	15.001	1090.303	177.118	55	173	6.156
CP9668	HW	15.657	1058.495	172.099	57	183	6.151
CP9668	WW	16.812	1005.937	182.79	90	270	5.503
CT0262	B	7.59	560.946	98.196	1	58	5.713
CT0262	FW	23.1	1394.026	192.138	59	177	7.255
CT0262	HW	23.817	1411.107	187.166	59	185	7.539
CT0268	B	18.5	285.397	73.363	15	359	3.89
CT0268	FW	19.165	642.63	104.826	68	194	6.13
CT0268	HW	19.134	843.712	129.306	53	184	6.525
CT0271	FW	23.031	641.968	107.97	54	186	5.946
CT0271	HW	18.001	663.117	111.113	58	188	5.968
CT0280	B	7.03	133.922	55.622	1	341	2.408
CT0280	FW	20.089	1728.374	220.767	74	175	7.829
CT0280	HW	20	1869.471	228.215	63	184	8.192
CT0562	B	24.475	473.605	90.697	47	20	5.222
CT0562	FW	24.748	1894.806	210.949	60	212	8.982
CT0562	HW	23.664	2132.324	239.352	55	196	8.909
CT0568	B	20.078	532.454	90.962	0	8	5.854
CT0568	FW	20.41	1382.796	179.239	57	176	7.715
CT0568	HW	20.279	941.076	138.032	62	184	6.818
CT9562	B	9.96	340.77	76.406	54	10	4.46
CT9562	FW	21.409	1461.018	185.022	68	187	7.896
CT9562	HW	21.86	1813.416	218.18	63	181	8.312
CT9862	B	18.239	389.525	84.687	1	257	4.6
CT9862	FW	19.106	1424.447	199.387	53	178	7.144
CT9862	HW	22.795	1344.258	186.988	59	190	7.189
CT9868	B	19.071	353.969	85.962	0	0	4.115
CT9868	FW	22.946	1304.748	178.311	61	177	7.317
CT9868	HW	21.091	1211.847	176.848	60	178	6.852
D0235A	B	14.668	215.716	59.03	0	265	3.654
D0235A	EW	28	780.514	113.189	90	280	6.896
D0235A	FW	14.971	503.299	97.164	90	10	5.18
D0235A	HW	14.998	522.16	190.773	72	187	4.757
D0235A	WW	29	781.088	113.109	90	280	6.906
D0238	B	7.322	109.099	49.509	21	185	2.204
D0238	FW	12.028	273.203	77.088	79	10	3.544
D0238	HW	11.36	259.164	78.612	58	193	3.297
D0238	WW	27.282	501.553	100.924	90	100	4.97
D0738	B	14.981	513.405	99.52	55	188	5.159
D0738	EW	30	948.048	129.888	90	100	7.299
D0738	FW	14.918	792.328	138.508	82	9	5.72
D0738	HW	14.987	448.992	89.956	55	10	4.991
DA0135	B	18.061	340.759	74.59	0	297	4.568
DA0135	FW	9.3	288.842	82.541	86	186	3.499
DA0135	HW	18.135	626.691	108.587	67	181	5.771
DA0135	WW	18.981	645.827	115.84	90	280	5.757
DA0138	B	9.403	158.966	52.933	35	11	3.003
DA0138	FW	16.098	433.773	85.814	67	194	5.055
DA0138	HW	18.73	658.477	117.025	60	178	5.627
DA0138	WW	19.593	451.55	99.285	90	280	4.548
DA0244	B	13.8	227.081	63.972	0	0	3.55

stope_name	surface	des_span_crit	des_area	des_perimeter	des_dip	des_dip_dirn	des_hr
DA0244	EW	37.178	820.089	147.8	82	290	5.549
DA0244	FW	13.9	468.81	95.48	78	194	4.91
DA0244	HW	13.8	453.964	98.096	56	219	4.628
DA0244	WW	31.79	811.918	140.908	90	100	5.762
DA0647	B	15.107	231.444	62.055	24	16	3.73
DA0647	FW	15.107	323.232	73.358	86	18	4.406
DA0647	HW	15.025	429.382	89.892	72	186	4.777
DA0647	WW	25.248	587.756	98.058	90	100	5.994
DA0650	B	27.875	147.081	64.969	11	20	2.264
DA0650	EW	15.046	333.436	95.699	80	298	3.484
DA0650	FW	28.164	793.335	117.721	63	199	6.739
DA0650	HW	26.149	824.201	118.687	52	199	6.944
DA0650	WW	20.126	343.474	92.555	90	100	3.711
DA0741	B	14.459	259.897	71.734	1	151	3.623
DA0741	EW	24.573	708.482	117.469	90	280	6.031
DA0741	FW	14.459	443.67	90.288	72	10	4.941
DA0741	WW	26	690.277	116.72	88	272	5.914
DA0744	B	15.574	334.373	76.248	2	172	4.385
DA0744	EW	22.649	758.327	122.534	90	99	6.189
DA0744	FW	15.4	465.414	91.026	72	177	5.113
DA0744	HW	15.9	520.474	97.671	66	183	5.329
DA0747	B	14.634	282.296	70.907	14	25	3.981
DA0747	EW	13.6	431.752	96.665	90	100	4.466
DA0747	FW	20.764	494.444	90.224	69	193	5.48
DA0747	HW	20.78	784.629	130.454	63	191	6.015
DA0747	WW	15.2	576.156	123.785	90	100	4.671
DA0835	B	19.824	386.942	77.924	0	0	4.966
DA0835	EW	29.506	682.186	99.208	90	100	6.876
DA0835	FW	19.954	617.511	104.814	75	189	5.891
DA0835	HW	19.956	596.782	113.44	88	12	5.261
DA0838	B	13.711	287.588	74.019	1	199	3.885
DA0838	EW	22.26	749.741	127.8	90	280	5.866
DA0838	FW	19.506	541.788	105.952	68	190	5.114
DA0838	HW	20.822	653	107.786	58	192	6.058
DA0841	B	11.748	212.771	61.973	13	13	3.433
DA0841	EW	23.852	511.911	102.895	90	280	4.975
DA0841	FW	19.141	455	89.685	80	190	5.073
DA0841	HW	18.972	682.298	109.577	61	188	6.227
DA0844	B	18.351	275.025	71.43	3	334	3.85
DA0844	EW	21.944	556.746	110.183	90	100	5.053
DA0844	FW	18.351	572.302	102.584	74	195	5.579
DA0844	HW	18.24	531.457	95.859	63	188	5.544
DA0859	B	14.562	234.615	62.2	2	284	3.773
DA0859	EW	15.16	225.009	67.1	90	90	3.353
DA0859	FW	14.67	344.364	79.806	63	191	4.315
DA0859	HW	14.562	300.505	71.315	82	180	4.214
DA0859	WW	17.3	276.844	70.94	90	270	3.903
DA1035	B	20.1	360.849	77.143	0	223	4.678
DA1035	EW	23	544.321	99.225	90	100	5.486
DA1035	FW	21.2	621.094	106.572	77	206	5.828
DA1035	HW	20.105	602.5	107.523	86	192	5.603
DA1038	B	6.273	122.33	52.37	49	10	2.336
DA1038	EW	17	570.204	104.102	90	280	5.477
DA1038	FW	20.013	650.456	107.511	80	190	6.05
DA1038	HW	19.996	840.3	131.436	57	182	6.393
DA1235	B		136.8	56.944	14	348	2.402
DA1235	EW	24.1	557.298	103.773	90	280	5.37
DA1235	FW	20.96	653.898	108.561	78	187	6.023
DA1235	HW	21.086	767.9	119.76	60	191	6.412
DB0135	B	11.86	178.875	55.917	0	0	3.199
DB0135	FW	18.533	974.689	166.41	90	20	5.857

stope_name	surface	des_span_crit	des_area	des_perimeter	des_dip	des_dip_dirn	des_hr
DB0135	HW	20.815	1425.055	181.076	90	29	7.87
DB0135	WW	29	1135.82	154.799	89	294	7.337
DB0235	B	14.984	449.431	91.318	2	35	4.922
DB0235	EW	30	770.807	115.605	88	278	6.67
DB0235	FW	12.411	393.658	99.179	72	191	3.969
DB0235	WW	30.039	820.551	115.1	90	100	7.133
DB0238	B	11.894	170.363	86.22	40	160	1.976
DB0238	EW	24.9	580	97	88	118	5.97
DB0238	FW	14	729.246	154.8	90	5	4.711
DB0238	WW	24	1161.897	167.7	90	281	6.928
DB0738	B	15.5	421.527	85.38	0	101	4.937
DB0738	EW	26.813	579.513	103.428	90	100	5.603
DB0738	FW	15.5	559.475	108.736	58	191	5.145
DB0838	B	17.567	193.67	58.09	14	14	3.334
DB0838	EW	25.1	1229.045	166.741	90	100	7.371
DB0838	FW	17.645	1031.318	170.461	87	188	6.05
DB1038	B	20.51	207.622	77.299	16	16	2.686
DB1038	EW	24	1253.858	170.673	90	280	7.347
DB1038	FW	20.521	1351.587	177.481	85	197	7.615
DC0238	B	12.53	191.378	63.79	20	12	3
DC0238	EW	14.4	423.952	92.583	89	277	4.579
DC0238	FW	12.594	813.827	173.6	85	213	4.688
DC0238	WW	21.9	1088.598	164.5	90	100	6.618
DC0741	B	15.29	398.72	82.5	0	204	4.832
DC0741	EW	26	521.55	96.2	90	100	5.42
DC0741	FW	15.01	492.4	96.3	66	198	5.11
DP0635	EW	35	2277.32	199.751	90	280	11.4
DP0635	FW	14.96	1115.8	187.273	58	177	5.958
DP0635	HW	15	1021.232	181.433	73	201	5.629
DP0635	WW	34.1	2273.125	200.302	90	100	11.348
DP0641	B	15.487	147.7	48.96	0	208	3.017
DP0641	EW	21	814.271	127.969	90	100	6.363
DP0641	FW	15.487	860.7	152.8	85	188	5.63
DP0641	HW	15.752	862.4	149.74	89	181	5.76
DP0641	WW	21.6	861.7	145.8	84	98	5.908
DP1159	B	15	126.4	47.57	14	359	2.657
DP1159	EW	16.5	1009.6	168.9	90	91	5.977
DP1159	FW	15	1055.377	170.7	60	183	6.18
DT0735	B	15.04	451.676	90.178	50	10	5
DT0735	EW	28.3	983.428	132.78	90	280	7.406
DT0735	FW	15.04	559.5	104.45	53	196	5.357
DT0735	HW	15.05	776.07	150.16	77	173	5.168
DT0735	WW	28	1062.495	135.17	90	280	7.861

stope_name	surface	des_hr_c	des_rf	elos	ello	depth_ob	depth_ub	depth_ave_ob	depth_ave_ub
AB01-1	FW	10.44	10.638	0.179	0.362	2.7	2.9	0.522	0.723
AB01-1	HW	10.427	10.638	0.402	0.303	2.4	1.6	0.769	0.811
AP02	EW	11.269	13.889	0.548	0.108	3.5	1.75	0.827	0.463
AP02	FW	8.76	7.576	0.733	0.027	1.9	1.5	1.306	1.093
AP02	HW	8.289	7.576	0.689	0.031	3.8	2.5	1.068	0.745
AP02	WW	12.784	14.706	0.22	0.283	4	2.6	0.502	0.698
AP07	B	5.114	5.952	0.287	0.018	3.25	4.75	0.797	0.137
AP07	EW	7.968	9.091	0.414	0.13	2.4	2.3	0.585	0.532
AP07	FW	7.784	7.143	0.299	0.248	2.7	2.5	0.885	0.588
AP07	HW	7.758	7.463	0.197	0.265	1.7	2.7	0.626	0.701
AP07	WW	8.326	9.259	0.449	0.281	3	2.9	1.007	0.646
AP12	B	8.228	8.197	1.392	0.031	6	2.8	2.243	0.467
AP12	EW	13.339	14.706	0.197	0.499	3.3	3.9	0.563	0.966
AP12	FW	10.007	8.929	0.186	0.838	3.6	8.1	0.801	1.64

stope_name	surface	des_hr_c	des_rf	elos	ello	depth_ob	depth_ub	depth_ave_ob	depth_ave_ub
AP12	HW	8.712	8.333	0.925	0.431	6.2	6.8	1.478	2.084
AP12	WW	10.679	12.5	0.326	0.124	2.9	2.5	0.514	0.527
AP18	B	7.142	8.065	0.575	0.544	3.5	3	1.168	1.468
AP18	EW	6.274	6.329	0.843	0.814	2.3	3.3	1.472	1.588
AP18	FW	9.824	10.204	0.832	0.601	6.3	9.5	1.64	2.159
AP18	HW	9.305	9.804	0.138	0.838	2.2	7.1	0.476	1.432
AP18	WW	9.752	9.804	0.553	0.429	3.6	3	0.978	1.191
AP86	EW	7.538	8.621	0.374	0.636	4.7	4	0.701	1.692
AP86	FW	11.54	11.628	0.843	0.642	3.6	3.2	1.694	1.843
AP86	HW	12.902	13.158	0.841	0.712	6.5	4.1	1.732	3.004
AP92	EW	11.16	11.628	0.231	0.31	1.2	2.5	0.459	0.637
AP92	FW	7.695	7.692	0.679	0.186	2	3.7	0.985	0.873
AP92	HW	8.407	7.937	0.264	0.514	4.1	3.6	0.397	2.505
AP92	WW	11.759	12.5	0.491	0.198	2.3	2.9	0.704	0.604
AP97	EW	11.34	12.821	0.894	0.068	3.6	1.5	1.066	0.385
AP97	FW	8.838	7.576	0.801	0.111	3.3	3	1.23	0.642
AP97	HW	8.127	7.813	0.397	0.397	3.7	4.5	0.775	1.06
AP97	WW	13.633	14.706	0.347	0.279	1.3	2.3	0.66	0.615
AS92	EW	8.813	10	0.223	0.984	2.7	4.5	0.706	1.417
AS92	FW	8.337	8.197	0.09	1.605	3.2	6.6	0.654	2.414
AS92	WW	9.719	12.5	0.531	1.024	4.3	5	1.285	1.87
AT04	FW	12.764	11.628	0.258	0.797	3.7	5	0.92	1.549
AT04	HW	11.767	11.628	0.565	0.337	7.4	4.2	1.552	0.724
AT09	FW	10.132	9.804	0.044	1.002	2.4	4.6	0.417	1.421
AT09	HW	7.957	10.417	1.035	0.637	7	5	1.803	2.153
AT15	FW	9.325	10.87	0.538	0.731	4.1	3.3	1.277	1.731
AT15	HW	9.007	10.67	5.614	0.52	17.5	2.9	8.246	3.609
AT99	FW	12.232	10.638	0.35	1.371	4.4	5.2	1.277	2.707
AT99	HW	12.039	11.111	0.109	1.147	2.2	3	0.484	1.757
C0080	B	3.151	3.497	0.061	0.08	0.5	2.1	0.543	0.628
C0080	FW	6.415	5.747	0.445	0.144	3.6	1.2	0.943	0.55
C0080	HW	5.826	5.682	0.418	0.317	4.4	3	1.164	0.859
C0080	WW	6.429	7.353	0.001	1.308	0.3	5	0.047	2.197
C0574	B	3.949	4.274	0.636	0.207	4.1	3.5	0.966	0.906
C0574	FW	7.609	7.692	0.135	1.515	2.8	9	0.613	1.977
C0574	HW	7.808	7.042	0.593	1.039	5	3.9	1.68	1.906
C0580	EW	3.645	3.906	0.578	0.029	4.4	0.9	0.938	0.2
C0580	FW	7.731	7.353	0.132	0.519	1	2.4	0.449	1.182
C0580	HW	7.463	7.246	0.249	0.248	3.3	1.2	0.954	0.549
C0774	B	4.255	4.854	0.489	0.077	3.5	0.5	1.584	1.194
C0774	EW	9.069	9.259	1.946	0.217	6.4	1.9	2.821	1.009
C0774	FW	7.415	6.757	0.052	1.442	1.8	2.9	0.68	2.068
C0774	HW	7.376	6.757	0.069	1.212	1.6	5	0.57	1.878
C0971	B	6.007	6.494	0.585	0.714	1.9	5.1	1.133	2.263
C0971	FW	7.679	8.772	0.086	2.583	2.2	10.1	0.739	3.942
C0971	HW	7.476	8.065	0.131	0.727	1.4	3.7	0.55	1.041
C0974	B	3.467	3.472	1.042	0.904	8.7	5.3	1.653	2.375
C0974	FW	6.177	6.494	0.018	2.528	1.4	9.7	0.432	2.911
C0974	HW	6.296	6.098	0.187	0.98	1.4	4.5	0.456	1.601
C0980	B	2.23	2.37	0	1.196	0	6	0	1.914
C0980	EW	6.124	6.41	0.619	0.383	4.2	2	1.093	1.292
C0980	FW	6.444	6.849	0.021	2.339	1.9	5	0.502	2.666
C0980	HW	6.715	6.944	0.415	0.593	2.9	2.9	1.326	1.294
C1068	B	3.692	4.386	1.103	0	4.7	0	1.553	0
C1068	EW	5.455	6.849	0.269	0.296	1.6	3.7	0.703	0.856
C1068	FW	5.622	6.494	0.346	0.224	4.4	2.1	1.007	0.603
C1068	HW	5.366	6.329	0.397	0.526	6.2	2.5	0.942	1.361
C1077	B	3.284	3.846	0.66	0	4	0	1.189	0
C1077	EW	3.992	4.348	0.299	0.036	1.5	1.6	0.549	0.398
C1077	FW	7.195	8.065	0.147	0.231	1.1	2.2	0.444	0.604
C1077	HW	6.97	7.937	0.033	0.433	0.9	4	0.233	0.704

stope_name	surface	des_hr_c	des_rf	elos	ello	depth_ob	depth_ub	depth_ave_ob	depth_ave_ub
C1080	B	2.812	2.778	0.206	0.044	0.7	1.5	0.491	0.216
C1080	EW	3.992	4.808	0.602	0.13	1.8	1	0.869	0.784
C1080	FW	7.906	8.475	0.323	0.29	2.2	0.9	0.947	0.754
C1080	HW	8.541	8.475	0.31	0.734	2.4	3.3	1.188	1.47
C1259	B	4.463	5.051	0	1.124	0.3	3.5	0.023	2.537
C1259	FW	7.644	7.143	0.16	0.595	1.9	3	0.526	1.446
C1259	HW	7.48	7.576	0.096	0.629	1.6	2.8	2.619	1.093
C1259	WW	6.551	6.757	0.112	1.014	1.6	4	0.728	1.424
C1268	B	6.693	6.579	0.881	0.233	5.5	2.9	1.917	0.822
C1268	EW	6.871	8.475	0.924	0.199	4.8	2.4	1.486	0.966
C1268	FW	7.249	6.757	0.562	0.051	2	1.5	0.92	0.458
C1268	HW	6.428	6.494	0	1.589	0	3.3	0	1.906
C1459	B	2.578	2.907	0.094	0	3.4	0	0.524	0
C1459	EW	5.848	6.25	0.158	0.412	1.6	1.6	0.455	0.97
C1459	FW	7.576	7.143	0.011	0.844	0.7	6.2	0.261	1.23
C1459	HW	7.145	7.246	0.383	0.342	1.8	3.4	1.202	0.883
C1468	B	7.84	8.333	0.099	0.232	1.2	0.9	0.371	0.781
C1468	EW	6.427	7.937	0.768	0.028	3.1	0.5	1.115	0.167
C1468	FW	8.907	9.091	0.258	0.178	1.3	0.6	0.561	1.037
C1468	HW	7.514	8.475	0.046	0.551	1.1	1.5	0.359	0.812
C8962	FW	7.886	7.576	0.713	0.091	3.3	0.7	1.217	0.796
C8962	HW	7.707	7.937	0.887	0.521	3.6	1.5	1.674	3.409
C8962	WW	7.781	8.33	0.103	0.308	2.3	1.2	0.356	0.595
C9162	B	5.678	6.41	1.299	0.825	4.2	5.5	2.281	2.64
C9162	FW	8.37	7.692	0.03	2.076	2	6.3	0.579	2.469
C9162	HW	8.378	7.937	0.513	0.491	4.5	7.7	1.021	1.052
C9168	B	4.338	4.902	0	0.018	0.4	1.1	0.029	0.417
C9168	FW	7.168	7.463	0.037	1.83	1.8	4.4	0.696	2.781
C9168	HW	7.507	7.576	1.189	0.389	9.6	4.8	2.784	1.832
C9168	WW	5.956	6.494	0.001	2.047	0.4	5	0.108	2.453
C9374	B	4.572	5.556	0.454	0.39	3	3.3	1.404	1.726
C9374	FW	6.39	7.246	0.208	0.801	2.2	3	1.105	1.389
C9374	HW	5.349	5.376	0.445	0.696	4.1	4.3	1.074	1.492
C9374	WW	8.764	10	3.31	0.059	9.7	0.2	4.079	0.869
C9568	FW	6.442	7.143	0.048	1.722	2	4	0.427	3.066
C9568	HW	6.259	6.849	0.053	0.553	1.2	3.2	0.496	1.139
C9571	FW	6.074	6.757	0.522	0.184	4.4	3	1.515	0.793
C9571	HW	6.453	6.944	0.068	0.616	1.6	3.4	0.566	1.546
C9674	B	5.245	6.329	1.133	0.723	5.1	6	1.896	3.123
C9674	EW	7.552	9.091	1.145	1.561	7.2	7.6	2.295	3.218
C9674	FW	9.543	9.091	0.05	2.815	2.4	9.2	0.398	3.971
C9674	HW	7.922	7.576	3.199	1.58	14.1	8.6	5.297	5.398
C9674	WW	6.62	6.757	1.45	1.814	9.3	5.4	2.996	3.374
C9874	B	5.8002	5.814	1.308	0.79	5.1	4.9	1.743	2.298
C9874	FW	7.147	6.494	0.196	1.412	2.2	5.7	0.747	2.467
C9874	HW	5.881	5.952	1.204	0.978	6	5.3	2.25	2.045
C9883	B	4.462	4.717	2.271	0.235	4.6	4.3	2.687	0.731
C9883	FW	7.416	7.246	0.156	1.557	4.7	6.2	0.842	1.966
C9883	HW	6.706	7.042	0.02	1.269	0.6	5	0.192	1.454
CD0062	B	2.953	3.427	0.001	0.306	0.4	3.8	0.012	1.84
CD0062	EW	5.858	6.41	0.595	0.663	2.5	1.8	1.22	1.871
CD0062	HW	6.356	5.952	0.29	0.329	1.5	3.4	0.623	1.081
CD0062	WW	6.217	6.757	0.146	0.599	0.9	4.2	0.374	1.528
CD0262	B	2.645	2.5	0	1.991	0	2.5	0	1.991
CD0262	FW	6.558	7.143	0.199	1.064	1.8	4.6	0.615	1.443
CD0262	HW	6.624	7.143	0.089	0.447	1.07	2.8	0.269	0.666
CP0062	EW	9.938	9.804	0.472	0.799	4.6	7.6	1.427	1.209
CP0062	FW	6.364	5.682	0.183	0.665	8.8	11.1	0.711	1.4
CP0062	HW	6.446	5.814	0.597	0.669	5.5	10.4	1.425	1.581
CP0062	WW	8.045	8.475	0.542	0.292	7.1	4.2	0.754	1.008
CP0062_68	B	4.621	4.95	0.031	2.785	2.5	18.2	0.553	6.849

stope_name	surface	des_hr_c	des_rf	elos	ello	depth_ob	depth_ub	depth_ave_ob	depth_ave_ub
CP0062_68	EW	10.286	10.204	0.373	0.854	4.7	5.8	1.114	1.248
CP0062_68	FW	6.711	5.882	0.237	0.722	2.1	14.7	0.628	1.479
CP0062_68	HW	6.87	5.952	0.796	0.969	6.3	4.1	1.864	4.156
CP0062_68	WW	8.593	9.434	1.099	0.229	10.7	4.2	1.31	0.931
CP0074	B	4.776	5.051	5.408	0.026	12.2	2.9	5.725	0.674
CP0074	EW	9.219	10	3.073	0.475	11.3	4.8	4.347	1.797
CP0074	FW	5.597	5.495	0.407	0.785	4.6	5	1.298	0.981
CP0074	HW	6.028	5.376	1.916	0.105	6.5	2.6	2.747	0.65
CP0074	WW	9.186	9.804	3.33	0.293	10.7	4.2	3.983	1.955
CP0362	EW	10.012	9.804	1.729	0.296	7.9	5	2.334	1.406
CP0362	FW	6.328	5.882	0.161	0.294	3	4.3	0.628	0.671
CP0362	HW	6.579	6.098	0.225	0.686	4	9.7	0.756	1.51
CP0362	WW	10.233	10.417	0.065	0.469	0.9	5	0.271	0.666
CP0362_68	B	4.479	4.762	0.003	2.225	0.6	12.9	0.123	5.423
CP0362_68	EW	10.464	9.615	1.518	0.418	9.1	5	1.9	1.612
CP0362_68	FW	6.69	5.747	0.557	0.274	7.6	10.9	1.188	0.823
CP0362_68	HW	6.965	5.882	0.329	0.939	6.1	13.3	1.211	1.224
CP0362_68	WW	10.1	10.204	0.088	0.62	5	5	0.374	0.82
CP0374	B	4.144	4.545	0.025	0.191	1.2	3.7	0.123	0.831
CP0374	EW	6.233	5.882	0.188	0.338	3.3	5.7	0.537	0.584
CP0374	FW	6.067	6.173	0.664	0.147	3.2	4.2	1.299	0.57
CP0374	HW	6.39	5.747	0.849	0.107	3	4.7	1.26	0.836
CP0374	WW	7.492	7.246	1.12	0.087	5.4	4.3	1.334	0.758
CP0380	B	1.106	1.131	0.003	0	0.3	0	0.011	0
CP0380	EW	5.122	5.376	0.777	0.187	3.8	3	1.593	0.703
CP0380	FW	6.379	5.682	0.391	0.17	3.7	3	1.011	0.587
CP0380	HW	6.298	5.435	1.236	0.015	4.6	1.3	1.891	0.2
CP0380	WW	5.06	5.556	0.551	0.079	3.1	1.3	0.823	0.683
CP0762	B	4.065	4.464	0.893	0.021	4.9	3.8	1.277	0.156
CP0762	EW	3.901	4.31	0.139	1.122	1.4	5	0.446	1.382
CP0762	FW	7.062	7.813	0.397	0.47	3.8	8.5	1.564	1.182
CP0762	HW	5.755	6.41	0.286	0.498	2.2	6.5	0.689	1.312
CP0762	WW	7.109	7.042	0.316	0.337	4.2	4.6	0.642	0.789
CP0768	B	4.481	5.376	0.406	0.063	3.2	3.1	0.926	0.413
CP0768	EW	6.122	6.25	0.536	0.257	4.2	4	1.047	0.466
CP0768	FW	6.933	6.579	0.219	0.997	3.6	15	0.875	1.966
CP0768	HW	6.16	5.435	0.286	0.225	2.4	3.5	0.568	0.48
CP0768	WW	8.925	9.259	0.05	1.06	2	5	0.381	1.141
CP9362	EW	6.519	6.494	0.194	0.598	3.2	4.8	0.521	0.945
CP9362	FW	6.266	6.098	0.613	0.222	10.5	7.4	1.228	0.796
CP9362	HW	6.29	5.208	0.002	0.85	0.2	4.9	0.076	1.111
CP9362	WW	5.082	4.587	0.063	0.907	1.3	5.1	0.35	1.046
CP9362_68	B	3.508	3.846	0	0.719	0.2	6	0	1.19
CP9362_68	EW	6.674	6.41	0.142	0.561	4.7	4.9	0.384	0.742
CP9362_68	FW	6.657	6.098	0.513	0.309	2.4	11.1	0.955	0.851
CP9362_68	HW	6.786	5.618	0.076	0.728	1.5	5.6	0.459	1.058
CP9362_68	WW	6.178	5.682	0.205	0.756	2.3	5.1	0.516	0.96
CP9662	B	4.22	4.545	0	0.928	0.1	6.3	0	1.129
CP9662	EW	8.228	7.937	0.735	0.608	4.3	3.8	1.361	1.436
CP9662	FW	6.066	5.618	0.157	0.543	2.1	7.8	0.451	1.08
CP9662	HW	5.975	5.682	0.154	1.154	1.5	10.4	0.514	2.038
CP9662	WW	7.953	7.813	0.702	0.371	3	5.1	1.106	0.968
CP9668	B	4.376	4.808	0.012	1.211	0.4	5.6	0.097	1.562
CP9668	EW	6.016	5.882	0.785	0.886	4	3.9	1.466	1.859
CP9668	FW	6.156	5.435	0.278	0.538	2	5.1	0.773	1.144
CP9668	HW	6.151	5.435	0.1	0.613	1.3	5.7	0.408	0.972
CP9668	WW	5.503	5.319	0.559	0.571	3.6	5.1	1.103	1.08
CT0262	B	5.713	6.098	2.262	0.046	6.2	1.8	2.66	0.524
CT0262	FW	7.255	6.849	0.293	0.565	4.6	5	1.298	0.981
CT0262	HW	7.539	6.849	0.181	0.438	3.7	8.7	0.551	0.961
CT0268	B	3.89	4.717	0.084	0.063	1.2	1	0.388	0.197

stope_name	surface	des_hr_c	des_rf	elos	ello	depth_ob	depth_ub	depth_ave_ob	depth_ave_ub
CT0268	FW	6.13	6.67	0.23	0.19	2.6	1.3	0.618	0.586
CT0268	HW	6.525	6.67	1.309	0.776	7	3	3.552	2.622
CT0271	FW	5.946	6.329	0.201	0.307	1.7	3	0.619	0.645
CT0271	HW	5.968	6.329	0.318	0.609	3.3	4.6	0.949	1.163
CT0280	B	2.408	2.347	3.554	0.299	6.1	2.9	3.911	1.449
CT0280	FW	7.829	7.353	0.37	0.632	4.2	8	0.74	0.986
CT0280	HW	8.192	7.143	0.618	0.616	4.2	3.8	1.156	1.27
CT0562	B	5.222	5.814	0.171	0.65	4.5	3.5	1.134	1.239
CT0562	FW	8.982	8.929	0.182	1.152	2.9	15.5	0.819	2.029
CT0562	HW	8.909	8.333	0.508	1.661	3.7	12	1.141	3.963
CT0568	B	5.854	6.173	1.715	0.599	5.7	5.5	2.088	3.621
CT0568	FW	7.715	7.143	0.624	0.683	3.3	8.1	1.175	0.856
CT0568	HW	6.818	6.944	0.055	1.222	1.4	6.8	0.399	1.581
CT9562	B	4.46	4.95	0.217	0.402	2.3	5	0.782	1.153
CT9562	FW	7.896	7.463	0.201	2.269	4.2	3.7	1.38	2.766
CT9562	HW	8.312	7.692	0.058	1.738	1.4	13.7	0.404	2.073
CT9862	B	4.6	5.263	0.87	0.023	5.3	1.7	1.121	0.396
CT9862	FW	7.144	6.849	1.325	0.362	7.9	4.1	2.369	1.094
CT9862	HW	7.189	6.667	1.619	0.64	6.5	7.1	3.221	1.679
CT9868	B	4.115	4.854	1.054	0.418	5.3	5	1.416	1.717
CT9868	FW	7.317	7.143	0.018	1.695	0.9	2.7	0.249	1.979
CT9868	HW	6.852	6.849	0.73	0.635	5.9	4.7	1.842	1.345
D0235A	B	3.654	4.132	0.821	0	3.9	0.1	2.341	0.067
D0235A	EW	6.896	7.692	1.904	0.573	7	2.7	3.785	2.528
D0235A	FW	5.18	5.376	0.25	0.149	1.6	1	0.631	0.439
D0235A	HW	4.757	5.495	1.434	1.737	6.9	5	3.518	4.759
D0235A	WW	6.906	7.692	0.615	0.166	2.3	1	0.901	1.738
D0238	B	2.204	2.591	0.742	0.001	3.8	0.4	2.389	0.045
D0238	FW	3.544	3.731	0.026	0.128	1.7	0.6	0.217	0.261
D0238	HW	3.297	3.401	0.343	0.772	3.9	5	1.18	2.594
D0238	WW	4.97	6.024	0.935	0.068	3.5	1.9	1.301	0.751
D0738	B	5.159	5.435	0.103	0.635	1.4	5.9	0.629	2.625
D0738	EW	7.299	7.937	1.169	0.177	2.9	1	1.755	1.828
D0738	FW	5.72	5.618	0.001	0.55	0.4	1.2	0.196	0.773
D0738	HW	4.991	5.319	0.002	1.354	0.3	2.8	0.052	2.257
DA0135	B	4.568	5.208	0.681	0.026	2.5	1	1.512	0.34
DA0135	FW	3.499	3.333	0	2.23	0.6	4.4	0.022	3.149
DA0135	HW	5.771	6.329	0.833	2.012	5	5	2.401	4.574
DA0135	WW	5.757	6.579	0.807	0.802	3	1	1.401	3.17
DA0138	B	3.003	3.247	0.006	0.132	0.1	1.2	0.049	0.847
DA0138	FW	5.055	4.495	0	0.98	0	3.3	0	1.325
DA0138	HW	5.627	6.173	0.693	0.363	3.9	1.4	1.709	2.076
DA0138	WW	4.548	5.376	1.014	0.038	2.6	0.1	1.295	0.654
DA0244	B	3.55	3.968	0.198	0.128	1	1.3	0.565	0.736
DA0244	EW	5.549	7.576	0.267	1.408	2.5	2	1.195	2.513
DA0244	FW	4.91	5.102	0.134	0.651	1	4	0.458	1.555
DA0244	HW	4.628	5.155	0.41	0.575	2.1	3	1.12	3.729
DA0244	WW	5.762	7.813	3.598	0.036	7.1	0.5	4.689	0.621
DA0647	B	3.73	4.274	0.622	0.004	1.6	0.8	0.96	0.238
DA0647	FW	4.406	4.902	0.071	0.13	0.7	0.6	0.262	0.341
DA0647	HW	4.777	5.155	0.526	0.953	2.8	5	1.205	3.141
DA0647	WW	5.994	6.849	0.604	0.168	1.6	0.5	0.884	1.594
DA0650	B	2.264	2.203	0.279	0	3.8	0	1.188	0
DA0650	EW	3.484	3.876	1.305	0.036	5.8	0.4	2.381	0.308
DA0650	FW	6.739	7.813	0.1	0.445	2	2	0.523	0.868
DA0650	HW	6.944	7.576	2.815	0	7.1	0	4.806	0
DA0650	WW	3.711	3.937	0.175	0.282	0.6	0.8	0.355	1.283
DA0741	B	3.623	4.032	0.135	0.012	1	0.4	0.296	0.081
DA0741	EW	6.031	7.246	0.327	0.202	2	0.5	0.631	0.823
DA0741	FW	4.941	5.102	0.379	0.097	2.1	1.4	0.708	0.509
DA0741	WW	5.914	7.042	0.488	0.711	2.6	1.9	1.065	1.892

stope_name	surface	des_hr_c	des_rf	elos	ello	depth_ob	depth_ub	depth_ave_ob	depth_ave_ub
DA0744	B	4.385	4.95	0.135	0.09	0.7	2.2	0.421	0.518
DA0744	EW	6.189	7.463	0.277	0.22	1.7	0.8	0.591	0.835
DA0744	FW	5.113	5.319	0	0.617	0.1	2.4	0	0.936
DA0744	HW	5.329	5.618	0	1.919	0	4	0	2.63
DA0747	B	3.981	4.505	1.24	0.234	6	2.4	3.673	1.098
DA0747	EW	4.466	5.155	0.025	0.831	0.6	2.5	0.259	1.201
DA0747	FW	5.48	6.25	0.061	0.281	0.9	1.5	0.288	0.594
DA0747	HW	6.015	7.042	0.363	0.475	1.5	0.4	0.77	1.918
DA0747	WW	4.671	5.682	0.191	0.266	3.1	0.6	0.553	0.839
DA0835	B	4.966	5.556	0.468	0.057	2	1	0.951	0.309
DA0835	EW	6.876	7.353	0.004	0.57	0.7	1.2	0.176	0.729
DA0835	FW	5.891	6.579	0.036	0.419	0.8	4	0.206	0.838
DA0835	HW	5.261	6.494	0.288	1.245	3.6	5	1.343	2.327
DA0838	B	3.885	4.386	0.344	0.031	1.7	0.8	0.76	0.196
DA0838	EW	5.866	7.143	0.172	0.389	1.1	1	0.545	0.792
DA0838	FW	5.114	6.024	0.317	0.282	3	3	0.879	0.879
DA0838	HW	6.058	6.41	0.291	0.706	2.8	2.5	0.974	1.932
DA0841	B	3.433	3.788	0.902	0.028	2.4	0.1	1.613	0.588
DA0841	EW	4.975	5.682	0.242	0.07	1.3	0.6	0.649	0.286
DA0841	FW	5.073	5.814	0.097	0.2	0.9	1.2	0.29	0.503
DA0841	HW	6.227	6.579	0.136	0.548	2	2.5	0.722	1.122
DA0844	B	3.85	4.587	2.393	0.004	5	0.1	3.592	0.217
DA0844	EW	5.053	6.329	0.731	0.244	2.5	0.5	1.245	1.314
DA0844	FW	5.579	6.173	0	1.37	0	3.7	0	1.806
DA0844	HW	5.544	6.098	0.76	0.015	2.6	0.3	1.113	0.328
DA0859	B	3.773	4.237	0	1.291	0	3	0	1.739
DA0859	EW	3.353	3.759	0	1.995	0.3	3	0.022	2.66
DA0859	FW	4.315	4.95	0.023	1.501	0.9	4.5	0.237	2.728
DA0859	HW	4.214	4.717	0.043	0.493	1	2.5	0.224	1.071
DA0859	WW	3.903	4.348	0.09	0.816	1	3	0.363	1.646
DA1035	B	4.678	5.263	0.574	0.011	2.9	0.3	1.422	0.207
DA1035	EW	5.486	6.579	0.004	0.645	0.4	1.3	0.141	0.82
DA1035	FW	5.828	6.667	0.193	0.821	3.4	2.5	1.329	1.387
DA1035	HW	5.603	6.579	0.573	0.574	4	3.1	2.058	1.174
DA1038	B	2.336	2.283	0	0.36	0	2.7	0	0.954
DA1038	EW	5.477	5.882	0.223	0.132	1.7	0.6	0.472	0.493
DA1038	FW	6.05	6.757	0.109	0.733	2.5	2.5	0.751	1.318
DA1038	HW	6.393	7.042	2.968	0.209	9.5	2	4.837	3.284
DA1235	B	2.402	2.488	0.073	0	1	0	0.369	0
DA1235	EW	5.37	6.329	0	0.931	0	1.9	0	1.095
DA1235	FW	6.023	6.849	0.425	0.165	3	1.2	0.935	0.527
DA1235	HW	6.412	7.143	0.983	0.457	5.9	4	2.208	2.055
DB0135	B	3.199	3.425	0.112	0.145	0.9	1.2	0.417	0.411
DB0135	FW	5.857	6.024	0.55	0.128	1.9	1.7	0.915	0.685
DB0135	HW	7.87	8.475	0.311	1.422	3.2	6	1.093	3.106
DB0135	WW	7.337	8.197	0.719	0.2	2.6	1.5	1.167	1.439
DB0235	B	4.922	5.263	0.069	0.223	1.1	0.9	0.509	0.641
DB0235	EW	6.67	7.692	0.309	0.143	2.2	1.3	0.666	0.465
DB0235	FW	3.969	4.274	0.003	0.257	0.4	1.2	0.098	0.5
DB0235	WW	7.133	7.937	0.05	0.296	0.8	1	0.2	0.531
DB0238	B	1.976	2.66	0.288	0	3.1	0	0.948	0
DB0238	EW	5.97	6.7	0.309	0.029	2	1	0.557	0.271
DB0238	FW	4.711	4.95	0.265	0.075	1.8	2	0.498	0.361
DB0238	WW	6.928	7.576	1.051	0.059	3.5	1	1.421	0.541
DB0738	B	4.937	5.319	0.536	0.076	2.5	0.6	0.963	0.767
DB0738	EW	5.603	6.329	0.109	0.112	0.9	0.6	0.382	0.323
DB0738	FW	5.145	5.618	0.08	0.4	1.4	2.1	0.509	0.786
DB0838	B	3.334	3.65	0.176	0.015	2	0.7	0.645	0.229
DB0838	EW	7.371	7.937	0.67	0.515	5.5	1.1	1.414	1.462
DB0838	FW	6.05	6.67	0.238	0.789	1.8	3.7	0.709	1.619
DB1038	B	2.686	3.623	0.053	0.65	1	2.6	0.542	1.151

stope_name	surface	des_hr_c	des_rf	elos	ello	depth_ob	depth_ub	depth_ave_ob	depth_ave_ub
DB1038	EW	7.347	7.463	0.932	0.076	4.4	0.3	1.388	0.524
DB1038	FW	7.615	7.813	0.174	0.286	2.2	1.8	0.592	0.648
DC0238	B	3	3.876	0.444	0.005	2.2	0.4	0.966	0.067
DC0238	EW	4.579	5.051	1.083	0.002	3.6	0.1	1.557	0.079
DC0238	FW	4.688	5.319	0.166	0.272	2.9	3.2	0.573	0.782
DC0238	WW	6.618	7.246	0.266	0.119	1.9	1	0.496	0.518
DC0741	B	4.832	5.1	0.697	0.01	2.4	0.4	1.655	0.235
DC0741	EW	5.42	6.173	0.002	0.995	0.4	1.7	0.059	1.232
DC0741	FW	5.11	5.376	0.026	0.404	0.9	1.7	0.334	0.785
DP0635	EW	11.4	11.905	0.043	0.013	0.7	0.7	0.274	0.347
DP0635	FW	5.958	5.618	0	0.056	0	0.6	0	0.487
DP0635	HW	5.629	5.952	0.372	0.051	2.9	1.2	1.174	0.463
DP0635	WW	11.348	12.195	1.215	0	10	0	1.904	0
DP0641	B	3.017	3.268	0.088	0.372	1	2.4	0.417	0.972
DP0641	EW	6.363	6.67	0.303	0.189	2	0.6	0.663	0.656
DP0641	FW	5.63	5.814	0.13	0.681	2.8	2.3	0.752	1.118
DP0641	HW	5.76	5.814	0.241	1.171	3.3	3	1.49	1.876
DP0641	WW	5.908	6.757	0.087	0.868	1.3	3.4	0.315	1.887
DP1159	B	2.657	2.924	0	0.095	0	0.5	0	0.212
DP1159	EW	5.977	6.173	0.368	0.743	3	1.5	1.133	1.569
DP1159	FW	6.18	5.556	0.359	1.108	2.4	2	1.075	2.751
DT0735	B	5	5.319	0.228	0.372	2.2	3	1.001	1.388
DT0735	EW	7.406	8.197	0.046	0.576	3.5	4	0.843	0.769
DT0735	FW	5.357	5.56	0.064	0.222	0.9	1.4	0.328	0.602
DT0735	HW	5.168	5.56	0.785	1.008	4.1	5.5	2.132	2.388
DT0735	WW	7.861	8.62	0.371	0.287	2.1	1.4	0.9	0.702

stope_name	surface	vol_ob	vol_ub	area_ob	area_ub	per_ob	per_ub	c_ob	c_ub	x_ob	x_ub	h_ob	h_ub
AB01-1	FW	382	772	732.3	1067.1	408.6	329.4	0.055	0.124	0.343	0.5	0.051	0.059
AB01-1	HW	873	658	1135.4	811.1	353.4	424.1	0.114	0.057	0.523	0.373	0.061	0.076
AP02	EW	2265.3	444.1	2739.9	958.7	767	475.5	0.059	0.053	0.663	0.232	0.042	0.04
AP02	FW	2251.1	81.9	1724	74.9	381.1	129.3	0.149	0.056	0.561	0.024	0.084	0.336
AP02	HW	1769.7	78.4	1656.5	105.2	517.3	105.2	0.078	0.119	0.645	0.041	0.07	0.193
AP02	WW	1016.2	1309.1	2025.2	1875.6	853.8	631.7	0.035	0.059	0.438	0.406	0.03	0.043
AP07	B	137.5	8.4	172.6	61.5	147.5	115.1	0.1	0.058	0.36	0.128	0.161	0.046
AP07	EW	649.8	204.7	1110.4	384.8	326.8	375.3	0.131	0.034	0.708	0.245	0.047	0.072
AP07	FW	438.6	364.8	495.841	620.311	241.8	257.1	0.107	0.118	0.338	0.422	0.106	0.063
AP07	HW	341.6	458.7	545.729	654.204	287	341.6	0.083	0.07	0.315	0.378	0.071	0.073
AP07	WW	752.8	471	747.8	729.5	270.3	296.9	0.129	0.104	0.447	0.436	0.098	0.064
AP12	B	2422.8	54.5	1080.1	116.8	245.1	160.7	0.226	0.057	0.62	0.067	0.181	0.115
AP12	EW	997.9	2530.4	1772.9	2618.3	701.1	792.5	0.045	0.052	0.349	0.516	0.036	0.05
AP12	FW	709.1	3197.2	885.678	1949.96	328.4	418.8	0.103	0.14	0.232	0.511	0.072	0.099
AP12	HW	2357.9	1098.5	1595.764	527.018	354	396.1	0.16	0.042	0.626	0.207	0.098	0.241
AP12	WW	1326.9	506.3	2581.6	960.8	719	449	0.063	0.06	0.634	0.236	0.027	0.045
AP18	B	528.3	499.9	452.2	340.5	134.8	172.8	0.313	0.143	0.492	0.371	0.146	0.212
AP18	EW	738.2	713	501.4	448.9	172	179.9	0.213	0.174	0.572	0.512	0.175	0.199
AP18	FW	1798.2	1298.4	1096.3	601.3	201.9	245.3	0.338	0.126	0.507	0.278	0.132	0.234
AP18	HW	265.4	1613.3	557.3	1126.3	282.4	432.5	0.088	0.076	0.29	0.585	0.054	0.113
AP18	WW	1125.9	874.1	1151.6	734.2	322	440.4	0.14	0.048	0.565	0.36	0.077	0.117
AP86	EW	922.1	1568.7	1315.6	926.9	491.3	519.9	0.068	0.043	0.533	0.376	0.051	0.148
AP86	FW	3454.4	2631.6	2039.7	1427.7	349.9	556.7	0.209	0.058	0.497	0.348	0.1	0.13
AP86	HW	3938	3333	2273.9	1109.7	517	560	0.107	0.044	0.486	0.237	0.097	0.24
AP92	EW	666.6	895.4	1451.1	1404.7	593	593.7	0.052	0.05	0.502	0.486	0.032	0.045
AP92	FW	1460.7	399.8	1483.4	458.2	394.1	445	0.12	0.029	0.689	0.213	0.068	0.108
AP92	HW	589.1	1147.7	1483.4	458.2	465.3	536.2	0.086	0.02	0.665	0.205	0.027	0.311
AP92	WW	1475.4	596	2096.3	986.9	554.7	638.2	0.086	0.03	0.697	0.328	0.041	0.051
AP97	EW	3462.8	261.8	3246.9	679.9	518.2	448.3	0.152	0.043	0.838	0.175	0.05	0.039
AP97	FW	2366.2	327.5	1923.5	509.8	460	524.6	0.114	0.023	0.651	0.173	0.075	0.076
AP97	HW	1085.6	1085.3	1400.9	1023.7	442.6	524.2	0.09	0.047	0.512	0.374	0.055	0.088

stope_name	surface	vol_ob	vol_ub	area_ob	area_ub	per_ob	per_ub	c_ob	c_ub	x_ob	x_ub	h_ob	h_ub
AP97	WW	1675.4	1347.9	2539.6	2192.7	667.5	739.4	0.072	0.05	0.526	0.454	0.035	0.035
AS92	EW	585.3	2582.6	828.5	1822.1	459.2	509.4	0.049	0.088	0.316	0.694	0.065	0.088
AS92	FW	193.8	3467.6	296.3	1436.6	213.3	447	0.082	0.09	0.137	0.665	0.101	0.169
AS92	WW	1471	2835.2	1144.8	1516.4	274.9	482.7	0.19	0.082	0.414	0.548	0.101	0.128
AT04	FW	1261.2	3888.6	1370.7	2509.6	444.6	762.6	0.087	0.054	0.281	0.514	0.066	0.082
AT04	HW	2508.9	1496	1616.3	2067.1	570.3	703.4	0.062	0.053	0.364	0.465	0.103	0.042
AT09	FW	111.6	2538.7	267.9	1786	180	387.2	0.104	0.15	0.106	0.705	0.068	0.089
AT09	HW	2312.6	1422.8	1282.7	660.7	310.7	333.6	0.167	0.075	0.574	0.296	0.134	0.223
AT15	FW	1979	2687.6	1550.3	1552.7	478.3	637.8	0.085	0.048	0.422	0.422	0.086	0.117
AT15	HW	20714.4	1920.4	2512	532.1	414	368	0.184	0.049	0.681	0.144	0.437	0.416
AT99	FW	1550.3	6072.4	1214.4	2243.2	310.4	609.9	0.158	0.076	0.274	0.506	0.097	0.152
AT99	HW	436.5	4594.2	901.8	2615	628.5	906.5	0.029	0.04	0.225	0.653	0.043	0.091
C0080	B	10	13	18.4	20.7	25.7	35.5	0.35	0.206	0.113	0.127	0.337	0.367
C0080	FW	592	191	628.1	347.1	219.8	209.2	0.163	0.1	0.473	0.261	0.1	0.079
C0080	HW	539	408	463.1	474.8	175.6	220.5	0.189	0.123	0.359	0.369	0.144	0.105
C0080	WW	1	985	21.2	448.4	25.1	115	0.423	0.426	0.028	0.596	0.027	0.276
C0574	B	166	54	171.9	59.6	112.7	71.5	0.17	0.147	0.659	0.228	0.196	0.312
C0574	FW	180	2014	293.6	1018.7	168.3	274	0.13	0.171	0.221	0.766	0.095	0.165
C0574	HW	845	1480	503.1	776.5	104.6	183.8	0.578	0.289	0.353	0.545	0.199	0.182
C0580	EW	455	23	485.1	114.8	209.8	150.1	0.138	0.064	0.616	0.146	0.113	0.05
C0580	FW	241	947	536.9	801.4	190.3	348.1	0.186	0.083	0.294	0.439	0.052	0.111
C0580	HW	439	436	460.2	794.3	161.5	323.8	0.222	0.095	0.261	0.451	0.118	0.052
C0774	B	153	24	96.6	20.1	75.7	23.9	0.212	0.442	0.309	0.064	0.428	0.708
C0774	EW	4241	472	1503.3	467.7	231.6	314.3	0.352	0.059	0.69	0.215	0.193	0.124
C0774	FW	92	2555	135.2	1235.2	69.3	289.1	0.354	0.186	0.076	0.697	0.156	0.156
C0774	HW	108	1900	189.4	1011.8	92.9	229	0.276	0.242	0.121	0.645	0.11	0.157
C0971	B	336	410	296.5	181.2	107.9	122	0.32	0.153	0.516	0.316	0.175	0.447
C0971	FW	88	2650	119	672.3	59.9	107.1	0.417	0.737	0.116	0.655	0.18	0.404
C0971	HW	119	658	216.4	631.8	80	206.4	0.425	0.186	0.239	0.698	0.099	0.11
C0974	B	219	190	132.5	80	62.8	74.8	0.422	0.18	0.631	0.381	0.382	0.706
C0974	FW	19	2729	44	937.5	41.2	937.5	0.326	0.013	0.041	0.868	0.173	0.253
C0974	HW	200	1051	438.4	656.6	173.6	305.6	0.183	0.088	0.409	0.612	0.058	0.166
C0980	B	0	151	0	78.9	0	47.9	0	0.432	0	0.625	0	0.573
C0980	EW	578	357	529	276.4	162.2	224	0.253	0.069	0.567	0.296	0.126	0.207
C0980	FW	21	2356	41.8	883.7	36	197.8	0.405	0.284	0.041	0.877	0.207	0.238
C0980	HW	470	671	354.4	518.4	91	211	0.538	0.146	0.313	0.458	0.187	0.151
C1068	B	291	0	187.4	0	60.6	0	0.641	0	0.71	0	0.302	0
C1068	EW	269	296	382.8	345.7	139.4	216.1	0.248	0.093	0.383	0.346	0.095	0.122
C1068	FW	347	224	344.6	371.6	180.8	234.5	0.132	0.085	0.344	0.371	0.144	0.083
C1068	HW	357	472	379.1	346.8	217.4	231.2	0.101	0.082	0.422	0.386	0.129	0.194
C1077	B	166	0	139.6	0	58.1	0	0.52	0	0.555	0	0.268	0
C1077	EW	118	14	214.9	35.2	125	94	0.173	0.05	0.545	0.089	0.1	0.178
C1077	FW	127	200	286.2	331.2	145.4	181.9	0.17	0.126	0.33	0.382	0.07	0.088
C1077	HW	28	362	120.1	514.2	153.8	207.8	0.064	0.15	0.144	0.615	0.057	0.083
C1080	B	37	8	75.3	37.1	46	61	0.447	0.125	0.419	0.206	0.151	0.094
C1080	EW	390	84	449	107.1	172.4	155.3	0.19	0.056	0.693	0.165	0.109	0.201
C1080	FW	461	414	486.9	548.9	309.5	330.7	0.064	0.063	0.341	0.385	0.114	0.086
C1080	HW	436	1032	367	702.2	94	130.7	0.522	0.517	0.261	0.499	0.165	0.147
C1259	B	0.1	380	4.4	149.8	13.7	57.9	0.295	0.562	0.013	0.443	0.029	0.551
C1259	FW	221	821	420	567.9	181.2	290.1	0.161	0.085	0.304	0.412	0.068	0.161
C1259	HW	132	864	50.4	790.2	144.4	319.6	0.03	0.097	0.037	0.576	0.981	0.103
C1259	WW	125	1130	171.6	793.4	62.6	233.6	0.55	0.183	0.154	0.712	0.148	0.134
C1268	B	819	217	427.2	264	131.3	131.8	0.311	0.191	0.459	0.284	0.247	0.134
C1268	EW	1144	246	769.9	254.6	159	142.9	0.383	0.157	0.622	0.206	0.142	0.161
C1268	FW	758	69	823.8	150.8	161.7	193.5	0.396	0.051	0.61	0.112	0.085	0.099
C1268	HW	0	1240	0	650.5	0	120.5	0	0.563	0	0.834	0	0.199
C1459	B	14	0	26.7	0	44.3	0	0.171	0	0.18	0	0.27	0
C1459	EW	154	402	338.8	414.6	169.3	199.3	0.149	0.131	0.347	0.425	0.066	0.127
C1459	FW	15	1165	57.5	947.2	42.9	199.5	0.393	0.299	0.042	0.686	0.091	0.106
C1459	HW	508	454	422.8	514	161.2	184.7	0.204	0.189	0.319	0.387	0.155	0.104
C1468	B	115	271	309.6	346.9	197.7	251.5	0.1	0.069	0.265	0.297	0.056	0.112

stope_name	surface	vol_ob	vol_ub	area_ob	area_ub	per_ob	per_ub	c_ob	c_ub	x_ob	x_ub	h_ob	h_ub
C1468	EW	854	31	765.6	185.2	190.9	169.1	0.264	0.081	0.688	0.167	0.107	0.033
C1468	FW	468	323	834.9	311.6	209.4	156.9	0.239	0.159	0.461	0.172	0.052	0.156
C1468	HW	46	547	128.3	674	76.3	139.6	0.277	0.435	0.129	0.68	0.084	0.083
C8962	FW	1118	142	918.4	178.5	179	124.5	0.36	0.145	0.586	0.114	0.107	0.158
C8962	HW	1408	828	840.9	242.9	134.7	94.4	0.582	0.343	0.53	0.153	0.154	0.582
C8962	WW	157	472	441.5	793.8	249.4	285	0.089	0.123	0.288	0.518	0.045	0.056
C9162	B	751	477	329.3	180.7	120.9	129.5	0.283	0.135	0.57	0.313	0.334	0.522
C9162	FW	50	3442	86.3	1393.9	63.3	193.1	0.271	0.47	0.052	0.841	0.166	0.176
C9162	HW	810	776	793.5	737.6	215.5	334.8	0.215	0.083	0.502	0.467	0.096	0.103
C9168	B	0.1	6	3.4	14.4	10.1	23.6	0.419	0.325	0.01	0.044	0.042	0.292
C9168	FW	52	2606	74.7	937	50.2	216	0.372	0.252	0.052	0.658	0.214	0.242
C9168	HW	1785	584	641.2	318.8	164.8	221.2	0.297	0.082	0.427	0.212	0.292	0.273
C9168	WW	1	2429	9.3	990.2	27.5	244.1	0.155	0.209	0.008	0.835	0.094	0.207
C9374	B	249	214	177.4	124	91.6	47.4	0.266	0.694	0.323	0.226	0.28	0.412
C9374	FW	232	892	210	642.4	69.8	188.41	0.542	0.227	0.188	0.577	0.203	0.146
C9374	HW	377	590	351.1	395.5	127.6	163	0.271	0.187	0.414	0.467	0.152	0.199
C9374	WW	5063	91	1241.3	104.7	187.1	109	0.446	0.111	0.811	0.068	0.308	0.226
C9568	FW	36	1297	84.4	423	40.9	113.2	0.634	0.415	0.112	0.562	0.123	0.396
C9568	HW	39	404	78.6	354.6	53.1	173.8	0.35	0.148	0.108	0.485	0.149	0.161
C9571	FW	347	122	229.1	153.9	82.4	106.2	0.424	0.171	0.345	0.232	0.266	0.17
C9571	HW	50	451	88.3	291.7	58.9	113.6	0.32	0.284	0.121	0.399	0.16	0.241
C9674	B	621	396	327.6	126.8	126	78.1	0.259	0.261	0.598	0.231	0.278	0.737
C9674	EW	1854	2528	807.8	785.7	181.8	202.9	0.307	0.24	0.499	0.485	0.215	0.305
C9674	FW	93	5202	233.9	1309.9	87.9	244.2	0.38	0.276	0.127	0.709	0.069	0.292
C9674	HW	4699	2320	887.1	429.8	136.2	84.8	0.601	0.751	0.604	0.293	0.473	0.692
C9674	WW	1665	2084	555.7	617.6	106.2	187.9	0.619	0.22	0.484	0.538	0.338	0.361
C9874	B	780	471	447.6	205	93.4	116.4	0.645	0.19	0.751	0.344	0.219	0.427
C9874	FW	258	1857	345.4	752.7	115.6	219.2	0.325	0.197	0.263	0.572	0.107	0.239
C9874	HW	1163	945	516.8	462.1	123.6	195.5	0.425	0.152	0.535	0.478	0.263	0.253
C9883	B	707	73	263.1	99.9	68.4	125.1	0.707	0.08	0.845	0.321	0.44	0.194
C9883	FW	171	1703	203.1	866.2	66.8	205.6	0.572	0.258	0.186	0.792	0.157	0.178
C9883	HW	20	1253	104.1	861.6	101.2	220.5	0.128	0.223	0.105	0.873	0.05	0.132
CD0062	B	0.1	46	8.3	25	16.7	37.7	0.374	0.221	0.055	0.166	0.011	0.978
CD0062	EW	597	665	489.3	355.5	151.5	267.2	0.268	0.063	0.488	0.354	0.147	0.264
CD0062	HW	339	385	544.4	356.3	179.2	170.5	0.213	0.154	0.466	0.305	0.071	0.152
CD0062	WW	152	625	406.9	409	195.7	242.9	0.134	0.087	0.39	0.392	0.049	0.201
CD0262	B	0	392	0	196.9	15	76.7	0	0.421	0	1	0	0.377
CD0262	FW	141	754	229.4	522.4	103.6	188.4	0.269	0.185	0.324	0.737	0.108	0.168
CD0262	HW	63	318	234.5	477.6	160.4	259.5	0.115	0.089	0.33	0.672	0.047	0.081
CP0062	EW	1015	1720	711.3	1423.2	224.7	375.2	0.177	0.127	0.33	0.661	0.142	0.085
CP0062	FW	237	861	333.5	614.9	207.8	254.9	0.097	0.119	0.258	0.475	0.103	0.15
CP0062	HW	728	815	511	515.4	193.9	281.4	0.171	0.082	0.419	0.423	0.168	0.185
CP0062	WW	930	502	1234	497.8	326.8	282.9	0.145	0.078	0.719	0.29	0.057	0.12
CP0062_68	B	11	1000	19.9	146	73.6	61.4	0.046	0.487	0.055	0.407	0.329	1.507
CP0062_68	EW	1364	3128	1224	2506.2	440.3	700.2	0.079	0.064	0.334	0.685	0.085	0.066
CP0062_68	FW	513	1565	817.4	1058.2	404.1	510.3	0.063	0.051	0.377	0.488	0.058	0.121
CP0062_68	HW	1971.7	2400.7	1057.6	577.6	304.9	338.6	0.143	0.063	0.427	0.233	0.152	0.46
CP0062_68	WW	3323	692	2536.6	743.1	465.2	548.6	0.147	0.031	0.839	0.246	0.069	0.091
CP0074	B	2512	12	438.8	17.8	103	21	0.52	0.507	0.945	0.038	0.727	0.425
CP0074	EW	5382	832	1238.2	463.1	218.3	218	0.327	0.122	0.707	0.264	0.328	0.222
CP0074	FW	409	788	315	803.5	35.8	229.1	3.089	0.192	0.314	0.8	0.195	0.092
CP0074	HW	1835	101	668	155.4	142.7	76.6	0.412	0.333	0.697	0.162	0.283	0.139
CP0074	WW	6089	536	1528.9	274.2	226.1	159.5	0.376	0.135	0.836	0.15	0.271	0.314
CP0362	EW	3945.5	674.8	1690.1	479.9	291.9	385.6	0.249	0.041	0.741	0.21	0.151	0.171
CP0362	FW	184.5	337.5	293.9	503	220.2	254.3	0.076	0.098	0.256	0.438	0.097	0.08
CP0362	HW	342.2	1041.9	452.9	690	194.1	345.6	0.151	0.073	0.298	0.454	0.094	0.153
CP0362	WW	153.3	1098.7	565.5	1649.4	492	672.7	0.029	0.046	0.241	0.704	0.03	0.044
CP0362_68	B	1	725	8.1	133.7	33.7	59.5	0.09	0.475	0.025	0.41	0.115	1.247
CP0362_68	EW	5745	1581	3024.2	980.6	445.5	578.1	0.191	0.037	0.799	0.259	0.092	0.137
CP0362_68	FW	1189	586	1000.7	711.7	335.4	397.5	0.112	0.057	0.469	0.333	0.1	0.082
CP0362_68	HW	844	2406	697.1	1966.4	327.7	535.3	0.082	0.086	0.272	0.768	0.122	0.073

stope_name	surface	vol_ob	vol_ub	area_ob	area_ub	per_ob	per_ub	c_ob	c_ub	x_ob	x_ub	h_ob	h_ub
CP0362_68	WW	325	2281	869.4	2783	614.4	923.4	0.029	0.041	0.236	0.757	0.034	0.041
CP0374	B	7	53	56.8	63.8	61.4	85.5	0.189	0.11	0.205	0.23	0.043	0.277
CP0374	EW	210	378	391.2	647.3	229.6	349	0.093	0.067	0.35	0.578	0.072	0.061
CP0374	FW	700	155	538.7	272	161.2	249.2	0.261	0.055	0.511	0.258	0.149	0.092
CP0374	HW	1027	129	814.8	154.3	210.2	210.4	0.232	0.044	0.674	0.128	0.117	0.179
CP0374	WW	1550	121	1161.6	159.7	270.3	182.3	0.2	0.06	0.839	0.115	0.104	0.159
CP0380	B	0.1	0	9.1	0	43.3	0	0.061	0	0.236	0	0.01	0
CP0380	EW	796	192	499.8	273	246.4	239	0.103	0.06	0.488	0.267	0.189	0.113
CP0380	FW	534	232	528.3	395.2	264.7	287.6	0.095	0.06	0.387	0.289	0.117	0.079
CP0380	HW	1530	18	808.9	89.8	179.5	130.6	0.315	0.066	0.654	0.073	0.177	0.056
CP0380	WW	545	78	662.1	114.2	270.4	128.4	0.114	0.087	0.67	0.116	0.085	0.17
CP0762	B	261	6	204.4	38.4	120.7	58.7	0.176	0.14	0.7	0.131	0.237	0.067
CP0762	EW	105	847	235.4	613.1	121.8	260	0.199	0.114	0.312	0.812	0.077	0.148
CP0762	FW	576	682	368.4	577.1	134	241.2	0.258	0.125	0.254	0.398	0.217	0.131
CP0762	HW	322	561	467.3	427.5	220.4	258.1	0.121	0.081	0.415	0.379	0.085	0.169
CP0762	WW	441	470	686.4	595.9	328.1	353.2	0.08	0.06	0.492	0.427	0.065	0.086
CP0768	B	234	36	252.8	87.2	85.9	94.7	0.431	0.122	0.439	0.151	0.155	0.118
CP0768	EW	602	288	575.1	618.4	213.8	276.5	0.158	0.102	0.512	0.551	0.116	0.05
CP0768	FW	278	1268	317.8	645.1	140	245.5	0.204	0.135	0.25	0.507	0.13	0.206
CP0768	HW	307	241	540.7	502.3	225.4	324.5	0.134	0.06	0.504	0.468	0.065	0.057
CP0768	WW	89	1891	233.5	1657.9	139.7	304.8	0.15	0.224	0.131	0.93	0.066	0.074
CP9362	EW	242	747	464.4	790.8	245.9	378.5	0.097	0.069	0.372	0.633	0.064	0.089
CP9362	FW	744	269	606	338	231.8	286.8	0.142	0.052	0.5	0.279	0.133	0.115
CP9362	HW	2	1015	26.4	913.3	68.6	226.6	0.07	0.224	0.022	0.765	0.039	0.098
CP9362	WW	62	895	177.3	855.6	134.4	271.3	0.123	0.146	0.18	0.867	0.07	0.095
CP9362_68	B	0	148	9.9	124.4	36.4	114.2	0.094	0.12	0.048	0.604	0	0.284
CP9362_68	EW	316	1250	823	1685.3	401.9	717.2	0.064	0.041	0.37	0.757	0.036	0.048
CP9362_68	FW	1144	688	1197.5	808.3	407.9	625.9	0.09	0.026	0.537	0.363	0.073	0.08
CP9362_68	HW	171	1640	372.6	1549.9	218.9	491.1	0.098	0.081	0.165	0.688	0.063	0.071
CP9362_68	WW	421	1554	815.8	1618.9	330.3	560	0.094	0.065	0.397	0.788	0.048	0.063
CP9662	B	0	268	15.8	237.4	22.1	160.5	0.407	0.116	0.055	0.822	0	0.195
CP9662	EW	1191	986	874.8	686.5	279.7	384.6	0.141	0.058	0.54	0.423	0.122	0.146
CP9662	FW	178	616	394.4	570.4	222.6	352.7	0.1	0.058	0.348	0.503	0.06	0.12
CP9662	HW	173	1295	336.3	635.5	191	279.4	0.116	0.102	0.3	0.566	0.075	0.215
CP9662	WW	1028	543	929.7	561.2	303.2	399.4	0.127	0.044	0.635	0.383	0.096	0.109
CP9668	B	4	404	41.1	258.7	51.7	132.3	0.193	0.186	0.123	0.776	0.04	0.258
CP9668	EW	885	999	603.6	537.3	179.3	282.6	0.236	0.085	0.535	0.477	0.159	0.213
CP9668	FW	303	587	392	513	135.9	209.5	0.267	0.147	0.36	0.471	0.104	0.134
CP9668	HW	106	649	260.1	667.7	134.6	260.2	0.18	0.124	0.246	0.631	0.067	0.1
CP9668	WW	562	574	509.4	531.4	183	292.4	0.191	0.078	0.506	0.528	0.13	0.125
CT0262	B	1269	26	477	49.6	142.5	60.1	0.295	0.173	0.85	0.088	0.324	0.198
CT0262	FW	409	788	315	803.5	166.4	303.8	0.143	0.109	0.226	0.576	0.195	0.092
CT0262	HW	255	618	463.2	643.2	314	380.5	0.059	0.056	0.328	0.456	0.068	0.101
CT0268	B	24	18	61.8	91.3	39.7	93.7	0.493	0.131	0.217	0.32	0.131	0.055
CT0268	FW	148	122	239.5	208.3	106	130.3	0.268	0.154	0.373	0.324	0.106	0.108
CT0268	HW	1104	655	310.8	249.8	75	90.7	0.694	0.382	0.368	0.296	0.536	0.441
CT0271	FW	129	197	208.3	305.2	76.6	134	0.446	0.214	0.324	0.475	0.114	0.098
CT0271	HW	211	404	222.3	347.5	95.2	166	0.308	0.158	0.335	0.524	0.169	0.166
CT0280	B	476	40	121.7	27.6	55.5	52.9	0.496	0.124	0.909	0.206	0.943	0.733
CT0280	FW	640	1093	864.7	1108.5	302.5	428.2	0.119	0.076	0.5	0.641	0.067	0.079
CT0280	HW	1156	1152	1000.2	906.8	219.9	387.9	0.26	0.076	0.535	0.485	0.097	0.112
CT0562	B	81	308	71.4	248.5	63.5	124.8	0.223	0.2	0.151	0.525	0.357	0.209
CT0562	FW	344	2182	420	1075.4	186.6	317.6	0.152	0.134	0.222	0.568	0.106	0.164
CT0562	HW	1083	3542	949.2	893.7	159.6	295.2	0.468	0.129	0.445	0.419	0.098	0.352
CT0568	B	913	319	437.3	88.1	85.5	87	0.752	0.146	0.821	0.165	0.265	1.026
CT0568	FW	863	944	734.6	1103.3	174.1	198.1	0.305	0.353	0.531	0.798	0.115	0.068
CT0568	HW	52	1150	130.2	727.4	97	196.2	0.174	0.237	0.138	0.773	0.093	0.156
CT9562	B	74	137	94.6	118.8	44.4	90.9	0.603	0.181	0.278	0.349	0.214	0.281
CT9562	FW	294	3315	213.1	1198.5	102.7	277.8	0.254	0.195	0.146	0.82	0.251	0.212
CT9562	HW	105	3152	259.9	1520.8	130.5	322.9	0.192	0.183	0.143	0.839	0.067	0.141
CT9862	B	339	9	302.3	22.7	124.1	27.5	0.247	0.377	0.776	0.058	0.171	0.221

stope_name	surface	vol_ob	vol_ub	area_ob	area_ub	per_ob	per_ub	c_ob	c_ub	x_ob	x_ub	h_ob	h_ub
CT9862	FW	1888	516	796.9	471.5	198.1	259.6	0.255	0.088	0.559	0.331	0.223	0.134
CT9862	HW	2177	860	675.8	512.3	132.6	156	0.483	0.265	0.503	0.381	0.329	0.197
CT9868	B	373	148	263.4	86.2	64.7	75.7	0.791	0.189	0.744	0.244	0.232	0.492
CT9868	FW	23	2212	92.5	1117.8	84.7	229.4	0.162	0.267	0.071	0.857	0.069	0.157
CT9868	HW	885	769	480.4	571.9	104.9	170.2	0.549	0.248	0.396	0.472	0.223	0.149
D0235A	B	177	0.1	75.6	1.5	40.2	8	0.588	0.295	0.35	0.007	0.716	0.145
D0235A	EW	1486	447	392.6	176.8	97.6	111.9	0.518	0.177	0.503	0.227	0.508	0.506
D0235A	FW	126	75	199.8	170.9	90.1	111.7	0.309	0.172	0.397	0.34	0.119	0.089
D0235A	HW	749	907	212.9	190.6	59.8	64.1	0.748	0.583	0.408	0.365	0.641	0.916
D0235A	WW	480	130	533	74.8	128.5	119.4	0.406	0.066	0.682	0.096	0.104	0.534
D0238	B	81	0.1	33.9	2.2	25.6	8.5	0.65	0.383	0.311	0.02	1.091	0.081
D0238	FW	7	35	32.2	133.9	53.7	96.6	0.14	0.18	0.118	0.49	0.102	0.06
D0238	HW	89	200	75.4	77.1	47.7	48.9	0.416	0.405	0.291	0.297	0.361	0.785
D0238	WW	469	34	360.5	45.3	79	80.6	0.726	0.088	0.719	0.09	0.182	0.296
D0738	B	53	326	84.3	124.2	39.3	77.2	0.686	0.262	0.164	0.242	0.182	0.626
D0738	EW	1108	168	631.4	91.9	117.5	153.6	0.575	0.049	0.666	0.097	0.186	0.507
D0738	FW	1	436	5.1	564.1	11.2	164	0.511	0.264	0.006	0.712	0.231	0.087
D0738	HW	1	608	19.1	269.4	18.9	93.6	0.672	0.386	0.043	0.6	0.032	0.366
DA0135	B	232	9	153.4	26.5	57.7	39.2	0.579	0.217	0.45	0.078	0.325	0.175
DA0135	FW	0.1	644	4.5	204.5	9.2	91.5	0.668	0.307	0.016	0.708	0.028	0.585
DA0135	HW	522	1261	217.4	275.7	60	81.9	0.759	0.517	0.347	0.44	0.433	0.732
DA0135	WW	521	518	371.8	163.4	82.5	114	0.686	0.158	0.576	0.253	0.193	0.659
DA0138	B	1	21	20.6	24.8	44.1	38.1	0.133	0.215	0.13	0.156	0.028	0.452
DA0138	FW	0	425	0	320.7	0	74.9	0	0.718	0	0.739	0	0.197
DA0138	HW	456	239	266.8	115.1	102	101.8	0.322	0.14	0.405	0.175	0.278	0.515
DA0138	WW	458	17	353.6	26	85.6	58.6	0.606	0.095	0.783	0.058	0.183	0.341
DA0244	B	45	29	79.6	39.4	48.9	25.4	0.418	0.767	0.351	0.174	0.168	0.312
DA0244	EW	219	1155	183.3	459.6	72.3	127.2	0.441	0.357	0.224	0.56	0.235	0.312
DA0244	FW	63	305	137.5	196.2	74.7	114.3	0.31	0.189	0.293	0.419	0.104	0.295
DA0244	HW	186	261	166	70	63.7	70.8	0.514	0.175	0.366	0.154	0.231	1.185
DA0244	WW	2921	29	622.9	46.7	103.8	50.7	0.726	0.228	0.767	0.058	0.5	0.242
DA0647	B	144	1	150	4.2	55.7	13	0.608	0.312	0.648	0.018	0.208	0.309
DA0647	FW	23	42	87.9	123.1	61.7	114.6	0.29	0.118	0.272	0.381	0.074	0.082
DA0647	HW	226	409	187.6	130.2	53.9	65.6	0.811	0.38	0.437	0.303	0.234	0.732
DA0647	WW	355	99	401.7	62.1	85.1	57.8	0.697	0.234	0.683	0.106	0.117	0.538
DA0650	B	41	0	34.5	0	42.3	0	0.242	0	0.235	0	0.538	0
DA0650	EW	435	12	182.7	39	76.5	50.9	0.392	0.189	0.548	0.117	0.468	0.131
DA0650	FW	79	353	151	406.9	84.4	150.2	0.266	0.227	0.19	0.513	0.113	0.114
DA0650	HW	2320	0	482.7	0	94.6	0	0.678	0	0.586	0	0.582	0
DA0650	WW	60	97	169.2	75.6	71.6	86.3	0.415	0.128	0.493	0.22	0.072	0.392
DA0741	B	35	3	118.3	37	66.9	59.5	0.332	0.131	0.455	0.142	0.072	0.035
DA0741	EW	232	143	367.6	173.7	133.7	185.1	0.258	0.064	0.519	0.245	0.088	0.166
DA0741	FW	168	43	237.4	84.5	80.8	64.9	0.457	0.252	0.535	0.19	0.122	0.147
DA0741	WW	337	491	316.4	259.5	114.4	159.7	0.304	0.128	0.458	0.376	0.159	0.312
DA0744	B	45	30	107	57.9	89	70.9	0.17	0.145	0.32	0.173	0.108	0.181
DA0744	EW	210	167	355.6	200.1	134.3	199.1	0.248	0.063	0.469	0.264	0.083	0.157
DA0744	FW	0	287	17.4	306.7	37.6	119.6	0.155	0.269	0.037	0.659	0	0.142
DA0744	HW	0	999	0	379.9	0	88	0	0.616	0	0.73	0	0.359
DA0747	B	350	66	95.3	60.1	53.3	32.5	0.422	0.715	0.338	0.213	1	0.377
DA0747	EW	11	359	42.5	299	37.6	102.6	0.378	0.357	0.098	0.693	0.106	0.185
DA0747	FW	30	139	104.3	234.2	106.5	121.5	0.116	0.199	0.211	0.474	0.075	0.103
DA0747	HW	285	373	370.1	194.5	99.8	127.7	0.467	0.15	0.472	0.248	0.106	0.366
DA0747	WW	110	153	199	182.4	118.1	178.4	0.179	0.072	0.345	0.317	0.104	0.165
DA0835	B	181	22	190.4	71.3	77.5	70.3	0.398	0.181	0.492	0.184	0.183	0.097
DA0835	EW	3	389	17	533.9	28.1	118.9	0.271	0.475	0.025	0.783	0.114	0.084
DA0835	FW	22	259	107	309.1	90.8	153.2	0.163	0.165	0.173	0.501	0.053	0.127
DA0835	HW	172	743	128.1	319.3	48.4	111.9	0.687	0.32	0.215	0.535	0.315	0.346
DA0838	B	99	9	130.3	46	56.2	81.7	0.518	0.087	0.453	0.16	0.177	0.077
DA0838	EW	129	292	236.7	368.5	88.7	180	0.378	0.143	0.316	0.492	0.094	0.11
DA0838	FW	172	153	195.7	174.1	97.5	134	0.259	0.122	0.361	0.321	0.167	0.177
DA0838	HW	190	461	195	238.6	59.5	123	0.692	0.198	0.299	0.365	0.186	0.333

stope_name	surface	vol_ob	vol_ub	area_ob	area_ub	per_ob	per_ub	c_ob	c_ub	x_ob	x_ub	h_ob	h_ub
DA0841	B	192	6	119	10.2	53.9	28.5	0.515	0.158	0.559	0.048	0.393	0.49
DA0841	EW	124	36	191.2	125.9	81.9	120.4	0.358	0.109	0.374	0.246	0.125	0.068
DA0841	FW	44	91	151.5	180.9	95.5	94.7	0.209	0.253	0.333	0.398	0.063	0.099
DA0841	HW	93	374	128.8	333.3	87	131.3	0.214	0.243	0.189	0.488	0.169	0.163
DA0844	B	658	1	183.2	4.6	55	33.3	0.761	0.052	0.666	0.017	0.706	0.269
DA0844	EW	407	136	327	103.5	86.5	110.3	0.549	0.107	0.587	0.186	0.183	0.343
DA0844	FW	0	784	0	434	0	87	0	0.721	0	0.758	0	0.231
DA0844	HW	404	8	363.1	24.4	87.4	34.1	0.597	0.264	0.683	0.046	0.155	0.176
DA0859	B	0	303	0	174.2	0	54.2	0	0.745	0	0.742	0	0.35
DA0859	EW	0.1	449	4.6	168.8	8.4	73.1	0.819	0.397	0.02	0.75	0.027	0.544
DA0859	FW	8	517	33.8	189.5	36.5	90.8	0.319	0.289	0.098	0.55	0.108	0.527
DA0859	HW	13	148	58.1	138.2	52.2	102.6	0.268	0.165	0.193	0.46	0.078	0.242
DA0859	WW	25	226	68.9	137.3	33.3	93.6	0.781	0.197	0.249	0.496	0.116	0.373
DA1035	B	207	4	145.6	19.3	100	23.2	0.183	0.451	0.403	0.053	0.313	0.125
DA1035	EW	2	351	14.2	427.8	39.4	92	0.115	0.635	0.026	0.786	0.099	0.105
DA1035	FW	120	510	90.3	367.7	52.9	116.9	0.405	0.338	0.145	0.592	0.372	0.192
DA1035	HW	345	346	167.6	294.6	69.8	129.2	0.432	0.222	0.278	0.489	0.423	0.182
DA1038	B	0	44	0	46.1	0	41.7	0	0.333	0	0.377	0	0.374
DA1038	EW	127	75	269.3	152.1	116.1	150.4	0.251	0.084	0.472	0.267	0.076	0.106
DA1038	FW	71	477	94.5	361.8	46.3	114.7	0.554	0.346	0.145	0.556	0.205	0.184
DA1038	HW	2494	176	515.6	53.6	102	41.2	0.623	0.397	0.614	0.064	0.566	1.192
DA1235	B	10	0	27.1	0	41.5	0	0.198	0	0.198	0	0.188	0
DA1235	EW	0	519	0	474.1	0	92.5	0	0.696	0	0.851	0	0.134
DA1235	FW	278	108	297.3	204.8	109.4	105.5	0.312	0.231	0.455	0.313	0.144	0.098
DA1235	HW	755	351	341.9	170.8	88.5	112.3	0.549	0.17	0.445	0.222	0.318	0.418
DB0135	B	20	26	48	63.2	35.6	53.5	0.476	0.277	0.268	0.353	0.16	0.138
DB0135	FW	536	125	585.7	182.4	181.6	114	0.223	0.176	0.601	0.187	0.101	0.135
DB0135	HW	443	2027	405.2	652.7	178	218.5	0.161	0.172	0.284	0.458	0.144	0.323
DB0135	WW	817	227	700	157.7	145.5	148.2	0.416	0.09	0.616	0.139	0.117	0.305
DB0235	B	31	100	60.9	156.1	41.5	90.7	0.444	0.238	0.136	0.347	0.173	0.136
DB0235	EW	238	110	357.6	236.7	133.2	151.8	0.253	0.129	0.464	0.307	0.094	0.08
DB0235	FW	1	101	10.2	201.8	30.1	125.9	0.141	0.16	0.026	0.513	0.082	0.094
DB0235	WW	41	243	204.9	457.7	150.1	260.3	0.114	0.085	0.25	0.558	0.037	0.066
DB0238	B	49	0	51.7	0	47.5	0	0.288	0	0.303	0	0.35	0
DB0238	EW	179	17	321.1	62.8	144.3	69.9	0.194	0.162	0.554	0.108	0.083	0.091
DB0238	FW	193	55	387.8	152.4	165	130.5	0.179	0.112	0.532	0.209	0.067	0.078
DB0238	WW	1221	68	859.2	125.6	156.2	124.7	0.443	0.102	0.739	0.108	0.129	0.128
DB0738	B	226	32	234.8	41.7	100.3	66.2	0.293	0.12	0.557	0.099	0.167	0.316
DB0738	EW	63	65	164.9	201.1	111.9	194.6	0.165	0.067	0.285	0.347	0.079	0.061
DB0738	FW	45	224	88.4	285.1	52.6	138.2	0.402	0.188	0.158	0.51	0.144	0.124
DB0838	B	34	3	52.7	13.1	33.2	21.4	0.601	0.359	0.272	0.068	0.236	0.168
DB0838	EW	824	633	582.8	433.1	174.4	251.5	0.241	0.086	0.474	0.352	0.156	0.187
DB0838	FW	245	814	345.4	502.9	122.3	188.1	0.29	0.179	0.335	0.488	0.101	0.192
DB1038	B	11	135	20.3	117.3	35	57.2	0.208	0.451	0.098	0.565	0.32	0.283
DB1038	EW	1168	95	841.3	181.3	204.6	114.6	0.253	0.173	0.671	0.145	0.127	0.103
DB1038	FW	235	386	396.8	596	207.1	268.7	0.116	0.104	0.294	0.441	0.079	0.071
DC0238	B	85	1	88	14.9	39	29.1	0.727	0.221	0.46	0.078	0.274	0.046
DC0238	EW	459	1	294.8	12.7	90.6	30	0.451	0.177	0.695	0.03	0.241	0.059
DC0238	FW	135	221	235.8	282.7	194.7	204.3	0.078	0.085	0.29	0.347	0.099	0.124
DC0238	WW	290	129	584.8	249	187.3	161.6	0.209	0.12	0.537	0.229	0.055	0.087
DC0741	B	278	4	168	17	60.7	37.1	0.573	0.155	0.421	0.043	0.339	0.152
DC0741	EW	1	519	17	421.1	23.5	123.3	0.387	0.348	0.033	0.807	0.038	0.16
DC0741	FW	13	199	38.9	253.6	39.6	113.6	0.312	0.247	0.079	0.515	0.142	0.131
DP0635	EW	98	30	358.1	86.5	151.8	85.1	0.195	0.15	0.157	0.038	0.038	0.099
DP0635	FW	0	62	0	127.2	0	113.8	0	0.123	0	0.114	0	0.115
DP0635	HW	380	52	323.7	112.2	124.7	68.9	0.262	0.297	0.317	0.11	0.173	0.116
DP0635	WW	2761	0	1449.8	0	246.1	0	0.301	0	0.638	0	0.133	0
DP0641	B	13	55	31.2	56.6	21.6	60.1	0.84	0.197	0.211	0.383	0.198	0.343
DP0641	EW	247	154	372.8	234.9	163.7	217.2	0.175	0.063	0.458	0.288	0.091	0.114
DP0641	FW	112	586	149	524.3	98.7	167.2	0.192	0.236	0.173	0.609	0.164	0.13
DP0641	HW	208	1010	139.6	538.4	50.7	146.9	0.682	0.314	0.162	0.624	0.335	0.215

stope_name	surface	vol_ob	vol_ub	area_ob	area_ub	per_ob	per_ub	c_ob	c_ub	x_ob	x_ub	h_ob	h_ub
DP0641	WW	75	748	238.4	396.4	173.8	206.1	0.099	0.117	0.277	0.46	0.054	0.252
DP1159	B	0	12	0	56.6	0	57.4	0	0.216	0	0.448	0	0.075
DP1159	EW	372	750	328.2	478.1	127.3	187.9	0.255	0.17	0.325	0.474	0.166	0.191
DP1159	FW	379	1169	352.5	425	94.2	160.6	0.499	0.207	0.334	0.403	0.152	0.355
DT0735	B	103	168	102.9	121	46.4	83	0.601	0.221	0.228	0.268	0.262	0.336
DT0735	EW	45	566	53.4	736.2	53.2	192	0.237	0.251	0.054	0.749	0.307	0.075
DT0735	FW	36	124	109.9	206	71.7	129.6	0.269	0.154	0.196	0.368	0.083	0.112
DT0735	HW	609	782	285.6	327.5	70.6	117.4	0.72	0.299	0.368	0.422	0.335	0.351
DT0735	WW	394	305	437.8	434.7	141.5	187	0.275	0.156	0.412	0.409	0.114	0.089

F.2 PROBABILITY DENSITY FUNCTION GRAPHS OF EXPECTED VOLUMES OF OVER-BREAK FOR BACK ANALYSED STOPES

